Pasquale Cavaliere *Editor*

Ironmaking and Steelmaking Processes

Greenhouse Emissions, Control, and Reduction

Springer

Ironmaking and Steelmaking Processes

Pasquale Cavaliere
Editor

Ironmaking and Steelmaking Processes

Greenhouse Emissions, Control, and Reduction

Springer

Editor
Pasquale Cavaliere
Department of Innovation Engineering
University of Salento
Lecce, Italy

ISBN 978-3-319-39527-2 ISBN 978-3-319-39529-6 (eBook)
DOI 10.1007/978-3-319-39529-6

Library of Congress Control Number: 2016946050

Printed on acid-free paper

This Springer imprint is published by Springer Nature
The registered company is Springer International Publishing AG Switzerland

Preface

Recently, many improvements have been made in ironmaking processes. Additionally, legislative regulations have been modified. As a result, an updated approach to, and description of, the new problems is not present in the literature as a scientific book. Recent technological and metallurgical improvements due to the new regulations and the provisional future regulations need a key point in the scientific literature. Our book offers a complete panorama of industrial steelmaking problems, leading to partial or total solutions of high-quality products with low greenhouse emissions impact.

The aim of the book is to provide readers with an in-depth knowledge of specific topics within the field of steelmaking with a focus on greenhouse emissions control and reduction. The chapters are written by acknowledged specialists in their fields. Beginners and experts will both find in the book a useful instrument and resource for topics relating to steel-production-product quality and plant efficiency-greenhouse emissions abatement. The book describes the main phases of steel production, from raw materials to refining, through the discussion of the control, operations, and instrumentation, always relating to the effect on the emissions and pollutants.

The book gives also a broad panorama of the different legal regulations all around the world, coupled with the different technological solutions, thanks to the contribution of scientists from 18 different countries.

The book is divided into four main parts reflecting the following broad areas of steelmaking:

- Sintering plants' operations, from raw material handling to the big plants' productivity to the most innovative technologies available for hazardous emissions control and reduction
- Blast furnace operations, from CO_2 mitigation to recent technologies finalized to the furnaces efficiency to the numerical modelling of blast furnaces operations
- Electric arc steelmaking, from the emissions control to the most recent technologies available for carbon and special steel
- Greenhouse emissions, from the energy consumption to the radically innovative technology to the future trends of steelmaking

Due to the importance of the topic, it is believed that the book will be revised in the future reflecting changes in technologies and legal regulations and standards.

My special acknowledgments to the passion and cooperation of all the authors and reviewers who made possible the realization of the book and the reduction of the publication time with their hard work and prompt responses.

My special thanks to the professionalism of the editorial office assistants. Finally, I would like to dedicate the work to my parents and to my children, Paolo and Alessandro.

Lecce, Italy Pasquale Cavaliere

Contents

Part I
Sintering Plants Operations

Chapter 1
Sinter Plant Operations: Raw Materials

Jin-Luh Mou and R. John Morrison

Abstract The raw materials for an integrated steelworks can be classified into four categories, which are iron ores, fluxes, fuels, and reverts. The characteristics of these raw materials strongly affect the metallurgical properties of iron ore sinter and sinter plant performance. An optimal ore blend design is therefore essential to produce low cost and high quality hot metal. Without doubt, some hazardous components are brought into the production process, and therefore, there are some associated pollutants. A good preparation of raw materials is the first step for in-process anti-pollution action. This chapter will introduce the common materials used in iron ore sintering and the handling procedures in an integrated steelworks.

1.1 Introduction to the Raw Materials Used in an Integrated Steelworks

1.1.1 Iron Ores

1.1.1.1 Iron Ore Fines

Based on the mineralogy, iron ores include hematite, magnetite, and goethite; a pure hematite (or others) is really rare but a mixture of different iron ore minerals is common. Most of the ores normally consist of hematite + magnetite + goethite; the ratio of mineral types can be roughly identified from the FeO and LOI content. The higher the FeO the higher magnetite will be, the higher LOI the higher the goethite content will be.

Based on the porosity, iron ores are classified as either a porous type or a dense type. Normally, the iron ores with crystalline water or combined water also have high porosity. More highly weathered deposits also usually have higher porosity.

J.-L. Mou
Formosa Ha-Tinh Steel Corporation, Ha-Tinh, Vietnam

R.J. Morrison (✉)
School of Earth and Environmental Sciences, University of Wollongong,
Wollongong, NSW 2522, Australia
e-mail: johnm@uow.edu.au

P. Cavaliere (ed.), *Ironmaking and Steelmaking Processes*,
DOI 10.1007/978-3-319-39529-6_1

1.1.1.2 Iron Ore Lump

Based on the particle size, iron ores are classified as iron ore fines (<10 mm) or iron ore lump (6.3–31.5 mm); iron ore fines are first processed in a sinter plant, while lump ores can be charged into the blast furnace (BF) directly. Iron ore lump is the lowest cost iron bearing material for the BF burden. Around 25–30 % under size lump (normally <10 mm) is screened out in the BF stock house and fed back to the sinter plant as iron ore fines.

1.1.1.3 Concentrate

If an iron deposit with a lower Fe content needs to be upgraded through a series crushing, milling, flotation, and magnetic separation processes, the product is called iron concentrate (<200 mesh or 75 μm). Concentrates are normally processed into iron ore pellet. A decade ago, Chinese steelworks followed the Japanese HPS (Hybrid Pelletized Sinter) process and developed the so-called mini-pellet sintering process, which uses lime milk as the binding matrix and uses a mixing drum to granulate the concentrate into mini-pellet; it is then put into a sinter machine to produce the grape type sinter, with excellent reducibility in blast furnaces.

1.1.1.4 Pellet

Pellet is made from iron concentrate with a nickname of “smoothing pill” because of its round shape and value for the burden permeability inside blast furnace. It is easy to roll under the distribution chute of blast furnace; therefore the blast furnace shape is slimmer when using high pellet ratio and squat for high sinter ratio.

1.1.1.5 Some Common Iron Ores

Magnetite (Fe_3O_4=FeO+Fe_2O_3, isometric crystal system)	
 http://webmineral.com/data/Magnetite.shtml	FeO:31.03 % Fe_2O_3:68.97 % Fe:72.2 % O:27.6 % Hardness : 5.5–6.5 specific gravity : 4.9–5.2 Originated from magmatic sources, contact metasomatic-hydrothermal reaction, metamorphic reaction, and a series of volcanic activities Strong Ferromagnetism, octahedron crystal form, with iron black luster, black streak, semi-metal luster

Hematite (α-Fe_2O_3, trigonal system)	
 http://webmineral.com/data/Hematite.shtml	Fe: 70 %, O: 30 % Hardness: 5.5–6.5, specific gravity : 5.26 Widespread mineral, arises from different geological processes. Hematite may be oxidized with water to form goethite. Streak shows bright cherry red or liver color. Metal to semi-metallic luster. Hematite may be in various forms: 1. Specularite: with metal luster of flake shape 2. Mica hematite: shape like fish scale 3. Oolitic hematite: oolitic or kidney shape
Martite (γ-Fe_2O_3, Isometric system) hematite but with magnetite appearance	
 http://www.mindat.org/min-2583.html	γ-Fe_2O_3, normally from the oxidation of magnetite, but with the appearance of magnetite Fe^{2+} in magnetite is replaced by Fe^{3+} ($3Fe^{2+} \rightarrow 2Fe^{3+}$), there are 1/3 of Fe^{2+} vacancy generated Martite is meta-stable in nature
Limonite	
 http://webmineral.com/data/Goethite.shtml	Limonite is not a mineral but a mixture of goethite, lepidocrocite, oxyhydroxides, and clays, without specific chemical composition and water content 1. Goethite α-FeO(OH), Fe 62.9 %. If contains absorption water, it is called water-goethite ($HFeO_2 \cdot nH_2O$) 2. Lepidocrocite γ-FeO(OH), Fe 62.9 %. If contains absorption water, it is called water-Lepidocrocite ($FeO(OH) \cdot nH_2O$)

Ilmenite ($FeTiO_3$, Trigonal system)	
 www.galleries.com/minerals/oxides/ilmenite/ilmenite.htm	Fe: 36.8 %, Ti: 36.6 %, O: 31.6 % Hardness: 5.0–6.5, specific gravity 4–5. Weak magnetism Ilmenite occurs in ultra-mafic, basic igneous, and metamorphic rocks Rhombohedron, irregular granular shape, fish scale, or plate shape It forms solid solution with hematite above 950 °C When temperature is dropping, segregation happened and brought fish scale inclusions into the crystal
Siderite ($FeCO_3$, Trigonal system)	
 http://webmineral.com/data/Siderite.shtml	FeO: 62.01 %, CO_2:37.99 % Hardness 3.5–4.5, specific gravity of 3.96 depends on the content of Mg & Mn Normally combined with Mg & Mn, shows rhombohedral shape with a curved crystal surface Crystalline shows grape shape, or earthy in yellow, brown yellow color

1.1.2 Fuel

1.1.2.1 Coke Breeze

Coke is the major reductant and heat source for blast furnace operation, where the lump coke (25–80 mm) is charged into blast furnace directly, and nut coke (15–25 mm) is mixed with the iron burden (sinter, pellet, or lump) and then charged into the furnace. The <15 mm under size portion (~15 % of coke production) is screened out in the coke oven screening station, and then crushed to <5 mm as the fuel for the iron ore sintering process.

The combustion heat from coke breeze provides the necessary energy for partial melting of the iron ore ultra-fines and fluxes to generate the bonding melt. The associated S and N contents in coke breeze convert to SOx and NOx and become the major pollutant sources of an integrated steelworks. Suppose a sinter plant consumes coke breeze of ~50 kg/t.sinter, and the BF coke rate is around 500 kg/t.HM. The estimated gases generated from sinter plant are SOx ~35 % and NOx ~28 % of the total emissions in an integrated steelworks (Mou 1998).

Owing to the incomplete combustion, the un-burnt carbon fragments and chlorine become bonded together under the catalytic effect of Fe or Cu (or their oxides) to form PCDD/Fs. The analysis data showed the toxicity fluctuates from ~0.5 to ~3.0 ng I-TEQ/Nm^3 depending on the materials being used and the operational condition (Kasai et al. 2001). A more detailed description will be discussed later.

Obviously, coke breeze is the major pollution source in the iron ore sintering process, where the S exists either in organic or inorganic phase, where the organic phase is hard to remove during the coal washing or the following coking process. Normally, using Australian coking coal would have 0.5–0.7 % of S remaining in the coke.

A sinter pot test conducted by Japanese steel mills using 79 % Ar + 21 %O_2 to check the NOx formation in sintering process concluded that fuel NOx is the major route rather than thermal NOx (Suzuki et al. 1975). N exists in coke in the amine form and is difficult to remove in the coking process. Not all the N in coke breeze converts to NOx; this depends on the coke breeze combustion conditions, the higher the sinter bed permeability the lower the NOx generated. Normally the conversion ratio is around 30–35 % (Hida et al. 1980).

1.1.2.2 Anthracite

Anthracite is a deeply metamorphosed type of coal with low volatile matter (VM—around 6–10 %) and high fixed carbon. It is a natural coke. Comparing the price with coke breeze, anthracite is much cheaper. Japanese steel mills use anthracite to replace coke breeze due to insufficient coke supply and reduce the sinter plant fuel costs.

Higher VM content generates another problem in the sintering process, the gas flow is from the top surface and passing through the sinter bed into the wind box and exhaust gas pipe, where VM is released out under the combustion zone before being ignited and sucked into the waste gases pipe, eventually adhering to the electrostatic precipitator plates and wires; for some time, the dust removal efficiency deteriorates and causes smolder, especially when the manhole is opened and fresh air flows into the EP during repair.

North Korea anthracite is an excellent clean fuel with the low sulfur content (S less than 0.3 % or even less than 0.18 %). It is used to replace coke breeze (30–50 %) to reduce SOx emissions; an example from China Steel Corporation had shown the actual SOx emissions were reduced from 110–130 to ~70 ppm. Low sulfur anthracite is now being applied in iron ore sinter plants as a countermeasure to reduce SOx emissions.

Table 1.1 Fixed C, heat value, VM, S content of different fuel for the sintering process

	Fixed C%	N%	S%	Total moisture%	VM%	Ash%	Heat value (Kcal/kg)
Coke breeze[a]	~82	~1.0	~0.6	<6	<2	~13	~7000
Low S Anthracite[b]	>80	<0.1	<0.2	<12	<6	<12	>6200
Carbonized palm shell	~85	0.1–0.5	~0.09	~13	~10	~3	~4800

[a]CWQ coke
[b]North Korea low S anthracite

1.1.2.3 Biomass (Carbonized Palm Shell)

Many kinds of biomass can be used in the iron ore sintering process, but two issues should be considered. The first is the processing cost, and the second is the VM level. For example, palm trees are popular in South East Asian countries; after the palm oil is extracted the shells are dumped as garbage or used as crude fuel in rural areas. Since the palm shell size is good for the sintering process, attempts have been made to use carbonized palm shell in the process. The collecting, transporting, and processing costs, however, are even higher than for coke breeze, and this eventually restricts the level of application. Another issue is the VM level of over 15 % after carbonization. The combustion speed in the sinter bed is too fast under such high VM levels and the sinter bonding strength becomes weak, and the quality deteriorates.

The advantages of using biomass are to reduce fossil fuel usage and reduce greenhouse gases emissions; the second is the S level is extremely low, which is effective in reducing SOx emission. The processing techniques need to be improved to reduce VM level; otherwise, the replacing ratio of coke breeze is low and cannot provide the advantage of using biomass. Table 1.1 shows the specifications of different fuels used in the sintering process.

1.1.3 Fluxes

1.1.3.1 Limestone

The chemical formula of limestone is $CaCO_3$; it is used in lime production and iron ore sintering. Limestone can be classified as primary sedimentary limestone and re-crystallized marble limestone.

Primary sedimentary limestone is known as reef limestone with relict fossil (commonly shell or coral reel) and porous texture. A strong water adhering ability, makes it good for granulation of the sinter raw mix, and therefore improves the sinter bed permeability and increases the productivity. In addition, the fine crystalline and porous texture provides a high reactivity of CaO with Fe_2O_3 to form a calcium ferrite bonding matrix. The generated liquid melt volumes are higher than from marble limestone, and increase the bonding portion and enhance bonding strength. Marble limestone also can be applied in the sintering process, but has lower reactivity, and the productivity and strength are poorer than using reef carbonate.

The size of limestone used in the sintering process will strongly affect the sinter plant performance; however, if we are looking for higher productivity, then a coarse limestone particle is required (<6.3 mm), if we want higher sinter strength, then finer particles are utilised (<3 mm).

Burnt lime is an essential flux for the steelmaking process, especially for desulfurization, converter slag forming, and the RH refining process. Normally, marble limestone is more suitable for producing burnt lime than reef material. Limestone decomposes at 900–950 °C; marble particles expand first and then shrink during the heating stage, micro fractures are generated and the lump particle breaks into small particles. If the marble has a micro-crystalline texture, the stress occurring during the heating stage would be absorbed as the grain boundary surface energy and reduce the breakage.

If reef limestone is used for lime production, its surface would become over burnt, partial melting occurs and the melt would become coated on its surface and reduce the lime reactivity. If some clay is associated with the reef limestone, some low melting point compounds such as di- or tricalcium silicate (C_2S, C_3S) will form and cause a clogging problem.

1.1.3.2 Dolomite

The chemical formula of dolomite is $CaMgCO_3$, it provides the MgO source for blast furnace slag formation. MgO does not participate in the bonding phase of iron ore sinter, nor does it help to improve sinter strength. MgO (periclase) exists independently in the SFCA (silico ferrite of calcium and alumina) or replaces Fe^{2+} of the crystal structure of magnetite.

Dolomite is also processed in lime kiln to produce light burnt dolomite for steelmaking. Since the converter refractory is MgO or MgO-C bricks, in order to protect the MgO base refractory, the converter slag should be oversaturated to control the MgO diffusion from slag to wall, rather than from wall to slag. In addition, MgO may improve the fluidity of slag.

Dolomite decomposes at two temperatures (~700 and ~950 °C), so the breakage portion is higher than limestone. Light burnt dolomite has strong water absorption capacity, and quickly loses its reactivity.

It is recommended that the light burnt material is utilized as soon as it is processed.

1.1.3.3 Serpentine or Olivine

The serpentine group describes a group of common rock-forming hydrous magnesium iron phyllosilicate ($(Mg, Fe)_3.Si_2O.5(OH)_4$) minerals; the most common serpentine mineral is antigorite. Olivine with a similar composition of $(Mg,Fe)SiO_4$, provides both MgO and SiO_2 for blast furnace slag formation in iron making process.

Serpentine and olivine are also used in the iron ore sintering process as a flux. Serpentine dehydrates around 400–700 °C and converts to Mg-olivine (forsterite) and amorphous $MgSiO_3$; under iron rich conditions, low melting compounds (such as fayalite + forsterite) turn into the bonding melt, where the MgO exists in a silicate melt rather than in Periclase form, and provides a silicate bonding phase. Normally, using serpentine or olivine as the MgO source will show better sinter strength and productivity than using dolomite.

The restriction on using serpentine or olivine in the sintering process is the SiO_2 level in iron ore fines; the blast furnace slag consists of four components,—CaO, MgO, SiO_2, and Al_2O_3—and among those certain fixing ratio ranges are important ($B2 = CaO/SiO_2 = 1.15–1.25$, $B3 = (CaO + MgO)/SiO_2 = 1.40–1.45$, $B4 = (CaO + MgO)/(SiO_2 + Al_2O_3) = 1.00–1.10$). If the SiO_2 were high in slag, then the other components will adjust accordingly to maintain the B2, B3, B4, this will increase the slag volume and need further fuel and decrease the productivity. In the last decade, owing to the strong demand for steel products in China, many iron ore deposits were mined out and dumped to the market without proper processing, and the gangue impurities such as Al_2O_3 and SiO_2 remaining in the iron ore fines are much higher than before, and this restricts the serpentine and olivine usage.

1.1.3.4 Silica Sand

Silica sand is normally used in the glass industry; the purpose of using silica sand in iron making is to maintain the B2, B3, B4 ratio in the blast furnace slag. The silica sand is added to the sinter raw mix and brought into the furnace within the sinter ores. The melting point of silica is 1750 °C, which makes the formation of bonding melt in sintering process difficult. A better option to adjust the SiO_2 level in sinter is by using serpentine or olivine, unless they are not available. Table 1.2 shows the chemical composition of fluxes for iron ore sintering.

1.1.4 Reverts

During the iron, steel making and rolling process, many dusts, slags, scales, slurries, and sludge are produced; these reverts contain valuable C and Fe, and are worth recovering. These reverts also contain some un-welcome compounds, such as PbO, ZnO, Na_2O, K_2O, sulfates, and chlorides. From the view point of physical

Table 1.2 Reference chemical composition of fluxes in iron ore sintering process (%)

	CaO	MgO	SiO_2	Al_2O_3	P	S	LOI
Limestone	>52.0	<3.0	<1.5	<0.15	<0.02	<0.03	42–44
Dolomite	>32.0	>18.0	<1.0	<0.5	–	–	–
Serpentine	–	34.5–37.5	38.5–41.5	<2.3	–	–	–
SiO_2-sand	–	–	>95	<2.5	$Na_2O + K_2O < 1.5\,\%$		

properties, their particles are extremely fine or extremely large, and need further processing. Many recovery processes have been developed, such as RHF (Rotary Hearth Furnace), oxy-cup, mini-pellet process, and so on, trying to recover these reverts at the lowest cost and without secondary pollution; a revert homogenization process will be introduced in the raw materials handling section.

1.1.4.1 Dust

Dust arises from fugitive particles being collected through dry processes, such as electrostatic precipitator (EP), cyclone, or bag filter. If the waste gas volume is large (>10^6 Nm^3/min) and having a high dust concentration (>1000 mg/Nm^3), then EP is recommended. Particles pass through an electric field and being polarized with electric charges are then collected by electric plates and wires; eventually, dust is collected in hoppers by rapping the plates and wire frames. Some high electric resistant materials such as alkali chlorides are difficult to polarize and difficult to remove from the waste gases. These particles are within the sub-micron range (<1.0 μm). The aerosols would take shape as these particles behave like nuclei, and acid gases condense on their surface, which scatter the visible light and cause the opacity problem.

If the gas volume was smaller and with coarse fugitive particles, then cyclone is recommended. The waste gas stream is conducted into a spiral channel, to reduce the gas diffusion speed and condense the particles under their own gravity, but dust removal efficiency is not as good as EP.

Bag filter is a pressure filtration device; particles are trapped by the filter cloth under the high pressure gas current. The waste gas handling capacity is flexible by installing different number of filtration tubes. The newest technique is able to remove the particles above 0.5 um, but the disadvantage of bag filter is the caking problem, especially under high moisture or sticky materials, the caking would block the filtration pores and shorten the filter life.

1.1.4.2 Scale

Mill scales are oxidized iron from the continuous casting line (CC), hot strip mill, or bar and wire rod mills; these oxidized iron materials are composed mainly of FeO and with TFe of >70 %. Mill scales are able to provide heat in the iron ore sintering process owing to the oxidation of FeO to Fe_2O_3, and save some fuel.

Water guns are installed for de-scaling from slab, bloom, or billet surfaces during the CC or rolling process. These scales are collected in sedimentation ponds, the coarse mill scales are trapped in a whirlpool, and the fine pit scales are trapped in an advection pool. Due to the leakage of lubricant oil or grease in the processing lines, these oils can accumulate in advection pools and seep in between the pit scale layers and make the pit scale become oily mill scale. The oil content can be sucked into the waste gas main and adhere to the EP plates when recovering pit scale in sintering process—this smoldering problem occurs when the oil content is too high. A routine check of oil content in EP dust is essential to prevent smoldering.

1.1.4.3 Sludge and Slurry

Sludge is a condensed viscous wet mixture and slurry is in a semi-liquid form, both are from the wet de-dusting or de-fume processes to trap fugitive fine particles. The major sources of sludge and slurry are from the blast furnace gas purification system and converter off-gases treatment system.

Two stage de-dusting devices are installed in the traditional blast furnace; the first is a gravity cyclone to trap coarse particles, and the second device is a wet type scrubber. Some steelworks apply dry dust catching systems by using cyclones and bag filters, the dust is removed but the acid gases, especially HCl and H_2SO_4, remain in the gas and condense to liquid phase with a very low pH value, eventually, causing a serious pipe corrosion problem. An alkali solution injection is required to maintain the pH value. However, dry cleaning processes need sophisticated operational skills.

Oxygen is injected into the steelmaking converter to burn C inside the liquid metal, hence, the liquid steel temperature increase to around 1700 °C, and the off-gases temperature is also high around 1500 °C; therefore, Venturi mist spraying systems are installed to reduce the gas temperature and trap the dust within the mist + dust particles. These particles are separated from the off-gas system by gravity and drop into the slurry tank. A vacuum filtration device is installed to remove the water and turn these particles into filtration cake. This cake contains very high FeO and C and recoveries are through the iron ore sintering process. The remaining slurry is injected into sinter blend mixing drums as granulation moisture.

Scraps are charged into the converter as coolants; some Zn and Pb from automobile scrap are also brought into the converter and evaporated into the waste gas system. Eventually, basic oxygen furnace (BOF) off-gas cake and slurry may contain ZnO and PbO and cause clogging problems in the blast furnace. Therefore, a proper treatment is required to separate ZnO and PbO before putting the cake and slurry into the sintering process.

1.1.4.4 Slag and Slag Tailing

Blast furnace slag (production) ratio is around 300 kg per tonne of hot metal; the typical chemical composition is shown in Table 1.3.

The slag can be cooled by air or water quenching; air cooled slag is a gravel paving material with low application value. Water quenched slag with amorphous texture is called Blast Furnace Granulated Slag (BFGS); after grinding to a specific surface area of >4000 cm^2/g, the slag powder has pozzolanic properties and is applied in concrete as a replacement of cement with higher application value.

Table 1.3 Typical chemical composition of BF slag (%)

FeO	MnO	P	S	SiO_2	Al_2O_3	CaO	MgO	B2
<1	0.3–0.5	<0.02	0.7–1.0	34–37	13–15	41–45	6–8	1.20 ± 0.05

Steel slags ratio is around 100–120 kg/t.Liq.Steel, which is a sum of de-S (actually, de-S slag is iron slag), de-C, de-P, de-Si slags, and cast residue. Normally, de-S slag associates with ~25 % of iron, and steel slag with 8–10 % steel. De-S slag is crushed and the iron content recovered by screening and magnetic separation. The steel and slag are bonded closely in steel slags, it needs further processing to recover the slag scrap. A steam box treatment by steam pressure has been developed in China and is widely applied in Chinese steel works; it is able to stabilize the free CaO and free MgO, and separate the steel and slag sufficiently, and allow recovery of a higher ratio of steel and make the slag tailings easy for resource use, such as application in steel slag cement.

1.1.4.5 Others

There are some other reverts generated in iron and steel making processes, such as kish graphite, coke dry quench (CDQ) dust, coke water quench (CWQ) sludge, lubricant oil, and grease. If entrusted to a contractor to clean these reverts, this would become a cost burden. However, these reverts have valuable contents and should be recovered internally in steelworks to fit well with a Zero Waste policy. Table 1.4 shows typical chemical composition of reverts.

Table 1.4 Typical chemical composition of reverts (%)

ITEM	CDQ dust	BF sludge	DW sludge	Oily mill scale	BOF dust	CRM sludge	IWI fly ash	Sinter EP dust
C-Fix	88.21	33.64	5.51	0.07	5.44	13.06	2.94	7.23
T.Fe	0.64	31.57	63.48	75.21	59.62	26.66	27.65	47.14
Fe_2O3	0.91	41.92	34.54	11.39	70.71	21.47	35.00	62.76
FeO	0.00	2.72	50.18	87.50	9.76	10.78	0.98	2.78
M.Fe	0.00	0.16	0.80	0.07	2.67	3.37	2.42	1.11
T.Cr	0.00	0.02	0.48	0.07	0.04	0.04	0.40	0.05
Cr_2O_3	0.00	0.03	0.69	0.09	0.06	0.06	0.58	0.07
M Cr	0.00	0.00	0.01	0.01	0.00	0.00	0.00	0.00
T.Ni	0.00	0.01	0.22	0.03	0.02	0.02	0.18	0.01
NiO	0.00	0.01	0.27	0.03	0.03	0.03	0.20	0.01
M. Ni	0.00	0.00	0.01	0.01	0.00	0.00	0.02	0.00
Pb	0.00	0.31	0.01	0.01	0.15	0.01	0.02	0.01
PbO	0.00	0.33	0.01	0.01	0.16	0.01	0.02	0.01
Zn	0.00	1.54	0.10	0.01	0.49	0.66	1.95	0.05
ZnO	0.00	1.92	0.12	0.01	0.61	0.82	2.43	0.06
Na	0.02	0.04	0.02	0.01	0.02	0.17	0.25	0.18
Na_2O	0.03	0.05	0.02	0.01	0.02	0.22	0.34	0.24
K	0.09	0.06	0.00	0.00	0.01	0.06	0.23	1.15
K_2O	0.11	0.08	0.00	0.00	0.01	0.07	0.28	1.38
P	0.00	0.06	0.07	0.01	0.08	0.63	0.88	0.05

(continued)

Table 1.4 (continued)

ITEM	CDQ dust	BF sludge	DW sludge	Oily mill scale	BOF dust	CRM sludge	IWI fly ash	Sinter EP dust
P_2O_5	0.00	0.13	0.17	0.02	0.17	1.44	2.01	0.12
S	0.32	0.55	0.11	0.01	0.09	0.31	1.25	0.36
SiO_2	5.79	5.49	0.73	0.01	1.78	5.30	11.11	5.33
Al_2O_3	3.20	2.36	0.15	0.07	0.50	0.84	3.47	1.86
CaO	0.00	4.82	3.49	0.02	4.59	16.47	23.67	8.32
MgO	0.00	0.65	0.24	0.01	0.45	3.51	3.61	1.03
MnO	0.00	0.22	0.54	0.29	0.37	0.15	0.74	0.18
TiO_2	0.00	0.12	0.01	0.01	0.07	0.05	0.25	0.10
Cl	0.00	0.05	0.01	0.01	0.03	0.45	0.97	1.46
F	0.00	0.06	0.10	0.01	0.15	0.03	0.43	0.19
Oil	0.20	0.19	1.68	0.22	0.17	5.77	0.18	0.23
Others	1.23	4.57	0.71	0.14	2.25	16.61	8.22	5.23
Total	100.00	100.00	100.00	100.00	100.00	100.00	100.00	100.00

1.2 Introduction to Raw Materials Handling

Raw materials handling is like a relay station and the artery system in the human body for blood transport. The materials receiving, stocking, reclaiming, and conveying systems would be different depending on the locations and the production capacity of a steelworks. Recently, raw materials supply by maritime transport has become the major trend; more and more steelworks are moving to ocean adjacent areas to take advantage of the cost savings of having their own wharf and unloading system. This section will give a brief introduction to the unloading devices, stock yard operations, and the related conveying systems.

1.2.1 Unloading and Conveying

1.2.1.1 Unloaders

Different kinds of unloading devices have been developed to meet the raw materials characteristics, so as to discharge these materials most smoothly and within the shortest duration. A brief introduction of some common unloaders follows.

Bucket Chain type: suitable for iron ore and coal unloading, designed for hard and heavy materials.
Screw Type: suitable for coal unloading, not suitable for iron ore.
Grab Type: suitable for iron ore, coal and fluxes. The unloading speed is low.

Bucket-Chain CSU

There are two types of Bucket-Chain CSU, one is catenary type (Fig. 1.1) without rigid support in the reclaiming section, where the hopper reaches onto the cargo surface and is able to adjust the angle when the waves are high, it also has the bottom clearance ability.

Another is L-shaped chain bucket CSU (Fig. 1.2), where the reclaimer can be rotated, and the boom can be tilted with rotation. The reclaiming procedure can be automatically controlled. There is no up and down grabbing movement, and with a closing system, so the dust emission during unloading is much lower than with grab types. It is an environmentally friendly system.

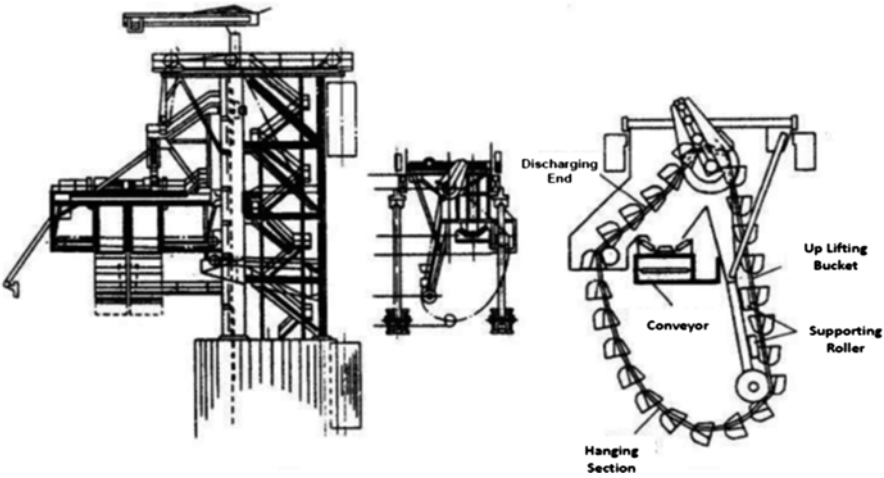

Fig. 1.1 Catenary type bucket-chain CSU (http://wiki.mbalib.com/zh-tw/)

Fig. 1.2 L type bucket-chain CSU

Fig. 1.3 Screw type CSU

Screw Type CSU

The dispensing head of screw unloaders is inserted into the pile cabin; a reverse rotating reclaimer moves the materials into a vertical screw conveyor, and then uplifted to the horizontal screw conveyor, and eventually transported into the transit silo and discharge to the stock yard by conveying system (Fig. 1.3). The biggest advantage is the operation process in a closed system, without dust pollution, but the abrasion is severe for hard materials, and the energy consumption is even higher due to the sophisticated mechanical structure. It is mainly used for coal, cement, bulk grain, fertilizer, potash, and other bulk materials unloading.

Grab Type Ship Unloader

The grab type unloader (Fig. 1.4) has been wildly applied in recent decades, and it is the most popular unloading system being used. The advantage is the suitability for different kinds of materials, e.g., coal, iron ores, and fluxes. Low efficiency is the disadvantage due to the return bucket not holding any materials. In addition, dust emissions are generated when the grab opens to discharge the materials into the receiving hopper.

1.2.2 Conveyor

Conveyors are designed to meet the operational requirements, and the most popular types of conveyors used in steel works are (1) steel cord conveyor, (2) canvas conveyor, and (3) aramid conveyor.

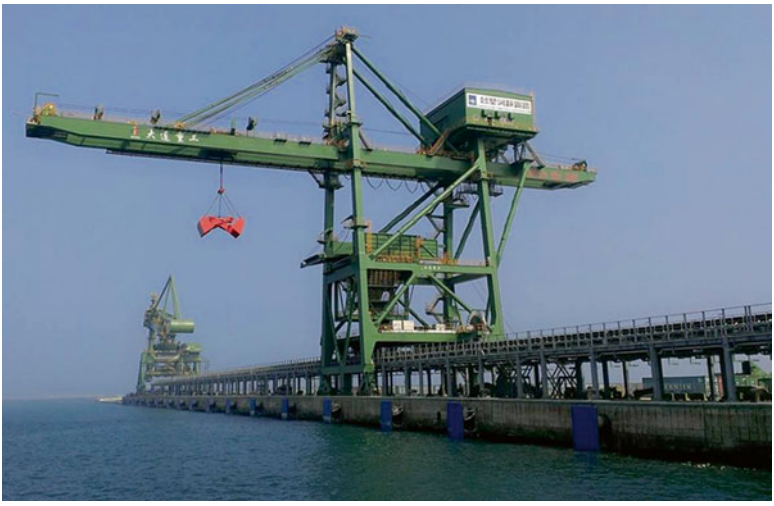

Fig. 1.4 Grab type unloader

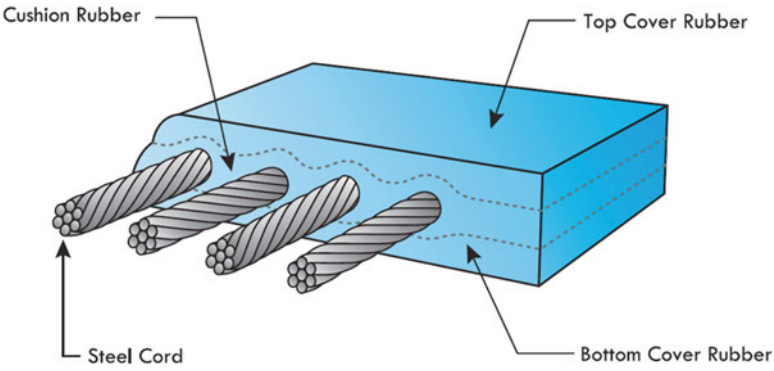

Fig. 1.5 Cross section of steel cord conveyor

1.2.2.1 Steel Cord Conveyor Belt

Steel cord conveyors are used for heavy loading transportation, or high flow rate transportation. The advantages are superior impact resistance, excellent trough ability, low stretch, suitable for long-distance transportation, and long working life. The cross section is shown in Fig. 1.5.

1.2.2.2 Canvas Conveyor Belt

Canvas conveyors are used in high moisture materials transportation, due to the high water proofing characteristics. The durability is not as good as in steel cord conveyors. These are in less load transportation and low flow rate conveying

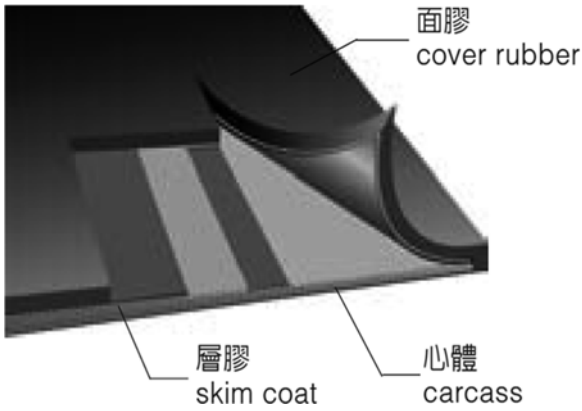

Fig. 1.6 Cross section of canvas conveyor

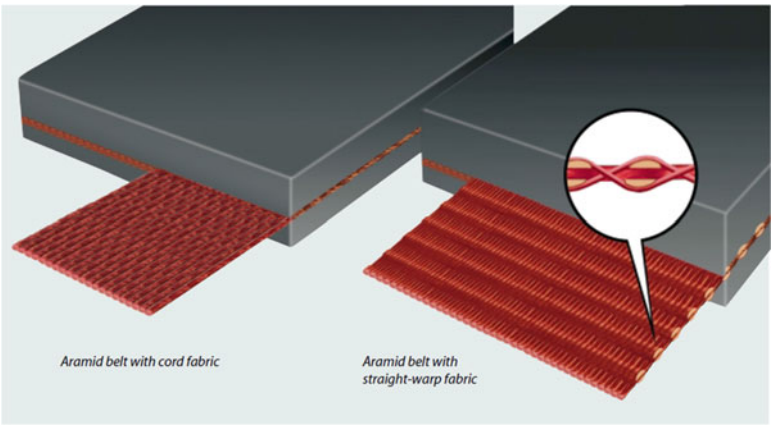

Fig. 1.7 Cross section of aramid conveyor

systems. The advantages are highly waterproof, low stretch, high tensile strength, high impact resistance, better mildew and moisture resistance. A cross section of a canvas conveyor is shown in Fig. 1.6.

1.2.2.3 Aramid Conveyor Belt

These are conveyors made of synthetic polymers with rubber to provide exceptional strength and thermal stability. They are durable for corrosion and moisture resistance, only the initial installation cost is higher than the other types of conveyors. The aramid conveyor features are superior impact resistance, corrosion and moisture resistance, long lifetime, easy installation and maintenance, and easy for recycling. The cross section of an aramid conveyor belt is shown in Fig. 1.7. A comparison of different conveyors characteristics is presented in Table 1.5.

Table 1.5 Conveyor belt comparison table

	Aramid	Steel cord	Canvas
Noncombustible	○	○	×
Nonconductive	○	×	○
No Spark	○	×	○
Corrosion resistance	○	×	○
Weight reduction	○	×	△
Low power consumption	○	×	△
High strength	○	○	×
Softness	○	×	○

○: Excellent △: Normal ×: Poor

1.2.3 Stock Yard

In order to balance the chemical composition and enhance mineral transformation during the sintering process, normally, several kinds of iron ores are being used at one time. How to adjust the sinter ore blending ratio by "drawing the sturdy portion to offset the weaknesses" has become the operation 'know how' for every steelworks. A preliminary experiment using a sinter pot test is conducted before choosing the ore type and ratio, followed by the integrated production plan to arrange the shipment and stocking; eventually, these raw materials are purchased and stored in the stock yard.

1.2.3.1 Open Yard

The most popular stock yard is an open yard. The materials with dense and coarse particles, resistant to wind blow and rainfall, are stocked in an open yard, but this would depend on the weather conditions. The excess or un-qualified sinter ores and coke are temporarily stocked in a dumping yard, which is ready to maintain the BF operation during the shutdown time of the sinter plant or coke oven. Figure 1.8 shows the stock yard and S/R (stacker and reclaimer), Fig. 1.9 shows the coke dumping yard.

1.2.3.2 Indoor Yards

Indoor yards are normally installed in the windy and heavy rain areas, but recently, steelworks have been requested to install indoor yards to prevent dust emissions. Two major types of indoor yards have been introduced, one is dome shaped and the second is a strip type. Figures 1.10 and 1.11 show a dome type indoor yard, and Figs. 1.12, 1.13, and 1.14 show the strip type indoor yard.

Fig. 1.8 Ore yard and S/R

Fig. 1.9 Coke dumping yard

Fig. 1.10 Dome indoor yard-exterior

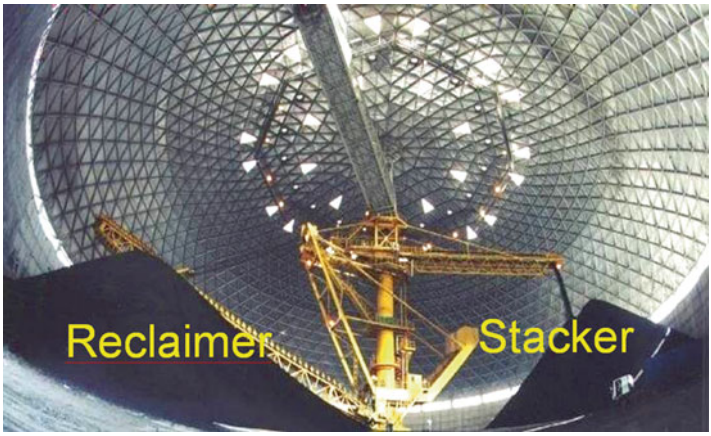

Fig. 1.11 Dome indoor yard-interior

1.2.4 Blending Silo and Blending Yard

1.2.4.1 Blending Silos

There are different ore blending schemes, some steel works blend iron ores only in the blending yard, and others may mix with fluxes, reverts, or BF return fines. However, the main purpose is to homogenize the ore mix and conform to the required chemical targets.

Fig. 1.12 Strip type indoor yard-exterior

Fig. 1.13 Strip type indoor yard-interior

Each silo contains different ores, fluxes, reverts, or others; through the chemical calculation to set the discharging rate of each bin, these materials are fed to a main conveyor and send to the blending yard for blending. The numbers of silos and holding capacity will depend on the ore usage and sinter plant capacity. Figure 1.15 shows the blending silos.

1.2.4.2 Blending Operations

Blending operations are to deploy these materials layer by layer through a walking stacker (Fig. 1.16), and reclaim the pile from cross section, Fig. 1.17 shows a roller drum type reclaimer.

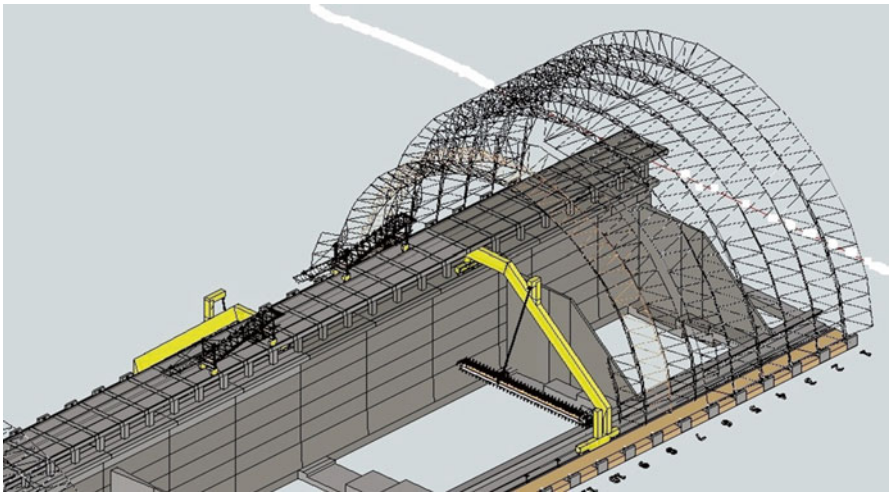

Fig. 1.14 Strip type indoor yard-sketch

Fig. 1.15 Blending silo

1.2.5 Reverts Homogenization Plant

A reverts treatment system is essential in any steelworks, because many iron, carbon, or CaO bearing wastes are worth recovering and feeding back into the production process. A reference typical Homogenization Plant is introduced in this section. A road map for reverts generation and utilization is shown in Fig. 1.18.

Fig. 1.16 Blending pile

Fig. 1.17 Roller drum type reclaimer

The basic ideas are as follows:

1. To remove alkali chloride elements from sinter plant EP dust by a stirring and washing system. This is a simple and easy method to depress PCDD/Fs formation by means of reducing Cl content, and also prevents the BF clogging by removal of low melting point alkaline salts;

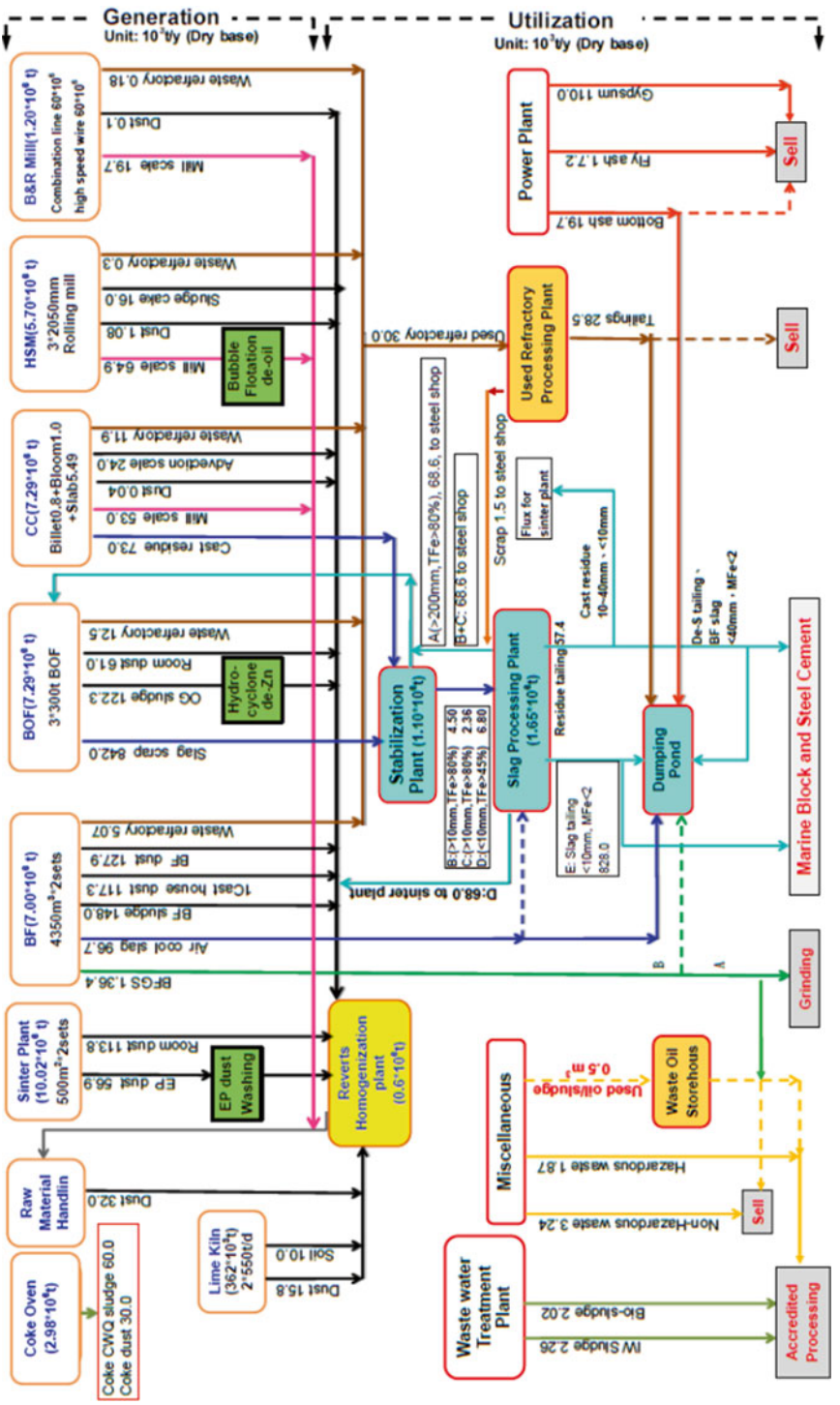

Fig. 1.18 Road map for reverts generation and utilization (example based on 7.29×10^6 t crude steel/year)

2. To separate high-Zn content of BOF OG slurry by hydro-cyclone, the Zn source may be from the head or tail chopping waste of the galvanization line, or using the auto scrap in BOF;
3. To remove the oil content from rolling mill pit scale by bubble flotation. The oil occurs in between the layers of the platy scale, these adhering scales have to be opened by strong bubble stirring and then remove the oil.
4. The wet sludge and dry dust are then mixed by an intensified mixer, followed by a blending and aging treatment before being sent to the blending silo as raw materials for the sinter plant. The reason for aging is that some of the Fe^{2+} or Fe^{0} in the waste should be changed into stable $Fe(OH)_2$ or Fe_2O_3 to prevent the clogging inside the silo.

The revert materials after removing the un-welcome elements, then, are classified into wet and dry groups, the dry dusts are transferred by tank lorry and stocked in bins, the wet reverts (H_2O <10 %) are transferred by truck and stocked in panel bunkers, where the sludges (H_2O >30 %) are transferred by tank and stocked in pits.

The key operational issues are to control the mixing reverts with the moisture content around 12 %, but having no water droplets fall out, and then feed into an intensified mixer before sending to the reverts blending pile. The deployed pile will be cured for about 1 week, with FeO or metal Fe becoming $Fe(OH)_2$ or/and Fe_2O_3 to avoid any clogging problem inside the blending bins. Revert mixture will be treated as one kind of materials to be used in sintering process.

Normally the ratios for wet and dry materials are not just made to balance the final moisture at 12 %; some iron rich tailings from converter slag, BF return fines are used as the dry materials.

Acknowledgements Assistance from colleagues at China Steel Corporation and Formosa Ha-Tinh Steel Corporation in providing the reference data and valuable information is greatly appreciated. However, the iron and steel making techniques are being updated all the time, and we are happy to share the information in this platform, hopefully, we can continue to update the new information in the future and make the world more sustainable ecologically.

References

Hida Y, Sasaki M, Ito K (1980) Consideration on the CO and NO formation around the coke specimen during combustion. Tetsu-to Hagane 66(13):21–29

Kasai E, Aono T, Tomita Y, Takasaki M, Shiraishi N, Kitano S (2001) Macroscopic behavior of dioxins in iron ore sintering plants. ISIJ Int 41(1):86–92

Mou J-L (1998) A study of in-plant de-NOx and de-SOx in the iron ore sintering process. PhD thesis, Environmental Science Department, University of Wollongong, Australia

Suzuki G, Ando R, Yoshikoshi H, Yamada Y, Nagaoka S (1975) A study of the reduction of NOx in the waste gas from a sinter plant. Tetsu-to-Hagane 61(13):3–11

Chapter 2
Predictions of PCDD/F, SO_x, NO_x, and Particulates in the Iron Ore Sintering Process of Integrated Steelworks

Jose Adilson de Castro, Daniele Aparecida Nogueira, Marcos Flavio de Campos, Vagner Silva Guilherme, and Elizabeth Mendes de Oliveira

Abstract This chapter is focused on the multiphase multicomponent model development and prediction of common hazardous compounds produced during the industrial iron ore sintering process within an integrated steelworks. The iron ore sintering process is a key technology in the steel industry due to its possibility of recycling waste solids or powders internally produced during the raw materials handling or subsequent process of steel production. However, this process is also recognized as one of the most critical unit with regard to the polychlorinated dioxins and furans (PCDD/F) emissions. In addition, as fossil fuels are used, the emissions of SO_x and NO_x are significant and must be strictly controlled. The process is dynamic and involves the cross flow of gas through the bed which can carry the fine particles. The outlet gas treatment involves the cleaning with electrostatic precipitator and filter bags. New technologies, however, have been introduced in order to treat PCDD/F and SO_x–NO_x compounds, which introduce significant increase in the cost of the production. New process concepts and technologies have been proposed such as gas recycling, fuel gas injection**,** and biomasses fuels. However, testing these technologies are expensive. In this context, comprehensive mathematical models based on transport phenomena are efficient tools to study and indicate new possibilities for designing operational conditions as well as resizing the machines for minimizing the hazardous emissions. In this chapter, the model principles and analysis cases are presented and discussed. The impacts of four technological proposal on the hazardous emissions of PCDD/F, NO_x, SO_x**,** and particulates are ana-

J.A. de Castro (✉) • D.A. Nogueira • M.F. de Campos • V.S. Guilherme
Universidade Federal Fluminense (UFF) – Escola de Engenharia Industrial Metalúrgica de Volta Redonda (EEIMVR), Av. Dos Trabalhadores, 420, Vila Santa Cecilia, Volta Redonda, Rio de Janeiro CEP 27255-125, Brazil
e-mail: joseadilsoncastro@id.uff.br

E.M. de Oliveira
Centro Federal de Educação Tecnológica Celso Suckow da Fonseca (CEFET), Rua Voluntários da Pátria, 30, Valença, Rio de Janeiro CEP 27600-000, Brazil

P. Cavaliere (ed.), *Ironmaking and Steelmaking Processes*,
DOI 10.1007/978-3-319-39529-6_2

lyzed, as follows: (a) effect of fuel gas injection; (b) effect of gas recycling and oxygen injection; and (c) effect of using biomass and biogas replacing the fossil fuel (coke breeze). The analysis is carried out comparing the actual operation of the industrial iron ore sintering machine with the new concepts proposed based on their specific hazardous emissions.

2.1 Introduction

The iron ore sinter process plays an important role at the integrated steel plant furnishing suitable raw materials for the blast furnace and recycling the inner fine dust produced within the whole steelmaking facilities. The size and capacity of the sinter machines vary widely and are mainly limited by the air suction systems. Larger machines, however, present small ability to handle low-grade raw materials although high-energy efficiencies are usually obtained. The small and compact machines are increasingly becoming attractive due to their ability to use different source of raw materials and low grade iron ores. The traditional sinter plant is composed of raw materials preparation, blowing and suction system, sinter strand, cleaning gas, cooling and sinter product classification. Figure 2.1 shows a schematic view of the sinter facilities.

In this study, the ignition furnace is modified and enlarged dividing ignition and gas burnout zones in order to allow gas fuel utilization and oxygen injection into five wind boxes length aiming to increase the sinter machine efficiency and decrease the emissions. The burner furnace is adapted to have two zones: (a) ignition zone using natural gas and (b) gas burner zone using steelmaking or biogas with oxygen enrichment. This concept is suitable for designing different gas utilization systems. The feeder system is adapted to have height control and allows bed adjustments with uniform distributions.

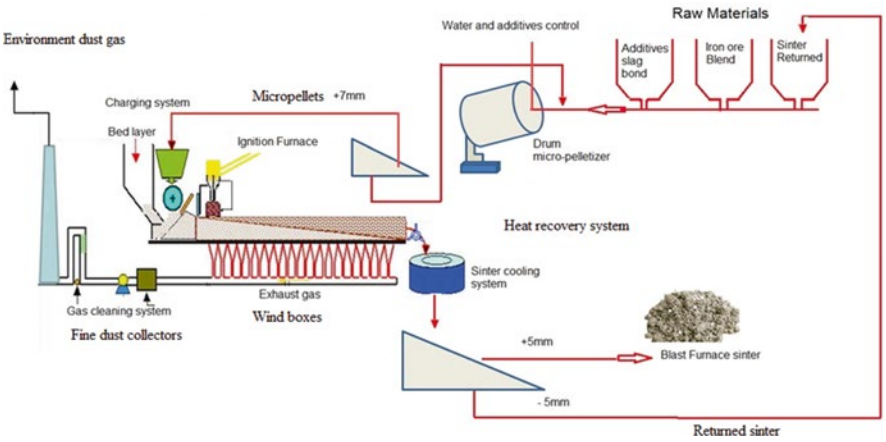

Fig. 2.1 Compact sinter machine and facilities

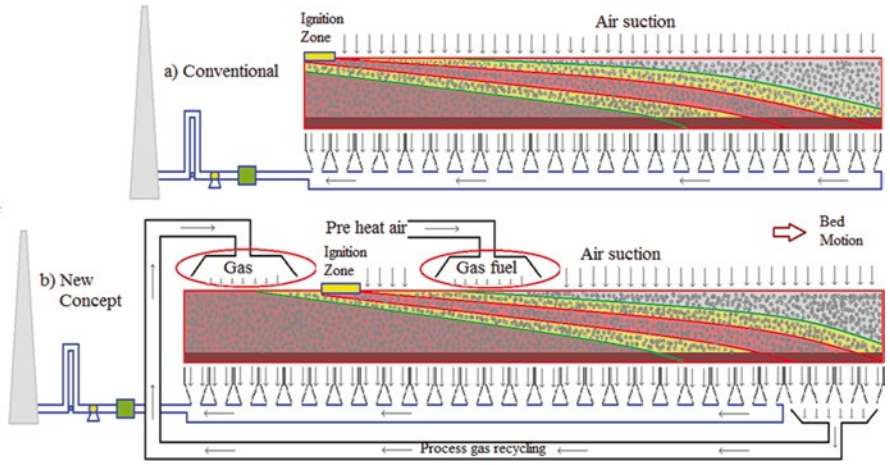

Fig. 2.2 Concept of new technology of gas recycling and gaseous fuels utilization

Many efforts have been made to develop new technologies aiming at decreasing the fossil fuels utilization due to the environmental restrictions and decrease the process carbon intensity (Oyama et al. 2011; Guilherme and Castro 2012). The process is complex and involves various physical and chemical phenomena such as heat, mass, and momentum transfer coupled with chemical reactions (Yamaoka and Kawaguchi 2005; Castro et al. 2012a, b, 2013a, b; Ahan et al. 2013; Kasai et al. 2005; Cumming and Thurlby 1990). These phenomena take place simultaneously increasing considerably the complexity of process analysis. Thus, an effective way of developing new concepts and their quantification is to develop comprehensive mathematical models capable of simultaneously considering the mass transfer using reliable rate equations for the chemical reactions, momentum transfer for complex bed structure and interphase heat transfer considering simultaneously convective, radiation and chemical reactions heat transfer. The proposal of this study is to adapt the actual sintering machine to improve the flexibility of the process and allow simultaneously operation with gas recycling, fuel gas utilization, operation with partial operation of mill scale and biomass together with fossil fuels as coke breeze or anthracite.

Figure 2.2 shows the new concept to attain these principles. As can be seen, the actual machine was modified adding new wind boxes and new furnaces and burners. Therefore, in the first furnace recycling gas can be used to pre-heat, water vaporization, calcination and transform partially the hematite to magnetite recovery the energy of the gas. The second furnace can be used to injection of fuel gas and oxygen at the region where in the traditional operation presents a deficit of heat and oxygen and consequently non-uniform sinter formation. Thus, with this comparatively small investment the process could be improved largely from the point of view of environmental impact and energy savings.

2.2 Theory

A mathematical model based on a set of partial differential equations represents the conservations of momentum, energy, and chemical species for gas, solid (raw material mix and solidified liquid), and melting phases. The domain is restricted to the control volume of the moving strand with the gas passing transversely through the bed, as shown in Fig. 2.2a, b.

The set of differential equations, Eqs. (2.1)–(2.4), are solved using the boundary conditions that represent the process of gas suction and solid inflow, as well as the heat losses to the environment by convections and radiation processes. The numerical solution is obtained by using the finite volume method based on the power law scheme to compute the algebraic coefficients and the SIMPLE (Semi Implicit Method for Pressure Linked Equations) algorithm to resolve the velocity components and pressure simultaneously in a staggered non-uniform grid (Melaen 1992). Additional relations accounting for interphase momentum and energy transfer are presented in Eqs. (2.5) and (2.6), while Eqs. (2.7) and (2.8) stand for the effects of the softening and melting properties of the raw materials, which strongly effects the bed permeability, heat and mass transfer.

$$\frac{\partial\left(\rho_i\varepsilon_i u_{i,j}\right)}{\partial t}+\frac{\partial\left(\rho_i\varepsilon_i u_{i,k}u_{i,j}\right)}{\partial x_k}=\frac{\partial}{\partial x_k}\left(\mu_i\frac{\partial u_{i,j}}{\partial x_k}\right)-\frac{\partial P_i}{\partial x_j}-F_j^{i-l} \tag{2.1}$$

$$\frac{\partial\left(\rho_i\varepsilon_i\right)}{\partial t}+\frac{\partial\left(\rho_i\varepsilon_i u_{i,k}\right)}{\partial x_k}=\sum_{m=1}^{\text{Nreacts}}M_n r_m \tag{2.2}$$

$$\frac{\partial\left(\rho_i\varepsilon_i H_i\right)}{\partial t}+\frac{\partial\left(\rho_i\varepsilon_i u_{i,k}H_i\right)}{\partial x_k}=\frac{\partial}{\partial x_k}\left(\frac{k_i}{C_{pi}}\frac{\partial H_i}{\partial x_k}\right)+E^{i-l}+\sum_{m=1}^{\text{Nreacts}}\Delta H_m r_m \tag{2.3}$$

$$\frac{\partial\left(\rho_i\varepsilon_i\varphi_n\right)}{\partial t}+\frac{\partial\left(\rho_i\varepsilon_i u_{i,k}\varphi_n\right)}{\partial x_k}=\frac{\partial}{\partial x_k}\left(D_n^{eff}\frac{\partial\varphi_n}{\partial x_k}\right)+\sum_{m=1}^{\text{Nreacts}}M_n r_m \tag{2.4}$$

$$F_j^{g-s}=\left[1.75\rho_g+\frac{150\mu_g}{\left|u_{g,j}-u_{s,j}\right|}\left(\frac{\varepsilon_s}{d_s\phi_s}\right)\right]\left(\frac{\varepsilon_s}{\left(1-\varepsilon_s\right)^3 d_s\phi_s}\right)\left|u_{g,j}-u_{s,j}\right|\left(u_{g,j}-u_{s,j}\right) \tag{2.5}$$

$$E^{g-s}=\frac{6\varepsilon_s}{d_s\phi_s}\frac{k_g}{\left(d_s\phi_s\right)}\left[2+0.39\left(\frac{\rho|U|}{\mu_g}\left(d_s\phi_s\right)\right)^{1/2}\left(\frac{\mu_g C_{p,g}}{k_g}\right)^{1/3}\right]\left(T_g-T_s\right) \tag{2.6}$$

$$\varepsilon_s=1-\left(0.403\left[100d_s\right]^{0.14}\right)\left(1-\text{MAX}\left(0,\ \text{MIN}\left(1,\left(\frac{T_s-T_m}{\Delta T_m}\right)\right)\right)\right)\frac{S_m}{100} \tag{2.7}$$

$$\varepsilon_g=1-\varepsilon_s \tag{2.8}$$

Table 2.1 Raw materials used in this study

Mass %	C	Fe_2O_3	Fe_3O_4	Fet	SiO_2	CaO	Al_2O_3	$(Ca,Mg)CO_3$
Iron ore		96.1	0.8	67.4	1.7		1.3	
Limestone					4.5		3.6	91.5
Mill scale	30.5	1.2	2.5	77.5	1.5	0.5	1.4	0.5
Fine dust	19.4	48.5	5.3	56.0	2.8	4.5	1.5	2.2

Fuel gas compositions (% vol)									
	C	volat	Ash	O_2	CH_4	CO	H_2	CO_2	N2
Coke breeze	84	1	11.5						
Biomass	75	22	3						
Coke oven gas					11.0	12.0	54.0	8.0	15.0
Gas mix				8.4	3.8	18.8	36.5	4.5	28.0
Biogas				1.5	2.5	32	52.0	6.0	6.0
Recycling gas (wind boxes WB16–WB20)				17.5	0.2	2.5	0.5	8.3	71.0

The thermo-physical properties of each phase thermal conductivity (k), heat capacity (C_p), viscosity (μ), and specific mass (ρ) are composition and temperature dependent. The symbols ε_g and ε_s stand for the individual solid and gas volume fractions, while d_s is the single particle diameter, S_m is the shrinkage melting down factor, and T_m is the initial softening and melting temperature. These parameters are obtained using standard softening and melting experiment for the raw materials (Nogueira and Fruehan 2006; Castro et al. 2013a, b). In this study, the raw materials used are listed in Table 2.1 with their respective composition. The chemical reactions that take place within the sinter bed involve gas and solid reactions. The water vaporization, partial softening, and melt and solidification are assumed to be controlled by the heat supply and cooling rates, while the combustion, reduction, and oxidation are assumed temperature and gas composition dependent. The rate equations for such mechanisms can be found elsewhere (Omori 1987; Castro et al. 2012a, b, 2013a, b; El-Hussiny et al. 2015; Lu et al. 2013). The NO_x and SO_x formation mechanisms take into account the oxygen potential and the temperature dependency of the rate equations. The PCDD/F net formation use a two steps mechanism of solid surface adsorption and decomposition and formation during cooling which depends on the local gas composition and temperature. The effect of raw materials composition is included on the rate equations based on empirical data (Mitterlehner et al. 2004; Kasai et al. 2005; Castro et al. 2013a, b; Kasama et al. 2006).

2.3 Results and Discussions

The proposal of the technological feasibility of the new concepts is analyzed using the multiphase multicomponent mathematical model. Base cases using actual operational data are used to model validation and verification on the compact machine

operating with coke breeze, granular biomass, and coke oven gas. In the following cases are considered the gas recycling, biomass and biogas utilization as well as oxygen addition on the post ignition chamber.

2.3.1 Model Verification

Figure 2.3 shows the new machine configuration and the temperature distribution for the gas phase using coke breeze as solid fuel. As can be observed, the temperature distribution shows a typical combustion front and cooling zones indicating feasible operation. Figure 2.4 shows the comparison of coke breeze, granular biomass, and fuel gas utilization. It is important to emphasize that the calorific heat values were used to determine the substitution factor of the fossil fuel by biomass and biogas aiming at recovering the energy input on the sintering zone. However, it is also important to point out that for biogas and biomass the fuel is renewable energy sources.

Figure 2.4 shows a comparison of the average temperatures measured and predicted by the model at the wind boxes channel using the new machine concept operating with coke breeze as solid fuel, granular biomass, and fuel gas with oxygen injection into the second burner chamber furnace. As can be observed, the average temperatures calculated at the outlet of the wind boxes entering into the suction channels of the wind boxes agreed well with the measured ones. The measured and calculated temperature demonstrated that for gaseous fuel utilization and oxygen injection on the second chamber covering win boxes 8–12 the outlet temperature of the gas is significantly shifted up compared with the coke breeze operation. The granular biomass operation with fuel adjustment on the sintering mixture based on the calorific values differences of the solid fuels presented similar pattern with

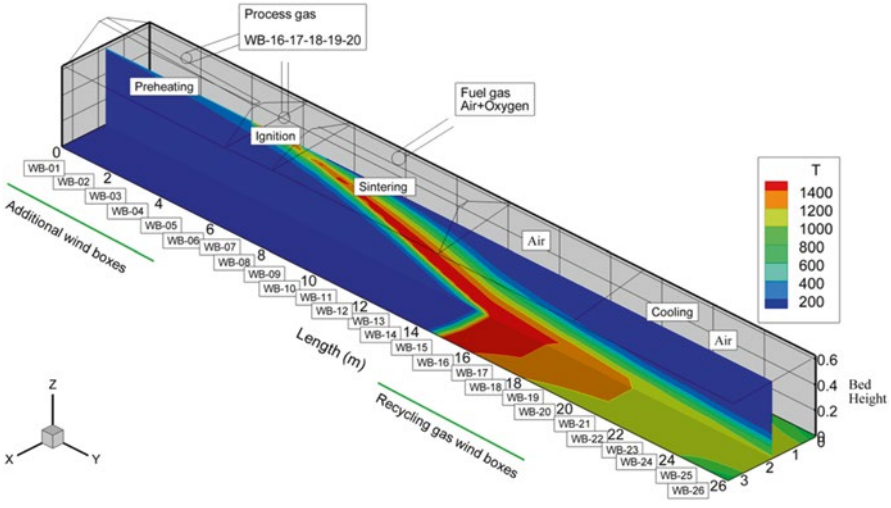

Fig. 2.3 Gas temperature distribution for the conventional operation conditions with the new machine design (fossil fuel operation—coke breeze)—base case

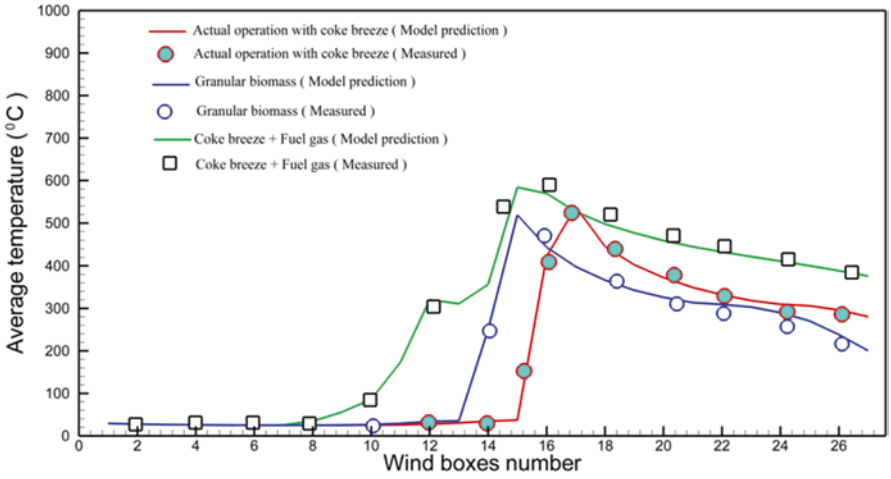

Fig. 2.4 Comparison of average temperature at the outlet of the wind boxes for coke breeze, granular biomass, and fuel gas operations

the thermal front shift back due to the higher reactivity of the granular biomass in comparison with the coke breeze. As a general trend, however, the model and measured values obtained by thermocouples positioned at the wind boxes suction outlet agreed very well and comparisons based on the simulation results could be obtained.

2.3.2 New Technologies Based on Fossil Fuels

In this section, new technologies using the modified sintering machine are considered. Scenarios of coke breeze solid fuel are compared with partial substitution by coke oven gas and process gas recycling. In order to illustrate the changes of the inner bed temperature distributions, Figs. 2.5 and 2.6 are shown. As can be seen, the temperature distributions and the thermal front zone significantly changes when fuel gas is used into the second chamber comprising the wind boxes length of 9–12 (WB9–WB12) and the product gas of the wind boxes (WB16–WB20) are recirculated to the first chamber which comprises the wind boxes length WB1–WB7 of the machine.

2.3.3 New Technologies Based on Biomass and Biogas Operations (Renewable Fuels)

In this section, new technologies based on renewable energy sources are summarized and analyzed using the multiphase multicomponent model developed by Castro et al. (2012a, b, 2013a, b). Previous results indicated that one severe shortcomings limiting the solid fuel operation leading to considerable generation of return sinter is a deficit of heat at the beginning of the combustion front.

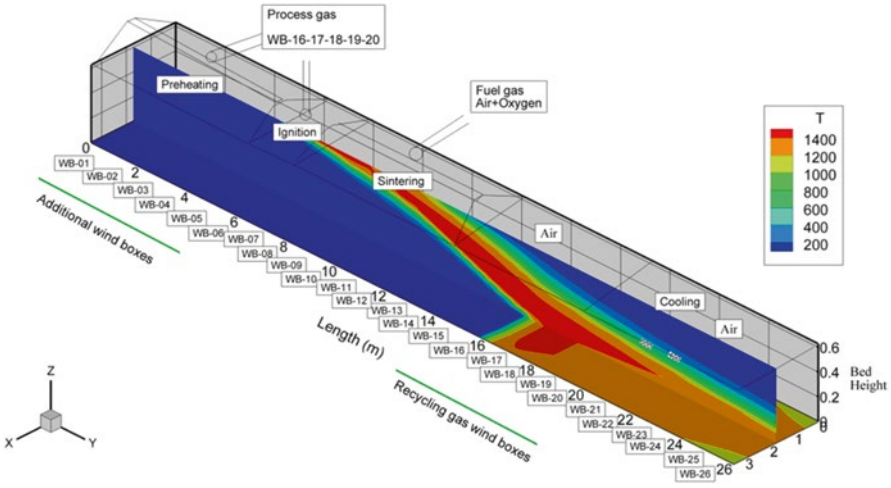

Fig. 2.5 Temperature distribution within the sinter bed for coke breeze and coke oven fuel gas utilization in the post ignition chamber

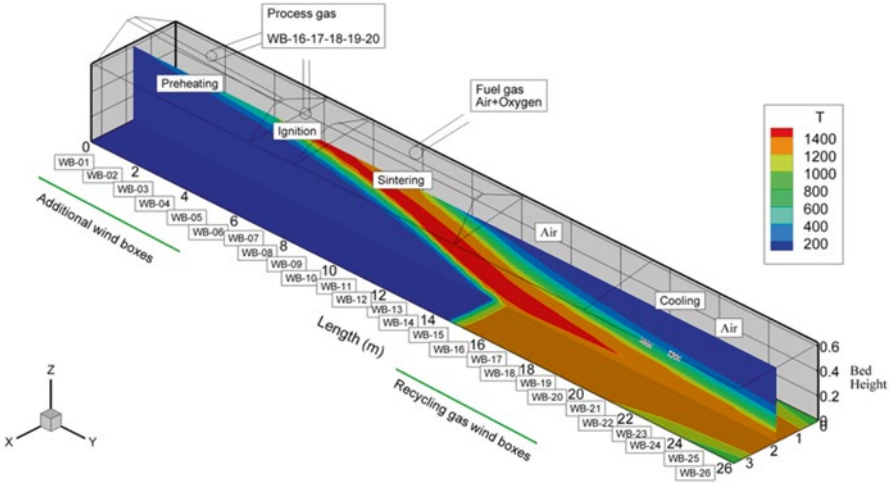

Fig. 2.6 Temperature distribution within the sinter bed for coke breeze, coke oven fuel gas utilization in the post ignition chamber, and process gas recycling of the first six wind boxes

The technologies based on fuel gas and oxygen injection within a post ignition chamber overcomes this limitation and drastically decreased the returned sinter promoting uniform heat distribution along the bed height. Figure 2.7 demonstrates this operation comparing with the actual operation technique. As can be observed, the operation with the post ignition chamber of fuel gas and oxygen furnishes additional heat on the surface of the sinter bed and significantly enlarges the sintering zone besides allowing narrow control of the temperature.

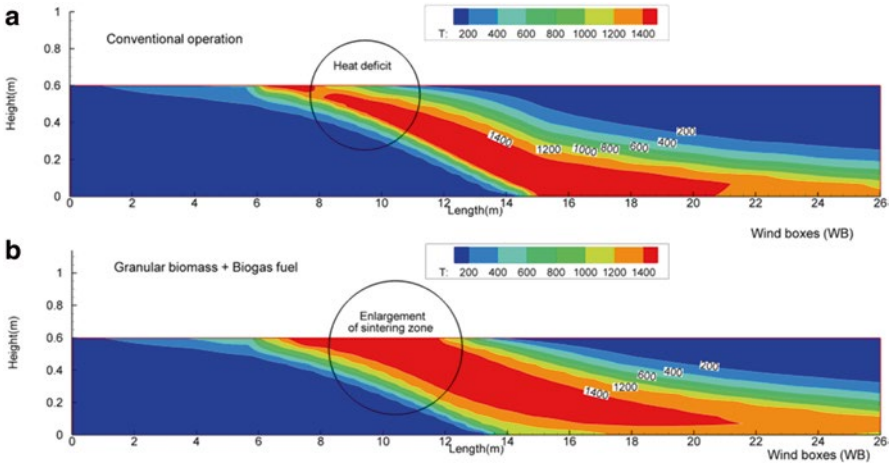

Fig. 2.7 Comparison of temperature distributions for coke breeze and biomass operation with biogas and oxygen injection within the post ignition chamber

Table 2.2 Summary of specific emissions for the cases analyzed

	Specific carbon intensity (kg ton^{-1})	SO_x (ppm)	NO_x (ppm)	PCDD (ng Nm^{-3})	PCDF (ng Nm^{-3})	Particulates (mg Nm^{-3})
Fossil fuels						
Base	68.45	35.32	23.34	0.44	0.91	15.45
Case 1	59.90	46.86	34.75	0.45	0.94	13.57
Case 2	54.62	46.22	33.85	0.01	0.81	9.82
Renewable fuels						
Case 3	74.41	1.25	21.35	0.34	0.71	15.86
Case 4	81.57	1.22	23.43	0.01	0.99	10.23
Case 5	50.41	0.88	19.23	0.19	1.08	7.34
Case 6	46.61	0.05	16.50	0.27	1.19	8.05

Base: Conventional operation with coke breeze and new sintering machine
Case 1: Partial replacement of coke breeze by coke oven gas
Case 2: Partial replacement of coke breeze by coke oven gas + Recycling gas
Case 3: Granular biomass (100 % renewable)
Case 4: Biomass + biogas (100 % renewable)
Case 5: Biomass + Biogas + Process gas recycling (100 % renewable)
Case 6: Biomass + Biogas + Process gas recycling + Oxygen (100 % renewable)

The concerns with regard to the new technologies are mostly due to the environmental impacts compared with the traditional ones. Table 2.2 shows the main environmental parameters for the new technologies and the traditional operation. Cases based on fossil fuels and renewable fuels were compared based on the emissions parameters. Regarding to carbon intensity case 2 for fossil fuels where coke oven gas and oxygen injection showed the best results. The scenarios of renewable fuels combining granular biomass, biogas with oxygen on the post ignition chamber combining

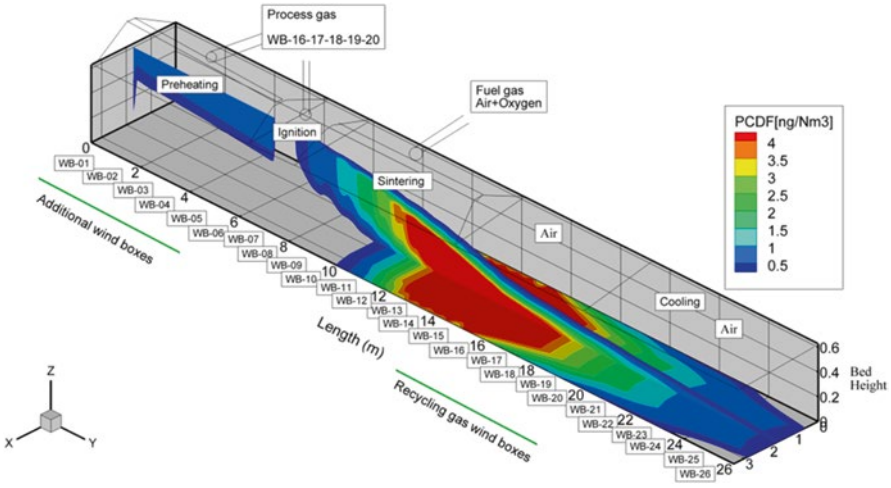

Fig. 2.8 PCDD/F inner bed distribution for best practice of coke breeze operation with process gas recycling

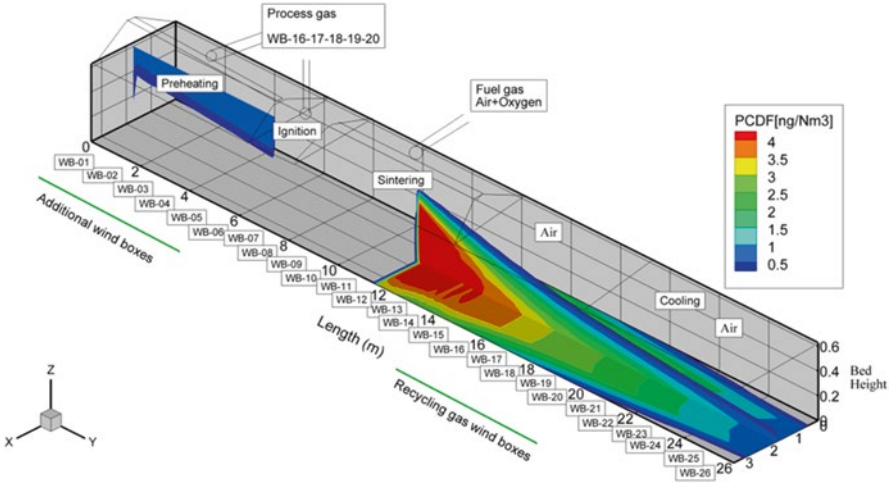

Fig. 2.9 PCDD/F inner bed distribution for best practice of biomass biogas with oxygen and process gas recycling

with the process gas recycling of wind boxes (WB16–WB20) into wind boxes (WB1–WB7) showed the best combination. For these best configurations, the emissions of particulates slightly decreased.

The emissions of SO_x drastically decreased for the cases of renewable fuels, while NO_x did not changed substantially indicating that the raw materials purities play the major role. The PCDD/F emissions strongly depends on the raw materials and the residency time of the process on the temperature range of 250–450 °C. As can be seen, the emissions of polychlorinated substances slightly decreased for the biomass and biogas utilization. Figures 2.8 and 2.9 show the inner bed PCDD/F

concentration distribution in the gas phase for the best cases analyzed of fossil fuels and renewable ones. As can be seen, the PCDD/F recycled into the gas in the first wind boxes are adsorbed into the bed at the lower temperature region and are released at the higher temperature zone where are partially destroyed and partly incorporated into the outflow gas.

2.4 Conclusions

A comprehensive mathematical model able to simulate a fuel flex compact sintering machine is proposed. The model is used to investigate feasible operations based on biomass, biogas, and steelmaking fuel gas together with process gas recycling. Simulation results indicated that feasible operation conditions could be obtained using 100 % of biomass fuel in a shorter machine with faster strand velocity due to higher combustibility of the granular biomass and biogas. Oxygen enrichment with fuel gas is recognized as an effective technology for reducing returned sinter and improve the strand productivity producing uniform sinter quality along the bed height. Regarding SO_x emissions the raw materials play the main role (mainly coke breeze and steelmaking gas). The 100 % of biomass and biogas reduced above 90 % of the SO_x emissions with negligible improvement on the particulate emissions. PCDD/F emissions are decreased for all gas recycling tested technology, but when dust fines are used the specific emissions increased as the percentage of fines is increased. The NO_x emissions are mainly affected by the combustion oxidizing conditions within the flame front. The results indicated that coke oven gas fuel utilization enhanced the NO_x emissions assuming the same raw materials and conversely the biogas and biomass decreased the specific emissions (see Table 2.2).

Acknowledgements This work is partially supported by CAPES, CNPq, and Faperj.

References

Ahan H, Choi S, Cho B (2013) Process simulation of iron ore sintering bed with flue gas recirculation. Part 2 – parametric variation of gas conditions. Ironmak Steelmak 40:128–137. doi:10.1179/1743281212Y.0000000072

Castro JA, Sasaki Y, Yagi J (2012a) Three dimensional mathematical model of the iron ore sintering process based on multiphase theory. Mater Res 15:848–858. doi:10.1590/S1516-14392012005000107

Castro JA, Guilherme VS, França AB, Sasaki Y (2012b) Iron ore sintering process based on alternative gaseous fuels from steelworks. Adv Mater Res 535:554–560. doi:10.4028/www.scientific.net/AMR.535-537.554

Castro JA, Pereira JL, Guilherme VS, Rocha EP, França AB (2013a) Model predictions of PCDD and PCDF emissions on the iron ore sintering process based on alternative gaseous fuels. J Mater Res Technol 2:323–331. doi:10.1016/j.jmrt.2013.06.002

Castro JA, França AB, Guilherme VS, Sasaki Y (2013) Estudo numerico da influencia de propriedades de amolecimento e fusão na cinetica de formação () na sinetrização de minerio de ferro, Tecnologia em Metalurgia, Materiais e Mineração. doi:10.4322/tmm.2013.003

Cumming MJ, Thurlby JA (1990) Developments in modeling and simulation of iron ore sintering. Ironmak Steelmak 17:245–254

El-Hussiny NA, Khalifa AA, El-Midany AA, Ahmed AA, Shalabi MEH (2015) Effect of replacement coke breeze by charcoal on technical operation of iron ore sintering. Int J Sci Eng Res 6:681–686

Guilherme VS, Castro JA (2012) Utilização de gás de coqueria na sinterização de minério de ferro. REM-Revista da Escola de Minas 65:357–362. doi:10.1590/S0370-44672012000300012

Kasai E, Komarov S, Nushiro K, Nakano M (2005) Design of bed structure aiming the control of void structure formed in the sinter cake. ISIJ Int 45:538–543. doi:10.2355/isijinternational.45.538

Kasama S, Yamamura Y, Watanabe K (2006) Investigation on the dioxin emission from a commercial sintering plant. ISIJ Int 46:1014–1019. doi:10.2355/isijinternational.46.1014

Lu L, Adam M, Kilburn M, Hapugoda S, Somerville M, Jahanshahi S, Mathieson JG (2013) Substitution of charcoal for coke breeze in iron ore sintering. ISIJ Int 53:1607–1616. doi:10.2355/isijinternational.53.1607

Melaen MC (1992) Calculation of fluid flows with staggered and nonstaggered curvilinear nonorthogonal grids-the theory. Numer Heat Transfer B 21:1–19. doi:10.1080/10407799208944919

Mitterlehner J, Loeffler G, Winter F, Hofbauer H, Smid H, Zwittag E et al (2004) Modeling and simulation of heat front propagation in the iron ore sintering process. ISIJ Int 44:11–20. doi:10.2355/isijinternational.44.11

Nogueira PF, Fruehan RJ (2006) Blast furnace burden softening and melting phenomena. Part III: melt onset and initial microstructural transformations in pellets. Metall Mater Trans B 37:551–558. doi:10.1007/s11663-006-0038-3

Omori Y (1987) The blast furnace phenomena and modeling. Elsevier Applied Science, London

Oyama N, Iwami Y, Yamamoto T, Machida S, Yguchi T, Sato H, Takeda K, Watanabe Y, Shimizu M (2011) Development of secondary-fuel injection technology for energy reduction in the iron ore sintering process. ISIJ Int 51:913–921. doi:10.2355/isijinternational.51.913

Yamaoka H, Kawaguchi T (2005) Development of a 3-D sinter process mathematical simulation model. ISIJ Int 45:522–531. doi:10.2355/isijinternational.45.522

Chapter 3
Dangerous Emissions Control and Reduction in Sinter Plants

Pasquale Cavaliere and Angelo Perrone

Abstract Sintering operations in steelmaking is one of the main sources of production of PCDD (polychlorinated dibenzo-p-dioxins), PCDF (polychlorinated dibenzo-furans), NOx, and SOx. The precise operating conditions through which a reduction of greenhouse emissions is described and analyzed by experimental-numerical approach. The goal is the recognition of optimized design as a function of the strong reduction of dioxins, furans, NOx, and SOx coupled with high productivity of the plant. Following the proposed approach, it was possible to reduce the emissions close to the legal limits with a high level of productivity and efficiency of the plant.

3.1 Introduction

Nomenclature

PCDD	Polychlorinated dibenzo-p-dioxins
PCDF	Polychlorinated dibenzo-furans
NOx	Nitrides
SOx	Sulfides
ESP	Electrostatic precipitator
WS	Wetfine scrubber
TCDD	2,3,7,8,-tetrachlorodibenzo-p-dioxin
TEQ	Toxicity equivalent
TEF	Toxic equivalency factor
Wb	Windbox number
Twbox	Windbox temperature
Twleg	Windleg temperature
O_2	Oxygen rate
CO_2	Carbon dioxide rate
CO	Carbon monoxide
Moi	Moisture

P. Cavaliere (✉) • A. Perrone
Department of Innovation Engineering, University of Salento,
Via per Arnesano, 73100 Lecce, Italy
e-mail: pasquale.cavaliere@unisalento.it; angelo.perrone@unisalento.it

P. Cavaliere (ed.), *Ironmaking and Steelmaking Processes*,
DOI 10.1007/978-3-319-39529-6_3

Rate	Air flow rate
Cu	Copper rate
Cl	Chlorine rate
S	Sulfur rate
Lim	Maximum value of the output
min	Minimum value of the output
D.O.F.	Design objective function
DoE	(Design of experiment
RS	Response surface

3.1.1 Process Description

Ironmaking and steelmaking are a highly material- and energy-intensive industrial operations. More than half of the mass input becomes outputs in the form of off-gases and solid wastes/by-products. The most dangerous emissions are those to air. Those from sinter plants dominate the overall emissions for most of the pollutants. The sintering of raw material is certainly one of the top steps in the steelmaking process for the production of steel components. Sinter plants agglomerate iron ore fines (dust) with other fine materials at high temperature, to create a product that can be used in a blast furnace. The final product, a sinter, is a small, irregular nodule of iron mixed with small amounts of other minerals. The process, called sintering, causes the constituent materials to fuse to make a single porous mass with little change in the chemical properties of the ingredients. The purpose of sinter is to be used converting iron into steel. Iron ore fines, other iron-bearing wastes, and coke dust are blended and combusted. The process of sintering to improve the physical and chemical properties of iron ore for use in blast furnaces is well documented (Nakano et al. 2009; Senk et al. 2006; Aries et al. 2006; Xhrouet and De Pauw 2004). The raw material for the production of iron and steel is made from solid oxides that are found in different layers of the earth's crust and that are extracted in huge quantities in order to be used in different stages of the metallurgical process. The compounds most exploited are generally metal oxides (micaceous iron, hematite, magnetite), hydrated oxides (limonite), carbonates (siderite), and sulfides (pyrite). The agglomeration process gives rise to many different physical and chemical phenomena. The process was largely explained by the authors (Cavaliere and Perrone 2013). Sintering, as already explained above, is a process that needs high temperatures that are always lower than the melting point of the crude; moreover we cannot forget the aspects related to the oxygen, carbon dioxide, and carbon monoxide level that influence the transformation; the same reasoning should also be done for the humidity level, the flow of intake air, the percentages of coke, and anthracite entered to get the mixture to be treated; furthermore, the choice of the raw material to be machined and the percentage of oxides, silicates, and sulfides of different nature that are pushed onto the conveyor belt into the furnace can change the mode the way in which the metallurgical process develops.

Many theories try to explain what really happens to the individual grains in these working conditions, and although they are debated in a large number of scientific

journals and numerous conference, in the end this process is still largely unknown. With regard to our work, it can be stated that we observed the development of a diffusion process that kicks off on the contact surfaces between two different grains and leads to their growth and compaction. Consequently a recrystallization of the grains and the decrease of porosity (i.e., the percentage of free volume) is observed.

An energy balance that pushes the particles toward the compaction is at basis of this transformation. Increasing the temperature, the crude loses the optimal conditions of equilibrium, as it has an excess of free energy due to the presence of numerous voids. At high temperatures, diffusion processes are activated in the material; they allow that given quantity of particles moves from the outside to the internal areas of the crude going to fill the voids. In this way, the overall volume is reduced, and consequently, there is an increase of the density. Therefore, the blocks are more compact.

The process is set up in a way that it is completed at the end of the agglomeration machine where the coke has to be completely combusted. The agglomeration process leads to a number of physical and chemical phenomena. During the cooking, the following main steps can be distinguished:

- Around 100 °C, drying of the mixture; at higher temperatures, the water of crystallization is removed.
- Between 600 and 800 °C, the first agglomeration of fine particles into a porous material takes place and the swelling grains adhere weakly to each other.
- More than 1000 °C, the grains soften, and we can see the same physical and chemical conditions that lead to the completion of the agglomeration process.

At the end of the grate, a sinter breaker is placed. It reduces the sintered material to the desired size (Anderson and Fisher 2002). Here PCDD/Fs form in the presence of carbon-containing materials (Ryan and Altwicker 2004; Tsubouchi et al. 2006); the process is favored by the presence of specific organic compounds or a carbonaceous matrix-sand sources of chlorine and oxygen, plus increased temperatures (200–800 °C, at higher temperatures PCDD/Fs will rapidly decompose). It was observed that the presence of catalytic metals (Cu) can be essential at modest temperatures (Kawaguchi et al. 2002). In the sinter bed, basically three layers can be recognized: raw material (wet and cold), the burning front, and the cooldown zone, consisting of sintered material. In this region, the products of incomplete combustion (PICs) surviving the heat of the burning front may condense, while the temperature is high enough to enable reactions with species in the raw materials acting as catalysts. Also, the native carbon-containing materials may react via the so-called de novo route. Obviously, during sintering, conditions are encountered wherein dioxins can be formed and for some part survive (Cieplik et al. 2003).

3.1.2 Emissions Formation

The gas temperature inside the wind box and wind legs is lower (100–500 °C) with respect to the sintering grate; such conditions lead to the optimal physical and chemical conditions for the formation of pollutants such as PCDD/F, NOx, and SOx (Iosif et al. 2008). Polychlorinated dibenzo-dioxins (PCDD) and polychlorinated

dibenzo-furans (PCDF) are persistent stable organic pollutants formed in all those high temperature processes with abundance of organic material in presence of chlorine and copper. Dioxins and furans are chlorinated tricyclic organic compounds resulting from the combination of organic compounds impregnated with halogens (i.e., fluorine, chlorine, bromine, or iodine) with a specific molecular heterocyclic structure (Menad et al. 2006). A deep and complete thermodynamic description of the PCDD/Fs formation has been presented in literature by Tan et al. (2001). These compounds are commonly grouped under the name "dioxins," but their chemical structures and their properties can be very different.

Dioxins are a class of heterocyclic organic compounds whose basic structure consists of rings with four carbon atoms and two oxygen atoms. On the other hand, furans have only one oxygen atom, and the two outer benzene rings are linked by a pentagonal structure. Among the 200 types of known dioxins, the most famous are certainly the PCDD, characterized by the presence of chlorine atoms that will complement the aromatic rings. The chemical stability of such compounds derives from the presence of these rings that make it resistant throughout. The most dangerous of dioxins, for serious problems of bioaccumulation and environmental contamination, is certainly TCDD.

A detailed description of their formation is presented in literature (Kulkarni et al. 2008; Raghunatan and Gullet 1996; Suzuki et al. 2004). The PCDD are generally measured in terms of toxicity equivalent (TEQ) relative to TCDD as a reference, being the most polluting and dangerous. The poly dibenzo-dioxins have different toxicities in relation to their structure. TEQ expresses the quantity of a "toxic" substance as the concentration of the reference substance that can generate the same toxic effects of TCDD. It is also possible to obtain the concentration of a PCDD with its toxic equivalency through the use of toxic equivalency factor (TEF). The TEF for TCDD is assigned equal to one, while the other dioxins have a factor less than one. This dimensionless parameter, multiplied by the actual concentration, results in the TEQ.

The World Health Organization (WHO) has identified the 7 most toxic PCDDs and the 10 most toxic PCDFs, giving them an international toxic equivalency factor (Eq. 3.1):

$$\mathrm{TEQ} = \sum_{1}^{7} (\mathrm{PCDD} * \mathrm{TEF}) + \sum_{1}^{10} (\mathrm{PCDF} * \mathrm{TEF}) \tag{3.1}$$

3.2 Experimental-Numerical Approach

The analysis of the sintering process was performed on a sintering plant belonging to an Italian steel company (Dwight-Lloyd sinter). For the development of such analysis, the emission levels of a period of 6 years and the corresponding inputs have been recorded to define the starting point of the problem. The corresponding productivity of the plant and the quality of the sintered material have been taken into account for comparison. The main goal is the reduction of dangerous emissions coupled with acceptable levels of productivity and quality of the material.

Each windbox was equipped with thermocouples (k-type) in order to monitor the off-gas temperature during sintering. The flue gases composition was monitored, according to EN1948 parts 2 and 3, EN-1948SS (sampling standards, Wellington Laboratories EN-1948ES (extraction standards, Wellington Laboratories), and EN-1948IS (injection standards, Wellington Laboratories), by employing a high-resolution gas chromatograph and a high-resolution selective mass detector.

The output variables (PCDD/F, NOx, and SOx) define a multigoal analysis and have been minimized, taking into account some constraints or limitations typical of the actual process of sintering.

In order to obtain a strong optimization and control of the industrial operations in sintering ore plants, different models were proposed and are available in literature, and many of those models refer to experiments performed on laboratory scale (Thurlby et al. 1979; Kucukada et al. 1994; Cross and Blot 1999; Young et al. 1979; Pomerleau et al. 2003).

In the present study, a model belonging to a multi-objective optimization analysis has been carried out from data belonging to a real industrial plant.

The sintering process is outlined in the workflow through the analysis carried out by modeFRONTIER, as shown in Fig. 3.1.

The workflow is divided into data flow (solid line) and logic flow (dotted line) which have a common node, the calculator node in which mathematical functions and chemical reactions representative of the process are introduced. In the data flow,

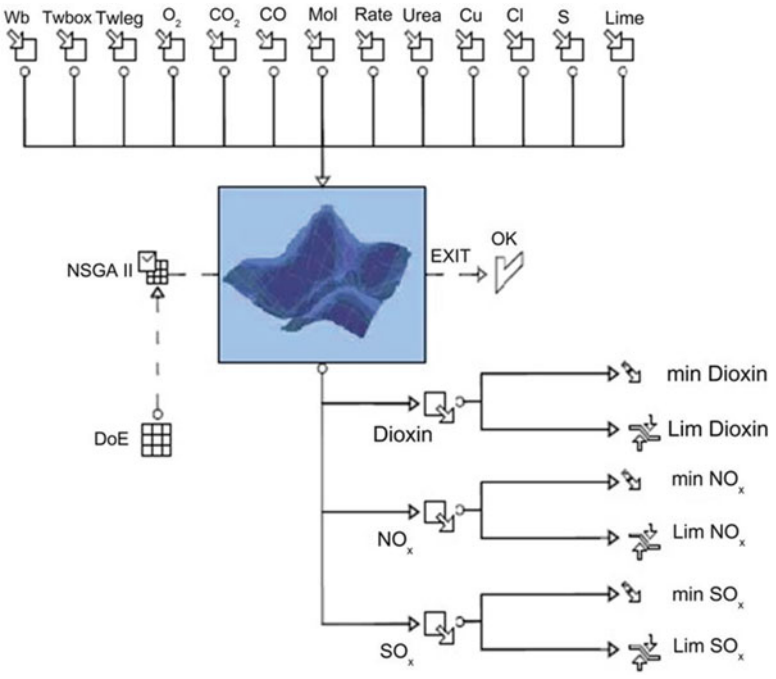

Fig. 3.1 Workflow of the analyses

all the input parameters are grouped; such input parameters should be optimized during numerical simulations as a function of the multi-objectives (in the present case the reduction of emissions). In the present case, the following input parameters are considered and then introduced:

- Number of the windbox: progressive value that indicates in which windbox there was a known level of emissions
- Gas temperatures in the wind box and wind leg
- Percentage of O_2, CO_2, CO, Moi inside the windbox that affects the development of PCDD/F
- Exit gas rate: expressed in meters per second. It appears to be an important parameter because it defines how long the gas remains within the wind box.
- Cl and Cu: both elements improve the production of PCDD/F, although in different ways. Chlorine is a key component of the structure of PCDD/F, and depending on the number of atoms on the rings, it defines the hazards and toxicity. Copper is a strong catalyst and thus fosters a series of chemical reactions, leading to the development of PCDD/F (Tan and Neuschutz 2004; Ogawa et al. 1996).
- Addition of S, according to the following three ways: through gas SO_2 added to the combustion gases, by the addition of coal containing sulfur with more impact than the previous case of pollutants SO_2, in the form of sulfur-based reagents added to the crude oil (Ogawa et al. 1996).
- Addition of urea, which has a dual effect of inhibition: it can act on the urea functional groups by blocking some surface complexes and thereby reducing the availability of catalytic metal sites and can coat the surface of the particulates and prevent chemical reactions (Boscolo and Padoano 2008).
- Addition of hydrated lime: capable of increasing the economic productivity of sintering; it is demonstrated to be a good suppressor of PCDD/F (Chen et al. 2009; Kurkin et al. 2007). Normally HCl reacts with oxygen to form water and Cl_2. The lime reduces the atmosphere of chlorination by setting HCl in $CaCl_2$ which has the lowest vapor pressure between the various metal chlorides (Boscolo and Padoano 2011).

3.3 Results and Discussion

Before starting to analyze the results of numerical simulation, the influence of input parameters should be evaluated. Concerning the gas temperature in windbox and windleg, it must be noted that their trends are very similar and differ only from 30 to 50 °C; the last box can reach even higher temperatures, up to 500–550 °C; from deep numerical analysis belonging to experimental setup of the plant, many fundamental results have been obtained in terms of input parameters (in a broad range of existence) influencing the dioxin and NOx and SOx emissions.

Dioxin emission shows a maximum in the windbox 19, in the temperature range of 350–480 °C (Fig. 3.2a); it increases also with increasing O_2 content up to very high levels (Fig. 3.2b); from the graph, it is clear how the emissions are very sensitive to such parameters.

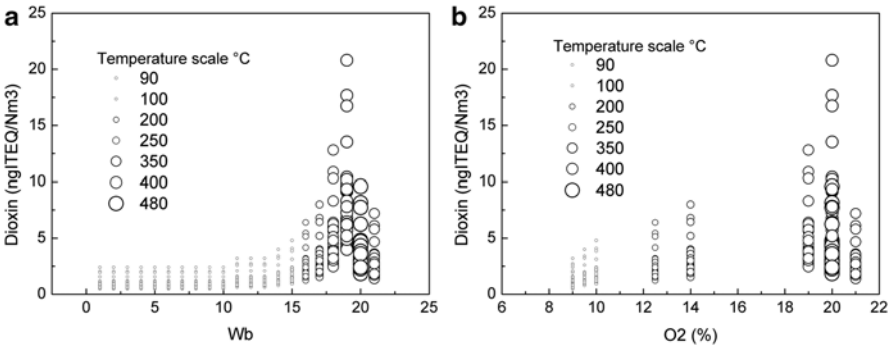

Fig. 3.2 Dioxin emission in the sintering plant monitored in the present study as a function of windbox number and temperature (**a**) and as a function of oxygen and temperature (**b**)

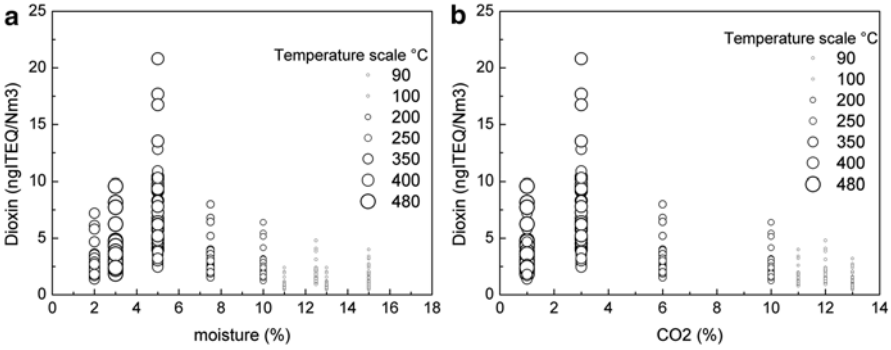

Fig. 3.3 Dioxin emission in the sintering plant monitored in the present study as a function of moisture and temperature (**a**) and as a function of CO_2 formation and temperature (**b**)

To obtain a sintered material of uniform quality, it is necessary to schedule heating and cooling on the grate in order to ensure that the thermal history of all the components is the same. This leads to the perfect control of temperature on the grate, taking into account that at temperatures below the red heat, the main mechanism of heating is through convection and conduction, while at higher temperatures, the main mechanism is radiation, such behavior is strongly related to the gas flow rate in the windboxes, and consequently the gas flow rate deeply influences the finale quality of sintered grains. Many elements and compounds are very active in dioxins formation, and, in particular, they lead to an increase in the levels of dangerous emissions; Cu and Cl lead to a strong increase in the levels of dioxins emissions as shown in Fig. 3.5.

Dioxin reaches highest values for high temperature and high moisture presence (Fig. 3.3a). In such conditions, also the CO_2 formation reaches its maximum values (Fig. 3.3b).

Dioxin emissions reach high values for high levels of flow rate in the windboxes (Fig. 3.4a); as shown in Fig. 3.4b, high values of dioxin correspond to low values of carbon monoxide. On the contrary, the addition of urea and $CaCO_3$ leads to a strong efficiency in dioxins emission reduction (Figs. 3.5 and 3.6).

Actually, also the NOx and SOx emissions were monitored during the present study, all the input parameters previously analyzed influence such emissions levels, and often the trend of reduction does not follow the dioxins one.

As shown in Fig. 3.7, for example, the addition of urea leads to a decrease in dioxin level, but, at the same time, such reduction of dioxin coincides with an increase in NOx levels. The influence of urea is very important in the reduction of polluting emission. In particular, the emission levels are reduced as the urea levels increase. For the PCDD/F, it occurs by means of a physical deposition or by poisoning the catalytic sites.

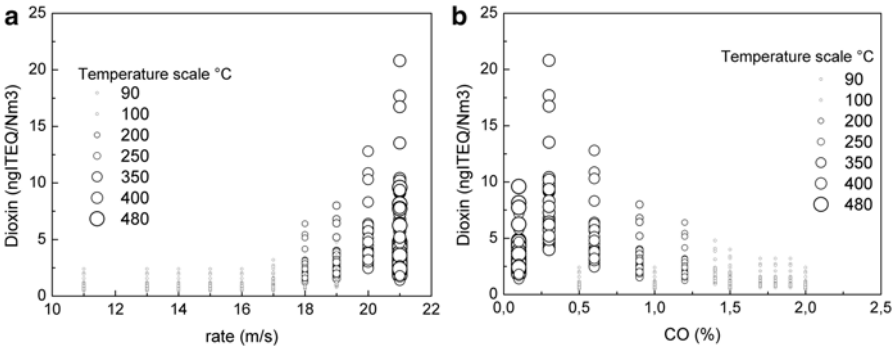

Fig. 3.4 Dioxin emission in the sintering plant monitored in the present study as a function of flow rate in the winboxes and temperature (**a**) and as a function of CO formation and temperature (**b**)

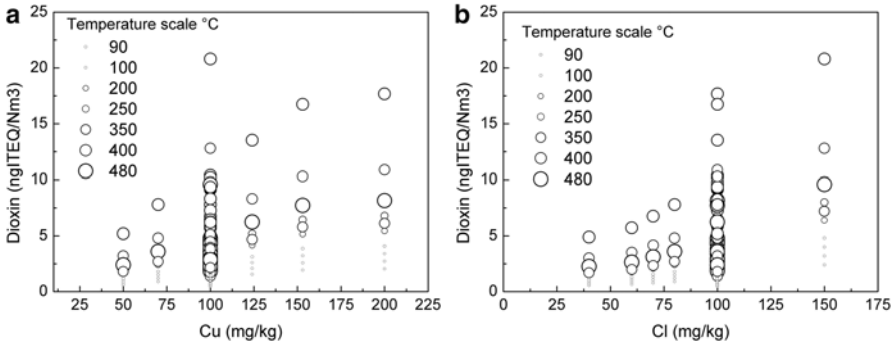

Fig. 3.5 Dioxin emission in the sintering plant monitored in the present study as a function of Cu and temperature (**a**) and as a function of Cl and temperature (**b**)

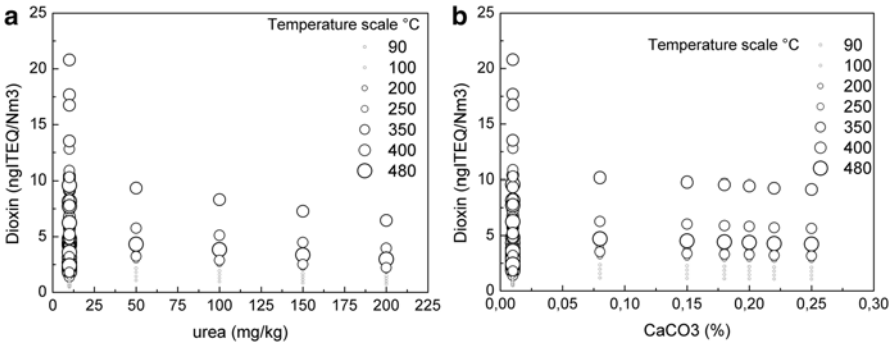

Fig. 3.6 Dioxin emission in the sintering plant monitored in the present study as a function of urea and temperature (**a**) and as a function of $CaCO_3$ and temperature (**b**)

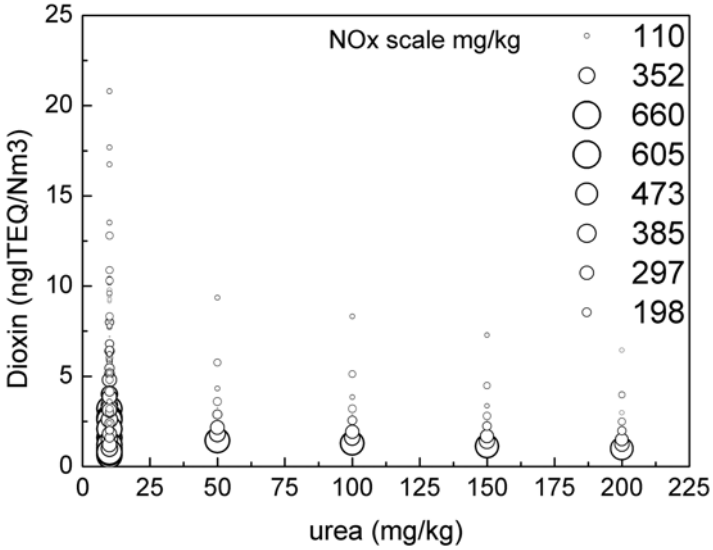

Fig. 3.7 Dioxin emission in the sintering plant monitored in the present study as a function of urea and NOx emissions

Another strong example is represented by the addition of sulfur; it is very efficient in reducing the dioxin emissions (Fig. 3.8a) but at the same time produces a strong increase in SOx emissions (Fig. 3.8b). The role of sulfur in the reduction of emissions in the sintering can be noted. In all three ways previously observed, there has been a reduction of PCDD/F, especially in the second case, and it is probably due to the presence of SOx in the flue gas. It is believed that these sulfides can be converted to SO_2, reducing the chlorine in HCl.

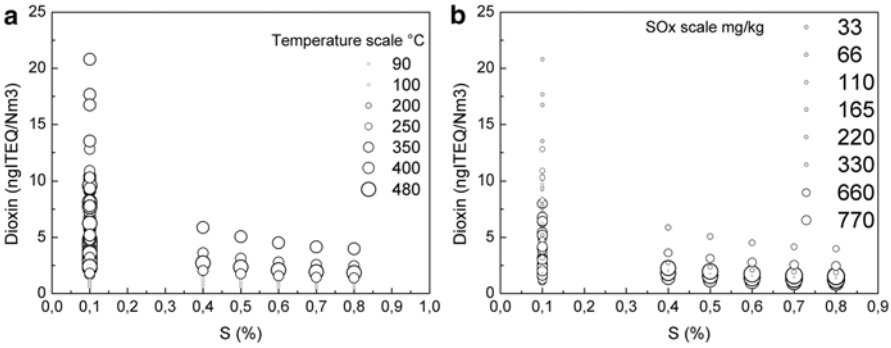

Fig. 3.8 Dioxin emission in the sintering plant monitored in the present study as a function of S and temperature (**a**) and as a function of S and SOx emissions (**b**)

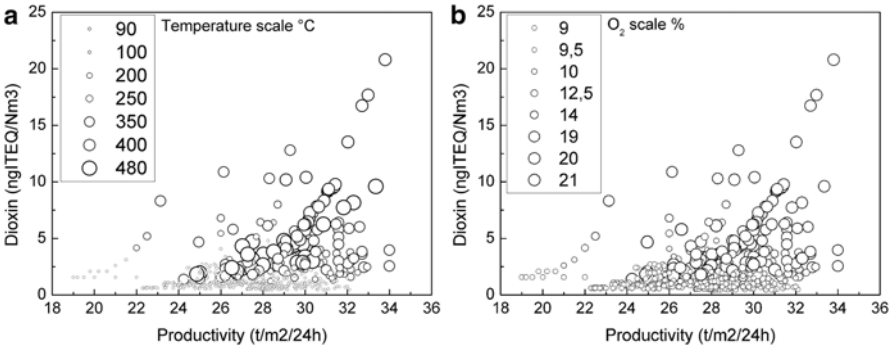

Fig. 3.9 Dioxin emission in the sintering plant monitored in the present study as a function of productivity and temperature (**a**) and as a function of productivity and O_2 (**b**)

The importance of lime in the reduction of PCDD/F has been largely outlined in the present paper. The emissions levels are reduced as the lime quantity in the raw materials increases. The lime also brings to a strong reduction of SOx and a moderate reduction of NOx.

Although the resultant optimal combination of input parameters is able to reduce the dangerous emissions from the plant, it is very important to examine the impact of the chosen input parameters on the sinter productivity. As a matter of fact, many different studies were performed on the productivity measurements for selected designs with controlled levels of dioxin and NOx and SOx emissions.

As shown in Fig. 3.9, high levels of dioxin emissions are found in correspondence of very low levels of productivity, and then productivity increases with increasing dioxins and then increases with decreasing dioxin emissions (Fig. 3.9a). By analyzing also the oxygen addition, it can be concluded that a decrease in O_2 shifts the same productivity to lower dioxin emissions (Fig. 3.9b).

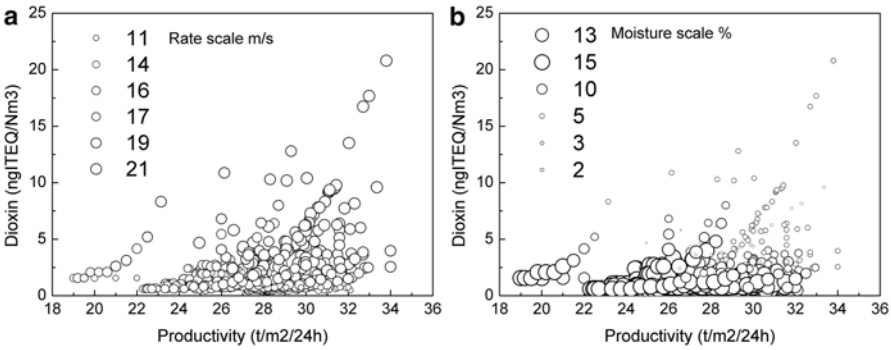

Fig. 3.10 Dioxin emission in the sintering plant monitored in the present study as a function of productivity and moisture (**a**) and as a function of productivity and gas flow rate (**b**)

Actually, temperature and oxygen flow influences moisture behavior in the sinter bed, and, as explained later in the paper, it is strongly related to the quality of the sinter; all the input parameter ranges were set in order to fix the quality of the pallets at a well-known level. High levels of productivity and low levels of dioxins can be reached with high level of moisture (Fig. 3.10a), and high levels of gas flow rate lead to an increase of productivity but unfortunately to an increase in dioxin emissions (Fig. 3.10b). Such parameter results are very important because it is strongly linked to the sinter permeability which can be directly related to the ore quality in terms of granule size and distribution, such parameter was taken strongly into account during the definition of the parameter ranges in order to set an acceptable pellets quality for all the analyzed input conditions. Also moisture strongly influences the sinter quality because it is strongly related to voidance, and also the range of such parameter was set to fix a given range of the product quality. Generally, low levels of moisture lead to a decrease in the spread of granule size distribution and to an increase in the spherical aspect of the product, such behavior leads to a material with improved voidance and consequently to good levels of productivity. In the conditions of higher levels of moisture, normally the sinter thickness decreases, and this leads to a tendency for voidance to decrease; in this way, the productivity tends to decrease.

Very low levels of dioxin and productivity are in correspondence oh high emissions of SOx and NOx (Fig. 3.11).

Actually, just focusing on the SOx and NOx levels as a function of productivity, it can be underlined how many input parameters play a key role in the overall behavior of the plant.

To obtain high levels of productivity and low SOx and NOx emissions, temperature plays a fundamental role (Fig. 3.12).

For all the productivity levels shown by the plant, the SOx and NOx levels can be reduced by reducing the oxygen flux (Fig. 3.13). In each case, from the previous analysis, it can be concluded that the effect of such input parameters leads to an effect on NOx and SOx emissions in a different way, and if they lead to a decrease

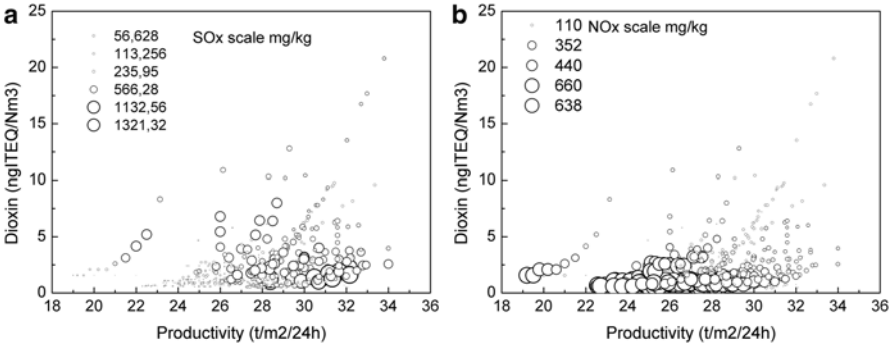

Fig. 3.11 Dioxin emission in the sintering plant monitored in the present study as a function of productivity and SOx (**a**) and as a function of productivity and NOx (**b**)

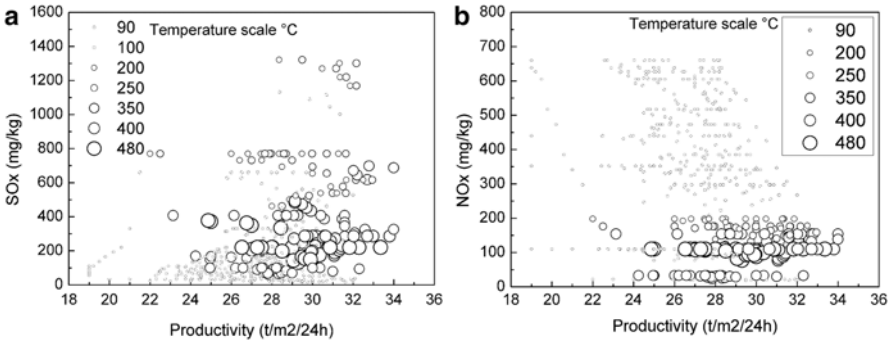

Fig. 3.12 SOx emission levels as a function of productivity and temperature (**a**) and NOx emission levels as a function of productivity and temperature (**b**)

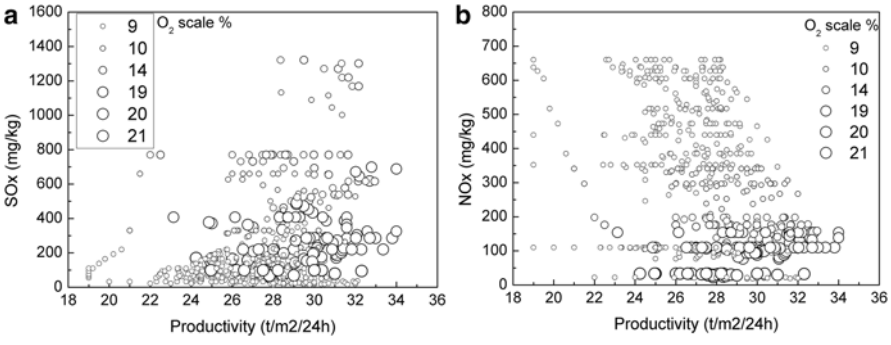

Fig. 3.13 SOx emission levels as a function of productivity and oxygen (**a**) and NOx emission levels as a function of productivity and oxygen (**b**)

in NOx, they produce an increase in SOx and vice versa, so the control of input parameters should be tuned in order to reach an optimum point of acceptable dioxins NOx and SOx levels coupled with input and operative conditions, maintaining good levels of productivity.

Another example is represented by the moisture effect; to reach good levels of productivity with low limits of SOx, NOx, it is necessary to fix lower levels of moisture (Fig. 3.14).

The increase of gas flow rate leads to an increase in SOx levels, while it leads to a decrease in NOx levels for all the values of productivity measured in the present study (Fig. 3.15). The effect on S addition on SOx and productivity and the effect of urea addition on NOx and productivity are shown in Fig. 3.16.

By increasing the lime content, it is possible to reach good values of productivity and, at the same time, to reduce the dioxin emissions (Fig. 3.17a). Lime is very effective in improving productivity with contemporary reduction of SOx emissions

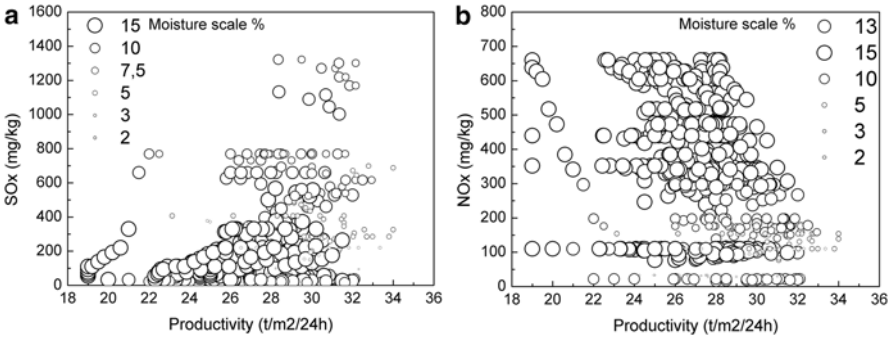

Fig. 3.14 SOx emission levels as a function of productivity and moisture (**a**) and NOx emission levels as a function of productivity and moisture (**b**)

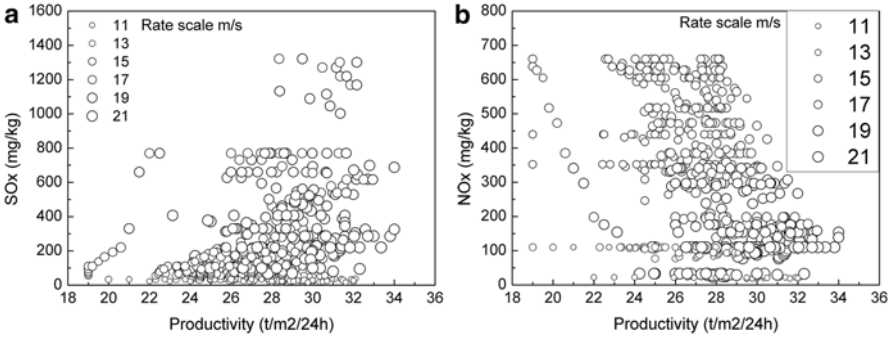

Fig. 3.15 SOx emission levels as a function of productivity and gas flow rate (**a**) and NOx emission levels as a function of productivity and gas flow rate (**b**)

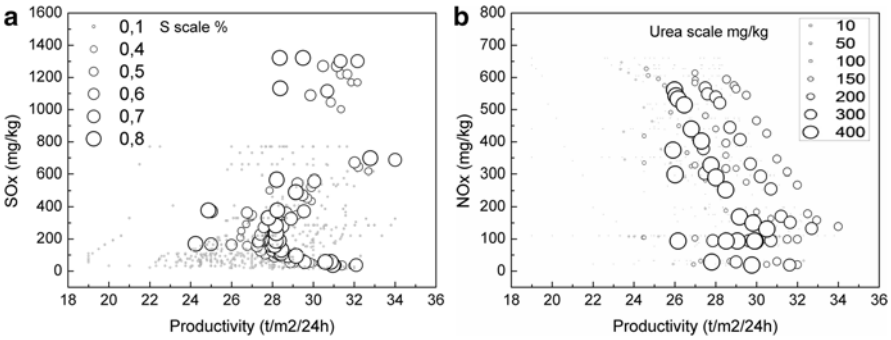

Fig. 3.16 SOx emission levels as a function of productivity and S (**a**) and NOx emission levels as a function of productivity and urea (**b**)

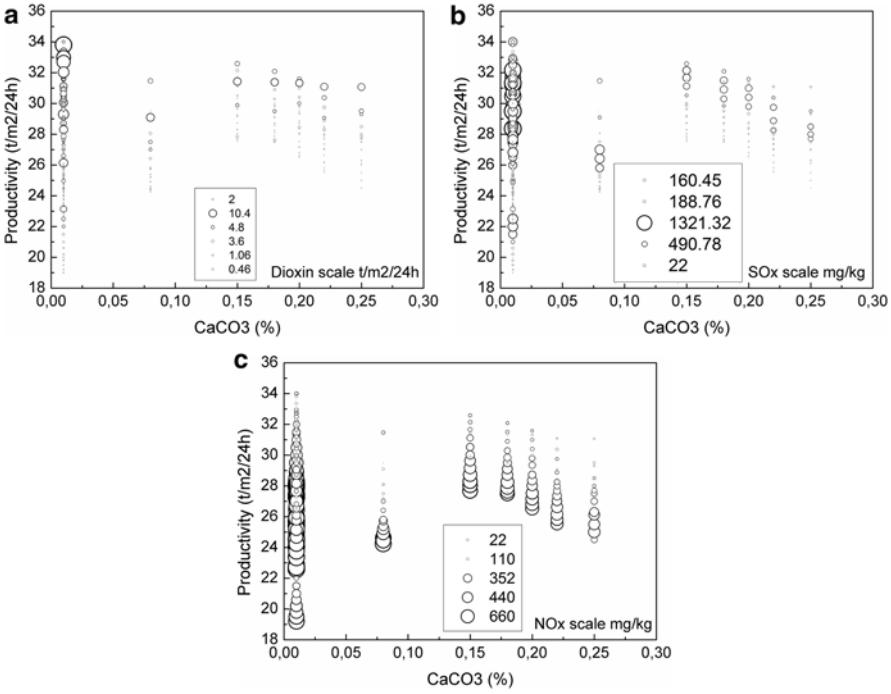

Fig. 3.17 Productivity as a function of lime and dioxin (**a**), productivity as a function of lime and SOx (**b**), and productivity as a function of lime and NOx (**c**)

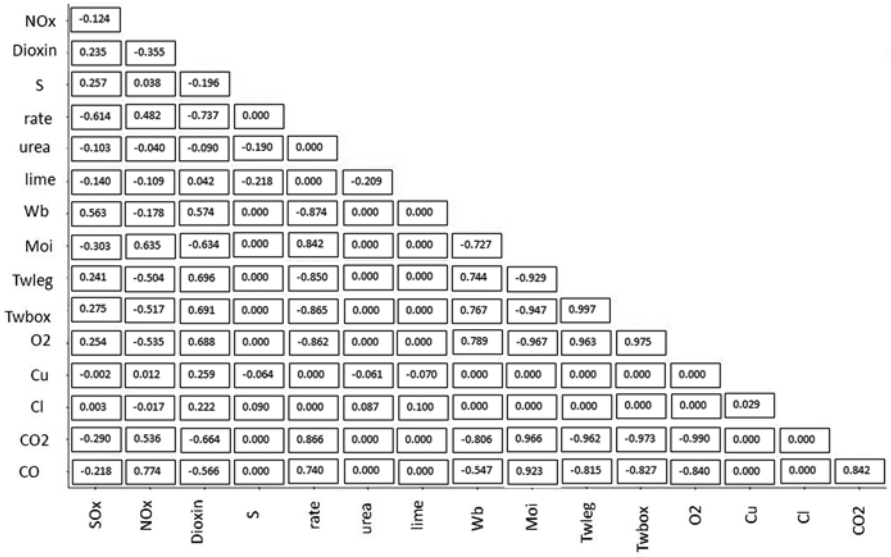

Fig. 3.18 Correlation matrix between the different variables taken into account in the present study

(Fig. 3.17b); the addition of lime leads to a moderate reduction of NOx for a given value of productivity (Fig. 3.17c). It is fundamental to underline that the quality of the sinter is inversely proportional to lime grain size; in the present study, a grain size dimension, individuated as optimal from previous studies, has been used in all the experiments.

By employing the so-called correlation matrix, it allows to immediately recognize how much the different variables are correlated between them; actually the parameters are strongly correlated if the corresponding value in the table is distant from zero in a range between −1 and 1; if the value is 1, the parameters are directly correlated, while if the value is −1, the parameters are inversely correlated. An example for the present study is given in Fig. 3.18. From such matrix, it is also possible to observe the different weights of all the parameters; the more the value differs from 0, the more it influences the corresponding variable. For example, there is a direct strong correlation between temperature, moisture, oxygen, and flow rate, while there is no relationship between the addition of elements and compounds to the raw material and the gas flow rate, position in the bed, and temperature.

For the output variables, it can be underlined that temperature, S, and potion of the windbox are directly related to SOx and urea, moisture CO, and CO_2 are inversely proportional to NOx. Temperature is proportional to dioxin, while flow rate, moisture, O_2, CO, and CO_2 are inversely proportional to such emissions. Focusing on the effect of the different input parameters on the sinter quality, we can summarize that:

– Flow rate is related to carbon monoxide and dioxide and consequently the combustion behavior with large influence on sinter strength, aspect, and voidance; it is related to moisture that strongly influences the quality parameters as largely indicated in the further discussion.
– Temperature strongly influences almost the main parameters with a strong effect on the sinter quality.

The range of existence of any input parameters is characterized by chemical and physical constraints that have to be respected to obtain realistic results from the analysis. For example, gas temperature in the windbox has to be higher than 450–500 °C because at this point, PCDD/Fs begin to decompose; but at the same time, the temperature should not increase too much because in this way the process would become too expensive.

Cu and Cl have to be reduced, but there is a physical and technological constraint that has to be respected by limiting the reduction of such elements in raw material. Urea, sulfur, and hydrated lime lead to a reduction of emissions, but too large an amount of these leads to deterioration of the mechanical and technological properties of the sintered material. If the sulfur percentage rises, the amount of SOx increases. For this reason, some designs have been excluded from the analysis.

During the preliminary analysis of the training database, the windbox with the highest level of emissions was noted to be number 19. So the first analysis was performed only on the said windbox to look for a set of values to be assigned to the different parameters in order to reduce the production of PCDD/F, NOx, and SOx. The optimum designs are summarized in Table 3.1.

It should be put in evidence that in all these cases there are high values of oxygen, while those of monoxide and carbon dioxide are relatively low, as well as the level of moisture.

The gas temperatures in the windbox turn out high; the chlorine and copper value is low, while the levels of additives cover upper-middle values. Maximum emissions of SOx and NOx are found respectively in windbox 17 and 7. When sulfur rises, the level of SOx emissions increases, while the increasing of the lime addition leads to a reduction in the levels of NOx and PCDD/F emissions. At this point, the best operating conditions of all the 21 windboxes of the system were fixed, and the medium value, weighed in the three different cases, was estimated. Some parameters, such as lime, sulfur, urea, chlorine, and copper, remain similar for all the 21 windboxes, while the remaining input (temperatures, moisture, oxygen, etc.) assume different values according to the position in the sintering bed (Cavaliere et al. 2011).

In all three cases, the medium values of emissions of SOx and NOx are largely below the legal limit. Unfortunately, with such operating conditions, the PCDD/F levels exceed the value limit of 0.4 ng I-TEQ/Nm^3. Besides offering the minimal value in the optimization regarding windbox 19, design 1 proposes valid operating conditions for the whole system and the lowest values of pollutants. In order to define the optimization strategy, reference to design 1 was chosen. The process parameters that result independent from the position on the belt conveyor were fixed. They are shown in the Table 3.2.

Table 3.1 Windbox optimum design N° 19

Wb N°	O_2 (%)	CO_2 (%)	Co (%)	Moi (%)	Twb (°C)	Twleg (°C)	Rate (m/s)	Cu (mg/kg)	Urea (mg/kg)	Cl (mg/kg)	S (%)	Lime (%)	SOx (mg/kg)	NOx (mg/kg)	PCDD/F (ng I-TEQ/Nm^3)
19	21	3	0.5	7	502	463	21	80	400	110	0.8	0.25	371	106	0.56
19	21	5	0.6	6	498	422	21	80	400	150	0.6	0.15	351	101	0.58
19	20	3	0.2	5	503	663	19	90	350	120	0.8	0.2	276	115	0.59

For remaining process parameters, the choice of the values to apply to the single windbox is necessary. The results offered from the first phase of optimization were not followed because the proposed profiles are discontinuous and inhomogeneous, difficult to apply to a real system. Therefore, another set of more homogenous profiles was proposed, taking into account the data of the first phase of analysis, defined new design. At last, the temperatures of the windboxes and windlegs for the new design were chosen and shown in the Table 3.3.

With these values attributed to the input variables, the minimum value of emissions obtained can be discovered. In Table 3.4 the results of the different designs are compared.

Some of the optimal operating conditions were removed in favor of profiles easier to apply to the system. In addition it was possible to obtain a value of productivity close to 30 in agreement with the industrial desires. Consequently an increase of the medium levels of emissions can be expected. In fact the level of PCDD/F was found to vary from 0.43 to 0.45 ng I-TEQ/Nm^3, with also a contemporary increase of NOx and SOx. With the exception of the latter, the PCDD/F still exceeded the legal limits. Despite an increase of emissions, the application of the set of parameters of the New Design was chosen because technologically simpler to realize. In addition it was possible to obtain a value of productivity close to 30 in agreement with the industrial desires.

Table 3.2 Parameters fixed for all the windboxes

Cu (mg/kg)	Urea (mg/kg)	Cl (mg/kg)	S (%)	Lime (%)
80	400	110	0.8	0.25

Table 3.3 Temperature fixed in windboxes and windlegs

Windbox/windleg	T windbox (°C)	T windleg (°C)
1–15	115	95
16	220	190
17–21	500	460

Table 3.4 Emission values

	SOx (mg/kg)	NOx (mg/kg)	PCDD/F (ng I-TEQ/Nm^3)	Productivity (t/m^2/24 h)
New design	297	201	0.45	29.8
Design 1	291	177	0.43	29.0
Legal limit	400	400	0.4	

This study made it possible to implement a setting of the system through which it is possible to obtain a clean reduction of the emissions of polluting substances. Thus, just acting on input parameters, all the values of PCDD/F below the legal limit were not possible to achieve. A further possible improvement was studied that consists in the application of a determined filtered device that can carry to a further reduction of pollutants (Cavaliere et al. 2011). In the authors of the previous chapter, such further reduction was strongly underlined, and in the present study, the attention was focused on the coupling between a decrease in dangerous emission and an acceptable productivity of the plant.

3.4 Conclusions

The crucial aspects related to dioxins emissions and plant productivity of the iron ore sintering process are underlined in the present work. The study outlines the influence of different parameters affecting it in order to establish a set of operating conditions capable of reducing the dangerous emissions. The way to tackle the problem consists in using numerical multi-objective optimization software modeFRONTIER with which to define optimal operating conditions. The analysis led to the definition of a series of three best design practices that lead to lower emissions. Since these results are obtained in dangerous working conditions, they represented the starting point necessary to define a particular setting of the system technologically easier to reproduce. A large attention was put on the analysis of the reduction of dangerous emissions coupled with an acceptable level for productivity. All the input parameters, before the optimization, were chosen in order to fall in a range, guaranteeing an acceptable quality of the sintered material in terms of dimension, sphericity, and voidance. The productivity of the plant, resulting from the chosen optimal input parameters, showed no significant differences from the required ones. The results confirmed the applicability of the obtained optimal conditions for the ordinary industrial production.

References

Anderson DR, Fisher R (2002) Sources of dioxins in the United Kingdom: the steel industry and other sources. Chemosphere 46:371–381

Aries E, Anderson DR, Fisher R, Fray TAT, Hemfrey D (2006) PCDD/F and "Dioxin-like" PCB emissions from iron ore sintering plants in the UK. Chemosphere 65:1470–1480

Boscolo M, Padoano E (2008) Investigations into dioxin emissions at Italian iron ore sintering plant. Ironmak Steelmak 35:338–342

Boscolo M, Padoano E (2011) Solutions for containing dioxin emissions from iron ore sintering at Italian plant. Ironmak Steelmak 38:119–122

Cavaliere P, Perrone A (2013) Analysis of dangerous emissions and plant productivity during sintering ore operations. Ironmak Steelmak 40:9–24

Cavaliere P, Perrone A, Tafuro P, Primavera V (2011) Reducing emissions of PCDD/F in sintering plant: numerical and experimental analysis. Ironmak Steelmak 38:422–431
Chen YC, Tsai P, Luhmou A (2009) Reducing PAH emissions from the iron ore sintering process by optimizing its operation parameters. Environ Sci Technol 43:4459–4465
Cieplik MK, Carbonell JP, Munoz C, Baker S, Kruger S, Liljelind P, Marklund S, Louw R (2003) On dioxin formation in iron ore sintering. Environ Sci Technol 37:3323–3331
Cross M, Blot P (1999) Optimizing the operation of straight-grate iron-ore pellet induration systems using process models. Metall Mater Trans B 30:803–813
Iosif A, Hanrot F, Ablitzer D (2008) Process integrated modelling for steelmaking life cycle inventory analysis. Environ Impact Assess Rev 28:429–438
Kawaguchi T, Matsumura M, Kasai E, Ohtsuka Y, Noda H (2002) Tetsu-to-Hagane 88:12–19
Kucukada K, Thibault J, Hodouin D, Paquet G, Caron S (1994) Modelling of a pilot scale iron ore pellet induration furnace. Can Metall Q 33:1–12
Kulkarni PS, Crespo JG, Afonso CAM (2008) Dioxins sources and current remediation technologies—a review. Environ Int 34:139–153
Kurkin VM, Tabakov MS, Kashkarov EA, Gurkin MA, Detkova TV, Reshetkin SV (2007) Effect of lime on sintering. Metallurgist 51:420–424
Menad N, Tayibi H, Garcia Carcedo F, Hernandez A (2006) Minimization methods for emissions generated from sinter strands: a review. J Clean Prod 14:740–747
Nakano M, Morii K, Sato T (2009) Factors accelerating dioxin emission from iron ore sintering machines. ISIJ Int 49:729–734
Ogawa H, Orita N, Horaguchi M, Suzuki T, Okad M, Yasuda S (1996) Dioxin reduction by sulfur component addition. Chemosphere 32:151–157
Pomerleau D, Pomerleau A, Hodouin D, Poulin E (2003) A procedure for the design and evaluation of decentralised and model-based predictive multivariable controllers for a pellet cooling process. Comput Chem Eng 27:217–233
Raghunatan K, Gullet BK (1996) Role of sulfur in reducing PCDD and PCDF formation. Environ Sci Technol 30:1827–1834
Ryan SP, Altwicker ER (2004) Understanding the role of iron chlorides in the de novo synthesis of polychlorinated dibenzo-p-dioxins/dibenzofurans. Environ Sci Technol 38:1708–1717
Senk D, Gudenau HW, Geimer S, Gorbunova E (2006) Dust injection in iron and steel metallurgy. ISIJ Int 46:1745–1751
Suzuki K, Kasai E, Aono T, Yamazaki H, Kawamoto K (2004) De novo formation characteristics of dioxins in the dry zone of an iron ore sintering bed. Chemosphere 54:97–104
Tan P, Neuschutz D (2004) Study on polychlorinated dibenzo-p-dioxin/furan formation in iron ore sintering process. Metall Mater Trans B 35:983–990
Tan P, Hurtado I, Neushutz D, Eriksonn G (2001) Thermodynamic modeling of PCDD/Fs formation in thermal processes. Environ Sci Technol 35:1867–1874
Thurlby JA, Batterham RJ, Turner RE (1979) Development and validation of a mathematical model for the moving grate induration of iron ore pellets. Int J Min Process 6:43–64
Tsubouchi N, Kuzuhara S, Kasai E, Hashimoto H, Ohtsuka Y (2006) Properties of dust particles sampled from windboxes of an iron ore sintering plant: surface structures of unburned carbon. ISIJ Int 46:1020–1026
Xhrouet C, De Pauw E (2004) Formation of PCDD/Fs in the sintering process: influence of the raw materials. Environ Sci Technol 38:4222–4226
Young RW, Cross M, Gibson RD (1979) Mathematical model of grate–kiln–cooler process used for induration of iron ore pellets. Ironmak Steelmak 1:1–13

Chapter 4
Pollutants Emission and Control for Sintering Flue Gas

Tingyu Zhu, Wenqing Xu, Yangyang Guo, and Yuran Li

Abstract The sintering process is an important part of iron and steel production. In the process of sintering, large amounts of SOx, NOx, HF, dioxins, particulate matters and other gaseous pollutants are produced. In order to control the sintering flue gas pollutants, the emission standard for iron and steeling sintering flue gas in China was published in 2012 and the control application of source, process and end treatment were applied. Based on a systematic description of relevant purification technologies, this chapter reviews the current situation for control of sintering flue gas in China and the trend of technology development. Aplication cases are described, with the purpose of providing an important reference for the choice of sintering flue gas emission control technology for domestic and international steel corporations.

Key words: Pollutants • Sintering • Flue gas • Control technologies

4.1 Overview

The sintering process is an important part of iron and steel production. During sintering, iron ore, pulverized coal (anthracite) and lime, blast furnace dust, mill scale, and steel slag are blended in a certain proportion and heated. Heat from fuel combustion melts part of the sintering materials and the bulk can bind into lumps. As a result, sintering materials are transformed into sinter with enough strength and grain size to be used as clinker for iron making. Sintering of iron ore fines is a comprehensive and complex process involving a variety of physical and chemical changes. Within a few minutes or less, due to the strong heat exchange, the temperature of the sintering material increases from less than 70 °C to 1300–1500 °C. Thus, large amounts of flue gas are produced. About 4000–6000 m^3 per ton flue gas sinter are produced during the sintering process. The temperature of the sintering flue gas fluctuates between 100 and 200 °C, the dust load is 1–5 g/m^3, and the water content of flue gas is approximately 10 % Vol. In the process of sintering, large amounts of

T. Zhu (✉) • W. Xu • Y. Guo • Y. Li
Institute of Process Engineering, Chinese Academy of Sciences, Beijing, China
e-mail: tyzhu@ipe.ac.cn

P. Cavaliere (ed.), *Ironmaking and Steelmaking Processes*,
DOI 10.1007/978-3-319-39529-6_4

SOx, NOx, HF, dioxins, and other gaseous pollutantsare produced, showing that steel sintering process is facing huge environmental pressure.

Generally speaking, sintering flue gas pollutants control technologies include control of source, process, and end treatment, and end treatment is the most common used method at present. The developed countries have removed from single control of dust and SO_2 to a comprehensive control of mutiple pollutants. It can be shown from related technology development the trends that synergetic and joint control the sintering flue gas pollutants is the direction for the future (Dickson et al. 1989). China began to focus on the control of sintering flue gas from 2000, and by the end of 2012, 389 sets of iron and steeling sintering desulfurization facilities had been constructed, and the total area of purified sintering machine reached 63,200 m^2. More than a dozen types of desulfurization technology for iron and steel sintering flue gas have been used, and about 80 % of the sintering machines use an Electrostatic precipitator . The dust emission concentration can normally be controlled under 50 mg/m^3. However, with increasing requirement from the government for environmental protection, the emission standard for iron and steel sintering flue gas has become stricter than before. In 2011, China's Ministry of Environmental Protection issued the Pollution Control Technology Policy for the iron and steel industry, in which a comprehensive prevention and control technology was put forward. According to this policy, the key point the iron and steel industry should be low-carbon and energy-saving. The industry should focus on clean production and be supported by effective pollution prevention and control technology with the purpose of synergetic control of atmospheric pollution by adopting end-treatment technology for emission reduction.

The existing emission standard for iron and steeling sintering flue gas in China was published in 2012. The mission standard for pollutants such as SO_2 in this new standard became stricter. In this standard, the Beijing–Tianjin–Hebei region, Yangtze River Delta, and the Zhujiang River Delta are designated as specific emission limited areas; in such areas, the requested emission value of pollutants are as follows: particles, less than 40 mg/m^3; SO_2, less than 180 mg/m^3; NOx, less than 300 mg/m^3; fluoride, less than 4.0 mg/m^3; and dioxin, less than 0.5 ng-TEQ/m^3. Therefore, it is important to select appropriate control technology for flue gas pollution. Based on a systematic description of relevant purification technologies, this chapter reviews the current situation for sintering flue gas control in China and the technology development trend. Application cases are described, with the purpose of providing an important reference for the choice of control technology for sintering flue gas emission for domestic and international steel corporations.

4.2 De-dust technologies for Sintering Flue Gas Control

The sintering process is the largest source of flue gas dust emission in the iron and steel industry. These emissions occupy 41 % of the whole iron and steel industry. Therefore, the key to emission reduction in the iron and steel industry is in the sintering (pelleting) process. There are various types of dust collector for sintering flue gas: mechanical dust collectors, electric dust collectors, bag de-dusting collectors,

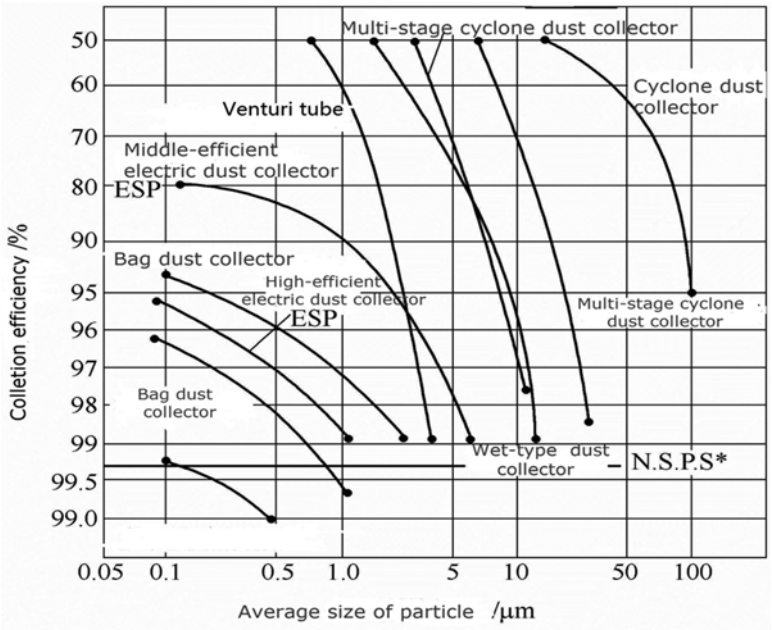

Fig. 4.1 Relationships between efficiency of de-dust technologies and the particle sizes

electric-bag composite dust collectors, new wet electric dust collectors, inorganic membrane dust collectors, etc. The relationship between the efficiency of de-dusting technology and the particle size of each technology is shown in Fig. 4.1.

4.2.1 Mechanical Dust Extractors

Mechanical dust extractors are mainly gravity sedimentation types or cyclone separating de-dusting systems. The mechanical extractors are usually characterised with simple structure, stable de-dusting efficiency, and being maintenance-free. However, their de-dusting efficiency is approximately 80 %, which makes it difficult to meet the standard of 30 mg/m^3, and even more difficult to meet the $PM_{2.5}$ aerodynamic diameter less than 2.5 μm) emission standard in the future.

4.2.2 Electrostatic Precipitators

About 80 % of sintering machines in China are equipped with electrostatic precipitators due to the large amount of flue gas with high temperature and humidity. The exit dust concentration of flue dust emission is 50–150 mg/m^3, which is much higher

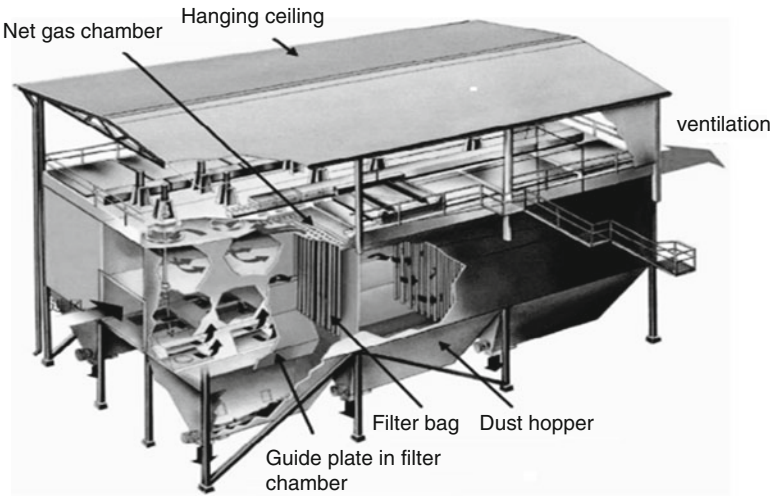

Fig. 4.2 Structure of a bag filter

than that in developed countries (20 mg/m^3). Some factors such as regional differences, technical quality, and economic, there is a certain gap in the level of environmental management between large enterprises and middle/small-sized enterprises as the electrostatic precipitators of a 214 m^2 sintering machine of the Anshansteel Group Corporation and the measured emission concentration at outlet is 45 mg/m^3. Electrostatic precipitators of a 400 m^2 sintering machine in the Anyang Iron & Steel Group Co., Ltd Sinter Plant adopts two sets of 300 m^2 double-rooms and four electric-field dust collectors were adopted; the measured dust emission concentration is $\leq$50 mg/m^3.

4.2.3 Bag Filters

Bag filters separate dust particle from the smoke flow by using a filter-bag made from porous filter cloth. Figure 4.2 shows the structure of a bag de-dusting collector. Flue gas flows from outside to the inside of the filter bag and the dust particles are blocked on the outside of the filter bag. Bag filters are characterized with high efficiency, high degree of automation (can be maintained on-line), long service life of the key component (the dust bag lasts 1.5 years), and high operation cost. Factors affecting the efficiency of bag filters are dust size, concentration power, bulk density of dust, dust cohesiveness, flue gas temperature, humidity, oxygen content, and pH value. In Shanxi Hanzhong iron and steel group, bag de-dusting collectors were adopted after the sintering machine expansion; the local environmental protection department reported a dust emission concentration is 20 mg/m^3.

4.2.4 Electric–Bag Composite Dust Collectors

Electric–bag composite dust collectors combine the advantages of electrostatic de-dusting and bag de-dusting. It is a highly efficient dust collector that removes large dust particles by electrostatic de-dusting before the filter bag. It makes full use of the advantages of electric dust collectors, bag dust collectors and exhibits new performance by the combination. The system can make up the shortcomings of the electrostatic precipitator and bag filter. The composite dust collector has many de-dusting advantages such as high efficiency, stable operation, low running resistance of the filter bag, long service life, and small cover area. Therefore, it is one of the main technologies used for the control of tiny particles of dust, $PM_{2.5}$, and other pollutants such as heavy metal mercury. Some electric–bag composite dust collectors have been successfully applied to sintering plants in China.

4.2.5 Wet-Type Electric Dust Collectors

Wet-type electric de-dusting technology has been developed on the basement of dry-type electric de-dusting. Before entering the wet-type electric de-duster, the flue gas should be wetted and saturated in a spray tower or the diffusing section of the entrance. Then, after the saturated flue gas enters the electric field, dust particles and droplets in the gas become charged and migrate down to the dust-collecting electrode under the influence of the electric field. Droplets attached to the plate connect with each other to form a liquid membrane that falls into the mud groove at the bottom of the dust collector, together with dust particles under the action of gravity. There is no need for shaking and hitting devices. This system can help to eliminate the secondary bolowing dust, so the efficiency of de-dusting will be improved. A wet-type electric dust collector has been successfully used by the Baoshan Iron & Steel Co., Ltd. of China and Qianan Iron & Steel Co., Ltd. After treatment, the flue gas emissions can meet the requirements of relevant environmental protection guidelines. This system will be gradually applied to the de-dusting of sintering flue dust in the future.

In addition to the above forms of dust collector, electric coagulation technology can help to remove fine particles and has good developmental prospects. The technology of rotation electrodes can effectively avoid shaking the dust, with a significant reduction in dust emission concentration. The high-frequency pulse-current transformer (HFPT) technology can be used in high-frequency pulse-current dust collectors and thus improve the efficiency of electric de-dusting. Furthermore, other dust collectors such as inorganic ceramic membranes and metal gauzes have the advantages of resistance to high temperature and corrosion with high mechanical strength and long service life; these kinds of dust collectors can also be used for de-dusting of iron and steel sintering flue gas.

4.3 SO_2 Control Technologies in Sintering Flue Gas

As the only large-scale commercial applicated desulfurization method in the world, FGD (flue gas desulfurization) now includes more than 200 kinds of desulfurization technology. On the basis of adding water or not, also the dry or wet forms of desulfurization by-product, sintering flue gas desulfurization can be divided into three categories: wet process, semidry process, and dry process, as show in Fig. 4.3.

Early treatment of sintering flue gas in European and North American countries mainly concentrated on dust and dioxin (PCDD/Fs). There were only a few devices for desulfurization of sintering flue gas, because the sulfur content in the raw materials originally used (iron ore and coke fuel) was low and the emission concentration of SO_2 can meet the emission standards. At present, the main sintering flue gas desulfurization technologies used in European and North American are (1) spray dryer absorption (SDA) semi-dry desulfurization, as used in the Duisburg Iron and Steel plant sintering machine in Germany; (2) novel integrated desulfurization (NID) dry desulfurization, as used by Alstom in France; (3) MEROS dry desulfurization, researched by Voestalpine in German and implemented in the Linz steel plant; and (4) circulating fluidized bed (CFB) semi-dry desulfurization, as used in the Dillinger Hütte sintering machine in Germany.

At present, the sintering flue gas desulfurization technologies being used in iron and steel enterprises in China mainly include (1) the limestone-gypsum sulfate method, as applied in the Baosteel (Group) company, Meishan (Shanghai) Iron & Steel Corp., Ltd., and Xiangshan Iron & Steel Group Co., Ltd.; (2) ammonia–ammonia sulfate method, as applied in the Liuzhou Iron and Steel (Group) Company, Xingtai Iron & Steel Corp., Ltd., Nanjing Iron and Steel Group Co., Ltd., Shandong Rizhao Steel Holding Group Co., Ltd., and Kunming Iron & Steel Holding Co., Ltd.; (3) CFB, as applied in the Fujian Sangang Group Co., Ltd., Meishan (Shanghai) Iron & Steel Corp., Ltd., and Han-Steel Group Co., Ltd.; (4) spray drying adsorption method, as applied in the Jiangsu Shagang Group Co., Ltd., Shan Steel Group Co., Ltd., Anshansteel Group Corporation, and Shandong Taishan Steel Group Co., Ltd.; (5) NID method, as applied in the Wuhan Iron and Steel (Group) Corp.; (6)

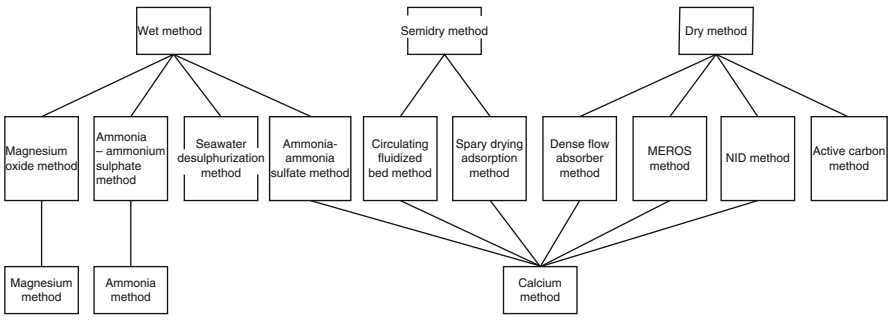

Fig. 4.3 Categories of sintering flue gas desulfurization technologies

organic amines method, as applied in the Laigang Group Co., Ltd.; (7) ionic liquid method, as applied in the Pansteel Group Co., Ltd.; and (8) dual-alkali method, as applied in the Guangzhou Iron and Steel Group.There are many desulfurization technologies have been used in China, but the iron and steel enterprises that have installed sintering flue gas desulfurization equipment shows different running effects. This is mainly because of the lackness of suitable and mature technology for sintering flue gas desulfurization in China. For iron and steel enterprises, investment in sintering flue gas desulfurization technology and evaluating the influence of desulfurization on the manufacture are extremly important.

4.3.1 Limestone–Gypsum Wet Method of Desulfurization

In November 2005, the Baoshan Iron & Steel Co., Ltd. of China set sintering flue gas desulfurization technology as their key research project and the Baoshan Research Institute took the lead in carrying out such research in China. This generated the technique and equipment technology of XPB (jet cyclone) sintering flue gas desulfurization. Three sets of large-scale sintering machines for full flue gas desulfurization projects were established in 2008. The No. 2 sintering machine desulfurization project was put into operation by a branch of Baoshan Iron & Steel Co., Ltd. in 2010. The basic information for four sets of projects is shown in Table 4.1.

4.3.2 Ammonia–Ammonia Sulfate Desulfurization

Many enterprises in China have selected the ammonia method for desulfurization of sintering flue gases like the 2×230 m^2 sintering machine in Weifang Iron & Steel Co., Ltd., 2×180 m^2 sintering machine of Shandong Rizhao Steel Holding Group Co., Ltd., 150 m^2 sintering machines of Hangzhou Iron & Steel Group Company and Xingtai Iron & Steel Corp., Ltd., 130 m^2 sintering machine of Kunming Iron & Steel Holding Co., Ltd., 360 m^2 sintering machine of Nanjing Iron & Steel Group Corp., and the 2×83 m^2, 265 m^2, and 110 m^2 sintering machines of Liuzhou Iron and Steel (Group) Company.

Table 4.1 Basic information for desulfurization project using limestone–gypsum wet method

Parameters	No. 3 180 m^2 sintering machine	No. 1 224 m^2 sintering machine	No. 3 495 m^2 sintering machine	No. 2 495 m^2 sintering machine
Flue gas volume [$\times 10^4$ m^3/h]	45–90 Designed 70	50–100 Designed 87.5	100–180 Designed 130	100–180 Designed 130
SO_2 concentration [mg/m^3]	1000–1300 Average 1800	300–1200 Average 500	350–1160 Average 400	350–1160 Average 400
Flue gas temperature [°C]	90–150	130–170	85–150	85–150
Year	2008	2008	2008	2010

Table 4.2 Desulfurization system of Liuzhou Iron and Steel (Group) Company

Parameters	Unit	Sintering machine		
		2×83 m^2	110 m^2	265 m^2
Flue gas flow	$\times 10^4$ m^3/h	52	32	85
Entrance SO_2	mg/m^3	637	687	783
Exit SO_2	mg/m^3	51	59	59
Desulfurization efficiency	%	92	91	92
SO_2 removal	ton	1449	865	2586
Dust concentration	mg/m^3	35	40	45

The 2×83 m^2 sintering machine–desulfurization project of the Liuzhou Iron and Steel (Group) Company began construction in July 2006 and was completed in February 2007. The total investment was about 60 million Yuan. The operational-parameters of the system are shown in Table 4.2.

4.4 Control Technologies for Nitrogen Oxide in Sintering Flue Gas

NO_x control technologies include process control and end-of-pipe technologies. (Table 4.3).

4.4.1 Flue Gas Circulation

The denitrification technique flowchart for sintering flue gas circulation is shown in Fig. 4.4. The system mainly consists of a changeover valve for circulating flue gas, an high efficient cyclone dust collector, flue gas mixing chamber, and circulating pipe. The flue gas from sintering process enters a mixing chamber through an induced draft fan to mix with partial cold ring waste gas after removing dust flue. Then, it enters a sealed air bells cap, which is filled with oxygen-enriched air to guarantee that the quality of sinter is not influenced.

To date, typical circulation techniques for waste gas include regional waste gas circulation technology developed by Nippon Steel of Japan, EOS (emission optimized sintering), LEEP (low emission and energy optimized sinter production) as well as Eposint (environmental process optimized sintering) developed by Voestalpine Profilform Co., Ltd.

4.4.2 Selective Catalytic Reduction Method

The denitration technology of selective catalytic reduction (SCR) refers to changing NOx to N_2 via reduction using a catalyst at a certain temperature. The technique has become one of the most widely applied for industrial flue gas denitrification

Table 4.3 Control technologies for NOx in sintering flue gas

Control Technologies		Process characteristics	Denitration efficiency
Process control	Flue gas circulation	Part of the hot waste gas is reintroduced to the sintering process and partial NO_x is thermal decomposition.	40–70 %
End-of-pipe technologies	Actived carbon adsorption	Activated coke (carbon) was used as adsorbent adsorption which could remove NOx or as a catalyst which could remove NOx under the presence of ammonia via SCR with the temperature at 120–150°C.	30–80 %
	SCR	NO_x was reduced into N_2 via using reducing agent under the action of catalyst with the temperature at 300–400°C.	>70 %
	Oxidative absorption	NO is oxidized to NO_2, N_2O_3, or N_2O_5 with high valence state; Then, they are absorbed and removed via using desulfurization equipments.	>50 %

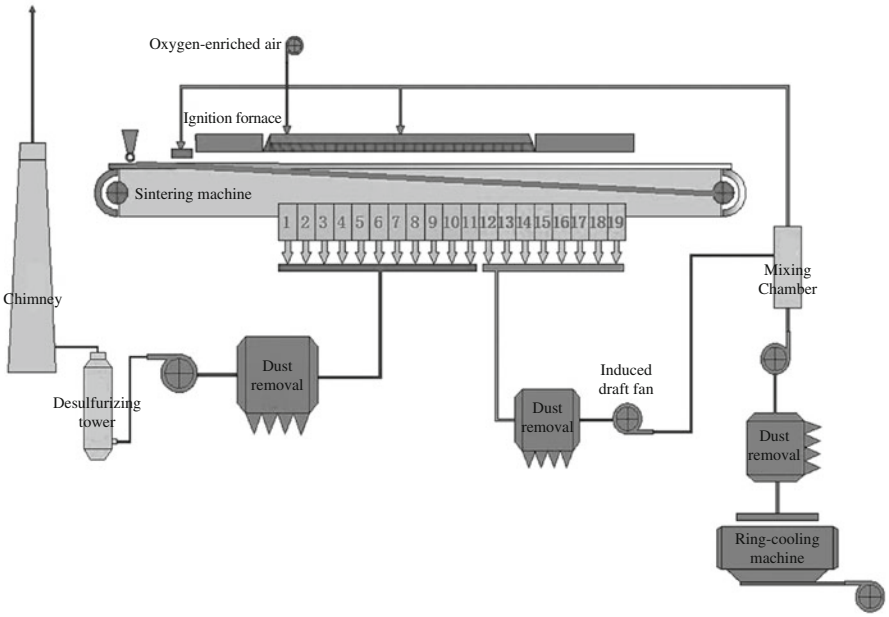

Fig. 4.4 Denitration flowchart for sintering flue gas circulation

technology, and its removal efficiency for the flue gas from coal-fired boilers is more than 90 %. SCR is the best denitration technology widely applied at present. The reaction mechanism of SCR is very complex and it mainly injects NH_3 to change NOx in flue gas into N_2 and H_2O under the presence of catalyst with reaction temperature at 250–450°C.

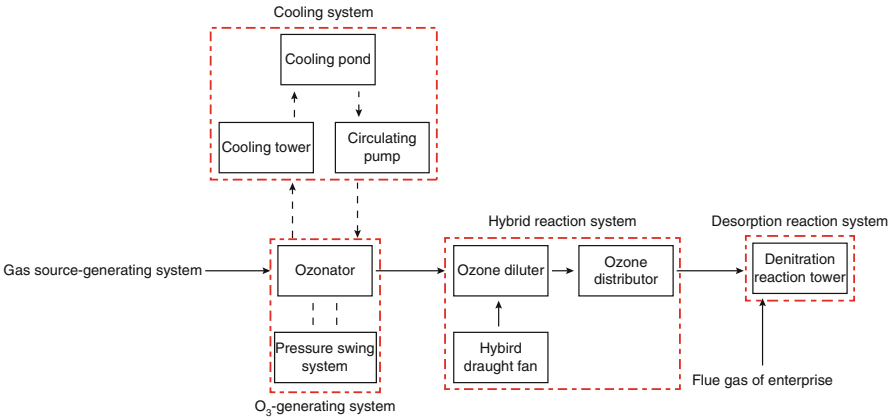

Fig. 4.5 Flow diagram for oxidation absorption denitrification technique using ozone

The catalyst is the key of the SCR technology. According to the different active components, it can be divided into metal oxide catalysts, molecular sieve catalyst and noble metal catalysts. Currently, the metal oxide catalysts is the most widely applied.. The catalysts as SCR denitration engineering application are three main types, including honeycomb catalyst, flat plate catalyst and corrugated plate catalyst. In terms of market share of SCR catalysts at present, the honeycomb catalyst plays a dominant role with 70 %, the flat plate catalyst accounts for approximately 25 %, and the corrugated plate catalyst accounts for approximately 5 %.

4.4.3 Oxidation Absorption Method

If NO is oxidized to NO_2, N_2O_3, or N_2O_5, it can be removed via absorption and desorption usingwater or alkaline substances in the desulfurization system. The oxidation absorption denitration technique mainly combines the gas-phase oxidation of ozone with an existing desulfurizing absorption tower to realize combined desulfurization and denitrification. The technological process is shown in Fig. 4.5.

4.5 Dioxin Control Technology for Sintering Flue Gases

4.5.1 Emission Characteristics of Dioxin in the Sintering Process

Because of different conditions in different the countries, the proportion of dioxin emission in the steel industry is different from that of total dioxin emissions. For example, the dioxin emissions mainly is from smelting in Germany and Australia,

but major from wood combustion in Austria, whereas about 45.6 % from production of steel and other metals in China. Research has shown that the emissions of dioxin by the Chinese steel industry are mainly concentrated in the sintering process. Its emissions account for more than 90 % of the total emissions of the steel industry.

Figure 4.6 shows the emission characteristics for 17 kinds of toxic PCDD/Fs from different sintering plants and a laboratory simulation of the sintering process. The maximum emission concentration is OCDD in the PCDD group; at the same time, 2,3,7,8-TCDF and 1,2,3,4,5,7-HpCDF are major emissions in polychlorinated dibenzofurans (PCDF) emissions. Analysis of dioxin species on the particles between in front of the Electrostatic precipitator and after the Electrostatic precipitator showed that dioxin on the particles does not exhibit a specific peak (McKay G 2002; Evans CS et al 2005; Guerriero E et al 2009).

4.5.2 Control of Dioxin in the Sintering Process

4.5.2.1 Source Reduction

According to the causes of dioxin formation, the presence of chlorine is an important factor in the process of dioxin formation; therefore, it is better to use material with low chlorine content. Because of the relatively high chlorine content in dust and in steel rolling, the content of chlorine in the mixed raw materials can be changed by changing the proportion of dust removal and steel rolling. The presence of copper in raw materials has a extremely catalytic effect on the formation of dioxin. Specific types of iron ore are likely to be the main source of copper, so choosing the right iron ore is very important. The return materials including dust, iron oxide scale, sludge and others which are served as raw materials in sintering could be treated via washing or high-temperature to reduce the chlorine and copper elements. In the end, sintering materials containing small amounts of dioxin precursor substances should be selected; for example, biomass fuels should be avoided (Dickson L C et al 1989).

4.5.2.2 Process Control

Studies have indicated that the addition of inhibitors can effectively block the formation of dioxin, and make it an effective method for controlling dioxin emissions. There are two categories of inhibitors, one is alkaline earth metal and the other is sulfur and nitrogen in inhibitor. So, there are two mechanisms for inhibitors. Alkaline earth metals can effectively reduce the content of HCl in flue gas, whereas sulfur and nitrogen inhibitors can make the catalyst which can generate dioxin "disabled". In addition, because of the high temperature of the sintering process (1200–1300 °C), the flue gas can be recycled so that the dioxin-rich gas passes through the high temperature zone again, enabling high temperature decomposition of formed dioxin.

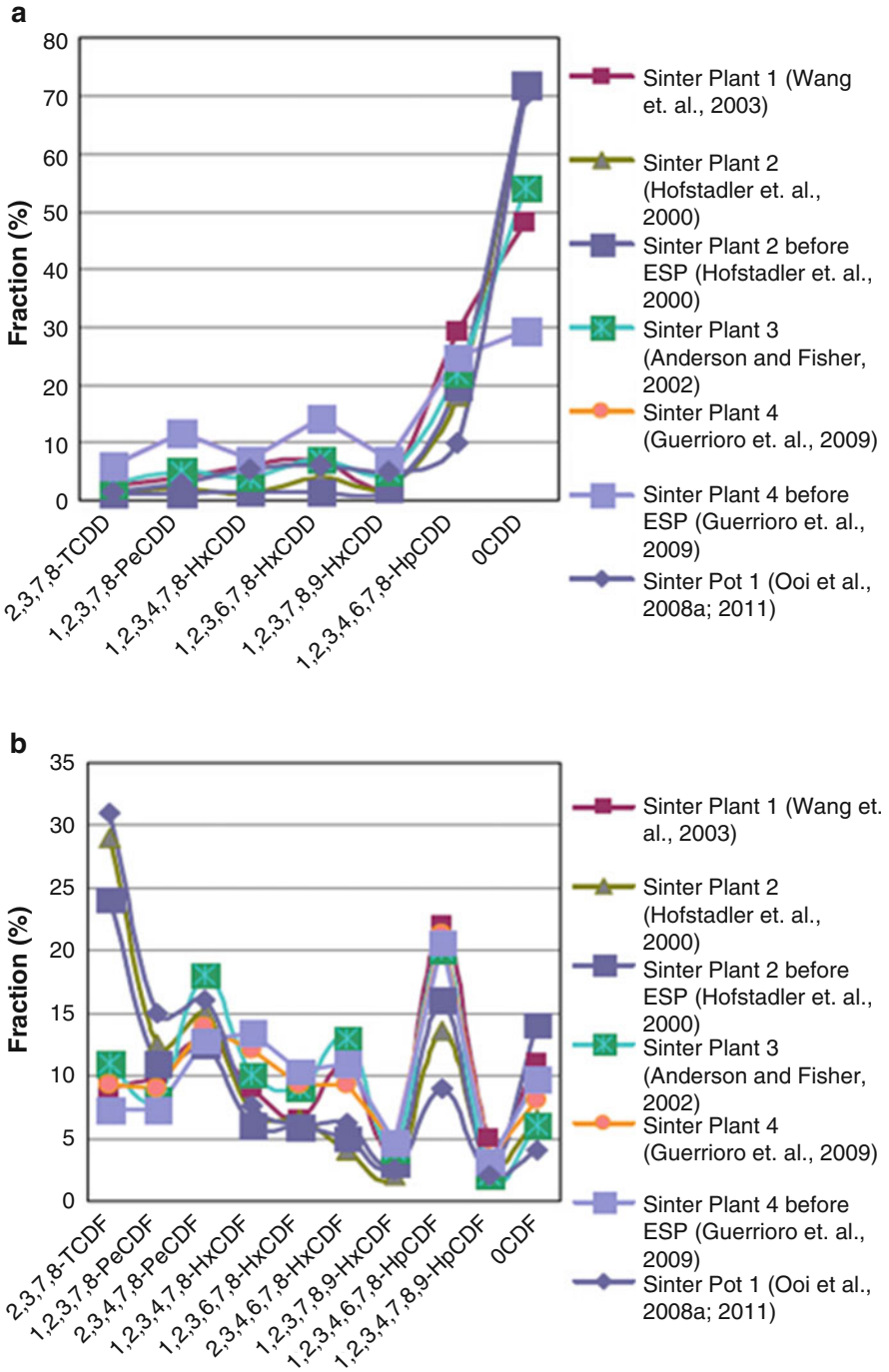

Fig. 4.6 Distribution of toxic dioxins (**a**) PCDDs and (**b**) PCDFs in the process of sintering (Gullett B K et al 1992)

4.5.2.3 Terminal Management

Generally speaking, the use of source reduction or process control cannot meet the strict dioxin emission standards for sintering flue gas. For the dioxin in the terminal of the flue gas emissions, special measures must be adopted. With the increasingly stringent environmental protection laws and regulations, processing for particulate matters and SO_2 have become very common in flue gas management. These terminal management methods remove a certain amount of dioxin together with the particles. However, dioxin in the gas phase must be further treated, and the original flue gas management equipment cannot be relied upon. The most efficient methods for controlling dioxin emissions are catalytic oxidation and activated carbon (jet or fixed bed) adsorption. Generally speaking, the cost of terminal management is much higher than that of process control. For countries or regions with more stringent emissions standards, management measures are usually selected according to the characteristics of flue gas emissions and the emission standards.

At present, terminal management for industrial operation mainly includes wet cleaning methods (such as Airfine and Wetfine systems), electrostatic dust or bag dust, SCR, and activated carbon adsorption (Ide Y et al 1996; Bertinchamps F et al 2006). Only the SCR process can provide directly decomposition of dioxin. Gas scrubber and filtering devices mainly realize the transfer of dioxin pollutants and need to manage further. Although these methods have proven effectively in reducing dioxin pollution, the operating expenses are higher.

4.6 Multiple Pollutants Control Technologies for Sintering Fuel Gas

Beside SO_2 produced in the flue from the sintering process, NO_x, CO_x, HF, PCDDs, PCDFs and other kinds of harmful gaseous pollutants are also produced. China has been implementing a single control strategy of pollutants, focused on period key pollution control as the main characteristics, established air pollution management system with the combination of total amount and concentration control and developed a series of more mature dust and sulfur separate removal technologies. However, China has generally used a hierarchical governance mode for single pollutants, with the increasing the types of pollution control, the number of sintering gas treatment equipments are more and more in the iron and steel industry. This has not only increased the cost of equipment and running, but also made the whole pollution control system much larger and more complex. Outstanding problems include the large amount of space needed for equipment, high energy consumption, and the greater risk of causing secondary pollution have emerged. The developmentof efficient and economic pollution control technology is a hot point from the point of international technologies (Knoblauch K et al. 1989).

With the aim of cooperative control of sintering flue gas pollution, the existing industrialized applications, which are mainly focused on separate pollutant control, have been developed to absorb many kinds of pollutions simultaneously, for example, by adding an annexing agent to a common gas desulfurization system. The importance of this for dry (active carbon) and semidry (humidifying) methods of flue gas decontamination are discussed in the rest of this section.

4.6.1 Actived Carbon Multiple Pollutants Control Technology

The Taiyuan iron and steel plant in China has adopted the dry active carbon method for desulfurization and denitrification. The multiple pollutants removal project was completed in 2006 with 450 m^2 sintering machine and the flue gas volume of 1.4×10^6 m^3/h. The annual sintering smoke SO_2 emissions are 6821 tons and for NOx 2744 tons; this is the first case in the Chinese sintering industry.

The system runs steadily after putting into use, with operability of over 90 %. The Taiyuan environmental monitoring central station measured the emissions in sintering smoke as SO_2 7.5 mg/m^3, NOx 101 mg/m^3, and dust 17.1 mg/m^3. Desulphurization efficiency was over 95 % and denitrification efficiency was over 40 %. Both of them reached design criterion and pollutant discharge standards. The annual secondary product (oil of vitriol) output was 9000 tons, and all of them were used in the steel rolling acid pickling process and the sulfur and ammonia production during coking, with turning waste into wealth and realizing an industrial chain of circular economy (Table 4.4).

4.6.2 Desulfurization with Actived Carbon Injection

4.6.2.1 MEROS Technology

Siemens industrial systems and the technology services of Voestalpine AG developed the maximized emission reduction of sintering technology (MEROS), which can produce a large reduction in sintering emissions. The technology as a continual treatment is able to reduce the dust, the harmful metal and organic matter to a lower emission level in the sintering fuel gas.

The MEROS method uniformly jets the adsorption and desulfurization additive(s) into the sintering smoke under backwash and high speed conditions, and uses efficient double-flow nozzle to cool wetting the sintering flue gas from the reactor. After leaving the modified reactor, the flue gas with dust passes through a pulse bag filter to remove dust particles. To enhance gas purification efficiency and reduce the cost of annexing agent, the separated dust in the pulse bag filter is recycled to the air flow after the adjusted reactor, and part of the dust leaves the system to go to a storage silo. The MEROS can simultaneously remove desulfurization,

Table 4.4 Operating performance test for 450 m^2 sintering smoke using the active carbon method of Taiyuan Iron and Steel Co

Project	Unit	Calculated value	Test value
Exit SO_2 concentration	mg/m^3 (T)	≤41	7.5
Desulphurization efficiency	%	≤95	98
Exit NOx concentration	mg/m^3 (T)	≤213	101
Denitrification efficiency	%	≤33	50
Exit dust concentration	mg/m^3 (T)	≤20	17.1
PCDD/F	ng/m^3TEQ (T)	≤0.2	0.15
NH_3 escape	ppm (T)	≤39.5	0.3
Relieving hyperacidity	98 % Sulfuric acid	Top quality goods	Top quality goods

T means the dry flue gas. The value of pollutant emission concentration in the table 4.4 is calculated under the condition of dry flue gas

HCl, HF, dioxin and other pollutants. And it aslo removes all the condensable volatile organic compounds (VOCs).

4.6.2.2 IOCFB Multiple Pollutants Control Technology

Inner and outer circulating fluidized bed (IOCFB) multiple pollutants control technology was developed by the Institute of Process Engineering, Chinese Academy of Sciences. IOCFB multiple pollutants control technology uses $Ca(OH)_2$ and other alkaline absorbents to absorb SO_2 and other acid gases in flue gas, and simultaneously uses activated carbon or activated coke adsorbent to adsorb the dioxin-like pollutants in flue gas. The method is based on the theory of a circulating fluidized bed, through multiple recirculation of absorbent and adsorbent, prolonging the contacttime of absorbent and adsorbent with flue gas, and improving the utilization rate of the absorbent and adsorbent. The desulfurization efficiency is stable at 90 % in the case of a low calcium to sulfur ratio (Ca/S < 1.3).

The 132 m^2 sintering machine of the Xuzhou Chengri Iron and Steel Co., Ltd produces a flue gas volume of 900,000 m^3/h. The IOCFB multiple pollutants coordinated control technology has been used as a pilot application demonstration in the plant and completely built in 2013. The system design parameters are shown in Table 4.5.

In March 2014, the project successfully passed the acceptance of the environmental protection department. Project monitoring showed that the concentration of SO_2 was 570 mg/m^3 before desulfurization and 20 mg/m^3 after desulfurization; The desulfurization efficiency reached 95 %. The dioxin concentration was 107.9 pg TEQ/m^3 before desorption and 22.2 pg TEQ/m^3 after desorption; The desorption efficiency was 79 %. The heavy metal Hg concentration was 20.3 μg/m^3 before desorption and 0.205 μg/m^3 after desorption; The desorption effiency was 99 %.

Table 4.5 Multiple pollutants control project parameters for a 132 m^2 sintering machine in Chengri Iron and Steel Co., Ltd

Entrance flue gas parameter		Technology design value	
Flue gas volume (operating conditions)	90×10^4 m^3/h	Flue gas temperature	<80° C
Flue gas volume (standard conditions)	64×10^4 m^3/h	Calcium/sulfur molar ratio	≤1.25
Flue gas temperature	120–150° C	Desulphurization efficiency	≥80 %
SO_2 concentration	1000 mg/m^3	SO_2 concentration	<200 mg/m^3
Dust concentration	100–200	Dust concentration	<30 mg/m^3
		Dedioxin efficiency	≥80 %

References

Bertinchamps F, Grégoire C, Gaigneaux EM (2006) Systematic investigation of supported transition metal oxide based formulations for the catalytic oxidative elimination of (chloro)-aromatics: Part II: Influence of the nature and addition protocol of secondary phases to VOx/TiO_2. Appl Catal Environ 66(1):10–22

Dickson LC, Lenoir D, Hutzinger O, Naikwadi KP, Karasek FW (1989) Inhibition of chlorinated dibenzo-p-dioxin formation on municipal incinerator fly ash by using catalyst inhibitors. Chemosphere 19(8):1435–1445

Evans CS, Dellinger B (2005) Mechanisms of dioxin formation from the high-temperature oxidation of 2-chlorophenol. Environ Sci Technol 39(1):122–127

Guerriero E, Guarnieri A, Mosca S, Rossetti G, Rotatori M (2009) PCDD/Fs removal efficiency by electrostatic precipitator and wetfine scrubber in an iron ore sintering plant. J Hazard Mater 172(2):1498–1504

Gullett BK, Bruce KR, Beach LO, Drago AM (1992) Mechanistic steps in the production of PCDD and PCDF during waste combustion. Chemosphere 25(7):1387–1392

Ide Y, Kashiwabara K, Okada S, Mori T, Hara M (1996) Catalytic decomposition of dioxin from MSW incinerator flue gas. Chemosphere 32(1):189–198

Knoblauch K, Richter E, Jüntgen H (1981). Application of active coke in processes of SO_2-removal and NO_x- removal from flue gases. Fuel 60(9):832–838

Otani Y et al (1986) Adsorption of mercury vapor on particles. Environ Sci Technol 20(7):735–738

Chapter 5
Sinter Plant Operations: Hazardous Emissions

Jin-Luh Mou and R. John Morrison

Abstract This article presents an outline of the iron ore sintering process, which introduces the blast furnace slag-forming requirements to allow an understanding of the required adjustments to flux addition in the sintering process; some basic concepts of the sintering reactions are also introduced. The recovery of miscellaneous wastes using high S, N, Cl content materials in sinter plants has been associated with some hazardous emissions, such as dust, NOx, SOx, and dioxins. The formation mechanism of these hazardous pollutants and some practical countermeasures are discussed.

5.1 Introduction

Before introducing the iron ore sintering process, some essential background information should be understood. This includes the following questions: why should iron ore fines be converted into lumpy materials? Why are fluxes added to the process? What are the chemical, physical, and metallurgical requirements of sinter ore?

The blast furnace operation is a bit like a black box; the gases and material flows interact counter-currently, and it is not possible to tell whether the iron burden is softening, melting, and dripping optimally inside the furnace. Only by checking the slag composition is it possible to tell whether the blast furnace is functioning satisfactorily or not.

A trigonal phase diagram of $CaO\text{-}SiO_2\text{-}Al_2O_3$ (Fig. 5.1) is an important guideline for blast furnace operations; accordingly, it is used to adjust the slag component ratio to reach near the eutectic point. This leads to the formation of the blast furnace slag with the lowest melting point, the best fluidity, and the best sulfur removal efficiency. Another important slag-forming component is MgO, which will facilitate the breaking of the slag silicate texture from framework, chain or double chain silicates into orthosilicates, or short-range silicates that enhances the fluidity.

J.-L. Mou
Formosa Ha-Tinh Steel Corporation, Ha-Tinh, Vietnam
e-mail: jinluhmou@gmail.com

R.J. Morrison (✉)
School of Earth and Environmental Sciences, University of Wollongong,
Wollongong, NSW, Australia
e-mail: johnm@uow.edu.au

P. Cavaliere (ed.), *Ironmaking and Steelmaking Processes*,
DOI 10.1007/978-3-319-39529-6_5

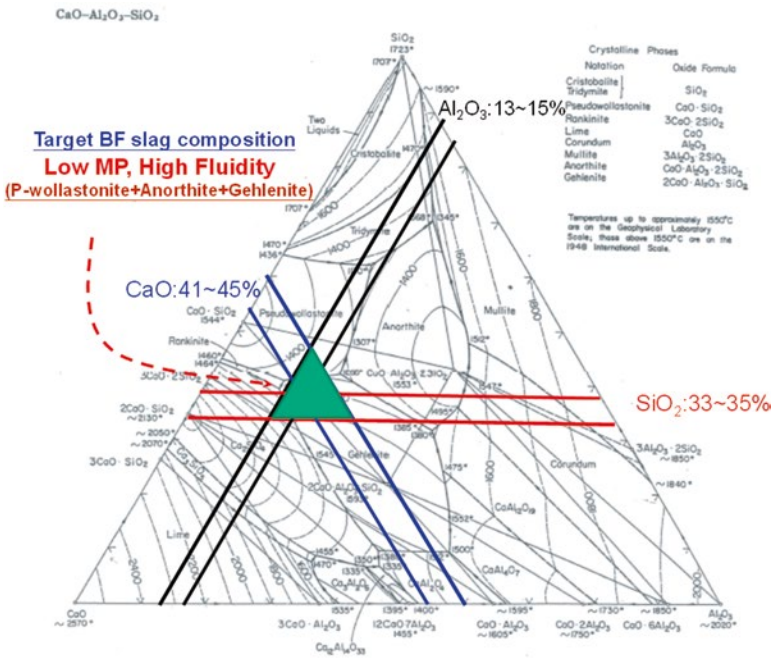

Fig. 5.1 Target BF slag composition based on the CaO-SiO_2-Al_2O_3 phase diagram

For the four major slag components, certain ratio ranges are required: $B_2 = CaO/SiO_2 = 1.15–1.25$, $B_3 = (CaO + MgO)/SiO_2 = 1.40–1.45$, and $B_4 = (CaO + MgO)/(SiO_2 + Al_2O_3) = 1.00–1.10$.

5.1.1 Size Requirements

A blast furnace is a "picky eater"; only the lumpy materials are fed into its belly. The size requirements of the iron burden for a blast furnace are iron ore lump, 6.3–31.5 mm; pellet, 9–18 mm; sinter, 5–50 mm; and coke, 25–80 mm. Iron ore fines, with the particle size of <10 mm, are not suitable as blast furnace feed. Several agglomeration processes have therefore been developed; if the ore type contains predominantly very fine particles (<0.075 mm), then a hot bond pelletizing process is applied. If the ore type has iron ore fines with coarser particles, then a sintering process is used.

5.1.2 Metallurgical Property Requirements

When the materials descend inside the furnace and the temperature reaches around 550 °C, Fe_2O_3 is reduced to Fe_3O_4 with around a 4 % volume expansion; some of the particles break down into small fragments and get blown out of the furnace with the

blast current. The breakage material is mainly composed of secondary hematite (the hematite that recrystallizes from the melt), therefore, to control the combustion atmosphere (to control the FeO level in sinter), and the chemical composition of sintering materials has become the key issue to minimize the reduction degradation.

When the temperature reaches 900–950 °C, magnetite (Fe_3O_4) is reduced to wustite (FeO); if the sinter has a compact texture without pores, then the reduction speed is low, and this reduces the burden descent speed, which leads to low BF productivity. The reducibility index is controlled mainly by the pore texture and is an important index for sinter ore.

When the temperature reaches 1400–1650 °C, the iron burden turns into liquid FeO or liquid Fe^0; softening and dripping occur in the cohesive zone. If the dripping melt has a high viscosity, then a coarser cohesive zone will be generated and will reduce the gas permeability, eventually resulting in low utilization of the reducing gas, and decrease the productivity. The softening and melting properties are controlled by slag components and the ratio among sinter, lump, and pellet; a good control of the burden ratio and slag-forming components is another important operational parameter.

5.2 Brief Background on Iron Ore Sintering

Modern sinter plants were developed in 1906 by Arthur S. Dwight and Richard L. Lloyd, and a chain grate strand type sinter machine which was able to operate continuously had been put into operation at Birdboro, Pennsylvania, USA, in 1911 (Vegman et al. 2004). The sintering process gained popularity quickly around the 1950s as positive links were found between blast furnace performance and ferrous burden of the sinter ratio.

5.2.1 Outline of Sintering Operations

Iron ore sintering is an agglomeration process, which combines fine mineral particles into a porous mass by partial liquefaction caused by heat generated from coke breeze combustion; a flow diagram of the iron ore sintering process is shown in Fig. 5.2.

The chemistry of the raw materials is calculated to fit BF slag formation requirements; under this operational guideline, iron ores together with fluxes (limestone, dolomite, serpentine) and reverts (mill scale, flue dust BOF OG sludge, etc.) are blended in the blending yard and conveyed to the sinter plant proportioning silos, where the coke breeze, sinter plant return fines (SP/RF), and tuning fluxes are added and granulated through mixing drums to form a sinter mixture that is laid onto the sinter strand. Eventually, the coke breeze is ignited by an ignition furnace to provide the energy for sintering.

The CaO and MgO slag components do not coexist with iron ores and are added separately; therefore, CaO (such as limestone) and MgO (such as serpentine or dolomite) are mixed with iron ore fines as the sinter raw mix for the sintering

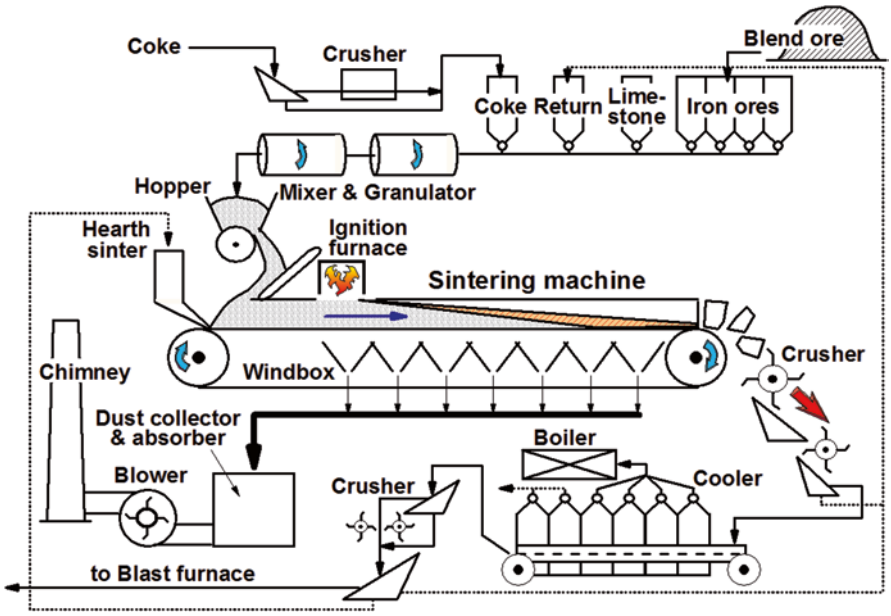

Fig. 5.2 Flow diagram of the iron ore sintering process

process. The ultrafine iron ore reacts with the fluxes and forms a bonding matrix (silico-ferrite of calcium and alumina, SFCA) at a reaction temperature of 1300 ± 50 °C from the combustion of coke breeze.

In order to promote the sinter plant productivity, a particle segregation device is installed to improve the sinter bed permeability. The main concept is to lay the coarse particles in the bottom layer and fine particles in the upper layer. There are several segregation devices, such as deflective plate, SSW (segregation slit wire, developed by Steel Plantech Corp.), ISF (intensified sifting feeder, developed by NSC), and MBF (magnetic braking feeder, developed by JFE).

Figure 5.3 shows a cross-sectional profile of sinter belt. The coke breeze is first ignited in the front end of the sinter strand; gas flow is sucked from upper surface and passes through the sinter bed to the bottom wind boxes. The combustion zone reaches the sinter bed bottom where sinter strand also reaches the tail end.

The inter-belt is thus classified into several regions; from the bottom part of the front end is a wet zone, where the moisture accumulates. A dry zone is found on top of the wet zone, as the moisture is driven down by the heat. On top of the dry zone are the coke breeze ignition and combustion zones, where the partial liquefaction occurs for sintering reaction. Cold gas is sucked in from the top surface and cools down the sinter cake in a cooling zone. After cooling, the sinter cake becomes brittle due to volume shrinkage. The wind box temperature is gradually increased from the front end to the tail and reaches the highest point, where the combustion zone reaches the bottom, and is called the burnt through point. The gas flow rate profile is similar to the temperature profile; the flow rate is higher in the tail end.

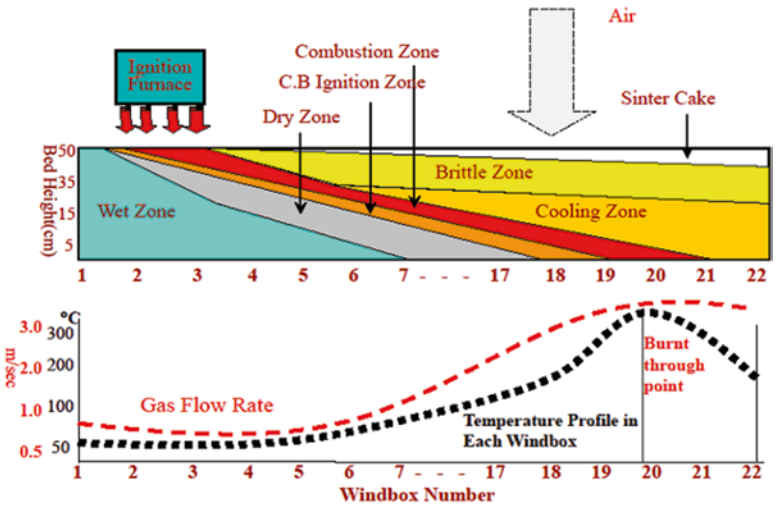

Fig. 5.3 Sinter belt cross section, temperature, and gas flow profiles in each wind box

5.2.2 *Fundamental Reactions of the Sintering Process (Pimenta 2012)*

In addition to the previous description of different temperature zones, a reduction region (rich in CO) is under the combustion zone, and an oxidation region, rich in O_2, is above the combustion zone. Below the material melting point, some reactions happen between solid-solid states, such as evaporation, dehydration, carbonate decomposition, reduction, or reoxidation.

The whole sintering process based on the heating stages can be split into five steps as shown in Fig. 5.4 (Pimenta 2012).

Step 1. Hematite (Fe_2O_3) reacts with CaO to generate the first calcium ferrites at around 1100 °C (solid–solid reaction). Around 1200 °C, these calcium ferrites start to convert into the liquid phase. The liquid is rich in CaO and Fe_2O_3 and begins to combine with ultrafine iron oxides, SiO_2, Al_2O_3, and MgO.

Step 2. Liquid phase starts to generate while temperature keeps on rising, and the superficial disintegration of hematite starts.

Step 3. The liquid melt assimilates with CaO and Al_2O_3, and the evolution of the reaction between liquid and hematite forms acicular calcium ferrites in the solid state (needle form), which are rich in Al_2O_3 and SiO_2.

Step 4. If the process temperature does not reach above 1300 °C or the residence time above 1300 °C is very short, the microstructure after cooling will be rich in acicular calcium ferrites in a bulk of crystalline silicates and granular hematite. That is the heterogeneous sinter.

Step 5. If the process temperature exceeds 1300 °C and the residence time above 1300 °C is long, columnar calcium ferrites and coarser recrystallized particles precipitate from melt. During the cooling step, skeletal rhombohedral hematite

precipitates from the liquid phase, and calcium ferrites crystallize as long columnar form flakes. That is the homogeneous sinter.

5.2.3 *Mineral Transformation During Iron Ore Sintering Process*

To convert the fine particles into lumpy agglomerates, the bonding matrix plays a major role (Fig. 5.5). When the coke breeze is combusted in the sinter bed, iron ore adhering fines together with the fluxes react and form the liquid melt; the wetting effect through this melt joins the iron ore particles together. Eventually, when the temperature cools down, this melt hardens, and the particles are bonded into lumpy

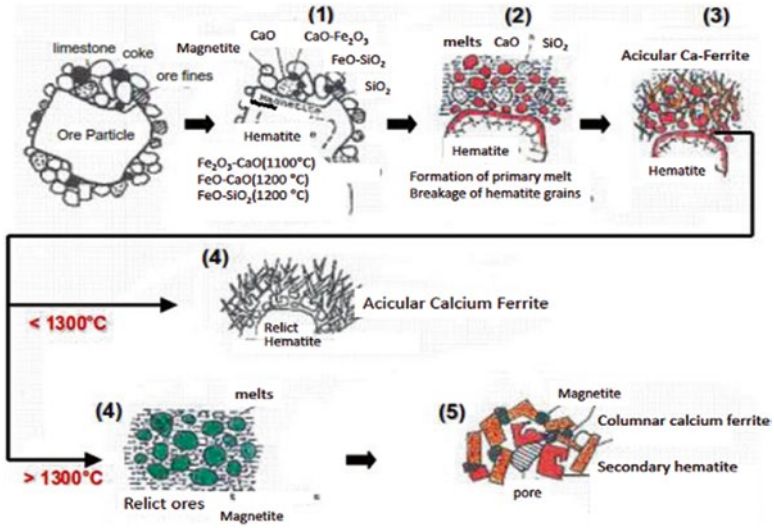

Fig. 5.4 Fundamental sintering process reactions

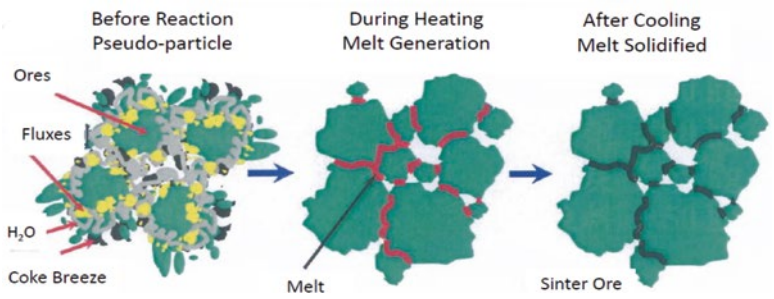

Fig. 5.5 Schematic diagram of the bonding matrix

agglomerate. Of course, dissolution, thermal decomposition, reduction, oxidation, recrystallization, etc., occur during the heating stage.

5.3 Hazardous Pollutant Emissions from Sinter Plants

Some of the hazardous elements, such as S and N, are brought into the process with the coke breeze or iron ores, and others, such as Pb, Zn, Na, K, S, Cl, and oil, may come from the revert materials. These unwelcome materials are brought into the system and are associated with the hazardous emissions. A sinter plant is the major pollutant source in an integrated steelworks; some estimated figures are summarized below, based on the assumed conditions.

Assumptions for a sinter plant emission:

An integrated steelworks produce 7.0 million tonnes of crude steel per annum (two sets of 4350 m^3 inner volume blast furnace), and the sinter ratio for the blast furnace is 80 %; then, two sets of 500 m^2 sinter plants are required to produce 10.2 million tonnes of sinter as the blast furnace iron burden. The fuel rate is 50 kg of coke breeze for per tonne of sinter, where the S content is 0.55–0.60 % and N is 0.8–1.0 % in the coke breeze. 2500 Nm^3 air is required to produce one tonne of sinter. Only a de-dusting electrostatic precipitator (EP) is installed, without installing the de-SOx, de-NOx, and de-DXNs devices. The estimated figures are as follows

O_2:	~15 %
CO:	8000–10,000 ppm
CO_2	5.0–6.0 %
Dust	40–50 mg/Nm^3
SOx	130–150 ppm
NOx	150–200 ppm
PCDD/PCDFs	0.8–2.0 ng I-TEQ/Nm^3

5.3.1 Dust

The off-gas dust concentration is about ~50 mg/Nm^3 with an EP removal efficiency of around 95 %; mostly the dust is composed of alkali chlorides and sulfates, which have high electric resistance and are hard to polarize in the electric field to be removed by the EP. These alkali chlorides are within the submicron particle range and generate the plume opacity together with the acid gases condensing on the surface as aerosols. A simple countermeasure is to install a multi-pulse type electric field generator and change the rapping frequency to clean the adhered particles off the electric plates and wires.

However, the most harmful PM2.5 is not monitored in the stack emissions. It has been assumed that PM2.5 forms 70 % of the PM10 measured in the waste gas (Wright 2014). This assumption is based on previous studies that have been undertaken by BlueScope Steel Limited that were considered as a reference index.

5.3.2 NOx (Mou 1998)

Suzuki et al. (1975) conducted sinter pot tests by replacing air with O_2(21 %) + Ar(79 %) and found no difference in the NOx emissions. This indicated that the NOx is fuel generated with almost no thermal NOx or prompt NOx in the sintering process.

An analysis of the chemical composition of the sinter raw materials showed that more than 90 % of the nitrogen comes from coke breeze (Mou 1992). It is difficult to identify what types of nitrogen compound exist in the coke breeze. However, it is believed that the nitrogen is tightly bound and for the most part in aromatic compounds. In the heating stage, the fuel-bound nitrogen compounds will, most likely, undergo some decomposition prior to entering the combustion zone; thus, it is not surprising that in the oxidation zone, the nitrogen compounds turn into the intermediates, such as HCN, CH, and amine radicals (Glassman 1987). These fragments react with oxygen in the continuous heating stage and form the nitrogen oxides. These intermediate compounds also contain hydrogen and carbon, which have a strong affinity with oxygen. In other words, the hydrogen or carbon will compete with nitrogen for the oxygen. Therefore, the presence C, CO, H, or OH in the combustion system will have some depression effect on the formation of nitrogen oxides.

Sasaki et al. (1990a, b) reported that a fast coke combustion rate led to higher $(CO + CO_2)/O_2$ and CO/O_2 ratio being found in the waste gases. Kasai et al. (1992) reported that faster coke combustion rate led to lower NO emissions. Obviously, the CO/O_2 ratio in the combustion zone is the major factor controlling the final NO emission. The combustion speed affects the atmospheric condition in the sintering process. Therefore, the improvement of coke combustibility would be a feasible countermeasure to depress the NO emission.

Not all the nitrogen content in the sinter raw mix would convert into nitrogen oxides in the sintering process; the conversion ratio will depend on the combustion condition especially the CO/O_2 ratio. Hida et al. (1980) and Kasai et al. (1992, 1993a, b) developed the conversion ratio formula. An estimated conversion ratio based on a real sinter plant operation data is around 36 % (Mou 1998).

5.3.3 De-NOx

Currently, there are less than five sets of de-NOx facilities being installed in the world sinter plants; the technique being applied is the SCR process. WO_3-TiO_2-V_2O_5 catalysts are applied for de-NOx operation, where the liquid NH_3 is injected into the reaction chamber under the operating temperature of 320–350 °C; the NOx removal efficiency can reach around 90 %. The reactions are summarized as follows.

$$4NO + 4NH_3 + O_2 \rightarrow 4N_2 + 6H_2O\,(\text{major reaction})$$

$$6NO + 4NH_3 \rightarrow 5N_2 + 6H_2O$$

$$2NO_2 + 4NH_4 + O_2 \rightarrow 3N_2 + 6H_2O$$

$$6NO_2 + 8NH_3 \rightarrow 7N_2 + 12H_2O$$

An in-process de-NOx study (Mou 1998) concluded that NOx emissions in iron ore sintering process depend mainly on the coke breeze combustion condition. A faster combustion speed results in lower NOx emission. To enhance the granulation and improve the permeability of the sinter mix has been shown to be an effective countermeasure by increasing the combustion speed and depressing the NOx emission.

This study also verified sugar is a strong binder in sinter mix granulation, improving sinter bed permeability and increasing the flame front speed; hence, the conversion ratio of nitrogen fragments to nitrogen oxides is greatly reduced. Sinter pot test results showed 1 wt% of sugar addition to the sinter mix decreased the NO mass from 533.8 to 283.3 g/t. sinter, with nearly 47 % NO mass reduction. The NOx concentration also decreased from 223 to 160 ppm with nearly 28 % concentration depression. Also, because of the shortened sintering time, sinter productivity is also significantly increased from 37.5 to 45.4 t/m^2/24 h as the sinter strength is maintained at the same level. Sugar is a potential additive for in-system de-NOx in the iron ore sintering process.

5.3.4 SOx

The sulfur compounds in the sinter mix may be in organic or inorganic forms. In iron ores, especially igneous magnetite, some pyrite (FeS_2) or chalcopyrite ($FeCuS_2$) is always present and difficult to get rid of through magnetic separation or washing processes. In coke breeze, there are either organic or inorganic sulfur compounds. Although in the coal washing process some of the pyrite can be removed through flotation and density separation, the removal efficiency is limited by the size of pyrite. It is very difficult to separate organic compounds from the coal. In the coking process, some of the sulfur compounds go into the by-products or escape to the atmosphere, and some others still remain in the coke, which is the major source of sulfur oxides in sintering.

SO_2 generated in the heating stage may be trapped by water (Martin 1984), limestone (Anderson and Galwey 1995), or iron ores (Tu and Liu 1992); SO_2 existing in water (referred to as S(IV)) occurs as three species, which are hydrated sulfur dioxide, bisulfite ion, and sulfite ion (Anderson and Galwey 1995).

$$\left[\mathrm{S(IV)}\right] = \left[SO_{2(aq)}\right] + \left[HSO_3^-\right] + \left[SO_3^{2-}\right] \tag{5.1}$$

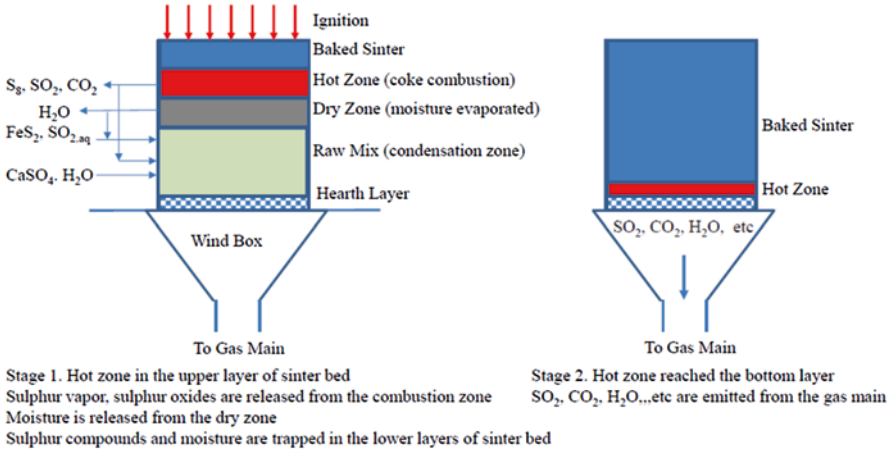

Fig. 5.6 SOx emission model for the iron ore sintering process

The unionized acid (H_2SO_3) has never been observed; the fraction of S(IV) in each species is a function of pH value. At pH < 2, $SO_{2(aq)}$ is dominant; pH at 2–8, HSO_3^- is formed; pH > 8, SO_3^{2-} is the preferred form.

A SOx emission model in sintering process is summarized as follows (Mou 1998). The sulfur released in the combustion stage is most likely to be absorbed and trapped below the dry zone. No matter whether the sulfur is liquid (S_8), sulfur dioxide (SO_2), or both, the sulfur is stored in several forms beneath the dry zone in the sintering process. When the combustion zone passes through the lower part of the sinter bed without any absorbent materials beneath it, the sulfur compounds oxidize to sulfur dioxide again and finally escape out to the atmosphere (Fig. 5.6).

5.3.5 Sulfur Journey in Iron Ore Sintering Process

Mou (1998) indicated that around 50–55 % of the sulfur in the sinter mix is from the coke breeze in the form of pyrite and organic sulfur; the other 45–50 % is from iron ores, fluxes, and reverts, mainly in the form of pyrite, chalcopyrite, and calcium sulfates. After heating, sulfur reacts with iron ores and limestone to form calcium sulfates and pyrite, which remain in the sinter. An estimated sulfur journey is summarized as follows (Mou 1998):

$$\text{Sulfur Raw Mix} = \text{Sinter} + \text{SP} / \text{RF} + \text{EP dust} + \text{Gases} \tag{5.2}$$

$$100\% = 18.9\% + 8.8\% + 1.1\% + 71.3\%$$

5.3.6 Conventional De-SOx Technologies

There are many applicable SOx removal technologies being applied in the combustion process. Most are off-gas treatment processes (Table 5.1). The side effects are the difficulties of resourcing these de-SOx by-products, especially the generated dust and sludge from the iron ore sintering process, which contain many impurities, such as iron ore powder, KCl, and NaCl. This causes a second pollution problem.

5.3.7 In-Process De-SOx Technology

Mou (1998) discovered an in-process de-SOx countermeasure by adding urea directly into the sinter mix. Urea decomposes to NH_3 at around 130 °C (Mcketta 1982) in the sinter bed dry zone and is trapped in the wet zone as NH_4OH and eventually released to the exhaust gas near the burnt through point (BTP), where the SOx (mainly SO_2) is also released out at the BTP, due to the strong affinity characteristic between NH_4SO_4 and SO_2. Eventually, $(NH_4)_2SO_4$, NH_4HSO_4, $(NH_4)_2SO_3$, and NH_4HSO_3 are formed inside the exhaust gas system. The SOx is converted to ammonium sulfates/sulfites/bisulfates/bisulfite, and therefore the SOx concentration in the outlet gases drops significantly.

Pot tests and plant trials have proven the de-SOx efficiency to 95 % (Mou 2001). The drawback is that the sticky $(NH_4)_2SO_4$ being brought out by the suction gas to the EP would adhere on the EP plate and wire and eventually lower the dust removal efficiency; the plume opacity becomes worse in a couple of days after the urea is added to the sintering process. Therefore, it is suggested to use wet EP or scrubber

Table 5.1 Conventional SOx removal processes

Process	Description	Reference
Active carbon absorption technology	SO_2 absorbed chemically or physically into the pores of active carbon	Slack (1975)
Metal oxide absorption technology	Metal oxides such as Mn, Fe, and Zn absorb SOx into sulfite or bisulfite at a lower temperature and desorb at a higher temperature	Slack (1975)
Lime base De-SOx technology	Limestone powder or hydrated lime reacts with SOx to form $CaSO_4 \cdot nH_2O$	Slack (1975)
Aqueous carbon process (ACP)	Sodium carbonate solution injected into the flue gases to form the sodium sulfite and/or sulfate to remove SOx	Slack (1975)
MgO De-SOx	$Mg(OH)_2$ injected into the flux gases to form $MgSO_4$(aq)	Burnett and Wells (1982)
Dry sorbent injection	Dry alkali sorbents injected into the flux gases to form the alkali sulfite or sulfate to remove SOx	Yet et al. (1982)

when urea is added. Actually, NH_3 is a basic reagent, besides its strong affinity to bind with SO_2 but also to bind with HCl. In other words, urea addition is capable of removing both SO_2 and HCl.

5.3.8 *Dioxins-PCDD/PCDF (Kasai 2002)*

Dioxins have been called the "century poison" with two congener groups being identified, polychlorinated dibenzo-p-dioxins (PCDD) and polychlorinated dibenzofurans (PCDF). In Japan, the coplanar polychlorinated biphenyls (Co-PCB) that have a similar toxicity are also treated as a subgroup of dioxins. The chemical structures of dioxins and their toxicity are shown in Fig. 5.7, and molecular structures are shown in Fig. 5.8.

Up to now, no conclusive evidence has been presented for the formation mechanism of PCDD/PCDFs. Two theories have been proposed, which are precursor condensation and de novo synthesis.

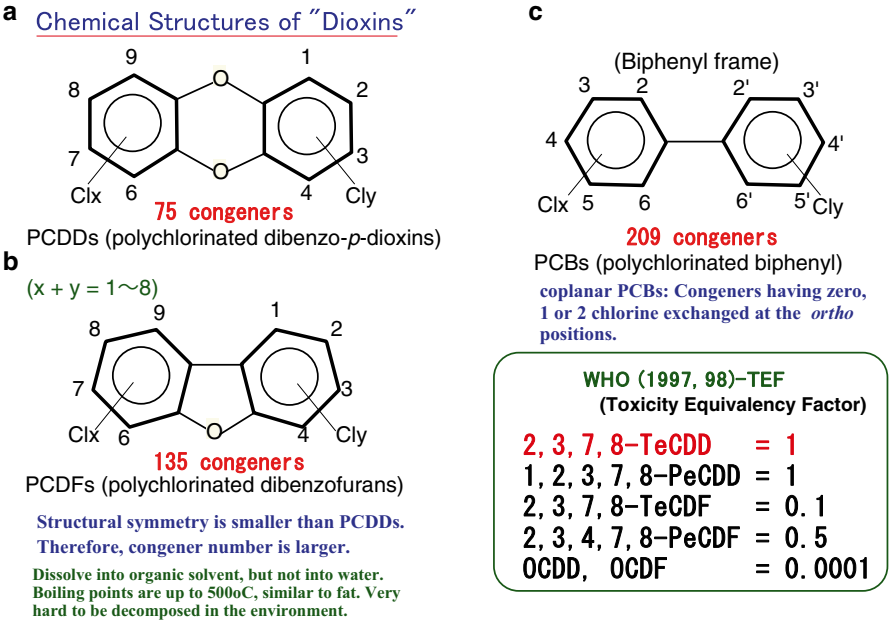

Fig. 5.7 Chemical structures of dioxins and their toxicities

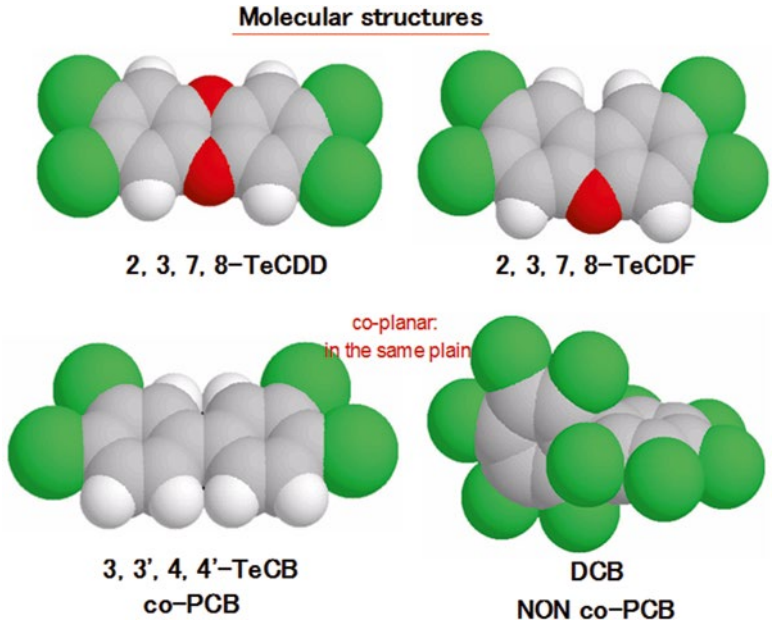

Fig. 5.8 Molecular structure of dioxins

5.3.9 Formation Mechanism of Dioxins (Kasai 2002)

1. Formation through precursors condensation
   Molecules with six-member ring structures, such as chlorobenzenes and chlorophenols, are heated in the combustion stage, where the chlorination, coupling reaction, and oxidation occur. Eventually, two six-member rings are joined together by two oxygen and the free radicals coupled with 1–8 Cl anions. The reaction temperature is above 800 °C, and the reaction is fast. The major congeners through precursors condensation are PCDDs. A schematic illustration of the precursor condensation route is shown in Fig. 5.9.
2. Formation through de novo synthesis
   Dioxins forming through de novo synthesis mean direct formation of dioxins from carbonaceous materials at relatively low temperature. Reactions to form dioxins involve the splitting of macromolecular compounds containing six-member rings. Normally, the reaction temperature is around 450 °C, and the major congeners are PCDF. An illustration of the de novo synthesis route is shown as Fig. 5.10.

Dioxin Formation in Sintering Process

Kasai (2002) established a dioxin formation model for the sintering process which explained the formation mechanism of dioxins in the sinter bed, as shown in Figs. 5.11 and 5.12.

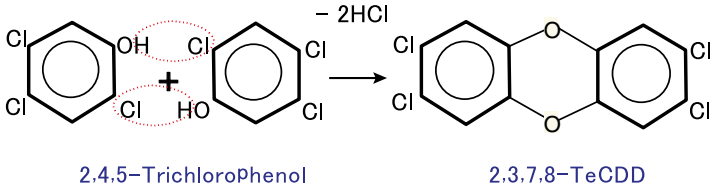

Fig. 5.9 Precursors condensation route for dioxin synthesis

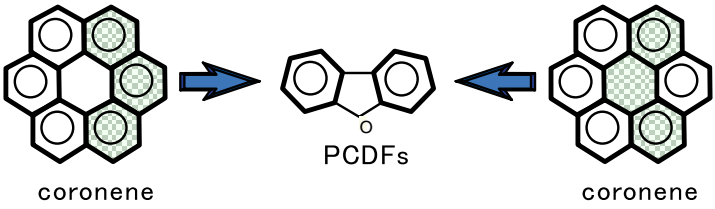

Fig. 5.10 De novo synthesis route for dioxin production

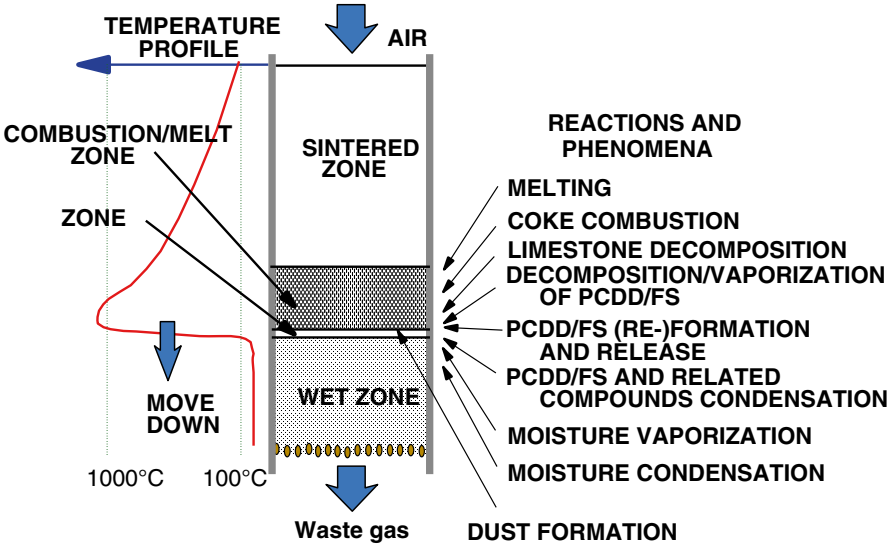

Fig. 5.11 Temperature profile and reaction zones in the sintering bed (Kasai, 2002)

Through the dioxin formation model, we can assume the dioxins would be released from the sinter bed when the combustion zone reaches the bottom; in other words, the dioxins are released out of the sinter bed around the BTP.

A survey result (Kasai 2002) indicated that the dioxin emission profile is similar to the temperature profile in each of the wind boxes. Additional surveys indicated that the major congeners of dioxins in the sintering process are PCDFs, the dominate congener is 23478-P5CDF, and the dominate congener for TEQ is 23478-P5CDF (Figs. 5.13 and 5.14).

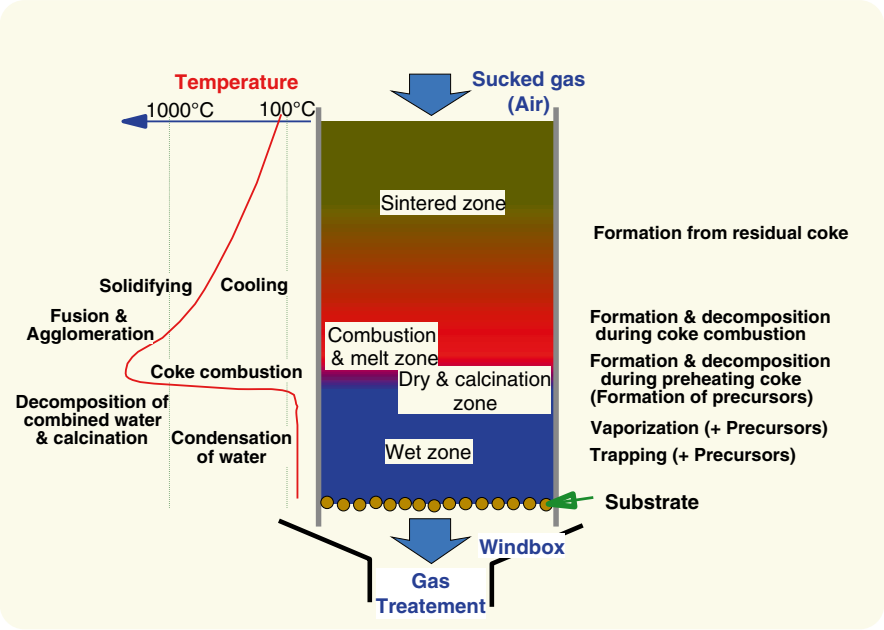

Fig. 5.12 Phenomena and reactions relating to the PCDD/PCDFs emission in the sintering bed PCDFs emission in the sintering (Kasai, 2002)

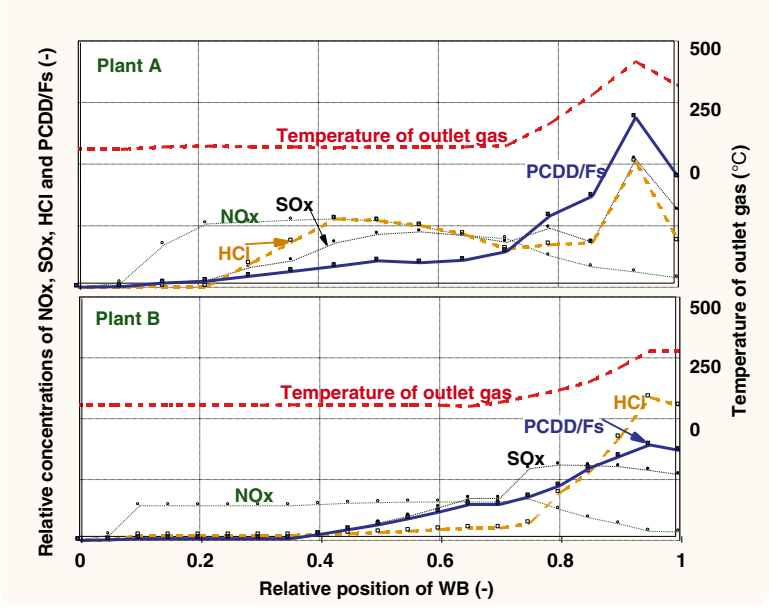

Fig. 5.13 Relative concentrations of PCDD/PCDFs and other gases in wind boxes with progress of sintering (Kasai, 2002)

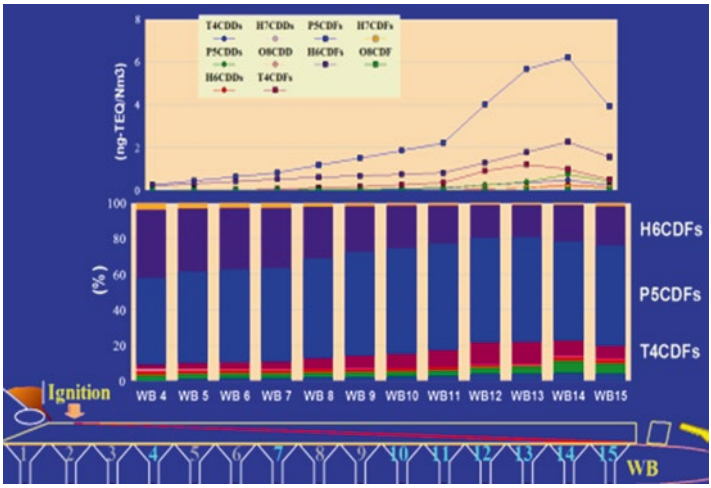

Fig. 5.14 Concentration and fraction of PCDD/PCDFs (TEQ) at the wind boxes of the sinter machine (Kasai, 2002)

Kasama et al. (2006) conducted a detailed analysis of the exhaust gas at the NSSMC Oita No. 1 sintering plant. This clarified and specified the strand positions where dioxins were released into the exhaust gas. The results are summarized as follows.

The release of dioxins was detected at two different positions. The first release position was located at the point where the drying zone reached the hearth layer, showing a broad peak containing a large amount of furans. The second release position was located at the point where the melting zone reached the heath layer, showing a sharp peak. Differences in dioxin congeners at the release positions imply a different mechanism of dioxin formation. The dioxins of the second release are considered to be formed in wind boxes at temperatures of 300 °C or more, with organic substances and chlorine supplied from incompletely sintered areas or with grease and dust in the wind boxes. This result has indicated that controlling the burn through point to the discharge end could be effective for decreasing the dioxin emissions in the second location. Figure 5.15 shows a schematic image describing the release of exhaust gas components.

Figure 5.15 also summarizes the results of the exhaust gas measurements in a commercial sinter plant. It seems that the drying zone begins to reach the grate surface near the sinter cake discharge side when the exhaust gas temperature reaches 100 °C. Thereafter, the exhaust gas temperature keeps on rising slowly, and the wet zone almost disappears within the subsequent strand as indicated by reading the moisture change. The dust ascends together with the dioxin ascent in the latter part, probably due to the loss of the capability of capturing them in the sintering bed as a result of the disappearance of the wet zone.

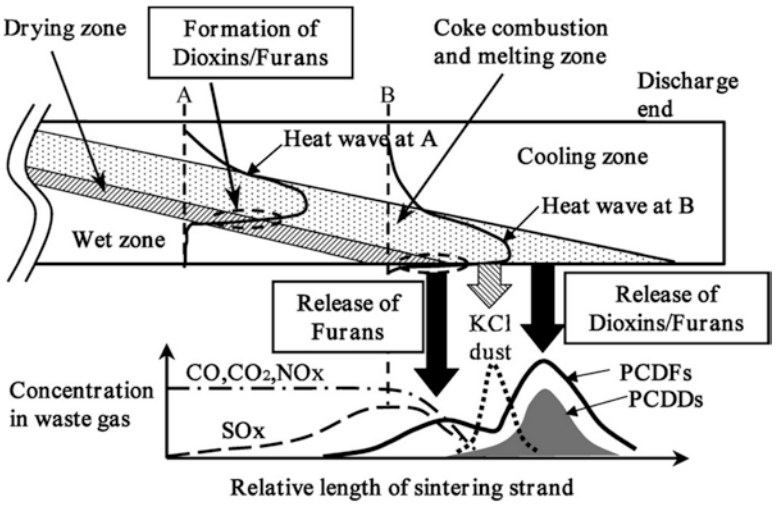

Fig. 5.15 Schematic image describing the release of exhaust gas components (Kasai, 2002)

From the results of the O_2, CO_2, and NOx measurements, the combustion of the fine coke seems to have been almost completed before it reached BTP. This may consequently indicate that, in the furthest area on the sinter cake discharge side after BTP, the coke combustion zone no longer exists and a high-temperature zone of over 1000 °C expands up to the hearth layer. Nevertheless, the wind box exhaust gas temperature rise is relatively slow because the sensible heat is consumed to increase the heat of the hearth layer and the grate.

From the next wind box, high-alkali and high-chlorine dust is affluently discharged. KCl and NaCl, which are considered to be the main components of the discharged dust, have a high melting point of 770 and 801 °C, respectively, and a high boiling point of 1510 and 1413 °C. In order to volatilize them, a condition near the highest temperature in the sintering bed is required. Therefore, the highest part of the sintering temperature must have reached up to the grate surface. This result agrees with the discussions of Kawaguchi et al. (2002) on the volatilization of chlorine. In BTP wind box, which comes after the chlorine release peak, a second-stage peak of dioxin release is observed. As regards the dioxins generated in the wind boxes close to the sinter cake discharge end, Tan and Neuschütz (2004) theoretically suggested the possibility of generation in the cooling process in the cooling zone, but no report has ever been made on this in commercial sintering equipment. The reason may be that, in production using sintering machines having a small number of wind boxes or in production where BTP is near the sinter cake discharge side, two phenomena occur in one wind box and these two could not be separately detected by the usual measurements.

The following two sources are conceivable for the supply of carbon and chlorine for the formation of dioxins in the second stage. One is the coke combustion zone that contains an un-sintered area where coke combustion remains incomplete until

it is discharged on account of sintering fluctuations. The incomplete combustion is often confirmed by the observation of sintered cakes on the discharge side. It is probable that small amounts of carbon and chlorine are supplied from this zone to cause dioxin formation such as the de novo synthesis reaction in the wind box. Although C and Cl are supplied in very small amounts, they are long exposed to a critical temperature zone, as long as several seconds, and may therefore be concentrated to a high level. The other source is grease and dust deposits on the inside surfaces of the wind boxes. Sealing grease is constantly fed to the slide surfaces of the sintering pallets. This grease loses its viscosity as it is heated in the latter half of the strand, is sucked into the wind box, and is deposited on its inside walls. Small amounts of chlorine contained in the grease and dust caught on the deposited grease are likely to cause dioxin generation slowly and progressively.

Kawaguchi et al. (2002) reported the memory effect of chlorine that remained in the wind box in their sinter pot test, seen in the form of re-volatilization and rediffusion of the chlorine in the drying process. Effects of said deposits in commercial operations need to be further analyzed in detail. Dioxins released in front of the BTP are reducible in quantity by strengthening the control of chlorine content or oil content in the raw materials for sintering, but different means of control are necessary for decreasing dioxins produced in the second stage. A practical effective means may be an appropriate control of the BTP position. There should be a control for setting a target BTP on the sinter cake discharge side within the tolerances of the operating conditions in terms of product yield, strength, exhaust gas temperature, etc. For high-productivity operation, BTP will be set on the utmost discharge side right from the start since the sintering rate cannot permit otherwise. For low-productivity operation, however, BTP may be set on the raw mixture feeding side of the strand as in the test being discussed. The operational results clearly show that the BTP position is varied on account of different factors and seem to indicate that holding the BTP stable on the discharge side can constrain dioxin release to a certain extent.

5.3.10 Countermeasures for Dioxin Reduction

5.3.10.1 Dioxin Reduction by SCR Catalyst

Mou (2005) conducted a pilot-scale test of dioxins reduction by using SCR catalysts in the No. 4 sinter plant of China Steel Corporation in year 2005. A test rig was installed adjacent to a sinter plant SCR de-NOx reactor (Fig. 5.16). Three types of catalysts had been tested: (1) plate-type $WO_3/V_2O_5/TiO_2$, (2) plate-type $MoO_3/V_2O_5/TiO_2$, and (3) honeycomb-type $(WO_3/V_2O_5/TiO_2)+(Pt/Al)$. The testing temperatures were set at 250, 290, 310, and 330 °C. The testing results are shown in Table 5.2 and summarized in the possible mechanism as follows:

1. Dioxin reduction efficiency reduced as the operational temperature increased.
2. The test results showed the reduction efficiency is around ~28 to ~45 %. The three types of catalyst removal efficiencies were all similar.

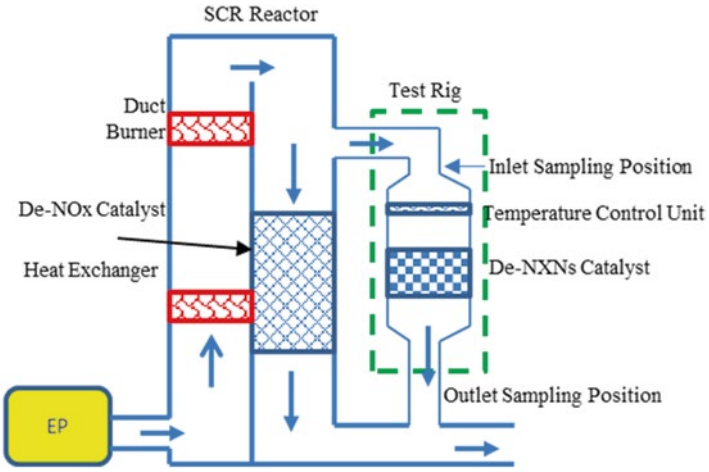

Fig. 5.16 SCR catalyst test rig for dioxin removal

Table 5.2 Toxicity removal efficiency (%) of SCR catalysts at different operational temperatures

°C	330	310	290	250
$WO_3/V_2O_5/TiO_2$	22.7	40.2	42.9	
$MoO_3/V_2O_5/TiO_2$	32.8	30.8	38.5	46.6
$(WO_3/V_2O_5/TiO_2) + (Pd/Al)$	29.1	27.5	36.8	44.4

3. The gas phase dioxin removal efficiency was higher than the solid phase.
4. During tests where dust accumulation on the catalyst surface was observed, these dusts contained rich KCl (source for Cl), unburnt coke breeze fines (source for C), and Fe_2O_3 (de novo catalyst); moreover, the SCR operation temperature is around 300–350 °C; hence, the surface of catalysts provided a suitable de novo synthesis environment. It was therefore assumed that dioxins formed on the surface of catalyst as the temperature stepped into the reaction window.
5. The removal efficiency of low chlorine (4, 5) dioxins was higher than high chlorine (6–8) dioxins. The removal efficiency of PCDD was higher than PCDF.
6. Sampling data showed the toxicity of PCDF was about 10 times that of PCDD.

5.3.10.2 Dioxin Removal by Lignite Coke Absorption

Mou and Passler (2008) conducted a demonstration scale test of lignite pack bed filter for dioxin removal in China Steel No. 2 sinter plant. The filter bed system is equipped with a long tube container with the $L \times W \times H = 6.05 \times 2.43 \times 2.90$ m^3. It

was a module design with the gas treating capability of 60,000 m^3 gas per hr per unit, and it could be connected in parallel in different units according to the required gas handling amount. The reason for choosing lignite coke was the pore diameter more suitable to trap the dioxin molecules than active carbon, and it also was more noncombustible than active carbon.

The basic concept was to deploy the lignite coke on top of an inclined screen net for around 10 cm; waste gases passing through the packed bed and those dioxins, submicron particles, alkali chlorides, sulfates, etc. were trapped on/in the packed bed. Purging air was introduced for backwashing when the pressure drop reached a certain level due to caking on the pack bed; this caking together with upper layer lignite coke was removed by screw discharger, and the fresh lignite coke continues to supplement on the pack bed. Figures 5.17, 5.18, 5.19, and 5.20 show the working principle of the filter bed.

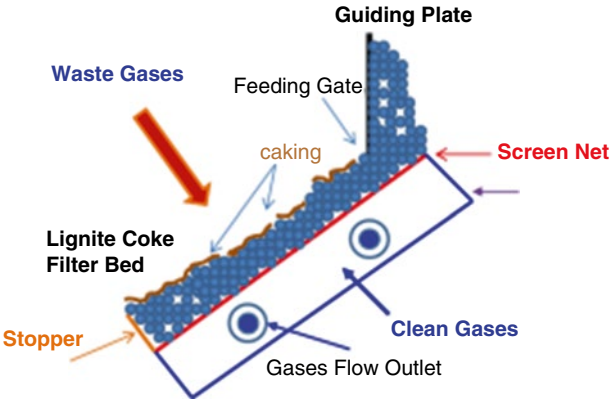

Fig. 5.17 Operation in gas purification stage

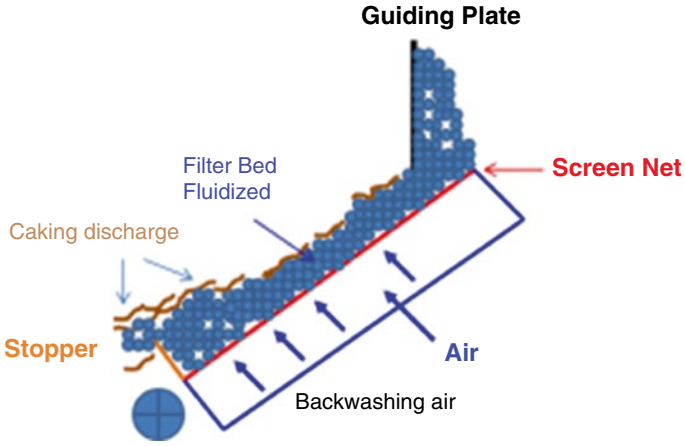

Fig. 5.18 Operation in air back washing stage

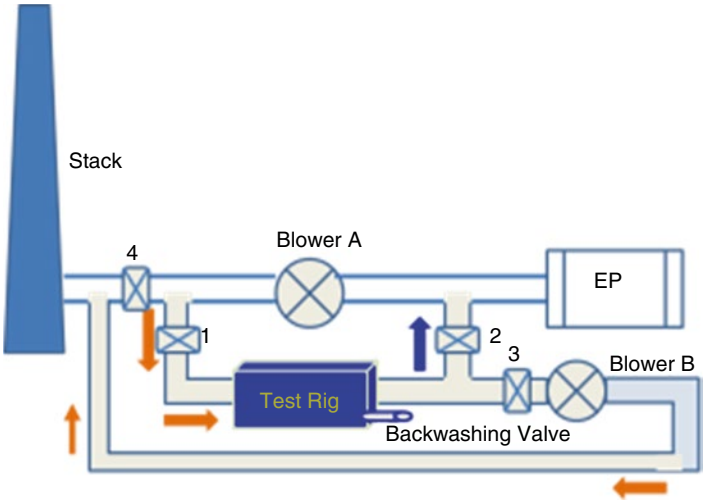

Fig. 5.19 Operational loop for testing module

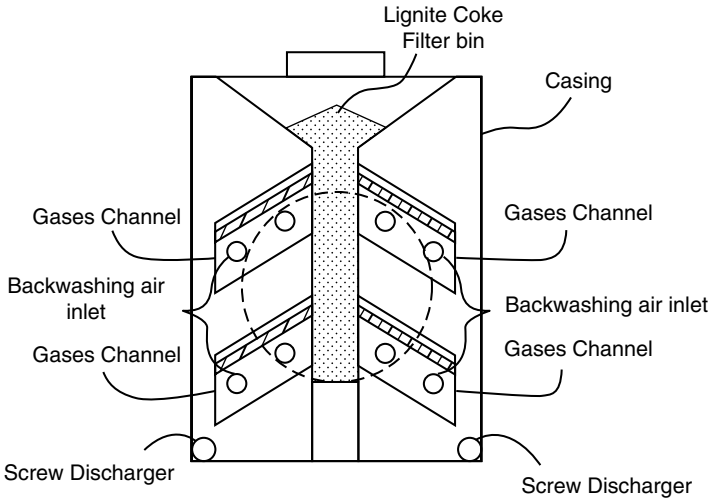

Fig. 5.20 Cross section of pack bed filter

Table 5.3 Average data for lignite pack bed testing results

	Filter Wt (B)	Filter Wt (A)	Sampling V (Nm^3)	Dust (mg/Nm^3)	O_2 (%)	O_2 corrected (ng I-TEQ/Nm^3)					
						Gas	Gas removal%	Solid	Sol removal%	Total	Removal%
In	0.338	0.359	1.761	12.054	15.37	1.028	NA	0.159	NA	1.289	NA
Out	0.559	0.563	2.106	2.342	14.44	0.017	98.3	0.013	92.1	0.029	97.7

For 3-month continuous testing, dioxin average removal efficiency reached around 98 % (Table 5.3). It is believed that the filter bed device is a potential apparatus for dioxins, submicron particle, and acid gas removal.

References

Anderson DC, Galwey AK (1995) Surface texture changes during reaction of $CaCO_3$ crystals with SO_2 and O_2, Air 3. In presence of coal combustion, 870–920 K. Fuel 74:101–1035

Burnett TA, Wells WL (1982) Conceptual design and economics of an improved magnesium oxide flue gas desulfurization process. In: Flue gas de-sulfurization, Chapter 18. American Chemical Society, pp 381–411

Glassman I (1987) Combustion, 2nd edn. Academic, New York, pp 318–361

Hida Y, Sasaki M, Ito K (1980) Consideration on CO and NO formation around the coke specimen during combustion. Tetsu-to-Hagane 66(13):21–29

Kasai E, Wu S, Sugiyama T, Inaba S, Omori Y (1992) Combustion rate and NO formation during combustion of coke granules in packed beds 1. Tetsu-to-Hagane 78(7):51–57

Kasai E, Wu S, Sugiyama T, Omori Y, Inaba S (1993a) Emission of nitrogen oxides during combustion of coke granules in packed beds. In: The third world conference on experimental heat transfer, fluid mechanism and thermodynamic, Honolulu, Hawaii, USA, Elsevier Science Publishers B.V., 31 Oct. to 5 Nov. 1993, pp 1065–1072

Kasai E, Sakata M, Sugiyama T, Omori Y, Yoshikawa O, Inaba S (1993b) Emission of nitrogen oxides and other nitrogen oxides from iron ore sintering process. In: Proceedings of sixth international symposium on agglomeration, Nagoya, Japan, pp 375–339

Kasai E (2002) Introduction of dioxins forming mechanism and their abatement countermeasures, presentation and discussions in China Steel Corporation, Kaoshiung, 2–5 July 2002

Kasama S, Yamamura Y, Watanabe K (2006) Investigation on the dioxin emissions from a commercial sintering plant. ISIJ Int 46(7):1014–1019

Kawaguchi T, Matsumura M, Hosotani Y, Kasai E (2002) Behavior of trace chlorine in sintering bed and its effect on dioxins concentration in exhaust gas of iron ore sintering. Tetsu-to-Hagané 88:59

Martin LR (1984) Kinetic studies of sulphur oxidation in aqueous solution, Chapter 2, SO_2, NO and NO_2 Oxidation Mechanism, Atmosphere Consideration. Jack G. Calvert, USA

Mcketta JJ (1982) Encyclopedia of chemical processing and design, vol 8, fertilizer components: ammonium sulfate. Marcel Dekker Inc., New York and Basel, pp 273–283

Mou JL (1992) A survey of the influence of sinter raw materials on NOx, SOx emission. TE-81023, Internal Technical Report of China Steel Corporation, Taiwan

Mou JL (1998) A study of in-plant De-NOx and De-SOx in the iron ore sintering process. PhD Thesis, Environmental Science Department, University of Wollongong, Australia

Mou JL (2001) In-plant reduction of NOx, SOx emission in iron ore sintering process, China Steel Technical Report No. 15, 31–36, Dec. 2001, Taiwan

Mou JL (2005) Evaluation of SCR catalysts for dioxins removal-pilot test, ST-94025, China Steel Corp. Internal Research Report

Mou JL, Passler K (2008) Report on NDF Demo Unit in CSC No. 2 SP. China Steel Corporation Taiwan

Pimenta FV (2012) Sintering process. Vale Training Course for Formosa Ha-Tinh Steel Corporation

Sasaki M, Hida Y, Enokio T, Ito K (1990a) The relationship between coke existing state and NO formation. Tetsu-to-Hagané 76:S57

Sasaki M, Hida Y, Enokio T, Ito K (1990b) A study of fuel NO formation and depression. Tetsu-to-Hagané 76:S58

Slack AV (1975) Sulfur dioxide removal from waste gases, 2nd edn. Noyes Data Corp., Park Ridge

Suzuki G, Ando R, Yoshikoshi H, Yamaoka Y, Nagaoka S (1975) A study of the reduction of NOx in the waste gas from sinter plants. Tetsu-to-Hagane 61, 3–13

Tan P, Neuschütz D (2004) Metall Mater Trans B 35B:983–991. doi:10.1007/s11663-004-0092-7
Tu LC, Liu GC (1992) A survey report of iron ore sinter plant De-NOx facilities. Engineering and Construction Dept. (V23), Internal Technical Report of China Steel Corporation, Taiwan
Vegman EF, Zherebin BN, Pochvisnev AN, Yusfin YuS, Kurunov IF, Parenkov AE, Chernousov PI (2004) Ironmaking. Akademkniga, Moscow, p 774
Wright J (2014) Review of human health risks – emissions from sinter plant. Principal/Director Environmental Risk Sciences Pty Ltd. Wollongong, Australia
Yet JT, Demski RJ, Joubert JI (1982) Control of SO_2 emission by dry sorbent injection. Chapter 16. In: Flue gas desulfurization. American Chemical Society, USA, pp 349–367

Part II
Blast Furnace Operations

Chapter 6
Recent Trends in Ironmaking Blast Furnace Technology to Mitigate CO_2 Emissions: Top Charging Materials

Hesham M. Ahmed, E.A. Mousa, M. Larsson, and N.N. Viswanathan

Abstract The iron- and steelmaking is the largest energy consuming in the industrial sectors. The high energy consumption is associated with emission of CO_2 and other pollutants. The most common ironmaking process used in the world is the blast furnace which contributes around 70 % of the world's steel production. Recently, blast furnace has undergone tremendous modifications and improvements to reduce the energy consumption and CO_2 emissions. The modifications are being focused on two main approaches: (1) development of top charging materials and (2) injections of auxiliary fuels through blast furnace tuyeres. The present chapter will discuss the recent modifications and development in the top charging burden and how it could participate in minimizing the energy consumption and CO_2 emissions for more efficient and sustainable iron and steel industry. The injection of auxiliary

H.M. Ahmed
MiMeR-Minerals and Metallurgical Engineering, Luleå University of Technology, SE-971 87 Luleå, Sweden

Minerals Technology Division, Central Metallurgical Research and Development Institute, P.O. Box 87-Helwan, Cairo, Egypt
e-mail: Hesham.Ahmed@ltu.se

E.A. Mousa (✉)
Minerals Technology Division, Central Metallurgical Research and Development Institute, P.O. Box 87-Helwan, Cairo, Egypt

Process Integration Department, Swerea MEFOS, SE-971 25 Luleå, Sweden
e-mail: Elsayed.Mousa@swerea.se

M. Larsson
Process Integration Department, Swerea MEFOS, SE-971 25 Luleå, Sweden

Energy Engineering, Department of Engineering and Mathematics, Luleå University of Technology, 971 87 Luleå, Sweden
e-mail: Mikael.Larsson@swerea.se

N.N. Viswanathan
Department of Metallurgical Engineering and Materials Science, Centre of Excellence in Steel Technology (CoEST), IIT Bombay, Mumbai 400076, India
e-mail: vichu@iitb.ac.in

P. Cavaliere (ed.), *Ironmaking and Steelmaking Processes*,
DOI 10.1007/978-3-319-39529-6_6

fuels will be discussed in details in another chapter. The enhancement of burden material quality and its charging mode into the blast furnace has resulted in a smooth and efficient operation. Recently, the usage of nut coke in the modern blast furnace is accompanied by higher production and lower reducing agent rates. An efficient recycling of in-plant fines by its conversion into briquettes with proper mechanical strength is applied in some blast furnaces to exploit the iron- and carbon-rich residues. Nowadays, novel composite agglomerates consist of iron ores and alternative carbonaceous materials represent a new trend for low-carbon blast furnace with lower dependence on the conventional burden materials. The recent investigations demonstrated that the novel composites are able to reduce the thermal reserve zone temperature in the blast furnace and consequently enhance the carbon utilization through its higher reactivity compared to fossil fuels. The top charging of bio-reducers and hydrogen-rich materials into the blast furnace is one of interesting innovations to mitigate the CO_2 emissions. Although some of previous approaches are recently applied in the modern blast furnace, others are still under intensive discussions to enhance its implementations.

6.1 Introduction

Blast furnace (BF) is considered to be the most important ironmaking unit. During 2014–2015 BF worldwide produced about 1155 million tonnes compared to 55 million tonnes by the direct reduced iron (DRI) (www.worldsteel.org). For the foreseeable future, it will continue to occupy a primary position because of its high efficiency on both reactions and heat exchange. BF is a continuously operating shaft furnace based on the counterflow principle. Carbon-bearing materials and burden are charged from the top as distinct layers. Charge materials descend under the influence of gravity. Through tuyeres (in the lower part of the furnace), hot blast is injected. The hot blast reacts with carbon in front of tuyere, forming carbon monoxide at high temperature. The hot ascending gases including carbon monoxide help in reduction of iron oxide as well as heating and melting of the descending materials. At the bottom of the hearth, molten iron and slag are collected and tapped (Biswas 1981).

The BF can be generally divided into three thermal zones; first is the preheating zone where the temperature of the ascending gases drops from 800 to 1000 °C down to 100–250 °C, and the raw materials heated up from room temperature up to 800–950 °C. Several reactions take place in this zone like the indirect reduction of hematite to magnetite and magnetite to wustite. Other reactions which occur in the zone are release of water vapor due to drying as well as that from hydrates, decomposition of carbonates (not calcium carbonates), deposition of carbon back from the ascending gas, etc. It is worth mentioning that the coke is relatively inert in this upper zone; it is heated up and loses its moisture and most of its volatile matter. In efficient furnace, by the time the iron reaches the thermal reserve zone (second zone), reduction would have completed and the gas composition would be corresponding that of wustite-Fe

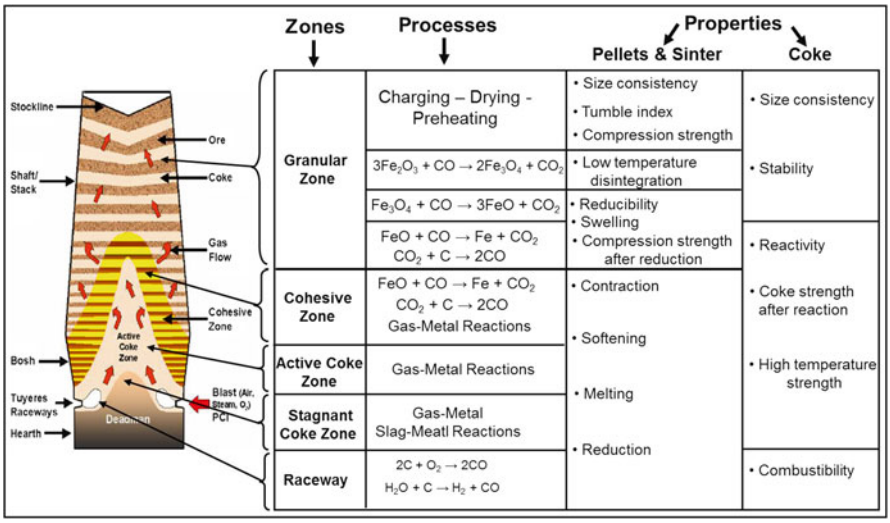

Fig. 6.1 Reaction zone and inner state of a blast furnace (Ranade and Chaubal 2004)

equilibrium. At the bottom of the thermal reserve zone, the indirect reduction of wustite to metallic iron takes place. This zone takes about 50 % of the BF height. The temperature of this zone is depended on the start of the gasification reaction, i.e., the coke reactivity. This zone is followed by the direct reduction zone where carbon gasification reaction rates are high, and the melting zone in which the molten material temperature approaches 1400–1450 °C. The ore softens in the cohesive zone, while the coke lumps act as windows for the gas to ascend through. The active coke zone starts below the cohesive zone and extends up to the raceway. The deadman zone consists of loosely packed coke through which droplets of melted material drip down to the hearth. In front of the tuyeres, the blast kinetic energy creates a semi void region with rapidly moving coke particles being combusted termed as the raceway. Dissolution of carbon into iron takes place in the melting zone when the metallic iron gets in direct contact with coke. The center area of coke zone which is known as stagnant coke zone extends through hearth and deadman zone and consists of densely packed coke. The most dominant reactions taking place in the BF and a schematic diagram showing the area where these reactions are most likely occurring are depicted in Fig. 6.1 (Mousa 2010; Peacey and Davenport 1979; Geerdes et al. 2015).

The charging system in modern BF is extremely important as it ensures good distribution of coke and burden materials inside the furnace which significantly affect the furnace performance and the productivity. The charging profile is an important tool for changing the gas distribution and to overcome the furnace irregularities such as uneven material distribution, channeling, scabs, scaffolds, hanging, etc. Bad distribution of feeding materials and ascending gases will result in poor permeability and limited access for the reducing gases through the burden materials resulting in poor reduction of descending oxides and thus consuming more carbon

down there in the dripping zone through direct reduction. Direct reduction does not result only in high carbon consumption but also in weakening the coke and adversely affecting the furnace permeability. An ongoing research activity at MiMeR laboratory, Lulea University of Technology, Sweden, showed that different distribution of feeding material can also have a significant impact on holding capacity of the descending bed for the generated fines. In modern blast furnace, the top is closed as they tend to operate under high top pressure.

Modern blast furnaces are usually equipped with "bell-less top" charging system invented by Paul Wurth in 1972. The bell-less top system allows easier burden distribution through a rotating chute and consequently uniform distribution of voidage and particles of charged materials inside the furnace. It is worth mentioning that proper feeding material distribution ensures good permeability and hence higher productivity, higher CO utilization, and thus lower coke rate. It also enhances the burden descent and lowers the thermal loads on the walls which ensure smooth operation, less heat losses, and longer refractory lifetime (Pandey and Yadav 1999).

6.2 Conventional Top Charging Materials

In the early days, BFs were quite often relied on charcoal and lump ores. Later the charcoal has been replaced by coke. Recently, BFs have grown considerably. In the early days, the hearth diameter was 4–5 m with annual production rate of 100,000 tonnes hot metal mostly from lump ore and coke. Nowadays, the bigger blast furnaces have hearth diameter up to 14–15 m with annual production rate of 3–4 million tonnes hot metal (Geerdes et al. 2015). The burden materials have changed from lump ore to more efficient materials like sinter and pellets. The reductant materials have developed as well from 100 % coke operation to use other injectant materials through tuyeres. Attempts are being made to charge other alternative reducing agents from the top along with burden material like biomass-based materials, plastics, etc. (Ahmed et al. 2014). Modern blast furnaces favor high Fe content in ore burden. Higher grade of iron ore burden can be realized after physical beneficiation process. This consequently creates more fine materials. These fine ores are too problematic to the BF operation. As a consequent, sintering and pelletizing as agglomeration processes are favored. Sinter constitutes 70–80 % of the iron-bearing material charged into the modern blast furnaces all over the world, while other blast furnaces in Europe apply 100 % iron ore pellets. A comparison of ferrous burden composition applied in 1990 and 2008 EU-15 is given in Fig. 6.2 (Luengen et al. 2012).

The quality demands for the blast furnace burden materials include chemical composition as well as mechanical durability. The chemical composition must meet the end product properties. The mechanical durability of the burden is related to the material property in cold, hot, and during reduction to ensure the furnace permeability and consequently good performance and less operational difficulties. The reducibility of the iron ores is for large extent controlled by how easy the reducing gases can get into the iron oxide particles. The intrinsic reducibility of the burden material

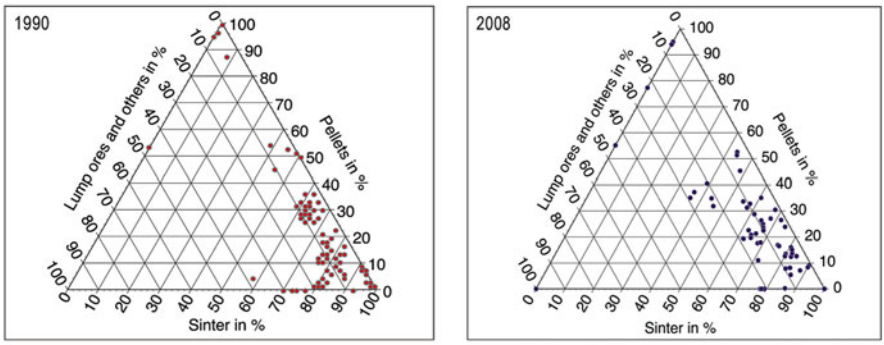

Fig. 6.2 Ferrous burden composition in 1990 and 2008 in EU 15 BFs (Luengen et al. 2012)

becomes a less important factor if no sufficient gas is transported to the reaction front and the produced gas is moved away from the reaction site. Ore burden materials are generally characterized by chemical composition, size and size distribution, cold strength, reduction, reduction disintegration, swelling, softening, and melting.

Although BF is a well-established and highly efficient process, there is a demand to enlarge its adaptability to reuse the in-plant residues and apply alternative reducing agents and novel charging composites. These modifications become essential to reduce the energy consumption and minimize the greenhouse gas emission (GHG) while keeping or even improving the furnace productivity. Therefore, the major part of this chapter will be devoted to brief the state of the art of attempts being made to meet these demands. Since these attempts are mostly based on decreasing the thermal reserve zone temperature and consequently shift the whole process toward lower CO/CO_2, it is more convenient to first discuss the fundamentals and different ways of shifting the process toward lower CO/CO_2 before discussing the developments of burden materials and alternative reducing agents.

6.3 Shifting the Process Toward Lower CO/CO_2

Enhancing the reducibility of the ore is always advantageous for blast furnace operation, especially in enhancing the productivity as well as smoother operation. If the ore can be reduced faster, then the production rate per unit volume of the furnace termed as productivity of the furnace can be enhanced. There is a possibility for further increase in the BF efficiency from the viewpoint of thermodynamics. If the rate of iron oxide reduction could be increased and the starting temperature of gasification reaction could be lowered, further increase in the efficiency of blast furnace process could be expected (Kashiwaya et al. 2001).

It is well known that an efficient blast furnace operation is characterized by a well-developed thermal reserve zone with a chemical reserve zone at the top of it.

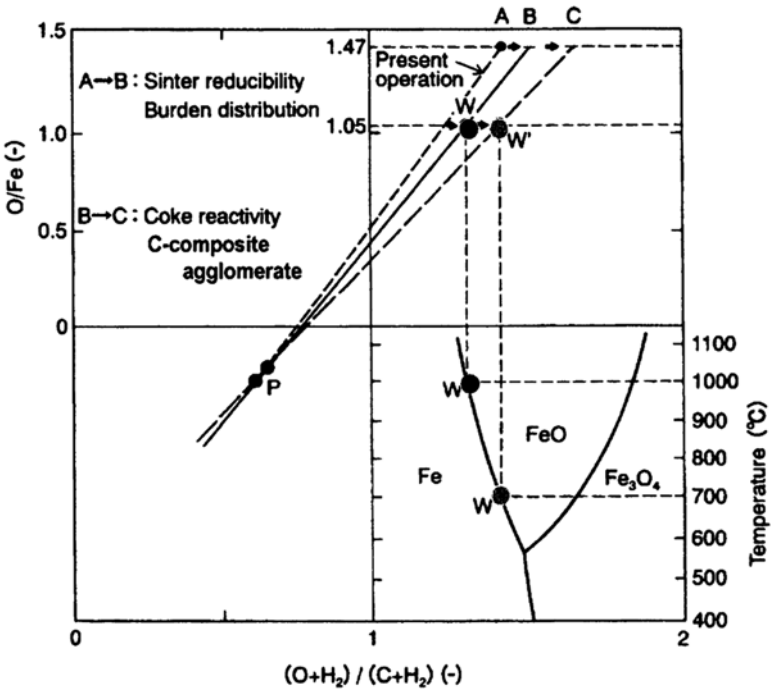

Fig. 6.3 Improvement technology of reaction efficiency on a blast furnace RIST diagram (Naito et al. 2006)

This is illustrated using the RIST diagram in Fig. 6.3 (Peacey and Davenport 1979). The point "W" corresponding to the chemical reserve zone is marked both in the RIST diagram and in the Fe-O equilibrium diagram. When the thermal reserve zone is equal to the W point (wustite-iron reduction equilibrium point) of the RIST diagram, the shaft efficiency of a blast furnace becomes 100 %, theoretically. In order to achieve that efficiency of furnace inner reactions, it would be necessary to shift the operation curve (the dotted line AP in Fig. 6.3) toward the W point, maintaining the present temperature condition of the thermal reserve zone unchanged (A → B), or to lower the thermal reserve zone temperature, shift the W point toward the high η_{CO} side ($\eta_{CO} = CO_2/(CO + CO_2)$).

Decreasing coke consumption in the blast furnace by means of shifting the equilibrium point of FeO-Fe reduction affecting decrease of thermal reserve zone temperature is being discussed intensively (Ariyama et al. 2005; Schmöle and Lüngen 2005; Nomura et al. 2005). Thermal reserve zone temperature is determined by the heat balance between the endothermic gasification reaction of coke and the heat supply from the gas flow. Thus, improving the gasification reaction, which is basically determined by the carbonaceous material reactivity, will reduce the thermal reserve zone temperature (Ueda et al. 2009a).

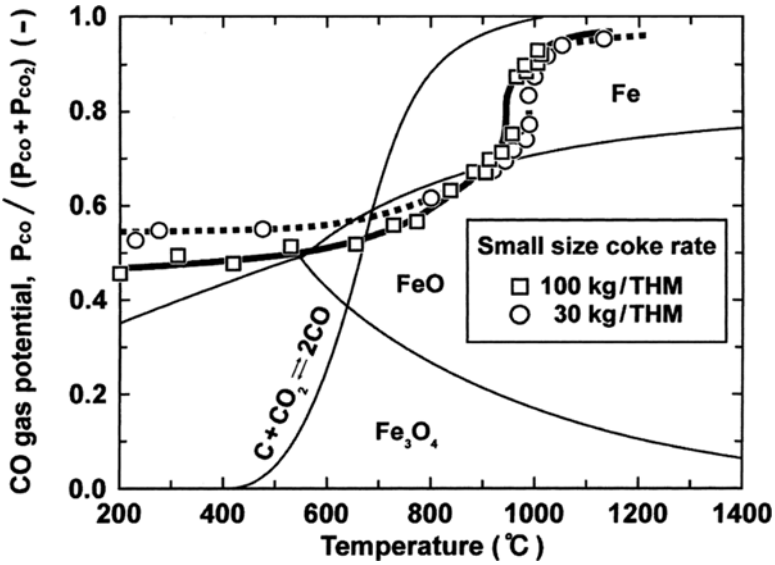

Fig. 6.4 Relationship between temperature and CO potential (Rist and Bonnivard 1963)

Using two facing sheets of hematite and graphite, the coupling between reduction and gasification was confirmed (Kashiwaya et al. 2001). Since mass transfer is a decisive variable in the reduction reaction inside the furnace, the degree of contact between the carbonaceous material and iron oxide would significantly affect the overall reaction rate. If the degree of contact between carbonaceous material and iron ore could be increased up to an ideal level, the starting temperature of the solution loss (gasification) reaction could be lowered (Kasai and Matsui 2004). Then, the equilibrium concentration at FeO-Fe reduction reaction will be shifted to higher CO gas utilization efficiency, resulting in the improved CO gas utilization efficiency at the furnace top and decreasing the reducing agents rate. This phenomenon is further explained by means of the Fe-C-O equilibrium diagram (Fig. 6.4) and the RIST diagram (Fig. 6.3). It was demonstrated experimentally that this phenomenon could be reached by using high reactive coke or carbon composite iron ore agglomerate (Kasai and Matsui 2004). Consequently, the gasification reaction could be improved, and the permeability and heat balance could also be improved, resulting in better performance under low reducing agent rate (Sawayama et al. 2009b).

It is worth mentioning that it would be a mistake to think that carbon consumption can be directly decreased and the process can be shifted toward the ideal blast furnace operation by just lowering the starting temperature of FeO-Fe reaction. However, decreasing the thermal reserve zone temperature using high reactive coke may intensify heat exchange and direct reduction in the lower zone. Carbon saving at lower reserve zone temperature can be realized only under certain conditions, for example, complete reduction of Fe_2O_3 to Fe_3O_4 at lower temperature such that no

Table 6.1 Effect of thermal reserve zone temperature on carbon and blast requirements

	Thermal reserve zone temperature, °C		
Parameter	823	923	1023
$(O/C)^{gwrz}$	1.34	1.30	1.28
$n_O{}^B$	94	0.99	1.05
$n_C{}^A$	49	1.58	1.65
Total carbon, moles of C/mol Fe	1.74	1.83	1.90

Note: $(O/C)^{gwrz}$ is the oxygen carbon molar ratio in the gas phase existing the wustite reduction zone, $n_O{}^B$s number of moles of oxygen in blast per mole of produced Fe, $n_C{}^A$s number of active carbon (carbon that goes to the gas phase) per mole of produce Fe

hematite or magnetite reaches the wustite reduction zone (Babich et al. 2009). Peacey and Davenport (1979) have presented predictions of carbon and blast requirements based on different reserve zone temperatures (Table 6.1). Their predictions are based on minimum heat demand (production of Fe, 5 % C from wustite, no flux, gangue nor heat losses) and blast temperature 1123 °C assumptions.

Ways of Shifting the Process Toward Lower CO/CO₂ The use of highly reactive or activated carbonaceous materials is suggested as one of the ways to reach this goal. Small-sized (Babich et al. 2009) or highly reactive coke usage significantly improves the gasification reaction (Naito et al. 2006). Coke reactivity can be enhanced significantly by means of catalytic effect (Babich et al. 2009). The activation energy could be lowered and the gasification rate increased on applying alkali vapor. When CRI (carbon reactivity index) is low, the catalytic effect appears strongly and almost disappears on using high reactive coke as well as on rising temperature. Fe and Ca are promising as catalysts to improve the coke reactivity at the condition of the thermal reserve zone in BF (Iguchi and Takada 2004). There are two basic ways to apply the catalyst to the coke (Nomura et al. 2005; Nomura et al. 2007): the post addition and the pre-addition of catalyst to the coke and coal blend, respectively. The selection of a suitable catalyst addition method could shift the reaction mode to a more homogeneous one at a lower reaction temperature, leading to an increase in the postreaction strength (Reddy et al. 1991). Additives such as Li_2O, $NaCO_3$, etc. can significantly affect the reduction rate by enhancing the rate of carbon gasification (Iguchi and Takada 2004; Reddy et al. 1991; Rao and Han 1984).

6.4 Recently Developed Top Charging Materials

6.4.1 Active Coke

Coke which is the reducing agent in blast furnace ironmaking is known to provide the structure through which the gas can ascend and distribute through the whole descending burden. Coke is a solid and permeable material up to very high temperature. Down

there in the blast furnace below the melting zone, coke is the only solid material. So the total weight of the blast furnace content is supported by the coke. Therefore, blast furnace requires special coke size as well as relatively low reactive coke to maintain the furnace permeability in lower part of the shaft (Lacroix et al. 2001). In addition, the size distribution should be narrow to maintain a stable operation and low coke rate (Podkorytov et al. 2009). The required size is in the range of 40–60 mm which can be achieved by screening the produced coke, the screening results in generation of undersieve coke which known as nut coke. Due to difficulties and GHG emissions to produce coke, there are several attempts that have been carried out to utilize this undersieve coke or nut coke in the blast furnace which of course will affect the furnace permeability and operation smoothness as well as productivity.

Several studies have been conducted to address the effect of charging nut coke with the burden material on the process efficiency and hence the productivity (Mousa et al. 2010b, 2011; Mousa 2010; Mousa et al. 2010a; Babich et al. 2008; Babich et al. 2009). The attempts started by charging this undersieve coke with different ratios (5–30 %) within the coke layer. It resulted in reducing the productivity by 0.9–6.5 %. It also led to nonuniform distribution of ascending gases (Nikitin et al. 1999). Other researchers (Loginov et al. 1976, 1977) have suggested charging the nut coke along with the burden material. The idea was successfully tested and followed by a good improvement in the blast furnace productivity and lowered coke rate. Figure 6.5 depicts how the size as well as its distribution affects the furnace permeability and liquid drainage.

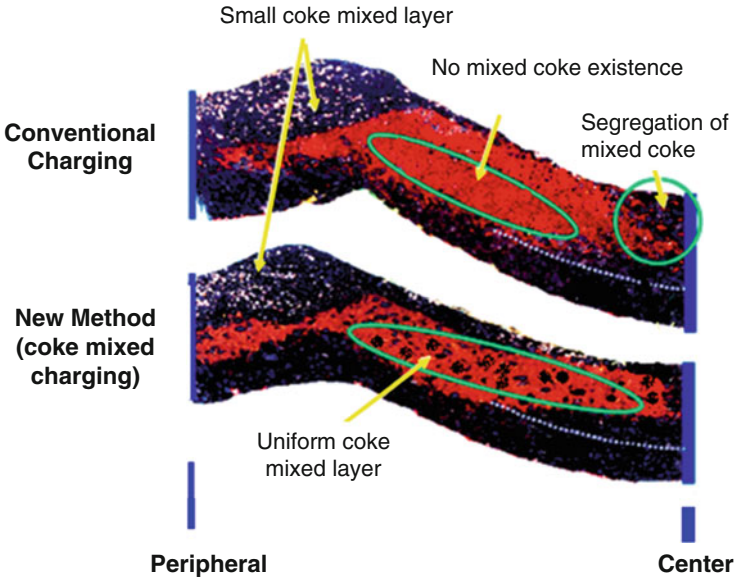

Fig. 6.5 Comparison between conventional charging method and coke-mixed charging method (Watakabe et al. 2006)

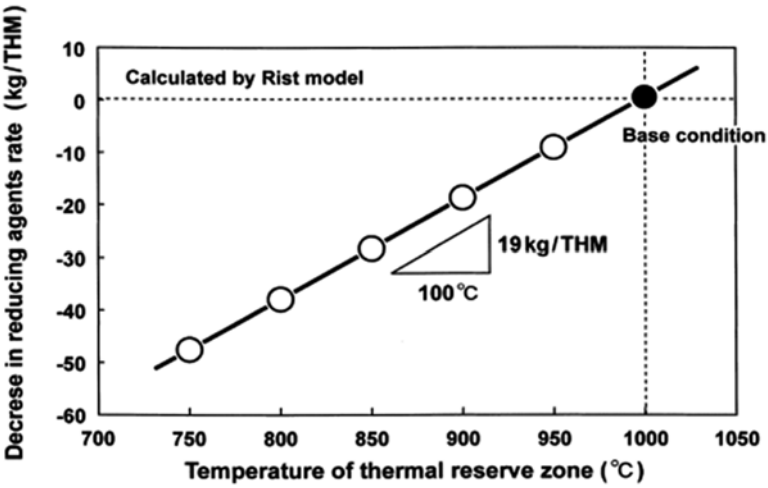

Fig. 6.6 Reducing agents rate and thermal reserve zone temperature (Kasai and Matsui 2004)

This success has inspired researchers to conduct an intensive research to study the effect of nut coke on different process parameters like permeability, reducibility, total coke consumption, etc. (Babich et al. 2009; Mousa et al. 2010a, b, 2011; Babich et al. 2008; Yaroshevskii et al. 2000; Watakabe et al. 2006). One of the important issues that should be taken care of is the uniform mixing of nut coke in the ore layer to maintain proper gas distribution and maintain the required permeability especially in the cohesive zone (Nikitin et al. 1999). Mixing of nut coke within the ore bed was very effective to increase the rate of carbon solution loss (Kasai and Matsui 2004). This further decreases the gasification reaction temperature which consequently decreased the lower limit of the thermal reserve zone temperature, thus decreasing the total coke consumption (Kasai and Matsui 2004). Figure 6.6 shows the relation between the thermal reserve zone temperature and coke rate consumption. Mixing of nut coke in the ore layer is not only expected to improve the solution loss reaction but also expected to protect the lump coke from gasification and consequently abrasion (Sawayama et al. 2009a).

The reactivity of small-sized coke was further increased by means of surface coating with compounds that contains hematite and Ca. It was found that activated nut coke shows even higher rates of gasification compared to original ones. The activation was more pronounced for coke with low coke reactivity index (CRI) values and further reduces the coke rate consumption (Ökvist et al. 1999).

6.4.2 In-Plant Fines

One more promising reducing agent is iron- and steelmaking residues. Large quantities of residues are annually generated during iron and steel production, a significant amount having potential of being valuable resources of carbon. Efforts have been

made during the past decades to return generated by-products as substitutes to raw materials in the steelmaking process. Part of the residues are therefore today recycled, mainly to the sinter strand but also to the blast furnace in the form of a cold-bonded briquette. Injection of dry BF dust into the BF is practiced at SSAB in Sweden. However, there are still substantial amounts of carbon-containing residues deposited. Examples of the latter include sludge from the blast furnace and sludge from the basic oxygen furnace (BOF), for which the recycling is limited due to impurity elements (zinc, lead, alkalis) or physical properties (particle size, wet material).

Most of the residues from the integrated steel industry are today recycled in the process either via the sinter plant or in cold-bonded agglomerates. Residues are also recycled through other applications outside the process, e.g., in road construction and in the cement industry or in external processes as the rotary hearth furnace (RHF) processes. When considering residues rich in carbon produced at the integrated steel plant, the blast furnace is the production unit responsible for the production of these. There are two such residues, namely, the blast furnace dust (BF dust) and the blast furnace sludge (BF sludge). As the dust is dry, it is more convenient to recycle. Typical carbon content for the dust from a production site in Sweden is 43.6 % making the residue eligible for utilization as reduction agent in the blast furnace. When operating the blast furnace on iron ore pellets, all the dry dust may be recycled through injection in the tuyeres and by cold-bonded agglomeration (Grip 2005).

The carbon content of a few different blast furnace sludges is reported to be in the range of 18.5–33.0 % (Itoh and Fieser 1982; Heijwegen and Kat 1984; Steer and Griffiths 2013; Vereš et al. 2012), making this residue eligible for utilization as reducing agent as well. However, problems arise when attempting to recycle both the dust and sludge from the gas cleaning system back to the blast furnace. The main issue is the accumulation of zinc in the furnace which may lead to high zinc loads which in turn disturb the smooth running of the process (Biswas 1981). An additional problem is the cost related to drying of the sludge prior to recycling.

Typically, the dominating output of zinc from the furnace is through the gas phase, in which the extent is determined by, e.g., the top pressure operated at the furnace. Therefore, in order to recycle both residues leaving the gas cleaning equipment of the blast furnace, a proper way of zinc removal has to be introduced. This can be achieved by upgrading the sludge using, e.g., physical separation, hydrometallurgical, or pyrometallurgical routes.

Upgrading of blast furnace sludge using a hydrocyclone has been demonstrated in previous studies (Butterworth et al. 1996; Heijwegen and Kat 1984; Itoh and Fieser 1982). Butterworth et al. (1996) have reported the results of laboratory and pilot plant trials using a one-stage hydrocyclone to remove zinc from the sludge. In average the pilot plant trials suggested that 66 % of the sludge can be recovered and recycled back to the process while removing 89 % of the zinc. Itoh and Fieser (1982) report that the hydrocyclone can be used in full-scale operation to remove zinc from the blast furnace sludge. The presented results suggest that the underflow, low in zinc, is enriched in both carbon and iron. Although some losses of carbon are realized through the zinc removal, a fraction with higher carbon content than the original sludge may be recycled and utilized for its iron content and reducing properties.

Another way to reduce the zinc content of the blast furnace sludge is by leaching. This has been realized in different leaching reagents such as sulfuric acid (Vereš et al. 2012), hydrochloric acid (Van Herck et al. 2000), and carboxylic acids (Steer and Griffiths 2013). The leaching of blast furnace sludge in 0.5 M sulfuric acid showed that almost 88 % of zinc can be recovered with an iron loss of about 9 % (Vereš et al. 2012). A pilot plant leaching experiment was conducted by Van Herck et al. (2000). The leaching was performed with hydrochloric acid under oxidizing conditions. The plant successfully removed an average of over 95 % of the zinc in the different sludges tested in the study.

On the other hand, effective utilization of carbon-rich integrated steelmaking residues based on pyrometallurgical treatments has been also investigated (Robinson 2005; Su et al. 2004). Producing agglomerates with self-reducing properties which is used further to produce DRI (direct reduced iron) has previously been suggested as a promising recycling method for the dust and sludge instead of landfills. Production of DRI by heat treatment also contributes to significant reduction of Zn, which enables introduction of carbon-rich by-products with high Zn contents to the blast furnace.

6.5 Novel Top Charging Materials (Iron Ore-Carbon Composite)

Composite pellets (Dutta and Ghosh 1994), carbon composite agglomerates (CCAs), briquettes (CCB), and self-reducing agglomerates, all refer to carbon-bearing materials mixed with iron-bearing materials into agglomerates. It can be mixtures of fine iron ore (hematite, magnetite, dust and pre-reduced iron-bearing ore fine, etc.) and fine carbonaceous materials (fine coke, fine coal, charcoal, char, etc.) adding some binding agents in most cases (Chu et al. 2004). Possibly, using these agglomerates in blast furnace as well as in other ironmaking processes, one can derive the following benefits simultaneously, i.e., (1) usage of alternate carbonaceous materials having significant hydrogen which can replace expensive coke like plastics and biomass and (2) shifting the BF operation toward lower CO/CO_2 ratio by shifting the thermal reserve zone to lower temperatures as explained earlier.

Therefore, in the context of process optimization, energy saving, waste recycling, and environmental concerns, CCAs have been attracting much attention as future raw materials for ironmaking. For blast furnace operation with CCAs or CCBs, the following advantages are being envisaged (Chu et al. 2004):

- Decrease the energy consumption and environmental loads through the less dependency on sinter and coke.
- The effective use of noncoking coal, and iron-bearing dust and sludge in steel industry, extends the variety of raw materials and promotes resource recycling.
- The short distance between close-packed fine iron ore and carbonaceous materials in the agglomerates ensures fast reduction reaction of iron oxide.

– Furthermore, carbon gasification reaction and iron ore reductions are mutually accelerated and occur at lower temperature due to the coupling effect (Dutta and Ghosh 1994; Kasai and Matsui 2004).

In light of the above, in the following sections, the current status and gaps in understanding of such composites as well as challenges and research needed for realizing them as an effective raw material for ironmaking have been presented.

6.5.1 Producing of Iron Ore-Carbon Composites

Carbon composites are made in the form of pellets (cold bonded with and/or without binder) or briquettes (which can be either hot or cold pressed). Specific studies on the production aspects of these pellets require further improvement, especially as usage in blast furnace calls for higher qualities in terms of strength. Currently, usage of cold-bonded ordinary pellets (not containing carbon) itself pose difficulties in terms of accommodating them in significant proportion for blast furnace process owing to their poor strength.

Possibly, improving the binding system could significantly reduce the accompanying operational difficulties that can arise from low strength composites. Experience on ordinary pellet production over the past decades has led to the identification of a number of criteria that a binder must satisfy (Qiu et al. 2003). They include good mechanical properties, while they are green, dry, and fired pellets, e.g., deformation under load, resistance to fracture by impact and by compression, and resistance to abrasion.

Bentonite is the most commonly used binder in iron ore pelletization and significantly improves physical properties of the pellets. However, there are some drawbacks with the use of bentonite. The most remarkable is the contamination of the product with gangue (silica). For example, addition of 1 % bentonite to an iron ore concentrate results in a lowering of acid pellet iron content by 0.6 % (Souza et al. 1984). In the case of direct reduction pellets, every percent of acid gangue addition is associated with an increased energy consumption of 30 kWh (Heerema et al. 1989).

Cold-bonded pellets (CBPs) containing metallurgical by-products and cement as binder have been investigated (Robinson 2008). The effect of particle size distribution and hydration extent on the cold strength of CBPs was carefully studied. They have concluded that an optimal blend of fine and coarse BOF sludge in CBPs significantly improves the particle size distribution as well as bonding during hydration therefore significantly improves the cold strength. On the other hand, several experiments were conducted with an aim to study the strength development with a focus on swelling (swelling has two consequences: loss of strength and degradation or disintegration during reduction) of briquettes of steel industry by-products during curing and reduction (Singh 2002). The briquette swelling was found to be significant only when the average particle size increases as well as in the presence of cement. However, swelling is significantly hindered when reduction of briquettes is carried out under load. Researchers (Adolfsson et al. 2008) have tried even to utilize steelmaking by-product (Ladle slag) in CBP as a supplement and/or partial substitute for ordinary cement.

Mantovani and Takano (2000) studied the behavior of self-reducing pellets at room temperature and upon heating. They have produced pellets of EAF dust with total iron between 30 and 50 %, coal fines (70.5 % fixed carbon, 15.4 % ash, and 17 % volatile matter), and additives (commercial Portland cement and $CaCO_3$) then left in open air for 28 days for gaining strength to handle. They could get cold strength up to 60 N/pellet for 5 % cements containing pellet, which is still not enough for charging in shaft furnaces. They found that pellets with Portland cement and low moisture content present low decrepitation. At 600 °C the formed hydrated component started to decompose, and consequently it loses its strength. In addition, at 1000–1100 °C the strength is critical due to swelling.

In addition, during reduction of CCA, large voidage is created by the consumption of carbonaceous materials and can lead to low strength values in the pellets during reduction. Therefore, special attention was devoted to understand the strength development in CCAs during reduction. Talano and Mourao (2001) studied the strength development of self-reducing pellets at high temperatures. The pellets face sharp decrease in their compression strength from room temperature to 900–950 °C due to the decomposition of the hydrates, which are the main components of the cold strengthening mechanism of curing when cement is used. As the temperature increases, iron starts sintering and therefore the strength increases (Adolfsson et al. 2008). Higher strength at room temperature correlates generally well with higher strengths at elevated temperatures.

Unlike inorganic binders, organic binders have no side effect on iron ore grade. It also improves the wettability as well as the chemical bonding and results in strong and heat-resistant organic chain skeleton. Qiu et al. (2003) investigated the functions and the molecular structure of organic binders for iron ore pelletization (no available data for CCA in literature) based on the basic principles of molecular design, interface chemistry, polymer science, and failure model of binding system. The authors suggest "Funa" as one of the best organic binders which is prepared from lignite or weathered coal and with humates as major constitutes. Min et al. (2009) proved the possibility of applying an organic synthetic binder referred SHN to iron ore pellets instead of inorganic binders (bentonite). Table 6.2 shows comparison between different binders and the effect of the pellet compression strength.

Another way of improving the agglomerate strength is by producing iron ore coal briquettes by hot pressing. The fluidity phenomenon of coal at temperature 350–600 °C can be utilized in gaining high density and high strength without the addition of any binding materials (Matsui et al. 2003). Utilization of thermal plasticity of coal is being under development as agglomerate without binder. Compared with other carbon-containing agglomerates, this briquette showed better reducing performance, lower cost, and higher strength due to thermal plasticity of coal (Chu et al. 2004). Hayashi (2009) has presented the behavior of coal composite iron ore briquettes at high temperatures. Also, this kind of binderless agglomerates offers less slag ratio and enables a high heat transfer thus higher reaction rate. On studying the reaction behavior and softening and melting of such briquettes (hot-pressed briquettes) under N_2 at 1400 °C, both density and cold crushing strength were increasing by increasing coal content in the briquettes. The thermal plasticity of coal could provide a strength more than required for practical blast furnace.

Table 6.2 Effect of binder types on the quality of iron ore pellets

Binder type	Dosage, %	Wet drop strength	Wet compressive strength	Shock temperature, °C	Dry compressive strength, N/P	Fired compressive strength, N/P
Ca-bentonite	4.00	3.6[a]	9.75	530	705	2813
Na-bentonite	2.00	4.1[a]	12.63	475	569	2768
SHN	0.06	4.0[a]	11.63	>600	488	2534
Funa	1.50	13.7[b]	27.8	780	287	NA[c]

[a]Times per 0.5 m
[b]Times per 1.0 m
[c]Not available

Briquettes with high amount of coal tend to melt at higher temperatures, while those having less amount of coal tend to melt earlier due to the melting of slag containing unreduced iron oxide. Higher coal content briquettes will be preferred in blast furnace to avoid forming low melting slag then maintaining the furnace gas permeability.

Thus, current understanding in making CCAs suitable for blast furnace process is very limited. Systematic and comprehensive studies on making of CCA suitable for blast furnace usage with new binders, carbonaceous, and iron ore sources followed by characterization in terms of strength and other metallurgical properties such as reducibility, swelling, pressure drop during reduction, etc. need to be conducted. While exploring new binders, care needs to be taken to not bring environmentally and metallurgically harmful elements such as P, S, As, etc., into the product. It should also not adversely affect iron grade and increase impurities such as silica.

6.5.2 Reduction Behavior of Composite Pellets

Understanding the reactions occur within a composite pellet is very essential for its usage in blast furnace as well as in other ironmaking processes. Both experimental and theoretical investigations have been carried out along this direction. A possible behavior of CCB in a blast furnace is described by Chu et al. (2004) assuming that the CCB consists of hematite, carbon, and gangue (SiO_2, CaO, MgO, and Al_2O_3), and it fits the BF requirements mechanically and chemically. After charging CCB into blast furnace, it gets heated up through heat exchange with the ascending gases. When CCB temperature reaches to a particular level, reduction of hematite and magnetite starts to happen by ascending reducing gas from the thermal reserve zone. Reduction of wustite to metallic iron starts at the thermal reserve zone. As the CCB descends further and enters high-temperature zone, softening and melting of reduced iron, iron oxide (if still exists), and gangue in CCB occur. They have theoretically evaluated the effect of charging carbon composite agglomerates on blast furnace operation based on multifluid blast furnace model (Austin et al. 1997, 1998; Castro et al. 2000) under constant inflow conditions of blast and pulverized coal and hot

metal temperature. On charging CCB, the predicted blast furnace productivity was improved, coke rate showed notable decrease, and total reducing agent rate tended to lower. For charging 30 % CCB, the productivity is increased by about 6.7 %; coke rate and reducing agent rate are reduced by 26.8 and 3.4 %, respectively, compared with base case without CCB charging. Kasai and Matsui (2004) have proposed a decrease in the thermal reserve zone temperature to 727 °C by charging of 20 % mass CCB which leads to a decrease in the reducing agent rate by 51 kg/tHM.

Several fundamental studies have been carried out on the reduction kinetics and mechanism of CCAs (Dutta and Ghosh 1994; Srinivasan and Lahiri 1977; Rao 1971; Sharma 1997; Fruehan 1977; Huang and Lu 1993). The main difference between iron ore agglomerates and CCAs is the rate-controlling step of the reduction of iron oxides. In case of iron ore agglomerates, the reduction takes place at gas-solid interfaces. Reducing gases move from the gas stream to the agglomerate surface then to the interior surface of the pores. In CCAs, carbon is present inside and so the chemical reaction can proceed very fast because of the large surface area available. Furthermore, mass transfer to and from reaction sites by gaseous diffusion could be also very fast because of the short traveling distance (Sun and Lu 1999a, b).

Reaction Sequence Reduction of hematite goes via three stages of reduction, hematite to magnetite then to wustite and finally to metallic iron. The reduction to wustite is relatively faster than to iron because the equilibrium CO_2-CO gas mixture consists almost of CO_2, while in the later the ratio becomes 0.4 (Fruehan 1977). The overall reaction and mechanism are represented by Eqs. (6.1), (6.2), and (6.3) and Fig. 6.7. Solid-solid reaction (reduction of iron oxide by solid carbon in the solid state) can be visualized as the early beginning as a result of the contact points between iron oxide and carbon particles which can be there only when gaseous products (CO and CO_2) are removed from the reaction system as fast as they are generated (Rao 1971). At thermodynamically reasonable temperatures, generation of carbon monoxide by carbon gasification (Eq. 6.3) and reduction of iron oxide by carbon monoxide (Eq. 6.1) start.

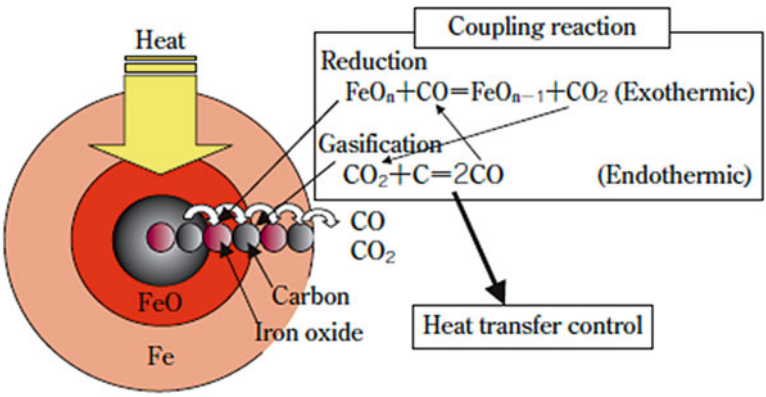

Fig. 6.7 Reduction mechanism of CCA (Michishita and Tanaka 2010)

$$\mathrm{Fe}_x\mathrm{O}_y(\mathrm{s}) + \mathrm{CO}(\mathrm{g}) = \mathrm{Fe}_x\mathrm{O}_{y-1}(\mathrm{s}) + \mathrm{CO}_2(\mathrm{g}) \tag{6.1}$$

$$\mathrm{Coal} = \mathrm{C} + \text{volatile matter} \tag{6.2}$$

$$\mathrm{C} + \mathrm{CO}_2(\mathrm{H}_2\mathrm{O}) = \mathrm{CO} + \mathrm{CO}(\mathrm{H}_2) \tag{6.3}$$

Factors Affecting the Reaction Rate and the Rate-Controlling Step The complexity of studying the reaction mechanism and kinetics of self-reducing pellets or CCAs arises from the simultaneous reactions such as direct reduction of iron oxide, indirect reduction by CO, carbon gasification, etc. The reaction mechanism would vary significantly with the change of degree of oxidation and type of iron ore, carbon type, density, diameter, particle size, size distribution, state and area of contact, and state of crystal. These conditions will affect the chemical reaction, heat transfer, and gas diffusion (Khaki et al. 2002). Also, coal fluidity seems to affect the composite reactivity; the higher the coal fluidity, the higher the composite reactivity. Increasing the fluidity improves the contact state between the iron ore and coal (Nishioka et al. 2009).

Srinivasan and Lahiri (1977) studied the reduction of a single hematite/carbon-containing pellet isothermally. Moisture and small amount of bentonite (1.5 %) were added as binder. They found that the CO_2/CO ratio tend to approach wustite equilibrium for low C/Fe_2O_3 ratio and Boudouard equilibrium for high values of this ratio. A decrease in C/Fe_2O_3 ratio leads to higher values of CO_2/CO ratio and lower rate of carbon gasification decreasing the partial pressure of CO inside the sample. The results indicated a changeover in the reaction mechanism; Boudouard reaction seems to be initially rate limiting and the final stages being probably controlled by the reduction of wustite by CO. Fruehan (1977) and Rao (1971) have observed that the gasification reaction is dominating at low temperatures, while it turns to be controlled by wustite reduction at higher temperatures. In their studies, higher reaction rates were observed on using catalysts such as lithium and slower rates in the presence of inhibitors such as sulfur reinforcing the argument of control by carbon gasification.

In fact, some investigators believed that the reaction of carbon composites is controlled by the gasification reaction at the initial stages, marked by large activation energy, while the heat transfer is dominating at the later stages of the reduction marked by significant reduction in apparent activation energy (Ueda et al. 2009a; Michishita and Tanaka 2010). In contradictory, some others (Sun and Lu 1999a, b) have reported that the rate-controlling step is the heat transfer from surrounding to the outer surface then to the interior partially reacted system. They have referred their thinking to that there is no heat generation within the agglomerates; the rate of the overall reaction is determined by the endothermic reaction (Eq. 6.3) which cools down the whole system. However, the approach of testing the possible rate-determining step by comparing the apparent activation energy values reported in the literature for the gasification, reduction reaction, or heat transfer may not be relevant under non-isothermal conditions (Seaton et al. 1983).

6.6 Alternative Reducing Agents

One of the most important benefits that could be realized upon charging carbon composites into BF is the possibility and flexibility of top charging hydrogen-rich and bio-carbon carbonaceous materials. The fact that cost reduction as well as GHG emission is greatly affected by coke led to increase effort to reduce the coke consumption rate in the BF. Production of 1 tonne of hot metal generates 1.5 tonne of CO_2 (Ng et al. 2012). The total worldwide CO_2 emission associated with blast furnace ironmaking in 2014–2015 is about 1733 million tonnes which mainly comes from the use of fossil fuel (www.worldsteel.org).

6.6.1 Plastic Materials

One alternative reducing agent is plastic-containing materials. The demand for plastics has grown significantly over the past decades and will continue. As carbon is a major constituent of waste plastics, clearly they have the potential to be a cheap and readily available auxiliary source of carbon. It has been reported that plastics have higher combustion and gasification efficiencies compared with pulverized coal (Hata et al. 2009). As plastics generally have high hydrogen content, these could also help reduce overall CO_2 gas emissions. Injection of waste plastic, excluding polyvinyl chloride (PVC), has been proposed to be a substitute reducing agent (Matsui et al. 2009), and injection of pure waste plastic and its behavior in a BF has been practiced (Grip 2005). Combustion and gasification behavior of waste plastic in a commercial BF is much different from that of pulverized coal. Plastic particles will be gasified completely in the raceway, which is claimed to improve process efficiency and sustain the gas permeability along the BF cohesive zone.

Plastics Xhave been used as reductants in blast furnaces to some extent, although the amount of plastic waste used for this purpose is quite low in comparison to the worldwide generation of plastic waste. For use in blast furnaces and in steelmaking in general, it is required to have pure plastic materials, free from other metal content than iron. Elaborated upgrading processes exist today, where such pure plastic material fractions can be generated. However, the price for these pure plastic fractions is comparably high in comparison to fossil carbon sources.

Upon heating plastics in absences of oxygen, it undergoes what is known as pyrolysis wherein the materials decompose into gases, oils, and chars. In pyrolysis of plastic polymers, macromolecular structures of polymeric materials are broken down into smaller molecules, and a wide range of hydrocarbons are formed. The quality of pyrolysis product and product distribution depends on temperature, residence time, and some other factors. Temperature is the most important operating variable. High temperature (>600 °C) favors the production of simple small gaseous molecules which is likely to be the case in the lower part of the BF shaft; low temperature (<400 °C), which is likely to be the case in the upper part of the furnace,

leads to more viscous liquid products. The residual solid after pyrolysis is known as char in which solid carbon is the major constituent. Quite often the residual solid carbon has higher reactivity compared to carbon from coke which makes it easy to gasify at relatively lower temperature.

6.6.2 Biomass

Biomass originating from forest residues, waste wood, etc. is today to large extent used or intended for use in a number of different applications in addition for use in production of pulp and paper. Some examples include district heating and production of biofuel. A tough competition for the raw material can therefore be foreseen which might result in a price which is not competitive with coal. The price for charcoal is today in Sweden not on a level which is competitive. Therefore, a lot of development is on the way to produce a partly carbonized or torrefied material. Again, as for the use of plastics as reductant, the possible interference of the volatiles with the process and to what extent the volatiles can be utilized for reduction will be crucial for the possibility to use a torrefied material.

The use of charcoal as a reductant in smaller blast furnaces is widely practiced in, e.g., Brazil (Assis et al. 2015). Utilization of biomass in metallurgical processes has been studied by many researchers, e.g., revealing high reactivity and high combustion degree for biomass (Janiana et al. 2009; Matsumura et al. 2008). Carbonization of biomass to attain selective removal of oxygen and improve the crushability, combustibility, and reactivity is required. The carbonized biomass char (400–1000 °C) would have the following features: (1) remaining duct structure of the wood, (2) larger specific surface area, and (3) noncrystalline structure. The above features make it highly reactive. The gasification of biomass char is reported to be faster than that of coke in couple of dozen times (Ueda et al. 2009b). The use of biomass as reducing agent for low-grade ores has been evaluated by Hata et al. (2009) and Matsui et al. (2009), and its high efficiency has been proved. The low crushing strength of biomass-derived reductant does not allow a complete substitution of coke on large BFs. Possibly a smaller part of the coke added from the top can be exchanged with biomass. A more promising route to introduce biomass in a BF is as replacement for coal injected through the tuyeres. An additional limitation refers to the high alkali content.

The use of biomass as a reductant in ironmaking has been investigated in the last few decades. Vladimir investigated the iron ore reduction with biomass “saw dust” (Strezov 2006). Urvashi et al. (Srivastava et al. 2013) and Yasuaki et al. (Ueki et al. 2013) studied the behavior of self-reducing iron oxide wood biomass composite pellets in an electrically heated furnace. Results showed that high-quality pig iron nuggets not only can be produced at various temperatures; they can also be produced at very short residence times.

6.7 Summary

The present article has thoroughly discussed the recent modifications and development which have been recently conducted in the blast furnace top charging materials to reduce energy consumption and CO_2 emissions. The conventional top-charged burden into the blast furnace including sinter, pellets, and metallurgical coke has reached a high level of quality that makes further improvement extremely hard. Although the blast furnace is nowadays working very close to the ideal conditions, there is still a demand to enlarge its adaptability to reuse the in-plant residues and maximize the overall efficiency. Successful trails have been done and implemented in the full-scale blast furnace on charging active/nut coke in the iron ore burden layers. The gas permeability, gas utilization, and iron ore reduction rate were improved which are accompanied by lower coke consumption and higher productivity of hot metal. The recycling of in-plant by-products and residues, which are rich with carbon and iron, into the blast furnace by its agglomeration in the form of sinter or cold-bonded agglomerates was succeeded in the mitigation of waste landfill and saving the virgin ores. Intensive work are being done on the partial replacement of conventional agglomerates with novel top charging materials including self-reducing pellets, carbon composite agglomerates, and carbon composite briquettes. The concept behind the novel composites is not only the efficient usage of the waste fines from carbonaceous materials and iron ores but also to reduce the coke consumption by using alternative sources of carbon. The recent investigations demonstrated that such novel composites are able to shift the wustite-iron equilibrium to a higher CO gas utilization at relatively lower temperature compared to that of conventional agglomerates. On the other hand, the mechanical strength of the novel composites is low for top charging into the blast furnace and required further investigations. The top charging of alternative reducing agents including waste plastics and biomass represent one of the promising ways to reduce the fossil fuel utilization in the blast furnace; however, the comparative prices and the required pretreatment of these materials represent the main challenges for its implementation.

Acknowledgment The partial financial support from the Centre of Advanced Mining and Metallurgy (CAMM) at Luleå University of Technology and the Postdoc grant at Swerea MEFOS funded by Swedish Research Council Formas are greatly acknowledged.

References

Adolfsson D, Robinson R, Blagojevic J et al (2008) Assessment of ladle slag as binder alternative for cold bonded briquettes. In: Global symposium on recycling, waste treatment and clean technology, Cancun, Mexico, October 12–15, 2008 Minerals, Metals & Materials Society, pp 117–123

Ahmed HM, Viswanathan N, Bjorkman B (2014) Composite pellets–a potential raw material for iron-making. Steel Res Int 85(3):293–306

Ariyama T, Murai R, Ishii J et al (2005) Reduction of CO_2 emissions from integrated steel works and its subjects for a future study. ISIJ Int 45(10):1371–1378

Assis SP, Calixto OK, Vasques FI et al (2015) Economical feasibility of the use of biogas in iron- and steelmaking. In: AISTech (ed) The iron and steel technology conference and exposition, AISTech and ICSTI, 4–7 May 2015, pp 652–655

Austin PR, Nogami H, Yagi J (1997) A mathematical model for blast furnace reaction analysis based on the four fluid model. ISIJ Int 37(8):748–755

Austin PR, Nogami H, Yagi J (1998) Analysis of actual blast furnace operations and evaluation of static liquid holdup effects by the four fluid model. ISIJ Int 38(3):246–255

Babich A, Senk D, Yaroshevskiy S et al (2008) Effect of nut coke on blast furnace shaft permeability. In: Proc. 3rd international conference on process development in iron and steelmaking (SCANMET III), 8–11 June 2008, Lulea, Sweden, vol 2, pp 227–236

Babich A, Senk D, Gudenau HW (2009) Effect of coke reactivity and nut coke on blast furnace operation. Ironmaking Steelmaking 36(3):222–229. doi:10.1179/174328108x378242

Biswas AK (1981) Principles of blast furnace ironmaking: theory and practice. Cootha Publishing House, Australia, 528 pp

Butterworth P, Linsley K, Aumonier J (1996) Hydrocyclone treatment of blast furnace slurry within British Steel. Revue de Metallurgie Cahiers d'Informations Techniques (France) 93(6):807–815

Castro JAd, Nogami H, Yagi J (2000) Transient mathematical model of blast furnace based on multi-fluid concept, with application to high PCI operation. ISIJ Int 40(7):637–646

Chu M, Nogami H, Yagi J (2004) Numerical analysis on charging carbon composite agglomerates into blast furnace. ISIJ Int 44(3):510–517

Dutta SK, Ghosh A (1994) Study of nonisothermal reduction of iron ore-coal/char composite pellet. MMTB 25(1):15–26. doi:10.1007/bf02663174

Fruehan RJ (1977) The rate of reduction of iron oxides by carbon. MTB 8(1):279–286. doi:10.1007/bf02657657

Greedes M, Toxopeus H, van der Vliet C (2009) Modern blast furnace ironmaking-an introduction. IOS Press BV, The Netherlands

Grip C (2005) Steel and sustainability: Scandinavian perspective. Ironmaking Steelmaking 32(3):235–241

Hata Y, Purwanto H, Hosokai S et al (2009) Biotar ironmaking using wooden biomass and nanoporous iron ore. Energy Fuel 23(2):1128–1131. doi:10.1021/ef800967h

Hayashi S (2009) Reaction behavior of coal composite iron ore hot briquettes in a laboratory scale blast furnace simulator. In: The 5th international congress on the science and technology of ironmaking, Baosteel Research Institute, Shanghai, China, pp 423–427

Heerema RH, Kortmann H, Kater T et al (1989) Improvements of acid, olivine and dolomite fluxed iron ore pellets using an organic binder. In: The 5th international symposium on agglomeration, Brighton, p 227

Heijwegen C, Kat W (1984) Beneficiation of blast furnace sludge. World Steel Metalwork Exp Man, pp 35–39

Huang BH, Lu WK (1993) Kinetics and mechanisms of reactions in iron ore/coal composites. ISIJ Int 33(10):1055–1061

Iguchi Y, Takada Y (2004) Rate of direct reactions measured in vacuum of iron ore-carbon composite pellets heated at high temperatures: influence of carbonaceous materials, oxidation degree of iron oxides and temperature. ISIJ Int 44(4):673–681

Itoh Y, Fieser A (1982) Zinc removal from blast furnace dust. Iron Steel Eng 59(8):33–36

Janiana M, Eduardo O, Antonio V et al (2009) Study of the behavior of biomass, coal and mixtures at their injection into blast furnace. In: The 5th international congress on the science and technology of ironmaking, Baosteel Research Institute, Shanghai, China, pp 804–808

Kasai A, Matsui Y (2004) Lowering of thermal reserve zone temperature in blast furnace by adjoining carbonaceous material and iron ore. ISIJ Int 44(12):2073–2078

Kashiwaya Y, Kanbe M, Ishii K (2001) Reaction behavior of facing pair between hematite and graphite: a coupling phenomenon of reduction and gasification. ISIJ Int 41(8):818–826. doi:10.2355/isijinternational.41.818

Khaki JV, Kashiwaya Y, Ishii K et al (2002) Intensive improvement of reduction rate of hematite–graphite mixture by mechanical milling. ISIJ Int 42(1):13–22

Lacroix P, Dauwels G, Dufresne P et al (2001) High blast furnaces productivity operations with low coke rates in the European Union. Revue de Métallurgie 98(03):259–268
Loginov V, Berin A, Solomatin S (1977) Effect of mixing burden with coke on blast furnace fluid mechanics and operation parameters. Stal 5:391
Loginov V, Solomatin S, Korzh A (1976) Experimental melts with blast furnaces charged with mixture of coke and sinter. Metallurgist 20(4):245–250
Luengen HB, Peters M, Schmoele P (2012) Ironmaking in Western Europe. Iron Steel Technol 9(3):63–69
Mantovani MC, Takano C (2000) The strength and the high temperature behaviors of self-reducing pellets containing EAF dust. ISIJ Int 40(3):224–230
Matsui K, Hata Y, Hosokai S et al (2009) Biotar ironmaking using wooden biomass and nano-porous iron ore. In: The 5th international congress on the science and technology of ironmaking, Baosteel Research Institute, Shanghai, China, pp 1292–1296
Matsui Y, Sawayama M, Kasai A et al (2003) Reduction behavior of carbon composite iron ore hot Briquette in shaft furnace and scope on blast furnace performance reinforcement. ISIJ Int 43(12):1904–1912
Matsumura T, Ichida M, Nagasaka T et al (2008) Carbonization behaviour of woody biomass and resulting metallurgical coke properties. ISIJ Int 48(5):572–577. doi:10.2355/isijinternational.48.572
Michishita H, Tanaka H (2010) Prospects for coal-based direct reduction process. Kobelco Technol Rev 69(29):76
Min G, Xiao-hui F, Zhen-hui Z et al (2009) Fundamental research on applying organic binder SHN to oxidized pellets. In: The 5th international congress on the science and technology of ironmaking, Baosteel Research Institute, Shanghai, China, pp 327–331
Mousa E, Senk D, Babich A (2010) Reduction of Pellets-Nut coke mixture under simulating blast furnace conditions. Steel Res Int 81(9):706–715
Mousa E, Senk D, Babich A et al (2010) Influence of nut coke on iron ore sinter reducibility under simulated blast furnace conditions. Ironmaking Steelmaking 37(3):219–228
Mousa E (2010) Reduction of iron ore burden materials mixed with nut coke under simulated blast furnace conditions. PhD thesis, RWTH Aachen University, Shaker verlag, Aachen
Mousa EA, Babich A, Senk D (2011) Effect of nut coke-sinter mixture on the blast furnace performance. ISIJ Int 51(3):350–358
Naito M, Okamoto A, Yamaguchi K et al (2006) Improvement of blast furnace reaction efficiency by temperature control of thermal reserve zone (UDC 669.162.263)
Ng KW, Giroux L, MacPhee T et al (2012) Combustibility of charcoal for direct injection in blast furnace ironmaking. Iron Steel Technol 9(3):70–76
Nikitin L, Mar'yasov M, Gorbachev V et al (1999) Blast-furnace operation with coke fines. Metallurgist 43(1):30–33
Nishioka K, Osuga K, Ueki Y et al (2009) Effect of iron and coal properties on reduction and gasification behavior of carbon composite iron ore briquette. In: The 5th international congress on the science and technology of ironmaking, Baosteel Research Institute, Shanghai, China, pp 1326–1330
Nomura S, Ayukawa H, Kitaguchi H et al (2005) Improvement in blast furnace reaction efficiency through the use of highly reactive calcium rich coke. ISIJ Int 45(3):316–324
Nomura S, Kitaguchi H, Yamaguchi K et al (2007) The characteristics of catalyst-coated highly reactive coke. ISIJ Int 47(2):245–253
Ökvist LS, Brandell C, Lundgren M (1999) Impact of activated nut coke on energy efficiency in the blast furnace. In: AISTech (ed) The iron and steel technology conference and exposition. AISTech, Indianapolis
Pandey B, Yadav U (1999) Blast furnace performance as influenced by burden distribution. Ironmaking Steelmaking 26(3):187–192
Peacey JG, Davenport WG (1979) The iron blast furnace: theory and practice. Pergamon, New York

Podkorytov A, Kuznetsov A, Dymchenko E et al (2009) Theoretical and experimental foundations for preparing coke for blast-furnace smelting. Metallurgist 53(5–6):322–328
Qiu G, Jiang T, Li H et al (2003) Functions and molecular structure of organic binders for iron ore pelletization. Colloids Surf A Physicochem Eng Asp 224(1–3):11–22. doi:10.1016/S0927-7757(03)00264-4
Ranade M, Chaubal P (2004) An intensive course—blast furnace ironmaking. McMaster University, Hamilton, pp 9–1
Rao YK (1971) The kinetics of reduction of hematite by carbon. MT 2(5):1439–1447. doi:10.1007/bf02913373
Rao YK, Han HG (1984) Catalysis by alkali carbonates of carbothermic reduction of magnetite concentrates. Ironmaking Steelmaking 11(6):308–318
Reddy GV, Sharma T, Chakravorty S (1991) Kinetic rate equation for direct reduction of iron ore by non-coking coal. Ironmaking Steelmaking 18(3):211–215
Rist A, Bonnivard G (1963) Reduction of an iron oxide bed with a gas. Rev Metal 60:23–38
Robinson R (2005) High temperature properties of by-product cold bonded pellets containing blast furnace flue dust. Thermochim Acta 432(1):112–123. doi:10.1016/j.tca.2005.04.015
Robinson R (2008) Studies in low temperature self-reduction of by-products from integrated iron and steelmaking. PhD thesis, Luleå University of Technology, Luleå, 69 pp
Sawayama M, Miyagawa K, Nozawa K, Matsui Y, Shibata K (2009a) Low coke rate operation of blast furnace by controlling size of coke mixed into ore layer. In Proceedings of the 5th international congress on the science and technology of ironmaking, ICSTI 09, 20–22 October 2009, pp 663–667, Shanghai
Sawayama M, Miyagawa K, Nozawa K et al (2009b) Low coke rate operation of blast furnace by controlling size of coke mixed into ore layer. In: The 5th international congress on the science and technology of ironmaking, Baosteel Research Institute, Shanghai, China, pp 659–663
Schmöle P, Lüngen H-B (2005) Ecological hot metal production using the coke plant and blast furnace route. Rev Metal 102(03):171–182. doi:10.1051/metal:2005140
Seaton CE, Foster JS, Velasco J (1983) Reduction kinetics of hematite and magnetite pellets containing coal char. Trans Iron Steel Inst Jpn 23(6):490–496
Sharma T (1997) Reduction of double layered iron ore pellets. Int J Mineral Process 49(3–4):201–206. doi:10.1016/S0301-7516(96)00020-8
Singh M (2002) Studies on the cement-bonded briquettes of iron and steel plant by-products as burden material for blast furnace. PhD thesis, Luleå University of Technology, Lulrå. ISSN 1402–1544
Souza RPd, Mendonca CFd, Kater T (1984) Production of acid iron ore pellet for direct reduction, using an organic binder. Mining Eng 36:1437
Srinivasan NS, Lahiri AK (1977) Studies on the reduction of hematite by carbon. MTB 8(1):175–178. doi:10.1007/bf02656367
Srivastava U, Kawatra SK, Eisele TC (2013) Production of pig iron by utilizing biomass as a reducing agent. Int J Miner Process 119:51–57
Steer JM, Griffiths AJ (2013) Investigation of carboxylic acids and non-aqueous solvents for the selective leaching of zinc from blast furnace dust slurry. Hydrometallurgy 140:34–41
Strezov V (2006) Iron ore reduction using sawdust: experimental analysis and kinetic modelling. Renew Energy 31(12):1892–1905
Su F, Lampinen H, Robinson R (2004) Recycling of sludge and dust to the BOF converter by cold bonded pelletizing. ISIJ Int 44(4):770–776
Sun S, Lu WK (1999a) Building of a mathematical model for the reduction of iron ore in ore/coal composites. ISIJ Int 39(2):130–138
Sun S, Lu WK (1999b) A theoretical investigation of kinetics and mechanisms of iron ore reduction in an ore/coal composite. ISIJ Int 39(2):123–129
Takano C, Mourao MB (2001) Comparison of high temperature behavior of self-reducing pellets produced from iron ore with that of dust from sintering plant. ISIJ Int 41(Suppl):S22–S26
Ueda S, Yanagiya K, Watanabe K et al (2009a) Reaction model and reduction behavior of carbon iron ore composite in blast furnace. ISIJ Int 49(6):827–836

Ueda S, Watanabe K, Yanagiya K et al (2009b) Improvement of reactivity of carbon iron ore composite with biomass char for blast furnace. ISIJ Int 49(10):1505–1512

Ueki Y, Yoshiie R, Naruse I et al (2013) Reaction behavior during heating biomass materials and iron oxide composites. Fuel 104(0):58–61. doi:10.1016/j.fuel.2010.09.019

Van Herck P, Vandecasteele C, Swennen R et al (2000) Zinc and lead removal from blast furnace sludge with a hydrometallurgical process. Environ Sci Technol 34(17):3802–3808

Vereš J, Lovás M, Jakabský Š et al (2012) Characterization of blast furnace sludge and removal of zinc by microwave assisted extraction. Hydrometallurgy 129:67–73

Watakabe S, Takeda K, Nishimura H et al (2006) Development of high ratio coke mixed charging technique to the blast furnace. ISIJ Int 46(4):513–522

Yaroshevskii S, Nozdrachev V, Chebotarev A et al (2000) Efficiency of using coke fractions smaller than 40 mm in a blast furnace. Metallurgist 44(11):598–605

Chapter 7
Dangerous Emissions in Blast Furnace Operations

Lei Gan and Huining Zhang

Abstract Blast furnace smelting is the dominant ironmaking method around the world. Blast furnace operations cover not only blast furnace smelting but also a set of auxiliary processes and equipments, including molten slag granulation, hot stoves and off-gas treatment systems. Dangerous emissions of SO_2 and H_2S are found in molten slag granulation sites; NOx are found from the hot stoves; heavy metals (mainly Zn and Pb) are found in the sludge and dust from off-gas treatment systems; fluorides are found in the off-gas. These emissions are generally in low concentrations. However, since the production of blast furnace is huge, the mass are still appreciable. The heavy metal emissions are mostly safely treated or recycled. However, few processes have been installed to treat emissions of H_2S, SO_2, NOx and fluorides.

7.1 Introduction

Blast furnace is the dominant metallurgical furnace for ironmaking around the world. The blast furnace iron production was 1.18 billion tons in 2014, accounting for 99 % of global production (World Steel Association 2015). In a modern blast furnace, the fuels (coke, charcoal), iron ores (sinter, pellet, lump ores) and fluxes (CaO, MgO, CaF_2) are continuously supplied through the top of the furnace, while hot blast with oxygen enrichment and pulverized coal is injected through tuyeres from the bottom of the furnace.

The product molten pig iron, or hot metal, is tapped from the bottom of the furnace, along with by-product molten slag. The hot metal is delivered to the next sector for further processing. The molten slag is either granulated by water or slow cooled in the air depending on the purpose of utilization. The by-product off-gas, or

L. Gan (✉) • H. Zhang
School of Metallurgical and Chemical Engineering, Jiangxi University of Science and Technology, Ganzhou, China
e-mail: ganlei2005@gmail.com; zhanghuining2008@126.com

P. Cavaliere (ed.), *Ironmaking and Steelmaking Processes*,
DOI 10.1007/978-3-319-39529-6_7

blast furnace gas (BFG), exits from the top of the furnace. After dedusting, it is distributed around the works and used as low-grade fuel for heating in hot stoves or for electricity generation in power plants.

The blast furnace system has also a set of auxiliary installations, including molten slag granulation, hot stoves and BFG treatment systems. Most of the molten slag is granulated in a water-quenching process. By slag granulation, the cooling and solidification speed is much faster than during dumpling and cooling in slag pit. The product usually is a fine slag sand with glassy structures, which is ideal for use in the cement industry (Shi et al. 2006). Gaseous sulphur emissions of H_2S and SO_2 are found during slag granulation process (Rehmus et al. 1973).

Each blast furnace has three or four associated hot stoves. The main function of the hot stoves is to provide the oxygen necessary for coke gasification and thus produce the gas that reduces iron oxides. The hot stoves preheat the air supplied to the blast furnace up to 1200 °C. The combustion temperature can reach higher than 1450 °C. NOx will form in such high temperatures (Chen et al. 2014).

The uncleaned BFG has a dust content of 20–40 g/m^3. It has to be reduced to lower than 10 mg/m^3 to meet the demand of fuel. The dedusting is finished in a wet or dry system. The collected sludge or dust can be recycled in the sintering sector due to its high Fe content. However, volatile heavy metals like zinc (Zn) or lead (Pb) also present in the sludge and dust. The dust and sludge with a high Zn or Pb content are usually not accepted as returns to the sinter plant or are only used in limited amounts (Remus et al. 2013). In addition, fluoride (HF and CaF_2) can be found in the BFG if high fluorine charges are used.

In this chapter, the sources, emissions and abatement methods for gaseous sulphurs, NOx, heavy metals and fluorides in blast furnace operations are briefly overviewed.

7.2 H_2S and SO_2 Emissions

7.2.1 Source

The sulphur burden of the blast furnace in China is 4–8 kg/t hot metal. Most of the sulphur comes from coke and injected pulverized coal, accounting for about 85 % of the total input sulphur (Cai et al. 2008; Hu et al. 2008). Roughly 10 % of the input sulphur solutes into the hot metal. Most of the soluble sulphur will be removed in the following processes to improve qualities of steel. Roughly 5 % of the input sulphur enters into the BFG. The BFG will be combusted in the hot stove or power plant, with emission of SO_2 into the atmosphere (Cai et al. 2008).

Majority of the burden sulphur is absorbed by molten slags. However, the sulphur in the slag is not necessarily stable; it may be released into the atmosphere in the form of gaseous sulphur during processing of molten slag. The molten slag can be either water-quenched to granulated blast furnace slag (GBFS) or slowly cooled to lump slag. The sulphur in the molten slag is mostly in the form of S^{2-} or sulphide. The

Fig. 7.1 Steam generation in a water granulation process of molten slag

sulphide is generally stable in neutral conditions, but may be oxidized to sulphate in the air. Therefore, it is found that the sulphur in GBFS existed mostly as sulphides with a minor amount as sulphate. In contrast, a slowly cooled blast furnace slag had most of the sulphide transformed to sulphate (Roy 2009).

In the ironmaking plants, most of the molten blast furnace slag is granulated by water, with the generation of large amount of steam, as shown in Fig. 7.1. The product GBFS is a valuable material for cement production. However, due to reactions between sulphur and water or steam, the quenching process gives rise to the generation of H_2S and SO_2, which are a cause of corrosion, worker exposure problems and odour complaints (Schmidt et al. 2003).

7.2.2 Emission

The blast furnace slag has a sulphur content of about 1–2 %, depending on raw material conditions. When the molten slag gets in contact with water or steam, gaseous sulphur compounds (H_2S and SO_2) will be generated according to the following possible reactions:

$$\mathrm{CaS} + \mathrm{H_2O} \rightarrow \mathrm{H_2S} + \mathrm{CaO} \tag{7.1}$$

$$\mathrm{CaS} + 3/2\mathrm{O_2} \rightarrow \mathrm{SO_2} + \mathrm{CaO} \tag{7.2}$$

These reactions mainly occur at temperatures above 1100 °C. Below 1000 °C only a small amount of gaseous sulphur compounds are generated (Schmidt et al. 2003).

Several measurements on the concentrations of H_2S and SO_2 emissions had been performed in laboratory or industrial works (Jablin 1972; Rehmus et al. 1973; Annamraju et al. 1984; Mishin et al. 1987; Schmidt et al. 2003; Remus et al. 2013). However, these measurements vary significantly depending on processing methods, slag flow rate and sample locations. Nevertheless, it is found that the sulphur loss in slag during granulation is from 15 to 20 % regardless of the physical-chemical variations of slags (Schmidt et al. 2003). The emission factors of H_2S and SO_2 are 14–300 and 13–142 g/t hot metal, respectively, in the EU (Remus et al. 2013).

Sulphur emissions are also found in the combustion of sulphur containing by-product gases, including BFG and coke oven gas (COG). The H_2S concentration is about 14 mg/Nm^3 for treated BFG and 50–500 mg/Nm^3 for desulphurized COG (Remus et al. 2013). In hot stove operations, the mixed BFG and COG are widely used as fuel. The sulphur compounds in the gases are emitted as SO_2 after firing. Emission concentrations for SO_2 are in the range of 4–154 mg/Nm^3 depending on the used gas, which corresponds to 1.6–154 g/t hot metal. In case of a mixture of BFG and non-desulphurized COG, the emission factor can be up to 400 g SO_2/t hot metal, which corresponds to up to the concentration of 267–1000 mg/Nm^3 (Remus et al. 2013).

7.2.3 Abatement

Because of the facts that sulphur emissions are always generated in the molten slag processing sites and H_2S can be detected by human nose in extremely low quantities, methods have been long investigated to abate the emissions. Generally, the emissions of H_2S and SO_2 have been found depending on the following issues:

1. Slag temperature
   The generations of H_2S and SO_2 can be greatly hindered at a low processing temperature based on a kinetic point of view. In a slag pit cooling investigation, it is shown that the reduction of H_2S emission is highly effective by lowering the slag temperature (Rehmus et al. 1973). For granulation processes, however, it is not easy to control the slag temperature, because lowering the temperature will result a rapid increase in viscosity (Gan and Lai 2014).
2. Physical-chemical properties of slag
   The physical-chemical properties of slag, like compositions and viscosity, surely have effects on H_2S and SO_2 emissions. Nevertheless, it is revealed that within the industrially acceptable range of physical-chemical variables, their effects on sulphur emissions are substantially constant (Schmidt et al. 2003). It is indicated that the H_2S and SO_2 emissions can hardly be influenced by variations of slag properties.
3. Temperature of granulation water
   The solubilities of H_2S and SO_2 decrease with rising water temperature. At cold water granulation systems, low gaseous sulphur compound emissions are

observed than at hot water systems (Schmidt et al. 2003). As far as granulation itself is concerned, the technique optimization should be that of controlling the temperature of the granulation water. Similarly, maintaining the right ratio between slag rate and water rate also helps reduce emissions (Société Belge de Filtration 1995).

4. Alkalization of granulation water

   The sulphur emissions tend to create acid compounds in the granulation water, which can be neutralized by alkali compounds. In a comparative analysis of industrial scale data, it is found the sulphur emissions can be cut by more than 80 % by the use of granulation water previously alkalized with lime to pH 11–12.5 (Mishin et al. 1987).

5. Oxidation of slag and granulation water

   The early laboratory studies show that the relative concentrations of H_2S and SO_2 are sensitive to the redox conditions of molten slag and atmosphere. Increase of partial pressure of O_2 produces a very great inhibiting effect on H_2S emission (Stoehr and Pezze 1975), whereas additions to slag of oxide agent like iron or manganese oxides greatly accelerate the rate of evolution of SO_2 (Pelton et al. 1974). Oxidization of molten slag by Fe_2O_3 or $KMnO_4$ and oxidization granulation water by $KMnO_4$ or H_2O_2 have been found effective in sulphur emission reduction (Schmidt et al. 2003; Rehmus et al. 1973).

6. End-of-line treatment

   The above-mentioned methods do make a significant reduction of sulphur emissions. However, they constitute only a partial solution. The end-of-line treatments are those treatments on exhaust air. It is needed for substantial reduction of sulphur emissions. Extensive operational measurements have been performed at laboratory trials and an industrial INBA slag granulation plants and show that NaOH, ferric EDTA, soda and hypochlorite scrubbings are good choices for H_2S absorption (Schmidt et al. 2003; Société Belge de Filtration 1995).

The demonstrated sulphur emission reduction effects of various methods are presented in Table 7.1.

7.3 NOx Emissions

7.3.1 Source

There are three fundamentally different mechanisms of NOx formation, which yield thermal NOx, fuel NOx and prompt NO (U.S. Environmental Protection Agency 1994, 1999). The thermal NOx mechanism arises from the thermal dissociation and subsequent reaction of N_2 and O_2 molecules in combustion air. The fuel NO mechanism arises from the evolution and reaction of fuel-bound nitrogen compounds with oxygen. The prompt NO mechanism involves the intermediate formation of hydrogen cyanide (HCN), followed by the oxidation of HCN to NO.

Table 7.1 Effect of various methods on H_2S and SO_2 emission reductions

Reference	Methods	H_2S reduction	SO_2 reduction	Notes
Rehmus et al. (1973)	Slag temperature reduction	Aver. 70 %	/	Longer pit filling periods
Rehmus et al. (1973)	Slag temperature reduction	Aver. 55 %	/	Three-day air cooling before quenching
Rehmus et al. (1973)	Granulation water oxidation	Aver. 75 %	/	100 ppm $KMnO_4$ in water
Mishin et al. (1987)	Granulation water alkalization	82–85 %	/	pH 11–12.5 by lime
Schmidt et al. (2003)	Molten slag oxidation	31–36 %	78–81 %	3 % Fe_2O_3 in slag
Schmidt et al. (2003)	Molten slag oxidation	26–32 %	44–52 %	3 % $KMnO_4$ in slag
Schmidt et al. (2003)	Granulation water oxidation	19–26 %	2–16 %	0.7 H_2O_2 in water
Schmidt et al. (2003)	Granulation water oxidation	28–34 %	1–15 %	2.8 H_2O_2 in water
Schmidt et al. (2003)	Exhaust air treatment	Nearly 100 %	Nearly 100 %	Scrubbing with NaOH or ferric EDTA solution

Both blast furnace smelting and hot stoves are operated at high temperatures, i.e. higher than 1200 °C. As a result, the NOx generation tends to be thermal NO. The atmosphere in blast furnace smelting is reductive, which is thermodynamically unfavourable for the formation of NOx. Therefore, the hot stoves are the main source of emissions of NOx in the blast furnace operations.

7.3.2 Emission

The blast furnace smelting is a closed process that does not have atmospheric emissions. However, the associated blast furnace hot stoves do generate NOx emission. It is shown that NOx in the hot stoves mainly exist in the form of NO. However, when gas temperature decreases, NO will be converted to NO_2 (Chen et al. 2014).

Because the stoves are heated primarily with low heat value BFG, the flame temperature is reduced. NOx concentrations from the stoves tend to be low. The emission factor is 373 mg/Nm^3 for the burning of BFG and 1296 mg/Nm^3 for COG (U.S. Environmental Protection Agency 1994). However, since the volume of BFG is huge, total NOx mass emissions are still large.

Currently relatively little NOx emission data are available relevant to hot stoves. The stove NOx emission in US steelworks is reported in the range of 1.4–32.6 ppm, with an average of about 30 ppm (U.S. Environmental Protection Agency 1994).

The data vary widely as the test conditions were seldom specified. In Europe, emission concentrations are in the range of 19–115 mg/Nm^3, which corresponds to 6–173 g/t hot metal produced (Remus et al. 2013).

7.3.3 Abatement

At the temperatures encountered in combustion air, the subsequent reactions are thought to proceed through mechanisms formulated by Zeldovich (1946):

$$\mathrm{N_2 + O \rightarrow NO + N} \quad k = 2 \times 10^{14} \exp\left(-76500 / RT\right) \tag{7.3}$$

$$\mathrm{N + O_2 \rightarrow NO + O} \quad k = 6.3 \times 10^{9} \exp\left(-6300 / RT\right) \tag{7.4}$$

where k is the rate constant, R is the gas constant and T is the temperature. Because of the high activation energy, these reactions are temperature sensitive. In fact, it reflects strong and exponential relationship between NOx emission and temperature (U.S. Environmental Protection Agency 1994). Therefore, the most effective measure to reduce thermal NOx formation is to lower the peak temperature.

It is suggested that the hot stove dome temperature should be controlled below 1420 °C in order to decrease NOx emission. Increasing excess air ratio is also beneficial to the reduction of NOx emission as it decreases the dome temperature (Chen et al. 2014).

7.4 Heavy Metal Emissions

7.4.1 Source

Blast furnace smelting typically uses high-grade ores with metal Fe content higher than 60 %. However, the low-grade ores with higher impurity content are becoming economical because of the depleting of high-grade ores. Dangerous heavy metals, i.e. Zn and Pb, can be found in most of the iron ores around the world. Also, dust and sludge are recycled as raw materials for sintering. These by-products always have high content of Zn. It significantly increases the Zn burden of the blast furnace. Heavy metals like Zn and Pb easily volatilize and deposit on different parts of the blast furnace during smelting. It may lead to severe environmental pollutions if not properly treated.

The zinc charged into the blast furnace is limited to 150–200 g/t hot metal in Japan (Ichikawa and Morishige 2002). The total zinc in the charge generally varies

from 100 to 250 g/t of hot metal produced in the EU (Remus et al. 2013). The value is averagely higher in China, which can reach even higher than 1500 g/t hot metal occasionally (Zheng et al. 2014).

7.4.2 Emission

Under the high temperature in the blast furnace, the Zn and Pb are easily removed with the BFG as fine ZnO and PbO particles. However, only 20–50 % of the total zinc in the charge are removed by the BFG (Zhou et al. 2010; Zheng et al. 2014). Most of the rest becomes scaffolding on the furnace line. The emission of zinc from the blast furnace is then estimated to be 20–125 g/t hot metal.

BFG treatment usually consists of pretreatment for the removal of coarse dust and subsequently wet scrubbing or electrostatic precipitation for the removal of fine dust (and thus heavy metals). Dust is removed with a high degree of efficiency during the two-stage treatment of BFG. The Zn and Pb concentrations are within 0.03–0.17 mg/Nm^3 and 0.01–0.05 mg/Nm^3, respectively, for cleaned BFG (Remus et al. 2013). Therefore, most of the heavy metals are then accumulated in the sludge or dust, depending on the use of wet or dry cleaning method in the second stage of BFG treatment. Typical compositions of sludge and dust from BFG treatment are listed in Table 7.2. The high contents of Zn and Pb make them difficult to be recycled in the steel plants.

Table 7.2 Compositions of sludge and dust from the treatment of blast furnace gas (%)

Source	C	Fe	CaO	SiO_2	Al_2O_3	MgO	Zn	Pb
Dust from Iran (Asadi Zeydabadi et al. 1997)	\	24	17.2	9.42	2.21	5.35	2.02	0.04
Sludge from Belgium (Van Herck et al. 2000)	3	8.6	0.83	4.1	1.89	0.63	3.9	0.8
Sludge from Germany (Mansfeldt and Dohrmann 2004)	19	15.8	11.6	16.5	6.76	3.42	3.26	1.03
Dust from China (Zhang et al. 2006)	32.0	22.1	8.0	5.1	2.53	2.46	1.1	0.51
Sludge from China (Li and Li 2009)	24.3	36.6	4.12	12.7	5.54	3.78	2.17	<1
Sludge from the USA (Vereš et al. 2012)	18.54	41.4	4.28	7.02	1.74	1.87	1.98	0.06
Sludge from the EU (Remus et al. 2013)	15–47	7–35	3.5–18	3–9	0.8–4.6	3.5–17	1–10	0.8–2

Table 7.3 A brief summary of methods for valuable metal recovery from blast furnace sludge and dust

References	Process	Methods
Asadi Zeydabadi et al. (1997)	Hydrometallurgical	Selective leaching by sulphuric acid at low acid concentration and room temperature
Van Herck et al. (2000)	Hydrometallurgical	Leaching under both acid (HCl) and oxidizing conditions and then passing through an anion exchanger
Stamatovic and Themelis (1994)	Hydrometallurgical	Leaching in NaOH and metal produced by electrolysis
Huang et al. (2007)	Hydrometallurgical	Leaching by sulphuric acid, ferric chloride or amine
Vereš et al. (2012)	Hydrometallurgical	Microwave-assisted leaching
Liu et al. (2012)	Hydrometallurgical	Low-acid leaching with waste acid from titanium dioxide plant
Steer and Griffiths (2013)	Hydrometallurgical	Leaching by organic carboxylic acids
Li and Li (2009)	Pyro- and hydrometallurgical	Reductive roasting and then reclaimed in CH_3COOH solution
Ichikawa and Morishige (2002); Koros (2003); Wang et al. (2011); Xu et al. (2012)	Pyrometallurgical	Rotary hearth furnace
Zhang et al. (2006)	Pyrometallurgical	High-temperature roasting and reduction by carbon
Gao et al. (2012)	Pyrometallurgical	Reductive roasting in H_2 or CO atmosphere

7.4.3 Abatement

Due to the high contents of Zn and Pb in the blast furnace sludge and dust, their recycling in the steel plant is limited. An alternative treatment, although very expensive, is to dewater the sludge and deposit it on a landfill for industrial waste after pretreatment (Van Herck et al. 2000). However, the present environmental policies encourage recycling and recovery for natural resource conservation, at the same time avoiding the very high landfilling cost.

Both hydro- and pyrometallurgical processes can be used to recover valuable metals in the sludge and dust. A brief summary of related methods is presented in Table 7.3. In order to recover zinc, the hydrometallurgical processes have been considered more eco-friendly and produce residues suitable for safe disposal, as zinc could be selectively dissolved in suitable lixiviants leaving other impurities in the residue (Jha et al. 2001). However, since the sludge and dust also have a high content of Fe, pyrometallurgical processes have been widely used to recover both Fe and Zn. The rotary hearth furnace process for separating Zn and recovering Fe from the sludge and dust has been commercially available (Xu et al. 2012). Figure 7.2 shows the main installations of a rotary hearth furnace in Shandong Province, China.

Fig. 7.2 A rotary hearth furnace plant in Shandong Province, China

7.5 Fluoride Emissions

7.5.1 Source

Fluorine is typically a minor element in iron ores with concentration lower than 0.1 %. However, for some special deposit like iron ore in Bayan Obo region in Baotou, China, its concentration can reach up to 4 % historically. The fluorine concentration of commercial Bayan Obo iron ore concentrate was still higher than 0.5 % in 2000 after years of relentless efforts on beneficiation (Pei 2002; Li and Yu 1990). In addition, fluorspar (CaF_2) is sometimes used as flux in the blast furnace to optimize smelting process. The fluoride emission is a serious environmental problem for smelting with high fluorine iron ores and flux in the blast furnace (Hu et al. 1982).

7.5.2 Emission

The fluorine in iron ores is mainly in the form of CaF_2. In the blast furnace, the temperature increases with descending of iron ores. Under high temperature, gaseous fluorides of HF, KF, and NaF are formed according to the following possible reactions (Zhang et al. 2015; Zhu and Zhou 1994):

$$CaF_2 + H_2O \rightarrow 2HF + CaO \tag{7.5}$$

$$K_2SiO_3 + 2HF \rightarrow 2KF + H_2O + SiO_2 \tag{7.6}$$

$$Na_2SiO_3 + 2HF \rightarrow 2NaF + H_2O + SiO_2 \tag{7.7}$$

The gaseous fluorides enter into the BFG and move upward to low-temperature region. The KF and NaF will react with CaO in the flux and generate CaF_2 again under lower temperature:

$$2KF + CaO \rightarrow CaF_2 + K_2O \tag{7.8}$$

$$2NaF + CaO \rightarrow CaF_2 + Na_2O \tag{7.9}$$

The newly formed CaF_2 is easily blown out of the furnace as dust by the high-speed off-gas. Experimental and small practical blast furnace investigations indicate that 78–96 % of the fluorine is absorbed by slag, 3.8–14.3 % is blown out as dust mainly in the form of CaF_2 and 0.05–8.55 % enters into the BFG mainly in the form of HF (Institute of Metallurgy and Ceramics Academia Sinica 1959; Chow et al. 1958, 1959). The fluorine concentration in BFG for smelting of iron ores with 3 % fluorine in an experimental blast furnace is 3–13 mg/Nm^3 (Chow et al. 1959) and 2.2–57.7 mg/Nm^3 in a small practical furnace (Institute of Metallurgy and Ceramics Academia Sinica 1959).

Uncontrolled fluorine emissions are also found in the cast house of the blast furnace. For a 100 m^3 practical blast furnace, the uncontrolled emission is found to be 1.29 % of the total fluorine input (Zhu and Zhou 1994).

7.5.3 Abatement

The primary method for fluorine emission abatement in the blast furnace is the reduction of fluorine input. The fluorine content in the iron ore concentrate should be restricted below 0.5 %. Removal of fluorine from sintering process rather than the blast furnace is a better choice from a technical point of view, because flue gas processing system is fully installed in most of the sintering plants.

The CaF_2 in the slag may react with water during granulation to form HF. The CaF_2 containing slag may also cause soil and water pollutions. However, investigations on emission and treatment of fluorine containing blast furnace slag have been seldom reported. The fluorine emissions from the BFG, both CaF_2 in the dust and HF in the gas, are mainly treated by either wet or dry dedusting processes. For newly built blast furnace, the flue gas treatment system is also installed in the cast house to reduce uncontrolled fluorine emissions (Song and Du 2008).

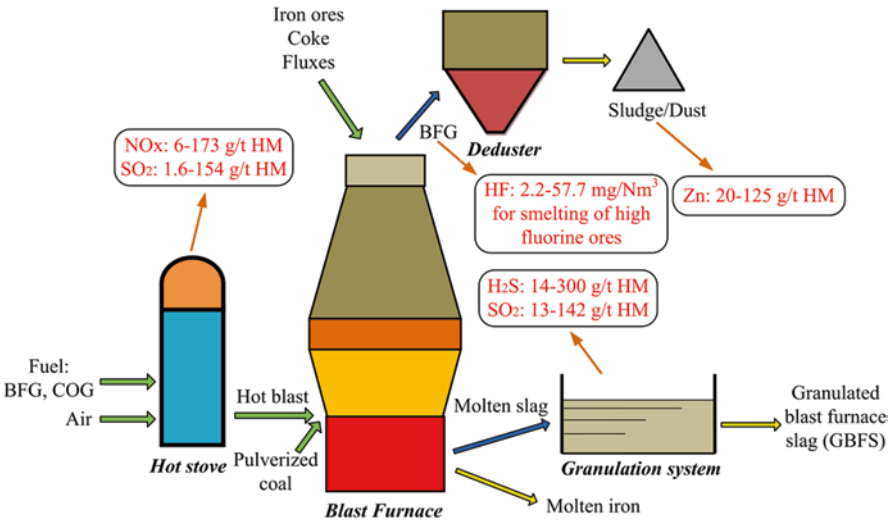

Fig. 7.3 Dangerous emissions in blast furnace operations

7.6 Conclusions

Gaseous sulphur (H_2S and SO_2), NOx, heavy metal (Zn, Pb) and fluorides are the primary dangerous emissions in blast furnace operations. The available emission factors are visually shown in Fig. 7.3. The emissions from the blast furnace are generally in low concentrations and depend strongly on operation conditions, which lead to difficulties in the application of abatement technologies. Since the production of the blast furnace is huge, the mass of these emissions are appreciable. The heavy metal emissions from the sludge and dust are further processed and recycled. However, few processes have been installed to treat emissions of H_2S, SO_2, NOx and fluorine from the blast furnace.

References

Annamraju G, Kemner W, Schworer PJ (1984) Assessment of atmospheric emissions from quenching of blast furnace slag with blast furnace blowdown water. EPA Report: EPA-600/S2-84-072

Asadi Zeydabadi B, Mowla D, Shariat MH, Fathi Kalajahi J (1997) Zinc recovery from blast furnace flue dust. Hydrometallurgy 47(1):113–125

Cai J-j, Wu F-z, Li J-q, Zhang J-z (2008) Sulphur flow analysis for blast furnace-converter process. Iron Steel 43(7):91–95

Chen C, Cheng S-s, Guo X-b (2014) Hazard control of NOx in hot stove. J Iron Steel Res Int 21(3):306–311

Chow J, Chou Y-H, Tsung-Li S, Hsu Y-S, Chow S-H, Wang W-Y, Mow P-K, Peng H-W, Tsung C-T (1958) Behavior of fluorine in blast furnace smelting II. Smelting Baotou iron ore in an experimental blast furnace. Acta Metall Sin 3(3):181–196

Chow J, Chou Y-H, Hsu Y-S, Hu C-L, Mow P-K, Wang W-Y, Chow S-H, Hsu P-L (1959) Behavior of fluorine in blast furnace smelting III. Movement of fluorine in a 1 m^3 experimental blast furnace smelting Baotou iron ore. Acta Metall Sin 4(1):1–15

Gan L, Lai C (2014) A general viscosity model for molten blast furnace slag. Metall Mater Trans B 45(3):875–888

Gao J, Li S, Zhang Y, Zhang Y, Chen P, Wang Y (2012) Separation technology of Fe and Zn from blast furnace dust at non-molten state. J Univ Sci Technol B 34(11):1268–1274

Hu R, Ruan Y, Ma L (1982) Study of fluorine pollution in soil in Baotou region. J Environ Sci (China) 2(2):143–149

Hu C-Q, Zhang C-X, Han X-W, Yin R-Y (2008) Sulfur flow analysis for new generation steel manufacturing process. J Iron Steel Res Int 15(4):12–37

Huang Z, Wu X, Peng G (2007) Removal of zinc from blast furnace dust by chemical leaching. Chin J Nonferrous Met 17(7):1207–1212

Ichikawa H, Morishige H (2002) Effective use of steelmaking dust and sludge by use of rotary hearth furnace. Nippon Steel Tech Rep 86:35–38

Institute of Metallurgy and Ceramics Academia Sinica (1959) Behavior of fluorine in blast furnace smelting IV. Mechanism of volatilization of fluorine and its movement in a 11 m^3 blast furnace smelting Baotou iron ore. Acta Metall Sin 4(2):95–106

Jablin R (1972) Expanding blast furnace slag without air pollution. J Air Pollut Control Assoc 22(3):191–194

Jha MK, Kumar V, Singh RJ (2001) Review of hydrometallurgical recovery of zinc from industrial wastes. Resour Conserv Recy 33(1):1–22

Koros PJ (2003) Dusts, scale, slags, sludges… Not wastes, but sources of profits. Metall Mater Trans B 34(6):769–779

Li L, Li K (2009) Recovery of iron and zinc from blast furnace sludge. Chin J Process Eng 9(3):468–473

Li Y, Yu Y (1990) Reducing fluorine and phosphorus contents of Baotou mine's iron concentrate from magnetic separation. Min Metall Eng 10(3):32–36

Liu S, Yang S, Chen Y, Min L (2012) A new process for recovery of zinc from blast furnace sludge (I): leaching using waste acid and removal of iron by neutralization. Hydrometallurgy China 31(2):110–114

Mansfeldt T, Dohrmann R (2004) Chemical and mineralogical characterization of blast-furnace sludge from an abandoned landfill. Environ Sci Technol 38(22):5977–5984

Mishin VF, Markman LG, Voronin AA, Seleznev VA, Zubkova LN (1987) Removing the harmful contents of vapor-gas emissions at a granulation unit. Metallurgist 31(4):104–105

Pei C (2002) Fluoride pollution and its present treatments in ironmaking plants of Baotou steel. Sci Technol Baotou Steel 28(3):64–65, 83

Pelton A, See JB, Elliott J (1974) Kinetics of evolution of SO_2 from hot metallurgical slags. Metall Trans 5(5):1163–1171

Rehmus FH, Manka DP, Upton EA (1973) Control of H_2S emissions during slag quenching. J Air Pollut Control Assoc 23(10):864–869

Remus R, Roudier S, Aguado-Monsonet MA, Sancho LD (2013) Best available techniques (BAT) reference document for iron and steel production: industrial emissions Directive 2010/75/EU: Integrated Pollution Prevention and Control Publications Office

Roy A (2009) Sulfur speciation in granulated blast furnace slag: an X-ray absorption spectroscopic investigation. Cem Concr Res 39(8):659–663

Schmidt B, Petersen J, Stubbe G, Brinckmann J, Miceli P, Perini G (2003) Optimised blast furnace slag water quenching with sulphur compounds control. European Commission Technical Steel Research Report: EUR 20584

Shi C, Roy D, Krivenko P (2006) Alkali activated cements & concrete. Taylor & Francis, London and New York

Société Belge de Filtration (1995) Odoriferous nuisances in steel industry: emissions at the blast-furnace slag granulation. European Commission Research and Innovation Report: 7261-01/501/02

Song W, Du Y (2008) Along the way of sustainable development with environmental protection and fluorine pollution control. In: Proceeding of development of metallurgical circulation economy forum, Metallurgical Industry Press, Beijing

Stamatovic M, Themelis N (1994) Recovery of zinc from ironmaking dusts by NaOH leaching. In: Proceedings of conference extraction and processing for the treatment and minimization of wastes, The Minerals, Metals and Materials Society, California, February 27–March 3, pp 533–542

Steer JM, Griffiths AJ (2013) Investigation of carboxylic acids and non-aqueous solvents for the selective leaching of zinc from blast furnace dust slurry. Hydrometallurgy 140:34–41

Stoehr RA, Pezze JP (1975) Effect of oxidizing and reducing conditions on the reaction of water with sulfur bearing blast furnace slags. J Air Pollut Control Assoc 25(11):1119–1122

U.S. Environmental Protection Agency (1994) Alternative control techniques document: NOx emissions from iron and steel mills. EPA 453/R-94/065

U.S. Environmental Protection Agency (1999) Nitrogen Oxides (NOx), why and how they are controlled. EPA 456/F-99-006R

Van Herck P, Vandecasteele C, Swennen R, Mortier R (2000) Zinc and lead removal from blast furnace sludge with a hydrometallurgical process. Environ Sci Technol 34(17):3802–3808

Vereš J, Lovás M, Jakabský Š, Šepelák V, Hredzák S (2012) Characterization of blast furnace sludge and removal of zinc by microwave assisted extraction. Hydrometallurgy 129–130:67–73

Wang C, Zhang J, Liu Z, Hu Z, Lin X, Su B (2011) Study on the treatment of zinc dust in ironmaking system by roasting-magnetic process at Baotou steel. Iron Steel 46(4):93–97

World Steel Association (2015) Steel Statistical Yearbook. Brussels

Xu H, Zhou H, Qi Y, Xie G (2012) Engineering and productive practice on rotary hearth furnace for steel dust and sludge. Iron Steel 47(3):89–93

Zeldovich YB (1946) The oxidation of nitrogen in combustion and explosions. Acta Physicochem URSS 21(4):577–628

Zhang J, Yan Y, Xu M, Zhao X, Zhang X (2006) Research on removal of Zn from blast furnace dust. Iron Steel 41(10):78–81

Zhang F, S-l A, Wang Y-c, Luo G-p, X-l S (2015) Thermodynamic analysis of formation of fluoride from Gangue in Bayan Obo iron concentrate containing fluorite. J Iron Steel Res Int 22(3):213–218

Zheng H, Xia J, Li B (2014) Analysis and control of zinc load in WISCO's No.5 blast furnace. Ironmaking 33(2):17–20

Zhou F, Peng Q, Chen B, Jin Z (2010) Analysis for zinc balance and scaffolding in blast furnace. China Metall 20(2):1–5

Zhu R, Zhou Q (1994) Uncontrolled fluorine emission from a 100 m^3 blast furnace. Sci Technol Baotou Steel 2:50–54

Chapter 8
Mathematical Simulation of Blast Furnace Operation

Jursová Simona, Pustějovská Pavlína, Brožová Silvie, and Bilík Jiří

Abstract This chapter deals with possibilities of mathematical modeling of blast furnace operation. This chapter summarizes various attitudes for evaluation of blast furnace operation. The chapter is aimed at modeling of kinetics of reduction processes. It presents a methodology developed at VŠB—Technical University of Ostrava—for interpreting of laboratory tests carried out according to international standards such as ISO 4695:2007. The designed model uses laboratory test results as inputs for mathematical simulation of the material processing in blast furnace aggregate. The model calculates kinetic constants of changes in iron oxides concentration during nondirect reduction and estimates coke consumption for it. It presents simulation of reduction gas consumption regarding the ratio of direct reduction in time. It carries out simulation for one-component and two-component blast furnace feedstock to find easily the optimum of production process.

8.1 Introduction

Centre ENET goes on with the development of mathematical model using Rist's diagram and former knowledge for simulation of reduction process in blast furnace (Bilík 1990). Reduction model was developed in three stages (from Fe_3O_4 to Fe_2O_3, then to FeO, and finally to Fe). In equations, it was required to use kinetic constants of single chemical reactions. Edge and initial conditions of partial differential equations were determined by two exercises (Pustejovska et al. 2013, 2015).

J. Simona (✉) • B. Jiří
Centre ENET, VŠB-Technical University of Ostrava, Ostrava Poruba, Czech Republic
e-mail: simona.jursova@vsb.cz; jiri.bilik@vsb.cz

P. Pavlína
Faculty of Metallurgy and Material Engineering, Centre ENET, VŠB-Technical University of Ostrava, Ostrava Poruba, Czech Republic
e-mail: pavlina.pustejovska@vsb.cz

B. Silvie
Faculty of Metallurgy and Material Engineering, VŠB-Technical University of Ostrava, Ostrava Poruba, Czech Republic
e-mail: silvie.brozova@vsb.cz

P. Cavaliere (ed.), *Ironmaking and Steelmaking Processes*,
DOI 10.1007/978-3-319-39529-6_8

The first exercise was reduction on rigid bed with a great surplus of reduction gas, which is enabled by experimental laboratory equipment. Solution of equations is analytic, in the form of formula where there was amount of sample mass loss on the left side and on the right side there was a complicated expression depending on the sample initial composition and kinetic constants, which cannot be found in any textbook or technical literature. Experimental data (sample mass loss in time) are possible to use to reveal a theoretic function such values of kinetic constants for which theoretic time flow and time of mass loss measured during the test is almost the same. These quasi(kinetic) constants of ore gas reduction gained from experimental data are fundamentally new partial result of the methodology.

The second exercise was reduction simulation in countercurrent in the blast furnace stack. The information about chemical composition and kinetic constants of chemical reactions found out from the first exercise are input data using for the calculation. Calculation result is "practically reachable" coke minimum specific consumption (ω). Classical heat balance needs reducing gas composition on the furnace top to check coke-specific consumption at blast furnace. To calculate "theoretic minimum" coke consumption, it is necessary to assume reaching chemical equilibrium between gas and charge, which can originate only after infinite time of charge holding at blast furnace. Presented use of kinetic constants enables calculation of coke consumption for actual charge under current conditions of present blast furnace (Jursová and Bilík 2013).

8.2 Kinetic Model of Reduction

8.2.1 Simulation of Reduction in the Fixed Bed

The laboratory tests of the blast furnace burden reducibility are carried out in a stationary fixed bed. The height of the burden bed is made small, and at the same time, the amount of reduction gas is large. Consequently, the change of the molar O/Fe ratio in the burden and the molar O/C ratio in the gas along the coordinate of the fixed bed is small, and the derivatives with respect to the coordinate can be dropped.

$$\frac{\partial C_i}{\partial t} = -K_i C_i \left(X - X_{e,i} \right) + K_{i-1} C_{i-1} \left(X - X_{e,i-1} \right) \tag{8.1}$$

where C_i is Fe concentration in the ith form as the fraction of the entire amount of Fe in the charge, K_i is kinetic constant (s^{-1}), X is molar O/Fe ratio in the burden, and $X_{e,i}$ is equilibrium molar fraction of CO with Fe in the ith form. The model yields a system of ordinary linear differential equations with initial determined by the values of the concentrations of Fe in the form i. The model can be solved analytically yielding the following result:

$$C_1 \left(t \right) = C_{1,0} e^{-N_1 t} \tag{8.2}$$

$$C_2(t) = C_{2,0} - \frac{C_{1,0}N_1}{N_2 - N_1}e^{-N_2 t} + \frac{C_{1,0}N_1}{N_2 - N_1}e^{-N_1 t} \tag{8.3}$$

$$C_3(t) = C_{3,0} - \frac{C_{2,0} - N_2}{N_3 - N_2} + \frac{C_{1,0}N_1N_2}{(N_3 - N_1)(N_3 - N_2)}e^{-N_3 t} + \frac{C_{2,0-}N_2}{N_3 - N_2} + \frac{C_{1,0}N_1N_2}{(N_3 - N_1)(N_3 - N_2)}e^{N_2 t} + \frac{C_{1,0}N_1N_2}{(N_3 - N_1)(N_3 - N_2)}e^{-N_1 t}. \tag{8.4}$$

where $C_{i,0} = C_i(0)$ is the initial concentration of Fe in the form $i = 1, 2, 3$ for $t = 0$, and N_i expressed (8.5).

$$N_i = K_i(X_0 - X_{e,i}), \quad i = 1,2,3 \tag{8.5}$$

The composition of the reduced burden is given by its content of Fe_2O_3 and FeO. In calculating the initial values of the concentration C_i, it is assumed that the sample does not contain elementary iron ($C_4 = 0$) and that iron is combined only in the form of Fe_3O_4 ($C_3 = 0$). e equilibrium constants were taken from the literature. The weighted sum of the concentrations C_1, C_2, and C_3 gives the molar O/Fe ratio in the sample of the burden. Of course, in order to calculate the time dependence $Y_{(t)}$ in the analytical form, it is necessary to determine the kinetic constants K_1, K_2, and K_3. These can be determined using the least squares method from the experimentally recorded time history of the mass loss of the oxygen in the sample during reduction and fitting them to the mass loss calculated from the analytical form of $Y_{(t)}$. The difference between calculated $Y_{(t)}$ and the experimental value Y_j forms the objective function (8.6)

$$F(K_1, K_2, K_3) = \sum_j \left(Y_j - Y_{(t_j)}\right)^2. \tag{8.6}$$

The objective function depends nonlinearly on the sought parameters, and it is therefore difficult to determine the global minimum. The optimization was therefore repeated for various initial estimation of the parameters K_1, K_2, and K_3 to locate global minimum. The kinetic constants for the given temperature of reduction characterize the reducibility in greater detail in comparison with the characteristics such as the amount of oxygen reduced in 1 h. To calculate the kinetic constants, it is necessary to have data describing the chemical equilibrium between the oxides of iron and between the composition of the reducing gas and the burden (Mihok and Baricová 2008).

Model simulation of reduction in countercurrent flow results from Rist's diagram. The slope of operating line in Rist's diagram (Fig. 8.1) represents the specific consumption of the reduction gas determined by the number of kmoles of CO per kg of Fe in the countercurrent phases (Konstanciak et al. 2003). Calculation of the

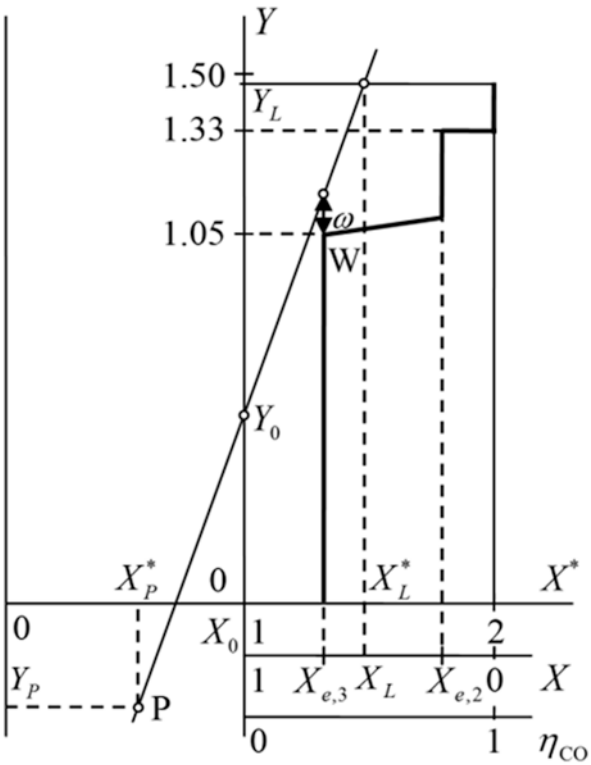

Fig. 8.1 Rist's diagram for iron ore reduction

position of the operating line is repeated for several values of the specific consumption of the reduction gas CS. This yields a set of operating lines whose positions are expressed by approximation Eq. (8.7). The parameter has been used for evaluation of the reducibility of the burden in the blast furnace by calculating this parameter from the O/Fe of the burden reduced in the direct way (r_d) and the composition of the burden, the gas at the top of the reduction zone (X_L, Y_L). The value of parameter determined from the laboratory tests of the ore reducibility can be compared with the value of the parameter determined from the operating data of the blast furnace. Better reducibility of the ore burden is characterized by the low value of the parameter ω.

$$\omega = a_0 + a_1 CS + a_2 CS^2. \tag{8.7}$$

8.2.2 Calculation of Specific Carbon Consumption

The specific consumption of the reducing gas is identical with the specific consumption of the carbon required to produce this gas (Babich et al. 2008). For the modeling, the calculation is carried out by Rist's diagram. Therefore, the set of the

operating straight lines for the given ore burden specifies the relationship between the specific consumption of the reducing gas and the degree of the direct reduction depending on the value of the parameter ω. The holding reaction time can be determined from a blast furnace production rate and volume. The production rate results also for the intensity of heat transfer in the lower and upper zone of the blast furnace. The heat balance equation of the lower zone for 1 kg of it is as follows:

$$\left(CS - Y_f - Y_0\right) q_v = Y_0 q_d + Q. \tag{8.8}$$

The quantity Y_f designates the consumption of carbon for reduction of accompanying elements. The left-hand side represents the heat released by imperfect combustion of carbon in front of the tuyeres and the sensible heat of the hot blast transferred to the burden by cooling to the temperature of the thermally ineffective zone. The first term on the right-hand side of Eq. (8.8) is the consumption of the heat for direct reduction, and the second term is the heat for reduction of accompanying elements, melting and heating the products of the melt to the tapping temperature and to cover heat losses. The thermal balance equation makes/enables us to write the equation of the operating line in the following form (8.9):

$$Y = Y_0 \left(X^* - \frac{q_d}{q_d + q_v} \right) \frac{q_v}{q_d + q_v} + \left(Y_f + \frac{Q}{q_d} \right) \left(X^* - 1 \right) \tag{8.9}$$

This form of equation of the operating line indicates that the position of its point P has the coordinates

$$X_p^* = \frac{q_d}{q_d + q_v}, Y_p = \left(Y_f + \frac{Q}{q_d} \right) X_p^* - Y_f. \tag{8.10}$$

As it is shown in Fig. 8.7, the position of the point P is determined by parameters controlled by composition of the burden and hot metal, blast temperature, the temperature of the isothermal zone, and slag and the heat losses. This indicates that the main problem of calculating the specific consumption of carbon is the construction of the operating line which passes through the point P and is also included in the set of the straight lines for the specific burden. The calculation results in the theoretically minimum consumption of carbon for production of hot metal which is discussed in literature as the ideal blast furnace operation in case that operating line passes through the point W, the calculation results in the theoretically minimum consumption of carbon for production of hot metal which is discussed in literature as the ideal blast furnace operation. The positive value of the parameter ω introduces into the calculation of the specific consumption CS the dependence on the reducibility of the ore burden. The result of calculation may be considered as the prediction of the consumption of carbon for a given ore burden in the blast. The calculation procedures also take into account the presence of hydrogen in the reduction gas and decomposition of carbonates.

8.3 Practical Modeling of Results of Reducibility Test

Parameters of measurement are indicated in Table 8.1. The Levenberg-Marquardt method was used for optimization of function $F(k_1,k_2,k_3)=\Sigma(Y_j-Y(t_j))^2$. Optimization was programmed using MATLAB mathematical library. Calculated kinetic constants are an important starting parameter during simulation of reduction processes of iron oxides in the stack of blast furnace. Calcualted kinetic constants are an important starting parameter during simulation of reduction processes of iron oxides in the stack of blast furnace (Bilík and Vu 2000). For practical modeling were used the samples of the properties presented in Table 8.2.

8.3.1 Example of Calculation of Reduction Run in the Area of Indirect Reduction

Results of reducibility test were used for simulation of different model options of indirect reduction of iron oxides (Pustějovská and Jursová 2013a, b). Proportion of direct/indirect reduction ideally represents proportion of wüstite in reduced charge when area-relative height of indirect reduction is zero. Below it, Boudouard's reaction already starts.

Figures 8.2 and 8.3 present reduction run of sinter of grain size amounting to 10–12.5 mm with time period of charge keeping in reaction space of duration of 3 h and with reducing gas-specific consumption amounting to 2 $kmol^{-1}$ of Fe.

Figure 8.4 presents reduction of two-component charge with different compositions: Two sinters were selected (sinter 1, 10–12.5 mm, and sinter 2, 10–12.5 mm). Dependence of controlled quantities (composition of reducing gas, concentration of iron oxides) is graphically represented. This calculation can serve in providing optimum charge composition for given technological conditions.

Mutual dependence among carbon consumption, direct reduction level, and process intensity following kinetic model application has generally tridimensional form. It is obvious that the lowest coke consumption is in the optimal rate between

Table 8.1 Parameters of reducibility tests

Sample weight	500 g
Measurement temperature	950 °C
Reducing gas composition	40 % CO, 60 % N_2
Gas equilibrium concentrations	$X_{r1}=0.01$; $X_{r2}=0.198$; $X_{r3}=0.675$

Table 8.2 Properties of samples

Sample	Fe [%]	FeO [%]	P_2	dR/dt
1	54.9	7.33	1.07	1.01
2	56.00	10.9	1.1	0.52

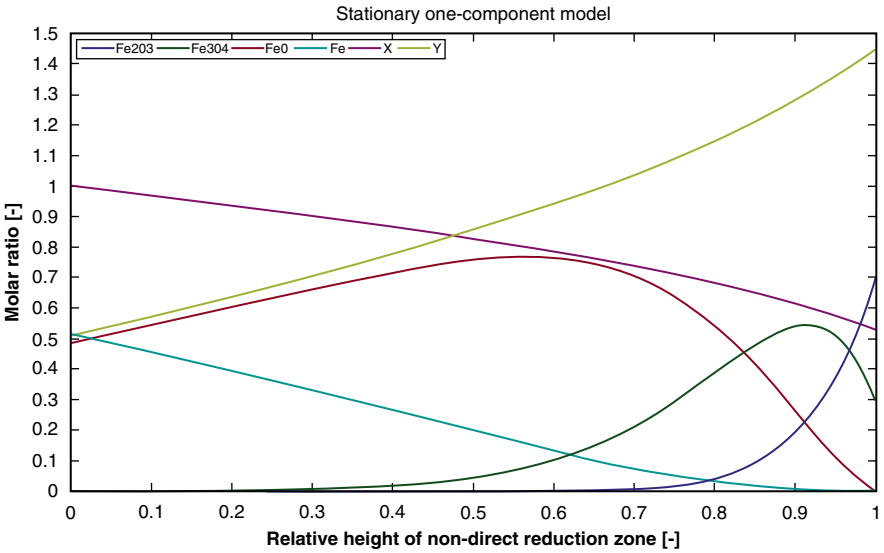

Fig. 8.2 Gas oxidation grade during decline of sinter 1 in the area of indirect reduction at the stack

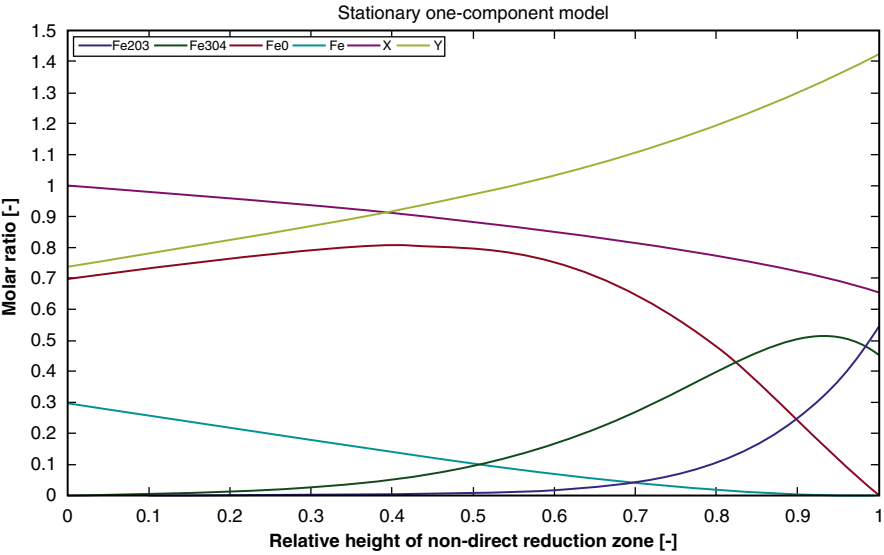

Fig. 8.3 Gas oxidation grade during decline of sinter 2 in the area of indirect reduction at the stack

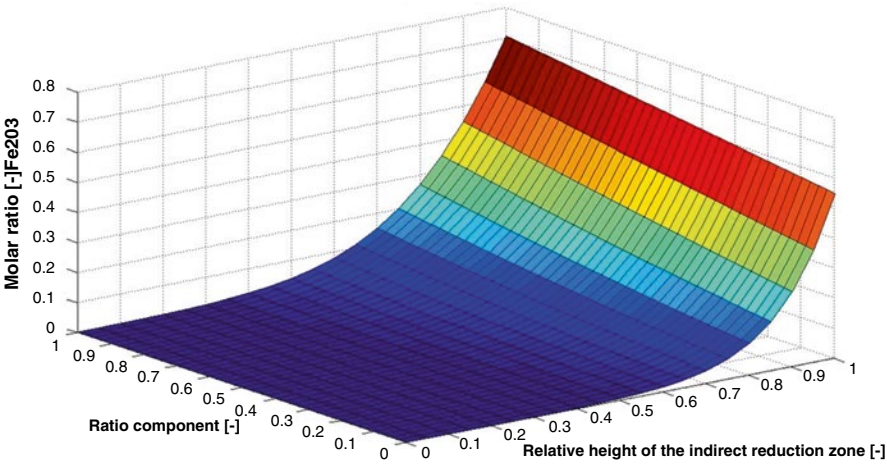

Fig. 8.4 Dependence of magnetite concentration on sinter relative height and its share in feedstock

direct and nondirect reduction. A different ratio results in an increase of coke consumption. The model interpretation has to respect the real dynamics of blast furnace technology. The productivity of blast furnace aggregate is affected by feedstock descent. The rate affects on the time of feedstock stay in the area of nondirect reduction. The shorter time results in the increase in ratio of direct reduction and the increase of heat demand relating to coke consumption (Jursová et al. 2015). An optimizing area for the specific consumption of reduction gas, relating to the time of stay in nondirect reduction area and direct reduction rate, is depicted Fig. 8.5. In case of usage of sinter 1, the optimizing area for the specific consumption of reduction relating to the time is typical with lower ratio of direct reduction, and for optimized blast furnace, feedstock processing in the zone of nondirect reduction rate is required shorter time. The comparison is obvious from Fig. 8.6.

Figures 8.6 and 8.7 present the time effect of feedstock stay in the area of nondirect reduction. It presents the changes in limit kinetic curves of carbon consumption at time of feedstock stay in the area of nondirect reduction. As the time is shorter, the limit kinetic curve of carbon consumption is of higher values.

8.3.2 Use of Kinetics Simulation for CDR Diagram Modification

By gaining kinetically well-founded dependence between reducing gas-specific consumption and level of direct reduction, it can be then determined chemical-kinetic limit of carbon consumption on indirect reduction of iron oxides expressed by the curve showed on Fig. 8.8. From the point of view of enthalpy balance, it is also necessary to provide that heat developed during carbon gasification to reducing gas will

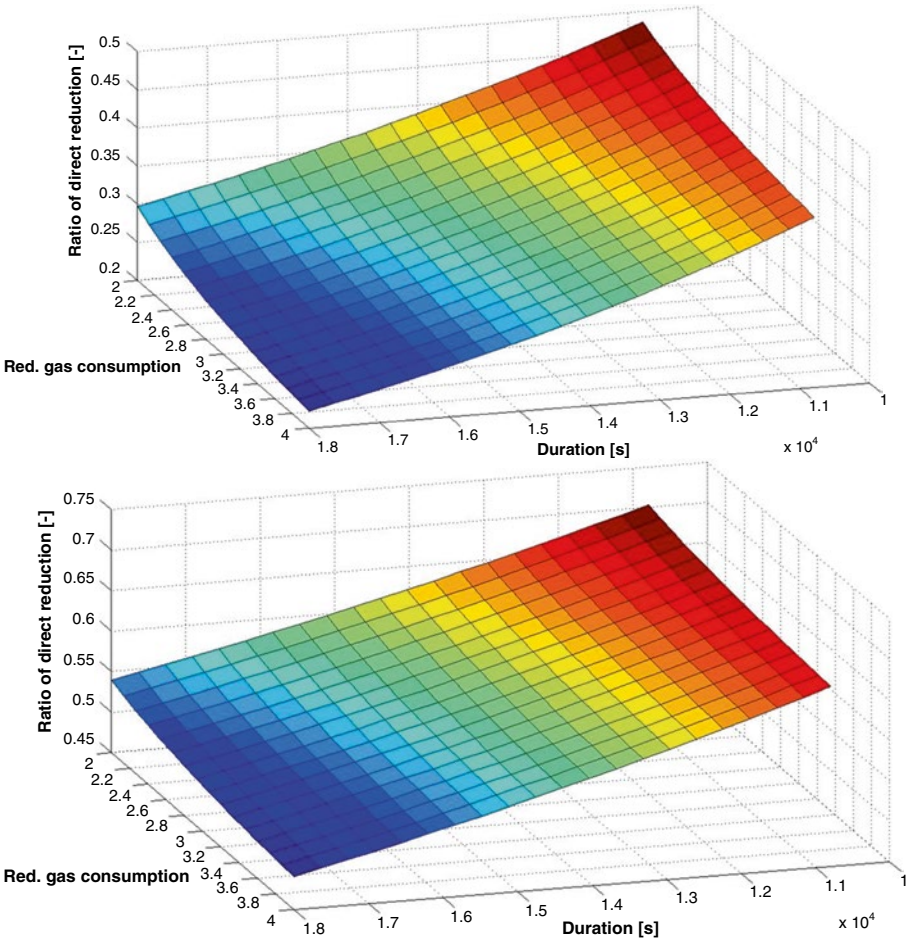

Fig. 8.5 (**a**) Optimizing possibilities for sinter 1; (**b**) Optimizing possibilities for sinter 2

cover also necessary heat needs of the process. Carbon needed for heat (heat limit) also depends significantly on the level of direct reduction. As indirect reduction is applied in the first phase of blast-furnace smelting, its run extent is in principle decisive for resulting mutual ratio of both reduction types (Jursová et al. 2013). Therefore the key role falls on kinetic simulation of indirect reduction run of iron oxides. Output of this simulation is a share of direct reduction on complete reduction extent—level of direct reduction rd. Mutual dependence between direct reduction share and resulting consumption of fuel carbon/deoxidizing agent represents a requirement on real minimum provision of reduction process by this fuel/deoxidizing agent.

In Fig. 8.9, there are kinetic curves as well as intersection of these curves with heat limit (point) calculated for conditions of present Czech process conditions. In comparison with currently used CDR diagram form, version mentioned in Fig. 8.8

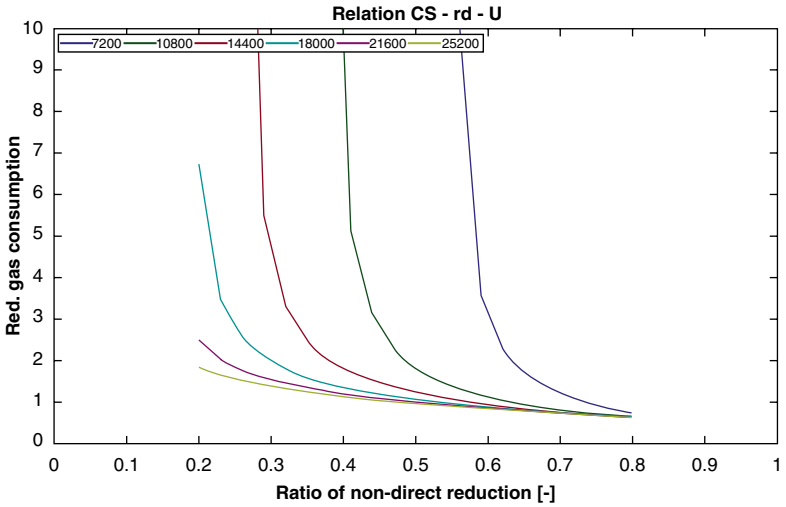

Fig. 8.6 Carbon consumption for processing of sinter 1 at nondirect reduction

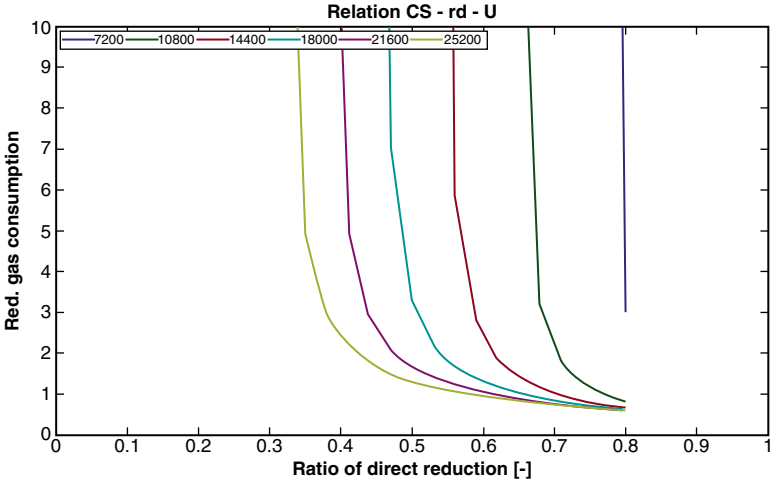

Fig. 8.7 Carbon consumption for processing of sinter 2 at nondirect reduction

shows not only theoretic but rather real limits of minimum specific consumption of reducing gas respecting actual charge reducibility and which can be reached only through better use of reducing gas (Bilík et al. 2013).

Mathematic model based on the indirect reduction describes well the reduction course in the area of the blast furnace where speed of Boudouard's reaction is small. But this model can also be successfully applied at simulation of reduction process of the so-called direct iron production where coke is not used or for estimation of proportion of direct/indirect reduction during processes of melting reduction.

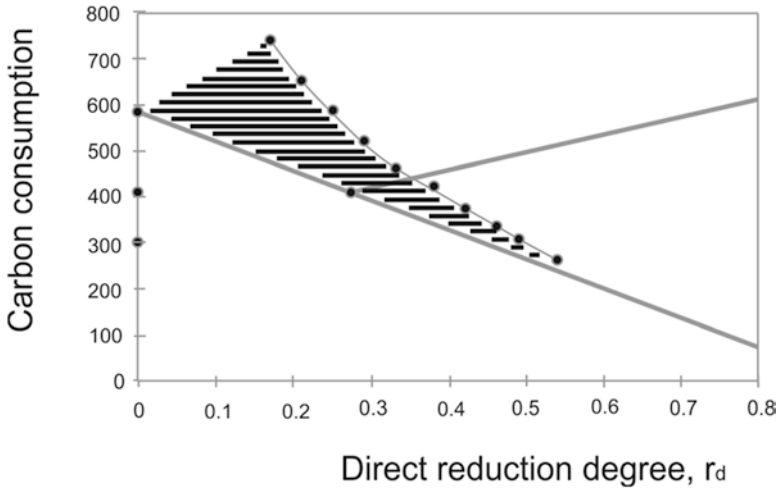

Fig. 8.8 Dependence of reducing gas (carbon)-specific consumption on the level of direct reduction

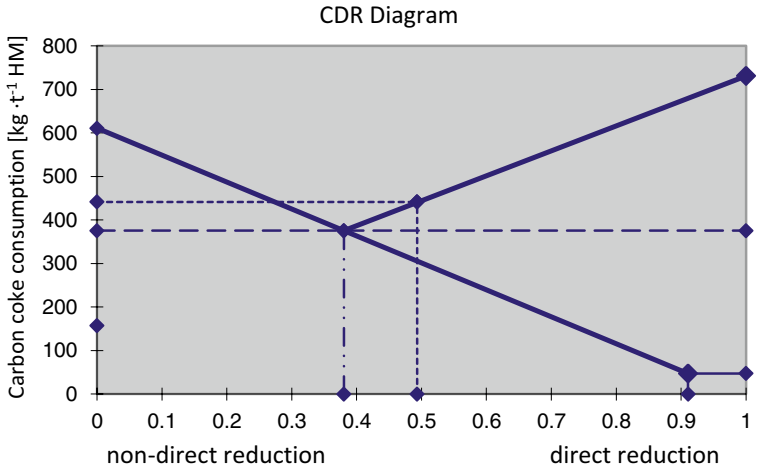

Fig. 8.9 Determination of kinetic and heat limits of carbon consumption (modified CDR diagram)

8.4 Conclusion

The mathematical model of indirect reduction describes well the reduction in the zone of blast furnace where the effect of the Boudouard reaction is insignificant. But this model might be also successfully employed for simulation of the reduction process of the so-called direct reduction iron (DRI) where coke is not a part of the burden. First of all, the degree of the charge metallization reached at the outlet of the charge from the bottom part of such a countercurrent reactor is important for

evaluation of the simulation results of these alternative iron production processes. The calculation of concentration profiles using mathematical modeling can be carried out for different specific consumptions of the reduction gas in this countercurrent reactor. The simulation then enables a prediction of the degree of metallization (pre-reduction) for various alternatives of ore charges (ore, pellets, sinters).

A simulation study of the reduction using kinetic model enables us to determine the limits posed by the thermal conditions and the kinetics of the reduction. It also enables more objective assessment of the impact of the considered innovations in the pig iron production.

Acknowledgments This chapter was conducted within the framework of the project LO1404: Sustainable development of ENET Centre.

References

Babich A, Senk D, Gudenau HW, Mavrommatis KTh (2008) Ironmaking, 1st edn. Wissenschaftsverlag Mainz, Aachen

Bilík J (1990) Matematický model degradace koksu ve vysoké peci. Hutnické listy XLV(4): 225–230

Bilík J, Vu HM (2000) Komplexní kinetický model redukce oxidů železa ve vysoké peci. Hutnické listy 4–7:7–10

Bilík J, Pustějovská P, Jursová S (2013) In: Kledusová J (ed) Modelování, analýza a predikce pochodů výroby železa z hlediska současných energetických a ekologických požadavků, 1st edn. Akademické nakladatelství Cerm, s.r.o. Brno

Jursová S, Bilík J (2013) Innovative research in the field of reductive processes. doi:10.5593/SGEM2013/BA1.V2/S04.008

Jursová S, Pustějovská P, Brožová S, Bilík J (2013) Optimization of blast furnace process according to metallurgical materials reducibility. In: Staniewska E, Górska M (eds) Doskonalenie procesów produkcyjnych i logistycznych, 1st edn. Wydawnictwo Wydziału Inżynierii Procesowej, Materiałowej i Fizyki Stosowanej Politechniki Częstochowskiej. Czestochowa

Jursová S, Pustějovská P, Brožová S, Bilík J (2015) Evaluation of low-reducible sinter in blast furnace technology by mathematical model developed at Centre ENET, VSB – Technical university of Ostrava. Int J Mech Aeros Ind Mechatron Eng 9(4):585–588

Konstanciak A, Jowsa J, Derda W (2003) Computer simulation of change in the chemical composition of coke ash in the blast-furnace. Mater Sci Forum 426–4:4535–4540

Mihok Ĺ, Baricová D (2008) Modern operating and verification methods in ironmaking and steelmaking metallurgy, 1st edn. Elfa, Košice

Pustějovská P, Jursová S (2013a) Effect of waste and alternative fuels on blast-furnace operation. Metallurgist 56(11):908–911

Pustějovská P, Jursová S (2013b) Process engineering in iron production. Chem Process Eng 34(1):63–76

Pustejovska P, Jursova S, Brozova S (2013) Determination of kinetic constants from tests of reducibility and their application for modelling in metallurgy. J Chem Soc Pak 35(3):565–569

Pustějovská P, Tůma J, Staněk V, Křišťál J, Jursová S, Bilík J (2015) Using a mathematical model of counter-current flow in a blast furnace to evaluate reducibility of iron-ore-bearing raw materials. Steel Res Int 86(4):320–328

Chapter 9
CO_2 Emission Reduction in Blast Furnaces

Pasquale Cavaliere and Alessio Silvello

Abstract Blast furnace (BF) represents the dominant hot metal-making process all over the world and one of the main energy-consuming processes. Modern research in the field focuses on the increase in plant productivity through energy saving and on the greenhouse emission reduction compatible with legal limits. The iron and steel industry is one of the biggest industrial emitters of CO_2. It is estimated that between 4 and 7 % of the anthropogenic CO_2 emissions originate from this industry in EU-27, which generated 252.5 million tons of CO_2 emissions on average during the period 2005–2008. Productivity is mainly governed by relevant input parameters such as material rates, material properties, and operating conditions. All the dominant input parameters and their variation have been analyzed in the present study, and they have been optimized in order to increase the plant productivity and reduce the greenhouse emissions. The study suggests new solutions in all processing parameters in order to improve plant productivity and to reduce the dangerous emissions.

9.1 Introduction

Blast furnace (BF) represents the dominant hot metal-making process all over the world and one of the main energy-consuming processes. Modern iron-making process development largely focuses on saving materials and energy, as well as on reducing environmental impact.

Nowadays, the most dominant hot metal-making process in the world is still the BF process, and modern research in the field focuses on the increase in plant productivity through energy saving and on the greenhouse emission reduction compatible

P. Cavaliere (✉) • A. Silvello
Department of Innovation Engineering, University of Salento,
Via per Arnesano, 73100 Lecce, Italy
e-mail: pasquale.cavaliere@unisalento.it; alessio.silvello@unisalento.it

P. Cavaliere (ed.), *Ironmaking and Steelmaking Processes*,
DOI 10.1007/978-3-319-39529-6_9

with legal limits. BF represents the main energy consumption operation in steelmaking industry; the increase in blast furnace productivity leads to a strong reduction in energy consumption.

The challenge, therefore, is to improve the technologies that will bring reduced consumption of energy, reduced consumption of raw materials, and reduced levels of emissions besides being cost effective. Steel being one of the major energy consumers in the manufacturing sector, major intervention will be required in this aspect.

The International Iron and Steel Institute identified 11 sustainable indicators in January, 2005, based on the information from 42 steel companies representing over 33 % of the world's crude steel production. The 11 sustainable indicators are:

1. Greenhouse gas emission
2. Energy intensity
3. Steel recycling
4. Environmental management system (EMS)
5. Investment in processes and products
6. Operating margin
7. Return on capital employed (ROCE)
8. Value added
9. Material efficiency
10. Employee training
11. Lost time injury frequency rate

The industries' environmental performance is measured by the indicators from nos. 1 to 4, the economic performance is measured by the indicators from nos. 5 to 9, and the social performance is measured by two indicators, i.e., nos. 10 and 11. On sustainable development, it is essential that the steel industry needs a systematic method to measure and report how the industries are performing with regard to the above 11 indicators.

The modern steelmakers continued to use the same carbothermic process discovered by the first iron-makers. The BF is a countercurrent continuous reactor occurring between the descending mix of iron ores, coke, and limestone and an ascending hot blast air. The objective of BF is to reduce iron oxides into iron metal within desirable specifications. High production capacity and very high employment have kept it the primary pig iron production. The most important raw material fed into the BF, in terms of operation efficiency and hot metal quality, is coke. Coke is produced by heating a coal blend in the absence of oxygen. The most common type of production technique is the so-called conventional or by-product coke plant. Coke performs three functions in a blast furnace, namely, a thermal function, as fuel providing the energy required for endothermic chemical reactions and for melting of iron and slag; a chemical function, as reductant by providing reducing gases for iron oxide reduction; and a mechanical function, as a permeable grid providing for the passage of liquids and gases in the furnace, particularly in the lower part of the furnace. Basically a BF is charged with alternate layers of coke and iron-bearing minerals. Such iron-bearing materials are a mixing of sinter, pellets, and iron ore with a varying ratio depending on the furnace. Different additives such as lime, dolomite, and quartz are inserted to control and regulate the slag composition, quality, and viscosity.

The main goals of recent research are decrease in coke use, increase in productivity, and reduction of dangerous emissions. In the last decade, three consistent themes have appeared pertaining to coke properties and blast furnace performance. They are related to the viability of the blast furnace, improvement in BF productivity and efficiency, and blast furnace operations at lower coke rates. The BF productivity depends strongly on the rate and degree of reduction; they are directly related to the reactivity of coke and to the composition and reducibility of the iron-bearing charge. In addition, it is interesting to note that if the iron bearing presents a good reduction strength, it is possible to reduce the coke consumption with optimal economic balance of the production process. Actually, one of the fundamental physical parameters for the reduction optimization is the mean dimension of the ores, pellets, and sinters; in general, the rate of reduction decreases with increasing size of the raw materials. Complex gas–solid, solid–solid, and liquid–liquid interactions take place in different zones of the BF.

9.2 Blast Furnace Operations

The BF is the first step in producing steel from iron oxides. The first blast furnaces appeared in the fourteenth century and produced 1 t per day. BF equipment is in continuous evolution, and modern, giant furnaces produce 13,000 t per day. Even though the equipment has improved and higher production rates can be achieved, the processes inside the blast furnace remain the same. BF will survive into the next millennium because the larger, efficient furnaces can produce hot metal at costs competitive with other iron-making technologies.

The purpose of a BF is to chemically reduce and physically convert iron oxides into liquid iron called "hot metal." The BF is a huge steel stack lined with refractory brick, where iron ore, coke, and limestone are dumped into the top and preheated air is blown from the bottom. The raw materials require 6–8 h to descend to the bottom of the furnace where they become the final product of liquid slag and liquid iron. These liquid products are drained from the furnace at regular intervals. The hot air blown from the bottom of the furnace ascends to the top in 6–8 s after going through numerous chemical reactions. Once a BF is started, it will continuously run for 4–10 years with only short stops to perform planned maintenance.

9.2.1 Blast Furnace Processes

Iron oxides can come to the blast furnace plant in the form of raw ore, pellets, or sinter. The raw ore is removed from the earth and sized into pieces that range from 0.5 to 1.5 in. This ore is either hematite (Fe_2O_3) or magnetite (Fe_3O_4), and the iron content ranges from 50 to 70 %. This iron-rich ore can be charged directly into a blast furnace without any further processing. Iron ore with a lower iron content must

be processed or beneficiated to increase its iron content. Pellets are produced from this lower iron content ore. This ore is crushed and ground into a powder so the waste material called gangue can be removed. The remaining iron-rich powder is rolled into balls and fired in a furnace to produce strong, marble-sized pellets that contain 60–65 % iron. Sinter is produced from fine raw ore, small coke, sand-sized limestone, and numerous other steel plant waste materials that contain some iron. These fine materials are proportioned to obtain a desired product chemistry and then mixed together. This raw material mix is then placed on a sintering strand, which is similar to a steel conveyor belt, where it is ignited by gas-fired furnace and fused by the heat from the coke fines into larger size pieces of 0.5–2.0 in. The iron ore, pellets, and sinter then become the liquid iron produced in the blast furnace with any of their remaining impurities going to the liquid slag.

The coke is produced from a mixture of coals. The coal is crushed and ground into a powder and then charged into an oven. As the oven is heated, the coal is cooked so most of the volatile matters such as oil and tar are removed. The cooked coal, called coke, is removed from the oven after 18–24 h of reaction time. The coke is cooled and screened into pieces ranging from 1 to 4 in. The coke contains 90–93 % carbon, some ash, and sulfur but compared to raw coal is very strong. The strong pieces of coke with a high energy value provide permeability, heat, and gases which are required to reduce and melt the iron ore, pellets, and sinter.

The final raw material in the iron-making process is limestone. The limestone is extracted from the earth by blasting with explosives. It is then crushed and screened to a size that ranges from 0.5 to 1.5 in. to become blast furnace flux. This flux can be pure high calcium limestone, dolomitic limestone containing magnesia, or a mixture of the two types of limestone.

Since the limestone is melted to become the slag, which removes sulfur and other impurities, the blast furnace operator may blend the different stones to produce the desired slag chemistry and create optimum slag properties such as a low melting point and a high fluidity.

All of the raw materials are stored in an ore field and transferred to the stockhouse before charging. Once these materials are charged into the furnace top, they go through numerous chemical and physical reactions while descending to the bottom of the furnace.

The iron ore, pellets, and sinter are reduced, simply meaning that the oxygen in the iron oxides is removed by a series of chemical reactions. These reactions occur as follows (Table 9.1).

Table 9.1 Iron oxide chemical reactions

$3\ Fe_2O_3 + CO = CO_2 + 2\ Fe_3O_4$	Begins at 850 °F
$Fe_3O_4 + CO = CO_2 + 3\ FeO$	Begins at 1100 °F
$FeO + CO = CO_2 + Fe$ $FeO + C = CO + Fe$	Begins at 1300 °F

At the same time, the iron oxides are going through these purifying reactions; they are also beginning to soften, then melt, and finally trickle as liquid iron through the coke to the bottom of the furnace.

The coke descends to the bottom of the furnace where the preheated air or hot blast enters the blast furnace. The coke is ignited by this hot blast and immediately reacts to generate heat as follows:

$$C + O_2 = CO_2 + \text{Heat}$$

Since the reaction takes place in the presence of excess carbon at a high temperature, the carbon dioxide is reduced to carbon monoxide as follows:

$$CO_2 + C = 2CO$$

The product of this reaction, carbon monoxide, is necessary to reduce the iron ore as seen in the previous iron oxide reactions.

The limestone descends in the blast furnace and remains a solid while going through its first reaction as follows:

$$CaCO_3 = CaO + CO_2$$

This reaction requires energy and starts at about 1600 °F. The CaO formed from this reaction is used to remove sulfur from the iron, which is necessary before the hot metal becomes steel. This sulfur-removing reaction is

$$FeS + CaO + C = CaS + FeO + CO$$

The CaS becomes part of the slag. The slag is also formed from any remaining silica (SiO_2), alumina (Al_2O_3), magnesia (MgO), or calcia (CaO) that entered with the iron ore, pellets, sinter, or coke. The liquid slag then trickles through the coke bed to the bottom of the furnace where it floats on top of the liquid iron since it is less dense.

Another product of the iron-making process, in addition to molten iron and slag, is hot dirty gases. These gases exit the top of the blast furnace and proceed through gas cleaning equipment where particulate matter is removed from the gas and the gas is cooled. This gas has a considerable energy value so it is burned as a fuel in the "hot blast stoves" which are used to preheat the air entering the blast furnace to become "hot blast." Any of the gas not burned in the stoves is sent to the boiler house and is used to generate steam, which turns on a turbo blower that generates the compressed air known as "cold blast" going to the stoves.

In summary, the blast furnace is a countercurrent reactor where solids descend and gases ascend. In this reactor, there are numerous chemical and physical reactions that produce the desired final product that is hot metal. A typical hot metal chemistry follows (Table 9.2).

Now that we have completed a description of the iron-making process, we will review the physical equipment comprising the blast furnace plant.

Table 9.2 Typical hot metal chemistry

Elements	Composition
Iron (Fe)	93.5–95.0 %
Silicon (Si)	0.30–0.90 %
Sulfur (S)	0.025–0.050 %
Manganese (Mn)	0.55–0.75 %
Phosphorus (P)	0.03–0.09 %
Titanium (Ti)	0.02–0.06 %
Carbon (C)	4.1–4.4 %

There is an ore storage yard that can also be an ore dock where boats and barges are unloaded. The raw materials stored in the ore yard are raw ore, several types of pellets, sinter, limestone or flux blend, and possibly coke. These materials are transferred to the "stockhouse/hiline" complex by ore bridges equipped with grab buckets or by conveyor belts. Materials can also be brought to the stockhouse/hiline in rail hoppers or transferred from ore bridges to self-propelled rail cars called "ore transfer cars." Each type of ore, pellet, sinter, coke, and limestone is dumped into separate "storage bins." The various raw materials are weighed according to a certain recipe designed to yield the desired hot metal and slag chemistry. This material weighing is done under the storage bins by a rail-mounted scale car or computer-controlled weigh hoppers that feed a conveyor belt. The weighed materials are then dumped into a "skip" car which rides on rails up the "inclined skip bridge" to the "receiving hopper" at the top of the furnace. The cables lifting the skip cars are powered by large winches located in the "hoist" house. Some modern blast furnaces accomplish the same job with an automated conveyor stretching from the stockhouse to the furnace top.

At the top of the furnace, the materials are held until a "charge" usually consisting of some type of metal (ore, pellets, or sinter), coke, and flux (limestone) has accumulated. The precise filling order is developed by the blast furnace operators to carefully control gas flow and chemical reactions inside the furnace. The materials are charged into the blast furnace through two stages of conical "bells" which seal in the gases and distribute the raw materials evenly around the circumference of the furnace "throat." Some modern furnaces do not have bells but instead have two or three air lock-type hoppers that discharge raw materials onto a rotating chute which can change angles allowing more flexibility in precise material placement inside the furnace.

Also at the top of the blast furnace are four "uptakes" where the hot, dirty gas exits the furnace dome. The gas flows up to where two uptakes merge into an "offtake." The two offtakes then merge into the "downcomer." At the extreme top of the uptakes, there are "bleeder valves" which may release gas and protect the top of the furnace from sudden gas pressure surges. The gas descends in the downcomer to the "dust catcher," where coarse particles settle out, accumulate, and are dumped into a railroad car or truck for disposal. The gas then flows through a "venturi scrubber" which

removes the finer particles and finally into a "gas cooler" where water sprays reduce the temperature of the hot but clean gas. Some modern furnaces are equipped with a combined scrubber and cooling unit. The cleaned and cooled gas is now ready for burning.

The clean gas pipeline is directed to the hot blast "stove." There are usually three or four cylindrical-shaped stoves in a line adjacent to the blast furnace. The gas is burned at the bottom of a stove, and the heat rises and transfers to the refractory bricks inside the stove. The products of combustion flow through passages in these bricks, out of the stove into a high "stack" which is shared by all of the stoves.

Large volumes of air, from 80,000 ft^3/min to 230,000 ft^3/min, are generated from a turbo blower and flow through the "cold blast main" up to the stoves. This cold blast then enters the stove that has been previously heated, and the heat stored in the refractory brick inside the stove is transferred to the "cold blast" to form "hot blast." The hot blast temperature can be from 1600 to 2300 °F depending on the stove design and condition. This heated air then exits the stove into the "hot blast main" which runs up to the furnace. There is a "mixer line" connecting the cold blast main to the hot blast main that is equipped with a valve used to control the blast temperature and keep it constant. The hot blast main enters into a doughnut-shaped pipe that encircles the furnace, called the "bustle pipe." From the bustle pipe, the hot blast is directed into the furnace through nozzles called "tuyeres." These tuyeres are equally spaced around the circumference of the furnace. There may be 14 tuyeres on a small blast furnace and 40 tuyeres on a large blast furnace. These tuyeres are made of copper and are water cooled since the temperature directly in front of them may be 3600–4200 °F. Oil, tar, natural gas, powdered coal, and oxygen can also be injected into the furnace at tuyere level to combine with the coke to release additional energy, which is necessary to increase the productivity (Cores et al. 2007). The molten iron and slag drip past the tuyeres on the way to the furnace hearth, which starts immediately below the tuyere level.

Around the bottom half of the blast furnace, the "casthouse" encloses the bustle pipe, the tuyeres, and the equipment for "casting" the liquid iron and slag. The opening in the furnace hearth for casting or draining the furnace is called the "iron notch." A large drill mounted on a pivoting base called the "taphole drill" swings up to the iron notch and drills a hole through the refractory clay plug into the liquid iron. Another opening on the furnace called the "cinder notch" is used to draw off slag or iron in emergency situations. Once the taphole is drilled open, liquid iron and slag flow down a deep trench called a "trough." Set across and into the trough is a block of refractory, called a "skimmer," which has a small opening underneath it. The hot metal flows through this skimmer opening, over the "iron dam" and down the "iron runners." Since the slag is less dense than iron, it floats on top of the iron and down the trough, hits the skimmer, and is diverted into the "slag runners." The liquid slag flows into "slag pots" or into slag pits (not shown), and the liquid iron flows into refractory-lined "ladles" known as torpedo cars or sub-cars due to their shape. When the liquids in the furnace are drained down to the taphole level, some of the blast from the tuyeres causes the taphole to spit. This signals the end of the cast, so the "mud gun" is swung into the iron notch. The mud gun cylinder, which

was previously filled with a refractory clay, is actuated, and the cylinder ram pushes clay into the iron notch stopping the flow of liquids. When the cast is complete, the iron ladles are taken to the steel shops for processing into steel, and the slag is taken to the slag dump where it is processed into roadfill or railroad ballast. The casthouse is then cleaned and readied for the next cast, which may occur in 45 min to 2 h. Modern, larger blast furnaces may have as many as four tapholes and two casthouses. It is important to cast the furnace at the same rate that raw materials are charged and iron/slag produced so liquid levels can be maintained in the hearth and below the tuyeres. Liquid levels above the tuyeres can burn the copper casting and damage the furnace lining.

9.3 CO_2 Emissions

Industrial processes produce about 21 % of total CO_2 emissions. According to the IEA (International Energy Agency), the steel industry accounts for approximately 4–5 % of the global CO_2 emissions.

On average, 1.9 t of CO_2 are emitted for every ton of steel produced. Therefore, it is vital for the steel industry to accelerate the pace of innovations undertaken to achieve production solutions with reduced CO_2 emissions.

Steel production from complete cycle inherently needs the carbon as a reducing agent: the iron must be transformed from the state of oxide (Fe_2O_3, Fe_3O_4) to the metal (Fe). The system used for this transformation is the blast furnace. The technology of the blast furnace involves the use of 400–500 kg of carbon per ton of cast iron. The carbon is used for the reduction of iron oxide into metallic iron, to generate heat and as a constituent of the cast iron. At the end of the blast furnace process, the residual carbon (in the form of CO gas) is used in other systems in which the processing takes place from CO to CO_2.

Therefore, in a full-cycle plant, the production of CO_2 is linked to the chemical–physical laws of the steel production process.

To be met by 2020, which is referred to as the 20-20-20 target, this means at least a 20 % reduction of greenhouse gas emissions below 1990 levels, 20 % of energy consumption to come from renewable resources, and a 20 % reduction in primary energy use compared to projected levels, to be achieved by improvements in energy efficiency. The iron and steel industry is one of the biggest industrial emitters of CO_2. It is estimated that between 4 and 7 % of the anthropogenic CO_2 emissions originate from this industry in EU-27, which generated 252.5 million tons of CO_2 emissions on average during the period 2005–2008. The ongoing increase in world steel demand means that this industry's energy use and CO_2 emissions continue to grow, so there is significant incentive to develop, commercialize, and adopt emerging energy efficiency and CO_2 emission reduction technologies for steel production. Furthermore, the iron and steel industry is the largest energy-consuming industry in the world, as well as the most important sources of CO_2 emissions.

Global warming has become a matter of real concern. The people all over the world are focusing on innovative green technologies in different sectors. Iron and steelmaking is critical from the perspective of greenhouse gases. Iron and steelmaking is among the largest energy consumer in the manufacturing sector, since it involves many energy-intensive processes that consume raw and recycled materials in large quantities. Raw materials with intensive carbon contents which are the primary resources for steel production influence climate changes materially. About half of the steel industry's energy derives from coal, and a large portion of this is consumed during the reduction of iron ore to pig iron.

Since conventional steelmaking processes are highly polluting, a search for some less polluting technology options is necessary. It is believed that coke making, steelmaking, and hot rolling areas hold vast scope for minimizing pollution levels leading to a cleaner and greener environment.

Coke oven by-product plants with complete gas tight collector headers in the by-product recovery plant lead to a higher eco-friendly process. Another eco-friendly option is to develop new coking process that reduces emissions at the source. The aim should be to approach zero pollution level. Opportunities for pollution minimization include the reduction of slag volume through better control of lime input to the furnace and improved control of silicon and sulfur in blast furnace hot metal.

Steel companies have both challenges and opportunities to improve their management practices and respond effectively to the needs of environment protection. Many leaders in the steel industry, as well as in other sectors, are beginning to practice new technologies and adopt management principles that reduce greenhouse gas emissions and minimize overall climate impact. They have, for example, launched voluntary emission reduction programs and are participating in emission trading markets. With the ushering in the Kyoto Protocol, the industry will be expected to calculate and manage actual reductions in greenhouse gas emissions, as opposed to improvements in emission intensity levels that occur normally over time. Purchasing and producing renewable energy, investing in low-carbon technologies, working to improve energy efficiency, and offering new products and services aimed at reducing emissions are all meaningful strategies for the steel industry to undertake. It is important to monitor the sustainability indicators for their mining as also iron and steelmaking so that both current and future generations will stand to derive economic advantages.

The challenge, therefore, is to improve the technologies that will bring reduced consumption of energy, reduced consumption of raw materials, and reduced levels of emissions besides being cost effective. Steel being one of the major energy consumers in the manufacturing sector, major intervention will be required in this aspect. So, a road map for achieving energy efficiency and energy conservation will be required.

The transition to a clean, green world will transform our whole economy. It will change our industrial landscape, our supply chain, and the way in which we all work and consume. Although the shift to a clean, green economy is an environmental and economic imperative, it is also an economic opportunity. Businesses and consumers can benefit from significant savings through energy and resource

efficiency measures. Supplying the demands of the clean, green economy offers a significant potential contribution to economic growth and job creation. The transition to a clean, green economy is necessary for two reasons. Primarily it is to stabilize greenhouse gas concentrations in the atmosphere. Secondly, the clean, green path is seen as a viable stimulus for a tipping economy. But it is also important to acknowledge that the "limits to growth" thesis has been confirmed after decades of poor criticism. The way forward to a sustainable future is to master and widely deploy clean engineering technologies.

For business, the transition to clean and green economy offers both commercial opportunities and the chance to save money and release productive resources through greater energy efficiency. At the heart of the clean, green industrial strategy are drivers of fundamental change in four key areas:

- Energy efficiency to save businesses, consumers, and the public service money
- Putting in place the energy infrastructure for the world's clean, green future in renewables, nuclear, carbon capture, and storage
- Development and production, for example, of clean, green technologies
- Ensuring skills, infrastructure, procurement, research and development, demonstration, and deployment policies to locate and develop a clean, green business and make sure international business recognizes that

So, the global shift to a clean, green economy could help to drive renewed growth that will lift us out of the economic downturn. It will be key in the long-term industrial future.

9.4 Experimental Procedure

Many of the blast furnace quality and performance indices are strictly dependent on sinter plant ones, and the quality and properties of raw materials must be analyzed before each blast furnace production cycle. The data can be collected from a plant in a definite period, and the working and useful volumes of the blast furnace are specified. The productivity data can be calculated referring to the working volume. Pellets, limestone, and coke compositional and quality ranges must be analyzed at each cycle, and the data must be reported. The material charges can be constantly monitored through the flux analysis of parallel bunkers at the top of the blast furnace. Then, the main independent variables can be underlined; the weight of such parameters on productivity and CO_2 emissions must be analyzed. The composition of the flue gases can be monitored according to EN-1948 parts 2 and 3, EN-1948SS (sampling standards, Wellington Laboratories), EN-1948ES (extraction standards, Wellington Laboratories), and EN-1948IS (injection standards, Wellington Laboratories), by employing a high-resolution gas chromatograph and a high-resolution selective mass detector, such as gas chromatograph "PCF Elettronica" and mass detector "Exactive," visible in Figs. 9.1 and 9.2.

Fig. 9.1 Gas chromatograph

Fig. 9.2 High-resolution selective mass detector

The automatic gas chromatograph can perform continuous analysis of a wide range of volatile organic compounds. It is based on the technique of the gas chromatographic separation and uses a flame ionization detection (FID). A pump downstream of the system fills a capillary which, brought to atmospheric pressure to obtain repeatable sampled volumes, is introduced via a rotary ten-way valve, in a gas chromatographic column for the separation of other organic substances of interest. The values obtained are integrated with a calculation software, by providing concentration by volume (ppmv) or weight (mg/m^3) (Table 9.3).

The aim of this paper is the research of an "optimum" condition in the development of the metallurgical BF process. The main goal is to analyze and optimize the emission of CO_2 and productivity in the BF after optimizing, for example, the emissions of PCDD/F, SOx, and NOx and productivity of a sintering plant.

Table 9.3 Example of information on input variable experimental setup for the blast furnace

Sinter productivity	Reduction rate	Coke rate	Sinter rate	Lime rate	O_2	T
30.6	42.5	645	910	102	44	2050
21.7	40.8	380	745	125	44	2000
25	40	310	1025	129	34	2100
22	80	300	388	145	31	2040
30.6	88	310	690	130	26	2050
25	82	298	388	108	24	2040

To do this, all the data must be collected in a broad period and can be analyzed by employing a multi-objective optimization tool, such as "modeFRONTIER" (ESTECO).

modeFRONTIER is an open system for the multi-objective and multidisciplinary optimization, based on the use of the Pareto limit frontier in space of the goals built on the industry needs. The system allows, for example, a multipurpose optimization (for problems with continuous, discrete, or mixed variables and variables compared to the limits/conditions that may develop during the process) or to formalize and manage a workflow to implement processes of any complexity in a flexible and dynamic way or to use a meta-model and the response surface methodology (RSM), to further reduce calculation times and increase information.

The optimization analysis can be achieved by considering the BF as a "black box" and applying the concept of input–output model. Thus by acquiring data from sensors located at the designated points of BF, various output parameters can be instantaneously determined and compared. Basically, an enormous number of data points each consisting of a setting of the critical input parameters of the blast furnace and the associated productivity values can be recorded on a real-time basis.

9.5 Results and Discussion

The target of the study is the definition of the main processing parameters leading to an optimization of blast furnace productivity with a decrease in CO_2 emissions. During blast furnace operations, many factors influence the behavior, and a serious selection of the independent variables affecting the productivity and the dangerous emissions has been performed. High productivity operation of a blast furnace requires enhancing reducibility and improving reduction behavior at high temperatures of sintered ore. The study can be started, for example, from the results previously obtained with optimization of a sintering plant (Cavaliere and Perrone 2013). It can be performed an analysis on the sinter plant operations in terms of productivity vs. reduction rate for different values of productivity of the blast furnace.

The optimal operating conditions of the sinter machine were fixed as shown in Table 9.4, corresponding to the underlined points in Fig. 9.3.

Table 9.4 Sinter output derived from the optimization study and employed as starting data for the BF operation analyses

	SOx (mg/kg)	NOx (mg/kg)	PCDD/F (ng I-TEQ/Nm^3)	Productivity (t/m^2/24 h)
Optimal design	297	201	0.45	29.8
Legal limit	400	400	0.40	

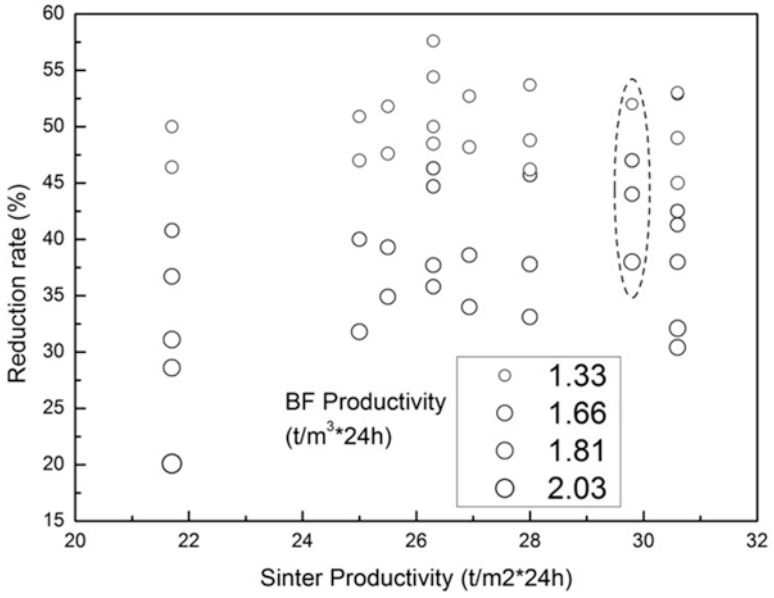

Fig. 9.3 Reduction rate as a function of sinter productivity and blast furnace productivity

Starting from such results, different BF operating conditions can be analyzed in order to increase the productivity taking into account the control of CO_2 emissions. In the sintering conditions described in Fig. 9.3, the different material qualities must be recorded, and the compositional and physical properties of the sintered material are indicated in Table 9.5.

The blast furnace is a reactor inside which gaseous, liquid, and solid phases coexist while consuming sinter, pellets, coke, and raw materials. All such phases influence the BF productivity through different physical–chemical, mechanical, and fluid processes and different endothermic and exothermic reactions, all acting simultaneously and affecting each others. In the blast furnace, formation of slag and the mineralogical transformation that the slag undergoes during the descending of burden inside the furnace influence the quality of hot metal. It is known that the components of slag, namely, silica and alumina, increase the viscosity, whereas the presence of calcium oxide reduces the viscosity. The melting zone of slag determines the cohesive zone of the blast furnace, and hence the fluidity and melting

Table 9.5 Sinter properties

Sinter	
Yield (%)	78–89
Fe (%)	58.3–59.1
FeO (%)	4.65–7.95
Al_2O_3 (%)	1.65–1.7
MgO (%)	1.5–1.6
Basicity ratio	1.8–2.21
Tumbler index	78–82.1

characteristics of slag play a major role in determining the blast furnace productivity; the way how ferrous burden materials soften and melt greatly affects the furnace's performance. Initially iron-rich slag is formed, and thereafter due to assimilation of CaO and MgO from the flux, the composition of slag varies. As the slag trickles down, it assimilates silica and alumina of ash, generated from the combustion of coke. The process of trickling down depends on viscosity of slag, which further is governed by the composition and temperature of the melt. The softening and melting behavior of ore is significantly affected by its rate of reduction, which is determined by its physical structure and chemical composition. The high levels of Fe and FeO coupled with the low levels of Al_2O_3 in the sinter guarantee further high levels of reducibility. Another important effect is the optimal composition in terms of MgO content leading to very high levels of sinter reducibility in the BF (Shen et al. 2006).

Many interesting papers describe the effect of raw material properties on blast furnace indexes (Jiang et al. 2010). This importance originates from the behavior of minerals during combustion. They can influence coal reactivity, and their transformations can have a detrimental impact on heat transfer process efficiency. High levels of basicity of the sinter allow to reduce the limestone addition, blast volume, and slag volume and consequently to reduce the coke consumption. An increase of basicity catalyzes the coke reactivity. In addition, heat loss decreases and furnace productivity rises. In general an increase in sinter basicity is well known to have a positive effect on all the quality and performance indices of the blast furnaces. In the last 50 years, more than 50 % of greenhouse emissions have been reduced especially through raw material rate and mixing optimization; anyway in normal blast furnaces, the consumed carbon is almost 30 % higher than the theoretical stoichiometric limit; a broad work can be made in such direction.

All the input parameters critically affecting the blast furnace indexes have been monitored for a long period and weighted. All the described description derives from long and deep analyses of the blast furnace behavior as a function of different input parameter variations. Coke quality is of fundamental importance in the operation of blast furnaces. Having coke that is of high quality with respect to its role as a reducing agent, a heat carrier, and a material which imparts good gas permeability to the charge is an important precondition for the stable operation of blast furnaces

(BFs). The importance of coke quality and its effect on the course of the smelting operation both increase with an increase in the size and capacity of the furnace. One of the main goals globally is to improve the coke-making process in order to prepare high-quality coke for low coke rate. Actually coke properties affect gas permeability, reduction efficiency, high-temperature properties, and segregation control. The coke size was strictly controlled in order to prevent deterioration of permeability and then of productivity of the BF (Sato et al. 1984; Nakagawa et al. 1992).

The relationships between the different parameters affecting the BF productivity and CO_2 emissions have been analyzed; actually just the parameters with heavy weight on such outputs were taken into account. Validation is important in order to determine if the model description is sufficient to solve the problems formulated. Both the model and model results have been validated.

Much attention must be taken in coke rate employment. In the blast furnace, the rate of consumption is governed by the reducibility of the ore and sinter and the reactivity of the coke. Coke rate and sinter rate have a strong effect on BF productivity, as shown in Fig. 9.4.

Coke rate and sinter rate have a strong effect on BF productivity. The furnace performance indices depend on the behavior of the coke throughout the entire volume of the furnace. It is necessary to analyze how an optimization of raw material utilization is compatible with the productivity of the blast furnace; one of the more direct ways is to couple the analysis of material flow and consequent productivity with the specific reducibility as a function of the variation of coke and sinter rate. The softening of burden materials is an extremely complex phenomenon, but the furnace investigations indicate that very significant productivity gains may be possible if the softening behavior of raw materials can be confined to a narrow temperature range after a high degree of reduction has been attained. In addition, a high reducibility of the materials is directly related to energy saving which represents a crucial need in the industrial practice. High productivity operation of a blast furnace requires enhancing reducibility and improving reduction behavior at high temperatures of sintered ore. The present analysis shows that productivity increases with the decreasing of coke rate and by increasing the sinter rate up to a limit in which an inversion of the trend can be underlined. In the case of sinter rate, productivity increases with sinter reducibility. Such behavior is due to a decrease in reduction time in the BF and an increase in the indirect reduction operations (Mousa et al. 2010). In this way it is possible to identify operating conditions coupling both a reduction in coke consumption and a good level of productivity in the blast furnace.

The variables which can be manipulated in a blast furnace can be divided into two classes, those entering the system from the top and those entering the system from the bottom. Between all the variables influencing productivity and emissions, the only ones to be considered are those with the heavier weight on such outputs; the manipulated variables entering from the top are the ore/coke ratio and the basicity ratio. The basicity ratio is related to the amount of flux material limestone and added per ton of hot metal produced. The manipulated variables from the bottom are the temperature and the fuel/ore ratio. For the efficient operation of the steelmaking

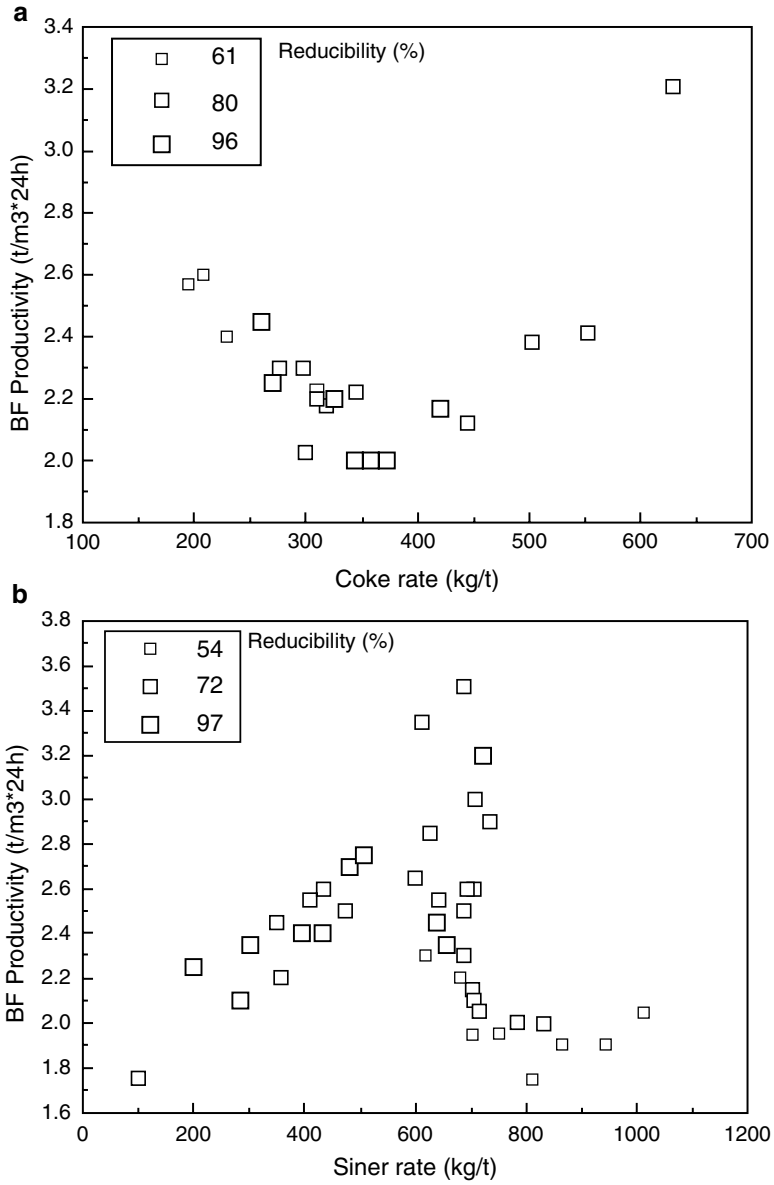

Fig. 9.4 Blast furnace productivity as a function of coke rate and reducibility (**a**) and as a function of sinter rate and reducibility (**b**)

process, the hot metal produced in the blast furnace has to meet stringent specifications with respect to composition and temperature (Fig. 9.5).

Combustion conditions strongly affect the blast furnace productivity; the external parameters easily tunable are represented by temperature and oxygen variation. Temperature and gas oxygen content strongly influences metal transformations and

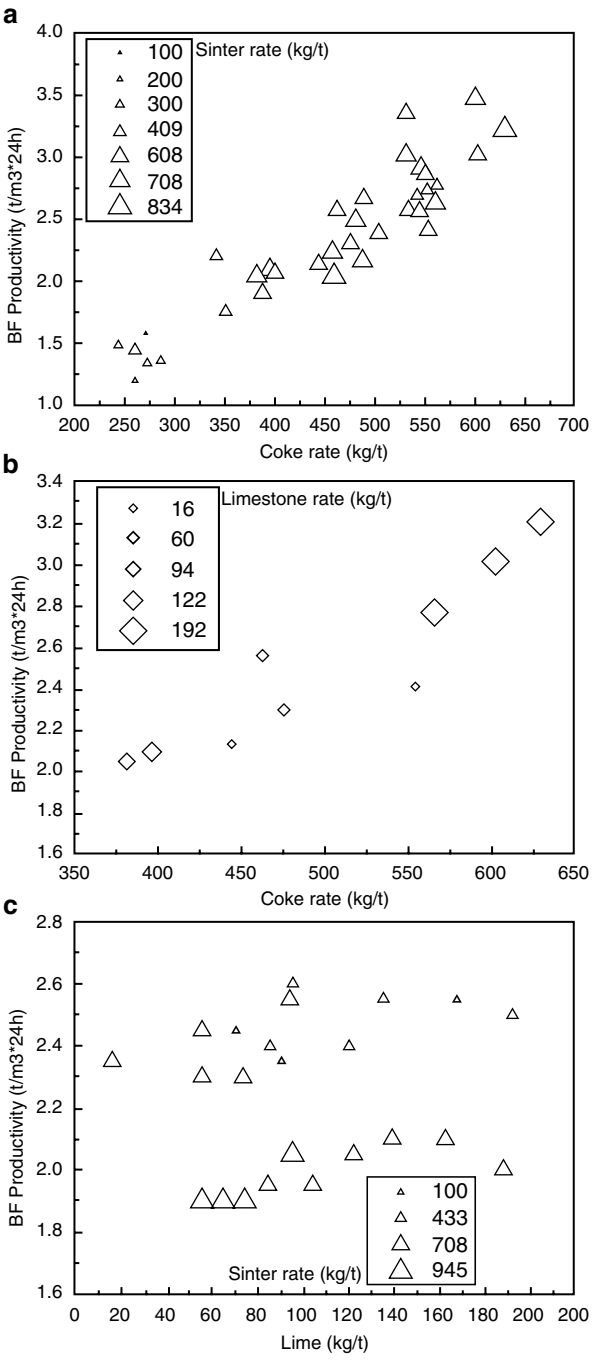

Fig. 9.5 Factors affecting BF productivity, coke and sinter rate (**a**), coke and limestone rate (**b**), and lime and sinter rate (**c**)

consequently BF productivity. An increase in productivity on the one hand requires an increase in the gas throughput, which implies improvement in furnace permeability, and on the other hand a reduction in the specific gas requirement, which finally means a reduction in the specific consumption of reducing agents. The blast furnace is a countercurrent reactor in which the reducing gas is produced by coke carbon gasification with the oxygen of the hot blast injected via tuyeres in the lower part of the furnace. This reducing gas flows upward reducing the iron-bearing materials charged at the top of the furnace. Permeability of the ferrous burden and coke column for the gas flow is inseparably linked together with the increase of gas throughput. In the recent years, oxygen enrichment has been indicated as a strong possible factor in reducing coke consumption in the blast furnace. Reduction of lower oxides can be controlled by tuning the oxygen potential. In spite of the variation of the direct reduction rate, coke saving and productivity are possible through the optimization of oxygen tuning in the blast. In addition, it is well known that over 30 % of the final cost of cast iron is dependent on energy consumption in the blast furnace. Temperature and oxygen addition influences BF productivity as shown in Fig. 9.6.

The maximum increase in oxygen content is also limited by the fact that the pressure of the blast air is theoretically and practically restricted. Basically CO_2 emissions depend on different parameters such as the improvement of shaft efficiency, the charge of metallic materials, the heat control in the BF, and the control of equilibrium FeO/Fe and then oxygen balance. Actually all the main input parameters influence CO_2 emissions, first of all coke and sinter rate (Fig. 9.7).

For further analysis coke rate/sinter rate ratio has been employed into the graphs; such ratio and limestone addition influences CO_2 emissions (Fig. 9.8); CO_2 emissions decrease considerably with coke rate decrease and low levels of limestone addition.

Finally, it is possible to underline an important relationship between sinter rate/coke rate ratio, CO_2 emissions, and productivity (Fig. 9.9) that can be interpolated by a cubic spline very useful in industrial operations.

9.6 Conclusions

The effect of the changing operating parameters on the plant productivity and greenhouse emissions has been investigated. In the study, several efficiency improvements were identified as regard to coke reduction, productivity, and CO_2 emissions. Multiple regressions have been established between the main operational parameters of the blast furnace and the productivity and CO_2 emissions.

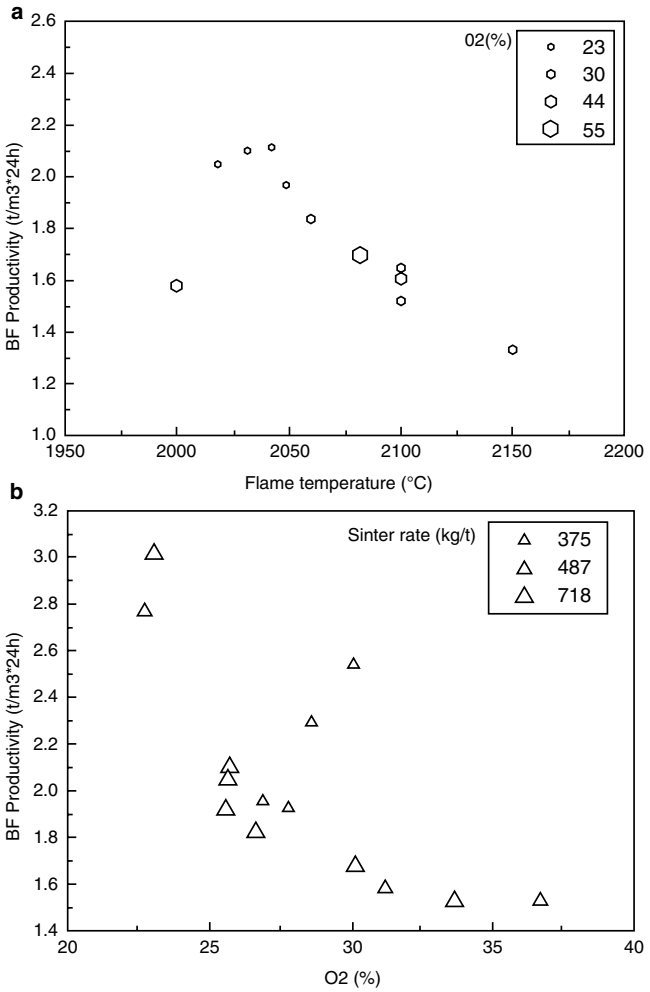

Fig. 9.6 BF productivity as a function of flame temperature and oxygen content (**a**) and as a function of oxygen content and sinter rate (**b**)

Sinter and coke properties were fixed into very strict ranges belonging to previous studies; such previous studies have been performed by focusing on a strong reduction of dangerous emissions. As a general point of view, the precise control of all the main processing parameters from the sintering operations to the BF ones leads to a strong reduction in dangerous emissions and to good levels of plants productivity.

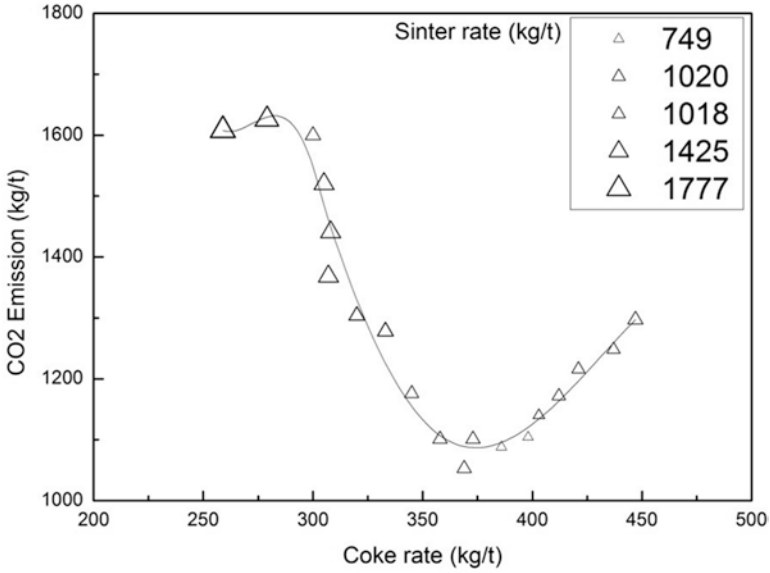

Fig. 9.7 Carbon dioxide emissions as a function of coke and sinter rate

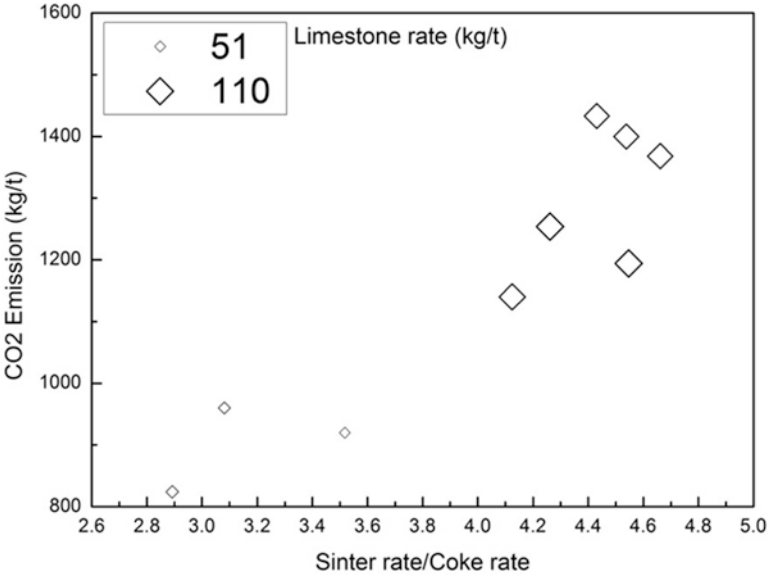

Fig. 9.8 Carbon dioxide emissions as a function of sinter/coke rate and limestone rate

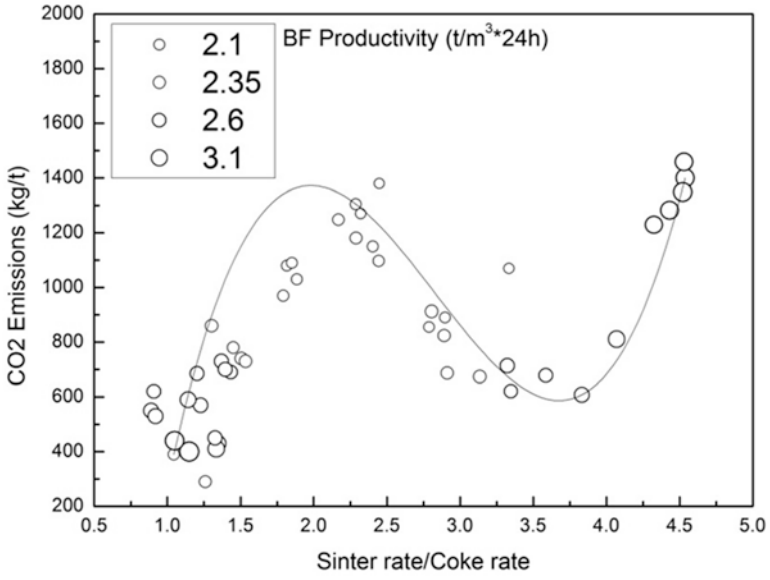

Fig. 9.9 Influence of raw materials and blast furnace productivity on carbon dioxide emissions

References

Cavaliere P, Perrone A (2013) Analysis of dangerous emissions and plant productivity during sintering ore operations. Ironmak Steelmak 40:9–24. doi:10.1179/1743281212Y.0000000019

Cores A, Babich A, Muñiz M, Isidro A, Ferreira S, Martín R (2007) Iron ores, fluxes and tuyere injected coals used in the blast furnace. Ironmak Steelmak 34:231–240. doi:10.1179/174328107X168066

Jiang T, Li GH, Wang HT, Zhang KC, Zhang YB (2010) Composite agglomeration process (CAP) for preparing blast furnace burden. Ironmak Steelmak 37:1–7. doi:10.1179/174328109X462995

Mousa EA, Senk D, Babich A, Gudenau HW (2010) Influence of nut coke on iron ore sinter reducibility under simulated blast furnace conditions. Ironmak Steelmak 37:219–228. doi:10.1179/030192309X12506804200906

Nakagawa Y, Sawai T, Hasegawa J (1992) Tetsu-to-Hagané 78:S55

Sato T, Sumigama T, Yamaguchi A, Kimura K, Shimomura A, Furuya S (1984) Tetsu-to-Hagané 70:S777

Shen F, Jiang X, Wu G, Wei G, Li X, Shen Y (2006) Proper MgO addition in blast furnace operation. ISIJ Int 46:65–69. doi:10.2355/isijinternational.46.65

Chapter 10
Recent Trends in Ironmaking Blast Furnace Technology to Mitigate CO_2 Emissions: Tuyeres Injection

E.A. Mousa, H.M. Ahmed, N.N. Viswanathan, and M. Larsson

Abstract Minimizing the coke consumption in the blast furnace is the key to achieve both ecological and economic aspects by reducing the CO_2 emissions and the overall hot metal production cost. Complementary injection of cheaper auxiliary fuels and waste materials into the blast furnace via tuyeres has been greatly modified in the recent years to reduce the expensive coke consumption. Nowadays, most of the blast furnaces all over the world use pulverized coal at different injection rates. The greatest influence of coal injection on lowering the production cost and enhancement of hot metal production rate has led to further investigations on the injection of various other auxiliary materials including coke oven gas, converter gas, blast furnace dust, waste plastics, charcoal and torrefied biomass. In addition,

E.A. Mousa (✉)
Process Integration Department, Swerea MEFOS, SE-971 25 Luleå, Sweden

Minerals Technology Division, Central Metallurgical Research and Development Institute, P.O. Box 87, Helwan, Cairo, Egypt
e-mail: Elsayed.Mousa@swerea.se

H.M. Ahmed
Minerals Technology Division, Central Metallurgical Research and Development Institute, P.O. Box 87, Helwan, Cairo, Egypt

MiMeR-Minerals and Metallurgical Engineering, Luleå University of Technology, SE-971 87 Luleå, Sweden
e-mail: Hesham.Ahmed@ltu.se

N.N. Viswanathan
Department of Metallurgical Engineering and Materials Science, Centre of Excellence in Steel Technology (CoEST), IIT Bombay, Mumbai 400076, India
e-mail: vichu@iitb.ac.in

M. Larsson
Process Integration Department, Swerea MEFOS, SE-971 25 Luleå, Sweden

Energy Engineering, Department of Engineering and Mathematics, Luleå University of Technology, 971 87 Luleå, Sweden
e-mail: Mikael.Larsson@swerea.se

P. Cavaliere (ed.), *Ironmaking and Steelmaking Processes*,
DOI 10.1007/978-3-319-39529-6_10

trials on the injection of iron ore fines, low reduced iron and BOF slag have been recently studied. The injection rate of auxiliary materials into the blast furnace should be optimized to attain the minimum coke consumption and stable operation. The present chapter will discuss the influence of various materials injection on the blast furnace operation. The injection limit and changing of the blast furnace operating conditions, hot metal quality and coke consumption will be explained based on the experimental trials and mathematical modelling.

10.1 Introduction

Iron and steel industry is one of the most important sectors which have a great impact on the global growth and economy. The steel production is sharply increased in the recent years to reach more than 1662 million tons in 2014, up by 1.2 % compared to 2013 (World Steel Association 2014). By 2050, steel use is expected to be increased by 1.5 times higher than present levels in order to meet the future needs. On the other hand steel manufacturing is one of the largest energy- and carbon-consuming sectors. The global energy consumption in steelmaking is estimated to be about 20 % of the annual industrial energy requirements. The fossil fuels represent the main source of heat and reducing agents in steelmaking and therefore a major contributor to the global anthropogenic CO_2 emissions. According to the International Energy Agency, the iron and steel industry accounts for approximately 6.7 % of total world CO_2 emissions (World Steel Association 2014; Brown et al. 2012). The CO_2 emission from iron- and steelmaking was 2.3 billion tons in 2007, and it is expected to reach 3.0 billion tons in 2050 (International Energy Agency 2010). Nowadays, the reduction of specific energy consumption and gas emissions is coming on the top priorities of iron- and steelmaking due to the dynamic growth of energy prices as well as the commitment of governments to decrease CO_2 emissions according to the Kyoto Protocol (Birat and Hanrot 2005). The ironmaking process is the highest CO_2 emission part in steel production due to the intensive utilization of fossil fuels for reduction of iron ore to iron and subsequent heating and melting of reduced iron. The most common ironmaking process used in the world is the blast furnace which produces about 70 % of total world steel production. Recently, the ironmaking processes have undergone tremendous modifications and improvements to reduce the energy consumption and CO_2 emissions; however, further reduction is still required to secure the future sustainability of this vital industry. The modifications and improvements in energy consumption have been offset by increasing the total production, and consequently the CO_2 emission has continued to rise dramatically. Projections of future energy use and CO_2 emissions show that without decisive action and innovative solutions, these trends will be continued. Therefore, reducing emissions from iron and steel industry requires sustainable and unlimited efforts for the development and deployment of new approaches and innovations.

Although the steel industry is energy and carbon intensive, it is important to mention that steel industry represents the core of green economy. The sectors and technologies which drive the green economy such as wind energy, low-carbon transport, clean energy vehicles, fuel-efficient infrastructure and recycling facilities are all dependent on steel products. According to EU ambition, an 80 % cut of fossil CO_2 emissions compared to 1990 levels has to be achieved by 2050. The utilization of auxiliary fuels in the blast furnace is one of the vital options to reduce the coke consumption and consequently the CO_2 emissions. An increasing attention has been recently paid on enhancing the replacing rate of coke by more environmentally friendly alternative sources. Injection of pulverized coal into the blast furnace is one of the most promising options to reduce the coke consumption. The maximum utilization of in-plant-generated gases and flue dust as a source of heat and reducing source can greatly enhance the overall efficiency of steel industry. The partial substitution of fossil fuels, namely, coal and coke, with renewable biomass products in ironmaking processes represents one of the few choices which could be introduced in short and middle terms to reduce the fossil CO_2 emissions (Babich and Senk 2013). The injection of these different materials in blast furnaces is a great option to reduce the production cost, reduce dangerous emissions and increase the productivity. The present work discusses and evaluates the recent activities which have been conducted on the blast furnace tuyere injectants to reduce the energy consumption and CO_2 emissions.

10.1.1 Iron- and Steelmaking Technologies

Steelmaking process can generally be classified into four main different routes including blast furnace/basic oxygen furnace (BF-BOF), direct reduced iron/electric arc furnace (DRI-EAF), smelting reduction/basic oxygen furnace (SR-BOF) and melting of scarp in electric arc furnace. The BF-BOF route is the most important way for steel production using mostly coke and coal as energy and reducing agents. The BF-BOF route represents about 70 % of the world steel production. The recycling and melting of steel scrap in EAF represent the second important route for steel production after BF-BOF and account for 25 % of world steel production. The DRI-EAF route uses mainly natural gas as a source of energy and reducing agent and produces approximately 5 % of the world steel. The SR-BOF route is based on the combustion of coal for the reduction of iron ores without agglomeration and produces only 0.4 % of the world steel production.

10.1.2 Energy Consumption and CO_2 Emissions in Steel Industry

In the last 20 years, technology has become one of the main drivers of economic and social development. As a result, in 2011, the global consumption of electricity and primary energy in the end-use sectors has been sharply increased to reach more than

22,000 TWh and 14,000 Mt, respectively (World Energy Council 2013). The CO_2 emission has been increased from 21 Gt in 1993 to 30 Gt in 2011 with an expectation to reach 42 Gt in 2020. The total CO_2 emission from the industrial sectors is about 9.0 Gt from which 2.0–2.3 Gt is emitted from iron- and steelmaking. The fossil fuels (coal, oil and natural gas) cover more than 70 % of the total energy usage in industrial sectors (Brown et al. 2012). Nowadays, the energy consumption and environmental pollution represent the main challenges for steel industry. The blast furnace is considered the major contributor to greenhouse gas emissions in steel industry (Kim and Choi 2003). The production of 1.0 ton of rolled coil steel is accompanied by about 1.8 tons of CO_2 emissions (Birat 2010). The blast furnace, sintering and cokemaking contribute together about 90 % of this amount (Pardo and Moya 2013). The energy usage in the BF and the accompanied CO_2 emission are the highest in steelmaking route and account for 12.31 GJ/tHM and 1.22 tCO_2/tHM, respectively. In the last decades, intensive work has been carried out to reduce the coke consumption in the blast furnace. Such efforts have been succeeded to sharply minimize the coke consumption by about 60 % since 1960 (Schmöle et al. 2009). The partial replacement of coke by injection of other auxiliary fuels such as pulverized coal (PC), natural gases (NG) and oil via blast furnace tuyeres has been commercialized to save coke. Other trials have been conducted on the injection of coke oven gas, BOF gas and waste plastics (Babich et al. 2008). In the recent past, the coke consumption is in the range of 286–320 kg/tHM, and PC injection is 170–220 kg/tHM at the majority of the modern blast furnaces (Babich et al. 2002). Over decades, the charged burden materials have been improved and adopted to achieve low coke consumption, but further improvements for the traditional burden become extremely hard. Recently, stable blast furnace operation with PCI rates of around 200 kg/tHM and coke rate below 300 kg/tHM have been successfully maintained. However, higher injection rate of auxiliary materials on account of coke requires high quality burden materials and higher oxygen enrichment with sophisticated control systems and modifications in the transport and injection systems (Carpenter 2006). The network gas connection in the integrated steel plant provides a novel solution to reach the highest credits through an efficient utilization of by-product gases (Mousa et al. 2013a, 2014a; Diemer et al. 2007). Under the impact of the global environmental regulations and post-Kyoto requirements, solutions to curtail emissions from ore-based steelmaking industry have been launched in the CO_2 Breakthrough Programme (Birat 2010). The modelling and experimental approaches are still in action to evaluate the potential for lowering the CO_2 emissions, energy consumption, operating cost and future sustainability. Based on this, the main challenge which strongly faces the ironmaking industry today is how to achieve the low energy consumption and reduce CO_2 emissions with cheaper energy carriers and lower-quality raw materials without losing the hot metal quality or the blast furnace efficiency. Under this restricted situation, maximizing the auxiliary fuel injection into the blast furnace is considered one of the vital options to lower the operating cost and maximize the productivity. Usage of cheaper fuels and H_2-rich materials for partial substitution of metallurgical coke can effectively reduce the CO_2 emissions. The next sections will thoroughly discuss the tuyere injection of different auxiliaries' materials into the blast furnace.

10.2 Pulverized Coal Injection into BF

Pulverized coal injection (PCI) is one of the essential methods to enhance the blast furnace profitability. Due to the ease of use, oil and natural gas were popular injectants in the 1960s, but due to the oil crises in the 1970s, many companies stopped the oil injection and turned to coal injection since the 1980s. Nowadays, the vast majority of blast furnaces all over the world apply PCI due to the relatively lower cost of coal compared to other fuels beside the beneficial effect on the blast furnace efficiency. Injection of PC into the blast furnace provides various economic and operational benefits (Bennett and Fukushima 2003). These benefits are including: (1) lower consumption of expensive coke, (2) replacing high-rank expensive coal with low-grade cheaper coals, (3) longer life period for coke oven, (4) higher blast furnace productivity, (5) higher flexibility in BF operation, (6) improving the hot metal quality and (7) lower CO_2 emissions. The influence of PCI on coke consumption in the blast furnace is given in Fig. 10.1 (Bennett and Fukushima 2003). The data has been taken from a range of blast furnaces in Europe (EU), Japan (JP) and China (CH). The replacement ratio of PC for coke is about 1.0 at injection rate up to 200 kg/tHM. At higher PCI (>200 kg/tHM), there is a reduction in the incremental replacement ratio of PC for coke. In contrast with other fuels which could be injected through tuyeres, PC has the minimum negative impact on the raceway flame temperature, and therefore, it has the highest possible injection rate than other fuels. Thermal coal which is a type of bituminous coal is often used for injection. Thermal coal is relatively cheaper than coking coal which is used for cokemaking,

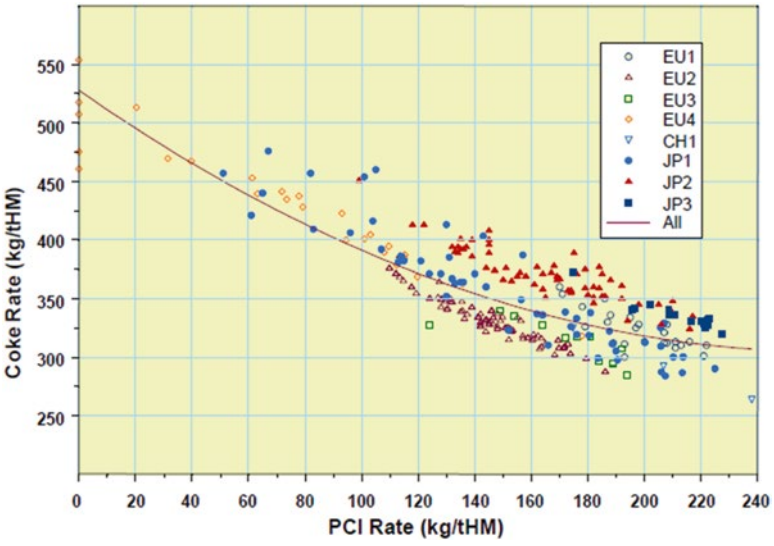

Fig. 10.1 Changing of coke rate with PCI in blast furnaces at various regions (Bennett and Fukushima 2003)

and this is another economical advantage of PCI. The combustion of PC in the raceway is a complex process that requires high control of various parameters. Efficient PCI is obtained by convenient coal treatment including the control of moisture content and grain size. The appropriate mixing of PC with hot blast, uniform distribution of PC across all tuyeres, low N_2 input into BF and maximizing retention time of coal in the tuyeres are necessary to achieve high combustion efficiency. The injection of coal through the tuyeres is certainly not new technology, but it has been recently developed to sustain optimum conditions.

10.2.1 PCI Technology

The first step in PCI technology is the production of pulverized coal particles followed by pneumatic conveying and then injection into the blast furnace. There are different processes that can be applied for PC injection into the blast furnace (Waguri 2003). The Armco pulverized coal injection system is represented schematically in Fig. 10.2 (Waguri 2003). The system consists mainly of raw coal feeder, pulverizer (mill), dryer, reservoir tank, distributor unit and pneumatic injection unit. The process started with coal screening to remove the tramp materials and then it is stored in raw coal bunker. The raw coal is pulverized (70–80 % <74 μm) and dried and then pneumatically conveyed to cyclone and filters. During this stage the PC is thoroughly dried to prevent saltation and compaction and to lower the negative effect of moisture on the combustion process. The PC is deposited in a single reservoir under inert atmosphere. The PC is fed, under the influence of gravity and pressurized nitrogen, into feed tanks which provide continuous flow of pulverized particles into the furnace. A single transport pipe carries the coal/gas mixture to a coal distributer in which the single stream is divided automatically into multiple equal streams of coal/gas mixture and conveyed by a pipe into each tuyere for injection into the blast furnace. The system is supported with block detector to avoid any blockage at tuyeres. The applied injection system has to be selected in order to accommodate the on-site design and the local conditions of the blast furnace. The injection rate can be also classified into (1) dilute phase and (2) dense phase (Weiser et al. 2006). The main difference between the dilute phase and dense phase of PCI system is the amount of gas that is used in conveying and injection (Schott 2015). The dilute phase is characterized by high gas velocity (more than 10 m/s) and low PC concentration (5–30 kg PC/m^3 of carrier gas), while the dense phase is characterized by low gas velocity (2–6 m/s) and high PC concentration (100–200 kg PC/m^3 of carrier gas). Due to the high energy consumption and the high wear resistance, the dilute phase is less economic compared to the dense phase. The oxygen-enriched hot blast (1100–1250 °C) is injected into the blowpipe at velocity 100–200 m/s (Sarna 2013). The coal/gas mixture (e.g. 150 kg coal/tHM) is injected by lance into the blowpipe at a rate equal to 150 g coal/m^3 of the blast. The residence time of PC

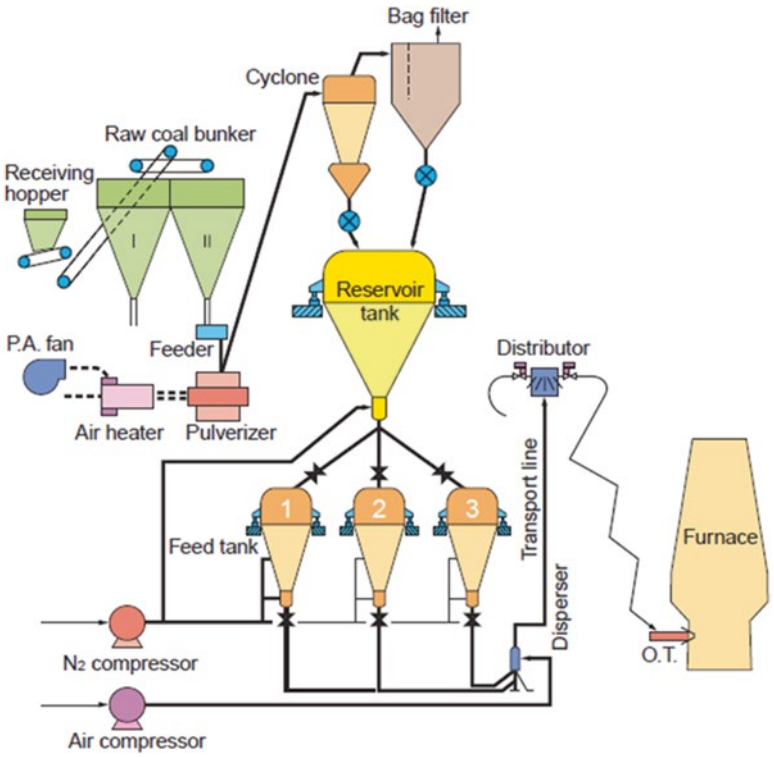

Fig. 10.2 Flowchart of ARMCO process for pulverized coal injection to BF (Waguri 2003)

in the raceway is very short: 20–30 ms. An alternative method of coal injection named granular coal injection (GCI) has been developed and evaluated at Bethlehem Steel (Hill et al. 2001). The GCI with a relatively bigger size (70–90 % >74 μm) has some economic benefits over normal PCI. The GCI required much less milling compared to PC which reduces the capital cost and saves about 60 % of grinding energy. At injection rate of 140 kg coal/tHM, it was found that the granular coal performs the same efficiency of pulverized coal which indicates that no intensive grinding of coal is required under this particular injection rate. On the other hand the construction of PC injection lance affects the efficiency of the combustion process. Three-dimensional computational fluid dynamics (CFD) model is applied to examine the coal combustion behaviour across the blowpipe, tuyeres and raceway of the blast furnace (Du et al. 2015). It was found that the coal combustion efficiency increased by 5.1 % using the double lance injection compared to single lance. On the other hand the oxy-coal injection lance showed higher coal combustion efficiency at oxygen enrichment higher than 90 %.

10.2.2 PCI Combustion

During the complete combustion of coal particles, three steps could take place. In the first step, the volatile matters of coal are released and combusted with the surrounding oxygen. These volatiles contain different gases including N_2, CO_2, H_2O and small portions of CO, H_2 and other types of hydrocarbon gases (C_xH_y). In the second step, the combustion of residual char takes place which has slower rate than combustion of volatiles. In the third step, ash is released after the complete combustion of char (Juniper and Schumacher 2013; Ishii 2000). A schematic view of the tuyeres and different zones and reactions in the raceway during PC injection is shown in Fig. 10.3 (Ishii 2000). The raceway can be classified into three main zones: (1) PC de-volatilization zone, (2) oxidation zone and (3) solution loss reaction zone. The concentration of oxygen sharply decreases in the oxidation zone due to its reaction with carbon of coke and coal to produce CO_2 as given in Eq. 10.1. As the oxygen concentration decreases, the solution loss reaction by CO_2 or steam takes place, as given in Eqs. 10.2 and 10.3, and the concentration of CO increases, while CO_2 decreases. Therefore, the reaction rate of PC is basically dependent on the oxygen content in the hot blast. The PC injection rate, blast condition (temperature, pressure, moisture and oxygen content), coal properties (carbon content, ash content, VM content, particle size), lance construction and properties of top-charged coke are important factors affecting the combustion efficiency of coal in the raceway:

$$C_{(s)} + O_{2(g)} = CO_{2(g)}; \quad \Delta H^\circ = -393.5\text{kJ / mol} \tag{10.1}$$

$$C_{(s)} + CO_{2(g)} = 2CO_{(g)}; \quad \Delta H^\circ = +172.46\text{kJ / mol} \tag{10.2}$$

$$C_{(s)} + H_2O_{(g)} = CO_{(g)} + H_{2(g)}; \quad \Delta H^\circ = +131.29\text{kJ / mol} \tag{10.3}$$

The raceway adiabatic flame temperature (RAFT) is defined as the temperature that the raceway gas reaches as soon as all C, O_2 and H_2O are converted to CO and H_2. The RAFT is a theoretical concept since not all reactions are accomplished in the raceway. The RAFT is normally in the range of 1900–2300 °C based on PCI rate, PC quality, blast temperature, blast moisture and oxygen enrichment. The RAFT is theoretically calculated from Eq. 10.4 (Greedes et al. 2009) developed using simple mass and heat balance. With increasing PCI, O_2 enrichment is an important factor that affects the RAFT. The O_2 content in the hot blast has to be adjusted with PCI amount at different production rates (Greedes et al. 2009). The higher the PCI rate, the higher O_2 enrichment is required to sustain the heat balance in the upper and lower part of the furnace. Too low RAFT results in very low top gas temperature which will delay the drying of the cold top-charged burden and consequently make the upper shaft less efficient. On the other hand too high O_2 enrichment in the blast is accompanied by relatively high RAFT which will result in an erratic descend of the burden. Therefore, the oxygen content in the hot blast has to be optimized very carefully to reach the proper RAFT and shaft efficiency:

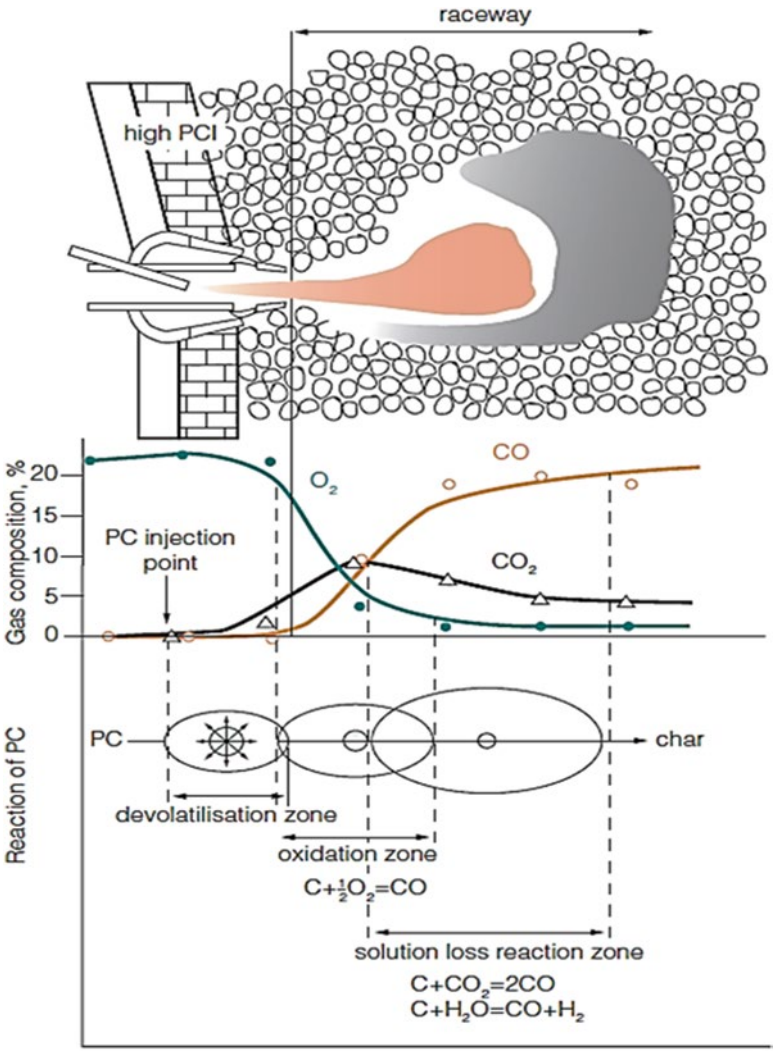

Fig. 10.3 Schematic diagram for PC reaction in raceway (Kamijou and Shimizu 2000)

$$\begin{aligned} \mathrm{RAFT} &= 1489 + 0.82 * \mathrm{BT} - 5.705 * \mathrm{BM} + 52.778 * \mathrm{OE} \\ &- 18.1 * \frac{\mathrm{Coal}}{\mathrm{WC}} * 100 - 43.01 * \frac{\mathrm{Oil}}{\mathrm{WC}} * 100 - 27.9 * \frac{\mathrm{Tar}}{\mathrm{WC}} * 100 \\ &- 50.66 \frac{\mathrm{NG}}{\mathrm{WC}} * 100 \end{aligned} \tag{10.4}$$

where BT is the blast temperature, °C; BM blast moisture, g/m^3; STP dry blast; OE oxygen enrichment (%O_2-21); Oil dry oil injection rate, kg/tHM; Tar dry tar injection rate, kg/tHM; Coal dry coal injection rate, kg/tHM; NG natural gas injection rate, kg/tHM; and WC wind consumption, m^3/tHM.

10.2.3 High Rate of PCI

For an optimal blast furnace operation using PCI, it is crucial to assure that the whole amount of the injected coal is gasified as fast as possible (Schott 2013). Estimating the average blast velocity in the raceway at 200 m/s, the residence time of small particles travelling with the gas would be ~10 ms (Bortz 1983). The transit time of the injected coal particles in the raceway could reach 20–30 ms (Mathieson et al. 2005). Within such limited time, the PC particles will not be completely combusted, and a considerable amount of char will escape from the raceway region to reach the active coke zone as can be seen in Fig. 10.4 (Mathieson et al. 2005).

Various problems could occur due to the high injection rate of PC as can be seen in Fig. 10.5 (Juniper and Schumacher 2013). The fine char particles tend to block the bed voids and consequently disturb the gas flow and increase the pressure drop inside the furnace, reduce the permeability of liquids and gases in the cohesive zone and reduce the shaft efficiency and the furnace productivity (Raask 1985; Lu et al. 2000). Moreover, the high PCI could enhance the carbon solution loss reaction at the lower part of the shaft and increase the CO content in the top gas. Since these fines are very light, it can be easily fluidized and elutriated which results in higher generation of carbon dust from the blast furnace. Therefore, various parameters have to be optimized when the blast furnace is working at a high rate of PCI as given in the countermeasure in Fig. 10.5. The particle size of the injected coal is another factor that significantly affects the efficiency of combustion. The optimum size range of PC normally contains ~80 % below 75 μm which has to be dried at 100–150 °C using an inert gas to remove the moisture (Ghosh and Chatterjee 2008). Intensive grinding of coal is not recommended as it will increase the power consumption and could deteriorate the particles flowability during the injection process. The hot blast temperature should be high (~1250 °C) to improve the efficiency of combustion. The combustion efficiency also depends on the coal rank which is related to the calorific value and the mineral contents (Bennett and Fukushima

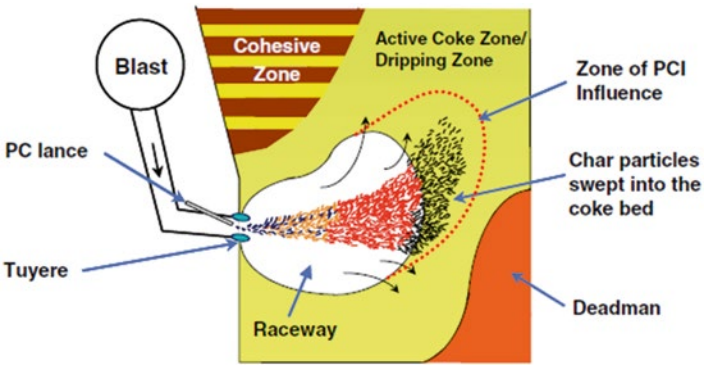

Fig. 10.4 Schematic of the lower zone of the blast furnace (Mathieson et al. 2005)

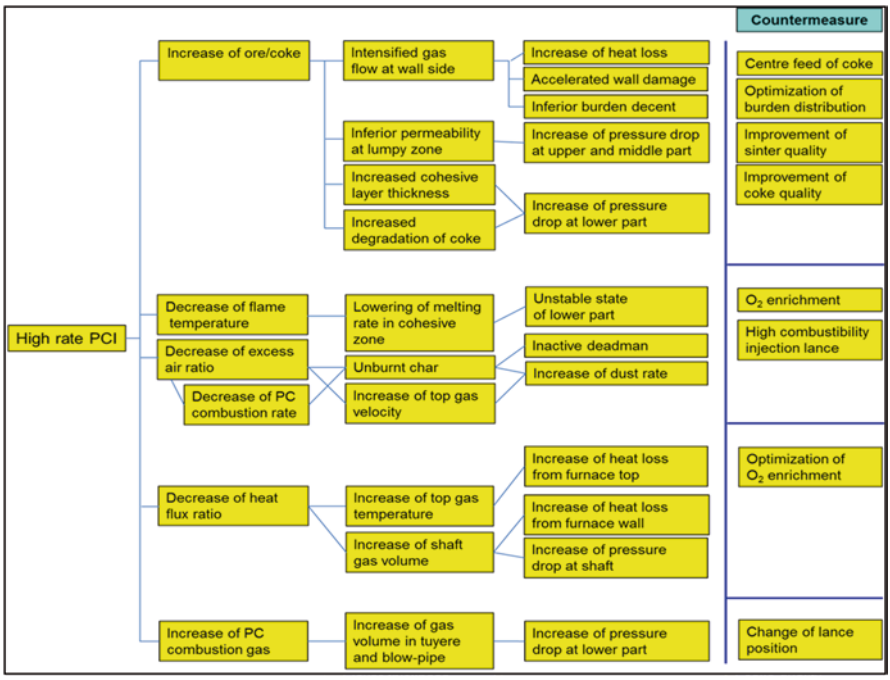

Fig. 10.5 Expected technical issues and countermeasure at high rate of PCI (Juniper and Schumacher 2013)

2003). The ash content of coal is an indicator of its mineral content, and it is considered an undesirable component because as the ash content increases, the carbon content decreases. Moreover, coals with high ash content will require additional basic fluxes which will increase the slag volume and energy consumption and reduce the productivity. Coals with higher volatile matter (VM) content exhibit superior combustibility due to the higher reactivity; however, coals with very high VM contain less carbon, and hence, the combustion efficiency in the raceway will be reduced (Ghosh and Chatterjee 2008). Also for high PCI, both sulphur and phosphorus should be kept as low as possible to avoid the negative effect on the hot metal quality.

10.3 Auxiliary Fuel Injection

10.3.1 Oil and Natural Gas Injection

The injection of oil and natural gas into the blast furnace was firstly implemented before PC, but the energy crisis during the 1970s resulted in more attention to pulverized coal injection. Nowadays, the countries which locally produce oil and

natural gas such as the USA, Russia and some other countries are still injecting these fuels into the blast furnace to reduce the coke consumption. It was reported that 1.0 ton of oil or natural gas replaces 1.2 tons of coke (Worrell et al. 2010; Lingiardi et al. 2001). The average consumption of natural gas is 70–100 m^3/tHM (~50–70 kg/tHM) but often exceeds to 150–170 m^3/tHM (~105–120 kg/tHM). The operation of blast furnaces using natural gas and oxygen-enriched blast is called composite blast technology. With oxy-oil technology the amount of injected oil could reach a level of 180 m^3/tHM (130 kg/tHM).

Oil and natural gas are decomposed and combusted in the blast furnace raceway (De Castro et al. 2002). The decomposition and combustion of hydrocarbons generate CO/CO_2 and H_2/H_2O. The CO_2 and H_2O in situ react with carbon of coke and PC or with hydrocarbons of natural gas to finally generate CO and H_2. The participation of hydrogen in the reduction of iron oxide leads to a decrease of CO_2 emissions. Furthermore, H_2 is a more effective reducing agent for wüstite than CO (Meschter and Crabaki 1979). The positive influence of H_2 on the reduction rate especially at elevated temperatures can be attributed to the higher gas diffusivity. The diffusivity coefficient of H_2/H_2O and H_2/N_2 gas mixtures is about 3–5 times as that of CO/CO_2 and CO/N_2 (Bogdandy and Engell 1971; Biswas 1981). In industrial blast furnace operation, the equilibrium shifted to more efficient gas utilization and consequently lower coke consumption by fuel oil injection (Strassburger et al. 1969). On the other hand the injected amount of auxiliary fuels such as heavy oil or natural gas into the blast furnace has to be carefully optimized to achieve the low energy consumption and high productivity since the reduction of wüstite with H_2 is an endothermic reaction and consequently more heat is required compared to the reduction with CO. Moreover, the C/H ratio in the injected fuel affects the RAFT. The heat of combustion increases as the C/H ratio increases because less heat will be consumed in the decomposition of hydrocarbons (Babich et al. 2002). The heavy oil and natural gas have higher percentage of hydrocarbons compared to coal/coke, and thereby, the endothermic effect of these hydrocarbons results in higher drop in RAFT (Babich et al. 2008). It was estimated that the RAFT will be decreased by 350–450 °C per 100 m^3/tHM of natural gas injection, 300–350 °C per 100 kg/tHM of heavy oil injection, 200–250 °C per 100 m^3/tHM of coke oven gas injection, 80–120 °C of low volatile coal injection and 150–220 °C of high volatile coal injection (Babich et al. 2002). To compensate the lowering of RAFT, the hot blast must be enriched with oxygen. However, the increase in the oxygen content of the blast reduces the nitrogen content and causes a drop in the top gas temperature. The top gas temperature must always be above the dew point to prevent any undesirable condensation of water vapour in the upper part of the furnace. Based on this concept, a minimum raceway adiabatic flame temperature (around 1900 °C) and a minimum top gas temperature (higher than 100 °C) must be maintained to ensure a stable blast furnace operation. Recent studies indicated that the rate of natural gas injection into the blast furnace could be increased significantly by injecting part of the natural gas in the shaft of the furnace. This will reduce the endothermic effect of natural gas injection on the RAFT, and the total oxygen consumption would be slightly lower compared with the tuyere-only injection (Jampani and Pistorius

2014). A mathematical model based on the heat balance in the bottom segment of the blast furnace has been developed to calculate the maximum injected amount of natural gas to attain the minimum value of RAFT, minimum possible coke consumption and the minimum direct reduction (Abdel Halim et al. 2009; Abdel Halim 2007). It was reported that the minimum coke consumption will be obtained when the coke carbon which is used as a source of heat is equal to the coke carbon which is consumed in the reduction processes (Abdel Halim et al. 2009).

10.3.2 Coke Oven Gas and Converter Gas Injection

The efficient utilization of integrated steel plant top gases becomes necessary to achieve profitability to steel mill operation from both economic and environmental aspects. The major fuel gases that could be recovered in the integrated steel works include blast furnace gas (BFG), coke oven gas (COG) and basic oxygen furnace gas (BOFG) (Wingrowe et al. 1999, Worrell et al. 2010). The COG has the largest net calorific value in the range of 16.4–18 MJ/Nm^3 (STP) compared to that of either BOFG (~8.8 MJ/Nm^3) or BFG (3.0–3.7 MJ/Nm^3) (Diemer et al. 2007; Diemer et al. 2004). The specific amount of generated coke oven gas is in the range of 410–560 Nm^3/t of coke, while the amount of BOFG is in the range of 50–100 Nm^3/t of steel in the suppressed combustion system, and it could reach 500–1000 Nm^3/t of steel in the open combustion system. The annual worldwide metallurgical coke production is more than 500 million tons which is produced from about 650 million tons of coking coals (Spirin et al. 2015). The cokemaking process is accompanied by more than 310 billion Nm^3 of COG (Yang et al. 2010). The COG is currently used after its cleaning from tar, naphthalene, raw benzene, ammonia and sulphur in heating of blast furnace stoves, ignition furnaces in sintering plant, heating furnace in rolling mills and electric power generation in power plant (Diemer et al. 2007; Diemer et al. 2004).

The estimations which have been carried out on optimizing the energy consumption in the integrated iron and steel works indicated that the utilization of COG for power generation is not always the optimal credits (Diemer et al. 2007). The composition of COG which is rich with hydrogen is attracting much attention for its utilization in the reduction processes (Tovarovskii and Merkulov 2011; Proface and Pivot 2011; Matsuzaki et al. 2012; Miwa et al. 2011). The flexibility of COG utilization in the integrated steel plant for DRI production through the addition of Midrex process is expected to be an efficient method that can introduce many benefits to the integrated steel mill (Diemer et al. 2004). The merging of the "traditional" ironmaking blast furnace with the "alternative" direct and smelting reduction processes is an innovative approach to achieve the economic and environmental targets of higher production and lower emissions. The recent studies which have been carried out to evaluate the reduction potential of original coke oven gas (OCOG) and reformed oven gas (RCOG) for direct reduction of iron ore pellets compared to reformed natural gas (RNG) indicated the high efficiency of these gases for DRI production

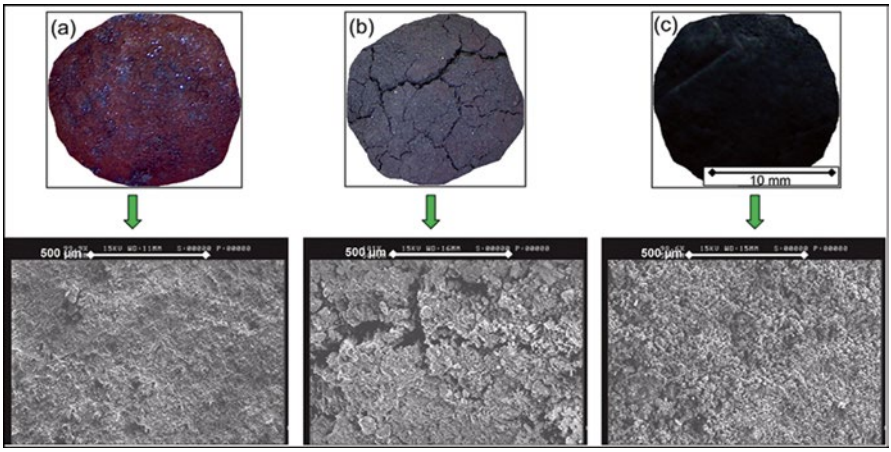

Fig. 10.6 External shape and outer surface of pellets: (**a**) original pellets, (**b**) after reduction with RCOG, (**c**) after reduction with OCOG (Mousa et al. 2013a, b)

(Mousa et al. 2013a, 2014a). An optimization for the reforming of coke oven gas is crucial to avoid the severe crack of pellets in the case of reduction with RCOG and the carbon deposition in the case of OCOG as shown in Fig. 10.6. The reduction potential of COG with/without mixing with converter gas (BOFG) has been studied for natural lump ore at 800–1050 °C (Mousa et al. 2014a, b). It was reported that the highest reduction rate was achieved with RCOG followed by OCOG. The reduction rate was decreased in the order of RCOG > OCOG > RNG > OCOG-BOFG > RCOG-BOFG at 900–1050 °C.

The injection of COG into the blast furnace through tuyeres has influence on the raceway conditions and iron ore reduction. The mathematical modelling on the injection of COG into the blast furnace tuyeres indicated better combustion conditions and higher injection rate by using two injection lances compared to one lance (Hellberg et al. 2005a, b; Slaby et al. 2006). The temperature distribution in the blast furnace with different levels of COG injection is given in Fig. 10.7, while the reduction distribution with different H_2 levels is given in Fig. 10.8 (Wang et al. 2011; Chu et al. 2012). The thickness of softening-melting zone decreases while the reduction is improved by increasing COG and H_2 injection into blast furnace, respectively. The combustion of COG hydrocarbons in the front of tuyeres by blast oxygen results in generation of carbon monoxide and hydrogen gases which increase the potential of reducing gas on account of inert N_2 (Hellberg et al. 2005a, b). The theoretical calculation and commercial trials which were carried out on the replacement of natural gas with coke oven gas in blast furnace showed lower coke consumption and higher hot metal production (Nogami et al. 2012). The high efficiency of COG is due to the fact that it contains 3.5–4.0 times less hydrocarbons compared to that of natural gas (Babich et al. 2008). This improves the combustion in the tuyere hearth, activates coke column and increases gas utilization in the furnace. A higher amount and higher heating value of blast furnace top gas under COG injec-

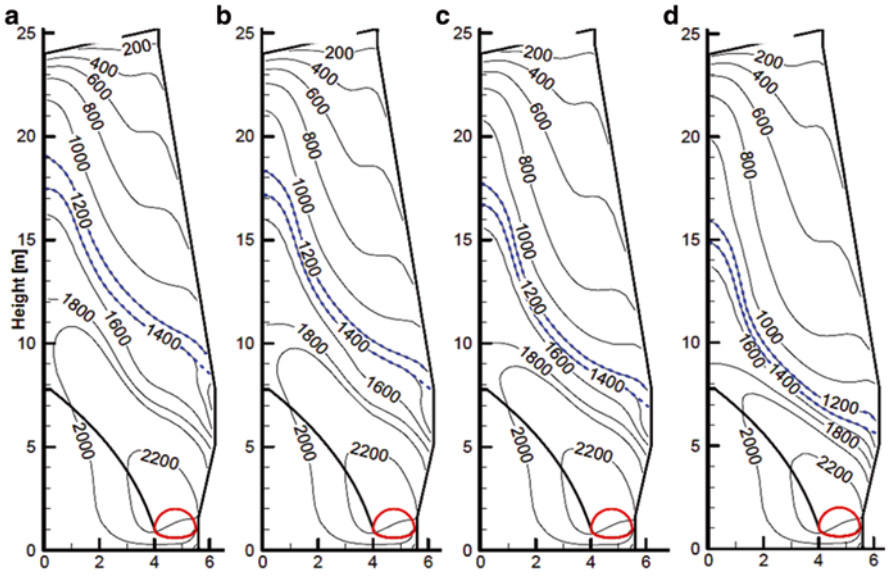

Fig. 10.7 Temperature distribution in BF under different injection levels of COG (Wang et al. 2011): (**a**) base case (**b**) 50 m^3 COG/tHM, (**c**) 100 m^3 COG/tHM, (**d**) 150 m^3 COG/tHM

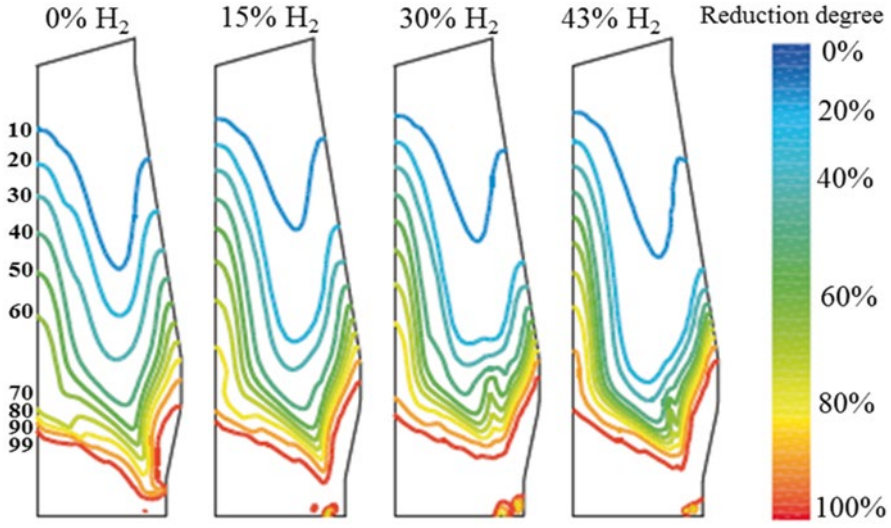

Fig. 10.8 Reduction distribution in BF under different levels of H_2 (Chu et al. 2012)

tion have been noticed (Nogami et al. 2012). The injection of COG into the blast furnace is practiced in some countries with different injection rates from about 30 to 280 m^3/tHM (Kovalenko et al. 1989; Bürgler et al. 2004). It was reported that the maximum level of COG injection into the blast furnace is 100 kg COG/tHM according

to the thermochemical conditions, while the replacement ratio is 0.98 ton of coke/t of COG (United State Environmental Protection Agency 2012). The reduction of iron ore sinter under simulated conditions of different injection levels (0–300 m^3 COG/tHM) of COG into the blast furnace has been investigated (Mousa et al. 2013b). The isothermal and non-isothermal reduction trials illustrated the enhancement of the reduction rate of sinter under the injection of COG due to the higher concentration of reducing agents (H_2 and CO) on account of inert N_2 (Mousa et al. 2013b).

10.3.3 Waste Plastic Injection

Recycling and utilization of waste plastics have received an increasing interest in the recent decades. The majority of this material is currently being landfilled or incinerated which causes environmental problems. The combustion of waste plastics generates hazardous pollutants, such as dioxins/furans, as well as undesirable carbon dioxide. The waste plastics can be efficiently utilized in blast furnaces as an alternative reducing agent and as a source of heat to reduce the coke consumption. As the plastics contain hydrogen and carbon, it can also provide additional benefits similar to oil and natural gas injection into the blast furnace. Due to the difficulty of waste plastic crushing, coarse particles were preferred to be injected into the furnace; however, the fine particles are better in combustion in the raceway. Therefore, a technology for fine pulverization of waste plastics has been developed and implemented in a full-scale industrial blast furnace in Japan. Since the collected waste plastics are a heterogeneous mixture from different types, it is recommended to conduct heat treatment at 200 °C before its injection into the blast furnace. The pretreatment will generate a homogenous pulverized waste plastic mixture (Asanuma et al. 2014). Moreover, the pretreatment of waste plastics will perform de-chlorination for the plastics containing chlorine such as polyvinyl chloride (PVC) and hence avoid the corrosive effect on the blast furnace tuyeres and the refractory materials in hearth lining.

The gasification and combustion behaviour of waste plastic were studied experimentally and followed by mathematical analysis (Murai et al. 2015). It was found that the rate of gasification of unburnt char depended on the rate of heating. As the rate of heating increased, the gasification process of waste plastic increased. The injection of relatively small particle size of plastics generates unburnt char with small size which leaves the raceway and flow up to be consumed at the cohesive zone by direct reduction of iron ore. On the other hand the coarse plastics generate bigger size of unburnt char which accumulates around deadman in the blast furnace and consequently reduces the permeability at the lower zone of the blast furnace. The injection of waste plastic could increase the coke reactivity; however, such effect will be correlated with the reactivity of coal char and the ash content of coke (Babich et al. 2009, 2015). It was reported that the gasification and combustion efficiency of waste plastics are improved by the implementation of co-injection

lance (Carpenter 2010). The small coal particles (75 μm) are adhering on the outer surface of larger plastic particle (~3 mm) and generate heat form combustion. This heat is supplied directly to the particles of waste plastic and enhances the combustion process. The theoretical limit of waste plastic injection is estimated to be 70 kg/tHM, while the higher injection rate will result in problems similar to that obtained with the relatively high PCI as previously illustrated in Fig. 10.5. Every tonne of plastics used in the blast furnace can replace 750 kg of coke (The Industrial Efficiency Technology Database 2013). Injection of waste plastics into the blast furnace is able to reduce the CO_2 emissions by 30 % due to the higher H_2 content (Carpenter 2010). On the other hand the cost of waste plastic collection and treatment is still representing one of the main challenges for its implementation in ironmaking. Efficient and effective systems are required to achieve sustainable and reliable supply of waste plastic into the blast furnace.

10.3.4 Secondary Material Injection

There are different types of secondary materials often generated in the integrated steel plant such as slags, filter dust and sludge. These materials are rich with iron and carbon and can be efficiently recycled to produce hot metal by its injection into the blast furnace. The injection of blast furnace flue dust and its influence on the coke consumption and hot metal quality have been tested in LKAB experimental blast furnace (EBF), and it has been applied in a full-scale blast furnace (Jansson and Sundqvist Ökvist 2004; Sundqvist Ökvist 2004a). It was found that the injection of flue dust improves the coal combustion efficiency and the slag formation in the raceway. In EBF, the injection of 23.4 kg flue dust/tHM reduced the coke and coal consumption by 21 kg/tHM. The silicon content in the hot metal was slightly decreased due to the relatively higher slag basicity with flue dust injection. The blast furnace flue dust contains about 23 wt.% of Fe_2O_3 which is directly reduced in the raceway and also improves the oxygen potential in this zone for the combustion of pulverized coal. The injection of iron ore fines into the blast furnace through tuyeres was actively studied in the 1980s in order to efficiently use the waste materials and increase the productivity. The tuyere injection of iron ore fines could achieve various advantages to the ironmaking blast furnace represented in lower top charging of pellets and sinter, more flexibility in controlling the raceway flame temperature and hot metal quality, utilization of low quality iron ore and possibility of higher productivity (Naito et al. 2006). On the other hand the injection rate of fine iron ore has to be adjusted with the injection rate of PC and the condition of hot blast. The calculation based on the raceway heat balance indicated that 184 and 100 kg/t of iron ore fines can be injected with 100 and 200 kg/tHM of PCI, respectively. The prereduction of iron ore fines up to 60 % can increase the injected amount to 594 kg/tHM provided that the temperature of hot blast has to be 1800 °C (Naito et al. 2006). This relatively high temperature of hot blast can be achieved by plasma superheating. The iron waste materials and the fines generated from direct reduction process such

as unexploited direct reduced iron (DRI) and low reduced iron (LRI) represent valuable materials and can be injected into the blast furnace. It was reported that the charging or injection of the pre-reduced iron ore into the blast furnace is expected to improve the efficiency of the overall process by increasing the productivity and decreasing the energy consumption (Naito et al. 2006; Kunitomo et al. 2006; Born et al. 2012a, b). The reduction behaviour of DRI/LRI in CO-CO_2-O_2 gas atmosphere was investigated (Born et al. 2011). Under reducing atmosphere (40 % CO–60 % N_2), LRI exhibited higher reduction rate compared to DRI due to the higher wüstite content. Under the effect of the oxidizing atmosphere of hot blast, reoxidation took place for DRI/LRI followed by full reduction to metallic iron.

Some blast furnaces all over the world are working with 100 % pellets (Sundqvist Ökvist 2004a). When fluxed pellets and basic fluxes are charged into the blast furnace, excessive basic slag is formed in the cohesive zone. Such phenomenon has a negative impact on the permeability of the cohesive zone and bosh region. Under such conditions, the injection of basic fluxes together with pulverized coal through tuyeres represents one of the possible solutions for this problem (Wikström et al. 2002). Trials on BOF slag injection into EBF have been conducted. The BOF slag has basicity of about 4.0 and has valuable amount of Fe and Mn (Sundqvist Ökvist 2004b). The furnace has achieved excellent performance with 11 kg/tHM reduction in the reducing agent compared to the reference case (Wikström et al. 2002).

10.3.5 Biomass Injection

Biomass comes back to appear in the horizon as one of the promising solutions to mitigate the CO_2 emissions in the steel industry. Biomass charcoal was used as energy source in ironmaking process till 1880; after that it became illegal, in many parts of the world, to use the biomass in the metallurgical applications in order to protect the natural forest against the irrational and oppressive exploitation at that time. Nowadays, the renewable energy has attracted more public and policy attention particularly for its impact in the mitigation of the greenhouse gas (GHG) emissions. The recent analysis of the long-term potential for renewable energy in industrial applications suggested that up to 21 % of total energy use in manufacturing industry in 2050 could be covered by renewable origin materials (Taibi et al. 2012). This will compensate about 50 exajoules per year (EJ/year) from the total energy (230 EJ/year) used in the industrial sectors. It was reported that the utilization of renewable biomass in the industrial sector has the potential to reduce the GHG emissions by 10 % in 2050 (Ladanai and Vinterbäck 2009). This represents 25 % of the total expected emission reductions of the industrial sectors and is equivalent to the total current CO_2 emissions from Germany, France, Italy and Spain together (Ladanai and Vinterbäck 2009). The global production of biomass and biofuel is growing rapidly due to the fluctuation of fossil fuel prices, growing environmental concerns and higher considerations regarding the security and diversification of energy supply. Although the world's bioenergy potential is large enough to meet the global energy demand in 2050, criteria to ensure the sustainable

production and supply of biomass are still unclear and required more attention (Taibi et al. 2012). The sustainable and constant supply of biomass resources is not the only challenge for its future impact, but the establishing of economic and efficient upgrading technologies to convert the raw biomass to valuable bioproducts with desired mechanical, physical and chemical properties represents another challenge for its efficient application in steel industry. The top charging of biomass into the large blast furnace still suffers from some problems which are related to the lower mechanical strength and the high volatile matter compared to coke. In order to overcome such problem, tuyere injection provides a flexible option for biomass utilization in the large modern blast furnace. In this case the mechanical strength is not required; however, the combustion behaviour of biomass is a very important factor affecting the RAFT. A static heat and mass balance model has been applied to investigate the substitution rate of biomass products (charcoal, torrefied material and wood pellets) for PCI (Wang et al. 2014, 2015). It was found that 166.7 kg/tHM charcoal is able to fully replace 155 kg/tHM PCI. The torrefied material and wood pellets could partially replace PCI by 22.80 % and 20 %, respectively (Wang et al. 2015). Charcoal demonstrated the highest potential for PCI substitution with almost insignificant change in top gas temperature. The oxygen enrichment in the hot blast has to be increased to 24.7 %. On the other hand the top gas temperature was found to be decreased by the injection of torrefied material and wood pellets. Based on these results, the maximum injection rate of torrefied material and wood pellets was found to be 134.2 kg/tHM and 98.9 kg/tHM, respectively, at the minimum allowed top gas temperature. Moreover, if the O_2 content in the blast is limited to 25.4 %, the maximum amount of torrefied biomass and wood pellets has to be decreased to 60.7 kg/tHM and 59.1 kg/tHM, respectively. The high level of volatile matter in the torrefied material and wood pellets reduces the RAFT, and hence, more O_2 enrichment in the hot blast is required. The reactive structure of charcoal improves the combustion process in raceway to become comparable to that of coal (Babich et al. 2010; Mathieson et al. 2012). It was reported that the maximum injection rate of charcoal will be in the range of 200–220 kg/tHM which is able to reduce the net CO_2 emissions by 40 % (Feliciano-Bruzual and Mathews 2013). Beside the environmental benefits, the injection of charcoal will result in lower amount of slag and higher production rate due to the low sulphur and ash content and higher content of CaO compared to PCI (Suopajärvi 2014). The results of mathematical modelling indicated an increase in the blast furnace productivity by about 25 % when 100 kg/tHM of charcoal is injected with 150 kg/tHM pulverized coal with an optimization of the oxygen enrichment (De Castro et al. 2013). Although the investigations and the commercial trials which have been conducted on biomass injection into the blast furnace demonstrated many benefits, its application is not practiced yet in the large modern blast furnaces. The practical limitations could be summarized in four main points (Feliciano-Bruzual and Mathews 2013): (1) less calorific value of biomass products compared to coal which required efficient pretreatment and pyrolysis, (2) difficulties in biomass injection at high rate due to the porous nature and the low density which required an optimization for the injection process, (3) wider particle size distribution of biomass after grinding which required an efficient sieving to get the proper particle size for injection and (4) higher alkalis in biomass products

which should be controlled and minimized before utilization to avoid its negative impact on the refractory materials. In addition, the higher cost of biomass products compared to that of fossil fuels represents another challenge for its implementation. Besides the policy instruments such as carbon tax or CO_2 allowance, it is important to reduce the production cost of biomass products. Both novel biomass upgrading processes and optimizing the existing process are required.

10.4 Summary

The blast furnace ironmaking has undergone tremendous modifications and improvements to reduce the energy consumption and CO_2 emissions. One of these modifications is injection of different auxiliary fuels into the furnace through tuyeres. Although the injection of pulverized coal through tuyeres has been applied a long time ago, continuous development is being done to sustain the blast furnace optimum conditions at the highest pulverized coal injection rate. The recent modifications in pulverized coal injection include development in the technology of pulverizing system and construction of the injected lance. An evaluation of the combustion process in the raceway and its influence on coke consumption, hot metal quality, process efficiency and furnace productivity are investigated. The injection of auxiliary fuels which are rich with hydrogen such as oil and natural gas is still applied in some blast furnaces in the world; however, it is based on the local availability of such fuels and the operation flexibility. The relatively higher hydrocarbon content in such fuels compared with pulverized coal reduces the flame temperature in the raceway and required higher oxygen enrichment in the blast to overcome the cooling effect. The generated coke oven gas and converter gas in the integrated steel plant can be used more efficiently in the integrated steel mill to achieve more consistent profits. These gases have relatively higher percentage of CO and H_2 in addition to higher calorific value compared to the blast furnace offgas. In addition, these gases have lower hydrocarbons compared to natural gas and fuel oil, and it can be injected at a higher rate to significantly reduce the coke consumption and CO_2 emissions. The waste plastics can be efficiently injected into the blast furnace as an alternative reducing agent to fossil fuels; however, the collection system and pretreatment methods are still representing the main challenges for its efficient implementation. The injection of secondary materials which are rich in iron and carbon such as BOF slag and flue dust is able to save the raw materials and reduce the solid and gas emissions. The partial replacement of fossil fuels with renewable biomass products represents one of the few options which can be introduced in short-medium terms to further reduce CO_2 emission from the steel industry. The mathematical modelling and system analysis demonstrated that charcoal has the highest potential for full substitution of pulverized coal; however, the higher price of charcoal compared to fossil fuels and the lack of knowledge about its future sustainability are representing the main challenges for its wide utilization in the steel industry.

Acknowledgement The financial support from the Swedish Research Council Formas for the postdoc grant at Swerea MEFOS and the partial financial support from the Centre of Advanced Mining and Metallurgy (CAMM) at Luleå University of Technology are greatly acknowledged.

References

Abdel Halim KS (2007) Effective utilization of using natural gas injection in the production of pig iron. Mater Lett 61:3281–3286

Abdel Halim KS, Andronov VN, Nasr MI (2009) Blast furnace operation with natural gas injection and minimum theoretical flame temperature. Ironmak Steelmak 36:12–18

Asanuma M, Terada K, Inoguchi T, Takashima N (2014) Development of waste plastics pulverization for blast furnace injection. JFE Technical Report No. 19, pp 110–117

Babich A, Senk D (2013) Biomass use in steel industry: back to the future. Stahl und Eisen 133:57–67

Babich A, Gudenau HW, Mavrommatis KT, Fröhling C, Formoso A, Cores A, Garcia L (2002) Choice of technological regimes of a blast furnace operation with injection of hot reducing gases. Revista de Metallurgia 33:288–305

Babich A, Senk D, Gudenau HW, Mavrommatis KT (2008) Handbook of ironmaking. Wissenschaftsverlag Mainz, Aachen. ISBN 3-86130-997-1

Babich A, Senk D, Gudenau HW (2009) Effect of coke reactivity and nut coke on blast furnace operation. Ironmak Steelmak 36:225–229

Babich A, Senk D, Fernandez M (2010) Charcoal behaviour by its injection into the modern blast furnace. ISIJ Int 50:81–88

Babich A, Senk D, Benkert S (2015) Interaction between injected waste plastics and coke bed in the blast furnace. In: Proceeding 7th international conference on the science and technology of ironmaking, Cleveland, OH, USA

Bennett P, Fukushima T (2003) Impact of PCI coal quality on blast furnace operations. In: Proceedings 12th ICCS 2003, Cairns, Australia

Birat JP (2010) Global technology roadmap for CCS in industry. Steel sectorial report: contribution to the UNIDO roadmap on CCS. http://hub.globalccsinstitute.com/sites/default/files/publications/15671/global-technology-roadmap-ccs-industry-steel-sectoral-report.pdf. Accessed on 05.11.15

Birat J, Hanrot F (2005) ULCOS – European Steelmakers' efforts to reduce greenhouse gas emissions. http://www.ulcos.org/en/docs/Ref18%20-%20ULCOSStockholm.pdf. Accessed on 06.11.15

Biswas AK (1981) Principles of blast furnace ironmaking-theory and practice. Cootha Publishing House, Brisbane. ISBN 0-949917-00-1

Bogdandy LV, Engell HJ (1971) The reduction of iron ores. Springer Verlag/Verlag Stahleisen, New York/Düsseldorf. ISBN: 3-540-05056-6

Born S, Stefan T, Babich A, Senk D, Gudenau HW (2011) Behaviour of DRI/LRI in CO-CO2-O2 atmospheres. In: Proceedings of METEC InSteel- Con, ECIC, VDEh, Düsseldorf, Germany

Born S, Babich A, Senk D, Gudenau HW, Stefan T (2012a) Injection of DRI/LRI into the blast furnace. In: SCANMET IV, 4th international conference on process development in iron and steelmaking, Lulea, Sweden, 10–13 June 2012

Born S, Senk D, Babich A, Gudenau HW, Stefan T (2012b) Investigations on the injection of DRI/LRI and char into the blast furnace. In: 6th international congress on the science and technology of ironmaking, 42nd ironmaking and raw materials seminar, 13th Brazilian symposium on iron ore, Rio de Janeiro, Brazil, 14–18 October 2012

Bortz S (1983) Coal injection into the blast furnace, Report EUR 8544 © ECSC-EEC, Commission of European Communities, Luxembourg, Brussel.

Brown T, Gambhir A, Florin N, Fennell P (2012) Reducing CO2 emissions from heavy industry: a review of technologies and considerations for policy makers. Grantham Institute for climate change, Imperial College London, Brief paper 7, pp 1–32

Bürgler TH, Braunnbauer G, Ferstl A (2004) Operational results of a new blast furnace gas injection system. Stahl und Eisen 124:39–42

Carpenter A (2006) Use of PCI in blast furnace. IEA Clean Coal Center report 2006. http://www.iea-coal.org.uk/documents/81520/6150/Use-of%C2%A0PCI-in-blast-furnaces. Accessed on 06.11.15

Carpenter AM (2010) Injection of coal and waste plastics in blast furnaces. IEA Clean Coal Centre. ISBN 978-92-9029-486-3.

Chu M, Guo T, Liu Z, Xue X, Yagi J (2012) Numerical analysis on blast furnace low CO2 emission operation with coke oven gas injection. In: Proceeding 6th international congress on the science and technology of ironmaking (ICSTI), Rio de Janeiro, Brazil, 14–18 October 2012

De Castro JA, Nogami H, Yagi J (2002) Numerical investigation of simultaneous injection of pulverized coal and natural gas with oxygen enrichment to the blast furnace. ISIJ Int 42:1203–1211

De Castro JA, Araújo GM, da Mota I, Sasaki Y, Yagi J (2013) Analysis of the combined injection of pulverized coal and charcoal into large blast furnaces. J Mater Res Tech 2:308–314

Diemer P, Killich HJ, Knop K, Lüngen HB, Reinke M, Schmöle P (2004) Potentials for utilization of coke oven gas in integrated iron and steel works. In: Proceedings of the 2nd international meeting on ironmaking/1st international symposium on iron ore, Vitoria, Brazil, 12–15 September 2004

Diemer P, Knop K, Lüngen HB, Reinke M, Wuppermann C (2007) Utilization of coke oven gas for the production of DRI. Stahl und Eisen 127:19–24

Du SW, Yeh CP, Chen WH, Tsai CH, Lucas JA (2015) Burning characteristics of pulverized coal within blast furnace raceway at various injection operations and ways of oxygen enrichment. Fuel 8:98–106

Feliciano-Bruzual C, Mathews JA (2013) Bio-PCI, charcoal injection in blast furnaces: state of the art and economic perspectives. Rev Metal 49:458–468

Ghosh A, Chatterjee A (2008) Ironmaking and steelmaking, theory and Practice. PHI Learning Private Limited, New Delhi. ISBN 978-8120332898

Greedes M, Toxopeus H, van der Vliet C (2009) Modern blast furnace ironmaking-an introduction. IOS Press BV, Amsterdam. ISBN 978-1-60750-040-7

Hellberg P, Jonsson TLI, Jönsson PG (2005a) Mathematical modelling of the injection of coke oven gas into a blast furnace tuyere. Scand J Metall 34:269–275

Hellberg P, Jonsson TLI, Jönsson PG, Sheng DY (2005b) A model of gas injection into a blast furnace tuyere. In: Fourth international conference on CFD in the oil and gas, Norway, Metallurgical & Process Industries SINTEF/NTNU Trondheim, 6–8 June 2005

Hill DG, Dwelly MG, Strayer TJ (2001) Why low volatile granular coal is the choice for coal injection at Bethlehem Steel's burns harbor blast furnaces. In: Proceedings of ironmaking conference, Baltimore, USA 60, pp 459–472

International Energy Agency (2010) Energy technology perspectives: scenarios and strategies to 2050. https://www.iea.org/publications/freepublications/publication/etp2010.pdf. Accessed on 27.07.15

Ishii K (2000) Advanced pulverized coal injection technology and blast furnace operation, 1st edn. Elsevier Science, Oxford/Pergamon. ISBN 80080546353

Jampani M, Pistorius PC (2014) Increased use of natural gas in blast furnace ironmaking. In: Proceedings of the iron & steel technology conference (AISTech), Indianapolis, IN, USA, 5–8 May 2014

Jansson B, Sundqvist Ökvist L (2004) Injection of BF flue dust into the BF- a full scale test at BF No. 3 in Luleå. In: Scanmet II, 2nd international conference on process development in iron and steelmaking, Luleå, Sweden, 6–9 June 2004

Juniper L, Schumacher G (2013) Advances in pulverized fuel technology: understanding coal comminution, combustion and ash deposition. In: The coal handbook: towards cleaner production, coal utilization, volume 2, Woodhead Publishing Series in Energy, pp 312–351. ISBN 978-1-78242-116-0

Kim JG, Choi JO (2003) CO_2 reduction in the ironmaking process by waste recycling and by-product gas conversion. Greenhouse Gas Control Technol 2:1037–1044

Kovalenko PE, Chebotarev AP, Pashinskii VF, Zamuruev VM, Tovarovskii IG, Boiko NG, Plevako VS, Trunov BS (1989) Improving the use of coke-oven gas in blast-furnace smelting. Metallurgist 33:169–170

Kunitomo K, Takamoto Y, Fujiwara Y, Onuma T (2006) Blast furnace ironmaking process using pre-reduced iron ore. Nippon Steel Technical Report, No. 94, pp 133–138

Ladanai S, Vinterbäck J (2009) Global potential of sustainable biomass for energy. Department of Energy and Technology, Report 13, Swedish University of Agriculture Sciences, Uppsala, Sweden. ISSN 1654-9406

Lingiardi O, Burrai O, Partemio C, Giandoménico F, Etchevarne P, Gonzalez JM (2001) High productivity and coke rate reduction at Siderar blast furnace 2. In: 1st international meeting on ironmaking, Belo Horizonte/MB-Brazil

Lu L, Sahajwalla V, Harris D (2000) Characteristics of chars prepared from various pulverized coals at different temperatures using drop-tube furnace. Energy Fuel 14:869–876

Mathieson JG, Truelove JS, Rogers H (2005) Towards an understanding of coal combustion in blast furnace tuyere injection. Fuel 84:1229–1237

Mathieson JG, Rogers H, Somerville MA, Jahanshahi S (2012) Reducing net CO_2 emissions using charcoal as a blast furnace tuyere injection. ISIJ Int 52:1489–1496

Matsuzaki S, Higuchi K, Shinotake A, Saito K (2012) Possibility of hydrogen reduction in ironmaking process (Course 50 Program in Japan). In: Proceeding international congress on the science and technology of ironmaking (ICSTI) Brazilian Metallurgical, Materials and Mining Association (ABM), Rio de Janeiro, Brazil

Meschter PJ, Crabaki HJ (1979) Kinetics of the water-gas shift reaction on an "FeO" surface. Metall Trans B 10B:323–329

Miwa M, Okuda H, Osame M, Watakabe S, Saito K (2011) Course 50-CO_2 ultimate reduction in steelmaking process by innovative technology for cool Earth 50: CO_2 emission reduction technology in Japan. In: METEC InSteelCon 2011, Proceedings of 1st international conference on energy efficiency and CO_2 reduction in the steel industry, Düsseldorf, Germany

Mousa EA, Babich A, Senk D (2013a) Reduction behaviour of iron ore pellets with simulated coke oven gas and natural gas. Steel Res Int 84:1085–1097

Mousa EA, Babich A, Senk D (2013b) Enhancement of iron ore sinter reducibility through coke oven gas injection into the modern blast furnace. ISIJ Int 53:1372–1380

Mousa EA, Babich A, Senk D (2014a) Utilization of coke oven gas and converter gas in the direct reduction of lump iron ore. Metall Mater Trans B 45B:617–628

Mousa EA, Babich A, Senk D (2014b) Reduction behaviour of iron ore agglomerates using coke oven gas. In: Proceeding 1st ESTAD & 31st JSI steel industry conference, Paris, France, 7–8 April 2014

Murai R, Asanuma M, Sato M, Inoguchi T, Terada K (2015) Flow behaviour of plastic particles in the lower part of blast furnace. ISIJ Int 55:528–535

Naito M, Yamaguchi K, Ueno H, Tamura K (2006) Ore injection into blast furnace through tuyeres. Nippon Steel Technical Report, No. 94, pp 139–146

Nogami H, Kashiwaya Y, Yamada D (2012) Simulation of blast furnace operation with intensive hydrogen injection. ISIJ Int 52:1523–1527

Pardo N, Moya JA (2013) Prospective scenarios on energy efficiency and CO_2 emissions in the European iron and steel industry. Energy 54:113–128

Proface E, Pivot S (2011) State of the art in coke oven gas treatment – a practical example. In: Proceeding METEC InSteelCon 2011, VDEh, Düsseldorf, Germany

Raask E (1985) Mineral impurities in coal combustion: behavior, problems, and remedial measures. CRC Press, Boca Raton. ISBN 978-0891163626
Sarna SK (2013) Pulverized coal injection in a blast furnace. http://ispatguru.com/pulverized-coal-injection-in-a-blast-furnace/. Accessed on 29.02.2016
Schmöle P, Lüngen HB, Endemann G (2009) Measures to reduce CO_2 and other emissions in the steel industry in Germany and Europe. In: Proceedings of 5th ICSTI'09, Shanghai, China, 2009
Schott R (2013) State-of-the art PCI technology for blast furnace ensured by continuous technological and economical improvement. Iron Steel Technol 10:63–75
Schott R (2015) Optimization strategies for pulverized coal injection into the blast furnace. In: Proceeding METEC & 2nd ESTAD, Düsseldorf, Germany
Slaby S, Andahazy D, Winter F, Feilmayr C, Bürgler T (2006) Reducing ability of CO and H_2 of gases formed in the lower part of the blast furnace by gas and oil injection. ISIJ Int 46:1006–1013
Spirin N, Shvidkiy V, Yaroshenko Y, Gordon Y (2015) Improvement in energy efficiency of blast furnace. In: Proceeding of METEC & ESTAD, Düsseldorf, Germany, 15–19 June 2015
Strassburger JH, Brown DC, Dancy TE, Stephenson RL (1969) Blast furnace, theory and practice. Gordon and Breach Science Publishers, New York
Sundqvist Ökvist L (2004a) Co-injection of basic fluxes or BF flue dust with PC into a BF charged with 100% pellets- effects on slag formation and coal combustion. PhD Thesis, Department of Chemical Engineering and Geosciences, Division of Process Metallurgy, Luleå University of Technology, Sweden
Sundqvist Ökvist L (2004b) High temperature properties of BOF slag and its behaviour in the blast furnace. Steel Res Int 75:792–799
Suopajärvi H (2014) Bioreducer use in blast furnace ironmaking in Finland. PhD Thesis, Oulu University, 2014. ISBN 978-952-62-0706-3. http://cc.oulu.fi/~kamahei/z/tkt/Suopajarvi_vk.pdf. Accessed on 05.02.15
Taibi E, Gielen D, Bazillian M (2012) The potential for renewable energy in industrial application. Renew Sust Energ Rev 16:735–744
The Industrial Efficiency Technology Database (2013) Blast furnace System. http://ietd.iipnetwork.org/content/plastic-waste-injection. Accessed on 09.02.2016
Tovarovskii IG, Merkulov AE (2011) Blast furnace smelting with the injection of natural gas and coke oven gas. Steel Translat 41:499–510
United State Environmental Protection Agency (2012) Available and emerging technologies for reducing greenhouse gas emissions from the iron and steel industry. http://www.epa.gov/sites/production/files/2015-12/documents/ironsteel.pdf. Accessed on 24.02.2016
Waguri S (2003) Pulverized coal injection for blast furnace. Ferram 8:371–372
Wang C, Karlsson J, Hooey L, Boden A (2011) Application of oxygen enrichment in hot stoves and its potential influence on the energy system in an integrated steel plant. In: International conference of World Renewable Energy Congress, IEE, Linköping, Sweden, May 2011
Wang C, Larsson M, Lövgren J, Nilsson L, Mellin P, Yang W, Salman H, Hultgren A (2014) Injection of solid biomass products into the blast furnace and its potential effects on an integrated steel plant. Energy Procedia 61:2184–2187
Wang C, Mellin P, Lövgren J, Yang W, Salman H, Hultgren A, Larsson M (2015) Biomass as blast furnace injectant- considering availability, pretreatment and deployment in Swedish steel industry. Energy Convers Manag 102:217–226
Weiser R, Braune I, Matthes P (2006) Control blast furnace pulverized coal injection to increase PCI rates. http://amepa.de/wp-content/uploads/2015/01/CFM-Publication-Weiser.pdf. Accessed on 30.11.15
Wikström JO, Sikström P, Sundqvist L, Zuo G (2002) Improved slag formation in the blast furnace by co-injection of basic fluxes, together with pulverized coal, through the tuyeres. In: International BF Lower Zone Symposium, Wollongong, Australia
Wingrowe G, Satchell D, Keeman B, Aswegen C (1999). In: Proceedings of gasification technologies conference, San Francisco, California, 17–20 Oct 1999
World Energy Council (2013) World energy resources 2013 survey. https://www.worldenergy.org/wp-content/uploads/2013/09/Complete_WER_2013_Survey.pdf. Accessed on 06.11.15

World Steel Association (2014) Crude steel statistics tables. https://www.worldsteel.org. Accessed on 22.01.15

Worrell E, Blinde P, Neelis M, Blomen E, Masanet E (2010) Energy efficiency improvement and cost saving opportunities for the U.S. iron and steel industry, LBNL-Report, United States Environmental Protection Agency, Oct. 2010. http://www.energystar.gov/ia/business/industry/Iron_Steel_Guide.pdf?25eb-abc5. Accessed on 05.02.2016

Yang Z, Zhang Y, Wang X, Zhang Y, Lu X, Ding W (2010) Steam reforming of coke oven gas for hydrogen production over a NiO/MgO solid solution catalyst. Energy Fuel 24:785–788

Chapter 11
Low CO_2 Emission by Improving CO Utilization Ratio in China's Blast Furnaces

Mingyin Kou, Laixin Wang, Jian Xu, Shengli Wu, and Qingwu Cai

Abstract In recent years, the CO_2 emission in China is the highest all around the world, accounting for about 30 %. China's 15 % CO_2 emission is produced from iron and steel companies, where blast furnace contributes more than 60 %. Therefore, blast furnace is the key to reduce CO_2 emission for iron and steel companies. Blast furnace is a countercurrent reactor between descending burdens and ascending gas. The higher the CO utilization ratio is, the lower the CO_2 emission. There are two main measures to improve CO utilization ratio—upper adjustment and lower adjustment. The upper adjustment is mainly about the burden distribution which includes adjusting batch weight, charging mode, stock line and so on. The lower adjustment is mainly about the gas distribution in the lower part of the blast furnace, which includes adjusting the gas volume, gas temperature, gas humidity and so on. The paper presents the upper and lower adjustments to improve CO utilization ratio in China's blast furnaces.

11.1 Introduction

In recent years, the CO_2 emission in China stays in the first place all around the world, accounting for about 30 % (Olivier et al. 2014). One of the largest CO_2 emission contributors is the iron and steel companies, whose CO_2 emission occupies

M. Kou (✉) • L. Wang • S. Wu
School of Metallurgical and Ecological Engineering, University of Science and Technology Beijing, No. 30 Xueyuan Road, Haidian District, Beijing 100083, China
e-mail: mingyinkou@gmail.com; wanglaixinustb@163.com; wushengli@ustb.edu.cn

J. Xu
College of Materials Science and Engineering, Chongqing University, Chongqing 400044, China
e-mail: jxu@cqu.edu.cn

Q. Cai
Engineering Research Institute, University of Science and Technology Beijing, No. 30 Xueyuan Road, Haidian District, Beijing 100083, China
e-mail: caiqw@nercar.ustb.edu.cn

P. Cavaliere (ed.), *Ironmaking and Steelmaking Processes*,
DOI 10.1007/978-3-319-39529-6_11

about 15 % of the total CO_2 emission in China. As the largest subsystem, the ironmaking process has about 90 % CO_2 emission of the iron and steel companies. And the CO_2 emission of the blast furnace exceeds 70 % of the ironmaking process. It can be found that blast furnace encounters very huge stress. Therefore, it is imperative to study blast furnace in order to reduce its CO_2 emission (Zhang et al. 2013; Liu et al. 2015).

Blast furnace is a countercurrent reactor between descending burdens and ascending gas, consisting of complicated transfer processes of heat, energy and momentum. Therefore, the smooth descending of burdens and the reasonable distribution of gas are the key to maintain a steady and smooth operation of blast furnace. The higher the CO utilization ratio is, the lower the CO_2 emission. There are two main measures to improve CO utilization ratio—upper adjustment and lower adjustment (Wang 2013a).

The upper adjustment is mainly about the burden distribution, which determines the second or third distribution of gas ascending from the lower part of blast furnace. The aim of burden distribution is to obtain reasonable radial distribution of ore/coke at throat. When burden is uniformly distributed at the throat, gas will be also uniform. In this way, the heating and reduction of burden by gas will also be adequate, which leads to a higher CO utilization. The upper adjustment mainly contains batch weight, charging mode, stock line and so on (Wang 2013a; Xiang and Wang 2014).

The lower adjustment is mainly about the initial gas distribution in the lower part of the blast furnace. The initial gas distribution is the priority of the second or third one. When the initial gas distribution is reasonable, there will be only little work to be done, or it is much easier to obtain a better gas distribution in the upper part of shaft furnace. The lower adjustment mainly contains the gas volume, gas temperature, gas humidity and so on (Wang 2013b; Xiang and Wang 2014).

Generally speaking, the effects of the lower adjustment are relatively timely and remarkable, while those of the upper adjustment will take a longer time to show. In practice, the upper adjustment and the lower adjustment are usually matched together to acquire a better gas distribution and a higher CO utilization.

11.2 The Upper Adjustment

11.2.1 Batch Weight

Batch weight has a critical value. When the batch weight is larger than the critical value, burden in the centre part of the blast furnace throat will become thicker with the increase of batch weight of ore, and the burden distribution will become evener; when the batch weight is smaller than the critical value, ore cannot reach the centre part of the furnace, and burden thickness in the peripheral part will become thicker with the increase of batch weight.

There is a relationship between the batch weight and the ratio of the burden thicknesses in peripheral and central area, which is illustrated in Fig. 11.1 (Liu 2005).

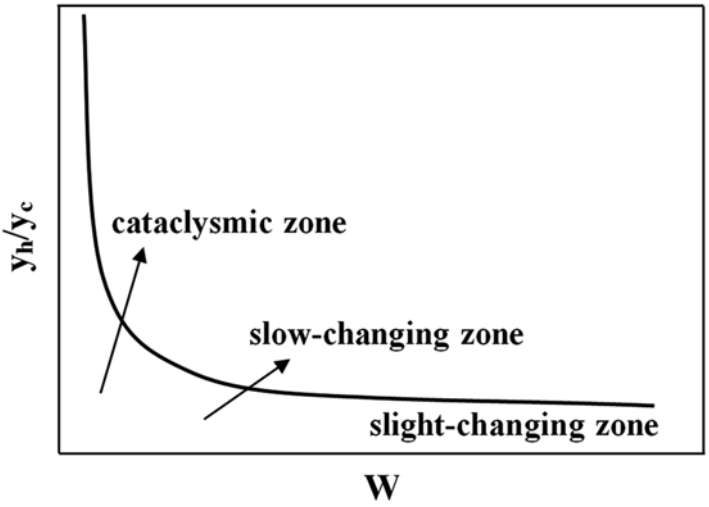

Fig. 11.1 Typical relationship between W and y_h/y_c

Where y_h is the burden thickness in peripheral part, y_c is the burden thickness in central part and W is the batch weight. The y_h/y_c line is usually divided into three zones, which are cataclysmic zone, slow-changing zone and slight-changing zone from left to right, respectively. When the batch weight belongs to the cataclysmic zone, the burden thickness in the central part will be thicker with the increase of batch weight; when it belongs to the slight-changing zone, the burden distribution can be hardly affected by the increase of batch weight; and when it belongs to the slow-changing zone, the effect of batch weight on the burden distribution will also be between the cataclysmic zone and slight-changing zone. In the slight-changing zone, the burden and gas distributions are stable, which are beneficial to obtain smooth operation and high CO utilization ratio. Therefore, the batch weight should be kept in the slight-changing zone. If there are too many powders in burdens, the batch weight should be kept in the slow-changing zone in order to prevent the burden blockages in central and peripheral areas (Liu 2005).

Channelling will be frequently occurred when the batch weight is too small. The gas will be blocked by overweighted burden when the batch weight is too large. The batch weight determines the thickness of the layered burdens. This means that when the batch weight increases, on one hand, the burden layers will be thicker, and the area of "coke window" will be also increased and the permeability will be also improved as a result. On the other hand, the number of burden layers will be reduced, then the "interface effect" between coke and ore will be also weakened, which also improves the burden permeability (Wang 2013b).

In the No. 3 Blast Furnace of Jiuquan Steel, the ore batch weight increased from 17.6 to 22.2 t, and the coke load increased from 4.0 to 4.2 (which means the coke batch weight increased from 4.40 to 4.78 t). The CO utilization ratio was increased, and the coke rate decreased from 438 to 428 kg/t (Bao 2008).

In No. 2 Blast Furnace of Shougang Jingtang United Iron & Steel Co. Ltd, the ore batch weight increased from 148 to 165 t, and the coke load increased from 5.00 to 5.44 at the same time in 2011. Smooth operation was enhanced, and the silicon content also kept about 0.3 % (Zhang et al. 2012a).

After three trials on large ore batch weight, the reasonable ore batch weight was found to be 100–115 t for 3200 m^3 blast furnace in Laiwu Steel. When the ore batch weight increased from 85 to 100–115 t, the fuel rate and the pressure drop decreased by 10 kg/t and 7 kPa, respectively (Mu et al. 2012).

In 2008, the ore batch weight went up from 10 to 21 t gradually in No. 4 blast furnace (inner volume: 400 m^3) of Nanjing Steel. Compared with the ore batch weight before adjustment, the CO_2 content in the top gas increased 0.2 %, and the blast furnace productivity increased by 0.49 $t/m^3\ d^{-1}$ (Lan and Wang 2009).

The ore batch weight was increased from 56 to 77 t in Benxi Steel. As a result, the gas distribution was stable, and CO utilization ratio was also increased by about 3 % (Zhu and Zhang 2009).

Huang et al. suggested that the coke layer thickness should between 500 and 700 mm, and the ore batch weight should be 0.95–1.20 % of daily production (Huang et al. 2015).

Hang and Wu thought the reasonable ore batch weight should be 0.012–0.015 of blast volume. The calculated ore batch weight was 55–68 t in No. 7 Blast Furnace of Jiugang Steel (Hang and Wu 2012).

11.2.2 Charging Mode

In the beginning, blast furnace is usually with bell top. The bell is used to store burdens and then goes down to discharge burdens into the blast furnace. However, the bell charging mode has some disadvantages, like bad sealing performance in the top, severe burden and gas segregations and so on. Therefore, the bell-less top blast furnace top is created. Blast furnaces are almost with bell-less top in China nowadays. The bell-less top will be only discussed in this paper.

The bell-less top blast furnace can be generally divided into three types based on the hoppers' location. The first type is parallel-type hoppers, which means that two hoppers are allocated on both sides of the centreline (see the left one in Fig. 11.2). The second type is serial-type hoppers, which means that two hoppers are allocated along the centreline of the blast furnace, and one is upper hopper, and the other is lower hopper (see the right one in Fig. 11.2). The third type is multi-hoppers, which means there are no less than three hoppers located around the centreline of blast furnace. There is no multi-hopper blast furnace yet in China, so it will not be discussed in this paper (Xiang and Wang 2014).

No matter parallel hopper or serial hopper, they both use rotating chute to discharge burdens from hopper into blast furnace. Therefore, charging mode of rotating chute is of significant importance to burden and gas distributions and further the CO utilization. The rotating chute usually has 8–12 rings corresponding to different angles. It can achieve many distributing modes due to its flexibility.

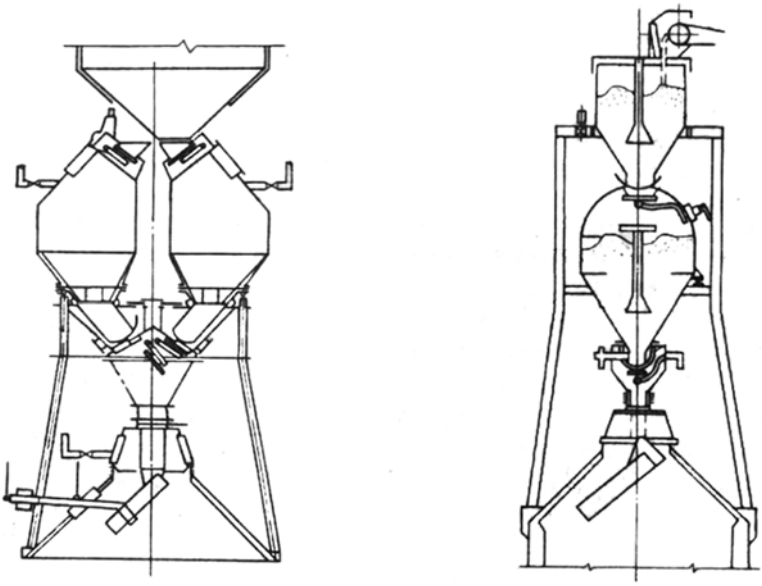

Fig. 11.2 Schematic diagram of bell-less blast furnace top

In general, there are four typical types of distributing modes: single-ring distributing, multiring distributing, fixed-point distributing and sector distributing. The former two modes are usually used in practical operation, while the latter two are only used when the gas distribution is not normal. The burden trajectory, burden stack shape and size distribution are directly determined by the rotating chute. The "terrace + funnel" burden stack shape is the most favourable one in China. Coke is easier to form a terrace, and the amounts of coke and ore can be adjusted based on the terrace. If the terrace is narrow and the funnel is deep, the burden stack will not be stable. On the contrary, if the terrace is wide and the funnel is shallow, the central gas flow will be suppressed. Once the terrace is developed, it should not be changed too much since the coke terrace controls the ore/coke ratio and size distribution in blast furnace.

Du and Guo proposed that the reasonable width of coke terrace should be 1.2–2 m for large-sized blast furnace and 0.8–1.2 m for middle-sized blast furnace. For example, the width of the coke terrace of the No. 2 blast furnace in Baosteel is 1.5 m (Du and Guo 1995). Li et al. suggested that the width of coke terrace should be 0.8 m and the depth of the funnel should be 1.5 m in the 1750 m^3 blast furnace of Ji'nan Steel (Li et al. 2006).

Wang et al. moved the main striking point of ore away from centre about 0.7 m and the main striking point of coke away from centre about 0.6 m by changing the charging modes in Shougang No. 2 blast furnace (inner volume: 1780 m^3) from March to April in 2008. As a result, the gas temperature in the top decreased from 200 to 180 °C, and the CO utilization ratio increased from 46 to 49 % (Wang et al. 2009).

Table 11.1 The CO utilization ratio corresponding to different charging modes in No. 5 blast furnace of TISCO

	Ore							Coke									
Rings	1	2	3	4	5	6	7	1	2	3	4	5	6	7	8	Fuel rate (kg t^{-1})	CO utilization ratio (%)
2008.02	0	3	3	3	3	3	1	2	2	2	2	2	2	2	2	508	49.9
2008.03	0	3	3	3	3	2	1	2	2	2	2	2	2	2	2	506	49.2
2008.11	2	3	3	3	1	1	2	1	2	3	3	3	1	1	1	503	50.1
2009.05	2	3	3	3	2	2	0	2	2	3	3	3	1	2	0	497	50.5
2010.04	3	3	3	3	2	1	1	3	2	3	3	3	1	1	0	503	50.05
2011.09	4	3	3	2	2	1	0	4	3	3	2	2	2	0	0	500	50.85
2012.03	4	3	3	2	2	2	0	4	4	3	2	2	2	0	0	507	50.5

Lu et al. used $C_3{}^{38°}{}_2{}^{36°}{}_2{}^{33.5°}{}_2{}^{30.5°}{}_2{}^{27.5°}{}_4{}^{17°}O_2{}^{38°}{}_3{}^{36°}{}_3{}^{33.5°}{}_3{}^{31.5°}{}_1{}^{28.5°}$to develop the gas flow in both peripheral and central gas at the beginning after the blow-in of No. 2 blast furnace (inner volume: 2500 m^3) of Chongqing Steel, then changed it to $C_2{}^{41°}{}_2{}^{39°}{}_2{}^{36.5°}{}_2{}^{33.5°}{}_2{}^{30.5°}{}_3{}^{23°}O_2{}^{41°}{}_3{}^{39°}{}_3{}^{36.5°}{}_2{}^{33.5°}{}_2{}^{30.5°}$ to inhibit the peripheral gas flow. After the adjustment, the CO_2 concentration increased from 18 to 20.0–21.0 %, and the comprehensive coke rate also decreased from 525 to 500 kg/t (Lu et al. 2012).

Table 11.1 shows the changes of charging mode from February of 2008 to March of 2012 in TISCO No. 5 blast furnace (inner volume: 4350 m^3). It can be seen that the CO utilization increased from 49.9 to 50.5 % (Li et al. 2013).

Another technique is also adopted to the burden charging in China, which is central coke charging. This technique charges coke in the central area of the blast furnace in order to develop central gas flow. Jingtang No. 1 blast furnace of Shougang group employed the central coke charging in 2011 to conquer the deterioration of raw and fuel materials and obtain a long and stable operation condition (Wang et al. 2013). However, this mode is not good to increase the CO utilization ratio in the blast furnace. When the amount of coke in the centre increased 1 %, the CO utilization ratio decreased 0.317 % (Teng et al. 2014). When the raw and fuel materials deteriorated, the central coke charging mode was adopted to keep a stable operation in No. 2 blast furnace of Shougang Jingtang. A higher CO utilization ratio was achieved, but it was still 1.5 % lower than the period with no central coke charging (Zhang et al. 2012b). Therefore, many companies cancelled the central coke charging to increase the CO utilization ratio, such as the No. 9 blast furnace in Xinyu Iron and Steel Co., Ltd., No. 2 blast furnace in Ji'nan Steel and so on (Zhou et al. 2015; Meng et al. 2010).

The advantages of the "terrace + funnel" are high CO utilization ratio and low fuel rate, but this mode requires a stable quality of raw and fuel materials. However, the central coke charging mode can adapt to the quality fluctuations of raw and fuel materials, but the disadvantage of this mode is low CO utilization ratio, which usually ranges at 46.5–48.5 % (Zhu 2014).

Table 11.2 Angle compensations at different stock lines in Baosteel

Level	1	2	3	4	5	6	7	8	9	10	11
Stock line base	52°	50.5°	48.5°	46°	43°	40°	36.5°	33°	29.5°	24°	15°
Stock line 1	51°	49.5°	47.5°	45°	42°	39°	35.5°	32°	28.5°	23°	15°
Stock line 2	50°	48.5°	46.5°	44°	41°	38°	34.5°	31°	27.5°	22°	15°
Stock line 3	49°	47.5°	45.5°	43°	40°	37°	33.5°	30°	26.5°	21°	15°
Stock line 4	48°	46.5°	44.5°	42°	39°	36°	32.5°	29°	25.5°	20°	15°

11.2.3 Stock Line

As for the bell-less top blast furnace, the stock line is defined as the vertical distance between the 0 m stock line and the burden stack surface. And the 0 m stock line is defined as the level of chute tip when the chute is vertically still or the position of top edge of steel brick in the blast furnace throat (Wang 2013b).

Changing the stock line equals to change the height of burden free falling zone and then to change the burden striking point. Therefore, it is matched with the initial angles of rotating chute. When the stock line is heightened, which means that it is close to the 0 m stock line, the burden striking point will move towards the centre, then the peripheral area is loosened and beneficial to developing peripheral gas. When the stock line is lowered, the burden striking point will move towards the wall, then it helps to develop the central gas (Liu 2005).

The stock line is related to the blast furnace throat, inside profile of the blast furnace top, burden properties and so on. Since the burden striking point can be controlled by the angles of the rotating chute, the stock line does not usually change once it is found suitable for the blast furnace operation. Generally, the stock line is controlled at 1–2 m (Xiang and Wang 2014).

When the practical stock line is higher than the preset stock line, the angles of the rotating chute should be adjusted to prevent burden from hitting on the furnace wall. Table 11.2 illustrates the angle compensations at different stock lines (Xiang and Wang 2014).

11.3 The Lower Adjustment

11.3.1 Gas Volume

Generally speaking, the more the gas volume is, the more the pig iron blast furnace produces, but the gas volume should not be too high. In order to have a high CO utilization and low fuel rate, the gas volume should be appropriate. The gas volume increases with the increase of blast furnace volume, but the ratio of gas volume to furnace volume almost stays at 1.6–1.7 Nm^3/m^3 (Li 2011). If the ratio of gas volume to furnace volume is too small, the blast furnace hearth will not be active enough, and permeability will be worsened, and the operation will not be smooth. Therefore,

Table 11.3 Main parameters corresponding to the change of tuyere area

Time	Tuyere area (m^2)	Gas volume ($m^3\ min^{-1}$)	Production ($t\ d^{-1}$)	Coke rate ($kg\ t^{-1}$)
2010.9.26	0.3476	4000	5200	438
2010.10.6	0.3599	4020	5155	447
2010.10.23	0.3732	4050	4180	533
2010.11.11	0.3486	4050	3900	544
2010.11.25	0.3609	4200	4350	510
2010.12.12	0.3742	4600	4890	487
2011.01.16	0.3619	4600	4620	495
2011.01.28	0.3558	4560	5760	423
2011.02.15	0.3520	4600	5380	425
2011.03.12	0.3398	4730	5440	417
2011.03.28	0.3340	4730	5740	404
2011.04.11	0.3463	4770	5810	403

a relative high ratio slows down the erosion of gas on the furnace wall and prevents the furnace accretion, then helps to keep smooth operation (Lin and Xiang 2012).

When the appropriate gas volume is reached, it will not be changed much anymore. Then a common way to adjust the gas is to change the tuyere area. Generally, reducing the tuyere area increases the gas velocity, and it is beneficial to the development of central gas; increasing the tuyere area decreases the gas velocity and helps to develop peripheral gas. When the amount of PCI (pulverized coal injection) increases or the quality of the raw and fuel materials deteriorates, the tuyere area should be reduced to develop central gas. For example, Qiu et al. decreased the tuyere area from 0.4248 m^2 in 2011 to 0.4076 m^2 in 2012 in order to perform the injection of bituminous coal for No. 3 blast furnace of Laiwu Steel (Qiu et al. 2014).

There were 24 tuyeres with 130 mm diameter and 8 tuyeres with 140 mm diameter in No. 5 blast furnace of WISCO, so the total tuyere area was 0.4417 m^2. However, the number of tuyere with 140 mm diameter was reduced to 2, and the total tuyere area was 0.4331 m^2, in order to cope with the deterioration of the raw and fuel materials (Hu 2012).

In 2011, the tuyere area was changed from 0.4278 to 0.3957 m^2 in the 3200 m^3 blast furnace of Laiwu Steel, and it turned out that the CO utilization ratio was improved, and the fuel rate decreased from 522 to 512 kg/t (Lin and Wang 2013).

The tuyere area was also changed to increase production and reduce fuel rate for No. 2 2500 m^3 blast furnace of Xuanhua Steel from 2010 to 2011, as shown in Table 11.3 (Hao 2011).

It can be seen that coke rate almost decreases with the decrease of tuyere area. And the gas volume should increase gradually after the reduction of tuyere area.

11.3.2 Gas Temperature

The main sources of the heat needed for blast furnace are the combustion heat of fuel and the physical heat of blast gas. The more heat the gas brings into blast furnace, the less heat the fuel needs to combust. Therefore, high gas temperature can

Table 11.4 The amount of saving coke corresponding to high blast gas temperature

Blast gas temperature (°C)	Around 950	950–1050	1050–1150	>1150
Saving coke (kg t^{-1})	About 20	About 15	About 10	About 8

Table 11.5 Typical technical index in some steel companies with high gas temperature in 2014

Company name	Gas temperature (°C)	Fuel rate (kg t^{-1})	Coke rate (kg t^{-1})	Coal rate (kg t^{-1})	Productivity (t m^{-3} d^{-1})
No. 6 blast furnace in Taiyuan Steel	1245	524	330	194	2.20
No. 5 blast furnace in Taiyuan Steel	1238	529	333	195	2.11
No. 3 blast furnace in Baosteel	1241	486	303	183	2.11
San'an Steel	1240	523	344	158	2.52
No. 9 blast furnace in Jingye Steel	1232	548	396	152	2.55
No. 10 blast furnace in Jingye Steel	1231	541	392	149	2.49

decrease the fuel rate and the cost of pig iron. At the same time, more coal can be injected to the blast furnace to replace some coke due to high gas temperature. Table 11.4 shows the amount of saving coke corresponding to the high gas temperature (Wen et al. 1996).

Many steel companies have high gas temperatures over 1200 °C, and typical technical indexes of some companies in 2014 are given in Table 11.5 (Wang 2015).

Table 11.6 shows some main technical and economical parameters of some advanced blast furnaces from January to June of 2011 in China (Zhang 2013).

Chen et al. reported that when the blast gas temperature increased from 1240.7 °C in 2008 to 1258.7 °C in 2009 in Qian'an Steel's No. 2 blast furnace, the coke rate decreased from 295 to 287 kg/t, while the coal rate increased from 164 to 172 kg/t (Chen 2010).

Guo et al. also tried to increase the gas temperature in No. 1 blast furnace of Chongqing Iron and Steel Company from 2010 to 2012. The main technical and economical parameters are given in Table 11.7. It can be found that the coke rate decreases greatly when the blast gas temperature increases (Guo et al. 2013).

Wang and Li reported the change of blast gas temperature in 2200 m^3 blast furnace in Angang Iron and Steel Company in 2006. Table 11.8 illustrates some typical parameters (Wang and Li 2007).

From 2004 to 2007, the blast gas temperature of No. 2 blast furnace in Meishan Steel increased from 1131 to 1223 °C, and the coal rate increased from 109 to 158 kg/t, while the coke rate decreased from 393 to 227 kg/t (Wang 2008).

Table 11.9 shows some main economic indicators of No. 7 blast furnace in Benxi Steel from 2005 to 2010 (Huang 2011).

Zhu reported that the blast gas temperature in 2500 m^3 blast furnace for Chengde Iron and Steel Company increased by 7.1 °C in 2012 from 1211.5 °C in 2011, the comprehensive coke rate decreased by 14.4 kg/t (Zhu 2013).

Table 11.6 Main technical and economical parameters of some advanced blast furnace from 2011.01 to 2011.06 in China

Company name	Effective volume (m^3)	Gas temperature (°C)	Fuel rate (kg t^{-1})	Coke rate (kg t^{-1})	Coal rate (kg t^{-1})	Productivity (t m^{-3} d^{-1})
No. 1 blast furnace in Shougang Jingtang	5500	1300	480	305	175	2.37
No. 3 blast furnace in Qian'an Steel	4000	1280	503	327	176	2.39
No. 3 blast furnace in Baosteel	4350	1236	–	306	185	2.50
No. 4 blast furnace in Baosteel	4747	1254	488	318	170	2.02
No. 8 blast furnace in WISCO	3800	1192	532	355	177	2.69
5800 m^3 blast furnace in Shazhou Steel	5800	1230	502	341	161	2.21
No. 5 blast furnace in Taiyuan Steel	4380	1243	502	315	187	2.50
No. 1 blast furnace in Ma'anshan Steel	4000	1225	514	338	140	2.22
No. 1 blast furnace in Bayuquan of Anshan Steel	4038	1225	523	372	151	2.11

Table 11.7 Main technical and economical parameters of No. 1 blast furnace in Chongqing Steel from 2010 to 2012

Time	Gas temperature (°C)	Coke rate (kg t^{-1})	Productivity (t m^{-3} d^{-1})
2010	1080	529	1.49
2011	1202	414	2.08
2012.01	1219	428	2.24
2012.02	1221	436	2.20
2012.03	1215	418	2.00
2012.04	1223	396	2.15
2012.05	1216	390	2.26
2012.06	1228	397	2.14
2012.07	1230	415	2.23
2012.08	1170	400	2.12
2012.09	1187	390	2.26
2012.10	1206	391	2.28
2012.11	1126	479	1.74
2012.12	1220	412	2.21

Table 11.8 Some typical parameters of 2200 m^3 blast furnace in Angang Steel in 2006

Time	Gas temperature (°C)	Coke rate (kg t^{-1})	Coal rate (kg t^{-1})	Productivity (t m^{-3} d^{-1})
2006.01–2006.03	1015	573	30	1.49
2006.04	1218	520	79	2.08
2006.05	1236	457	111	2.24
2006.06	1199	404	137	2.20
2006.07	1218	388	150	2.00
2006.08	1189	383	150	2.15
2006.09	1192	383	143	2.26

Table 11.9 Some typical parameters of No. 7 blast furnace in Benxi Steel from 2005 to 2010

Time	Gas temperature (°C)	Coke rate (kg t^{-1})	Coal rate (kg t^{-1})
2005	986	466	39.9
2006	1070	388	93.8
2007	1109	386	106.5
2008	1091	374	90.3
2009	1140	347	119.0
2010	1155	348	124.6

11.3.3 Gas Humility

At the beginning, the gas humility keeps at the value it originally has. However, the gas humility varies day by day, which results in unstable blast furnace operation. In order to solve the problem of the variation of gas humility, there are two ways: one is humidified blast and the other is dehumidified blast. Humidified blast is to fix the humility at a relatively high value to keep a stable furnace operation. But the water vapour brought by humidified gas needs to be decomposed, which consumes the heat in blast furnace. When the gas humility increases by 1 %, the coke rate will be increased by 4–5 kg/t, otherwise, the gas temperature needs to be increased by 25 °C. Dehumidified blast is to fix the humility at a low value. It reduces the heat consumed by the decomposition of water vapour and increases the theoretical combustion temperature, then decreases the coke rate. Therefore, the amount of CO generated at the lower part of blast furnace will decrease, then the CO utilization will increase as a result. Generally, when the gas humility decreases by 1 g/m^3, the coke rate can be decreased by 0.8–1.0 kg/t (Xiang and Wang 2014).

The dehumidified blast has been applied to No. 1 blast furnace in Liuzhou Steel since 2010. The gas humility decreased from 20 to 6~7 g/m^3, and the fuel rate decreased by 9.2 kg/t as a result (Huang et al. 2013).

Yao et al. also reported that the gas humility decreased from 18.3 to 10 g/m^3 for No. 3 blast furnace in Hangzhou Steel from 2011. As a result, the coke rate decreased from 373 to 357 kg/t, and the CO_2 content at the top of the furnace increased from 18.81 to 19.23 %, which indicated a better CO utilization ratio (Yao et al. 2012).

Table 11.10 Some parameters before and after the application of dehumidified blast technique in No. 8 blast furnace of Nanjing Steel in 2011

Time	Gas humility ($g\ m^{-3}$)	Productivity ($t\ m^{-3}\ d^{-1}$)	Fuel rate ($kg\ t^{-1}$)	Coke rate ($kg\ t^{-1}$)	Coal rate ($kg\ t^{-1}$)	Gas temperature (°C)
Before dehumidified blast technique (2011.07–2011.08)	18	2.47	542	357	151	1209
After dehumidified blast technique (2012.07–2012.08)	8	2.63	509	325	166	1220

In 2011, the No. 8 blast furnace in Nanjing Steel adopted the dehumidified blast technique, and some main technical and economical parameters before and after the dehumidified blast technique are shown in Table 11.10 (Wang 2013b).

The coke rate also decreased by 17.3 kg/t when the gas humility decreased by 7.7 g/m^3 for No. 2 blast furnace in Meishan Steel (Tao 2010).

Zhang et al. reported that the fuel rate decreased by 18.40 kg/t, while the production increased by 27.51 t/d after the application of dehumidified blast in 2005 in 2500 m^3 blast furnace of Stainless Steel Branch of Baosteel (Zhang et al. 2006).

11.4 Conclusions

The principle of upper adjustment and lower adjustment is that they should be suitable for each other. When the peripheral gas in the lower part of blast furnace is developed, then the upper adjustment should not block the peripheral gas heavily. The upper adjustment should gradually open the central gas and control the peripheral gas at the same time in order to prevent the sudden block of peripheral gas, which may affect the smooth operation of blast furnace. Likewise, when the central gas in the lower part is overdeveloped, the upper adjustment should not block the central gas immediately, but should open the peripheral gas properly and then release the overdevelopment of central gas. Above all, the upper adjustment and lower adjustment should not form confrontation. The CO utilization ratio can be increased remarkably with the cooperation of the upper adjustment and lower adjustment.

Acknowledgements The financial support from the Fundamental Research Funds for the Central Universities (Grant No. FRF-TP-15-065A1) and China Postdoctoral Science Foundation (2016M591076) is gratefully acknowledged. The authors also gratefully acknowledge the helpful comments and suggestions of the reviewers, which have improved the paper.

References

Bao W (2008) The practice of large batch operation in No. 3 blast furnace of Jiuquan Steel. In: Medium and small blast furnace annual conference, Qingdao, 2008

Chen G (2010) Discussion on high blast temperature of blast furnace. Research on Iron and Steel. 38(5):53–55

Du H, Guo K (1995) A key link of burden distribution in the bell-less blast furnace top – the formation of terrace. Ironmaking 14(3):33–36

Guo D, Yang B, Liu P (2013) The application of high blast temperature technique in the No. 1 blast furnace of Chongqing Steel. Ironmaking 32(6):43–45

Hang W, Wu L (2012) Discussion about operation system of 2500 m^3 blast furnace of Jiuquan Steel. Hebei Metall 8(23):31–35

Hao L (2011) The practice of reducing tuyere area in No. 2 blast furnace of Xuanhua Steel. In: Hebei ironmaking annual academic conference, Xingtai, 2011

Hu Z (2012) Strategy for improving in utilization rate of No. 5 blast furnace in WISCO and its practice. WISCO Technol 50(2):8–11

Huang Y (2011) Influence of high blast temperature on blast furnace. Benxi Steel Technol 1:5–6,21

Huang R, Li H, Cai Y (2015) The decreasing cost practice of "Four high and one large" technique in blast furnaces of Liuzhou Steel. Ironmaking 34(2):43–46

Huang Q, Zhang H, Qiang Q (2013) The application of dehumidified blast in No. 1 blast furnace of Liuzhou Steel. Ironmaking 32(4):56–57

Lan H, Wang Y (2009) The practice of large ore batch operation in No. 4 blast furnace of Nanjing Steel. Ironmaking 28(1):28–30

Li W (2011) Operation and management outline of large sized blast furnace. Ironmaking 30(3):1–7

Li C, An M, Gao Z, Dai J (2006) Research and practice of burden distribution in blast furnace. Iron Steel 41(5):6–10

Li H, Liang J, Yang Z, Tang S (2013) The characteristics and control of proper gas distribution in large size blast furnace. In: The 14th national annual academic conference of large-size blast furnace, Jiayuguan

Lin X, Wang L (2013) Production practice of adjusting tuyere area of Laiwu Steel's 3200 m^3 blast furnace. Shandong Metall 35(2):6–8

Lin C, Xiang Z (2012) Design feature and operation practice for Baosteel No. 3 blast furnace long campaign life. In: National annual technical conference on ironmaking production, Wuxi, 2012

Liu Y (2005) Burden distribution law in blast furnace, 3rd edn. Metallurgical Industry Press, Beijing

Liu Z, Zhang J, Yang T (2015) Low carbon operation of super-large blast furnaces in China. ISIJ Int 55(6):1146–1156

Lu D, Zhao S, Gao Z, Gao T, Li T (2012) The application and practice of burden distribution parameters measured by laser in the No. 2 blast furnace of Chongqing Steel. Ironmaking 31(3):39–42

Meng L, Li B, Chen X, Fan P (2010) The research on cancelling central coke charging in No. 2 1750 m^3 blast furnace in Ji'nan Steel. Shandong Metall 32(3):21–23

Mu X, Lang D, Yang L (2012) The application of large ore batch in 3200 m^3 blast furnace of Laiwu Steel. Ironmaking 31(3):30–32

Olivier JG, Janssens-Maenhout G, Muntean M, Peters JA (2014) Trends in global CO_2 emissions: 2014 report. PBL Netherlands Environmental Assessment Agency, Hague

Qiu G, Yin Z, Zhu H, Jiang Z (2014) Increasing utilization rate of blast furnace gas to decrease fuel consumption. China Metall 24(1):47–51

Tao Z (2010) The application of dehumidified blast in No. 2 blast furnace of Meishan Steel. Ironmaking 29(2):50–52

Teng Z, Cheng S, Zhao G (2014) Influence of central coke charging on the gas distribution and utilization for a blast furnace. J Iron Steel Res 26(12):9–14
Wang Q (2008) Practice of high blast temperature technology on Meishan No. 2 blast furnace. Metall Collection 3:9–10,13
Wang X (2013a) Ferrous metallurgy (Ironmaking part). Metallurgical Industry Press, Beijing
Wang Y (2013b) Application of dehumidified blast in No. 8 blast furnace. Technol Manage Nanjing Steel 3:28–31
Wang W (2015) Technical discussion on high blast temperature in blast furnace. World Met Bull 9:1–3
Wang S, Li C (2007) Production practice of high blast temperature on 2200 m^3 blast furnace in Anyang Steel. Metallurgical Collection 4(11–12):15
Wang X, Wang S, Chen J, Wei H, Ma H (2009) Adjustment of gas flow distribution in Shougang No. 2 blast furnace. Ironmaking 28(1):8–11
Wang X, Wang Y, Li H (2013) The practice of cancelling central coke charging in Shougang Jingtang's No. 1 blast furnace. Ironmaking 32(2):24–27
Wen X, Mi K, Shen Z (1996) Ironmaking process in Baoseel. Heilongjiang Science and Technology Press, Harbin
Xiang Z, Wang X (2014) Blast furnace design: the theory and practice of ironmaking process design. Metallurgical Industry Press, Beijing
Yao K, Fan W, Ma J, Gao W (2012) The application of dehumidified blast in No. 3 blast furnace of Hangzhou Steel. Zhejiang Metall 5:32–34
Zhang F (2013) Developing prospects on high temperature and low fuel ratio technologies for blast furnace ironmaking. China Metall 23(2):1–7
Zhang Z, Zhang J, Gong T (2006) The application and results of dehumidified blast device in 2500 m^3 of Stainless Steel Branch of Baosteel. Ironmaking 25(3):31–33
Zhang H, Ren L, Chen Y, Wang G, Zhen K (2012a) Production under large batch ore charging system in No. 2 blast furnace of Shougang Jingtang United Iron and Steel Company. Ironmaking 31(3):6–9
Zhang H, Wang X, Wang Y, Wang G, Li H (2012b) Technical features of central coke charging for No. 2 blast furnace of Shougang Jingtang. Ironmaking 31(6):7–10
Zhang Q, Jia G, Cai J, Fengman S (2013) Carbon flow analysis and CO_2 emission reduction strategies of ironmaking system in steel enterprise. J Northeast Univ (Nat Sci) 34(3):392–394, 403
Zhou L, Hu X, Chen L, Gu Y (2015) Practices on cancelling central coke charging operation under low quality burden in No. 9 blast furnace. Jiangxi Metall 35(5):15–17, 25
Zhu J (2013) Research about high blast temperature utilization in 2500 m^3 blast furnace in Chengde Steel. Hebei Metall 10:1–4
Zhu R (2014) Technique and management of large-size blast furnace operation in Baosteel. Ironmaking 33(4):1–6
Zhu W, Zhang F (2009) The study and apply about large batch of ore in the No. 7 blast furnace of Benxi Steel. Met World 6:9–14

Part III
Electric Arc Steelmaking

Chapter 12
Dioxin Emission Reduction in Electric Arc Furnaces for Steel Production

Pasquale Cavaliere

Abstract Steel production through electric arc furnaces has strongly increased in the past decade. Dibenzo-p-dioxins and dibenzofurans (PCDD/Fs) are the main type of greenhouse emissions in such kind of plants. The main factors influencing the emissions levels are the composition of raw materials, the processing conditions employed during melting, and the adsorbent effects of additional compounds added before filtering. Many techniques have been experienced in the recent past to improve the abatement of emissions levels. In the present chapter, the greenhouse emissions belonging to an industrial steel electric arc furnace are monitored in different processing condition setups. The effect of lignite and CuCl addition on the dangerous emission levels have been deeply investigated.

12.1 Introduction

Electric arc furnaces (EAFs) are employed in the steel industry to melt scraps at very high temperatures by using electric arcs (normally divided into high-pressure and low-pressure arcs). Graphite electrodes are the main sources of electrical energy; the electric arc leading to the material melting burns between the electrodes and the metal; those arcs are normally divided into high current and ultrahigh current (if the current exceeds 10 kA). Normally, oxygen is blown into the furnace using an oxygen lance; such oxygen, combined with the carbon, leads to the formation of a foam slag that works as a protective agent. Many studies focus on the efficiency of reducing the chemical energy loss by increasing the oxygen content in the furnace. During refining, the removal of carbon and further inorganic impurities, such as phosphorus, sulfur, silicon, manganese, aluminum, chromium, etc., is carried out by the oxygen lances. The oxidized elements are risen and enter the slag phase, which coats on the surface of the molten steel. This phase consists of the oxides of the impurities and slag former materials (CaO, MgO). Once the impurities

P. Cavaliere (✉)
Department of Innovation Engineering, University of Salento,
Via per Arnesano, 73100 Lecce, Italy
e-mail: pasquale.cavaliere@unisalento.it

P. Cavaliere (ed.), *Ironmaking and Steelmaking Processes*,
DOI 10.1007/978-3-319-39529-6_12

are removed from the steel, their separation is carried out during the deslagging phase, when the furnace is tilted and the slag is poured out through the slag door. Apparently, during each phase of normal EAF operation, emission of fumes and gases is presented and can be divided into primary and secondary emissions. Generally, if carbon monoxide content in the exiting gases diminish below the flammability limit and the rest cannot be burned at the combustion gap, if the temperature remains high, the generated carbon dioxide could dissociate to carbon monoxide and oxygen, which would form dioxins in the downstream of the off-gas system. Consequently, the carbon monoxide and dioxin content of the off-gases are very high. The homogenous temperature is achieved through the employment of oil burners. Electric arc furnace and sintering plants (Cavaliere and Perrone 2013) represent the main sources of polychlorinated dibenzo-p-dioxins and dibenzofurans (PCDD/Fs) during steel production processes. Even if sinter plants are considered the main sources of dangerous dioxin emissions, the use of EAF for steel production is strongly increased, and this fact leads to a strong attention in their use and management. The high energy consumption of the EAF motivates the development of control and optimization strategies that would reduce production costs, while maintaining targeted steel quality (steel grade) and meeting environmental standards. The knowledge about optimized melting conditions of various types of scraps is limited to results belonging to statistical analyses, and the description of the relationships between the system efficiency and the greenhouse emission levels is very poor. Both PCDDs and PCDFs are persistent stable organic pollutants formed in all those high-temperature processes with an abundance of organic material in the presence of chlorine and copper. Dioxins and furans are chlorinated tricyclic organic compounds resulting from the combination of organic compounds impregnated with halogens (i.e., fluorine, chlorine, bromine, or iodine) with a specific molecular heterocyclic structure. A deep and complete thermodynamic description of the PCDD/F formation has been presented (Tan et al. 2001). These compounds are commonly grouped under the name "dioxins," but their chemical structures and their properties can be very different. Dioxins are a class of heterocyclic organic compounds whose basic structure consists of rings with four carbon and two oxygen atoms. On the other hand, furans have only one oxygen atom, and the two outer benzene rings are linked by a pentagonal structure. Among the 200 types of known dioxins, the most famous are certainly the PCDDs, characterized by the presence of chlorine atoms that will complement the aromatic rings. The chemical stability of such compounds derives from the presence of these rings. The most dangerous of dioxins, for serious problems of bioaccumulation and environmental contamination, is certainly TCDD. A detailed description of their formation is presented in the literature (Kulkarni et al. 2008; Raghunatan and Gullet 1996; Suzuki et al. 2004). The PCDDs are generally measured in terms of TEQ relative to TCDD as a reference, being the most polluting and dangerous. The polydibenzo-dioxins have different toxicities in relation to their structure. The TEQ expresses the quantity of a "toxic" substance as the concentration of the reference substance that can generate the same toxic effects of TCDD. It is also possible to obtain the concentration of a

PCDD with its toxic equivalency through the use of the TEF. The TEF for TCDD is assigned equal to 1, while the other dioxins have a factor of <1. This dimensionless parameter, multiplied by the actual concentration, results in the TEQ. Many studies presented in literature report the effect of processing factors and off-gases filtering on dioxin emissions (Prüm et al. 2004; Öberg 2004; Chang et al. 2006). The main factors influencing the emissions levels are the composition of row materials, the processing conditions employed during melting, and the adsorbent effects of additional compounds added before filtering. Many techniques have been investigated in order to improve the abatement of dioxin levels. The techniques converge on the activated carbon adsorption or catalytic oxidation (Everaert and Baeyen 2004). From these studies, the employment of activated carbon results in the best available technique to reduce the dioxin levels from EAF. Anyway, these techniques require a very precise control of gas temperature in order to result efficient. Another efficient solution is the Cu chloride addition; in presence of urea, the addition leads to a strong reduction in PCDD/F formation (Li et al. 2008). Normally, dioxin compounds are destroyed at higher temperatures, but dioxins reform in the off-gas at lower temperatures. Such parameter is fundamental in monitoring the dioxin behavior and in the setting of optimal plant parameters in order to reduce dangerous emissions. In the present paper, both the process parameter tuning and the additive addition, all finalized to the PCDD/F reduction, are analyzed and the results presented. It is demonstrated how the optimal management of processing parameters and the precise utilization of additives lead to a strong reduction in dangerous emissions from EAFs.

12.2 Electric Arc Furnace Operations

The electric arc furnace investigated in the present study is a 100 t furnace designed for a maximum flow rate of 1500 Nm^3/h. The stack off-gases are emitted in the atmosphere through a 32 m height stack. In EAF, graphite electrodes carry the current through the furnace roof into the charge of metal. The electric arc formed melts the charge at very high temperatures. The melting sequence for the electric arc furnace comprises the different stages: charging, melting, oxidization, and tapping. The waste gases produced in the furnace are extracted through an aperture in the furnace roof and the dust from various sources in the housing. The waste gas is cooled to recover heating as steam, hot water, or electric energy and is then dedusted by cloth filters. In some operating conditions, the dust from the electric furnace can contain considerable quantities of heavy metals, such as zinc and lead, and so it is worth recovering them. After filtering, the examinations of the off-gases were performed according to EN 1948 parts 2 and 3, EN 1948SS (Sampling Standards, Wellington Laboratories), EN 1948ES (Extraction Standards, Wellington Laboratories), and EN 1948IS (Injection Standards, Wellington Laboratories), by employing a high-resolution gas chromatograph and a high-resolution selective

Table 12.1 Electric arc furnace processing parameters

Parameters	Value
Flow rate (Nm^3/h)	300–1100
Coke (t/h)	0.2–1.2
Gas temperature (°C)	60–350
Lignite (kg/h)	0–100

mass detector. The emission levels of polychlorinated dibenzo-p-dioxins and polychlorinated dibenzofurans are determined through a 12 h monitoring per each experimental condition in a time range of 4 years. Many experimental conditions belonging to different plant setup were monitored. These conditions are summarized in Table 12.1 in terms of plant processing parameters. Flow rate, coke, and gas temperature were considered as processing parameters of the electric arc furnace. In all the conditions, different quantities of lignite were added in order to monitor the effect on dioxin emissions. For selected experiments, 5 mmol of CuCl were added to the charge.

12.3 Greenhouse Emission Reduction

The main results of this study can be summarized as follows. Dioxin emissions decrease as flow rate increases (Fig. 12.1); very low rates of coke lead to an increase in dioxin emissions for low flow rate.

In correspondence of high flow rates, dioxin emissions decrease in correspondence of intermediate values of coke rate. Such behavior is a good indicator of plant efficiency; a high flow rate corresponding to a high plant efficiency leads to emission lowering. Also for high efficiency, coke rate should remain from low to intermediate values. Dioxin emissions decrease as the gas temperature and the flow rate increase (Fig. 12.2).

Dioxin compounds form in a temperature range of 200–600 °C with a maximum in the range 250–400 °C. The maximum levels of dangerous emission concentration are recorded at intermediate values of temperature and flow rate. Such behavior is time dependent; in this way, the more time off-gases remain at a stable temperature, the more dioxin formation is allowed. In this way, it is easy to demonstrate that, as increasing the gas flow and tuning the gas temperature far from the dangerous range, the emission levels are strongly reduced. In this way, it is not only the temperature that plays a role in the reaction kinetic but also the reaction rate due to the gas flow. The rapid cooling of off-gases coupled with high flow rate represents an optimal solution in reducing dioxin formation and improving the plant efficiency. Such a process control system can be used to regulate the furnace stability by working at operating parameters that reduce dioxin production in the plant. As a matter of fact,

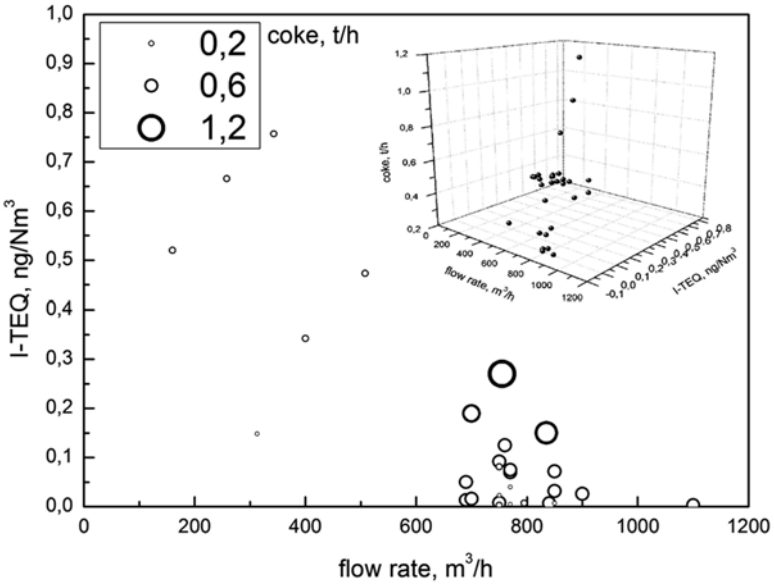

Fig. 12.1 Dioxin emissions as a function of flow and coke rates showing a decrease in dioxins level by increasing the flow rate and by fixing the coke rate to intermediate values

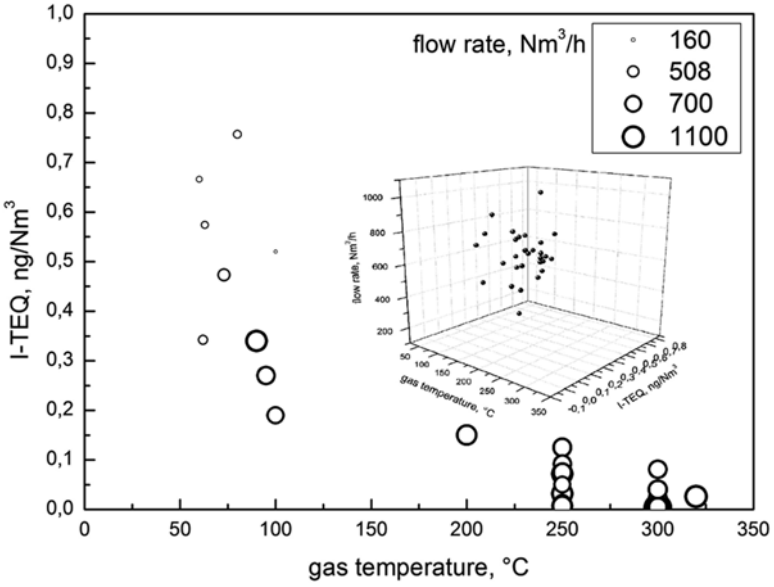

Fig. 12.2 Dioxin emissions as a function of temperature and flow rate showing the abatement of emissions by increasing both gas temperature and flow rate

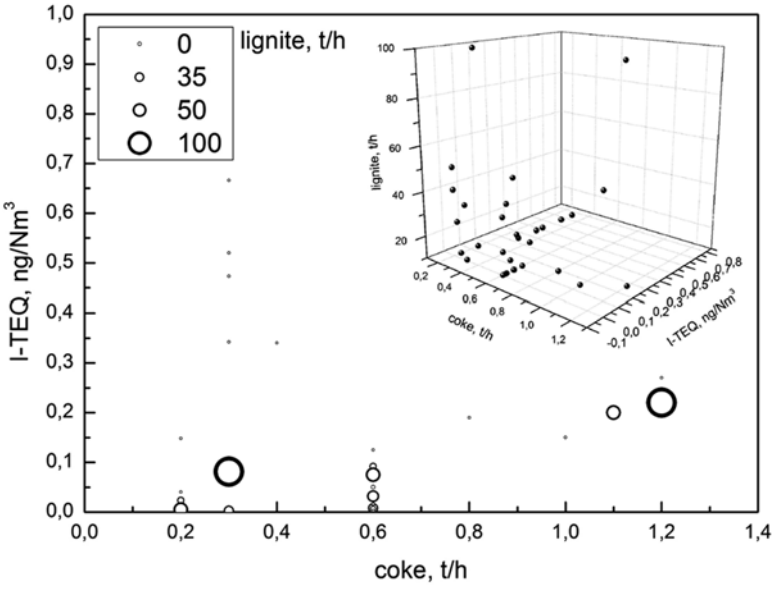

Fig. 12.3 Dioxin emissions as a function of coke rate and lignite addition, lignite injection contributes to the emissions reduction at fixed values of coke rate

many plant layouts employ off-gas post-combustion to destroy PCDD/Fs, but such system does not eliminate dangerous product formation.

Dioxin emissions decrease from low to intermediate values of coke rate; such reduction is amplified by lignite injection (Fig. 12.3).

Lignite coke can be employed to reduce dioxin/furan concentration when it is used as an adsorbent to the waste gas flow. PCDD/Fs are strongly reduced thanks to the lignite addition because of its strong bonding irreversible action on dangerous emissions and the further decomposition during heat treatment phase. Lignite is injected into the gas flow acting as a strong redactor of dioxin and furan emissions. Normally, the lignite injection is operated in different points of the gas flow pattern with various percentages; in the present study, the global addition of lignite to the exhaust gases is considered. For high coke rate levels, dioxin emission increases also with lignite injection. By taking a look to the dioxin evolution as a function of gas temperature and lignite injection, a strong decrease of emissions as temperature and lignite increase can be underlined (Fig. 12.4) even if lignite injection is still active at high gas flow temperatures.

A strong effect on the reduction of dioxin emissions is noted for the addition of CuCl. In Fig. 12.5, a strong reduction of emission level for the same lignite addition is due to the presence of CuCl.

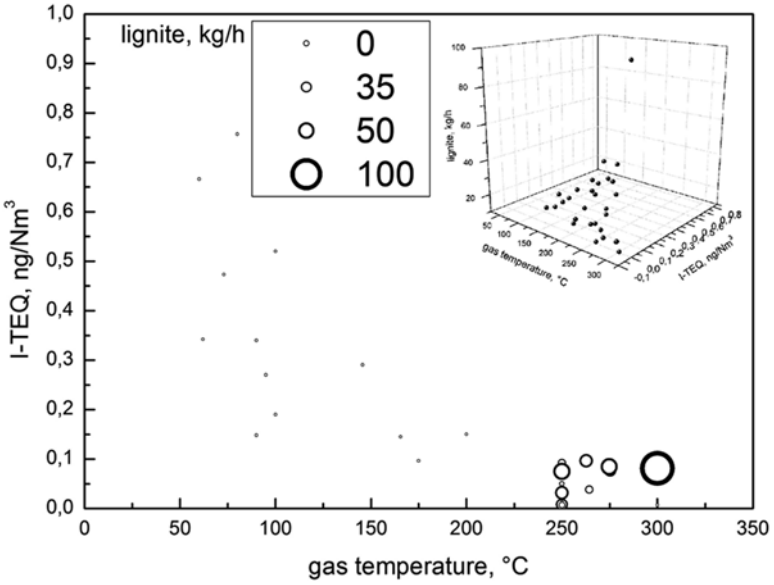

Fig. 12.4 Dioxin emissions as a function of gas temperature and lignite addition, high efficiency in emissions reduction is achieved by increasing temperature and lignite injection

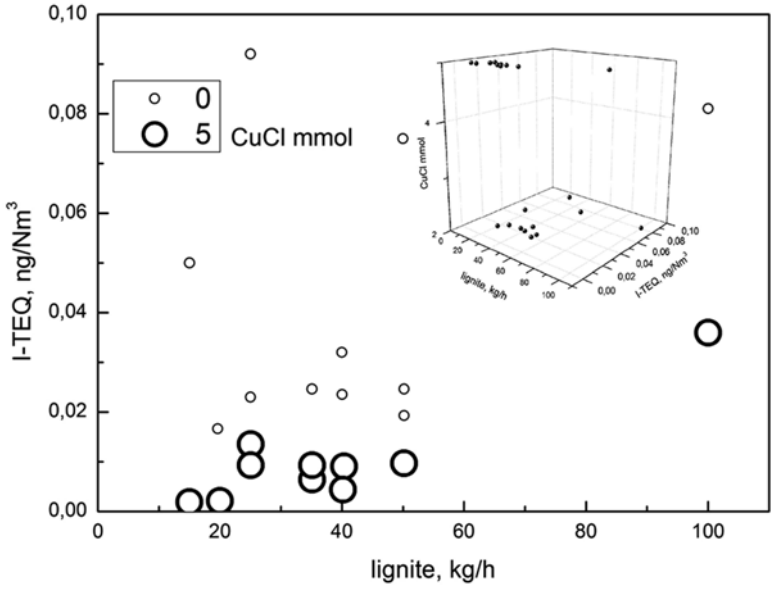

Fig. 12.5 Dioxin emissions as a function of lignite and CuCl, addition of CuCl is very efficient in reducing emissions levels

12.4 Conclusions

An electric gas furnace designed for a maximum flow rate of 1500 Nm^3/h was monitored in the present study. Different processing parameters were employed in order to measure the variation of dioxin and furan emissions to atmosphere. The results of the experimental analyses conduced to the main following conclusions:

- Dioxin emissions reach low levels at high flow rate and intermediate coke rates. Such result has been identified as a good instrument to control the PCDD/Fs control during the process.
- Also the temperature increase has a beneficial influence on dioxin and furan reduction.
- Lignite injection leads to a reduction in greenhouse emissions.
- An important effect on emission reduction is due to the addition of CuCl during processing.

References

Cavaliere P, Perrone A (2013) Analysis of dangerous emissions and plant productivity during sintering ore operations. Ironmak Steelmak 40:9–24. doi:10.1179/1743281212Y.0000000019

Chang MB, Huang HC, Tsai SS, Chi KH, Chang-Chien GP (2006) Evaluation of the emission characteristics of PCDD/Fs from electric arc furnaces. Chemosphere 62:1761–1673. doi:10.1016/j.chemosphere.2005.07.054

Everaert K, Baeyen J (2004) Removal of PCDD/F from flue gases in fixed or moving bed adsorbers. Waste Manage 24:37–42. doi:10.1016/S0956-053X(03)00136-3

Kulkarni PS, Crespo JG, Afonso CAM (2008) Dioxins sources and current remediation technologies-a review. Environ Int 34:139–153. doi:10.1016/j.envint.2007.07.009

Li HW, Lee HW, Tsai PJ, Moud JL, Chang-Chien GP, Yang KT (2008) A novel method to enhance polychlorinated dibenzo-p-dioxins and dibenzofurans removal by adding bio-solution in EAF dust treatment plant. J Hazard Mater 150:83–91. doi:10.1016/j.jhazmat.2007.04.077

Öberg T (2004) Halogenated aromatics from steel production: results of a pilot-scale investigation. Chemosphere 56:441–448. doi:10.1016/j.chemosphere.2004.04.038

Prüm C, Werner C, Wirling J (2004) Reducing dioxin emissions in electric steel mills. Stahl Eisen 124:61–67

Raghunatan K, Gullet BK (1996) Role of sulfur in reducing PCDD and PCDF formation. Environ Sci Technol 30:1827–1834. doi:10.1021/es950362k

Suzuki K, Kasai E, Aono T, Yamazaki H, Kawamoto K (2004) De novo formation characteristics of dioxins in the dry zone of an iron ore sintering bed. Chemosphere 54:97–104. doi:10.1016/S0045-6535(03)00708-2

Tan P, Hurtado I, Neushutz D, Eriksonn G (2001) Thermodynamic modelling of PCDD/Fs formation in thermal processes. Environ Sci Technol 35:1867–1874. doi:10.1021/es0002181

Chapter 13
Emission of High Toxicity Airborne Pollutants from Electric Arc Furnaces During Steel Production

João F.P. Gomes

Abstract The present chapter describes the determination of emissions of high toxic airborne pollutants (dioxins, dibenzofurans, polycyclic aromatic hydrocarbons, and polycyclic carbonyl biphenyls) from electric arc furnaces during the production of steel. By using the European Standard method CEN 1948 for dioxin-like compound sampling and measurement, it was possible to determine the characteristic fingerprint of these micropollutants emitted by this particular stationary source.

13.1 Introduction

Several well-known experimental evidences (Anderson and Fisher 2002; Wang et al. 2003) have concluded that steel production is an industrial activity characterized by atmospheric emission sources potentially emitting microorganic pollutants to the atmosphere (Buekens et al. 2001).

Electric arc furnace (EAF) steel production from ferrous scrap has been recognized as a potential source for organic micropollutant emission such as dioxins (polychlorodibenzodioxins—PCDDs), dibenzofurans (PCDFs), polycyclic aromatic hydrocarbons (PAHs), and polycyclic carbonyl biphenyls (PCBs). Usually, the formation of dioxin-like compounds requires the presence of organic compounds known as precursors such as phenols, chlorobenzenes, PCBs, and chlorine, catalytic substances such as cooper or any other heavy metals, and a reaction temperature between 200 and 600 °C (Altwicker et al. 1989).

PCBs, unlike other highly toxic compounds, such as PCDDs and PCDFs, are almost noncombustible, have very low vapor pressures at room temperature, are nonvolatile and non-soluble, have considerable thermal and chemical stability, and

J.F.P. Gomes (✉)
CERENA – Center for Natural Resources and Environment, Instituto Superior Técnico, Universidade de Lisboa, Av. Rovisco Pais, 1049-001 Lisbon, Portugal

ADEQ – Chemical Engineering Departmental Area, ISEL – Instituto Superior de Engenharia de Lisboa, Rua Conselheiro Emídio Navarro, 1959-007 Lisbon, Portugal
e-mail: jgomes@deq.isel.ipl.pt

P. Cavaliere (ed.), *Ironmaking and Steelmaking Processes*,
DOI 10.1007/978-3-319-39529-6_13

are resistant both to acid and alkali substances (Erickson 1997). Therefore, they have been used as dielectric fluids in electrical transformers and condensers, as adhesive, paints, hydraulic lubricants, etc. Nevertheless, its toxicity has been widely demonstrated, resulting in the restriction of PCB involvement in several applications. Both PCBs and PAHs have been reported as emitted from the steel and metallurgic industries, namely, when scrap is melted again in recycling processes, such as steel making from scrap via the EAF process (Anderson and Fisher 2002; Buekens et al. 2001).

Therefore, the study of the formation mechanism regarding these compounds during steel production in the EAF is quite important in order to define effective measures so that the emissions of dioxin-like compounds could be controlled by means of its operational parameters.

13.2 EAF Plant Description

Experimental measurements were made on an EAF installed in a steel mill in Northern Portugal. The EAF is a DEMAG unit, originally built in 1976, type UHP, having a power consumption of 48 MVA which produces 77 t of melted steel per heat, from 92 t of inlet material. Each production cycle lasts 2 h, operating continuously in day and night shifts. The type of scrap and raw materials used is presented in Table 13.1. Table 13.2 shows the actual quantities of raw materials, products, and

Table 13.1 Scrap type ranges

Scrap type	%
Fine scrap	13.3/19.6
Fragmented scrap	13.2/16.1
Average scrap	24.9/31.9
Industrial scrap	27.4/41.9
Ferrous rejects from foundries	5.0/5.4

Table 13.2 Quantities of raw materials, products, and by-products during measurement tests (ton)

Test code	Raw materials			Product	By-products	
	Scrap	Lime	Coke	Steel	Slag	Dust
54668	90.6	2.8	1.2	75.5	17.4	1.4
54671	82.3	2.5	1.2	72.4	13.8	1.2
54673	84.9	3.1	1.2	70.8	16.8	1.3
54682	95	2.5	1.2	83.1	14.1	0.8
54694	85.7	2.3	1.2	73.9	20.2	1.6
54696	92.5	2.3	1.2	77	18.6	1.6
54724	90.4	2.4	1.2	74.7	17.4	1.4
54728	92	2.3	1.2	76.5	18.5	1.5

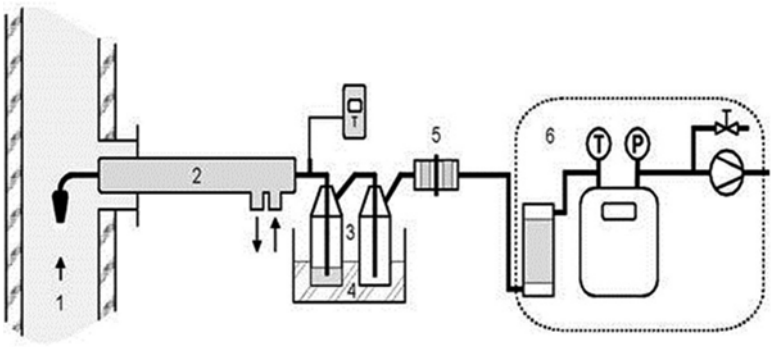

Fig. 13.1 Sampling apparatus: 1. flue gas, 2. water-cooled sampling probe, 3. condensate flask, 4. ice bath, 5. filter cartridge (PUF plugs and plane filter), 6. suction device

by-products (in ton) during measurement tests. Exhaust gases are collected in a hood and send through a pipe of two independent stacks, working simultaneously, the extraction flow being 135,000 Nm^3/h.

Each stack is equipped with different dedusting systems, each consisting of a bag filter device, indicated here as "A, Old system," and "B, New system." The flow sheet concerning the gas cleaning section is presented on Fig. 13.1. The total gas handling capacity is of 180,000 Nm^3/h. Both units work simultaneously in order to achieve a better abatement of pollutants. Unit "A, Old system," has a gas handling capacity of 80,000 Nm^3/h and a filtering area of 2480 m^2, whereas the unit "B, New system," has a capacity of 100,000 Nm^3/h and a filtering area of 2800 m^2.

The nominal design outlet concentration for total suspended dust is 20 mg/Nm^3.

13.3 Emission Measurements

Stack sampling measurements were made after the dedusting units both for "A, Old system," and "B, New system," units. A partial volume of the flue gas—e.g., gas including dust—is extracted via a glass tube from the flue gas duct and led into the collection system. The glass probe is installed centrically in a water-cooled probe of titanium. By the means of cooling water, a rapid cool down of the sample is executed (Fig. 13.1). The collection system consists of a condensate flask, receiving the accumulating condensate and a part of the dust, and of a cartridge with two polyurethane foams, a special sorbent with proven efficiency for the separation of organic substances. The foams are installed on both sides of a plane filter with high collection efficiency.

Connecting to this is an equipment group consisting of drying tower, gas pump, and gas volume meter. A sampling standard (C-13-labeled 1,2,3,7,8-PeCDF, 1,2,3,7,8,9-HxCDF, 1,2,3,4,7,8,9-HpCDF) is added to the condensate flask before

sampling. The flow of the sampled gas stream is adjusted to isokinetically[1] conditions on the sampling nozzle.

The sampling procedure is in compliance with the EU-Standard EN 1948, part 1 (CEN 1996a), using the alternative C-water-cooled probe. Emission samples were analyzed according to the European Standard EN 1948 parts 2 and 3 (CEN 1996b, c). Quantitative determinations of PCDD/PCDF in various samples were made according to the isotope dilution method with the use of the following 2,3,7,8-substituted 13C-UL internal standards. Afterward the extraction of the samples with appropriate solvents from the condensate, the PU foam, the plane filter was made. Additionally, the glass sampling tube was cut into pieces and extracted too. Cleanup was done in multicolumn systems involving carbon-on-glass fiber or carbon-on-celite. HRGC/HRMS measurements were made with VG-AutoSpec using SP2331 and/or DB-5 capillary columns. For each substance, two isotope masses were measured. Quantification is carried out with the use of internal/external standard mixtures. Seventeen congeners of PCDD/PCDF were determined, according to standard EN 1948, part 3 (CEN 1996c), as follows:

(a) PCDD:
2,3,7,8-TCDD(D1);1,2,3,7,8-PCDD(D2);1,2,3,4,7,8-HxCDD(D3);1,2,3,7,8,9-HxCDD (D5); 1,2,3,6,7,8-HpCDD; 1,2,3,7,8,9-HxCDD; 1,2,3,6,7,8-HpCDD; 1,2,3,4,6,7,8-HpCDD (D6); 1,2,3,4,6,7,8,9-OCDD (D7)

(b)PCDF:
2,3,7,8-TCDF (F1); 1,2,3,7,8-PCDF (F2); 2,3,4,7,8-PCDF (F3); 1,2,3,4,7,8-HxCDF (F4); 1,2,3,6,7,8-HxCDF (F5); 1,2,3,7,8,9-HxCDF (F6); 2,3,4,6,7,8-HxCDF (F7); 1,2,3,4,6,7,8-HpCDF (F8); 1,2,3,4,7,8,9-HpCDF (F9); 1,2,3,4,6,7,8,9-OCDF (F10).

Regarding polycyclic aromatic hydrocarbons and polycyclic carbonyl biphenyls, the sampling technique was again based on the European Standard method EN 1948 (CEN 1996a), which specifically concerns dioxin and dibenzofuran sampling and analysis, as previously mentioned. However, certain modifications were introduced in order to isokinetically sample PAHs and PCBs. The analytical determinations were performed in a HRGC/HRMS, VG-AutoSpec using capillary column DB5. PAH analysis included the determinations of 16 congeners, defined according USEPA, using deuterated extracts ranging from D^8 to D^{14} as follows:

Naphthalene	Benz(a)anthracene
Acenaphtalene	Chrysene
Acenaphtene	Benzo(b)fluoranthene
Fluorene	Benzo(k)fluoranthene
Phenanthrene	Benzo(a)pyrene
Anthracene	Indene(1,2,3)-cd-pyrene
Fluoranthene	Benzo(ghi)perylene
Pyrene	Dibenz(ah)anthracene

[1] Isokinetic sampling is a sampling at a rate such that the velocity of the gas entering the sampling nozzle is the same as that of the gas in the duct at the sampling point (ISO 2003).

Regarding PCBs, the analysis covered the isomers 28, 52, 101, 138, 153, and 180 and total homologue using internal standards marked with ^{13}C. For the utilized sampling volumes, the detection limit both for PAHs and PCBs was determined at 0.01 mg/m^3. The basic sampling procedure, using a cooled probe, was the same already described for dioxins and dibenzofurans. However, the sampling time was now considerably reduced to about an hour. Particulate matter was collected on a filter, and the gaseous phase was collected by condensation on an adsorbent agent. After sample recovery, the sampling train was decontaminated using water and acetone. Filters and adsorbents are mixed together for extraction with an organic solvent by Soxhlet and then concentrated in a rotovapor device. It is necessary to remove any interferents from the final extract before performing the chromatographic analysis by HRGC/HRMS. The determinations are made by adding internal and external deuterated standards as follows:

Naphthalene	D^8
Acenaphthylene	D^{10}
Phenanthrene	D^{10}
Pyrene	D^{10}
Benzo(k)fluoranthene	D^{12}
Benzo(a)pyrene	D^{12}
Dibenz(ah)anthracene	D^{14}
Benzo(ghi)perylene	D^{12}

The same sample was used for determination of PCB 28, 52, 101, 138, 153, and 180 and total homologue. This later determination was made using the following internal standards:

2,4,4′-Tri-PCB (PCB 28)	^{13}C-UL
2,2′,5,5′-Tetra-PCB (PCB 52)	^{13}C-UL
2,2′,4,5,5′-Penta-PCB (PCB 101)	^{13}C-UL
2,2′,3,4,4′,5′-Hexa-PCB (PCB 138)	^{13}C-UL
2,2′,4,4′,5,5′-Hexa-PCB (PCB 153)	^{13}C-UL
2,2′,3,4,4′,5,5′-Hepta-PCB (PCB 180)	^{13}C-UL

After the addition of standards, samples were extracted with nanograde-specific solvents. The procedure for interferent removal, already described for PAHs, was also used here prior to the chromatographic determination.

13.4 Discussion

The summary of obtained results is presented in Table 13.3.

Our experience shows that, in general, uncertainties in the range of 10–20 % for the components listed in the above tables. For values close to the detection limit, the uncertainties are higher. Based on the measurements made, Figs. 13.2 and 13.3 show the existence of individual species of dioxins and furans, in the picogram

Table 13.3 Summary table of dioxins/furans in the new and old dedusting systems: concentration of the determined components, referring to standard conditions (1013 hPa, 273 K), expressed as I-TEQ (pg/m^3)

Measurements	A—Old system	B—New system
1	67	84
2	105	53
3	832	129
4	121	86
Average	281	88

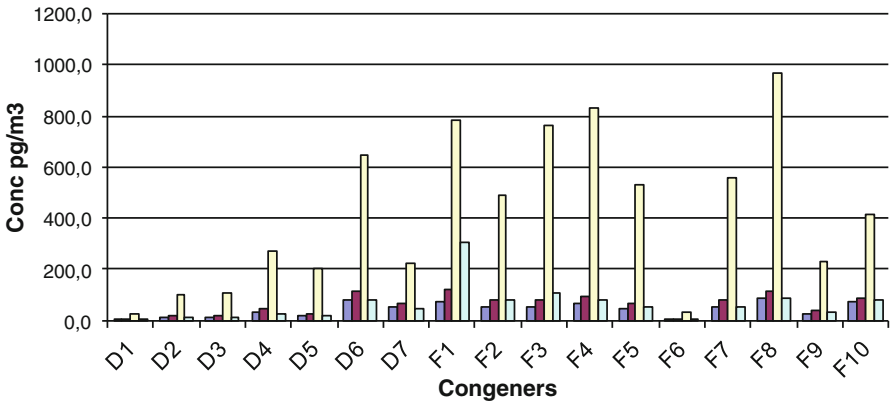

Fig. 13.2 Diagram of 17 dioxin and furan congeners in eight measurements of dioxins and furans in the stack of the new dedusting system

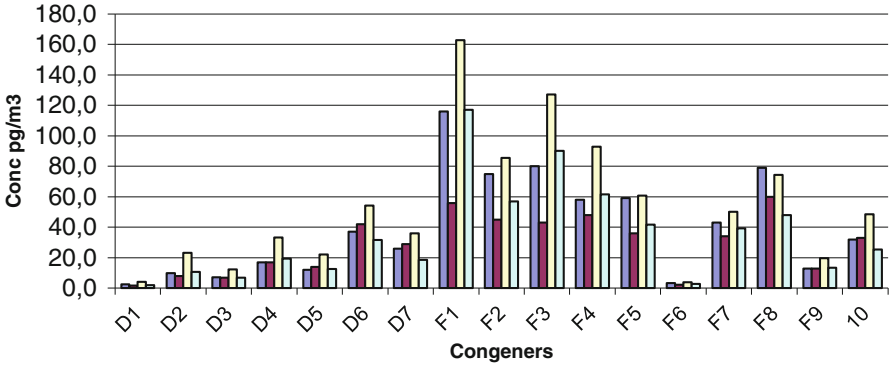

Fig. 13.3 Diagram of 17 dioxin and furan congeners in eight measurements of dioxins and furans in the stack of the old dedusting system

range, with a prominence of 2,3,4,7,8-pentaCDF in all measurements. In this plot, the existence of 17 searched compounds was verified. The obtained values are not homogeneous with some dispersion of the obtained results, for congeners and also for the total of the dioxins/furans. However, observing Figs. 13.4 and 13.5, the

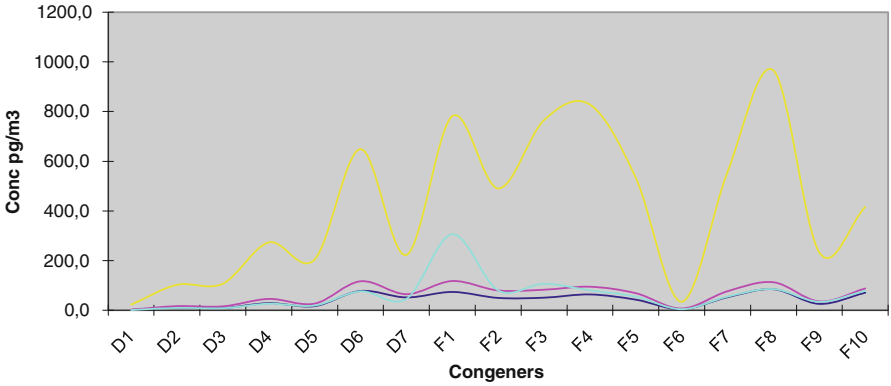

Fig. 13.4 Profile of 17 congeners in eight measurements of dioxins and furans in the stack of the new dedusting system

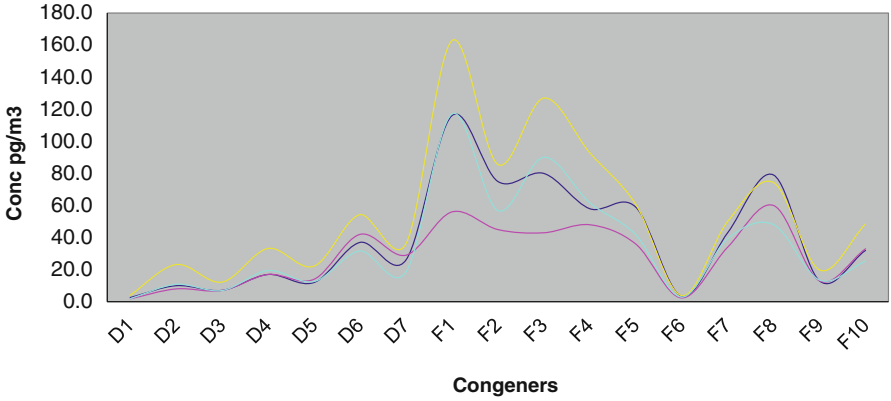

Fig. 13.5 Profile of 17 congeners in eight measurements of dioxins and furans in the stack of the old dedusting system

existence of a coherent profile is verified. It can be noted that this kind of profile is always observed during the operation of this EAF system and is nondependent of the gas flow rate neither of the EAF actual processing capacity. The average value obtained in these measurements is of 0.18 I-TEQ ng/m^3. However, registered values are very high (in the order of the 0.83 I-TEQ ng/m^3), but very low values (approximately 0.05 I-TEQ ng/m^3) were also measured. The variations observed can possibly be explained by different production regimes, using different loads for the furnace, which were observed during sampling operations. These measurements are considerably long, about 6 h, and generally 4–6 different charges (comprising different loads) each, which contributes to the observed variability in the amount of micropollutants. Nevertheless, it can be noticed that the profile of analyzed congeners seems to be nearly the same for all the sampling trials.

It should be noted that, within the scope of the mentioned European Standards, there is no standardized method for the determination of the uncertainty of measurement that covers both sampling and the analytical procedure as well as the uncertainty related with the conditions of the sampling site in special. For this reason, the single results are not supplied with information on uncertainty.

Our experience shows that, in general, uncertainties lie in the range of 10–20 % for the components listed in the above tables. For values near the detection limit, the uncertainties might be higher.

Based on the performed measurements, Fig. 13.6 shows the existence of individual species of PAHs, where a prominence of naphthalene, acenaphthylene, phenanthrene, and fluorine could be noticed. Other species such as fluoranthene, pyrene, acenaphtene, and chrysene were also found in lower amounts. As a whole, the existence of 12 of the 16 searched species of PAHs was verified, as benzo(a)pyrene, indene(1,2,3)-cd-pyrene, benzo(ghi)perylene, and dibenz(a,h)anthracene were not detected. Carefully observing this figure, with a zoom from anthracene on, the existence of a coherent profile is also verified, and this is the actual "fingerprint" of this process in terms of PAH emissions. In fact, it can be noted that this profile is always observed during the operation of this EAF system and is nondependent of the gas flow rate neither of the EAF actual processing capacity.

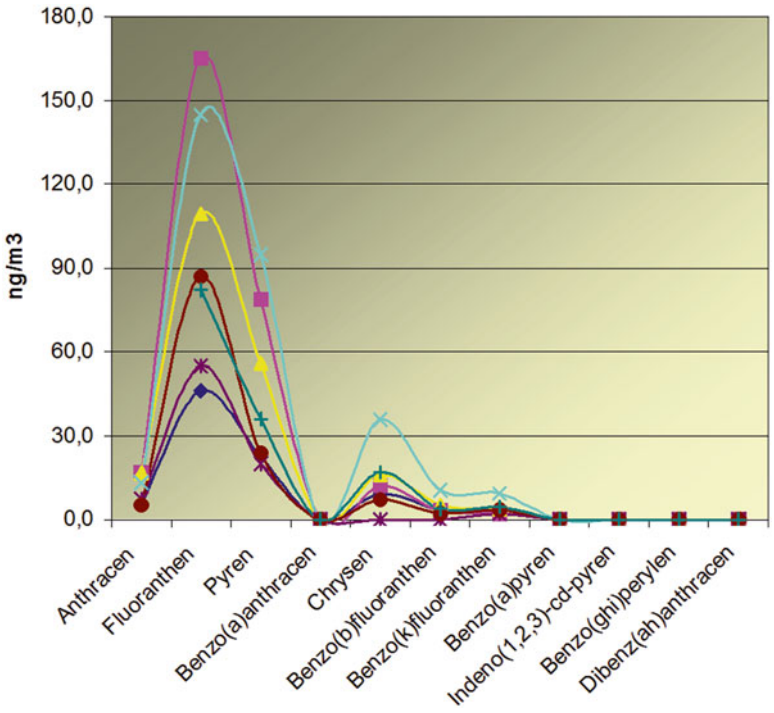

Fig. 13.6 Profile of PAHs obtained in 7 measurements

Table 13.4 Physical-chemical properties of PAHs (Erickson 1997)

PAHs	Number of rings	Mol. weight (g/mol)	Fusion point (°C)	Boiling point (°C)	Chemical formula
Naphthalene	2	128	80.6	218	$C_{10}H_8$
Acenaphthylene	3	152	94	265	$C_{12}H_8$
Phenanthrene	3	178	99.5	340	$C_{14}H_{10}$
Fluorene	3	166	116	295	$C_{13}H_{10}$
Acenaphtene	3	154	95	279	$C_{12}H_{10}$
Anthracene	3	178	217	370	$C_{14}H_{10}$
Fluoranthene	4	202	110.8	375	$C_{16}H_{10}$
Pyrene	4	202	156	404	$C_{16}H_{10}$
Chrysene	4	228	255	448	$C_{18}H_{12}$
Benz(a)anthracene	4	228	159.8	437.6	$C_{18}H_{12}$
Benzo(a)pyrene	5	252	176	495	$C_{20}H_{12}$
Dibenz(a,h)anthracene	5	278	266	524	$C_{22}H_{14}$
Benzo[k]fluoranthene	5	252	215.7	480	$C_{20}H_{12}$
Benzo[b]fluoranthene	5	252	167	357	$C_{20}H_{12}$
Indene(1,2,3)-cd-pyrene	6	276	162.5	536	$C_{22}H_{12}$
Benzo(ghi)perylene	6	276	278	500	$C_{22}H_{12}$

The observed variations can possibly be explained by different production regimes, using different loads for the furnace, which were observed during sampling operations.

Table 13.4 presents the main physical and chemical properties (Erickson 1997) of the measured PAHs. It can be noticed that the species that were not found present in the stack emissions are the species with five and six benzene rings, which have strongly adhered to dust particles and, thus, are collected by bag filters as dust-capturing devices (Fig. 13.7).

It was also found that the dedusting systems, apart from retaining dust and fine particulate, are mainly maintaining the presence of the compounds that are solid samples, as they are not producing different concentration profiles but are only attenuating them, that is, are reducing its concentration, as can be seem on Fig. 13.8 for PAHs.

From the measured, the following observations should be highlighted:

For the gaseous phase, before the dedusting unit, high quantities of all micropollutants are detected, while after the dedusting unit, only residual quantities are detected in the gaseous effluent samples (Table 13.5).

The fingerprint profile of PCDDs/PCDFs determined in gaseous samples collected in the main duct shows a consistent profile. The relative amount of concentrations for micropollutant species are higher for PAHs and then PCBs and lowest for PCDDs/PCDFs, both for samples collected before and after the dedusting unit. The observed profiles for PCDDs/PCDFs are slightly different from samples collected before and after the dedusting unit. While for samples before the dedusting unit, OCDD and OCDF show concentration peaks, in samples collected after the

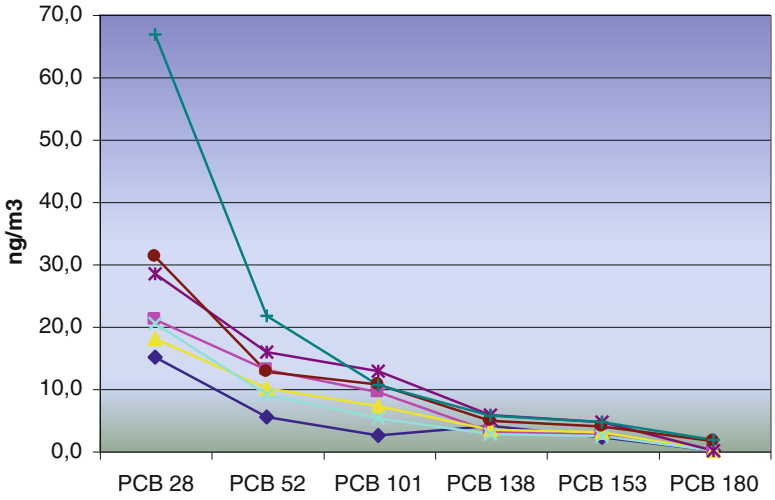

Fig. 13.7 Profile of PCBs obtained in 7 measurements

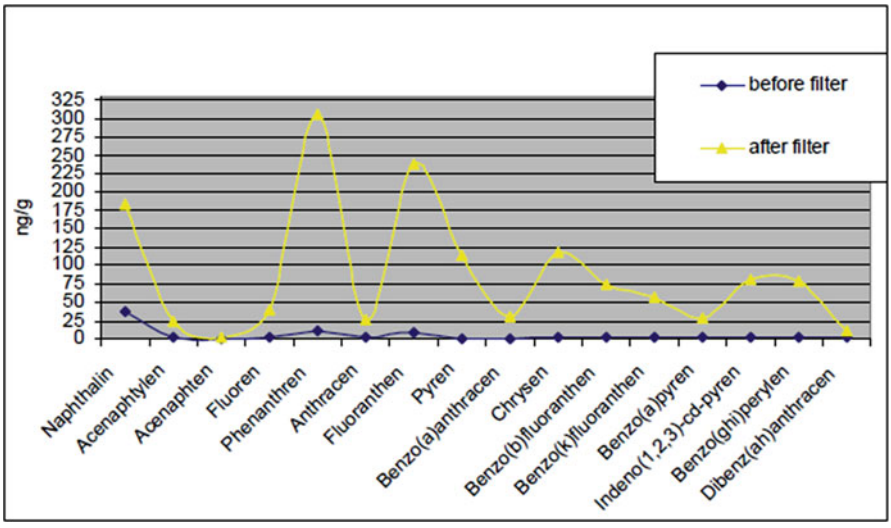

Fig. 13.8 Profile of PAHs in solid samples before and after dedusting unit

dedusting unit, these same compounds exhibit the lowest concentrations. The observed profile for PAHs is slightly similar both from samples collected before and after the dedusting unit.

In what regards PCBs, the same does not happen and a slight variation on the "fingerprint" profile before and after the dedusting system occurs.

For the particulate phase, samples of dust collected from the dedusting unit show high quantities of micropollutants, mainly of PAHs and PCBs but not PCDDs/PCDFs,

Table 13.5 Physical-chemical properties of PCBs (Erickson 1997)

PCBs	N° of chlorine atoms	Mol. weight (g/mol)	Boiling point (°C)	Fusion point (°C)	Vapor pressure at 25 °C (Pa)	Evaporation rate at 25 °C (g/m^2 h)
PCB 28	3	256	28–87	337	0.054	0.017
PCB 52	4	290	47–180	360	0.012	4.2×10^{-3}
PCB 101	5	324	76.5–124	381	2.6×10^{-3}	1.0×10^{-3}
PCB 138	6	358	77–150	400	5.8×10^{-4}	2.5×10^{-4}
PCB 153	6	358	77–150	400	5.8×10^{-4}	2.5×10^{-4}
PCB 180	7	391	122.4–149	417	1.3×10^{-4}	6.2×10^{-5}

when compared with samples of dust collected from the bottom of the stack, before the dedusting unit. Samples of dust collected from the bottom of the stack, before the dedusting unit, are almost free of PCBs as the detected concentrations for these compounds are only very near the detection limits of the analytical methods. The fingerprint profile for all micropollutant species (PCDDs/PCDFs, PAHs, and PCBs) is slightly similar for both samples collected before and after the dedusting unit.

These observations suggest that the installed dedusting units seem efficient for removal of particulate matter from the gaseous effluent. As these species of micropollutants usually are aggregated into the particulate phase, this also makes the dedusting units efficient for removal of micropollutants from the gaseous effluent. Thus, micropollutants are then collected in the dust removed in the dedusting unit. Apparently, the observed difference between fingerprint profiles for the micropollutant species in the gaseous phase indicate that highly chlorinated species such as OCDD and OCDF were formed near the EAF, and they reduce their relative amounts probably due to the temperature reduction in the dedusting unit itself. As a whole, there are considerable reductions of PCDDs/PCDFs from samples before and after the dedusting unit, when comparing both gaseous and particulate phases. For PAHs, the latter behavior is the opposite, when comparing gaseous and particulate phases. For PCBs, these species diminish in the gaseous phase from before to after the dedusting unit and become apparent in the particulate phase after the dedusting unit, which could be due to the decrease in temperature that makes for its aggregation to the particulate phase, and thus less higher molecular weight PCBs are detected in the gaseous phase. This similar behavior, regarding higher molecular weight compounds, is also true for PAHs.

All these suggest that two different mechanisms exist regarding two different zones having considerably different temperatures: one mechanism is responsible for the generation of these compounds near the EAF (where temperature is higher) governed by the de novo synthesis and possibly facilitated by the presence of metallic catalysts.

In the duct and after the EAF, where temperature is lower, a mechanism based on organic precursors coming from contamination of the scrap seems to govern. This latter mechanism could also be enhanced by the presence of metallic catalysts as heavy metals are also frequently detected in the flue gas.

13.5 Conclusions

The principal kind of emissions from electric arc furnace operations is described in the present chapter. A very clear profile of dioxins and dibenzofurans does exist which can be considered as the emission fingerprint for this process. The obtained concentrations are higher in the new system, where the majority of gas flow (55 %) and also the filtration area are bigger (53 %), and thus a higher concentration of reactive species could be expected to exist in the new system. Dispersion is observed in each group for both the old and new system. As this scrap is considered to be non-contaminated and thus precursors are, a priori, nonexistent, there is a possibility of occurrence of heterogeneous reactions over particulate surface at temperatures higher than 300 °C, but as the oven temperature is higher than 1500 °C, certain organic species are destroyed. However, it is believed that the basic conditions for occurrence of de novo synthesis (without organic precursors) do exist. This can be enhanced at temperatures higher than 250 °C and by the occurrence of metallic species acting as catalysts.

These studies have, so far, allowed to derive some important conclusions on the emission of gaseous micropollutants, making possible to determine the characteristic profile (also known as “fingerprint”) of PCDDs/PCDFs, as well as PAHs and PCBs.

In fact, in spite of some observed variability in successive sampling campaigns, it was possible to determine regular concentration profiles of the gaseous emissions of the sampled compounds. This is the basic information that will allow, further on, to derive further conclusions on the mechanisms of formation/destruction of these species and, at a later stage, to define operational strategies to perform the abatement of these emissions.

It should be noted that the observed existence of PAH and PCB species, which are PCDD/PCDF precursors, could easily result in the formation of PCDD/PCDF congeners by the means of heterogeneous reactions, on the surface of particles and dust that occur at temperatures higher than 300 °C (Wang et al. 2003).

Acknowledgments This work was partially supported by the European Commission under contract N° 7210-PR-200 (Figueira and Gomes 2004; Gomes 2008).

References

Altwicker ER, Schonberg JS, Konduri RK, Milligam MS (1989) Polychlorinated dioxin/furan formation in incinerators. Hazard Waste Mater 7:73–87. doi:10.1089/hwm.1990.7.73

Anderson DR, Fisher R (2002) Sources of dioxins in the United Kingdom: the steel industry and other sources. Chemosphere 46:371–381. doi:10.1016/S0045-6535(01)00178-3

Buekens A, Stieglitz L, Hell K, Huang H, Segers P (2001) Dioxins from thermal and metallurgical processes: recent studies for the iron and steel industry. Chemosphere 42:729–735. doi:10.1016/S0045-6535(00)00247-2

CEN (1996a) CEN/EN 1948 – Part 1: stationary source emissions – determination of the mass concentration of PCDDs/PCDFs, Brussels

CEN (1996b) CEN/EN 1948 – Part 2: stationary source emissions – determination of the mass concentration of PCDDs/PCDFs, Brussels

CEN (1996c) CEN/EN 1948 – Part 3: stationary source emissions – determination of the mass concentration of PCDDs/PCDFs, Brussels

Erickson MD (1997) Analytical chemistry of PCBs. Lewis Publishers, New York

Figueira SL, Gomes JF (2004) Emissions of dioxin and dibenzofuran from electric arc furnaces. Revista de Metalurgia Madrid 40:164–168

Gomes JF (2008) Emissions of polycyclic aromatic hydrocarbons and polycyclic carbonyl biphenyls from electric arc furnaces. Revista de Metalurgia Madrid 44:280–284. doi:10.3989/revmetalm.2008.v44.i3.117

ISO (2003) ISO Norm 9096. Stationary source emissions – manual determination of mass concentration of particulate matter, Geneva

Wang T, Anderson DR, Thompson D, Clench M, Fisher R (2003) Studies in the sintering process used in the iron and steel industry. 1. Characterization of isomer profiles in particulate and gaseous emissions. Chemosphere 51:585–594. doi:10.1016/S0045-6535(02)00784-1

Chapter 14
Use of Sustainable Inorganic Binders in the Treatment of Bag-House Dust

Beste Cubukcuoglu

Abstract Cementitious materials are the most popular binding agents used in the treatment of hazardous waste to convert it from an unstable to a more stable form. The use of ordinary Portland cement (PC) or other hydraulic binders (such as pozzolanic power plant fly ash) in the solidification/stabilisation (S/S) process is one of the best available methods for the treatment of waste that cannot be reduced, destroyed or recycled.

There are many other studies and researchers who agree that PC is the main binder being used to solidify and immobilise pollutants into a solid form (Li et al., J Hazard Mater 82:215–230, 2001). In addition to cement, pozzolanic materials are also used for this purpose. These mainly include PFA, blast furnace slag, silica fume, natural or modified clays and sand (Poon et al., Waste Manage Res 3:127–142, 1985). Although cement was selected as the main binder in the S/S technique, it was realised in the past century that it has detrimental effects on the environment and human health. The production of cement causes large amounts of carbon emissions to be released into the environment and involves an overuse of natural resources (Middendorf et al., Lime pozzolan binders: an alternative to OPC, 2005).

This has incited the use of different types of additives and binders as substitutes for cement. Many different formulations have been developed for the S/S process mainly based on the type of waste or heavy metals it might include. It has been proved that PC can be modified and/or replaced using fly ash, hydrated lime, steel slag, soluble silicates, clay and magnesium oxide (MgO) for suitable S/S process (Mayers and Eappi, Laboratory evaluation of stabilization/solidification technology for reducing the mobility of heavy metals in New Bedford Harbour superfund site sediment, stabilization of hazardous radioactive and mixed wastes, 1992; Singh and Garg, Cem Concr Res 29:309–314, 1999; Fernandez et al., J Environ Eng 129:275–279, 2003; Turkel, J Hazard Mater 137:261–266, 2006; Tsakiridis et al., J Hazard Mater 152:805–811, 2008; Fernandez-Pereira et al. Fuel 88(7):1185–1193, 2009; Zhang et al., Cem Concr Res 41:439–442, 2011).

B. Cubukcuoglu (✉)
Department of Civil Engineering, Faculty of Engineering, Antalya International University, Antalya, Turkey
e-mail: Beste.cubukcuoglu@antalya.edu.tr

P. Cavaliere (ed.), *Ironmaking and Steelmaking Processes*,
DOI 10.1007/978-3-319-39529-6_14

An industrial by-product may be used in the cement manufacturing process in two different ways. One could be the use of the by-product as the raw material feed to the kiln in the manufacture of PC in place of coal. Alternatively, by-products could be used together with PC by mixing slag cements or PFA as pozzolans (Gutt, Manufacture of cement from industrial by-products, 1971; Tsakiridis et al., J Hazard Mater 152:805–811, 2008). Alternative binding agents to cement are discussed in detail with the aim of achieving the most sustainable material that could be used in the treatment of industrial wastes as binding agents which would allow them to be used as construction materials. The S/S treatment is based on binders and waste mixtures where the binders used in these systems are most likely alkaline materials that reduce the leachability of the metals in a high-pH matrix.

14.1 Introduction

Steel industry is the key element in the industrialisation and economic development of a country due to its high input within all manufacturing sectors. Moreover, most buildings are structurally made from steel which means that there is a huge need of steel products even for construction industry. The global crude steel production is reported as 1646 mega tonnes (Mt) for the year 2014 (World Steel Association 2015). However, steel-making industry is one of the main and biggest hazardous waste producers in the world. Throughout the world, steel foundries are faced with the major problem of dealing with the hazardous waste generated from the electric arc furnaces.

Hazardous waste and hence its disposal has been problematic issues since industrialisation began. The increasing awareness of the environmental impact arising from the disposal of these types of wastes has forced the authorities to make the driving legislations more stringent. Recent amendments in the legislations all over the world introduced the mandatory treatment of all hazardous wastes prior to their disposal in landfill. Accordingly, all hazardous wastes have to be pretreated before landfill disposal. In addition, the increasing cost of landfill disposal has incited industries, including waste management companies, to find novel alternative options to deal with the complexity of hazardous waste disposal.

Electric arc furnace dust (EAFD) is generated as an air pollution control (APC) residue during the melting of scrap steel in the electric arc furnaces. These dusts are extremely fine particles formed by the metal vaporisation process in the electric arc furnaces and collected in the bag-house dust. EAFD is an industrial waste and is classified as hazardous according to the European Waste Catalogue (EWC) under the code of 10 02 07*, mainly due to its heavy metal content, i.e. lead (Pb), cadmium (Cd), zinc (Zn) and chromium (Cr) (European Union Council 2002). The disposal of EAFD has been a problematic and costly issue as the amounts produced worldwide are extremely high. In the electric steel process, the specific dust proportion per tonne of crude steel is about 10–20 kg, i.e. the mass of dusts produced corresponds to about 1–1.5 % of the mass metal produced in the electric arc furnace (Stegemann et al. 2000; Menad et al. 2003).

Reduction in the mobility of the waste and hence the leachability of pollutants of concern is the main aim of the S/S processes. After pretreatment, S/S products can either be disposed of in landfill or be considered for reuse in the construction industry, depending on the structure and physical and chemical characteristics of the final products (Wiles and Barth 1992).

14.2 Solidification/Stabilisation (S/S) Treatment of Hazardous Wastes

Solidification/stabilisation (S/S) technology is one of the most commonly used treatment technique for the hazardous wastes. Therefore, it has been also proposed as a treatment method for the wastes that are generated by the steel manufacturing industry. During S/S treatment of hazardous waste, Portland cement type I (hereafter PC) was commonly used to effectively solidify and hence encapsulate the toxic content of the waste within the solid matrix (Li et al 2001). Therefore, there is a need of huge amount of cement to be used in this process. However, due to cement's detrimental impact on the environment during its manufacturing process, scientists have been looking for alternative materials which may be proposed to replace cement (Gutt, 1971; Mayers and Eappi, 1992; Singh and Garg, 1999; Fernandez et al. 2003; Middendorf et al. 2005; Turkel, 2006; Tsakiridis et al. 2008; Fernandez-Pereira et al. 2009; Zhang et al. 2011). This should be a material which is as cheap and effective as cement.

Cement has the ability to gain strength very quickly as soon as it reacts with water. Therefore, it is a must that the proposed material should possess similar chemical characteristics and be more environmental friendly than cement. Accordingly, it is found out that pulverised fuel ash (PFA) which is a by-product of coal-fired power stations can replace cement efficiently as it possesses pozzolanic characteristics which allow it to react with cement and gain strength by time. This is a well-known material which was proposed as a cement replacement. When it comes to dealing with hazardous wastes with a variety of toxic content, it is important to evaluate the leaching potential of each toxic material contents of the waste. Relying on this important consideration, it is required to test the leaching potential of PFA-blended waste matrices. It is clear from the literature that PFA has been successful in the treatment of EAFD with effective leaching test results (Poon et al. 1985, 2001; Fuessle and Taylor 2004; Atis and Bilim 2007; Pereira et al. 2001, 2007; Fernandez-Pereira et al. 2009). However, due to some unexpected leaching potential of some toxic content of EAFD, it was observed that PFA was not effective in molybdenum leaching.

In the meantime, another by-product material has been proposed for the S/S treatment of EAFD which is a hard-burned low-grade magnesium oxide (hereafter LGMgO), obtained from the calcination process of magnesite (Cubukcuoglu and Ouki 2012). An LGMgO-blended waste matrix was proposed in order to formulate a better option for PFA to assure the immobilisation of all toxic elements with leaching potential. Accordingly, the compression strength value of the matrix was reduced, but a better toxic encapsulation was achieved. This is due to the high pH range

Table 14.1 Chemical composition of materials

Compound	PC (%)	MgO (%)	PFA (%)	Lime (%)	S.slag (%)	EAFD (%)
CaO	63.78	9.80	1–5	10.2	29.36	7.15
SiO_2	20.33	3.09	45–51	0.20	0.19	1.71
Al_2O_3	4.47	0.38	27–32	0.05	9.73	0.52
SO_3	3.09	4.14	0.3–1.3	–	–	–
Fe_2O_3	2.52	2.45	7–11	0.2	31.37	50.75
MgO	1.07	65.34	1–4	3.2	20.57	2.32
$K_2O + Na_2O$	0.81	0.23	1–5	–	–	0.57
Cl	0.03	–	0.05–0.15	–	–	–
Mn	–	0.11	–	–	5.05	3.34
TiO_2	–	–	0.8–0.11	–	–	0.07
$Ca(OH)_2$	–	–	–	57.6	–	–
$CaCO_3$	–	–	–	23.6	–	–
Zn	–	–	–	–	0.08	16.08
P	–	–	–	–	0.38	<0.01
Pb	–	–	–	–	0.10	3.09
Mo	–	–	–	–	0.02	0.05
Cr	–	–	–	–	–	0.82
Insoluble	–	–	–	0.32	–	–
Loss on ignition	2.33	–	–	–	–	–
Non-detected	1.57	14.46	–	4.63	3.15	13.53

(9–11) of MgO which controls and minimises the solubility of metal hydroxides. Ion exchange between magnesium and other metal cations and possible complexation between contaminants and OH groups on the MgO surface provides the superior immobilisation capacity to LGMgO (Garcia et al. 2004; Cubukcuoglu and Ouki 2012; Tresintsi et al. 2013; Valle-Zermeno et al. 2015; Jin et al. 2015).

Steel slag is another very commonly used material for the S/S process of heavy metals. There are different types of steel slags that are generated as by-products from the steel manufacturing industry. They do all have different chemical compositions which bring their own characteristics alongside with them. The chosen steel slag is effective in S/S process due to its high MgO content compared to other materials like PFA and lime (see Table 14.1). Steel slag and LGMgO are both by-products generated by the industrial processes, and hence they are pertinent binders in this particular research. It is therefore important to evaluate their performance as a cement replacement binder to potentially improve the sustainability of this technique for the treatment of this particular waste product in discussion.

The aim is to produce solidified waste products that comply with the landfill waste acceptance criteria (WAC) and could have potential for beneficial reuse. This may only be achieved by performing comprehensive and controlled laboratory-based experiments to evaluate the viability of this technique for the remediation of EAFD by implementing the following objectives:

- Perform a detailed chemical characterisation of the materials and waste products used in the study in order to establish the chemical nature and level of the pollutants of concern present in the waste.
- Perform a preliminary screening programme in order to select the potential mix designs (CEMI: binder, water: solid (w/s) ratios and % of EAFD addition) for further detailed investigations.
- Evaluate the effects of different binders on the physical characteristics of the final solidified products by examining the following relevant parameters: unconfined compressive strength (UCS), setting time, bulk density (BD), consistency, specific gravity and moisture content (MC). Most of these parameters require close monitoring if the waste is to be disposed of in a landfill environment.
- Evaluate the leaching characteristics of the untreated and treated waste products with respect to the pollutants of concern (Cd, Cr, Pb, Zn, Mo and chloride (Cl^-)) in order to establish a better understanding of the leaching mechanisms involved and hence optimise the immobilisation capability of the systems studied. An acid neutralisation capacity (ANC) test coupled with granular and monolith leaching tests will provide pertinent information regarding the buffering capacity of the treated and untreated wastes as well as the long-term leaching behaviour under conditions that nearly simulate practice.
- Perform extended and advanced microstructural and mineralogical testing on a selection of treated and untreated specimens with a view to develop a better understanding of the chemical nature of the products formed, the location of the pollutants before and after treatment and, consequently, the effectiveness of S/S in the immobilisation of the pollutants of concern.

14.3 Effect of EAFD Addition on S/S Products Using PC, Lime, LGMgO, Steel Slag and PFA

Basic characterisation of EAFD has shown that its hazardous properties are due to the concentration of Pb (699.1 mg/kg) and Zn (111.4 mg/kg) which exceeded the hazardous waste landfill (BS EN 12457-3) set limits of 50 and 30 mg/kg respectively. The waste sample was found to be toxic for reproduction and ecotoxic. The results show that almost all blended mix ratios studied were successful in terms of physical integrity including UCS, setting time and consistency tests, but only few were capable of stabilising heavy metals. The setting and strength development were delayed mainly due to the heavy metal content of the waste. Best physical performances were achieved in the following order: CEMI-only>CEMI-slag>CEMI-PFA>CEMI-LGMgO. However, most of the slag-blended samples achieved higher UCS values than CEMI-only samples at longer curing ages (≥28 days). UCS results of potential mix designs at 28 days curing age are shown in Fig. 14.1. A legend has been prepared for this UCS data analyses: CEMI-only (C), CEMI-EAFD 60:40 (C1), CEMI-EAFD 30:70 (C2), CEMI-LIME 33:67 (L1), CEM-LIME 20:80 (L2), CEMI-LIME-EAFD 20:40:40 (L3), CEMI-LIME-EAFD

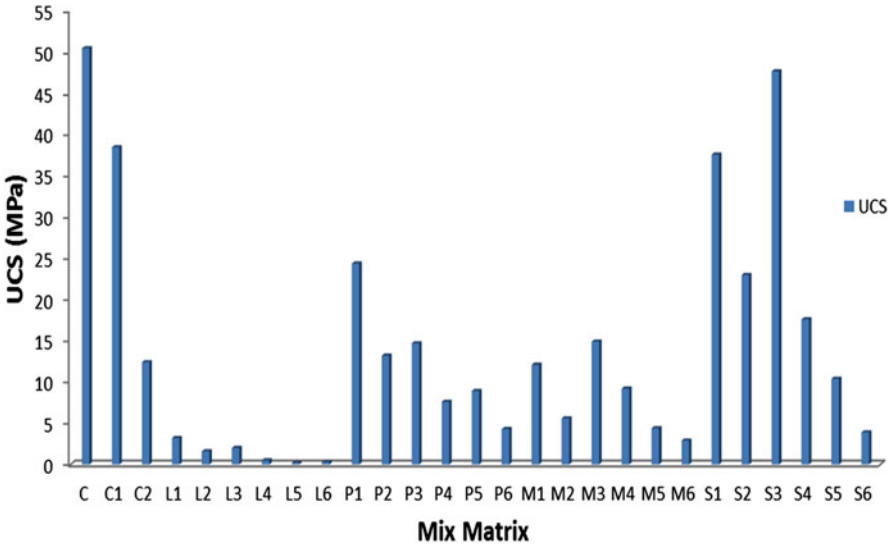

Fig. 14.1 UCS values of mix matrices at 28 days curing age

Table 14.2 pH values of as-received materials

Material	pH
PC	12.67
LGMgO	11.78
Steel slag	12.25
Lime	12.36
PFA	9.93
EAFD	12.16

12:48:40 (L4), CEMI-LIME-EAFD 10:20:70 (L5), CEMI-LIME-EAFD 6:24:70 (L6), CEMI-PFA 33:67 (P1), CEM-PFA 20:80 (P2), CEMI-PFA-EAFD 20:40:40 (P3), CEMI-PFA-EAFD 12:48:40 (P4), CEMI-PFA-EAFD 10:20:70 (P5), CEMI-PFA-EAFD 6:24:70 (P6), CEMI-LGMgO 33:67 (M1), CEM-LGMgO 20:80 (M2), CEMI-LGMgO-EAFD 20:40:40 (M3), CEMI-LGMgO-EAFD 12:48:40 (M4), CEMI-LGMgO-EAFD 10:20:70 (M5), CEMI-LGMgO-EAFD 6:24:70 (M6), CEMI-SLAG 33:67 (S1), CEM-SLAG 20:80 (S2), CEMI-SLAG-EAFD 20:40:40 (S3), CEMI-SLAG-EAFD 12:48:40 (S4), CEMI-SLAG-EAFD 10:20:70 (S5) and CEMI-SLAG-EAFD 6:24:70 (S6).

Metal mobility of Pb, Cd and Zn is associated with pH. Low pH values (<7) increase the solubility of the metals in question, whereas pH values in the range of 8–11 decrease the mobility of those metals. Mo usually forms mobile oxy-anions and present as MoO_4^{2-} above pH 5. It is believed that the existence of $PbMoO_4$ and

$CaMoO_4$ phases control Mo solubility in the leachate within pH range of 4 and 7. The pH values of as-received materials are given in Table 14.2. Accordingly, it is clear to understand that all materials have very alkaline characteristics which lead to the fact that any mix combination of these binders with waste will not produce any material with a pH value less than 9. XRD and SEM/EDX analysis could not detect any $CaMoO_4$ and $PbMoO_4$ phases which are required to control Mo leaching. Therefore, Mo leaching could be linked to the fact that there was no information of $CaMoO_4$ and $PbMoO_4$ in the systems. The trend of heavy metal emissions, including Zn, Cd, Cr, Mo, Cl and Pb is not linear with continuous changes in the sign of the slopes. Very few samples had a leaching behaviour that is mainly dominated by diffusion. A very high proportion of samples showed a mode dominated mostly by depletion.

14.4 Conclusions

The results proved that S/S of various hazardous waste exhibits much better product performance in terms of granular leaching test regime when compared to the monolithic one. The leaching test results showed that the leaching test according to EA NEN 7375 provides a more conservative scenario than the one presented by the standard BS EN 12457-3 for granular waste. The new crystalline compounds formed in the stabilisation process included calcite and zincite and appeared in the waste samples but were not originally present in the pure cement. The high MgO and Fe content of steel slag resulted in the formation of magnetite and magnesioferrite for CEMI-slag mix matrices.

Microstructural analysis revealed that waste solidification is governed by the formation of crystalline calcium zincate hydrate $CaZn_2(OH)_6{\cdot}2H_2O$ by reaction of ZnO with the cement hydration product portlandite ($Ca(OH)_2$). SEM analysis is able to detect the formation of cement hydration products (portlandite and ettringite) and the effect of heavy metals, including Zn, Mo, Cd and Cr, on the formation of C–H and/or C–S–H cement hydration products. The SEM/EDX results demonstrate the existence of zinc in EAFD waste with Pb, Cd and Cr bearing phases being very small to be detected. Anhydrite ($CaSO_4$) and anglesite ($PbSO_4$) are considered as the main mineralogical phases of the leaching residue; however, these were not detected in either the SEM/EDX or XRD analysis of this study.

Both LGMgO and steel slag may replace cement up to 70 % including waste at a range of 40–70 %. These ratios may be suggested as the optimum mix designs that are successful in the S/S of EAFD and satisfied all the WAC requirements. Therefore, effective replacement of cement by LGMgO and steel slag (both waste by-products) at a ratio of (20:80) significantly improves both the economics and sustainability characteristics of this treatment technique.

Acknowledgements This work is fully supported by Dr. Sabeha K. Ouki, University of Surrey, UK. This research is funded by the Technology Strategy Board (TSB) UK and the materials supplied by Tata Steel Europe (CORUS, formerly), Castle Cement-UK and Magnesitas Navarras, Spain. It is also supplemented by a grant provided by Funds for Women Graduates (FfWG).

References

Atis CD, Bilim C (2007) Wet and dry cured compressive strength of concrete containing ground granulated blast-furnace slag. Build Environ 42:3060–3065

British Standards Institution (2002) BS EN 12457-3:2002, Characterisation of waste. Leaching. Compliance test for leaching of granular waste materials and sludges. BSI, London

Cubukcuoglu B, Ouki SK (2012) Solidification/stabilisation of electric arc furnace waste using low grade MgO. Chemosphere 86:789–796

Environment Agency (2004) EA NEN 7375:2004 Leaching characteristics of moulded or monolithic building and waste materials. Determination of leaching of inorganic components with the diffusion test. 'The tank test' based on the translation of the Netherlands Normalisation Institute Standard, Version 1.0, Environment Agency, UK

Environment Agency (2005) Guidance on sampling and testing of wastes to meet landfill waste acceptance procedures (WAC). Environment Agency, UK

European Union Council (2002) European waste catalogue and hazardous waste list by commission decision 2002/532/EC

Fernandez AI, Chimenos JM, Raventos N, Miralles L, Espiell F (2003) Stabilisation of electrical arc furnace dust with low-grade MgO prior to landfill. J Environ Eng 129:275–279

Fernandez-Pereira C, Luna Y, Querolb X, Antenuccic D, Valea J (2009) Waste stabilization/solidification of an electric arc furnace dust using fly ash-based geopolymers. Fuel 88(7):1185–1193

Fuessle RW, Taylor MA (2004) Long-term solidification/stabilisation and toxicity characteristics leaching procedure for an electric arc furnace dust. J Environ Eng 130:492–498

Garcia MA, Chimenos JM, Fernandez AI, Miralles L, Segarra M, Espiell F (2004) Low-grade MgO used to stabilize heavy metals in highly contaminated soils. Chemosphere 56:481–491

Gutt W (1971) Manufacture of cement from industrial by-products. Building Research Station, Garston

Jin F, Wang F, Al-Tabbaa A (2015) Three-year performance of in-situ solidified/stabilized soil using novel MgO-bearing binders. Chemosphere 144:681–688. doi:10.1016/j.chemosphere.2015.09.046

Li XD, Poon CS, Sun H, Lo IMC, Kirk DW (2001) Heavy metal speciation and leaching behaviours in cement based solidified/stabilised waste materials. J Hazard Mater 82:215–230

Mayers E, Eappi ME (1992) Laboratory evaluation of stabilization/solidification technology for reducing the mobility of heavy metals in New Bedford Harbour superfund site sediment, stabilization of hazardous radioactive and mixed wastes. ASTM, Philadelphia

Menad N, Ayala JN, Garcia-Carcedo F, Ruiz-Ayucar E, Hernandez A (2003) Study of the presence of fluorine in the recycled fractions during carbothermal treatment of EAF dust. Waste Manag 23:483–491

Middendorf B, Martirena JF, Gehrke M, Day RL (2005) Lime pozzolan binders: an alternative to OPC. In: International building lime symposium proceedings, Orlando, FL, 9–11 March

Pereira CF, Rodriguez-Pinero M, Vale J (2001) Solidification/stabilization of electric arc furnace dust using coal fly ash: analysis of the stabilization process. J Hazard Mater 82:183–195

Pereira CF, Galiano YL, Rodriguez-Pinero MA, Parapar JV (2007) Long and short-term performance of a stabilized/solidified electric arc furnace dust. J Hazard Mater 148:701–707

Poon CS, Clark AI, Peters CJ, Perry R (1985) Mechanisms of metal fixation and leaching by cement based fixation processes. Waste Manage Res 3:127–142

Poon CS, Lio KW, Tang CI (2001) A systematic study of cement/PFA chemical stabilisation/solidification process for the treatment of heavy metal waste. Waste Manage Res 19:276–283

Singh M, Garg M (1999) Cementitious binder from fly ash and other industrial wastes. Cem Concr Res 29:309–314

Stegemann JA, Roy A, Caldwell RJ, Schilling PJ, Tittsworth R (2000) Understanding environmental leachability of electric arc furnace dust. J Environ Eng 126:112–120

Tresintsi S, Simeonidis K, Katsikini M, Paloura EC, Bantsis G, Mitrakas M (2013) A novel approach for arsenic adsorbents regeneration using MgO. J Hazard Mater 265:217

Tsakiridis PE, Papadimitriou GD, Tsivilis S, Koroneos C (2008) Utilization of steel slag for Portland cement clinker production. J Hazard Mater 152:805–811

Turkel S (2006) Long-term compressive strength and some other properties of controlled low strength materials made with pozzolanic cement and class C fly ash. J Hazard Mater 137:261–266

Valle-Zermeno R, Giro-Paloma J, Formosa J, Chimenos JM (2015) Low-grade magnesium oxide by-products for environmental solutions: characterisation and geochemical performance. J Geochem Explor. doi:10.1016/j.gexplo.2015.02.007

Wiles CC, Barth E (1992) Solidification/stabilization: is it always appropriate? In: Gilliam TM, Wiles CC (eds) Stabilization and solidification of hazardous, radioactive, and mixed wastes. ASTM, Philadelphia

World Steel Association (2015) Crude steel production. https://www.worldsteel.org/statistics/crude-steel-production.html. Accessed 26 Jan 2012

Zhang T, Cheeseman CR, Vandeperre LJ (2011) Development of low pH cement systems forming magnesium silicate hydrate (M-S-H). Cem Concr Res 41:439–442

Chapter 15
Dangerous Emissions During Steelmaking in Electric Arc Furnaces

Dana-Adriana Iluţiu-Varvara

Abstract The steelmaking in the electric arc furnaces (EAFs) is in the category of industrial processes with high degree of pollution. In the air environmental factors are transferred the following dangerous substances: carbon oxides, sulphur dioxide, nitrogen oxides, volatile organic compounds, polychlorinated dibenzodioxins, polychlorinated dibenzofurans and particulate matter. This chapter presents the categories of dangerous emissions generated from the steelmaking in the EAFs; potential sources that generate the dangerous emissions from the steelmaking in the EAFs; generation mechanisms of dangerous emissions from the steelmaking in the EAFs; methods of minimizing the dangerous emissions from the steelmaking in the EAFs.

15.1 Categories of Dangerous Emissions Generated from the Steelmaking in the Electric Arc Furnaces

In order to identify the categories of dangerous emissions generated from the electric arc furnaces (EAFs), one must know the inputs of the steelmaking process. In Fig. 15.1 are presented the inputs and outputs from the steelmaking in the EAFs.

The categories of dangerous emissions generated from the steelmaking in the EAFs are carbon oxides (CO_x), sulphur oxides (SO_x), nitrogen oxides (NO_x), volatile organic compounds (VOCs), polychlorinated dibenzodioxins (PCDDs), polychlorinated dibenzofurans (PCDFs) and particulate matter (PM).

D.-A. Iluţiu-Varvara (✉)
Faculty of Building Services, Technical University of Cluj-Napoca,
28 Memorandumului Street, 400114 Cluj-Napoca, Romania
e-mail: dana.varvara@gmail.com; dana.adriana.varvara@insta.utcluj.ro

P. Cavaliere (ed.), *Ironmaking and Steelmaking Processes*,
DOI 10.1007/978-3-319-39529-6_15

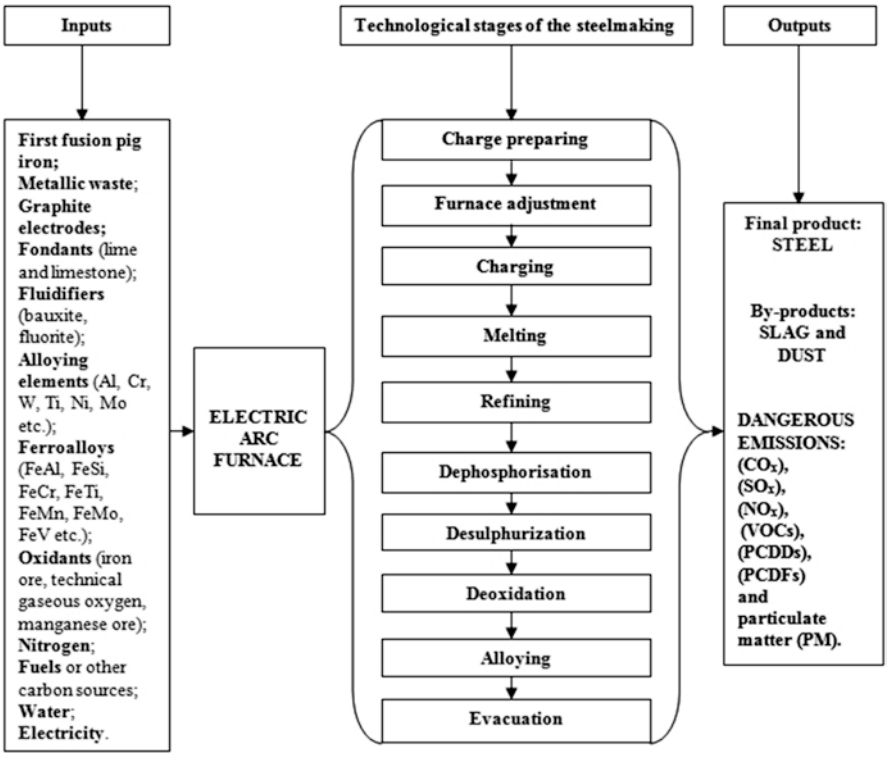

Fig. 15.1 Inputs and outputs from the steelmaking in the EAFs (Iluţiu-Varvara 2007a)

15.1.1 What Are Dangerous Emissions?

Carbon monoxide (CO) is an odourless, tasteless and colourless gas produced by the incomplete burning of materials which contain carbon. It combines with haemoglobin to form carboxyhaemoglobin, resulting in hypoxia with serious consequences for various tissues and cell respiration, which is manifested clinically by headache, dizziness, drowsiness, nausea and arrhythmias. It also transformed into carbon dioxide (CO_2, which is also directly emitted when fuels are being burnt. Carbon dioxide is the most anthropogenic greenhouse gas emitted through human activities and has no direct adverse health effects. One of the anthropogenic activities which emitted carbon oxides is the steelmaking in the EAF (Iluţiu-Varvara 2010; Iluţiu-Varvara et al. 2015a, b).

Sulphur oxides (SO_x) refer to all sulphur oxides, ones being sulphur dioxide (SO_2) and sulphur trioxide (SO_3). Sulphur dioxide is a colourless gas with a pungent, irritating odour and taste. It is highly soluble in water forming weakly acidic sulphurous acid. When sulphur dioxide combines with the oxygen in the air some sulphur trioxide is slowly formed. Sulphur trioxide rapidly combines with water to produce sulphuric acid (Iluţiu-Varvara et al. 2011, 2013; Iluţiu-Varvara and Rădulescu 2013).

Nitrogen oxides include nitrous oxide (N_2O), nitrogen monoxide (NO), nitrogen dioxide (NO_2), nitrogen trioxide (NO_3), dinitrogen trioxide (N_2O_3), dinitrogen tetroxide (N_2O_4) and dinitrogen pentoxide (N_2O_5) (Greenwood and Earnshaw 1997). Nitrogen oxides are in the category of most polluting substances emitted into the environment. The nitrogen dioxide is the second most producing greenhouse effect (Negrea and Sandu 2000).

VOCs, as defined in Directive 2010/75 (European Union Directive 2010/75/EU, Drotloff 2014), are organic compounds having at 293.15 K a vapour pressure of 0.01 kPa or more, or having a corresponding volatility under the particular conditions of use. Due to their characteristics, the use of VOC solvents in certain installations generates emissions of organic compounds that contribute directly to air pollution and climate change and are also ozone precursors, i.e. they react chemically with nitrogen oxides in the presence of sunlight to form ozone. While ozone is beneficial in the upper atmosphere, where it shields the earth from dangerous UV rays, it can be harmful when present in high concentrations at ground level. According to Directive (European Community Directive 1999/13/EC), an organic compound is defined as any compound containing at least the element carbon and one or more of hydrogen, halogens (e.g. chlorine, fluorine or bromine), oxygen, sulphur, phosphorus, silicon or nitrogen, with the exception of carbon oxides and inorganic carbonates and bicarbonates. An even wider definition is used in the EU National Emissions Ceilings Directive (Directive 2001/81/EC), where a VOC is any organic compound of anthropogenic nature, other than methane, that is capable of producing photochemical oxidants by reaction with nitrogen oxides in the presence of sunlight (Iluţiu-Varvara et al. 2016).

PCDDs and PCDFs are types of persistent organic pollutants with a wide range of toxic responses and carcinogenic properties. These pollutants can be considered as environmental quality indicators of anthropogenic activities. One of the most important anthropogenic sources of PCDDs and PCDFs from the ferrous metals industry includes steelmaking in the EAFs (Iluţiu-Varvara 2016; Varvara 2006a; Anderson and Fisher 2002; Chang et al. 2006; Grochowalski et al. 2007; Sofilic et al. 2012). The generation of these compounds requires carbon, oxygen and chlorine, as well as metallic catalysts and adequate temperature. The optimal temperature range for pyrosynthesis of these compounds is between 400 and 700 °C (Van den Berg et al. 2006).

In order to achieve a higher level of uniformity and comparability of results defining PCDDs and PCDFs content in samples of different materials of different origin, there was adopted the International Toxicity Equivalent Factor (I-TEF). Nowadays, the analysis of PCDDs/Fs in various samples commonly includes 17 compounds (7 PCDDs and 10 PCDFs) and their level in the sample is described as toxic equivalent (I-TEQ) in correlation with 2,3,7,8-tetrachlorinated dibenzo-*p*-dioxin (2,3,7,8-TCDD). In Table 15.1 is presented the I-TEF reported in various references from specialized literature.

Particulate matters (PM) refer to a suspension of solid, liquid or a combination of solid and liquid particles in the air. Air pollution originating from PM is generally characterized by its highly complex nature. Particulate matters are a mixture of

Table 15.1 International toxicity equivalent factors (I-TEF) for dioxin and furan congeners

PCDD and PCDF congeners	I-TEF[a]	I-TEF[b]
2,3,7,8-Tetrachloro dibenzo-*p*-dioxin (2,3,7,8-TCDD)	1	1
1,2,3,7,8-Pentachloro dibenzo-*p*-dioxin (1,2,3,7,8-PeCDD)	1	0.5
1,2,3,4,7,8-Hexachloro dibenzo-*p*-dioxin (1,2,3,4,7,8-HxCDD)	0.1	0.1
1,2,3,6,7,8-Hexachloro dibenzo-*p*-dioxin (1,2,3,6,7,8-HxCDD)	0.1	0.1
1,2,3,7,8,9-Hexachloro dibenzo-*p*-dioxin (1,2,3,7,8,9-HxCDD)	0.1	0.1
1,2,3,4,6,7,8-Heptachloro dibenzo-*p*-dioxin (1,2,3,4,6,7,8-HpCDD)	0.01	0.01
1,2,3,4,6,7,8,9-Octachloro dibenzo-*p*-dioxin (1,2,3,4,6,7,8,9-OCDD)	0.0003	0.001
2,3,7,8-Tetrachloro dibenzofuran (2,3,7,8-TCDF)	0.1	0.1
1,2,3,7,8-Pentachloro dibenzofuran (1,2,3,7,8-PeCDF)	0.03	0.05
2,3,4,7,8-Pentachloro dibenzofuran (2,3,4,7,8-PeCDF)	0.3	0.5
1,2,3,4,7,8-Hexachloro dibenzofuran (1,2,3,4,7,8-HxCDF)	0.1	0.1
1,2,3,6,7,8-Hexachloro dibenzofuran (1,2,3,6,7,8-HxCDF)	0.1	0.1
1,2,3,7,8,9-Hexachloro dibenzofuran (1,2,3,7,8,9-HxCDF)	0.1	0.1
2,3,4,6,7,8-Hexachloro dibenzofuran (2,3,4,6,7,8-HxCDF)	0.1	0.1
1,2,3,4,6,7,8-Heptachloro dibenzofuran (1,2,3,4,6,7,8-HpCDF)	0.01	0.01
1,2,3,4,7,8,9-Heptachloro dibenzofuran (1,2,3,4,7,8,9-HpCDF)	0.01	0.01
1,2,3,4,6,7,8,9-Octachloro dibenzofuran (1,2,3,4,6,7,8,9-OCDF)	0.0003	0.001

[a]Iluţiu-Varvara (2016) and Van den Berg et al. (2006)

[b]Iluţiu-Varvara (2016), Sofilic et al. (2012) and European Standard EN 1948-1:2006

particles and droplets in the air, consisting of a variety of components such as organic compounds, metals, acids, soil and dust. These suspended particles vary in size, composition and origin. Particles are often classified by their aerodynamic properties because (Rai 2015) these properties govern the transport and removal of particles from the air; they also govern their deposition within the respiratory system and they are associated with the chemical composition and sources of particles.

PM_{10} (the fraction of particulates in air of very small size (<10 μm)) and $PM_{2.5}$ particles (<2.5 μm) are of major current concern, as they are small enough to

penetrate deep into the lungs and so potentially pose significant health risks. Larger particles, meanwhile, are not readily inhaled and are removed relatively efficiently from the air by sedimentation.

15.2 Potential Sources That Generate the Dangerous Emissions from the Steelmaking in the Electric Arc Furnaces

15.2.1 Potential Sources That Generate Carbon Oxides

The sources with carbon oxides generating potential to the steelmaking are (Varvara 2007a; Iluţiu-Varvara 2007a) the carbon from the charge; scrap iron; first fusion pig iron; fuel material and the carbon from the graphite electrodes, which are gradually consumed, until destruction.

15.2.2 Potential Sources That Generate Sulphur Oxides

The sources with sulphur dioxide generating potential in the electric arc steelmaking are (Varvara 2006b, 2007a) the metallic charge; additions of auxiliary materials; first fusion pig iron (0.05–0.07 % S) and EAF atmosphere, when using fuels containing sulphur.

The sulphur may derive from some impurities of the charge and from the electrodes. The sulphur from the charge in the form of metal sulphides <MeS> can undergo the reaction:

$$\langle \mathrm{MeS} \rangle + 2\{\mathrm{O_2}\} = \langle \mathrm{MeSO_4} \rangle \tag{15.1}$$

$$2\langle \mathrm{MeSO_4} \rangle \rightarrow 2\langle \mathrm{MeO} \rangle + 2\{\mathrm{SO_2}\} + \{\mathrm{O_2}\} \tag{15.2}$$

15.2.3 Potential Sources That Generate Nitrogen Oxides

The EAF atmosphere is source that generates nitrogen oxides because it contains gases, like as oxygen and nitrogen, at high temperatures (~1800 °C). The fuels used in steelmaking and some oils introduced with the charge contain nitrogen. During combustion processes, the fuels are oxidized and a substantial fraction of them contain nitrogen, which is oxidized, thus forming (NO_x).

15.2.4 Potential Sources That Generate Volatile Organic Compounds

The potential sources that generate the VOCs from the steelmaking are organic matters, paints and plastics from the charge (Iluţiu-Varvara 2007a, 2009c; Iluţiu-Varvara et al. 2016). Sources of VOCs from EAFs include (Environmental Agency of London 1999) scrap preparation with solvent degreasers; combusting auxiliary fuel; hydrocarbons contained in the oils, wire casing, foam and plastics found in the steel scrap feedstock can vapourize when melting takes place; decarburization of scrap; charging of the furnace and tapping of the molten metal and slag.

15.2.5 Potential Sources That Generate Polychlorinated Dibenzo-p-Dioxins and Polychlorinated Dibenzofurans

Scrap metal can be contaminated with paint, organic matter (oil and cutting fluids) and plastic (polyvinyl chloride). Organic and inorganic forms of chlorine may also be present. Scrap may be thermally pre-treated to remove contamination by burning, drying to evaporate water, or by partial pyrolysis. Burning and pyrolysis of contaminated scrap give rise to products of incomplete combustion such as particulate matter, carbon monoxide, organic compounds and may emit dioxins and furans (Iluţiu-Varvara 2016; Cavaliere and Perrone 2015).

15.2.6 Potential Sources That Generate Particulate Matter

The potential sources that generate the particulate matter in the steelmaking are (Iluţiu-Varvara 2007b; Varvara 2007b; Li and Tsai 1993) the charge components of the EAF; the physico-chemical interaction of the charge components; the furnace lining (acid or alkaline); melting method used and the possibility of metal oxides volatilization and other slag components in the gas phase above the EAFs.

The emission sources of particulate matter containing (Iluţiu-Varvara 2007a):

- zinc are dip galvanized and auto industry wastes;
- lead, cadmium, chromium and nickel are the presence in charge of the nickel plating surfaces, cadmium plating surfaces, chromate surfaces, brassed surfaces, paints and auto industry wastes;
- sodium, potassium and chlorine are associated with the auto industry wastes; the chlorine can originate from oils, organic materials and plastics;
- calcium is lime (CaO);
- fluorine is calcium fluoride (CaF_2), used as fondant;
- silicon is lining of the EAF.

15.3 The Generation Mechanisms of Dangerous Emissions from the Steelmaking in the Electric Arc Furnaces

15.3.1 The Generation Mechanisms of Carbon Oxides

The carbon oxidation in the metal bath can be performed by direct reaction with oxygen and through the iron oxide. The chemical reactions that lead to the generation of carbon oxides (CO_x) from the steelmaking in EAFs are (Varvara 2007a; Iluţiu-Varvara 2007b; Turkdogan 1996)

$$[C]+[O]=\{CO\} \tag{15.3}$$

$$[C]+[FeO]=[Fe]+\{CO\} \tag{15.4}$$

$$[C]+2[FeO]=2[Fe]+\{CO_2\} \tag{15.5}$$

$$[C]+[O_2]\leftrightarrow\{CO_2\} \tag{15.6}$$

At high temperatures, the following reactions can also occur:

$$5[C]+([P_2O_5])=5\{CO\}+2[P] \tag{15.7}$$

$$2[C]+([SiO_2])=2\{CO\}+[Si] \tag{15.8}$$

$$[C]+([MnO])=\{CO\}+[Mn] \tag{15.9}$$

In the slag, the following CO emitting reactions take place:

$$3(C)+(CaO)=(CaC_2)+\{CO\} \tag{15.10}$$

$$3(FeS)+(CaC_2)+2(CaO)=3(CaS)+3[Fe]+2\{CO\} \tag{15.11}$$

$$(CaCO_3)\leftrightarrow\{CO_2\}+(CaO) \tag{15.12}$$

$$2(C)+\{O_2\}=2\{CO\} \tag{15.13}$$

15.3.2 The Generation Mechanisms of Sulphur Oxides

The reactions of sulphur dioxide and sulphur trioxide formation are (Varvara 2007a; Iluţiu-Varvara 2007a)

$$[S]+2[O]=\{SO_2\} \tag{15.14}$$

$$[S]+3[O]=\{SO_3\} \tag{15.15}$$

$$\{SO_2\}+1/2\{O_2\}\leftrightarrow\{SO_3\} \tag{15.16}$$

$$[FeS]+2[O]\rightarrow\{SO_2\}+[Fe] \tag{15.17}$$

$$[FeS]+3[O]\rightarrow\{SO_3\}+[Fe] \tag{15.18}$$

$$[FeS\cdot MnS]+4[O]=2\{SO_2\}+[Fe]+[Mn] \tag{15.19}$$

Sulphur can be usually found in the iron ore in the form of pyrite (FeS_2) or pirotin (FeS). When entering the ore in the furnace the following processes occur: dissociation and oxidation of iron sulphides (Iluţiu-Varvara 2007a; Varvara 2007b; Iluţiu-Varvara et al. 2013).

Pyrite dissociates easily at 600 °C and $p=1$ atm. according to this reaction:

$$2(FeS_2)=2(FeS)+S_2 \tag{15.20}$$

then the pirotin oxides according to this reaction:

$$3/5(FeS)+\{O_2\}=1/5(Fe_3O_4)+3/5\{SO_2\} \tag{15.21}$$

It can take place also this reaction:

$$(FeS)+10(Fe_2O_3)=7(Fe_3O_4)+\{SO_2\} \tag{15.22}$$

The presence of sulphur dioxide in the furnace atmosphere is a potential source of sulphuring and oxidation of metal bath.

The sulphuring and oxidation of metal bath in the presence of $\{SO_2\}$ take place according to this reaction:

$$2\{SO_2\}=\{S_2\}+2\{O_2\} \tag{15.23}$$

15.3.3 The Generation Mechanisms of Nitrogen Oxides

Nitrogen oxides emissions are due to the oxidation of nitrogen at high temperature. The highest temperatures during steelmaking in EAF are in the arc area and in the oxygen blowing area. So, the best conditions for the generation of (NO_x) are particularly in the electric arc area (Iluţiu-Varvara 2009a, b).

The mechanisms after which the generation of nitrogen oxides may occur are (Zeldovich et al. 1947, 1985) thermal mechanism; prompt mechanism and fuel mechanism.

In the case of the thermal mechanism, the nitrogen oxides formed are a consequence of not only the oxidation of the nitrogen from the fuels composition, but also the oxidation of the nitrogen from its dissociation.

The dissociation reaction is

$$\{N_2\} \leftrightarrow 2N_{ad.} \tag{15.24}$$

The adsorbed nitrogen atoms are dissolved in the slag and metal bath. In contact with the oxygen at temperatures above 1800 K, the nitrogen monoxide is formed. The oxidation reactions may be with the molecular nitrogen or with the nitrogen in atomic state (resulting from dissociation).

$$N + O \leftrightarrow 2NO \tag{15.25}$$

$$N_2 + O = NO + N \tag{15.26}$$

$$1/2\{O_2\} + 1/2\{N_2\} \leftrightarrow NO \tag{15.27}$$

$$N + O_2 = NO + O \tag{15.28}$$

$$N + OH = NO + H \tag{15.29}$$

It results that the nitrogen monoxide can be formed by direct combination at high temperature (>1000 °C) of the oxygen with the nitrogen from the EAF atmosphere.

The nitrogen monoxide can react with the oxygen and thus forming the nitrogen dioxide, based on the reaction:

$$2\{NO\} + \{O_2\} = 2\{NO_2\} \tag{15.30}$$

The prompt formation mechanism of nitrogen oxides refers to the formation in the arc area, which is also a thermal mechanism. This mechanism is more complex and controlled by the formation of CH radicals. The CH radicals react with nitrogen to HCN, which then react in several steps to nitrogen oxides according to the reaction (Echterhof et al. 2011):

$$CH + N_2 \rightarrow HCN + N \ldots \overset{\rightarrow NO}{\underset{\rightarrow N_2}{}} \tag{15.31}$$

The prompt NO_x is dependent on the concentration of CH radicals, which in turn is strongly controlled by local fuel concentration.

The fuel mechanism of nitrogen oxides formation refers to the direct formation from the fuels used. In this case, the nitrogen oxides are generated by the oxidation of fossil fuel (coal and heavy oil) bound nitrogen. The specific reaction of this mechanism is

$$2\left[\mathrm{N}\right]_{\mathrm{fuel}} + \mathrm{O}_2 \rightarrow 2\mathrm{NO} \tag{15.32}$$

The predominant generation mechanism of nitrogen oxides at high temperatures is the thermal type.

Nitrogen monoxide (NO) is generated because of the atmospheric nitrogen oxidation (thermal NO by dissociation at high temperature and via the reaction of nitrogen radicals and hydrocarbons) or due to the oxidation of the nitrogen compounds contained in fossil fuels (fuel NO). As fuel gas in the steel industry does not contain chemically bounded nitrogen, the thermal NO formation is the dominant source of NO_x from the EAF. Thermal NO occurs by dissociation of the air in the electric arc in accordance with the Zeldovich mechanism (Capitelli et al. 2000; Warnatz et al. 1999; Malikov et al. 2002).

15.3.4 The Generation Mechanisms of Volatile Organic Compounds

VOCs are generated in the EAFs from combustion of auxiliary fuel, oil contained in the scrap and decarburization of the scrap (Unamuno et al. 2008).

VOCs emissions may result from organic substances adhering to the raw materials (solvents, paints) charged to the furnace. In the case of the use of natural coal (anthracite), compounds such as benzene may degas before being burnt off (Eurofer 2007).

*15.3.5 The Generation Mechanisms of Polychlorinated Dibenzo-*p*-Dioxins and Polychlorinated Dibenzofurans*

The generation of these compounds requires carbon, oxygen and chlorine, as well as metallic catalysts and adequate temperature. The optimal temperature range for pyrosynthesis of these compounds is between 400 and 700 °C (Sofilic et al. 2012).

By thermal processes the compounds may be formed by two mechanisms:

- "de novo synthesis"; dioxins and furans are formed from its basic elements—carbon, hydrogen, oxygen and chlorine. The process is taking place at temperatures between approximately 250 and 500 °C on catalytically active surfaces. In particular copper compounds are regarded as effective catalysts.
  - formation from precursors; dioxins and furans are formed from chlorinated organic compounds, such as chlorinated phenols that serve as precursors for the process. Similarly, these reactions may take place at temperatures between approximately 200 and 500 °C on catalytically active surfaces, but also spontaneously at the relevant temperatures.

Whereas dioxins are likely to be decomposed at very high temperatures (above 800–1000 °C) assuming adequate residence time at this temperature level, formation of dioxins may take place again at lower temperatures in the flue gas or on active surfaces by "de novo synthesis". This sets the focus on all kinds of high temperature processes. The source of chlorine could be the material itself, or it could be the fuel (Tysklind et al. 1989).

Molecular chlorine is thought to be responsible for the formation of "de novo synthesis" of dioxins, according to the following reactions:

$$CuCl_2 + 1/2O_2 \rightarrow CuO + Cl_2 \tag{15.33}$$

$$CuO + 2HCl \rightarrow CuCl_2 + H_2O \tag{15.34}$$

$$2HCl + 1/2O_2 \rightarrow H_2O + Cl_2 \tag{15.35}$$

In the case of fossil fuels, the reaction will be

$$Cl_2 + SO_2 + H_2O \rightarrow SO_3 + 2HCl \tag{15.36}$$

Dioxins tend to form both at low and high temperatures. At temperatures between 200 and 400 °C, in combustion gas exhaust streams, highly chlorinated dibenzo-*p*-dioxin and dibenzofuran are formed from phenol and benzene prior to particle collection equipment. Chlorination at lower temperatures on particle surfaces is a potential source of chlorinated dibenzofuran (Ryu et al. 2003). At high temperatures, between 500 and 800 °C, mainly the less chlorinated dibenzofuran congeners are formed. The chlorination can occur on metals, in particular, copper (II) chloride ($CuCl_2$) by the Deacon reaction. Hydrogen chloride is converted catalytically to Cl_2, which then can lead to gas-phase DF chlorination (Wikstrom and Marklund 2000):

$$4HCl + O_2 \rightarrow 2Cl_2 + 2H_2O \tag{15.37}$$

The formation of chlorinated dibenzofurans by the chlorination of aromatic molecules with conversion of $CuCl_2$ to CuCl takes place according to the following reactions (Stieglitz et al. 1991):

$$ArH + CuCl_2 \rightarrow ArHCl + CuCl \tag{15.38}$$

$$ArHCl + CuCl_2 \rightarrow ArCl + CuCl + HCl \tag{15.39}$$

For all thermal processes the presence of precursors may be anticipated to increase the probability of dioxin formation and may reduce the need for catalytically active surfaces.

In Table 15.2 there are shown the percentage concentrations of PCDDs and PCDFs in the stack flue gases from steelmaking in the EAF (Iluţiu-Varvara 2016).

Table 15.2 Percentage concentrations of PCDDs and PCDFs from steelmaking in the EAF

PCDDs and	Concentrations [%]	PCDFs	Concentrations [%]
TCDD	12.5	TCDF	40.55
PeCDD	10.7	PeCDF	19.4
HxCDD	3.4	HxCDF	10.5
HpCDD	0.7	HpCDF	1.7
OCDD	0.3	OCDF	0.25

The variations of dioxin and furan emissions from the steelmaking in the EAF are dependent on the quality of the scrap used; degree of contamination with chlorine compounds of the charge components; conditioning and gas cleaning systems and efficiency collection of particulate matter.

15.3.6 The Generation Mechanisms and Compositions of Particulate Matters

The particulate matters from steelmaking in the EAF are the end product of a series of phenomena such as the

- transfer of the particles from the metal bath and slag;
- transfer of the particles together with gases emitted;
- physical (changes phase, agglomeration) and chemical transformations (reactions between the phases and with the gaseous phase) during the process capture.

The generation mechanism of particulate matter takes place in two steps (Guézennec et al. 2005):

- the emissions of the particulate matter "precursors" (vapours, metal droplets and solid particles) inside the furnace;
- the precursors conversion into particulate matter by agglomeration and physico-chemical transformation.

The emission mechanisms of the particulate matter "precursors" are

- the volatilization of the elements from the charge composition (Zn, Pb, Cd, etc.) prevails mostly in the electric arc area and the oxygen jet zone;
- the emission of the droplets from metal bath, at the impact of electric arc with oxygen jet;
- projection of fine droplets by bursting of CO bubbles during the decarburization of the metal bath;
- the expulsion of metal and slag droplets in contact with oxidizing atmosphere of the furnace;
- direct removal of solid particles, during the introduction of powdered material into the furnace (scrap, coal for slag foaming, additive materials and recycled dusts);

- entrainment of the large slag droplets;
- entrainment of the solid materials.

The "precursors" are further transformed during their transport within the furnace and then in the fume extraction system. They can undergo

- physical transformations: condensation of the vapours, rapid solidification of the fine projections in contact with a colder atmosphere, in-flight agglomeration and coalescence of dust particles.
- chemical reactions (oxidation) with the carrier gas, whose temperature and composition vary and they can possibly react with other precursor particles. For a reaction between condensed phases (liquid or solid) to occur, particles must first be brought into contact. Therefore, there is a strong link between the mechanisms of agglomeration and the chemical evolution (Huber 2000).

The projection of liquid steel and slag droplets by bursting of carbon monoxide bubbles has been recognized as the principal mechanism of particulate matter emissions from the steelmaking in the EAF (Han and Holappa 2003).

The chemical compositions of the particulate matter from steelmaking in the EAFs vary considerably depending on the steel type produced, raw materials used, auxiliary materials used, operational parameters, melting methods used and furnace type and heats (Varvara 2007b).

Particulate matters from EAF containing a number of oxides (lead oxides, nickel oxide, aluminium oxide, magnesium oxide, manganese oxides and silica and calcium oxide) which are generated according to the reactions (Iluţiu-Varvara 2007b; Varvara 2007a, b):

$$2Pb + O_2 = 2PbO \tag{15.40}$$

$$\frac{3}{2}Pb + O_2 = \frac{1}{2}Pb_3O_4 \tag{15.41}$$

$$Pb + O_2 = PbO_2 \tag{15.42}$$

$$2Ni + O_2 = 2NiO \tag{15.43}$$

$$\frac{4}{3}Al + O_2 = \frac{2}{3}Al_2O_3 \tag{15.44}$$

$$2Mg + O_2 = 2MgO \tag{15.45}$$

$$2Mn + O_2 = 2MnO \tag{15.46}$$

$$6MnO + O_2 = 2Mn_3O_4 \tag{15.47}$$

$$4Mn_3O_4 + O_2 = 6Mn_2O_3 \tag{15.48}$$

$$2Mn_2O_3 + O_2 = 4MnO_2 \tag{15.49}$$

$$Si + O_2 = SiO_2 \tag{15.50}$$

$$2Ca + O_2 = 2CaO \tag{15.51}$$

Compared to carbon steel plant dust, stainless steel plant dust has a low zinc concentration, but is enriched in metallic components since high alloy scrap is used in the production of stainless steel.

Stainless steel dust consists mainly of oxide phases that are rich in iron, chromium, calcium, zinc, magnesium, manganese and nickel, with minor amounts of phases that contain alkaline metals (potassium and sodium), halogens (chlorine and fluorine), silicon, molybdenum, lead and sulphur. Chromium and iron oxides (CrO and Fe_2O_3) as well as spinel phases (such as $FeCr_2O_4$, $(Mg, Fe, Mn, Cr)_3O_4$, $MnFe_2O_4$ and $ZnFe_2O_4$), and some raw materials (CaO, CaF_2 and $CaCO_3$) are the major crystalline phases present in the particulate matter from stainless steel. Minor phases include pure metallic particles (iron, zinc and nickel), oxide phases (NiO, MgO, PbO, SiO_2 and ZnO), halogens ($PbCl_2$, $ZnCl_2$, KCl and NaCl), SiC, fayalite (Fe_2SiO_4), sulphates and hydrates ($ZnCl_2 \cdot 4Zn(OH)_2$, $Ca(OH)_2$) (Ma and Garbers-Craig 2006; Iluţiu-Varvara 2007b; Varvara 2007b).

Particulate matters from the EAF are formed mainly from (Iluţiu-Varvara 2007a) metallic oxides; refractory oxides and volatile elements from the charge.

In Table 15.3, there are presented the minimum and maximum concentrations of the elements in the EAF particulate matters (USEPA 1988). The gathering of the particulate matters from EAFs is performed with baghouses or scrubbers. The particulate matters from EAF are in the category of hazardous waste.

15.4 Methods of Minimizing the Dangerous Emissions from the Steelmaking in the Electric Arc Furnaces

The minimizing of carbon oxides emissions from the steelmaking in the EAFs is possible by (Varvara 2007a; Iluţiu-Varvara 2007b, 2010; Lotun and Pilon 2005) the charge component selection; the use of raw materials with reduced carbon content and using "foaming slag" technology.

The foaming slag can be obtained at the end of fusion of ferrous materials before the disappearance of the last melt by simultaneously injecting through the cleaning door of the coal in the slag; oxygen at the surface or inside the metal.

The foaming slag is not stable, once formed, is degrading, as a consequence the coal must be continuously injected. This technology has the following effects: decreasing the air flow rate entering the furnace, which results in lower emissions of carbon oxides; decreasing the melting stage duration and decreasing the graphite electrodes consumption.

Table 15.3 The total concentrations of the elements in the EAF particulate matters

Elements	Minimum concentrations [mg/kg]	Maximum concentrations [mg/kg]
Antimony	5	294
Arsenic	10.2	400
Barium	24	400
Beryllium	<0.5	8.1
Cadmium	1.4	4988
Chromium	<0.05	106,000
Lead	1.3	139,000
Mercury	<0.001	41
Nickel	<10	22,000
Selenium	0.07	600
Silver	2.5	71
Thallium	0.8	50
Vanadium	24	475
Zinc	3900	32,000

The pollution prevention and control techniques to reduce the air pollution with sulphur oxides (SO_x) from the steelmaking include the following: the selection feedstocks and scrap with low sulphur content; the usage of fuel with low sulphur content, such as natural gas; the usage of wet scrubbing systems before dry scrubbers as part of collecting and dedusting system and emissions control technologies such as sorbent injection and flue gas desulphurization (methods may include wet or dry processes) (Iluţiu-Varvara et al. 2013; Iluţiu-Varvara and Rădulescu 2013).

The reduction of NO_x emissions from steelmaking is possible through general ventilation of the electric steel mill, encapsulation of the EAF and exhaust systems (Iluţiu-Varvara 2009a, b).

The reduction of pollution with VOCs from the steelmaking in the EAFs is possible by charge component selection (scrap should be free of dirt, oil and grease); the use of raw materials without organic compounds and scrap management program for the prevention/minimization of potential contaminants in the steel scrap (Iluţiu-Varvara et al. 2016).

The reduction of pollution with dioxins and furans from the steelmaking in the EAF is possible by charge component selection and by the use of raw materials with reduced plastics content (Iluţiu-Varvara 2016).

Baghouses and cyclones can be used to control particulate matter emissions. There are two possibilities to manage these EAF dusts: hydrometallurgical and pyrometallurgical processes. They consisted in the extraction of nonferrous metals, i.e. zinc, in order to recycle the residue in the steelmaking industry; however, the hydrometallurgical processes are regarded as more eco-friendly for treating materials having a relatively low zinc content. A third option that can be considered for these dusts is their inactivation, i.e. their stabilization prior to permanent disposal (Jha et al. 2001; Varvara 2006b).

15.5 Conclusions

The dangerous emissions generated from the steelmaking in the EAFs are carbon oxides (CO_x); sulphur oxides (SO_x); nitrogen oxides (NO_x); VOCs; PCDDs; PCDFs; particulate matter (PM).

The generation sources of emissions with dangerous potential in the electric arc steelmaking are the charge components of the EAF; the physico-chemical interaction of the charge components; the furnace lining (acid or alkaline); melting method used; the possibility of metal oxides volatilization and the contamination degree of the charge components.

Because of the extremely high toxic potential of dioxins and furans, it is very important to keep dioxin emission at a minimum by focusing on additional measures aimed at reducing human exposure to high levels of dioxins in the short to medium term and to maintaining exposure at safe levels in the long term. Additionally, measures should be taken in order to minimize the levels of dioxins and furans precursors from the steelmaking in the EAF.

The conditions for the generation of dioxins and furans from the steelmaking in the EAF are the presence in the charge of chlorine or fluorine ions; the presence of organic carbon; temperature between 200 and 450 °C; oxidizing atmosphere and the presence of copper, iron, zinc or manganese ions.

The emissions generated from the steelmaking in the EAF have a negative impact on the human health and the environment.

The reduction of dangerous emissions to the steelmaking is possible by charge component selection and by the use of raw materials without impurities.

Acknowledgements The authors also gratefully acknowledge the helpful comments and suggestions of the reviewers, which have improved the presentation.

References

Anderson DR, Fisher R (2002) Sources of dioxines in the United Kingdom: the steel industry and other sources. Chemosphere 46:371–381

Capitelli M, Ferreira CM, Gordiets BF, Osipov AI (2000) Plasma kinetics in atmospheric gases. Springer, Berlin

Cavaliere P, Perrone A (2015) Optimization of processing conditions leading to dangerous emissions in steelmaking plants. In: Engineering solutions for sustainability: materials and resources II, pp 93–102

Chang MB, Huang HC, Tsai SS, Chi KH, Chang-Chien GP (2006) Evaluation of the emission characteristics of PCDD/Fs from electric arc furnace. Chemosphere 62:1761–1773

Directive 2001/81/EC of the European Parliament and of the Council of 23 October 2001 on national emission ceilings for certain atmospheric pollutants

Drotloff H (2014) Reduction of emissions by chemical industry from the German emission control act to the Industrial Emission Directive (IED). Procedia Technol 12:637–642

Echterhof T, Gruber J, Pfeifer H (2011) Measurements and simulation of NOx formation in the electric arc furnace. In: 2nd international conference clean technologies in the steel industry, Budapest, Hungary, 26–28 September

Environmental Agency of London (1999) Process subjected to Integrated Pollution Control. IPC Guidance Note, Series 2 (S2), Metal Industry Sector, S2 2.01 Iron and Steel Making Processes, London. http://ea-lit.freshwaterlife.org/archive/ealit:1909. Accessed 15 November 2015

Eurofer (2007) Review of the EAF chapter of the current BREF. 42

European Community Directive 1999/13/EC (as amended by Directive 2004/42/CE and Directive 2008/112/EC) on the limitation of emissions of volatile organic compounds due to the use of organic solvents in certain activities and installations

European Standard EN 1948-1:2006 Stationary source emissions – Determination of the mass concentration of PCDDs/PCDFs and dioxin-like PCBs – Part 1: sampling of PCDDs/PCDFs

European Union Directive 2010/75/EU of the European Parliament and the Council of 24 November 2010 on industrial emissions (Integrated Pollution Prevention and Control), Official Journal of the European Union

Greenwood NN, Earnshaw A (1997) Chemistry of the elements, 2nd edn. Elsevier, Amsterdam

Grochowalski C, Lassen M, Holtzer M, Sadowski M, Hudyma T (2007) Determination of PCDDs, PCDFs, PCBs and HCB emission from the metallurgical sector in Poland. Environ Sci Pollut Res Int 14:326–332

Guézennec AG, Huber JC, Patisson F, Sessiecq P, Birat JP, Ablitzer D (2005) Dust formation in electric arc furnace: birth of the particles. Powder Technol 157:2–11

Han Z, Holappa L (2003) Bubble bursting phenomenon in gas/metal/slag systems. Metall Mater Trans B 34:525–532

Huber JC (2000) La formation des poussières dans un Four Electrique d'Aciérie. Doctorate Thesis, INPL, France

Iluţiu-Varvara DA (2007a) The generation and transfer of pollutant substances in industrial processes (in Romanian). UT Press, Cluj-Napoca. Romania ISBN 978-973-662-344-8

Iluţiu-Varvara DA (2007b) Experimental researches regarding the constituted phases of the dusts exhausted during steelmaking in the electric arc furnace. Acta Technica Napocensis - Scientific Bulletin of the Technical University of Cluj-Napoca. Series: Machine Building. Materials 50:121–125

Iluţiu-Varvara DA (2009a) Study on generation mechanisms of nitrogen oxides (NO_x) during the steelmaking. Acta Technica Napocensis - Scientific Bulletin of the Technical University of Cluj-Napoca. Series: Machine Building. Materials 52:86–88

Iluţiu-Varvara DA (2009b) Experimental research on nitrogen oxides (NO_x) emissions generated from the steelmaking. Acta Technica Napocensis - Scientific Bulletin of the Technical University of Cluj-Napoca. Series: Machine Building. Materials 52:97–100

Iluţiu-Varvara DA (2009c) Experimental researches concerning the volatile organic compounds (VOCs) emissions to the steelmaking. Metalurgia Int 7:38–44

Iluţiu-Varvara DA (2010) Research about the greenhouse gases emissions from metallurgical processes. Environ Eng Manag J 6:813–818

Iluţiu-Varvara DA, Pică EM, Brânduşan L (2011) Assessment of air environmental factor pollution to the steelmaking. Bulletin of the Polytechnic Institute of Jassy, Construction. Architecture 3:113–118

Iluţiu-Varvara DA, Brânduşan L, Pică EM (2013) Researches regarding the air pollution with sulfur dioxide (SO_2) to the steelmaking. Adv Eng Forum 8–9:115–126. doi:10.4028/www.scientific.net/AEF.8-9.115

Iluţiu-Varvara DA, Rădulescu D (2013) Assessment of air pollution with sulphur dioxide (SO_2) to the electric arc furnaces. Stud Univ Babes-Bolyai Chem 2:143–150

Iluţiu-Varvara DA, Mârza CM, Sas-Boca IM, Ceclan VA (2015a) The assessment and reduction of carbon oxides emissions at electric arc furnaces-essential factors for sustainable development. Procedia Technol 19:402–409. doi:10.1016/j.protcy.2015.02.057

Iluţiu-Varvara DA, Brânduşan L, Arghir G, Pică EM (2015b) Research about the characterization of metallurgical slags for landfilled waste minimization. Environ Eng Manag J 14:2115–2126
Iluțiu-Varvara DA (2016) An assessment of pollution with polychlorinated dibenzodioxins (PCDDs) and polychlorinated dibenzofurans (PCDFs) at steelmaking. Procedia Technol 22:445–451. doi:10.1016/j.protcy.2016.01.084
Iluțiu-Varvara DA, Mârza CM, Aciu C, Hădărean A, Domniţa FV, Sas-Boca IM, Mihu AM (2016) An assessment of pollution with volatile organic compounds in the electric arc furnaces. Procedia Technol 22:452–456. doi:10.1016/j.protcy.2016.01.086
Jha MK, Kumar V, Singh RJ (2001) Review of hydrometallurgical recovery of zinc from industrial wastes. Resour Conserv Recycl 33:1–22
Li CL, Tsai MS (1993) Mechanism of spinel ferrite dust formation in electric arc furnace steelmaking. ISIJ Int 33:284–290
Lotun D, Pilon L (2005) Physical modeling of slag foaming for various operating conditions and slag compositions. ISIJ Int 45:835–840
Ma G, Garbers-Craig AM (2006) A review on the characteristics, formation mechanisms and treatment processes of Cr (VI)-containing pyrometallurgical wastes. J South Afr Inst Min Metall 106:753–763
Malikov GK, Lisienko VG, Malikov KY, Viskanta R (2002) A mathematical modeling and validation study of NOx emissions in metal processing systems. ISIJ Int 10:1175–1181
Negrea V, Sandu V (2000) Combating pollution in road transport (in Romanian). Technical Press, Bucharest
Rai PK (2015) Multifaceted health impacts of particulate matter (PM) and its management: an overview. Environ Skept Crit 4(1):1–26
Ryu JY, Mulholland JA, Chu B (2003) Chlorination of dibenzofuran and dibenzo-p-dioxin vapor by copper (II) chloride. Chemosphere 51:1031–1039
Sofilic T, Jendricko J, Kovacevic Z, Cosic M (2012) Measurement of polychlorinated dibenzo-p-dioxin and dibenzofuran emission from EAF steel making process. Arch Metall Mater 57:811–821
Stieglitz L, Vogg H, Zwick G, Beck J, Bautz H (1991) On formation conditions of organohalogen compounds from particulate carbon of fly ash. Chemosphere 23:1255–1264
Turkdogan ET (1996) Fundamental of steelmaking. The University Press, Cambridge
Tysklind M, Söderström G, Rappe C (1989) PCDD and PCDF emissions from scrap metal melting processes at a steel mill. Chemosphere 19:705–710
Unamuno I, Laraudogoitia JJ, Almeida SM (2008) Sidenor Basauri EAF emissions reduction through analysis and modeling. Arch Metall Mater 2:379–384
US Environmental Protection Agency (USEPA) (1988) Final BDAT background document for KO61. Washington, DC, August
Varvara DA (2006a) The problematic of pollution with dioxins and furans to the steelmaking in the electric arc furnace. Acta Technica Napocensis - Scientific Bulletin of the Technical University of Cluj-Napoca. Series: Machine Building. Materials 49:151–157
Varvara DA (2006b) The problematic of interphase transfer of pollutant substances to the steelmaking. Acta Technica Napocensis - Scientific Bulletin of the Technical University of Cluj-Napoca. Series: Machine Building. Materials 49:147–150
Varvara DA (2007a) Studies concerning the substances transfer between the steelmaking phases. PhD Thesis, Technical University of Cluj-Napoca, Cluj-Napoca, Romania
Varvara DA (2007b) Experimental researches about of the particulate matter emitted in the steelmaking process. Foundry J (Revista de Turnătorie) 7(8):12–16
Van den Berg M, Birnbaum LS, Denison M, De Vito M, Farland W, Feeley M, Fiedler H, Hakansson H, Hanberg A, Haws L, Rose M, Safe S, Schrenk D, Tohyama C, Tritscher A, Tuomisto J, Tysklind M, Walker N, Peterson RE (2006) The 2005 World Health Organization reevaluation of human and mammalian toxic equivalency factors for dioxins and dioxin-like compounds. Toxicol Sci 93:223–241

Warnatz J, Maas U, Dibble RW (1999) Combustion. Springer, Berlin
Wikstrom E, Marklund S (2000) Secondary formation of chlorinated dibenzo-p-dioxins, dibenzofurans, biphenyls, benzenes, and phenols during MSW combustion. Environ Sci Technol 34:604–609
Zeldovich Y, Barenblatt G, Librovich V, Makhviladze G (1985) The mathematical theory of combustion and explosions. Plenum Publishing Corporation, New York
Zeldovich Y, Frank-Kamenetskii D, Sadovnikov P (1947) Oxidation of nitrogen in combustion (M. Shelef Trans.). Academy of Sciences of USSR, Institute of Chemical Physics, Moscow-Leningrad

Chapter 16
Electric Arc Furnace

Jorge Madias

Abstract In this chapter, electric steelmaking is introduced with a short review: share, raw materials, operation, typical equipment, off-gas treatment, emissions. Electric-based steelmaking enjoys a much comfortable position than integrated classical blast furnace—oxygen steelmaking facilities, regarding greenhouse emissions. This is compared both for regions and for the world. For instance, the mostly EAF-based NAFTA countries are nowadays the region where the production of steel generates lower specific emissions. This said (and detailed), the chapter continues with a discussion of the CO_2 emissions of the electric arc furnaces. A reference is be made to the use of alternative raw materials, as DRI/HBI, pig iron and hot metal. In relation with the EAF design, factors to be analyzed are the effects of different furnace designs on emissions: conventional, twin shell, conveyor scrap preheating, and shaft scrap preheating are considered. The use of chemical energy is reviewed, as well as the effect of an external factor: how electric energy is generated.

16.1 Electric Steelmaking

The electric arc furnace applied in steelmaking was invented in 1889 by Paul Héroult. Emerging new technology started in the beginning of the twentieth century when wide-ranging generation of relatively cheap electric energy started at that time. First-generation furnaces had a capacity in between 1 and 15 t. The EAF had Bessemer/Thomas converters and Siemens Martin furnaces as strong competitors, initially. But its niche was the production of special steels requiring high temperature, ferroalloy melting, and long refining times. In the 1960s, with the advent of billet casting, the EAF occupied a new niche: the melting unit of choice for the so-called minimills, feeding billet casters for the production of rebar and wire rod (Madias 2014).

J. Madias (✉)
Metallon – 432, 9 de Julio Street, San Nicolas, Buenos Aires B2900HG, Argentina
e-mail: jorge.madias@metalllon.com.ar

P. Cavaliere (ed.), *Ironmaking and Steelmaking Processes*,
DOI 10.1007/978-3-319-39529-6_16

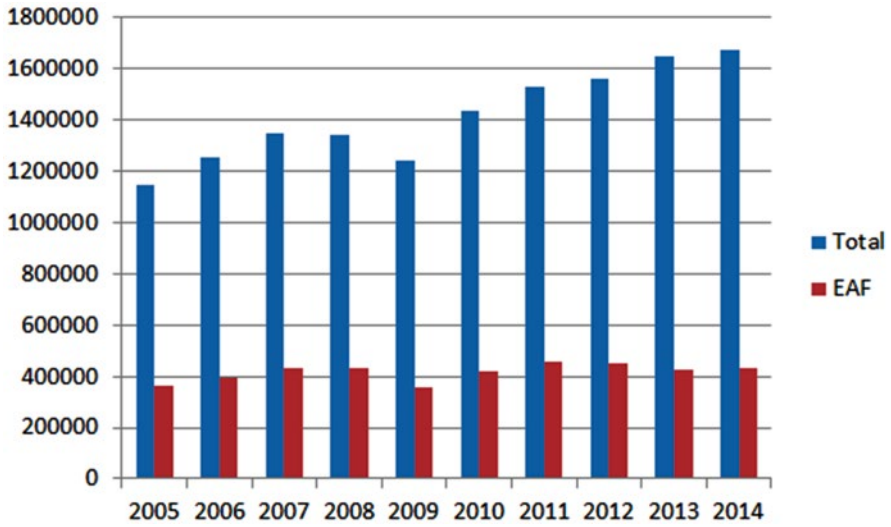

Fig. 16.1 Worldwide crude steel production (EAF vs. total) 2005–2014 (Worldsteel Association 2015)

Table 16.1 Ten top producers of steel through electric arc furnace in 2014 (Worldsteel Association 2015)

Country	EAF production (t)
United States	55,174,000
India	50,211,000
China	49,938,000
Japan	25,679,000
South Korea	24,197,000
Turkey	23,752,000
Russia	21,852,000
Italy	17,200,000
Iran	13,607,000
Mexico	13,311,000

In the following two decades, to better support the short tap-to-tap time required by billet casters, the EAF reinvented itself as a melting-only unit. Steel refining was left for the recently introduced ladle furnace. Large transformers were introduced; ultrahigh-power furnaces developed, which were made possible by adopting foaming slag practice. This way, tap-to-tap time became close to casting time.

By 1985, a new niche for electric steelmaking began to be taken: flat products, through thin slab casting, and direct rolling.

This process route has achieved a significant role in world steel production, being close to 26% share by 2014 (Fig. 16.1). The three top producers are the United States, India, and China (Table 16.1).

Table 16.2 Estimation of raw materials for EAF steelmaking for 2014

	Annual production/ consumption	% share	Assumptions
EAF crude steel production (t)	430,251,000		From [2]
Estimated metallics required (t)	478,056,667	100	90 % yield
Scrap (t)	382,425,834	80	Balance
DRI/HBI production (t)	73,209,000	15.3	All DRI/HBI production consumed in EAFs
Hot metal + pig iron	22,421,833	4.7	BOF mix 85 % hot metal, 15 % scrap, 90 % yield

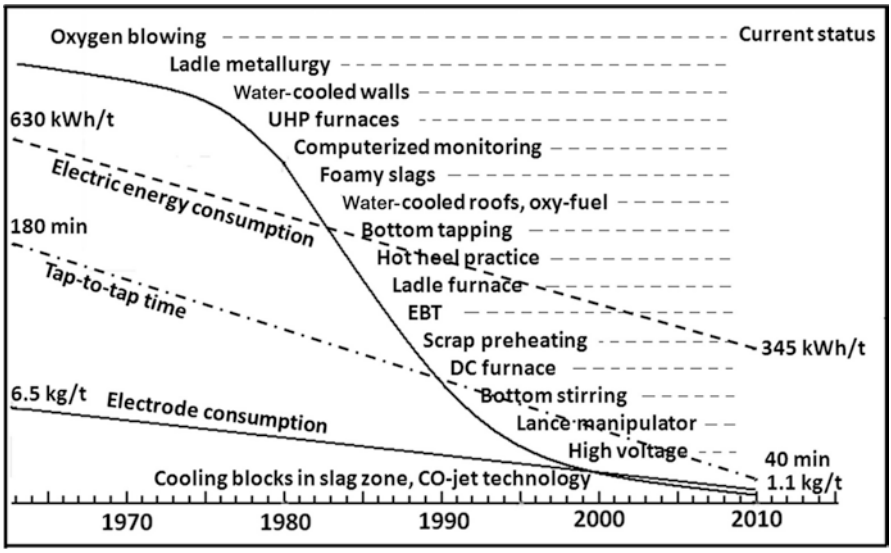

Fig. 16.2 Evolution of EAF technology 1965–2010

Most of the ferrous scrap worldwide is recycled and refined to steels via electric furnaces. EAFs are versatile, charging everything from all sorts of scrap to hot briquetted iron (HBI), direct reduced iron (DRI), pig iron, hot metal (Table 16.2).

EAFs may produce all type of steels: long and flat, carbon and alloyed, merchant and special products.

The developments in the EAF technologies since 1965, promoting lower electric energy consumption, shorter tap-to-tap time, and less electrode consumption, are shown in Fig. 16.2 (Lüngen et al. 2013). Furnace size enlarged up to 350 t maximum, which together with the shortening of tap-to-tap time made possible to have more than 1 Mtpy capacity with just one furnace. Electric energy consumption

decreased down to 350 kWh/t for 100 % scrap operations. Chemical energy increased at levels not far from those of Basic Oxygen Furnace (BOFs). Refractory consumption fell down due to the replacement by cooled roof and panels, slag foaming, and refractory quality improvement. Power-off time is now of <10 min for the best operated furnaces. For a large number of ArcelorMittal group meltshops, average electrode consumption was 1.43 kg/t.

16.1.1 Equipment

The increase in furnace electric power has been the key factor in the development of EAF technology during the past 50 years. As in the 1960s, a common EAF power was 250–300 kVA/t liquid steel; today standard ultra-high-power EAFs have 900–1000 kVA/t steel available in the transformers. These furnaces are equipped with water-cooled panels and EBT tapping. EBT stands for eccentric bottom tapping, a tapping system that yields a uniform steel jet falling into the ladle, with slag carry over controlled to a certain extent. In Fig. 16.3, a scheme of such state-of-the-art EAF is presented.

The current furnace includes three water-cooled parts: roof, panels, and off-gas duct. Although some heat is lost due to the heat extraction by the cooling

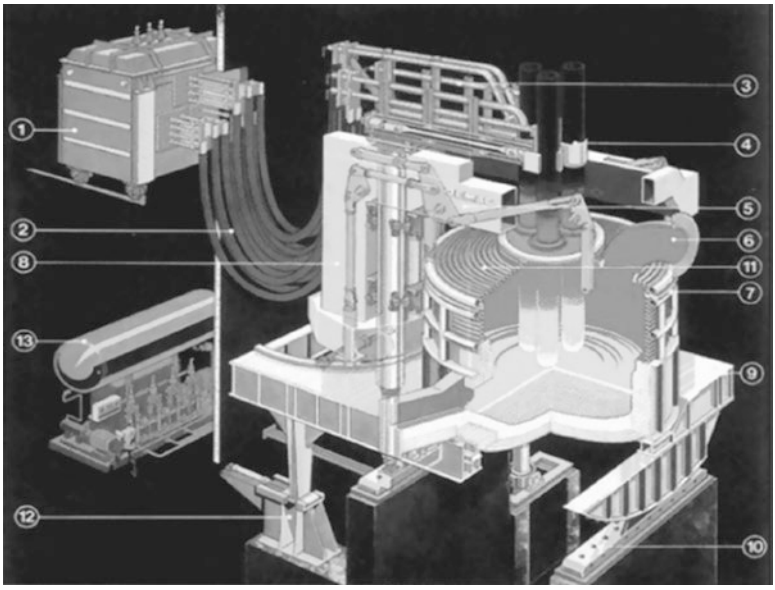

Fig. 16.3 Current EAF standard design. (*1*) Transformer, (*2*) flexible cable connection, (*3*) electrode arms, (*4*) electrodes clamping, (*5*) arms, (*6*) cooled off-gas duct, (*7*) cooled panels, (*8*) structure, (*9*) basculating structure, (*10*) rack, (*11*) cooled roof, (*12*) basculating device, and (*13*) hydraulic group

water, this design makes possible less refractory consumption (because they replace refractory linings) and the use of high power. At the time the panels were first introduced, some fears arose on safety risks, but after realizing the cost advantage, almost all EAF adopted them. They may be made of steel or copper (much longer life) and with different designs (conventional, flip and turn, etc.). Recently, more attention has been paid to safety with water cooling. First, to detect, limit, and avoid the possibility of water leakage, and second, to cut the need of repairing work in the hot furnace. Off-gas analysis, when hydrogen is included, is a useful tool to detect leakage. To limit leakage and maintenance work, solid cast or machined water panes have been introduced. Split shell, with spray-cooled upper shell means less risk as non-pressurized water tends to penetrate less in case of leakage.

There are variations on the standard design:

- Use of direct current instead of alternative current, with one large electrodes (or two) instead of three, and a refrigerated anode in the hearth bottom. Main aim is to decrease electrode consumption and flickers.
- Use of scrap preheating on a continuous scrap transporter, using the off-gas heat, in counter-current. Main aim is to decrease energy consumption and to avoid bucket charging.
- Use of scrap preheating in a shaft, using the off-gas heat. Main aim: to decrease energy consumption.
- Twin shell.

16.1.2 Melting Practice

The basic principle of electric steelmaking today is that the furnace is a "melting machine" that produces liquid steel with required chemistry, temperature, and mass in time to feed steel to successive ladle treatments and continuous caster, which finally determines the production rhythm. Typical tap-to-tap times are in the range of 40–60 min, which is also the total furnace time per heat.

Although Ultra High Power (UHP) furnaces are used, fast melting by using only electric power is difficult and not the most economic practice either. Importing extra energy and assisting melting technique can greatly accelerate scrap melting and bring economic benefits. Accordingly, the current state of the art in EAF steelmaking is to use as much as possible chemical energy, besides electric energy, to accommodate tap-to-tap times to the pace of the downstream continuous caster.

Regarding the application of electric energy, at the start of melting, after basket charge, not all the available power can be applied, as the electrodes may be still in a high position, too close to the roof. Then, when the melting operation has advanced further, changing to the tap maximum power may be applied. This is not the case for 100 % flat bath operations like in Consteel EAFs or 100 % DRI/HBI charging through the fifth hole. Chemical energy is introduced by oxygen, carbonaceous

materials, and natural gas, more and more through injectors rather than lances. The energy generating reactions are:

$$C + \tfrac{1}{2}O_2 = CO \rightarrow 2.55\,\text{kWh/kg C}$$

$$C + O_2 = CO \rightarrow 9.1\,\text{kWh/kg C}$$

$$C + \tfrac{1}{2}O_2 = CO_2 \rightarrow 2.81\,\text{kWh/kg C}$$

$$Fe + \tfrac{1}{2}O_2 = FeO \rightarrow 1.32\,\text{kWh/kg Fe}$$

The refining step usually does not require full power, which with already flat bath could be dangerous for the lining. At that time, the foaming of the slag is a must. For the slag to foam, the production of CO gas is necessary, by means of the injection of carbon and oxygen through lances or burners. For foaming purposes, several carbonaceous materials are useful, depending on local cost and availability: anthracite, petroleum coke, coke breeze.

16.2 EAF CO_2 Emissions

There is a specific methodology to calculate GHG emissions from EAF steel facilities (Climate leaders 2003). It includes calculating emissions from carbonate flux and use of carbon electrodes. Emissions of CO_2 from use of carbonate flux are calculated based on the amount of flux used and the stoichiometric ratio of CO_2 to $CaCO_3$ and $MgCO_3$. The emissions from use of electrodes are estimated based on the number of electrodes used and the carbon content of the electrodes. CO_2 emissions from any coke or coal used in the process are estimated using the Climate Leaders Stationary Combustion guidance. The steps involved with estimating iron and steel process related CO_2 emissions from EAF facilities are shown below.

Step 1: Determine the amount of carbonate flux used. This should be in terms of pure $CaCO_3$ and $MgCO_3$. Therefore, the total amount of flux used needs to be adjusted for purity.

Step 2: Calculate the flux carbon factor. This is based on the stoichiometric ratio of C to $CaCO_3$ and $MgCO_3$. Default values are given in Climate Leaders 2003, Sect. 3.2.

Step 3: Determine the amount of electrodes used. This could be based on the actual amounts used or could be estimated based on the amount of steel produced.

Step 4: Determine the electrode carbon factor. This is based on the carbon content of the electrode

Equation 16.1 represents the method used to calculate CO_2 emissions from steel production at EAF facilities. More explanation of emission factors and default values is provided in Sect. 16.3 of the reference.

$$\text{Emission} = \left[\left(\text{Flux} \times \text{CF}_{\text{Flux}}\right) + \left(\text{Electrode} \times \text{CF}_{\text{E}}\right)\right] \times \frac{\text{CO}_2\,(\text{m.w.})}{\text{C}(\text{m.w.})}$$

where :

$$\text{Flux} = \text{mass of flux used}$$

$$\text{CF}_{\text{Flux}} = \text{flux carbon factor}\left(\frac{\text{mass C}}{\text{mass flux}}\right) \tag{16.1}$$

$$\text{Electrode} = \text{mass of carbon electrode used}$$

$$\text{CF}_{\text{E}} = \text{electrode carbon factor}\left(\frac{\text{mass C}}{\text{mass of electrode}}\right)$$

$$\text{CO}_2\,(\text{m.w.}) = \text{molecular weight of carbon}$$

If the CO_2 emissions related to the production of electric energy are considered, the source of this energy has a very strong influence. A case study has been carried out for a conventional EAF in Canada and an EAF equipped with shaft preheater in the UK (Thomson et al. 2000). Both countries have a different profile of electricity sources (see Table 16.3). In Fig. 16.4 the share of GHG emissions (including the generation of electricity) is shown for the two cases.

It is well known that emissions from EAF-based steelmaking are much lower than for integrated plants. Electric steelmaking represented in 2013 29 % of the world steel production, but only 1 % of the energy consumption and just 12 % of CO_2 emissions (see Fig. 16.5).

Worldwide figures have been collected by Worldsteel in 2013 from 72 BF/BOF mills and EAF plants, to benchmark emissions. Results are presented in Fig. 16.6. In weighted average, for BF/BOF plants CO_2 intensity is 2.26 t CO_2/t crude steel, while for EAF plants the figure is 0.62 t CO_2/t crude steel (Reimink 2015).

In Table 16.4, a comparison is made for the case of the USA, where the dominant process route is electric steelmaking.

Thanks to its higher share of EAF, NAFTA (Mexico, USA, Canada) has the lower specific energy consumption and CO_2 emissions in comparison with other OECD countries (Europe 27 + TK and Australasia), see Fig. 16.7.

Recycling scrap in EAFs is the most efficient available technology, not just for energy. Steel, like all metals, is indefinitely recyclable without loss of properties. Steel is not “consumed” but “used,” over and over again. The energy needed to

Table 16.3 Electricity generation source distribution

	Canada	UK
Coal (%)	25	50
Fuel (%)	3	5
Natural gas (%)	4	13
Nuclear (%)	30	29
Hydroelectricity (%)	38	3

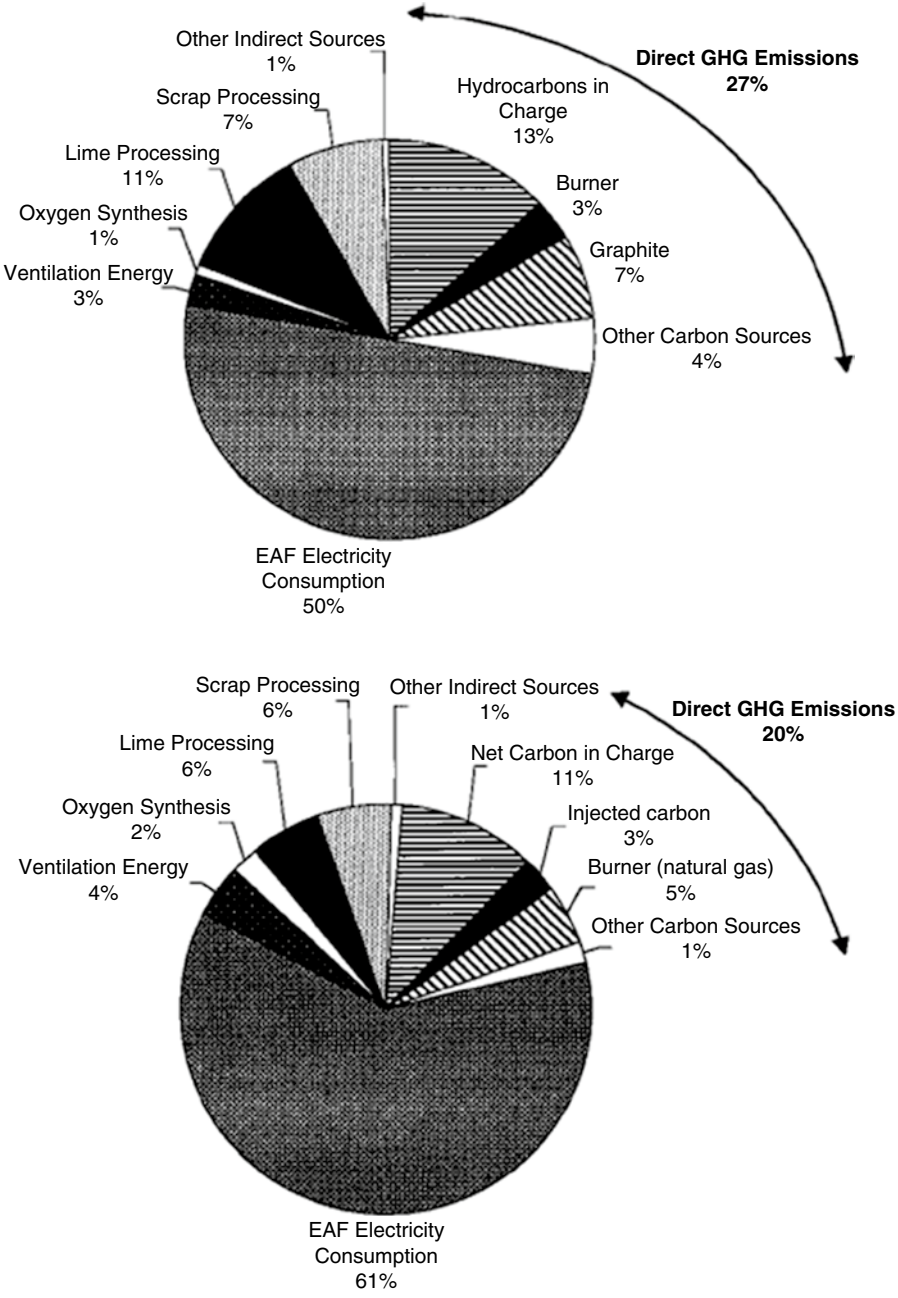

Fig. 16.4 Direct and indirect GHG sources for two cases. *Top*: convention EAF using Canadian electricity generation source distribution; *bottom*: scrap preheating EAF with UK electricity generation source

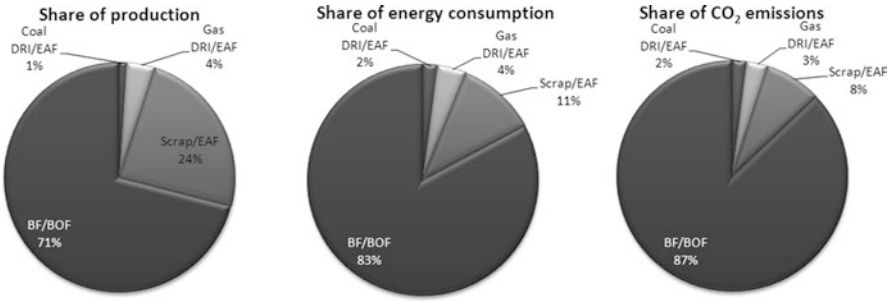

Fig. 16.5 EAF vs. BF/BOF route worldwide: a comparison of production, energy consumption, and CO_2 emissions (Laplace Conseil 2013). * Includes share of CO_2 from electricity needed; assume same mix of primary energies for electricity production

melt scrap represents 40 % of the energy and 30 % of CO_2 to smelt iron ore in a modern BF/BOF integrated mill. In addition, capital cost per ton of capacity is 60–70 % lower; maintenance costs are decreased in the same proportion. Labor productivity is twice as high and smaller size of mill usually leads to better social relationship.

16.3 Technologies to Decrease EAF CO_2 Emissions

In Europe, some technologies are being considered as Best Available Technology to decrease energy consumption and CO_2 emissions. In Table 16.5 those BAT are listed, taking into account if they are add-on, process control, or new technology (Pardo et al. 2012). Those selected as the most promising are scrap preheating and oxy-fuel burners.

In the USA, several technologies have been identified to decrease energy consumption and in consequence CO_2 emissions in EAFs (EPA Office of Air and Radiation 2012), see Table 16.6.

In the following, a short discussion of the two more promising technologies mentioned above is carried out.

Scrap Preheating Some 20 % of all the energy input for melting the scrap in an EAF disappears in the form of waste gas. Preheating of scrap is a technology that can reduce the power consumption in the EAF process by using the waste heat of the furnace to preheat the incoming scrap charge. There are 99 Scrap Preheating systems currently installed in the EU. In the case of adoption of this technology, total and direct CO_2 emissions should decrease by 0.037 t CO_2/t crude steel.

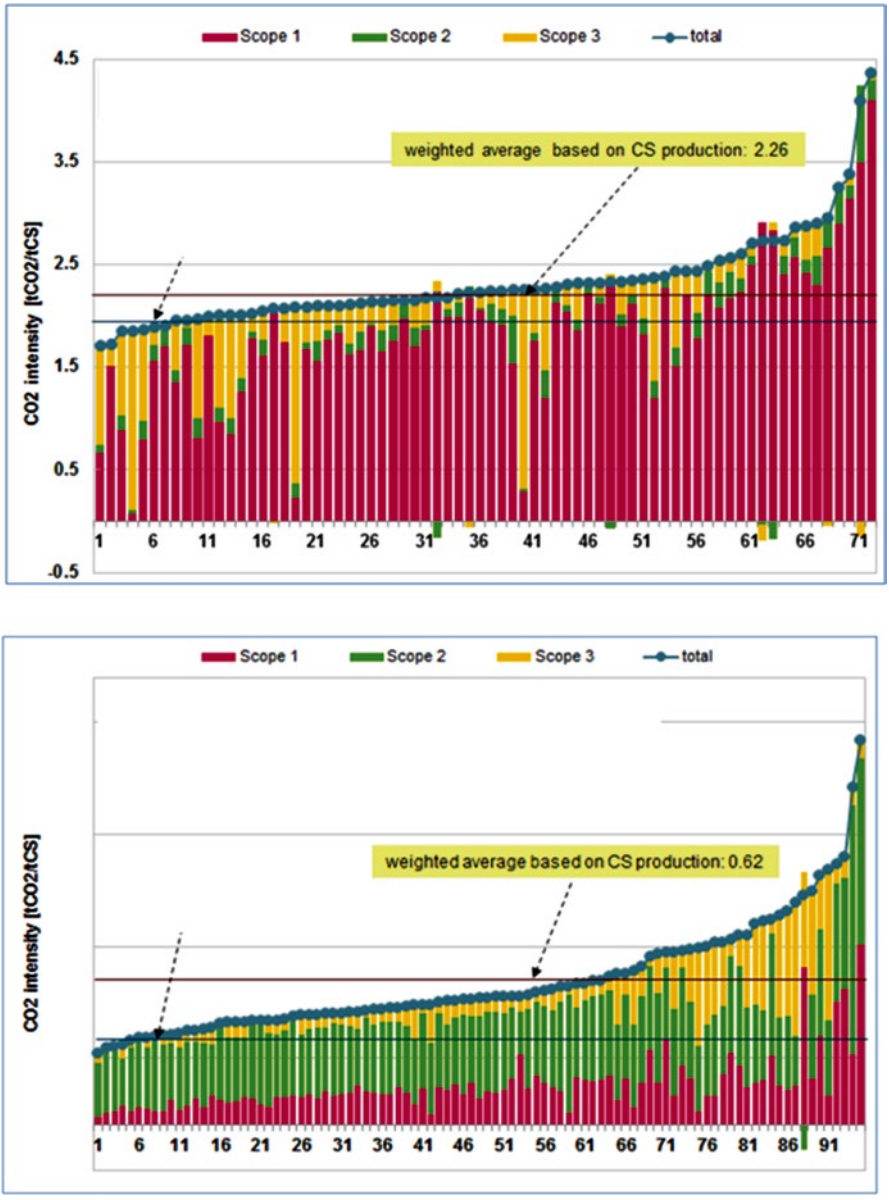

Fig. 16.6 2013 CO_2 intensity for BF/BOF (*top*) and EAF (*bottom*) plants

Table 16.4 Estimates of GHG emissions for iron and steel sector using emission factors (million tons of CO_2/year)

	Number of facilities	Process units	Miscellaneous combustion units	Indirect emissions (electricity)	Industry total	Average per plant
All EAF	87	5.0	19	24	48	0.6
All integrated	17	33	17.5	6.8	57	3.4

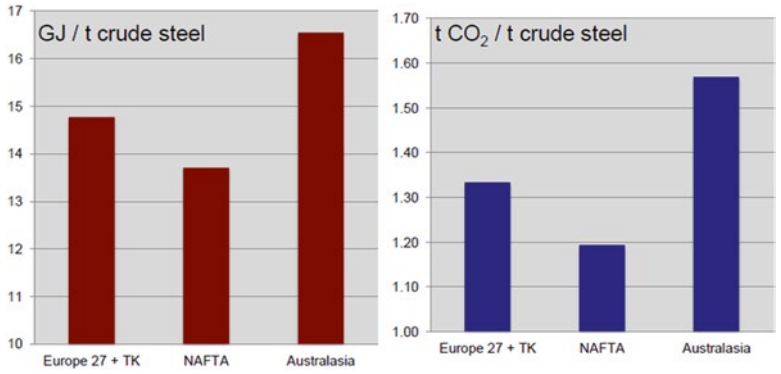

Fig. 16.7 Energy consumption and CO_2 emissions per ton of crude steel in OECD regions (Laplace Conseil 2013)

Table 16.5 Best available technologies to decrease energy consumption and CO_2 emissions being considered in Europe

Best available technology	Feature
Scrap preheating	Add on
Oxy-fuel burners	Add on
Bottom stirring/gas injection	Add on
Foamy slag practices	Process control
Improved process control	Process control
Eccentric bottom tapping	New technology
Twin shell furnace	New technology
Direct current (DC) arc furnace	New technology

Table 16.6 Energy efficiency technologies and measures available for electric arc furnace steel production in the USA

Option	Applicability and feasibility codes	Payback time (years)
Improved process control (neural network)	EX	0.5
Adjustable speed drives	EX	2–3
Transformer efficiency—ultra high power transformers	C, EX	5.2
Bottom stirring/stirring gas injection	C, EE, N	0.2
Foamy slag practice	C, EX	4.2
Oxy-fuel burners	C, EX	0.9
Post-combustion of the flue gases	C, EX	
DC arc furnace	C, EE, S	
Scrap preheating—tunnel furnace (Consteel)	C, EE, N, S	
Engineered refractories		
Airtight operation	P	
Contiarc furnace	C, N, S	
Flue gas monitoring and control	C, EX	4.3
Eccentric bottom tapping on existing furnace	C, N, S	6.8
DC twin shell with scrap preheating	C, EE, N	3.5

C = Site-specific variables may affect costs and/or practicality of use of the option at all facilities. EE = Options that could improve energy efficiency and potentially lower GHG emissions but may increase other pollutants. EX = Process already widely implemented at many existing facilities. N = Only feasible for new units. P = Immature process that is still in research and/or pilot stage as applied to Iron and Steel. S = Specialized process only technically appropriate for some equipment configurations or types

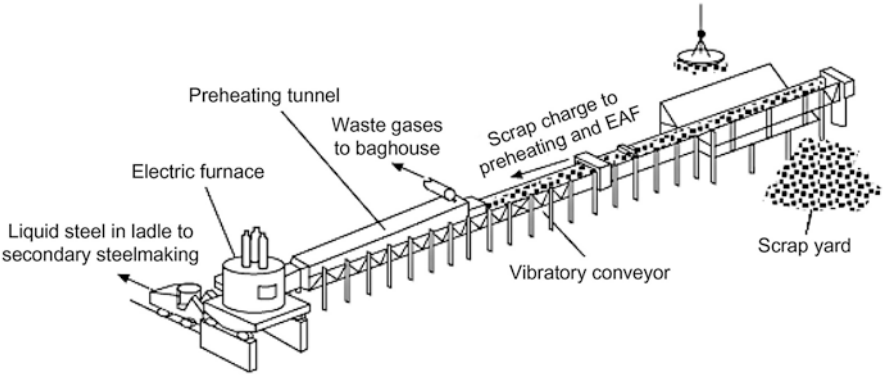

Fig. 16.8 Continuous scrap charging and off-gas energy recovery with Consteel EAF

Basically, there are three ways of preheating the scrap that are being used currently: in a conveyor, using continuous charging (Consteel EAF), or in a shaft, with batch charging.

In the Consteel EAFs, preheating is carried out continuously with the off-gas exiting the furnace over a conveyor feeding the scrap to the EAF (Fig. 16.8). The upper part of the scrap enters the furnace hotter than the lower part, which is not so much exposed to the heat. Most advantages of the furnace type come from the full flat-bath operation, although energy recovery through preheating is even significant. A current trend in these furnaces is to have a large hot heel, even 50 % of the heat weight, thus favoring heat transfer from liquid to solid steel, as long as there is bottom stirring. Here the mechanism of radiation from the electrodes to the scrap around the electrodes does not exist. More than 40 Consteel EAFs have been built and more than 30 are in operation, with some more under construction. The emphasis in the first decade of this century has been more on high productivity, large EAFs installed in Asia, rather than in the energy recovery feature. Here there is potential for more efficiency (Jones et al. 1998).

As previously mentioned, continuous charging lets us use maximum power from the start of the heat, as a difference with batch charging, where lower tap is applied after charging of each bucket to avoid damage to the roof. Obviously, power-off time for bucket charging is avoided. Recently, the Consteel Evolution concept has been proposed, including natural gas burners for charge preheating before entering the off-gas preheated tunnel, and off-gas analysis to improve post-combustion in the tunnel (Memmoli et al. 2012).

Preheating in Shaft The other industrially applied way of preheating the scrap is the shaft furnace. They are often DC EAFs with one central electrode and some of them operating in twin mode. Currently, more than 20 such furnaces are in operation (Fuchs, Eco-Arc, and Quantum type). In Fig. 16.9, a scheme of a Fuchs shaft furnace is shown, together with the typical charging/melting cycle.

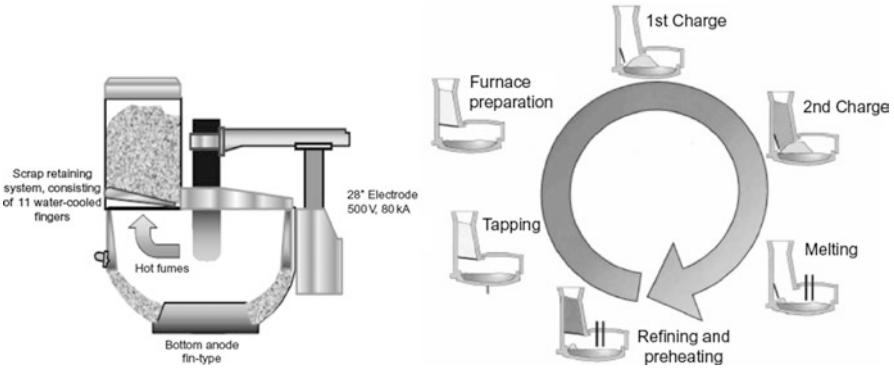

Fig. 16.9 Electric furnace with off-gas energy recovery by preheating scrap in a shaft. *Left*: scheme for a DC shaft furnace, with one electrode. *Right*: Operating cycle for a shaft furnace charging two scrap baskets

Formation of dioxine has been reported for some of these operations. Main reasons for dioxine formation are (a) plastics in the scrap and (b) critical temperature range. In a Japanese version of shaft furnace (Eco-arc by J. P. Plantech), charging is performed by means of a skip car instead of a bucket. The shaft has no device for keeping the scrap inside. The off-gas treatment includes a post-combustion chamber to decompose dioxines and a fast cooling chamber to avoid De Novo synthesis.

Oxy-Fuel Burners Modern furnaces use oxygen-fuel burners to provide chemical energy to the cold-spots, making the heating of the steel more uniform. Oxy-fuel burners reduce electricity consumption by substituting electricity with fuels and increase heat transfer. Some 136 Oxy-fuel burners are currently installed in the EU. The expectation is that this technology may decrease total and direct CO_2 emissions by 0.006 t CO_2/t crude steel.

Oxy-fuel burners have a long story of optimization and enlargement. Initially, Oxygen was introduced in the furnace through the slag door to accelerate melting by cutting scrap parts. The combination of Oxygen and Carbon lances was useful then to create a foamy slag protecting panels, roof and refractories form the arc radiation. After that, lance manipulators were devised to facilitate the lancing operation. Finally, burners were introduced through the furnace walls, to inject Oxygen, Carbon, natural gas, and lately lime. This equipment resulted easy to maintain and effective for its different tasks. Besides, their operation can be automated to a large extent.

Lately, chemical energy tends to contribute with 30 % of the EAF energy input. Since the heat duration is short, the large specific oxygen consumption (40 m^3/t crude steel, in average) requires quite high-intensity injection. In modern furnaces, the specific intensity of oxygen blowing is usually 0.9–1.0 m^3/t per minute and may also reach 2.5 m3/t per minute if hot metal and reduced iron are used in large amounts (Toulouesvski and Zinurov 2010).

16.4 CO_2 Emissions and the Future of the Electric Arc Furnace

As in China and other emerging countries start to have more scrap availability, and taking into account that these countries will have a commitment to decrease their emission, it is reasonable to expect an increased EAF share in world production, instead of the decrease of recent years. The International Energy Agency (IEA) has prepared forecasts regarding process routes and consumption of metallic till year 2050 (International Energy Agency 2012). They defined three scenarios for global average temperature increase: 6 °C, 4 °C, and 2 °C. 6 °C is an extension of current trends; 4 °C takes into account commitments assumed by countries regarding emission limits and energy efficiency improvement, and 2 °C is a very restrictive scenario regarding CO_2 emissions.

In Table 16.7, the aforementioned scenarios are presented, in relation with their influence on process routes and utilization of metallics, in comparison with the base situation, year 2010.

Although this forecast has spurred controversy (Mendes de Paula 2013), it reflects the current expectations on the future growth of this process route.

16.5 Conclusions

Electric arc furnace-based steelmaking is the low-CO_2 alternative to make steel, as long as scrap is available at a competitive price. Still, this process route may advance in lowering emissions, through the spreading of several technologies that are already available and working at industrial scale.

EAF total emissions have a large dependence on the source of electricity: hydroelectric, nuclear, natural gas, wind, or coal-based.

Table 16.7 Scenarios of increased global average temperature under low and high steel demand, and its influence on process route and metallics consumption for the year 2050, according to International Energy Agency

		Year 2010	Year 2050: low demand			Year 2050: high demand		
			6 °C	4 °C	2 °C	6 °C	4 °C	2 °C
Process route	EAF (%)		50.2	51.6	50.6	50.4	51.7	51.0
	BOF (%)	71.5	49.8	48.4	49.4	49.6	48.3	49.0
Metallics	Hot metal/pig iron (%)	68.6	45.6	44.3	40.8	45.5	44.2	37.9
	Gas-based DRI (%)	3.5	7.0	7.0	9.5	7.0	7.0	9.7
	Coal-based DRI (%)	1.3	4.8	4.8	0.0	4.7	4.7	0.0
	Smelting reduction (%)	0.0	0.5	0.5	4.8	0.4	0.4	7.4
	Scrap (%)	26.6	42.1	43.4	44.8	42.4	43.7	45.0

It is expected that in the future there will be more availability of scrap. This situation, together with the already mentioned low emission, and other advantages like lower investment, less manpower, more flexibility, easier maintenance, would make EAF the route of choice for the following decades.

Acknowledgments The author gratefully acknowledges the helpful comments and suggestions of the reviewers, which have improved the presentation.

References

Climate Leaders (2003) Direct emissions form iron and steel production. Climate leaders greenhouse gas inventory protocol core module guidance

EPA Office of Air and Radiation (2012) Available and emerging technologies for reducing greenhouse gas emissions from the iron and steel industry, pp 1–78

International Energy Agency (2012) Energy technology perspectives 2012 – pathways to a clean energy system

Jones JAT, Bowman B, Lefrank PA (1998) Chapter 10, Electric furnace steelmaking in The Making, Shaping and Treating of the Steel, The AISE Steel Foundation, Pittsburgh, USA

Laplace Conseil (2013) Impacts of energy market developments on the steel industry. In: 74th Session of the OECD Steel Committee, Paris, France, July 2013

Lüngen H-B et al (2013) Measures to increase efficiency and to reduce CO_2 emissions in iron and steelmaking in Germany and Europe. In: AISTech 2012 Proceedings, 2012, pp 109–119

Madias J (2014) Electric Furnace steelmaking in Treatise on Process Metallurgy – Industrial Processes part A, Elsevier, Amsterdam, The Netherlands

Memmoli F, Guzzon M, Giavani C (2012) Iron & steel technology, vol 9, pp 70–78

Mendes de Paula G (2013) Controversial forecast – IEA conclusion of electric steelmaking explaining more than 50% of steel production generates controversy. Revista ABM – Metalurgia, Materiais e Mineração, Jan/Feb, pp 21 (in Portuguese)

Pardo N, Moya JA, Vatopoulos K (2012) Prospective scenarios on energy efficiency and CO_2 emissions in the EU Iron & Steel Industry. Joint Research Centre, Report EUR 25543 EN

Reimink H (2015) Benchmarking systems designed for improvement. Worldsteel presentation

Thomson MJ, Evenson EJ, Kempe MJ, Goodfellow HD (2000) Control of greenhouse gas emissions from electric arc furnace steelmaking: evaluation methodology with case studies. Ironmak Steelmak 27(4):273–278

Toulouesvski YN, Zinurov IY (2010) Innovation in electric arc furnaces – scientific basis for selection. Springer, Heidelberg, London New York, p 14

Worldsteel Association (2015) Steel statistical yearbook. Worldsteel Association, Brussels

Part IV
Greenhouse Emissions

Chapter 17
Technological Methods to Protect the Environment in the Ukrainian BOF Shops

B.M. Boichenko, L.S. Molchanov, and I.V. Synegin

Abstract BOF process is one of the most productive ways of steel manufacturing. Byproducts of this process are metallurgical slag, gases (volatile-rich oxide and other chemical compounds), metallurgical dust, and excessive heat. Nevertheless there are developed a large number of waste gas cleaning systems and recycling technologies, these factors still have negative impact on whole biosphere. The greatest effect it makes on the atmosphere since during melting, a substantial amount of carbon and nitrogen oxides are released into the environment. The steelmaking dust can be classified by its origin. The main types of waste dust include: fragments of the raw material (as a result of technological overload and crushing of the raw materials), products of evaporation and condensation (vaporized molten slag and graphite ripe). For their capture in conditions of Ukrainian manufacturing developed a number of specific technological schemes involving precipitation of dust component in special units (Venturi tubes, cyclones, and scrubbers). Their use can reduce the concentration of hazardous substances and to the regulated legal framework limit.

17.1 Introduction

Metallurgy is the basis of the Ukrainian economic (11th place in world ranking of crude steel production). The most widespread method of steel production is Basic Oxygen Process (BOP) with top blowing. This high productivity technology allows producing low-carbon and carbon steel of ordinary quality. Steelmaking has a negative impact on the environment because of such wastes as slag, dust, and technological gases containing harmful volatile and dangerous substances and excessive heat. The greatest impact steel production has on atmosphere. Therefore, the main part of the technical solutions for environment protection in Ukraine is reducing emissions in atmosphere.

The aim of this work is to generalize and clarify information about the ways of protecting the environment that are used at the Ukrainian metallurgical plants and

B.M. Boichenko (✉) • L.S. Molchanov • I.V. Synegin
National Metallurgical Academy of Ukraine,
Gagarina Ave, 4, Dnipropetrovsk 49600, Ukraine
e-mail: boichenko@metal.nmetau.edu.ua

P. Cavaliere (ed.), *Ironmaking and Steelmaking Processes*,
DOI 10.1007/978-3-319-39529-6_17

development of technical solutions for complex improvement of technological schemes of steelmaking in order to reduce the negative impact on the environment.

17.2 Affection of Harmful Factors of Steelmaking Production on the Biosphere

The share of ferrous metallurgy in Ukraine accounts for about 20–25 % of total harmful emissions into the atmosphere, and in the areas of the large steel plants is more than 50 % of all contaminants. Annually Ukrainian metallurgical plants emit in the atmosphere a huge amount of harmful substances (Table 17.1).

In addition, the steel industry is one of the largest water consumers. Modern steel plant consumes 180–200 m^3 of water to produce 1 t of rolled steel. Daily water consumption may exceed 3 million m^3. It includes cooling equipment—48 %, waste gas cleaning—26 %, metal processing—12 %, hydraulic transport—11 %, and others—2 % of water needs. Discharge wastewater from the steel plants in the pond increases the amount of suspended solids, much of which are deposited near the drain, raises water temperature, deteriorates oxygen regime. On the surface of the pond, an oily film can form due to emission lubricant products with water. If the effluents contain acid, it leads to change the water acidity and disturbing biological processes. Pollutants emission causes the death of aquatic organisms and interferes in the process of pond self-cleaning. Most metals, their compounds, and other inorganic substances contained in wastewater of metallurgical plants have harmful effects on humans and warm-blooded animals, flora, macro- and microorganisms.

Processes of steel production cause to forming large amount of solid waste, which accumulated on large areas and which have a harmful effect on the soil, flora, water sources, and air. Solid Waste Dumps now occupy thousands of hectares of mineral lands. Slag and dust waste are generated on almost all stages of steelmaking. According to approximate estimation to produce 1 t of steel used 4.7 t of raw materials, which produced 0.406 t of waste.

Now Ukrainian metallurgical plants have accumulated about 94 million tons of slag produced by steelmaking and ferroalloy industries that occupy about 800 ha. And this value significantly increases if we take into account the area occupied by waste of refractory from the worn lining of furnaces, ladles, and other aggregates. Thus it should be noted that the most dangerous factors is atmosphere pollution, which will be discussed further.

Volume of the gases produced by Basic Oxygen Furnace (BOF) is cyclical (Fig. 17.1) and depends on the rate of carbon oxidation and conditions of oxygen blowing.

Table 17.1 Average gross emissions of harmful substances into the atmosphere by metallurgical plants per year

Harmful substances	Dust	CO	SO_4	NO_x	H_2S	Suspended substances
Amount of emission, 1000 t	337.2	2638.9	207.4	296.5	3.3	194.8

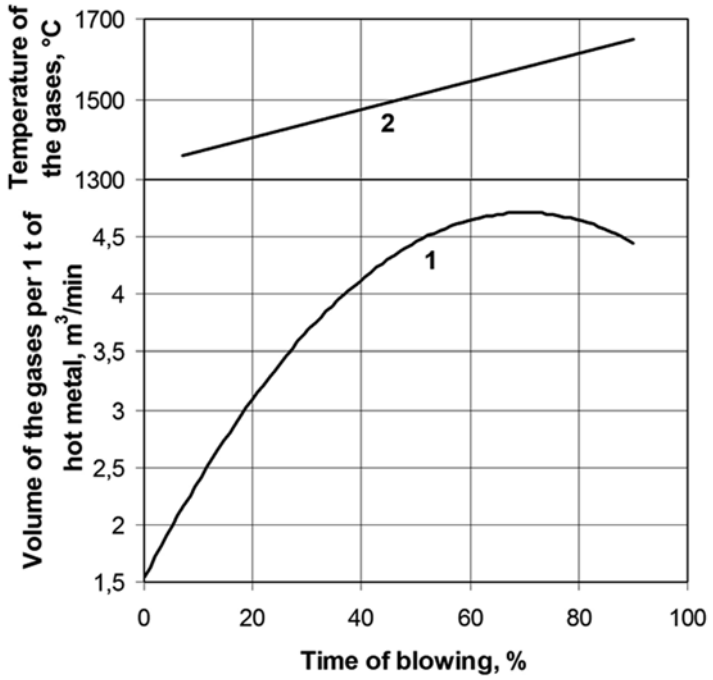

Fig. 17.1 Change of the BOF gases volume (*1*) and temperature (*2*) during oxygen blowing

Table 17.2 The chemical composition of BOF gases

	Chemical composition of the gases, %			
Sampling point	CO	CO_2	O_2	N_2
Near the BOF throat	85.0–90.0	8.0–14.0	1.5–3.5	0.5–2.5
In pipeline after full CO post-combustion	–	31.0	9.0	60.0

According to the practical data, volume of BOF gases that emits from the converter throat is 70–90 m^3/t of steel. The ratio of the maximum decarburization speed to the medium with using multinozzle lance is about 1.4. Table 17.2 shows the chemical composition of BOF gases.

In addition to the compounds indicated in Table 17.2 the following gas contents were revealed: 50 mg/m^3 SO_2; 100 mg/m^3 F_2 and 10 mg/m^3 Cl_2. Nitrogen oxides are not formed in the BOF workspace. However, the post-combustion CO to CO_2 leads to the formation of nitrogen oxides in amount of about 100 mg/m^3 or 50 g/t of crude steel. Nitrogen oxides are also formed in the post-combusted gases on the stack outlet in an amount of 30 g/t of steel. The BOF gases temperature at the outlet of its throat constantly increases during oxygen blowing. In the beginning of blowing it is 1250–1300 °C, and in the middle and at the end—1600–1700 °C.

During oxygen blowing BOF gases carry 1.5–2.0 % dust per 1 t of hot metal. Concentration of dust in the gases during blowing varies from 20 to 250 g/m^3 (or even more) and depends on many factors: the fume extracting and cooling system,

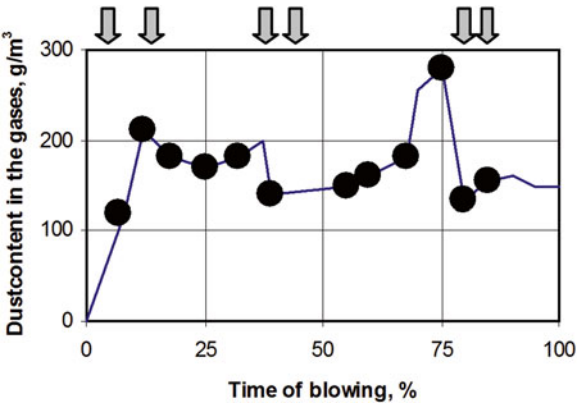

Fig. 17.2 Change of the gases dustiness during the blowing

Table 17.3 Average grain-size distribution of the dust emitted with the gases from the BOF

Particle size, μm	<3	3–60	60–250	>250
Mass fraction, %	65.0	7.0	9.0	19.0

oxygen blowing mode, quality, size distribution, and humidity of lime and other bulk materials charged during BOF blowing (Fig. 17.2). The maximum value of dust emissions observes at the time of charge the bulk materials (indicated by arrows).

The chemical composition of the dust little depends on the intensity of oxygen blowing, but varies greatly during periods of melting. Grain-size composition of dust can be divided into two groups: Fine, which is formed by the iron oxidation (<3 mm) and larger factions, which is formed by removal of slag and bulk materials particles (>3 μm). Grain-size and chemical composition of dust change during the melting. In periods of scrap and hot metal charging and also in the first minutes of oxygen blowing dust consists of large fractions (scrap pollution, particles of lime, etc.). Then the dust becomes fine disperse because of intensive combustion of iron in a reaction zone. Averaged grain-size distribution of dust emitted with the gases from the BOF is presented in Table 17.3.

The next stage of exploration was the complex analysis of technical solution for the atmosphere protection on Ukrainian metallurgical plants.

17.3 Technical Solutions for the Atmosphere Protection on the Metallurgical Plants

17.3.1 Cleaning and Cooling of the BOF Waste Gases

As though temperature of the gases emit from the vessel throat is very high, they must be cooled before the gas cleaning. Cooling can be carried out by injection of water in the gases. The disadvantage of this method is a significant increase of gas volume caused by forming of water vapor and inability of heat recovery. Thus this method is used only for partial cooling.

Application of waste heat boilers (WHB) is much better method that is widely used nowadays. Cooling by this method almost does not change the gases volume and allows recovering their warm.

17.3.2 BOF Pipeline

By way of the BOF gases emissions into the atmosphere pipelines are divided into three groups:

1. systems with air leakage through the slit between the BOF and WHB and the full post-combustion of CO to CO_2, i.e., air flow factor $\alpha > 1$;
2. systems with partial post-combustion of carbon monoxide in the WHB, i.e., at $0.0 < \alpha < 1.0$;
3. systems without air leakage in the pipeline and without post-combustion of carbon monoxide, i.e., at almost $\alpha < 0.15$.

Mode of pipeline is determined by the pressure maintained in the slit between the BOF and the WHB.

If at the slit there is kept sufficiently large rarefied, then ambient air is injected in WHB with the BOF gases. Amount of injected ambient air is sufficient for combustion of the BOF gases, i.e., $\alpha > 1.0$. In this case, the pipeline works in a mode of full post-combustion of carbon monoxide.

If at the slit there is kept little rarefy, the volume of injected ambient air is insufficient to complete post-combustion of carbon monoxide and pipeline works in a mode of partial post-combustion of CO to CO_2.

Depends on rarefy at the slit through the pipeline will pass complete combustion products, not post-combusted BOF gases or partially post-combusted gases. It should be noted that converter gas is explosive when $\alpha < 0.75$. To avoid explosion it needs to exclude the possibility of a collision BOF gases with air, especially in low temperatures areas, where the gases do not burn and form explosive mixtures.

This requires good hermetic of pipeline and complete exclusion of air leak in it. It is also necessary to move volume of inert gas right afore and behind explosive gases (CO_2 and H_2).

For slit pressures higher than the atmospheric one, air does not leak in the pipeline and post-combustion of carbon monoxide does not occur ($\alpha \approx 0$). Since in this mode the gases can be released into the shop atmosphere, then minimal rarefy at the slit is maintained ($\alpha = 0.11$–0.15).

The rarefy value in slit is regulated by the flap in the pipeline before the smoke exhauster.

Volume of the gases that come to the gas clearing system with full post-combustion of carbon monoxide is 3–5 times more than volume of the gases formed during the blowing. It results to increase in size of the pipeline, the system of gas clearing, power and energy consumption of smoke exhauster. Use of such system with the BOF capacity over 200 t is economically inefficient. But it should be installed for the BOF of smaller capacity, because of complete safety.

Table 17.4 Dependence of volume of the gases from the air flow rate

Air flow rate, α	1.0	0.75	0.15	0.07
Volume of emitted BOF gases, m^3/h	1000	1200	1700	3600
%	100	120	170	360

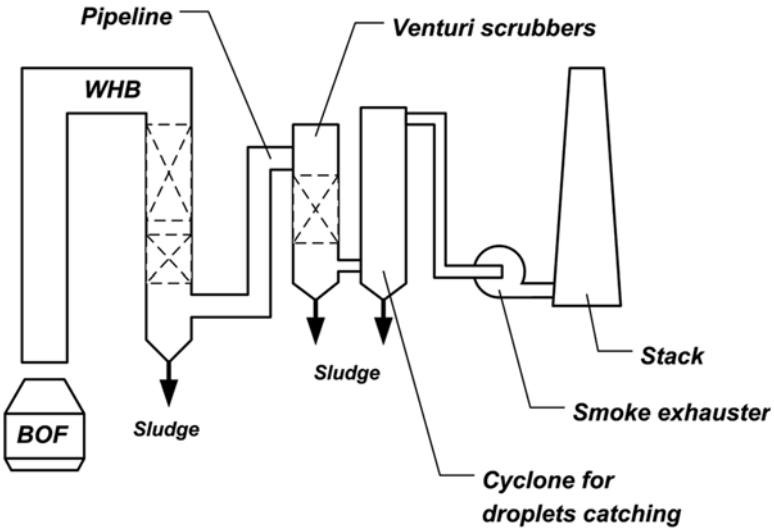

Fig. 17.3 Scheme of system for cooling and cleaning of the BOF gases with full post-combustion CO

The value of the air flow rate α for post-combustion of carbon monoxide significantly impacts on the capacity of the pipeline (Table 17.4).

Thus, the same volume of BOF gases would need much smaller pipeline if value of air rate α is small. Switching BOF from a full system of CO post-combustion ($\alpha > 1.0$) to the partial post-combustion system or without any post-combustion of carbon monoxide can significantly increase the intensity of blowing and consequently improve BOF productivity.

17.3.3 Units with Full Post-Combustion of Carbon Monoxide

Plants of this type are widely used in Ukraine (Fig. 17.3). In the fireplace above the BOF CO burns by air which leaks through the fully open slit between the BOF and the fireplace.

After passing through the WHB the dusty gases significantly change chemical composition and size of dust particles. Because of particle precipitation, especially its large fractions of dust in WHB pipes the concentration of dust in the gases before

Table 17.5 Grain-size composition of dust before cleaning, %

	Dust fraction, μm			
Time of blowing, min	<3	3–60	60–250	>250
1–5	60	15	15	10
18–14	82	3	5	10
18–22	86	5.5	5	3.5

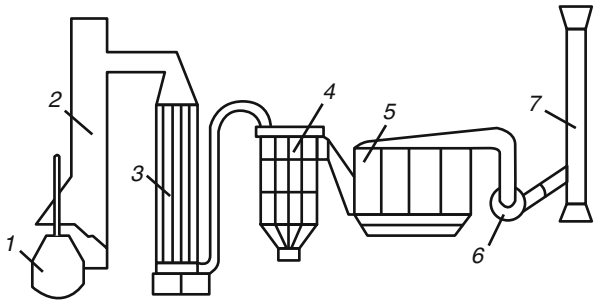

Fig. 17.4 Scheme of gas cleaning in baghouse: (*1*) the BOF; (*2*) cooled fireplace; (*3*) regenerator; (*4*) evaporative scrubber; (*5*) baghouse; (*6*) smoke exhauster; (*7*) stack

cleaning is up to 25–60 g/m^3. On this stage dust mostly consists of iron oxides. Mass fraction of fine fraction increases to the end of blowing (Table 17.5).

After WHB gases flow to the clearing, which in all Ukrainian BOF plants is carried out in Venturi scrubber. Since after Venturi scrubbers cleaned gases still contain dust within water droplets that have harmful effect on the pipes and smoke exhausts, they are treated in droplet catcher and then thrown through the chimney in the atmosphere.

In many countries dry and wet electrostatic precipitators (ESP) and sometimes baghouse are widely used for cleaning of the BOF gases. Fabric filters are used in France, Belgium, USA etc. (Fig. 17.4) for BOF gases cleaning.

In case of BOF gases cleaning without heat recovery, the gases from the converter (1) flow in the cooled fireplace (2), where they are post-combusted and cooled, and then sent to the regenerator (3). When flowing through vertical refractory channels of regenerator, gases give them their heat. Final cooling of gases before baghouse (5) is carried out in evaporation scrubber (4). After the BOF blowing atmosphere air is flown through the regenerator and cooled its checker. The final concentration of dust in the gases that released into the atmosphere through the smoke exhauster (6) and chimney (7) is 4.7 mg/m^3.

The cleaning of the BOF gases by cloth filters is also performed with heat recovery. In this case for cooling of the gases instead of regenerator the WHB is used.

17.3.4 Units with Partial Post-Combustion of Carbon Monoxide

There are two modes of the unit with partial post-combustion of carbon monoxide: in the first mode the system does not combust CO completely ($0.75 < \alpha < 1$); the second—with the partial combustion of carbon monoxide at $0.3 < \alpha < 0.6$. The principal difference between these modes is that in the first case gases in pipeline cannot burn, and the second—they are explosive.

Saturated with moisture gases flare up and burn if consist of at least 20–25 % CO. The disadvantage of the first mode ($0.75 < \alpha < 1$) is that the amount of carbon monoxide in the gases at the outlet of the stack are much lower. Thus the gases cannot be post-combusted and significant volume of toxic CO is emitted in atmosphere.

In the mode of partial post-combustion of CO ($0.3 < \alpha < 0.6$), CO content is more than 25 % during the most of the blowing time and gases post-combust. The slit between the BOF and the WHB is entirely open in this mode. Smoke exhauster is set up to constant productivity that is on 10–15 % more than volume of the BOF gases in the period of maximum gas emission.

In the initial period of BOF blowing when exhaust gases consist little CO, the system operates in the mode of full post-combustion and there are oxygen and carbon dioxide in the pipeline, but not carbon monoxide. That is not explosive exhaust gases.

Excess volume of oxygen in the exhaust gases rapidly decreases with increase of the total volume of gases emits from the BOF (i.e. air flow through the leak remains the same and the volume of CO in the gases increases) and when $\alpha = 1$ is about zero. At this time exhaust gases almost do not content CO that completely combusted to CO_2. Formed volume of inflammable gas ($CO_2 + H_2$), is blown through pipeline and clears it from remaining oxygen. Right after the volume of inflammable gas another gases flow that consists of carbon monoxide but no oxygen. After the end of blowing the same processes occur in the opposite direction. So volume of inflammable gas that is formed in the initial period and at the end of blowing reliably separates the transported gas. That does not allow mixing transported gas with air and CO to form explosive gas mixtures. In this mode BOF gases cannot be used as fuel. The BOF gases with a high content of CO are formed and flow out the throat in the pipeline just for 6–10 min, i.e., less than 50 % of blowing time.

Waste gas could not be used as a fuel in the last period of the BOF melting because of reduces of CO content. Thus in all systems with partial post-combustion of CO the BOF gases is burnt on the stack before release in the atmosphere.

In systems with partial post-combustion of CO dust content in the gases before cleaning is a little more (30–80 g/m^3 of gases) than in systems with full post-combustion of CO because of less air leak in the gases. Weight of the formed dust is the same as in the full post-combustion, but dust concentration is more as a result of the much less air leak in the gases and consequently less volume of waste gases.

The chemical and grain-size composition of dust in systems with partial post-combustion of CO are almost the same as in the system with full post-combustion CO.

By employing wet dust-catcher (Venturi scrubber) the mode of full CO post-combustion can be easy shifted on partial CO post-combustion. It is needed just to seal pipelines, mainly in its coldest part (gas temperature below 800–900 °C), to eliminate the possibility of formation of dead air zones, equip the stack with burner,

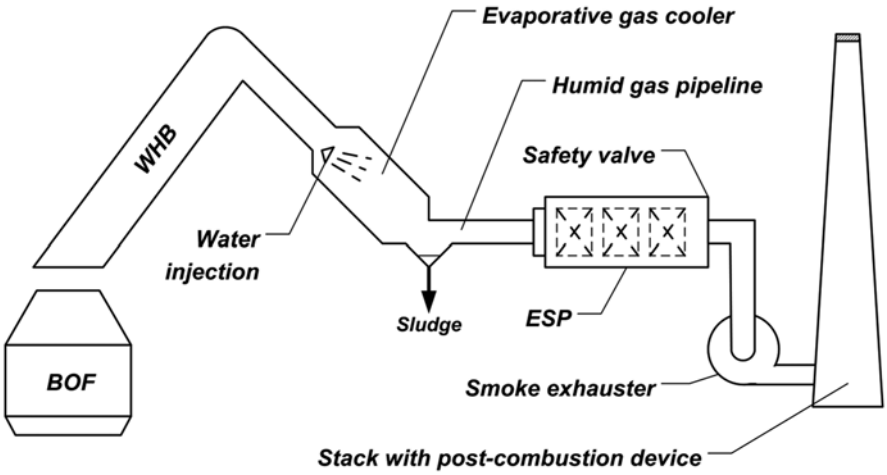

Fig. 17.5 Scheme of unit for cooling and cleaning in ESP the BOF gases with the partial CO post-combusting

and make the pipeline of the each BOF unit autonomous. Operation of gas-path does not become more complicated, but rather simplifies, since there is no need for any regulation while maintaining complete safety.

One of the reasons of the wide application of wet type units (Venturi scrubber) to clean the BOF gases regardless of a number of disadvantages (high water consumption, systems for its cleaning, sludge processing, corrosion of equipment, etc.) is dangerously explosive gas mixture in the case of ESP application. Some of the European and US plants use gas cleaning system with ESP (Fig. 17.5).

The unit includes evaporative gas cooler, through which the high-temperature gases (~1000 °C) are flown. Their temperature depends on the top blowing mode in the BOF and the effectiveness of the WHB. In the evaporative gas cooler the gases temperature is reduced to about 200 °C due to injection of carefully regulated volume of water that completely evaporates. Then gases are directed, by smoke exhauster to the stack with post-combustion device.

Such gas-cleaning units operate with minimal air flow rate of $\alpha = 0.2–0.6$ and provide clean gases emitted through the stack to dust concentration of about 30–50 mg/m^3.

17.3.5 Units Without Carbon Monoxide Post-Combustion

When using the BOF of more than 250 t and blowing intensity more than 4.0 m^3/(t·min) the volume of the gases significantly increases. Calculations show that in that case installation of the unit with complete CO post-combustion is economically inefficient. The unit without CO post-combustion is more rational because the volume of the treated gases and therefore the size of the gas pipeline reduce 3–5 times. Smaller size of the pipeline favours installation and operation.

Before treatment the gases consist of (volume): CO_2—17 %; N_2—16 %; and CO—67 %. In addition, the gases contain (mg/m^3): SO_2—70; H_2S—30; F—200; and Cl—20. After treatment gases can be recycled and used as fuel.

Due to the lack of combustion in the pipeline chemical and grain-size composition of dust emitted from the BOF almost do not change and are the same as when using devices with full or partial CO post-combustion. The dust content in the gases at the BOF throat is up to 200 g/m^3.

Without CO post-combustion the possibility of formation of explosive mixtures of oxygen and carbon monoxide in the pipeline significantly increases. That's why all Ukrainian BOF plants, without CO post-combustion, are equipped with wet type (Venturi scrubber) gas cleaning units.

Safety of operation, as in units with partial CO post-combustion, is provided by forming volume of inflammable gas mixture (CO_2+N_2) that in the initial period and after the blowing reliably separates explosive volumes and prevents their mixing. Formation of the volume of inflammable gas provides a hood, which hangs over the BOF.

A rectangular Venturi tube with an adjustable throat section is widespread in the big BOF plants working without CO post-combustion (Fig. 17.6).

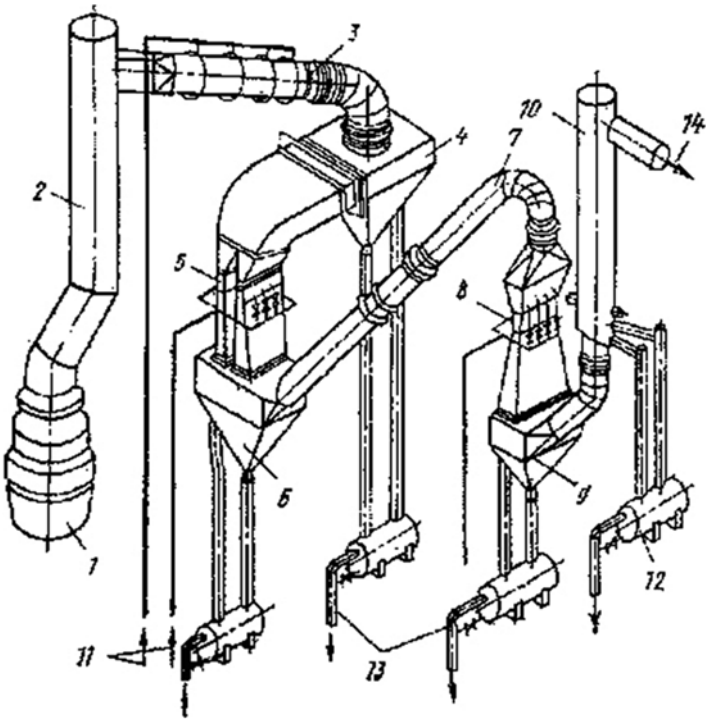

Fig. 17.6 Scheme of gas cleaning units equipped with Venturi scrubbers for the 300 t BOF capacity: (*1*) the BOF unit; (*2*) the WHB; (*3*) pipeline with water injection; (*4*) hopper of water injection pipeline; (*5*) Venturi tubes of the first stage; (*6*) hopper of the first stage; (*7*) connecting pipeline; (*8*) adjustable Venturi tube of the second stage; (*9*) hopper of the second stage; (*10*) droplet catcher; (*11*) water supply to the water injection pipeline; (*12*) hydraulic lock; (*13*) removal of sludge; (*14*) supply of gas to the smoke exhauster

After the WHB (2) gases with a temperature of 750–1000 °C are directed into water injection pipeline (3). Water supply (11) to the pipeline is carried out with circulating. The water cools the gases to 250–300 °C. The hopper of water injection pipeline (4) is adjacent to two Venturi tube of the first stage cleaning (5). From the Venturi tubes hopper (6) gases make the turn by connecting pipeline (7) and flow to the second stage of treatment—the adjustable Venturi tube (8). Then after the hopper (9) the gases come to droplet catcher (10), from which through the pipeline (14) sucked by smoke exhausters and post-combusted in the stack outlet.

Such BOF cleaning units mostly equipped with shortening Venturi tubes with disk spraying (Fig. 17.7).

The gases that flow out of the BOF (1) after WHB (2) with a temperature of 750–1000 °C reach the unit of preliminary water injection and then are directed into the shortened Venturi tube (4) equipped with moisture separator (5) and the hopper of the first stage (6). Then the gases are sent through the shortening Venturi tubes of the second stage (7) in the hopper of the second stage (9). After that the gases through

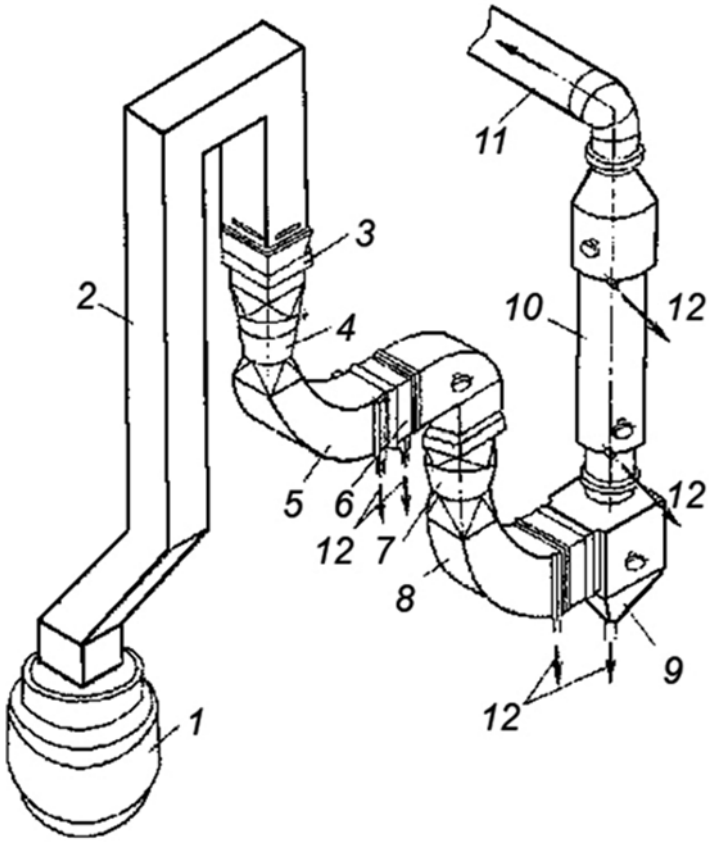

Fig. 17.7 Scheme of the BOF gas cleaning units with shortening Venturi tubes for capacity 350–400 t: (*1*) the BOF; (*2*) WHB; (*3*) unit of preliminary water injection; (*4*) the shortening Venturi tubes of the first stage; (*5*) moisture separator; (*6*) hopper of the first stage; (*7*) the shortening Venturi tubes of the second stage degree with disk control; (*8*) droplet catcher; (*9*) hopper of the second stage; (*10*) centrifugal droplet catcher; (*11*) pipeline to smoke exhauster; (*12*) removal of sludge

the centrifugal droplet catcher (10) by pipeline (11) are sucked by smoke exhausters and emitted through the stack. The gases are post-combusted on the stack outlet.

In order to improve the reliability of operation the following amendments in gas cleaning units were made.

– highly dispersed water injection in the top of the lifting pipeline in order to faster solidification and cooling of dust particles, and to avoid slagging of WHB top lid;
– replacement of pipeline with water injection and the shortening Venturi tubes of the first stage by hollow scrubber with water injection. These amendments simplify pipeline, reduce its hydraulic resistance, allow to get rid of large fractions of dust and pieces of sludge, reduces abrasive wear and prevent clogging of sludge duct;
– installation of the second droplet catcher before the smoke exhauster to protect the last from drops formed due to cooling gas saturated with moisture.

17.4 Decrease of Unorganized Emission of Harmful Substances into the Atmosphere on Metallurgical Plants

Gas and dust emissions directly emitted in the atmosphere are called unorganized emissions.

In steelmaking shops unorganized fugitive emissions happen while overloading charge materials (scrap, limestone, lime, etc.), filling and pouring hot metal in mixers, removing of slag from mixers and ladles, tilting of the BOF for charging sampling and tapping, secondary treatment of steel and casting in ingots or continuous casting machine (CCM), preparation for work and repairing of technological units.

There are no forced ventilation systems in the steelmaking shops. Ventilation is carried out by aeration lanterns. Therefore, in all areas where there are unorganized emissions of gas and dust in the atmosphere an aspiration system needs to be installed. The most simple aspiration system for the treatment of unorganized emissions is shown in Fig. 17.8.

When using this system gas and dust emissions from the source are caught by umbrella and by the fan or smoke exhauster transported through pipeline to the hopper chamber. In the hopper chamber dust particles are deposited due to gravitational forces and purified air (smoke) emits through the stack into the atmosphere. Hopper chamber, smoke exhauster, and stack are installed out of shop.

Among the steelmaking units the mixer is one of the main suppliers of unorganized emissions in the atmosphere (Table 17.6). While pouring hot metal 0.02–0.05 % of its weight becomes the dust.

For mixers 2500 t capacity as the first stage of gas cleaning system the cyclones are recommended, and for the second stage—baghouse or ESP. Baghouse cannot fire because the red-hot iron particles, talc, and graphite foam are completely caught in the cyclone. Electrostatic breakdown of ESP insulation is also impossible, because after the first stage of treatment there is no electrically conducting graphite foam in the gas.

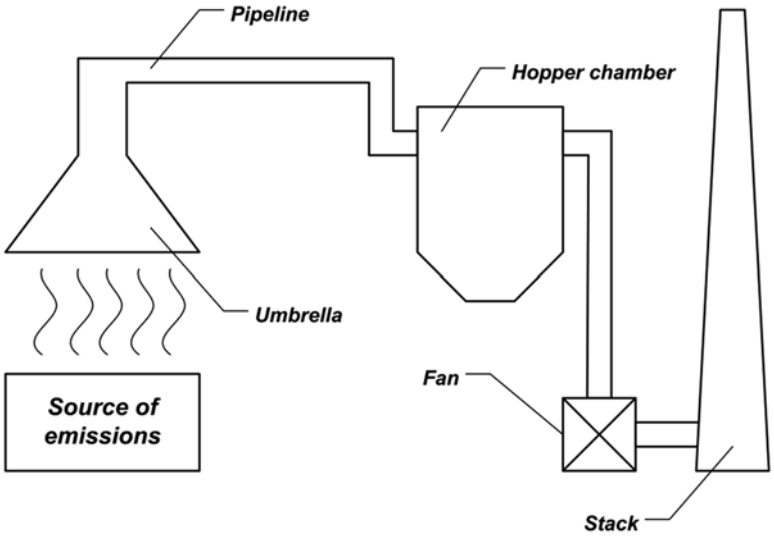

Fig. 17.8 Aspiration system for unorganized emissions

Table 17.6 Parameters of the gas and dust emission from mixers

	Mixer capacity, t			
Technological process	600	1300	2500	Temperature of gases, °C
Filling of hot metal	114/0.22[a]	139/0.45	150/0.52	30–40
Slag skimming	82/3.1	67/1.9	61/2.2	70–90
Pouring of hot metal	44/0.46	65/1.06	85/4.13	50–180

[a]Numerator—volume of the gases, m^3/s; denominator—dust content in the gases, mg/m^3

In order to reduce air leakage in the pipeline the smoke exhausters should be installed before gas cleaning unit. Thanks to lubricating qualities of graphite foam, there is no abrasion wear of smoke exhausters in this case.

The unorganized emissions also can be decreased by the formation of a neutral atmosphere in the iron ladle. It can be done by filling the ladle with neutral gas or by burning natural gas in it. The neutral atmosphere in the iron ladle prevents formation of iron oxides and emission of brown smoke.

In the BOF shops the unorganized emissions reach its maximum value while filling hot metal after scrap charging. The emissions include up to 35 % FeO and 30 % graphite foam in the form of particles smaller than 100 μm. Volume of emissions mostly depends on scrap quality and filling speed. Its value can be reduced by using less contaminated scrap. During steel tapping in a teeming ladle a dense smoke is formed that contains dust (less than 100 μm), which consists of up to 75 % FeO.

The aspiration system is employed to catch unorganized emissions there are successfully used the aspiration system, which include umbrella, although they suck a lot of air. The umbrellas require minimal workspace and do not disturb staff. On the contrary, local extraction near the sources of dust is more effective, but its operation is more complicated.

Sometimes, to catch unorganized emissions caused by the BOF charging the umbrellas in combination with fabric filters or scrubbers are used. Aeration systems are also installed in the department of bulk materials at the transport devices and supply hoppers.

The optimal solution to eliminate unorganized emissions is the isolation of the BOF vessel using gas-tight storage ("dog house"). Efficiency of this system is about 90–95 %.

There is performed different kind of operation with refractory in yard of teeming ladles preparation. Replacement or partial repair of lining forms significant amounts of dust. According to various sources its value can range from 0.01 to 0.2 kg of dust per 1 t steel. While drying and heating the recorded emissions were (kg/t of steel): SO_2—0,01; CO—0.1; NO_x—0.1; and some CH_4. At this site there are widely used the aspiration systems with umbrella, local extraction of contaminated air, and lids on the ladles. Application of unshaped refractory lining in the form of liquid concrete as well helps to reduce emissions.

17.5 Conclusions and Recommendations

Volume of gases produced during the BOF melting depends on:

- blowing mode,
- type of additives,
- lance design,
- height above the bath surface,
- hot metal composition,
- blowing intensity,
- vessel capacity.

and according to practical data is 70–90 m^3 per 1 t of vessel capacity.

One of the effective ways to reduce emissions is application of multinozzle lance.

Volume of the BOF gases depends on oxygen consumption for carbon oxidation. Application of the modes with partial or without CO post-combustion significantly reduces the volume of the BOF gases and dust. It also could be reached by the following measures:

- fast forming of a homogeneous slag,
- use of bulk materials without fine fractions,
- optimal composition of hot metal,

– scrap clean of nonmetallic materials,
– reducing the blowing intensity at the time of bulk materials charging.

Reducing the amount of the dust also occurs when charging bulk materials in the vessel before or at the very initial stage of the blowing with small volume of the formed gases.

Chapter 18
State of the Art in Air Pollution Control for Sinter Plants

Christof Lanzerstorfer

Abstract In integrated steel mills, the sinter plant is one of the major sources of emissions to the atmosphere, whereas the emissions of waste water and solid residues from the sinter plant are usually less significant. Therefore, state-of-the-art emission control technology for off-gas treatment is essential in order to comply with stringent emission limits. In the first part of this chapter, the sinter process is described, the resulting emissions are characterized and primary measures to reduce the off-gas volume and the emission of various pollutants are presented. The second part gives an overview of the state-of-the-art emission control technologies applied in sinter plants for the reduction of particulate emissions, emissions of SO_2 and other acid gases, NOx emissions and emissions of dioxins. In the third part, methods of treating and recycling the residues from sinter plant off-gas cleaning are described. The last part describes some possible future developments in air pollution control for sinter plants.

18.1 Introduction

In an integrated steel mill, the sinter is an important feed material for the production of pig iron in the blast furnace. The sinter is produced in the sinter plant by agglomeration of the charge which consists of iron ore fines, fluxes and fine-grained recycled iron-containing materials such as dusts, sludge and scale. Due to the high volume of off-gas from the sintering process, sinter plants are responsible for a significant proportion of the atmospheric emissions from integrated steelworks.

The process off-gas from a sinter plant is usually de-dusted in an electrostatic precipitator (ESP). At some sinter plants, a subsequent process for off-gas desulphurization (DeSOx), reduction of dioxin emissions and/or further de-dusting has been installed in order to comply with tighter emission limits. In a few sinter plants, a process for the reduction of NOx emissions (DeNOx) is also applied.

C. Lanzerstorfer (✉)
University of Applied Sciences Upper Austria, School of Engineering/Environmental Sciences, Wels, Austria
e-mail: c.lanzerstorfer@fh-wels.at

P. Cavaliere (ed.), *Ironmaking and Steelmaking Processes*,
DOI 10.1007/978-3-319-39529-6_18

Table 18.1 Emission limits for sinter plant primary off-gas in mg/Nm^3 dry

	Europe			China
Source	2010/75/EU[a] and 2012/135/EU[b]			GB 28662–2012[c]
Dust	Bag filter <1–15	Advanced ESP[d] <20–40		50
SOx as SO_2	Using low S content coke and ore for the charge <350–500	Injection of adsorption agent into the off-gas before de-dusting by bag filter <350–500	Wet desulphurization or regenerative activated carbon process <100	200
NOx as NO_2[e]	Off-gas recirculation; low NOx burner for ignition <500	Regenerative activated carbon process <250	Selective catalytic reduction (SCR) <120	300
PCDD/F[f]	Injection of adequate adsorption agents into the off-gas duct of the sinter strand before bag filter <0.05–0.2	Injection of adequate adsorption agents into the off-gas duct of the sinter strand before ESP[d] <0.2–0.4		0.5
HF	–			4.0
Hg	Activated carbon or activated lignite coke injection[g] <0.03–0.05			–

[a]European Parliament and Council of the European Union (2010)
[b]European Commission (2012)
[c]Ministry of Environmental Protection of the People's Republic of China (2012)
[d]When bag filters are not applicable
[e]Related to an oxygen content of 15 %
[f]In ng I-TEQ/Nm^3 dry
[g]When selecting raw materials with a low mercury content is not applied

Other sources of dust emissions in sinter plants are the handling and conveying of the feed material, the sinter cooler and the crushing and screening of the sinter produced. These emissions are extracted by a ventilation system, often referred to as the room de-dusting system (Remus et al. 2013).

18.2 Emissions from the Sintering Process and Primary Methods of Emission Reduction

The limits for emissions to the atmosphere from sinter plants have been tightened in recent years. The current emission limits for Europe and China are summarized in Table 18.1. The best available technique-associated emission levels (BAT-AELs) for air emissions from sinter plants are defined in the commission implementing decision of 28 February 2012, establishing the best available technique (BAT) conclusions under Directive 2010/75/EU of the European Parliament and of the council on industrial emissions for the iron and steel production. The BAT-AELs in Europe depend on the applied BAT technology for emission reduction.

For China, fixed emission limits are valid. The limit values are within the range of the European limits. For dust and polychlorinated dibenzo(p)dioxins and furans (PCDD/Fs), the emission limits are somewhat higher than the European limits, while the limit for SOx is lower with the exception of that for the wet DeSOx process and the regenerative activated carbon process.

BAT for the secondary emissions, the emissions from sinter strand discharge, sinter crushing, cooling, screening and conveyor transfer points, is to achieve an efficient extraction and subsequently to reduce dust emissions by using a bag filter or an ESP. The respective BAT-AEL for dust is <10 mg/Nm^3 for a room de-dusting bag filter and <30 mg/Nm^3 for de-dusting with an ESP. The Chinese emission limit for the secondary dust emissions is also 30 mg/Nm^3.

18.2.1 The Sintering Process

The feed material of the sintering process—iron ore, fluxes, recycling fines and a solid fuel, usually coke breeze—is mixed and then placed on a continuous, travelling grate called the sinter strand. A burner at the beginning of the strand ignites the fuel in the mixture after which the combustion is self-supporting. Underneath the strand, there are several wind boxes to draw air and combustion gases down through the sintering bed into a duct which is connected to the induced draft (ID) fan. As the sinter mixture proceeds along the sinter strand, the combustion front is drawn downwards through the mixture.

The combustion of the coke—approximately 4–6 % of the charge—creates sufficient heat (1300–1480 °C) to sinter the fine particles together into porous sinter. The off-gas from the sinter strand contains considerable amounts of entrained particulate matter and various gaseous pollutants. It is usually de-dusted in an ESP

before it is released into the air via the main stack. The ESP is installed upstream of the ID fan to protect the fan impeller. In some older sinter plants, cyclones are still used for this purpose.

The fused sinter is discharged at the end of the sinter strand and subsequently crushed and screened. The undersize material is recycled back to the feed. The remaining sinter product is cooled in a cooler where air is used for the cooling. The cooled sinter is crushed and screened again. The fines are recycled and the product is sent to the blast furnace (Remus et al. 2013).

18.2.2 Emissions from the Sintering Process

The particulate matter contained in the off-gas from the sinter strand originates from two sources. Firstly, fine-grained feed material can be carried by the gas flow out of the lower parts of the bed. Secondly, some components like alkali chlorides can be volatilized in the high-temperature zone of the bed. These components recondense and form very fine particles when the off-gas cools down. Typical particle size distributions of the particulate matter from the de-dusting of various sinter plants can be found in the literature. The mass median diameter of the ESP dust is in the range of 2.8–40 μm, while cyclone dust is coarser (Kasama et al. 2006; Lanzerstorfer 2015a). The dust remaining in the off-gas downstream of the de-dusting stage is considerably smaller. Its mass median diameter is typically less than 1 μm (Fleischanderl et al. 2007).

The chemical composition of dust emitted from sinter plants has been investigated in several studies (Xhrouet et al. 2002; Ahn and Lee 2006; Tsai et al. 2007; Sammut et al. 2010; Sinha et al. 2010; Lanzerstorfer and Steiner 2015). The main components of the dust are Fe, C, K, Ca, Cl and S. The dust also contains increased amounts of volatile heavy metals, especially Pb and to a lesser extent Cd and Zn (Remus et al. 2013). In one study, no difference was found in the Hg concentration in the off-gas before and after the ESP (Park et al. 2008). Therefore, it can be assumed that at sinter off-gas temperature nearly all Hg is gaseous.

In the sintering process, coke breeze is usually used as the solid fuel to supply the thermal energy for sintering. Due to the short residence time of the gas in the combustion zone and the rapid cooling of the combustion off-gas when it flows through the bed of feed material below the flame front, some products of incomplete combustion remain in the off-gas. The main component from incomplete combustion is CO. Its concentration in sinter off-gas is in the range of 0.5–1.5 % (vol) (Leuwerink and van der Panne 2001; Eisen et al. 2004; Kasama et al. 2006; Remus et al. 2013).

The S contained in the fuel is oxidized in the combustion zone, and some of it is discharged with the off-gas as SO_2. In sinter pot tests, it was found that approximately 20–50 % of the S was emitted as SO_2 depending on the basicity of the sinter mixture and the specific S input (Lanzerstorfer et al. 2015a). Typical SO_2 concentrations in the sinter off-gas are between approximately 100 and 500 mg/Nm^3 dry (Remus et al. 2013). However, S-containing recycled material in the feed can significantly increase the SO_2 emissions.

The emitted NOx consists mainly of NO. Usually the dominating source is the N contained in the coke breeze (Mo et al. 1997, Remus et al. 2013). The typical NOx concentration in the sinter off-gas is between approximately 150 and 500 mg/Nm^3 dry (Remus et al. 2013).

The emissions of HF and HCl depend on the F and Cl content of the feed material and on the basicity of the sinter mixture. The reported sinter off-gas concentrations for HF are in the range of 0.2–4 mg/Nm^3 dry and for HCl 0.7–400 mg/Nm^3 dry (Remus et al. 2013).

Residues which contain oil are the major source of hydrocarbon emissions from sinter strands. Hydrocarbons can evaporate before they are reached by the combustion front moving downwards through the bed. Additionally, some hydrocarbon emissions result from incomplete combustion of the fuel. The concentration of non-methane volatile organic compounds (NMVOC) in the sinter off-gas is in the range of 0.7–120 mg/Nm^3 dry (Remus et al. 2013). In another study, the composition of the NMVOC emissions was reported (Tsai et al. 2008).

Due to the incomplete combustion process in the sinter bed, some polycyclic aromatic hydrocarbons (PAH) can be found in the sinter off-gas. A PAH concentration in the off-gas after the ESP of 0.01 mg/Nm^3 was reported (Guerriero et al. 2008).

Iron ore sintering is one of the most important emission source types for PCDD/Fs (Quaß et al. 2004) and other organohalogen compounds. An overview on the formation of PCDD/F in the sinter process is given in several articles. For sintering, it is generally accepted that PCDD/Fs are formed through the de novo reaction (Ooi and Lu 2011; Wang et al. 2003b). The typical emissions concentration of PCDD/F in the off-gas is 0.07–2.86 ng I-TEQ/Nm^3 (Remus et al. 2013). Measurements showed that the congener pattern of PCDD/Fs and polychlorinated biphenyls (PCBs) is substantially the same for all sinter plants. The contribution of the PCDFs to the I-TEQ emission is 80–90 % (Hofstadler et al. 2000; Kasai et al. 2001a; Wang et al. 2003b; Chang et al. 2007).

PCBs are essentially precursors of the formation of PCDD/F. They are relatively volatile and may be driven off ahead of the combustion zone as the sinter bed is heated by the gaseous combustion products. PCDD/Fs contained in the recycled material can also contribute to PCDD/F formation in the off-gas. Even as they are destroyed in the sinter strand while decomposing, the resulting compounds can contribute as precursors to the de novo synthesis. The contribution of PCBs to the total TEQ emission (PCDD/Fs and PCBs) is in the range of 5–7 % (Aries et al. 2006; Grochowalski et al. 2007).

The concentration of polychlorinated naphthalenes (PCNs) was found to be in the range of 0.4–23.3 pg TEQ/Nm^3 (Liu et al. 2012).

The steps for crushing, raw material handling, belt charging and discharging from the screens all involve the generation of considerable amounts of entrained particulate matter. The emissions are normally extracted by the room de-dusting system and discharged through a separate stack. The dust concentration after de-dusting is in the range of 7–50 mg/Nm^3 depending on the type of de-dusting equipment installed (Remus et al. 2013). The PCDD/F concentration in this gas was measured in the range of <0.001–0.060 (Anderson and Fisher 2002).

The composition of the off-gas extracted from individual wind boxes varies considerably along the sinter strand. Characteristic curves are available for the temperature and CO_2, CO, O_2, H_2O, HCl, SO_2, NOx and PCDD/F content (Kasai et al. 2001a; Brunnbauer et al. 2006; Remus et al. 2013). These profiles are especially important for selective off-gas recirculation.

18.2.3 Primary Measures for Emission Reduction

There are different ways of reducing the emissions produced in the sintering process. The addition of recycling materials to the sinter feed usually increases the emissions. Therefore, limits for the quality and the quantity of these recycled materials lead to a reduction of the emissions produced.

Another way of reducing the amount of pollutants emitted is partial recirculation of the off-gas. By this technique, the amount of off-gas produced is reduced while the concentration of the pollutants in the off-gas stays the same or is increased by a factor which is smaller than the reduction factor for the off-gas volume.

The emissions of PCDD/F can be reduced by the use of inhibitors like urea, monoethanolamine (MEA) and triethanolamine (TEA). Usually, the inhibitors are added to the charge, but there are reports of tests where an aqueous solution of the inhibitor was sprayed into the off-gas in the wind boxes.

Increasing the basicity of the sinter to reduce the emissions of acid gases would be another primary measure for emission reduction. However, the basicity of the sinter is usually a requirement set by the blast furnace operation.

Another measure to reduce emissions can be the optimization of the operation conditions of the sinter plant. The Taguchi experimental design was used for sinter pot tests to optimize sinter plant operation with respect to PAH and PCDD/F emissions (Chen et al. 2008, 2009). A multi-objective optimization tool was employed for sinter plant process optimization targeting emission reduction and productivity (Cavaliere et al. 2011; Cavaliere and Perrone 2013). Numerical and experimental analyses allowed the definition of the optimal conditions for the minimization of pollutants at acceptable productivity of the sinter plant.

18.2.3.1 Control of Recycling Material

In integrated steel mills, fine-grained materials rich in iron and carbon-like dust, sludge and mill scale are usually recycled through the sinter plants (Hansmann et al. 2008). The recycling is generally controlled depending on the analysis of the material because the recycled residues also have some effect on sinter quality, strength and productivity. For example, an increased input of Zn into the blast furnace has to be avoided because Zn can cause operational problems there (Esezobor and Balogun 2006), and the sintering process is typically not very efficient in reducing the Zn content (Lanzerstorfer et al. 2015a). There are further constraints on the materials

that can be recycled to avoid operational problems in the sinter plant. In particular, the concentration of hydrocarbons must be controlled to avoid glow fires in the ESP (Remus et al. 2013), and the concentration of alkali metals (Na and K) has to be limited because of their adverse impact on the removal efficiency of the ESP (Schuster et al. 2003; Remus et al. 2013).

18.2.3.2 Off-Gas Recirculation

The recirculation of off-gas is an efficient technique to reduce the amount of off-gas discharged through the main stack and to save some fuel at the same time. The CO contained in the off-gas recycled to the sinter strand is oxidized when it passes the flame front. The concentration of CO in the off-gas discharged from the sinter process remains more or less unchanged because of the reaction equilibrium between O_2, CO and CO_2 prevailing in the flame front. However, the total amount of emitted CO is reduced by the same factor as the off-gas volume. Also the organic pollutants (VOC, PAH, PCDD/F) are destroyed when the recycled off-gas passes the high-temperature zone of the flame front. When recirculated off-gas passes through the sinter bed, most of the dust is filtered out, and the acid gases SO_2, HCl and HF can react with base components in the sinter bed.

Fuel saving results from two effects: firstly, when CO is oxidized, the heat of reaction of 283 kJ/mol (Haynes 2012) is released and secondly, from the sensible heat of the recycled off-gas.

There are various process designs used for off-gas recirculation systems. In the EOS system, a part of the off-gas collected in the wind boxes is recirculated after de-dusting into a hood covering the whole sinter strand. The required O_2 content in the hood atmosphere is achieved by the controlled addition of fresh air. Thus, only a reduced amount of off-gas has to be discharged through the main stack (Leuwerink and van der Panne 2001). Reported results for the fuel saving and the emission reduction achieved by the EOS system at Tata Steel, Ijmuiden, are summarized in Table 18.2.

The LEEP process at the sinter plant of HKM, Duisburg aims to recirculate the off-gas with the highest pollutant concentrations and energy content. Therefore, the off-gas from the wind boxes of the second half of the sinter strand is recirculated into hoods covering the whole length of the sinter strand, while the off-gas from the wind boxes of the first half of the sinter strand is discharged. As the temperature of the off-gas from the first half is substantially lower than the temperature of the off-gas from the second half, a Ljungström heat exchanger is installed to reduce this difference. Heating-up the off-gas from the first half to a temperature above the acid dew points is required to prevent corrosion. Both off-gas streams are de-dusted in ESPs before they enter the ID fans (Eisen et al. 2004).

In the Eposint system (voestalpine Stahl, Linz, and Dragon Steel, Taichung), the recirculated off-gas is also from the second half of the sinter strand. In contrast to the LEEP system, the off-gas from the last two wind boxes is added to the off-gas from the first half of the sinter strand thus increasing the temperature of this gas

Table 18.2 Reported results for the various off-gas recirculation systems

		EOS	LEEP	Eposint
Source	Calculation basis for the reduction	Leuwerink and van der Panne (2000, 2001)	Bastürk et al. (2009), Eisen et al. (2004)	Brunnbauer et al. (2006), Reidetschläger et al. (2012)
Off-gas volume	m^3/h	−47 %	−45 %	−40 %
Reduction of coke breeze consumption	kg/t_{sinter}	12	5	2–5
SO_2 emission	kg/h	−28 %	>−60 %	−29 %
Dust emission	kg/h	−55 %	−45 %	−37 %
NOx emission	kg/h	−39 %	−49 %	−24 %
CO emission	kg/h	−47 %	−45 %	–
HCl emission	kg/h	−15 %	−63 %	–
HF emission	kg/h	–	>−55 %	−56 %
VOC emission	kg/h	−42 %	–	–
PCDD/F emission	g/h	−63 %	−80 %	–

without a heat exchanger. The hood above the sinter strand for off-gas recycling does not cover the whole strand but leaves approximately the last quarter of the strand uncovered. The air added to the recycled off-gas is collected at the sinter cooler outlet because of its higher temperature (Brunnbauer et al. 2006; Reidetschläger et al. 2012).

Reported results for the fuel saving and the emission reduction achieved are summarized in Table 18.2. When the reduction of the emission of a pollutant is lower than the reduction of the off-gas volume, the concentration of this pollutant in the off-gas is increased due to the off-gas recirculation. With selective off-gas recirculation for some pollutants, the reduction can be even higher than the reduction of the off-gas volume.

A selective off-gas recirculation using four different off-gas zones is installed at a sinter plant of NSSC, Yawata Works (Sakuragi et al. 1994). The off-gas volume was reduced by 28 %, and the reported reduction in coke breeze consumption was 7 %. The reductions in dust and SO_2 emissions are not really comparable because of the existing wet DeSOx system for the off-gas from one of the zones.

18.2.3.3 Suppression of PCDD/F Formation

Primary abatement of PCDD/Fs can be achieved through process optimization (Chen et al. 2008; Cavaliere et al. 2011; Cavaliere and Perrone 2013) and feed material selection (Xhrouet and De Pauw 2004; Nakano et al. 2009). A significant increase in the discharged amount of PCDD/Fs was found in the case of the recycling of ESP dust to the sinter feed (Kasai et al. 2001b).

The formation of PCDD/Fs can be suppressed by the addition of substances which have an inhibiting effect on the formation. Two different methods are described in the

literature. In the first method, nitrogen compounds are added to the solid sinter mix in order to inhibit catalytic reactions on the surfaces involved. Tests with the addition of MEA, TEA or urea were carried out in different sinter plants. With an addition of 0.02 % urea to the charge, a reduction in PCDD/F emissions of approximately 50 % was achieved (Schofield et al. 2004; Anderson et al. 2007). Also CaO was found to be a PCDD/F suppressing agent when added to the charge (Nakano et al. 2009).

The second method was tested in one sinter plant. The inhibitors MEA and TEA were dissolved in water and introduced into the wind boxes by way of spraying nozzles. After some time of operation in which the inhibitor was injected continuously, the PCDD/F concentration was measured and compared with the results of reference tests without inhibitor injection. MEA as well as TEA were both effective in preventing PCDD/F formation, up to 90 % inhibition was reached using MEA (Xhrouet et al. 2002; Xhrouet and De Pauw 2003).

18.3 Emission Reduction Processes

In the last 25 years, a second-stage off-gas cleaning system was installed at several sinter plants to comply with lower emission limits for dust, SO_2 and PCDD/F. This additional cleaning stage can be a wet system or a dry system (Menad et al. 2006; Delwig et al. 2007; Guerriero et al. 2009). However, dry systems using a sorption process are predominantly used for the separation of acid gases and PCDD/F and a fabric filter for final de-dusting (Weiss 1998; Leroy et al. 2007; Lanzerstorfer et al. 2008; Yu et al. 2009). In some sinter plants, a DeNOx process is also applied (Wang et al. 2009; Remus et al. 2013; Putz 2015).

An overview of the state-of-the-art technology for sinter plant off-gas cleaning is summarized in the "Best Available Techniques (BAT) Reference Document for Iron and Steel Production" (Remus et al. 2013).

18.3.1 Advanced Dry De-dusting of Sintering Off-Gas

In several sinter plants, advanced ESPs were installed to achieve lower dust emissions. The main problem in sintering dust separation with an ESP arises from the high specific resistivity of the dust (Lee et al. 2001; Lanzerstorfer and Steiner 2015). There are two systems in use at sinter plant ESPs to deal with this problem.

The first is pulse energization using microsecond pulses. With pulse energization, the peak voltage is higher, providing better particle charging in the precipitator. Reported clean dust concentrations after ESP are in the range of 20–75 mg/Nm^3 (Kim et al. 1997; Grass et al. 2004; Remus et al. 2013).

The second is a moving electrode electrostatic precipitator (MEEP). In this ESP type, the movable precipitation electrodes are cleaned externally by brushes. Thus back corona effects can be reduced (Bastürk et al. 2009). Reported clean gas dust concentrations are in the range of 25–50 mg/Nm^3 (Buchwalder et al. 2008; Ando et al. 2011; Remus et al. 2013).

Bag filters are usually applied downstream of the ID fan. The removal of dust can be easily combined with the removal of SO_2 and other acidic gases (DeSOx) by injection of a base chemical and the removal of PCDD/F and other persistent organic pollutants by injection of an adsorbent. All the dust, the un-reacted reagents and the reaction products as well as the adsorbent are filtered off by means of the filter. A significant proportion of the removed dust is recirculated to the off-gas in order to increase the utilization of the consumables and thus reduce the costs. The rest is discharged out of the system for disposal. When DeSOx is applied, the solid residues are usually not recycled to the sinter strand due to the release of the SO_2 at sinter temperature. The clean gas dust concentration after the filter is generally <10 mg/Nm^3 (Remus et al. 2013).

18.3.2 Reduction of SOx Emissions

The first DeSOx systems installed at sinter plants applied wet processes. The off-gas was desulphurized by scrubbers using $Ca(OH)_2$, $Mg(OH)_2$, NaOH or a solution of NH_3 as reactants. Most of these systems were installed in Japan (Remus et al. 2013). In 1998 a semidry DeSOx process was installed at the sinter plant of DK, Duisburg. Lime milk is atomized in a spray absorber. After evaporation of the water, the dry residue is separated from the off-gas in a fabric filter (Moore et al. 2003).

The new DeSOx systems comprise a dry sorption process in combination with a fabric filter (Weiss 1998; Leroy et al. 2007; Hartig et al. 2007; Lanzerstorfer et al. 2008; Remus et al. 2013; Wisse 2014). In some systems, entrained flow sorption is applied (Fleischanderl and Aichinger 2009), while other systems use various kinds of reactors (Schuster et al. 2003; Yu et al. 2009). When $Ca(OH)_2$ is used as base reactant, some water is added to the off-gas or the reactant because SO_2 separation efficiency is higher at lower temperatures (Fleischanderl et al. 2006). When $NaHCO_3$ is used, no cooling is required. This is especially advantageous in the case of a subsequent DeNOx system (Fleischanderl and Aichinger 2009). The ranges for the stoichiometric factor for $Ca(OH)_2$ and $NaHCO_3$ consumption are 2–4 and 1.1–1.4, respectively. Reported clean gas SOx concentrations after dry sorption processes are in the range of 225–400 mg/Nm^3 (Remus et al. 2013). By mixing a carbon-containing sorbent to the reactant for acid gas separation, the PCDD/F emissions can be reduced simultaneously.

18.3.3 Reduction of PCDD/F Emissions

At some sinter plants, adsorbent is injected prior to the ESP to reduce the PCDD/F emissions by an entrained flow adsorption process. Usually, lignite coke or activated carbon is used as adsorbent. To minimize the risk of glow fires in the ESP, the carbon content of the captured dusts typically has to be limited to <20 %. Thus, limestone or hydrated lime is added as an inert material. In order to minimize the risk of fires, the off-gas temperature has to be <180 °C. With increasing dosing rate the

separation efficiency improves, dosing rates up to 300 mg/Nm^3 lignite coke are reported. However, a PCDD/F concentration of <0.1 ng/Nm^3 cannot be safely achieved because of the limited injection rate of the carbon-containing adsorbent due to the risk of an explosive mixture in the ESP (Bastürk et al. 2009). The adsorbent and the inert material are dosed into the turbulent stream of the off-gas and dispersed by a static mixer. During the flow in the ducts, the PCDD/Fs and other organohalogen compounds are adsorbed. The residence time between the injection point and the gas cleaning device is typically in the range of some seconds. In the ESP, the adsorbent and the inert material are collected together with the sinter dust. Usually, this ESP dust is recycled to the sinter strand where the PCDD/Fs are cracked in the high-temperature zone.

At ArcelorMittal, Ghent, a yearly average concentration of PCDD/Fs of 0.5 ng I-TEQ/Nm^3 is achieved with a typical dosing rate of 80 mg/Nm^3 of activated coal and 200 mg/Nm^3 of limestone. Additionally, only strictly limited amounts of grease, oil and chloride are added to the raw mix with recycled materials (Bonte et al. 2003; Remus et al. 2013). At ArcelorMittal, Eisenhüttenstadt, 80 mg/Nm^3 of pulverized lignite coke is injected. The PCDD/F concentrations were 0.115–0.255 ng I-TEQ/Nm^3 (Buchwalder et al. 2008). At Thyssen Krupp, Duisburg, zeolite and lignite coke is injected. The average PCDD/F concentrations were 0.152–0.22 ng I-TEQ/Nm^3 (Remus et al. 2013).

For dry sorption processes in combination with a fabric filter, reported PCDD/F concentrations were <0.05–0.23 ng I-TEQ/Nm^3 (Remus et al. 2013).

Activated carbon adsorption systems compete with coupled DeNOx and dioxin destruction systems gases (Finocchio et al. 2006). The removal efficiency for PCDD/Fs in a tail-end DeNOx system (SCR) on an ng I-TEQ basis was approximately 70 % (Kasai et al. 2001a; Wang et al. 2003a). Laboratory studies show that the reduction efficiency increases with temperature (Chang et al. 2007, 2009).

18.3.4 Reduction of NOx Emissions

For the reduction of NOx emissions, selective catalytic reduction (SCR) plants were installed at some sinter plants. In the SCR process, the NOx reacts with the added NH_3 to N_2 and H_2O. This reaction takes place in a reactor that contains a catalyst which is usually V_2O_5–WO_3/TiO_2. In sinter plants, SCR systems are tail-end installations, where the SCR is installed as the last cleaning stage before the off-gas is discharged through the stack. Because of the required reaction temperature, the off-gas has to be heated from the discharge temperature (typically 120–180 °C) to the operation temperature of the catalyst, which is in the range of 250–425 °C (Heck 1999) depending on the SOx concentration in the off-gas (Institute of Clean Air Companies 2009). The off-gas is heated in two steps: firstly, some of the heat contained in the off-gas after the catalyst is transferred to the off-gas before the catalyst in a heat exchanger. Secondly, a gas-fired burner is used to finally reach the required temperature. Before the off-gas enters the catalyst, NH_3 is added and mixed as homogeneously as possible into the off-gas by a static mixer.

The reported reduction efficiency of the SCR systems at the CSC, Kaohsiung, sinter plants is approximately 80 % (Lee et al. 1999). The catalyst operation temperature is 350 °C (Wang et al. 2003a). At voestalpine Stahl, Linz, the sinter plant was equipped with a SCR system a few years ago. The sinter off-gas is heated from 140 °C to about 260 °C in a heat exchanger. Heating to the catalyst operation temperature of 280 °C is done by burners fired with coke oven gas. The required clean gas concentration for NOx of <100 mg/Nm^3 is reached at a NH_3 slip of <0.1 mg/Nm^3. After 12,000 operating hours, the measured activity of the catalyst was 98.6 % of the original value (Putz 2015).

18.3.5 Simultaneous Reduction of SOx and NOx Emissions

Simultaneous reduction of SOx and NOx emissions can be achieved by the regenerated activated carbon (RAC) process. SO_2 is adsorbed on activated carbon (AC) which is thermally regenerated. Sulphuric acid is yielded in the regeneration process as a by-product. By this process, HCl, HF, Hg, PCDD/F and optionally NOx are also removed from the off-gas. The system can be designed as a single-stage or a two-stage process. In the single-stage process, the off-gas is led through a bed of AC where the pollutants are adsorbed. NOx removal only occurs when NH_3 is injected into the gas stream before the AC bed. In the two-stage process, the off-gas is led through two beds of AC. The NH_3 for NOx reduction is injected before the second bed.

The reported DeSOx efficiency of a one-stage system is 95 % and the DeNOx efficiency is 15–20 % (Kasama et al. 2006). RAC systems are operated at sinter plants in Japan, Korea and Australia (Remus et al. 2013).

18.3.6 Advanced Wet Emission Reduction Processes

Typical wet scrubbers show limited efficiency in the collection of fine dust. The reported clean gas dust concentrations after a two-stage gas cleaning system consisting of cyclones and a subsequent venture scrubber was 70–90 mg/Nm^3 (Shvets et al. 2003). In the 1990s, some advanced wet second-stage off-gas cleaning systems were installed at sinter plants (Hofstadler et al. 1999; Leuwerink and van der Panne 2001; Brunnbauer et al. 2006). In an AIRFINE scrubber system, circulating water is sprayed into the off-gas by compressed air. The reported dust separation efficiency was 80–90 %, and the dust concentration after the scrubber was in the range of 30–40 mg/Nm^3. A simultaneous reduction of the PCDD/F emissions (Smit et al. 1999) as well as a reduction of acid gases emissions was reported (Hofstadler et al. 1999). However, both installations of this technique were replaced by bag filter systems in the recent years.

At another sinter plant, a wet ESP was installed as second-stage dust separator. The reported de-dusting efficiency is 83 % (Boscolo et al. 2008), and the reduction of PCDD/F emissions is approximately 70 % (Guerriero et al. 2009).

18.4 Residues from Dry Off-Gas Cleaning at Sinter Plants

In dry sinter off-gas de-dusting and DeSOx, the residues are fine-grained dusts; no waste water is produced. The dry consistency of the residues and the absence of waste water are major advantages in comparison with wet off-gas cleaning systems.

18.4.1 Residue from De-dusting of Sintering Off-Gas

The solid residues from de-dusting with ESPs or cyclones are usually recycled to the charge of the sinter plant. In some sinter plants, the dust collected in the last electrical field of the ESP is excluded from recycling because of the high concentration of chloride (Remus et al. 2013). The reason for the exclusion is that chloride is volatilized to a great extent in the sintering process in the form of alkali chlorides and discharged with the off-gas (Debrincat and Loo 2007). The chlorides are present as KCl and to a lesser extent as NaCl (Ahn and Lee 2006; Peng et al. 2008, 2009; Zhan and Guo 2013). When the off-gas temperature decreases, the alkali chlorides condense on the dust and are collected as dust in the ESP. Thus, higher recycling rates of chlorides lead to an up-cycling of chloride in the sintering process resulting in a higher alkali chloride concentration in the off-gas which negatively influences the performance of the ESP (Schuster et al. 2003). Therefore, ESP dust with a higher chloride concentration is not recycled in the sintering process but has to be disposed of in landfill sites (Eisen et al. 1996).

For reduction of the amount of chloride-containing dust which has to be excluded from recycling, air classification of ESP dust was investigated (Lanzerstorfer 2015b). The results showed that this would be a feasible process for the treatment of the ESP dust. By separating off the finest fraction with the highest chloride content, the amount of recycled dust can be increased while keeping the recycled amount of chloride constant.

18.4.2 Residues from Desulphurization of Sintering Off-Gas

The residue from dry second-stage off-gas cleaning is a fine-grained powder. Its flowability is poor, especially when $NaHCO_3$ is used instead of $Ca(OH)_2$ as reagent (Lanzerstorfer 2015c). The residue has to be disposed of in landfills because of the high concentrations of S and Cl which are the result of the separation of SO_2, HCl and the finest dust fraction (Peng et al. 2008, 2009). Recycling of this residue in the sinter process would result in increased SO_2 emissions (Remus et al. 2013). In order to avoid landfill disposal, leaching of this residue with water was investigated. The yielded material can be reutilized in the cement industry (Xu et al. 2012) or can be recycled to the sinter plant (Lanzerstorfer et al. 2015b). However, a significant amount of salty water, which has to be discharged, is generated by these processes. Therefore, such a process is only feasible for sinter plants located near the sea.

Guo et al. (2009) investigated the utilization of the residue from semidry desulphurization as cementing material. After thermal treatment of the residue at 450 °C, the addition of up to 20 % of the residue did not negatively influence the properties of the produced samples.

18.5 Future Developments

Some developments for improved sinter plant off-gas cleaning are currently under investigation. If the technical reliability and the economy of these technologies are proved, their application could influence state-of-the-art off-gas cleaning of sinter plants.

18.5.1 Reduction of NOx Emissions in Sinter Plants with Catalytic Bags Filters

This technology combines de-dusting and DeSOx with entrained flow injection in a fabric filter with membrane filter bags and DeNOx with an additional catalytic membrane placed inside the fabric membrane. The fabric membrane provides the protection of the catalytic support by the removal of dust and acid gases. Tests with off-gas from a sinter plant were performed in a small pilot unit. The off-gas was heated to 220 °C before it entered the bag filter. The reported results from small-scale pilot tests at a sinter plant showed up to 80 % reduction of NOx when the SOx concentration was kept below 15 mg/Nm^3. The destruction efficiency for PCDD/F was approximately 90 %. However, maintaining such a low SOx concentration by a dry sorption process required a high injection rate of the sorbent (Iosif et al. 2015).

18.5.2 Single-Stage Gas Cleaning with a Bag Filter

The use of a fabric filter for sinter plant de-dusting upstream of the ID fan did not gain widespread acceptance (Kazyuta et al. 2004; Remus et al. 2013). The recently installed fabric filters with a dry sorption process for removal of acid gases are all installed downstream of the ID fan. There are two reasons for this arrangement. Firstly, the static pressure difference for the filter casing is lower because upstream of the ID fan there is negative pressure of 15–20 kPa. Secondly, the two-stage design enables the separate collection of the residues. Usually, the residue from the first de-dusting stage can be recirculated to the sinter process, while the residue from the second cleaning stage has to be disposed of in landfill sites to avoid a build-up of Cl and S in the system.

A single-stage off-gas cleaning concept for new sinter plants was suggested (Lanzerstorfer and Neuhold 2015). It comprises an entrained flow sorption process and a fabric filter, installed upstream of the suction fan. In this way, the investment

costs for the off-gas cleaning system could be reduced. Air classification of the residue was investigated to avoid landfilling of the whole residue. In laboratory tests the residue was split into two fractions: one fraction with a low Cl and S content for recycling to the sinter feed and a second fraction that contains most of the Cl and S.

18.5.3 Metal Mesh Dust Filter

A new off-gas filtration process was tested in pilot tests using metallic filter screens. A filter cake is built on the mesh from the particles in the off-gas which then acts as a filter medium. This cake has to be formed in a recirculation operation mode. A dust outlet concentration of <10 mg/Nm^3 was achieved (Briggs et al. 2004; Schofield et al. 2004).

18.6 Conclusions

Off-gas cleaning at iron ore sinter plants is still an area of importance for integrated steel mills. The emission limits for sinter plants have been tightened in recent years. Several competing technologies are available to reduce the emission of dust, SO_2, NOx, HCl, HF and PCDD/Fs to these limits. Due to different operating conditions and raw materials, the emissions and, therefore, the requirement for emission control systems differ from sinter plant to sinter plant. Thus, the selection of the appropriate technology is a demanding task. The overview of the state of the art in air pollution control for sinter plants given in this chapter attempts to present a survey of off-gas cleaning technologies applied in sinter plants.

Acknowledgements Translation of the document GB28662-2012 from Chinese by Mrs. Xu Qi and proofreading by Mr. Peter Orgill is gratefully acknowledged. The author also gratefully acknowledges the helpful suggestions of the reviewers.

References

Ahn YC, Lee JK (2006) Physical, chemical, and electrical analysis of aerosol particles generated from industrial plants. J Aerosol Sci 37:187–202. doi:10.1016/j.jaerosci.2005.04.008

Anderson DR, Fisher R (2002) Sources of dioxins in the United Kingdom: the steel industry and other sources. Chemosphere 46:371–381

Anderson DR, Fisher R, Johnston S, Aries E, Fray TAT, Ooi TC (2007) Investigation into the effect of organic nitrogen compounds on the suppression of PCDD/Fs in iron ore sintering. Organohalogen Compd 69:2470–2473

Ando H, Shiromaru N, Mochizuki Y (2011) Recent technology of moving electrode electrostatic precipitator. Int J Plasma Environ Sci Technol 5:130–134

Aries E, Anderson DR, Fisher R, Fray TAT, Hemfrey D (2006) PCDD/F and "Dioxin-like" PCB emissions from iron ore sintering plants in the UK. Chemosphere 65:1470–1480. doi:10.1016/j.chemosphere.2006.04.020

Bastürk S, Delwig C, Ehler W, Hartig W, Hillmann C, Lüngen HB, Richter J, Schneider H, Zirngast J (2009) Technologien und Trends zur Abgasreinigung an Sinteranlagen. Stahl Eisen 129(5):51–59

Bonte L, Buttiens K, Fournelle R, Merchiers G, Pieters M (2003) New coal injection plant for dioxin reduction at the Sidmar sinter plants. Stahl Eisen 123(1):47–50

Boscolo M, Padoano E, Tommasi S (2008) Identification of possible dioxin emission reduction strategies in pre-existing iron ore sinter plants. Ironmak Steelmak 35:146–152. doi:10.1179/174328107X247815

Briggs AMW, Carcedo FG, Sedeno JV, Estrela MA (2004) Reductions in dust and gaseous emissions from sinter strands. Final Report. Office for Official Publications of the European Communities, Luxembourg

Brunnbauer G, Ehler W, Zwittag E, Schmid H, Reidetschläger J, Kainz K (2006) Eposint – a new waste gas recirculation system concept for sinter plants. Szahl Eisen 126(9):41–46

Buchwalder J, Hensel M, Richter J, Lychatz B (2008) Verminderung der Staubemissionen an der Sinteranlage von ArcelorMittal Eisenhüttenstadt. Stahl Eisen 128(9):111–117

Cavaliere P, Perrone A (2013) Analysis of dangerous emissions and plant productivity during sintering ore operations. Ironmak Steelmak 40:9–24. doi:10.1179/1743281212Y.0000000019

Cavaliere P, Perrone A, Tafuro P, Primavera V (2011) Reducing emissions of PCDD/F in sintering plant: numerical and experimental analysis. Ironmak Steelmak 38:422–431. doi:10.1179/1743281211Y.0000000034

Chang MB, Chi KH, Chang SH, Yeh JW (2007) Destruction of PCDD/Fs by SCR from flue gases of municipal waste incinerator and metal smelting plant. Chemosphere 66:1114–1122. doi:10.1016/j.chemosphere.2006.06.020

Chang SH, Chi KH, Young CW, Hong BZ, Chang MB (2009) Effect of fly ash on catalytic removal of gaseous dioxins over V_2O_5-WO_3 catalyst of a sinter plant. Environ Sci Technol 43:7523–7530

Chen Y-C, Tsai P-J, Mou J-L (2008) Determining optimal operation parameters for reducing PCDD/F emissions (I-TEQ values) from the iron ore sintering process by using the Taguchi experimental design. Environ Sci Technol 42:5298–5303

Chen Y-C, Tsai P-J, Mou J-L (2009) Reducing PAH emissions from the iron ore sintering process by optimizing its operation parameters. Environ Sci Technol 43:4459–4465

Debrincat D, Loo CE (2007) Factors influencing particulate emissions during iron ore sintering. ISIJ Int 47:652–658

Delwig C, Hartig W, Hoffmann M, Lüngen HB (2007) Developments in sinter technology. Stahl Eisen 127:S51–S66

Eisen HP, Groß J, Hüsig K-R, Kersting K, Stedem K-H (1996) Reduction of dust emissions in German sinter plants. In: Proceedings of 3rd international ironmaking congress, Gent, pp 165–169

Eisen HP, Hüsig K-R, Köfler A (2004) Construction of the exhaust recycling facilities at a sintering plant. Stahl Eisen 124(5):37–40

Esezobor DE, Balogun SA (2006) Zinc accumulation during recycling of iron oxide wastes in the blast furnace. Ironmak Steelmak 33:419–425

European Commission (2012) Commission implementing decision of 28 February 2012 establishing the best available techniques (BAT) conclusions under Directive 2010/75/EU of the European Parliament and of the Council on industrial emissions for iron and steel production; notified under document C(2012) 903, (2012/135/EU)

European Parliament and Council of the European Union (2010) Directive 2010/75/EU of the European Parliament and of the Council of 24 November 2010 on industrial emissions (integrated pollution prevention and control)

Finocchio E, Busca G, Notaro M (2006) A review of catalytic processes for the destruction of PCDD and PCDF from waste gases. Appl Catal B Environ 62:12–20. doi:10.1016/j.apcatb.2005.06.010

Fleischanderl A, Aichinger C (2009) New developments to achieve environmentally-friendly sinter production. In: Proceedings of the iron & steel technology conference 2009, vol I. Association for Iron & Steel Technology, Warrendale, pp 191–200

Fleischanderl A, Neuhold R, Meierhofer G, Lanzerstorfer C (2006) MEROS® - improved dry-type gas-cleaning process for the treatment of sinter offgas. In: Proceedings of iron & steelmaking conference 2006, Linz, Paper No. 11.4, pp 1–6

Fleischanderl A, Plattner T, Lanzerstorfer C (2007) Efficient reduction of PM 10/2.5 emissions at iron ore sinter plants. In: Proceedings of DustConf2007, Maastricht, S2/3, pp 1–12
Grass N, Hartmann W, Klöckner M (2004) Application of different types of high-voltage supplies on industrial electrostatic precipitators. IEEE Trans Ind Appl 40:1513–1520
Grochowalski A, Lassen C, Holtzer M, Sadowski M, Hudyma T (2007) Determination of PCDDs, PCDFs, PCBs and HCB emissions from the metallurgical sector in Poland. Environ Sci Pollut Res 14:326–332. doi:10.1065/espr2006.05.303
Guerriero E, Lutri A, Mabilia R, Tomasi Scian MC, Rotatori M (2008) Polycyclic aromatic hydrocarbon emission profiles and removal efficiency by electrostatic precipitator and wetfine scrubber in an iron ore sintering plant. J Air Waste Manag Assoc 58:1401–1406. doi:10.3155/1047-3289.58.11.1401
Guerriero E, Guarnieri A, Mosca S, Rosetti G, Rotatori M (2009) PCDD/F removal efficiency by electrostatic precipitator and wetfine scrubber in an iron ore sintering plant. J Hazard Mater 172:1498–1504. doi:10.1016/j.jhazmat.2009.08.019
Guo B, Ren A, Gao J, Fang Z, Zhu T (2009) Sintered flue gas semidry processing desulphurization ash as cementing materials. In: Proceedings 3rd international conference on bioinformatics and biomedical engineering, Beijing, IEEE. doi:10.1109/ICBBE.2009.5163404
Hansmann T, Fontana P, Chiappero A, Both I, Roth J-L (2008) Technologies for optimum recycling of steelmaking residues. Stahl Eisen 128(5):29–36
Hartig W, Hoffmann M, Reufer F, Weissert H (2007) Commissioning and first operational results of the new gas cleaning installation with the Paul Wurth Entrained Flow Absorber (EFA) at ROGESA No 3 sinter strand. In: Proceedings METEC Congress, Düsseldorf, Germany, pp 322–330, 11–15 Jun 2007
Haynes WM (ed) (2012) CRC handbook of chemistry and physics, 93rd edn. Taylor & Francis, Boca Raton
Heck RM (1999) Catalytic abatement of nitrogen oxides–stationary applications. Catal Today 53:519–523
Hofstadler K, Lanzerstorfer C, Gebert W (1999) Fine dedusting and waste gas cleaning of ore sintering plants with AIRFINE. Revue Metallurgie-CIT 96:1191–1196
Hofstadler K, Friedacher A, Gebert W, Lanzerstorfer C (2000) Dioxin at sinter plants and electric arc furnace – emission profiles and removal efficiency. Organohalogen Compd 46:66–69
Institute of Clean Air Companies (ed) (2009) White paper – selective catalytic reduction (SCR) control of NOx emissions from fossil fuel-fired electric power plants. Institute of Clean Air Companies, Arlington
Iosif AM, Havelange O, DeMontard B, Ebert J (2015) Reduction of NOx emissions in sinter plants with catalytic bags filter. In: Proceedings METEC & 2nd ESTAD conference, Düsseldorf, Germany, 15–19 Jun 2015
Kasai E, Aono T, Tomita Y, Takasaki M, Shiraishi N, Kitano S (2001a) Macroscopic behaviors of dioxins in the iron ore sintering plants. ISIJ Int 41:86–92
Kasai E, Hosotani Y, Kawaguchi T, Nushiro K, Aono T (2001b) Effect of additives on the dioxins emissions in the iron ore sintering process. ISIJ Int 41:93–97
Kasama S, Kitaguchi H, Yamamura Y, Watanabe K, Umezu A (2006) Analysis of exhaust gas visibility in iron ore sintering plant. ISIJ Int 46:1027–1032
Kazyuta VI, Mantula VD, Shvets MN (2004) Ecology and resource conservation: bag filters for cleaning sintering gases. Steel Translat 34(11):68–73
Kim JR, Lee KJ, Hur NS (1997) Reduction of dust emission in sinter plant at Kwangyang Works. Curr Adv Mater Process 10:799
Lanzerstorfer C (2015a) Mechanical properties of dust collected by dust separators in iron ore sinter plants. Environ Technol 36:3186–3193. doi:10.1080/09593330.2015.1055821
Lanzerstorfer C (2015b) Application of air classification for improved recycling of sinter plant dust. Resour Conserv Recycl 94:66–71. doi:10.1016/j.resconrec.2014.11.013
Lanzerstorfer C (2015c) Mechanical and flow properties of residue from dry desulphurization of iron ore sinter plant off-gas. Environ Eng Sci 32:970–976. doi:10.1089/ees.2015.0180
Lanzerstorfer C, Neuhold R (2015) Residues from single-stage dry de-dusting and desulphurization of sinter plant off-gas: enabling partial recirculation by classification. Int J Environ Sci Technol 12:2939–2946. doi:10.1007/s13762-014-0709-6

Lanzerstorfer C, Steiner D (2015) Characterization of sintering dust collected in the various fields of an electrostatic precipitator. Environ Technol. doi:10.1080/09593330.2015.1120787
Lanzerstorfer C, Fleischanderl A, Plattner T, Ehler W, Zwittag E (2008) Emissionsminderung bei Eisenerz-Sinteranlagen. In: VDI-Bericht 2035. VDI Verlag, Düsseldorf, pp 161–170
Lanzerstorfer C, Bamberger-Straßmayr B, Pilz K (2015a) Recycling of blast furnace dust in the iron ore sinter process: investigation of coke breeze substitution and the influence on off-gas emissions. ISIJ Int 55:758–764. doi:10.2355/isijinternational.55.758
Lanzerstorfer C, Xu Q, Neuhold R (2015b) Leaching of the residue from the dry off-gas de-dusting and desulphurization process of an iron ore sinter plant. Int J Miner Metall Mater 22:116–121. doi:10.1007/s12613-015-1051-9
Lee C-S, Charng C-T, Hong G-W (1999) DeNOx system in sinter plant at CSC. SEAISI Q 1999:44–50
Lee JK, Hyun OC, Lee JE, Park SD (2001) High resistivity characteristics of the sinter dust generated from the steel plant. KSME Int J 15:630–638
Leroy J, Ravier E, Wajs A (2007) New abatement technique of the atmospheric emissions of large sinter plant. First results of industrial pilot in Arcelor's Fos-sur-mer. In: Proceedings DustConf2007, Maastricht, p.S2/2,1
Leuwerink T, van der Panne A (2000) Reduced emissions from Hoogovens sinter and pellet plants. In: Seminar on sinter and pellets 1999, International Iron and Steel Institute, Committee on Raw Materials, Brussels, pp 176–183
Leuwerink T, van der Panne A (2001) Operation results of emission optimized sintering with Airfine gas cleaning. Stahl Eisen 121:29–34
Liu G, Zheng M, Du B, Nie Z, Zhang B, Liu W, Li C, Hu J (2012) Atmospheric emission of polychlorinated naphthalenes from iron ore sintering processes. Chemosphere 89:467–472. doi:10.1016/j.chemosphere.2012.05.101
Menad N, Tayibi H, Carcedo FG, Hernández A (2006) Minimization methods for emissions generated from sinter strands: a review. J Clean Prod 14:740–747. doi:10.1016/j.jclepro.2004.03.005
Ministry of Environmental Protection of the People's Republic of China (2012) Emission standard of air pollutants for sintering and pelletizing of iron and steel industry, GB28662-2012
Mo C-L, Teo C-S, Hamilton I, Morrison J (1997) Admixing hydrocarbons in the raw mix to reduce NOx emission in iron ore sintering process. ISIJ Int 37:350–357
Moore C, Deike R, Hillmann C (2003) Minimization of dioxin emissions during sintering of iron residues. In: Proceedings 3rd international conference on science & technology of ironmaking (ICSTI), Düsseldorf, Germany, pp 578–581, 16–20 Juni 2003
Nakano M, Morii K, Sato T (2009) Factors accelerating dioxin emission from iron ore sintering machines. ISIJ Int 49:729–734
Ooi TC, Lu L (2011) Formation and mitigation of PCDD/Fs in iron ore sintering. Chemosphere 85:291–299. doi:10.1016/j.chemosphere.2011.08.020
Park KS, Seo Y-C, Lee SJ, Lee JH (2008) Emission and speciation of mercury from various combustion sources. Powder Technol 180:151–156. doi:10.1016/j.powtec.2007.03.006
Peng C, Guo Z-C, Zhang F-L (2008) Discovery of potassium chloride in the sintering dust by chemical and physical characterization. ISIJ Int 48:1398–1403
Peng C, Zhang F-L, Guo Z-C (2009) Separation and recovery of potassium chloride from sintering dust of ironmaking works. ISIJ Int 49:735–742
Putz B (2015) Operational experience in the field of sintering with the new installed DeNOx plant at voestalpine Linz. In: Proceedings METEC & 2nd ESTAD conference, Düsseldorf, Germany, 15–19 Jun 2015
Quaß U, Fermann M, Bröker G (2004) The European dioxin air emission inventory project—final results. Chemosphere 54:1319–1327. doi:10.1016/S0045-6535(03)00251-0
Reidetschläger J, Stiasny H, Hötzinger S, Aichinger C, Fulgencio A (2012) Selective waste gas recirculation system for sintering plants. Stahl Eisen 132(1):25–30
Remus R, Aguado-Monsonet MA, Roudier S, Sancho LD (2013) Best available techniques (BAT) reference document for iron and steel production, industrial emissions Directive 2010/75/EU, Integrated Pollution Prevention and Control. Publications Office of the European Union, Luxembourg

Sakuragi J, Kubo S, Terada J, Mochida J (1994) Operation results of the exhaust gas recirculation system in Tobata No. 3 sinter plant. Revue Metallurgie-CIT 94:899–908

Sammut ML, Noack Y, Rose J, Hazemann JL, Proux O, Depoux M, Ziebel A, Fiani E (2010) Speciation of Cd and Pb in dust emitted from sinter plant. Chemosphere 78:445–450. doi:10.1016/j.chemosphere.2009.10.039

Schofield N, Fisher R, Anderson DR (2004) Environmental challenges for the iron- and steelmaking process. Ironmak Steelmak 31:428–432

Schuster E, Zirngast J, Zellner H, Pössler J (2003) Improved flue-gas cleaning by bag filter at the sinter strand of voestalpine Stahl Donawitz. In: Proceedings METEC Congress, Düsseldorf, Germany, pp 574–577, 16–21 Jun 2003

Shvets MN, Brekhunov AV, Kachmarchik YA, Yurchenko VN, Savenchuk SV (2003) Reconstruction of gas-purification systems for sintering machines. Steel Translat 33(2):9–12

Sinha M, Ramna RV, Sinha S, Bose G (2010) Characterization of ESP dust sample from sinter plant. ISIJ Int 50:1719–1721

Smit A, Leuwerink THP, van der Panne ALJ, Gebert W, Lanzerstorfer C, Riepl H, Hofstadler K (1999) Reduction of dioxin emissions from Hoogovens sinter plant with the AIRFINE® system. Organohalogen Compd 40:441–444

Tsai J-H, Lin K-H, Chen C-Y, Ding J-Y, Choa C-G, Chiang H-L (2007) Chemical constituents in particulate emissions from an integrated iron and steel facility. J Hazard Mater 147:111–119. doi:10.1016/j.jhazmat.2006.12.054

Tsai J-H, Lin K-H, Chen C-Y, Lai N, Ma S-Y, Chiang H-L (2008) Volatile organic compound constituents from an integrated iron and steel facility. J Hazard Mater 157:569–578. doi:10.1016/j.jhazmat.2008.01.022

Wang L-C, Lee W-J, Tsai P-J, Lee W-S, Chang-Chien G-P (2003a) Emissions of polychlorinated dibenzo-p-dioxins and dibenzofurans from stack flue gases of sinter plants. Chemosphere 50:1123–1129

Wang T, Anderson DR, Thompson D, Clench M, Fisher R (2003b) Studies into the formation of dioxins in the sintering process used in the iron and steel industry. 1. Characterisation of isomer profiles in particulate and gaseous emissions. Chemosphere 51:585–594. doi:10.1016/S0045-6535(02)00784-1

Wang JB, Hung CH, Hung CH, Chang-Chien GP (2009) Polychlorinated dibenzo-p-dioxin and dibenzofuran emissions from an industrial park clustered with metallurgical industries. J Hazard Mater 161:800–807. doi:10.1016/j.jhazmat.2008.04.026

Weiss W (1998) Maßnahmen zur Verbesserung der Entstaubung einer Eisenerzsinteranlage mit nachfolgenden Untersuchungen zur Minderung der PADD/PCDF-Emissionen, Stahlwerke Bremen

Wisse AM (2014) Installation von Gewebefiltern an der Sinteranlage von Tata Steel in IJmuiden. Stahl Eisen 134(3):41–50

Xhrouet C, De Pauw E (2003) Prevention of dioxins de novo formation by ethanolamines. Environ Chem Lett 1:51–56

Xhrouet C, De Pauw E (2004) Formation of PCDD/Fs in the sintering process: influence of the raw materials. Environ Sci Technol 38:4222–4226

Xhrouet C, Nadin C, De Pauw E (2002) Amines compounds as inhibitors of PCDD/F de novo formation on sintering process fly ash. Environ Sci Technol 36:2760–2765

Xu S, Liu J, Song M (2012) Water-washing of iron-ore sintering gas cleaning residue for beneficial reutilization as secondary construction material. Procedia Environ Sci 16:244–252

Yu Z, Li Q, Xu H, Lin C (2009) Design and application of the Dry-FGD process in sanming steel No. 2 sintering plant. In: Yan K (ed) Electrostatic precipitation - 11th international conference on electrostatic precipitation. Springer, Berlin, pp 620–623

Zhan G, Guo Z-C (2013) Water leaching kinetics and recovery of potassium salt from sintering dust. Trans Nonferrous Met Soc China 23:3770–3779

Chapter 19
Risk Assessment and Control of Emissions from Ironmaking

Tao Kan, Tim Evans, Vladimir Strezov, and Peter F. Nelson

Abstract Processing of raw materials to valuable products results in the formation of undesired compounds due to feedstock impurities and process inefficiencies. During the iron and steelmaking process, iron ore is converted to iron and steel at high temperatures using carbon energy sources. As the iron ore and carbon sources contain minor and trace element impurities and the combustion of carbon is incomplete, certain undesirable compounds may be formed that can be detrimental if emitted to the environment. These emissions can pose significant risks to humans and to the health of the ecosystem. This chapter outlines the various emissions associated with ironmaking, the risks these emissions pose to the environment and the technologies employed to minimise or eradicate the pollutants.

19.1 Introduction

The iron and steelmaking industry is a highly material and energy-intensive process contributing to pollutant emissions and significantly affecting the air, water and soil quality. For example, in China, the atmospheric emissions of SO_2, NO_x (nitrogen oxides), $PM_{2.5}$ (particulates with size of less than 2.5 μm) and VOCs (volatile organic compounds) from the iron and steelmaking industry were estimated to be approximately 2.2, 0.9 and 0.6 Mt respectively with the total crude steel production of 731, 040 Mt in 2012 (World Steel Association 2015; Wu et al. 2015). Pollutants are mainly formed from the conversion of minor and trace element impurities as well as other contained compounds during the processing of iron ores and other raw materials.

Iron and steel production typically consist of:

1. Ironmaking processes:
   (a) Integrated ironmaking plants

T. Kan • T. Evans • V. Strezov (✉) • P.F. Nelson
Department of Environmental Sciences, Faculty of Science and Engineering, Macquarie University, Sydney, NSW 2109, Australia
e-mail: vladimir.strezov@mq.edu.au

P. Cavaliere (ed.), *Ironmaking and Steelmaking Processes*,
DOI 10.1007/978-3-319-39529-6_19

Pelletising: agglomeration of fine iron ores to produce pellets using a pellet plant
Sintering: agglomeration of fine iron ores to produce sinter using a sinter plant
Cokemaking: metallurgical coke production using coke ovens
Ironmaking: pig iron production using ironmaking blast furnaces

(b) Direct reduced iron (DRI) plants

2. Steelmaking processes:

(a) Steel production:

Steelmaking using basic oxygen furnaces (BOF) which is typical for integrated plants
Using electric arc furnaces (EAF) which is typical for DRI plants

(b) steel refining, casting and shaping:

Ladle metallurgy furnaces (LMF)
Continuous casters and batch casting in ingot moulds
Shaping the steel in rolling mills

The ironmaking processes account for the majority of pollutant emissions from the entire iron and steelmaking industries. This chapter is thus mainly focused on the pollutant emissions from the main processes of an integrated ironmaking plant, including sintering, pelletising, cokemaking and ironmaking blast furnaces.

These processes emit pollutants of different amounts. For example, in the sintering process, significant amounts of SO_2 are contained in the exhaust gas while in blast furnaces most sulphur partitions to the iron and slag. Sinter plants contribute the largest share of pollutant emissions in the ironmaking plants and are the second largest emitter after municipal solid waste (MSW) incineration (Philip 1999). For example, in China, sinter plant emissions are responsible for around 70 % of the atmospheric emissions of SO_2 and VOCs, 50 % of NO_x, 25 % of $PM_{2.5}$, 98 % of PCDD/Fs (dioxins and furans) and 10 % of CO_x (carbon oxides) (Gan et al. 2012; Wu et al. 2015).

Pollutant minimisation and recycling are major concerns for retaining the sustainability of industrial operations. The updating and implementing stricter environmental regulations by global governments (e.g. US Environmental Protection Agency and European Commission) are driving technological improvements in the iron and steel industry. For developing countries (e.g. China and India), there is much room for technological improvement and huge investments are required to avoid further lagging behind the developed countries. To comply with legislations, a variety of technologies and facilities have been employed to minimise or even eliminate the pollutant emissions.

This chapter is intended to give an introduction to the types of pollutant emissions, material inputs and outputs (especially the pollutant outputs) of ironmaking plants, and the commonly adopted abatement measures (primary and secondary) of various pollutant emissions. The effects of pollutant emissions on environment and human health as well as the quantitative assessment of the corresponding risks are also presented in the final section of this chapter.

19.2 Pollutant Types and Their Effects

Pollutant emissions can be categorised into several groups based on the affected environmental media: (1) pollutant emissions to atmosphere, (2) pollutant emissions to water and (3) pollutant emissions to soil. These emissions are further subcategorised according to their chemical nature. The majority of research has been devoted to the pollutant emissions to atmosphere which mainly consist of SO_x, NO_x, particulate matter (PM), heavy metals, polycyclic aromatic hydrocarbons (PAHs), volatile organic compounds (VOCs) and dioxins and furans (PCDD/Fs). Among these, SO_x, NO_x, CO, Pb and PM (PM_{10} and $PM_{2.5}$) are priority pollutants. PCDD/Fs and PAHs have been of great research interest in recent years. They are air toxics in the category of persistent organic pollutants (POPs) that are resistant to environmental degradation and pose severe effects to human health and environment (Zhang et al. 2012).

Gaseous and particulate pollutants have different negative impacts on the environment and human health. CO_2, CH_4 and N_2O are greenhouse gases (GHG) that can contribute to the radiative forcing of the atmosphere. NO_x and SO_2 are acidic gases contributing to wet and dry acid deposition. CO, CH_4 and NO act as precursors for tropospheric ozone formation through photochemical reactions, which then make the major component of smog.

The atmospheric particulate matter (PM) is one of the most vital indices of ambient air quality. It can result in severe damage to the respiratory and cardiovascular systems of human beings. According to the particle diameter, for regulation purposes, PM emissions are generally defined as PM_{10} (<10 μm) and $PM_{2.5}$ (<2.5 μm).

VOCs refer to a variety of organic compounds with low boiling points (usually < 100 °C), such as benzene and derivatives (e.g. toluene and p-xylene) and formaldehyde. Some of the VOCs will cause the generation of ozone and other photo oxidants, which subsequently cause harm to the environment and human health. Generally, VOCs can cause irritation to the eyes, nose and throat and possibly other long-term health effects and even cancer. The target annual limit of average benzene concentration for VOCs from 2010 was set to be 5 $\mu g/m^3$ by the European Commission (Ciaparra et al. 2009).

The persistent organic pollutants, PAHs and PCDD/Fs, have also attracted much concern for environmental regulation, specifically for iron and steelmaking. PAHs have been determined to expose high risk of carcinogenicity for which the concentration value of benzo [*a*] pyrene (B[*a*]P) is selected as the indicator. They are also harmful to the skin and respiratory systems of human bodies. In Europe, the B[*a*]P in air was targeted at 10^{-9} g/m^3 by the end of 2012 (Ciaparra et al. 2009). Among all the iron and steelmaking sectors, cokemaking, sintering and ironmaking blast furnaces are the main sources of PAH emissions.

The formation of PCDD/Fs may take place during any combustion reactions in the presence of C, O and Cl (Demirbas 2008). Dioxins and furans have specific molecular heterocyclic structures with impregnated halogen atoms such as chlorine. PCDD/Fs refer to polychlorinated dibenzo-*p*-dioxins and dibenzofurans, which are highly hazardous and carcinogenic. The total toxicity of PCDD/Fs in gas is commonly expressed as international toxicity equivalents (I-TEQ).

19.3 Material Inputs and Outputs of Iron Industrial Processes

19.3.1 Sintering Process

The sintering process aims to agglomerate fine iron-bearing particles into larger porous clinkers (sinter product) that are suitable for use in blast furnaces. The input materials generally include ferrous materials (e.g. natural iron ores, fine iron ore powder from screening, slag, mill scales and sludge from iron and steelmaking), fluxes (e.g. limestone or dolomite) and 5 % solid fuels (e.g. coke breeze or anthracite). The simplified flow diagram of a sinter plant with inputs and emissions is shown in Fig. 19.1.

In a sintering process, the blend of input materials is loaded onto the travelling sinter strand to form a sintering bed, where the sintering reactions take place. At the start point of the sinter strand, the ignition burners ignite the coke breeze in the blend, and the combustion initiates as air is sucked through the bed. Very high bed temperatures (>1300 °C) cause the bed material to melt and agglomerate to form the sinter product. The produced combustion gas is pulled down through the sinter bed height into the wind boxes beneath the strand by suction fans. An entire sintering cycle occurs from the ignition of coke breeze in the sinter mixture to the burn-through point (Lu et al. 2015).

The exhaust gas in the wind boxes is a complex mixture of (1) fine particle matter which comprised of contains heavy metals and organic compounds; (2) low concentrations of CO, NO_x (e.g. 200 ppm) and SO_2 (e.g. <500 ppm); (3) low concentrations of PCDD/Fs; and (4) miscellaneous minor constituents such as HCl, HF and moisture (Chen et al. 2008a; Zhang et al. 2012).

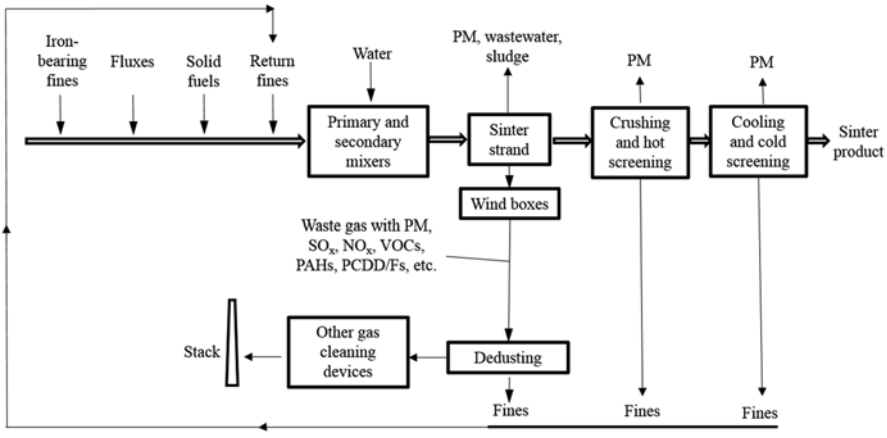

Fig. 19.1 A simplified flow diagram of a sinter plant with inputs and emissions

The exhaust gas also possesses other properties, such as a wide temperature range and fluctuating gas amounts with large flow rates (e.g. 100 $m^3/(m^2\ min)$). As shown in Fig. 19.1, particulate matter is emitted along the entire flow of the sintering process. Materials handling, wind box exhaust gas, sinter discharge (crushing and hot screening) and cold screening contribute to the major emissions of particulate matter. Wind boxes experience the most noteworthy concentrations of PM emissions and carry iron and sulphur oxides, carbonaceous materials, heavy metals, metal chlorides, aliphatic hydrocarbons, dioxins and other possible contaminants, e.g. NH_3 (ammonia), As (arsenic), and fluorides. The main components of PM emissions from sinter crushing and hot screening are generally iron oxides and calcium oxides. The particle size of sinter plant dusts mostly ranges below 10 μm which is different from the blast furnace particle size distribution which can range up to 1000 μm in size (Formoso et al. 2000). The effective removal of fine particulates and aerosols at sinter plants is a difficult technical problem (Menad et al. 2006).

The concentrations of CO_x, NO_x, SO_x, VOCs, HCl and HF depend on the quality of the input raw materials as well as the reaction conditions. CO_2 and NO_x are discharged into the wind boxes throughout the entire sintering cycle. The combustion of fuels contributes more than 90 % of the NO_x emissions with the rest from other components of the sinter mixture. For example, in China the iron and steelmaking industry annually produced NO_x of up to millions of tons, most of which was caused by the sinter plants (Chen et al. 2008b).

The majority of generated SO_2 is firstly detained by the wet zone in the lower sinter bed and then released when the burn-through point approaches (Lu et al. 2015). SO_2 arises from the combustion of sulphur in the charged solid fuels, such as coke breeze or anthracite, and the oxidisation of the sulphur contained in the fluxes and other sulphur-bearing materials (e.g. ferrous fines).

VOCs are also produced mainly due to the evaporation of oils contained in certain materials (e.g. mill scale) and are pulled into the wind boxes before the formation of the sinter (Carmichael and Carson 1998).

PCDD/Fs can be also present in the exhaust gas. Sinter plants are a significant source of PCDD/F emissions. According to the statistical data by the European Environment Agency (EEA), during 1993–1995, sinter plants in Europe emitted flue gases with dioxin content of $1–10 \times 10^{-9}$ g I-TEQ (International Toxic Equivalent) per m^3 (Menad et al. 2006) which accounted for more than 90 % of the total dioxin emitted by the entire iron and steelmaking industry (Babich et al. 2008). In China, PCDD/F emissions from sinter plants are responsible for nearly 60 % of the metallurgical plants or about 26 % of the total national PCDD/F emissions (Yu et al. 2012).

The formation of PCPP/Fs during the sintering process may be due to (1) the combustion of the chlorinated precursors (e.g. chlorinated aromatics) in the sinter bed and/or (2) the de novo synthesis reaction of chlorinated precursors with hot fly ash which is catalysed by Cu and other metals such as Fe (Lu et al. 2015).

Other molecules such as HCl, Cl_2 and gaseous chlorides presented in the exhaust gas should be the result of high-temperature reactions of chlorine-containing compounds such as sodium and potassium chlorides.

19.3.2 Iron Ore Pelletising

19.3.2.1 Iron Ore Pelletising Process

With the depletion of high-grade lump ores and sinter fines, iron ore pelletising has gained popularity during the past 2–3 decades (Cameron et al. 2015). Pellet plants are nowadays confronted with less stress from the increasingly stricter environmental legislations than the sinter plants due to the following three reasons (Poveromo 2006):

(a) The majority of the global pellet plants were constructed during the past 30–40 years and equipped with relatively more modern pollutant abatement systems than sinter plants.
(b) Release of lower emissions from pelletising than sintering due to the different nature of the two processes.
(c) Considerable degradation and mass loss of sinter feed occur during handling and transportation. On the contrary, for pellet feed, the effect is minor. Most pellet plants are located at or close to the remote mining areas contrary to the sinter plant location at iron and steelmaking plants in urban areas with stringent laws.

Pelletising process involves three major steps of:

(a) Pretreatment: mixture preparation of iron ore concentrate, coal or coke breeze, fluxes (e.g. limestone, dolomite, olivine and quartz), binders (mainly bentonite, hydrated lime and organic binders), moisture and other additives
(b) Balling: production of green pellets in balling drums or discs followed by screening
(c) Induration, cooling and final screening: heating of green balls to very high temperature (1250–1400 °C) in induration furnaces to form hard pellets (Carvalho et al. 2015) External fuels are used to supply the required heat, including liquid (e.g. fuel oils), gaseous (e.g. natural gas and coke oven gas) and solid (e.g. coal) fuels. Solid carbonaceous materials (e.g. coal) may be added into the iron ore concentrate in advance. Final pellets of 6–18 mm after screening are ready for use in blast furnaces.

The induration is the core operation of the pelletising and typically consists of four distinct phases: drying, preheating, firing and cooling. Three commercially available induration furnaces are (1) shaft, (2) straight/travelling grate and (3) grate–kiln system wherein the induration of green pellets takes place in the rotary kiln. Other new emerging induration technologies such as circular pelletising are underway (Cameron et al. 2015). The overall inputs and outputs of the pelletising process can be described by Fig. 19.2.

The waste gases from pellet plants mainly include CO_2, CO, CH_4, NO_x and SO_2. Other pollutant emissions such as PM, VOCs, PCDD/Fs, fluorides, heavy metals (lead and mercury) and other trace elements are also commonly present.

Among these, the NO_x emissions are of particular concern. There are three main mechanisms for explaining the formation of NO_x (Dean and Bozzelli 2000).

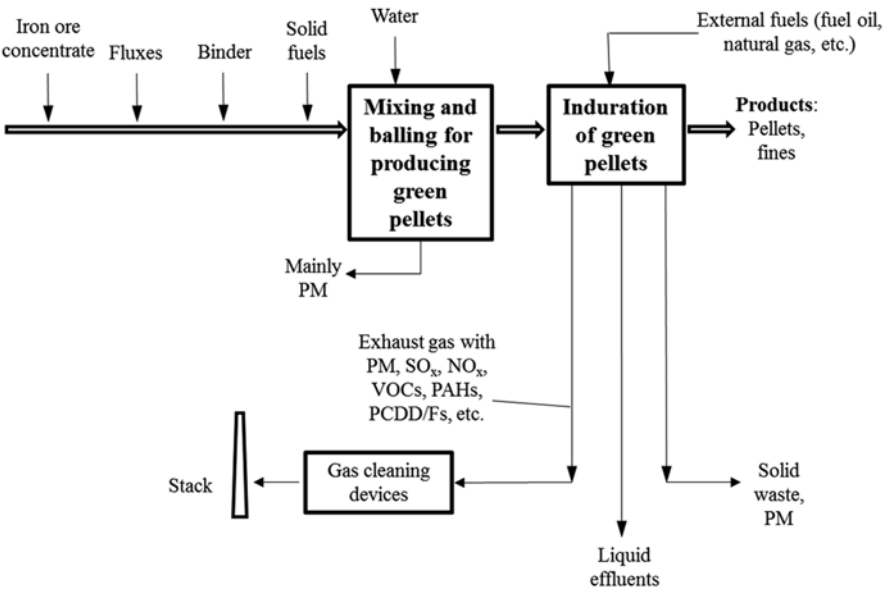

Fig. 19.2 Overall inputs and outputs of the pelletising process

For the pelletising process, the NO_x emissions are primarily generated through the fuel—NO_x route followed by the thermal—NO_x formation. However, the generation of induration NO_x is dominated by the thermal—NO_x route (Bolen 2014).

Several technologies have been applied to reduce the NO_x pollutant emissions in most modern pellet plants. Wet scrubbers, bag houses and ESPs are used for fugitive particulate removal at some points of the material handling such as cooler discharge (Bolen 2014). The recycled dust can be reused as a raw material for pelletising.

The fuel type and amount used in the pellet induration largely determine the NO_x emissions from pellet plants where NO_x is typically NO (Zahl et al. 1995). Generally, the combustion of the natural gas produces more NO_x than coal due to the reaction of nitrogen in the excessive air at the extremely high-temperature flame generated by the natural gas (Engesser 2004). It was also found that the NO_x amount increases with flame temperature. Thus, the addition of coal into the green pellets could be able to reduce NO_x production during the induration. 1 % coal addition succeeded to decrease the NO_x production by 10–12 % in the peak pellet temperature range of about 1200–1260 °C (Engesser 2004). An investigation into the NO_x formation in a rotary kiln test facility showed that the use of coal or biomass could result in lower NO_x emissions than the use of oil or gas (Johannes 2014). Reduction reactions of NO_x on char could also be responsible for decreases in observed NO_x.

Contrary to NO_x, SO_2 is hard to reduce during the pelletising process. SO_2 is formed by oxidisation of sulphur which may be present in most raw materials and external fuels. Thus, reduction in SO_2 emissions can be achieved by using low-sulphur content raw materials and external fuels. More recently built pellet plants may also have installed desulphurisation devices for SO_2 removal, such as lime slurry, to react with SO_2.

19.3.2.2 Comparison of Sintering and Pelletising

Figure 19.3 presents typical amounts of several emissions from pelletising and sintering according to the date provided by Poveromo (2006). The amounts of different emission types from pelletising and sintering are distinct, especially SO_2, CO and CO_2. Pelletising of hematite and magnetite typically emits SO_2 of 200 and 100 g/t pellet respectively while sintering produces around 1700 g/t sinter. CO emissions from pelletising are lower than 1 kgt/t pellet compared to the value of about 40 kg/t sinter for sintering. CO_2 production from pelletising is only 1/7–1/8 of that from sintering (Poveromo 2006).

The differences in emissions between the above pelletising of hematite and magnetite are mainly related to the variation in their fuel requirements. In addition, compared to sinter plants, pellet plants generally emit much less non-methane volatile organic compounds (NMVOCs) and PCDD/Fs but more heavy metals (such as Pb, Cd, Hg, Cr, Cu, Ni and Zn) and other hazardous nonmetal elements (such as As and Se) per unit mass of sinter or pellet product. For example, according to the data from the European Commission in 2001, sinter plants emitted uncontrolled NMVOCs of 138 g/t and Pb of 3.5 g/t sinter (European Environmental Agency 2013). For pellet plants, the emissions of uncontrolled NMVOCs and Pb are 14 and 20 g/t pellet respectively.

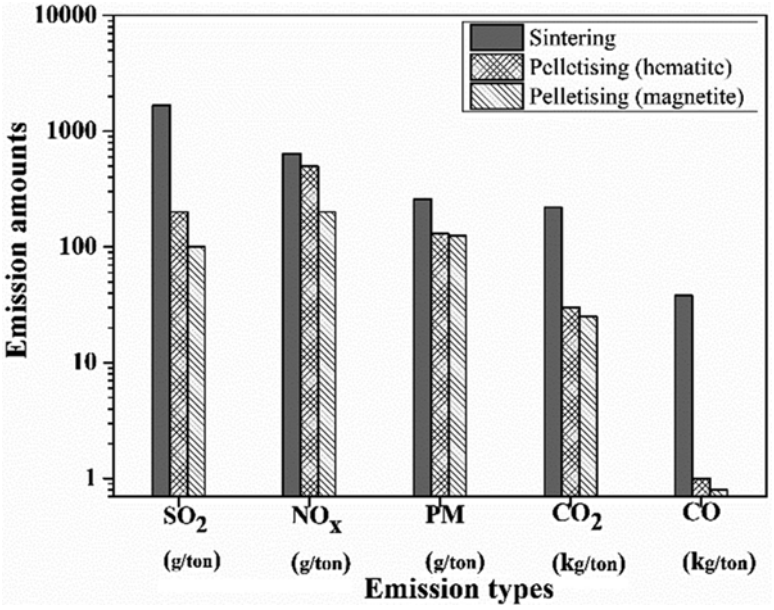

Fig. 19.3 Comparison of emissions from sintering and pelletising processes (Poveromo 2006)

19.3.3 Cokemaking

Cokemaking involves the decomposition of bituminous coals in the absence of oxygen to remove volatile matter, producing a solid residual of coke, and by-products including coke oven gas, coke breeze, tar, light oils and other chemicals. Cokemaking takes place in batteries which house 10–100 ovens. Coal is charged into the ovens from their top, and the heat required for coal decomposition is supplied by the combustion of recycled coke oven gas, natural gas or other gas fuels. Most coking plants integrate by-product facilities that are used to collect distilled volatile matters and purify the untreated coke oven gas ('foul' gas). By-product chemicals such as tar, light oils, naphthalene and ammonia can be recycled from the gas.

Figure 19.4 illustrates typical yields (wt%, based on the coal feed) of major products/by-products from cokemaking. The yields were calculated from the data found in the literature (Energetics 2000). Coke and coke breeze are the dominant solid products with yields of 63.5 and 6.8 %, respectively. A considerable amount of the coal feed is converted to the coke oven gas with a yield of approximately 15 %. Ammonia liquor and coal tar are the most outstanding liquid products with respective yields of around 6.5 and 5 %. Other products such as light oil and ammonia sulphate are formed at yields of less than 4 %.

Figure 19.5 illustrates a typical composition (vol%) of major species in coke oven gas. Hydrogen and methane are the dominant components with contents of around 52 and 30 % respectively. The concentrations of other components are below 10 %. The contained minor gas species generally involve benzene (C_6H_6) of 21–36 g/m^3, PM of 2–36 g/m^3, toluene (C_7H_8) of 2–3 g/m^3, hydrogen cyanide (HCN) of 0.1–4 g/m^3, etc. (US Environmental Protection Agency 1988; Nelson et al. 1991; Association of Iron and Steel Engineers 1998).

The cokemaking process with corresponding emission sources can be schematically described as illustrated in Fig. 19.6. The process is comprised of more than 10 modules, including production of blast furnace coke (consisting of coal preparation, coke oven batteries, coke removal with water quenching and coke screening with storage) followed by downstream treatments of foul gas consisting of ammonia spray, condenser/exhauster, tar extractor, saturator and condenser, absorption tower and a scrubbing tower. The final clean coke oven gas after treatment can be combusted for heat supply to the coke oven batteries, used in other processes or sold.

PM is released during the physical handling (e. g., pushing, charging and loading) of the raw coal material and the coke product as well as during the cokemaking in battery ovens. VOCs and other small-molecule gases, such as SO_2, NO_x and CO, are primarily generated as by-products of coking. Other dominant emissions include ammonia, coal tar, wastewater, sludge and tar residue which are produced along the streamline of foul gas treatment.

During cokemaking, ammonia results from the high-temperature (>700 °C) degradation of nitrogen-containing organics as part of the secondary decomposition reactions. Ammonia is irritating to skin, eyes and the respiratory system and can cause damage to lungs or even death if the ammonia concentration in the air is very

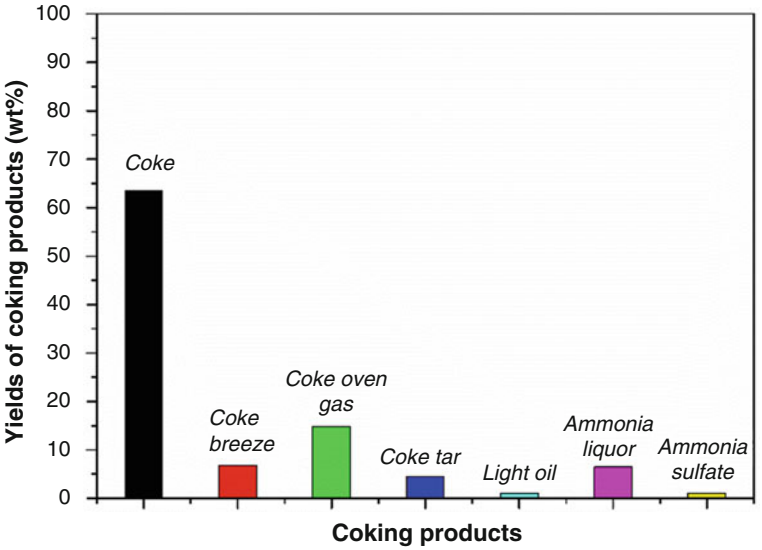

Fig. 19.4 A typical distribution (wt%, based on the coal material) of major products/by-products from cokemaking

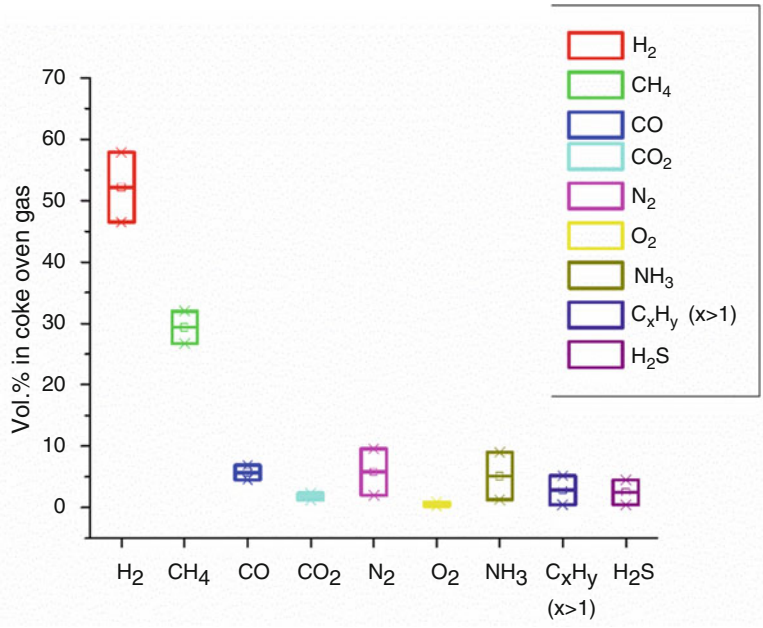

Fig. 19.5 A typical composition (vol%) of major species in coke oven gas

high. Ammonia may aggravate the eutrophication of some water resources. It can react with sulphate ions and return to the earth surface by rainfall. PAHs are released as fugitive emissions from leakages in the coke oven doors, lids, pipes and charging and pushing operations.

Large amounts of pollutant emissions are generated due to the enormous coke demand in ironmaking plants. Table 19.1 exhibits an example of pollutant production amounts (kg) per one tonne of coke manufactured.

19.3.4 Ironmaking in Blast Furnaces

The majority of ironmaking takes place in blast furnaces, although other ironmaking technologies have been developed. The basic process of blast furnace ironmaking with inputs and outputs is shown in Fig. 19.7. The overall inputs mainly include iron-bearing materials (lump ore, sinter, pellets, scrap, etc.), fluxes (e.g. limestone and dolomite), coke, other types of fuels (e.g. coal, coke breeze and coke tar), hot air blast, air, oxygen, coke oven gas, natural gas or fuel oil and water.

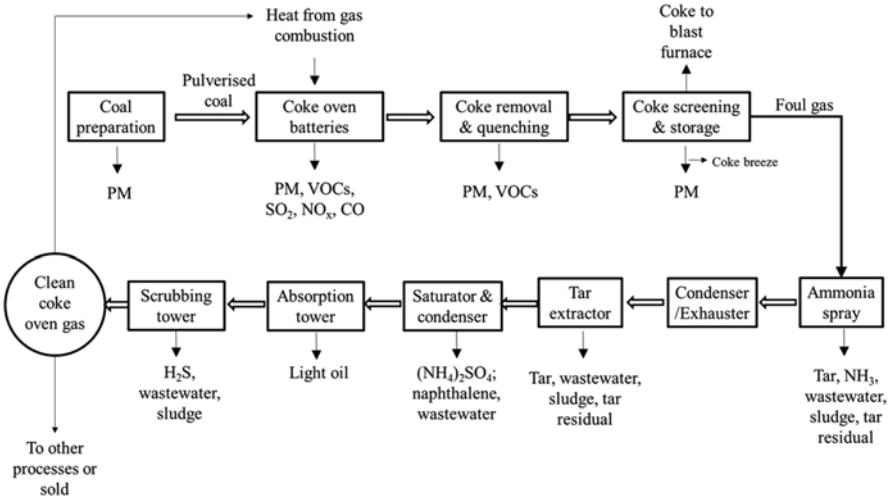

Fig. 19.6 The coking process and pollutant emissions (Energetics 2000)

Table 19.1 An example of pollutant production from cokemaking based on one ton of coke manufactured (Yaroshevskii et al. 1995)

Amount of pollutant emissions (kg pollutant per ton coke)					
H_2S	SO_2	CO	NH_3	NO_x	Phenol
2.3	1.0	0.46	0.3	0.16	0.09

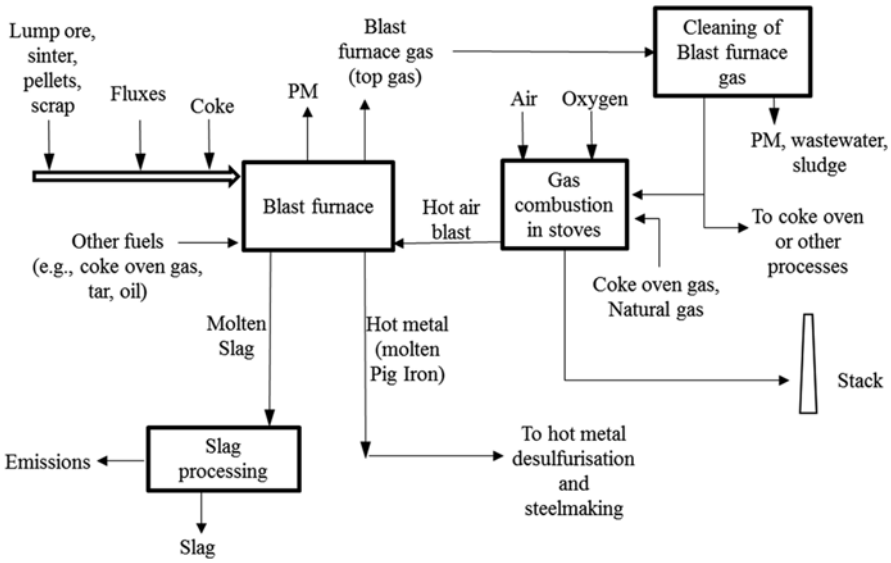

Fig. 19.7 Schematic diagram of blast furnace ironmaking process with inputs and outputs (Energetics 2000)

The outputs primarily include molten pig iron (iron saturated with carbon) which is then sent to steelmaking, molten slag, blast furnace gas, PM and wastewater and sludge.

Tapping of the blast furnace to extract pig iron and slag releases considerable emissions. During tapping, some metal oxides, such as magnesium oxide, and carbonaceous materials are released as particulates (European Environmental Agency 2013). Particle emissions also arise from the charging and conveying operations. VOCs can be released from the heating of the transport trough (after coating) and the plugging material (European Environmental Agency 2013).

The most abundant by-product from ironmaking in blast furnace is the slag which is then generally used as construction material or directly sent for landfilling. The slag contains large quantities of unwanted impurities such as sulphur. The generation rate of slag generally depends on the impurity content of the feed materials and is typically around 300 kg/t pig iron.

The blast furnace generates gas emissions mainly from the top where the blast furnace gas (top gas) is released. The blast furnace gas leaving the furnace top is hot, combustible and contains considerable dust. The size of the dust particles in the raw blast furnace gas ranges between several μm and about 6 mm. Multistage operations are employed for de-dusting. The first-stage dry cyclones or gravity dust catchers can remove over 60 % of the particles from the gas stream. Besides the dust, the blast furnace gas typically contains CO_x (CO and smaller content of CO_2) of up to 40 %, N_2 of 55–57 %, H_2 of 1–5 % and small amounts of other components such as VOCs, SO_2 and H_2S with a typical heating value of 2.5–3.6 MJ/Nm^3 (Energetics

2000). SO_2 and H_2S are formed due to the sulphur content of coke and other materials. In Europe, NAFTA (North American Free Trade Agreement) countries and Japan, the sulphur content of coke charged to blast furnaces are generally 0.5–0.9, 0.6–0.7 and 0.5–0.6 wt%, respectively (Babich et al. 2008). The cleaned blast furnace gas is extensively used in blast furnace stoves to preheat the inlet air to supply hot air blast or for heat recovery to generate steam and electricity.

19.4 Emission Abatement Measures

Commonly used emission abatement measures can be utilised in ironmaking processes; however, some technologies are exclusively designed to fit the special requirements of ironmaking plants (mainly coking, sintering, pelletising and ironmaking blast furnaces).

Solid by-products from these plants, e.g. slag from blast furnaces, are treated and/or recycled by customised methods. Wastewater is processed in wastewater treatment plants prior to discharge to the environment. The measures for gas emission abatement include (1) primary measures aiming to prevent and minimise emissions during the production processes and (2) secondary (end-of-pipe) measures applied to abate emissions after their generation. Generally, primary measures should be given more priority, but the related environmental, economic and technical aspects should be also taken into consideration.

The commonly used primary and secondary measures for gas emission abatement in different production plants are depicted in Tables 19.2 and 19.3. Due to the low pollutant concentrations and huge amount of gases involved in these processes, the introduction of pollution control measures generally incurs high investment cost. Beside the measures listed in Tables 19.2 and 19.3, there are also measures for comprehensive control of pollutants specially developed for sintering and pelletising processes. These measures include (1) for sintering (emission optimised sintering (EOS®) (Menad et al. 2006; Bolen 2014), low emission and energy optimised sintering process (LEEP) (Eisen et al. 2004), environmental process optimised sintering (Eposint) (Alexander et al. 2007)) and (2) for pelletising (LKAB KK4 (operating) and Essar Steel Minnesota (under construction) (Bolen 2014)). Integrated 'co-control' of multi-pollutants and energy consumption is believed to be more efficient than single measures. Environmental regulations are putting pressure on the iron and steel industry to develop more efficient emission control technologies.

19.5 Conclusions

Iron production processes (including sintering, pelletising, cokemaking and blast furnace ironmaking) release significant amounts of pollutant emissions to the air, water and soil. This work is focused on the pollutants emitted to the air including CO, SO_2, nitrogen oxides (NO_x), acid gases (H_2S, HCl, HF), polycyclic aromatic

Table 19.2 Measures for gas emission abatement in different iron industrial plants (US EPA 1994; Engesser 2004; Menad et al. 2006; Chen et al. 2008; Bolen 2014)

Emission types	Primary measures			
	Sintering	Pelletising	Coking	Ironmaking in blast furnace
PM	Restrict generation of SO_x and NO_x which are precursors for $PM_{2.5}$ Equipping charging cars with dust collector Ensuring sealing of pipes and holes	Restrict generation of SO_x and NO_x which are precursors for $PM_{2.5}$ Equipping charging cars with dust collector Ensuring sealing of pipes and holes	Equipping ascension pipe ejector with steam or NH_3 liquor systems Quenching tower with emission control system	Suppression of pollutant formation by minimising the contact between hot metal and air. It can be achieved by installing evacuated runner cover systems and local hooding ducted to a baghouse. This primary measure also applies for other pollutant emissions
SO_2	Use low-sulphur raw materials (e.g. coke breeze) Substitution of solid fuels by suitable biomass Use of additives, e.g. CaO, MgO and urea	Use low-sulphur raw materials	Use low-sulphur raw materials	In blast furnaces, most of sulphur is absorbed in slug by reaction
NO_x	Selective use of fuel with low N content Substitution of coke breeze by s suitable biomass Use of additives, e.g. rice husk and sugar Minerals in coke generally suppress the transformation of coke N into NO_x	Selective use of materials of low N content Addition of coal or biomass into the green pellets Lowering the amount and temperature of the combustion air Adopting low NO_x burners in traditional air re-coup ducts with NO_x removal efficiency of 10–50 % Adopting low or ultra-low NO_x burners in separate combustion chambers with NOx removal efficiency of up to 95 % Lowering the flame temperature by expanding the flame zone Generating partial reducing atmosphere within the flame	Improved heating system to avoid excessive oxygen Waste gas recirculation to reduce the local temperature and increase the residence time of the recirculated NO_x	Decreasing the flame temperature when blast furnace gas burns The NO_x concentration in blast furnace gas and stove flue gas is very low and thus is not a concern. Generally, no special NO_x controlling measures are needed

VOCs	Removing oil from mill scale before its use in sinter plants Restricting oil content in sinter mixture	Process and equipment modifications	/	Similar to SO_2 and NO_x, these emissions are of less concern
PAHs	Optimising the main sintering conditions such as the water content, suction pressure, bed height and type of hearth layer	Process and equipment modifications	Minimising leakages of coke oven batteries at doors, lids, pipes and charging and pushing operations	
PCDD/Fs	Minimising the chloride and oil loading in the sinter bed Use of additives, e.g. ammonia and urea Setting the burn-through point at the sinter discharge Setting the burn-through point at the sinter discharge Using Taguchi experimental design to optimise process parameters, including oxygen and moisture contents of inlet gas, temperature in combustion chamber, temperature of outlet flue gas, residence time in cooler	Optimising process parameters	Optimising process parameters	

Table 19.3 Secondary measures for gas emission abatement in different iron industrial plants (Bolen 2014; Philip 1999)

Emission types	Secondary measures	Comments		
PM	PM removal devices/technologies	PM removal efficiency (%)	Typical discharge PM contents (mg/m^3)	Several devices/ technologies could be combined to enhance the PM removal
	Mechanical collectors (e.g. cyclones and dropout boxes)	50–80	45–150	
	Fabric filters (baghouse)	90–99.99	10	
	Dry electrostatic precipitators (ESPs)	90–99.99	20	
	Wet electrostatic precipitators	90–99.99	20	
	Wet scrubbers	70–99+	45	
SO_2	SO_2 removal devices/technologies	SO_2 removal efficiency (%)	Typical discharge SO_2 contents (ppmv)	These technologies typically use reaction of SO_2 with CaO or $CaCO_3$ and by-products of $CaSO_3$ or $CaSO_4$ will be produced
	Circulating fluidised bed or gas suspension absorber	95–99	5	
	Wet lime/limestone scrubbing	80–95	10	
	Spray dryer absorption	70–90	25	
	Wet electrostatic precipitator	~80	/	
	Lime/limestone injection	30–50	/	
NO_x	NO_x removal technologies	NO_x removal efficiency (%)	Reactions	
	Selective catalytic reduction (SCR)	60–90	Ammonia or urea + $NO + O_2 \rightarrow N_2 + H_2O$ (+ CO_2 for urea) on vanadium-based catalysts at 300–500 °C	
	Low temperature oxidation (LoTOx)	~80	$O_3 + NO_x \rightarrow HNO_3 + H_2O$ at ~150 °C	
	Selective noncatalytic reduction (SNCR)	30–50	Direct injection of urea or aqueous ammonia into hot gas stream at 900–1010 °C	
VOCs and PAHs	Adsorbents (e.g. activated carbon)	/		

PCDD/Fs	Airfine system	/
	Optimised de-dusting facilities, e.g. ESP with rotating electrode	/
	Entrained flow process	It mainly comprises of an adsorbent component of lignite coke of very fine particles and an electrostatic precipitator (ESP) where dust is separated. Results showed that this processing technology was able to restrain the PCDD/Fs concentration to 0.3–0.4 ng I-TEQ per m^3
	Oxidative catalysis method	PCDD/Fs can react with H_2O and O_2 and break down to form small molecules of CO_2, HCl and H_2O
Heavy metals	Heavy metals significantly adhere to particulates which can be removed by PM removal devices such as wet scrubbers. Zn, Pb and Cd emissions are the main concerns in sinter plants. Mercury emission is of concern in pellet plants. Soluble oxidised mercury can be removed by wet scrubbers. Elemental mercury can be removed by activated carbon injection into the off gas duct followed by carbon particle capture by PM removal devices	
Waste water	Solids removal by sedimentation, heavy metal precipitation by physical/chemical processing, and filtration	Recycling and reuse of up to 98 % of water can be achieved by applying advanced technologies

hydrocarbons (PAHs), volatile organic compounds (VOCs), dioxins and furans (PCDD/Fs), heavy metals and particulate matter (PM). Their effects on the environment and human health are summarised. The inputs and emission outputs for the above four iron production processes are also introduced, aiming to give readers the information on the sources and production mechanism of the major pollutants in each production process. Sintering contributes the largest share of most types of pollutant emissions among the iron production processes. Waste gases produced from the sintering bed reactions are the primary sources of emissions. Emissions from pellet plants are mainly generated during the thermal induration of green pellets. Comparison of these two iron ore aggregation processes shows that pelletising generally emits much less NO_x, SO_2, CO, non-methane VOCs and PCDD/Fs but more heavy metals per unit mass of sinter or pellet product. Cokemaking is responsible for severe emissions of H_2S, SO_2, NO_x, CO, PM, VOCs and heavy metals from the coke oven batteries and coke quenching process. As to the blast furnace ironmaking process, tapping generates the primary emissions due to the contact of hot metal and slag with the air. Furtherly, the work describes the commonly used primary and secondary measures for gas emission abatement. More efficient and cost-saving measures and technological advances are required to respond to the increasing pressure from environment regulations.

References

Alexander, F, Andreas, K, Anton, S (2007) New developments for achieving environmentally friendly sinter production-eposint & meros. In: The 6th ironmaking conference proceedings

Association of Iron and Steel Engineers (1998) Steelmaking and refining volume. In: Fruehan RJ (ed) The making, shaping, and treating of steel, 11th edn. The AISE Steel Foundation, Pittsburgh

Babich A, Senk D, Gudenau HW, Mavrommatis KT (2008) Ironmaking. RWTH Aachen University, Aachen

Bolen J (2014) Modern air pollution control for iron ore induration. Miner Metall Process 31:103–114

Cameron I, Huerta M, Bolen J, Okrutny M, O'Leary K (2015). Guidelines for selecting pellet plant technology. In: AusIMM iron ore conference, 13–15 July 2015

Carmichael KR, Carson JR (1998) Process reduction of volatile organic compound emissions at a steel mill sinter plant. In: Environmental innovations in the metals industry for the 21st century: proceedings of a specialty conference

Carvalho MMO, Cardoso M, Vakkilainen EK (2015) Biomass gasification for natural gas substitution in iron ore pelletizing plants. Renew Energy 81:566–577

Chen YC, Tsai PJ, Mou JL (2008a) Determining optimal operation parameters for reducing PCDD/F emissions (I-TEQ values) from the iron ore sintering process by using the Taguchi experimental design. Environ Sci Technol 42:5298–5303

Chen YG, Guo ZC, Wang Z (2008b) Application of modified coke to NOx reduction with recycling flue gas during iron ore sintering process. ISIJ Int 48:1517–1523

Ciaparra D, Aries E, Booth MJ, Anderson DR, Almeida SM, Harrad S (2009) Characterisation of volatile organic compounds and polycyclic aromatic hydrocarbons in the ambient air of steelworks. Atmos Environ 43:2070–2079

Dean AM, Bozzelli JW (2000) Chapter 2. Combustion chemistry of nitrogen. In: Gardiner WC (ed) Gas-phase combustion chemistry. Springer Science+Business Media, New York
Demirbas A (2008) Hazardous emissions from combustion of biomass. Energy Source Part A 30:170–178
Eisen P, Husig KR, Kofler A (2004) Construction of the exhaust recycling facilities at a sintering plant. Stahl Eisen 124:37–40
Energetics (2000). Energy and environmental profile of the U.S. iron and steel industry. Prepared for U.S. Department of Energy
Engesser J (2004) Nitrogen oxide (NOx) emission reduction during pellet induration by fuel addition to the green pellets and decreased excess air. Miner Metall Process 21:9–16
European Environmental Agency (2013) EMEP/EEA air pollutant emission inventory guidebook – 2013
Formoso A, Moro A, Fernandez-Pello G, Muniz M, Jimenez J, Moro A, Cores A (2000) Study of the iron ores mixture granulation in the sintering process. Part 2. Granulation index. Rev Metal Madrid 36:254–265
Gan M, Fan XH, Chen XL, Ji ZY, Lv W, Wang Y, Yu ZY, Jiang T (2012) Reduction of pollutant emission in iron ore sintering process by applying biomass fuels. ISIJ Int 52:1574–1578
Johannes H (2014) Evaluation of the NOx formation in a rotary kiln test facility. Master's thesis, Chalmers University of Technology Göteborg, Sweden
Lu L, Ooi TC, Li X (2015) Sintering emissions and their mitigation technologies. In: Lu L (ed) Iron ore: mineralogy, processing and environmental sustainability. Elsevier, Cambridge
Menad N, Tayibi H, Carcedo FG, Hernandez A (2006) Minimization methods for emissions generated from sinter strands: a review. J Clean Prod 14:740–747
Nelson D, Scheff P, Keil C (1991) Characterization of volatile organic compounds contained in coke plant emissions. Presented at the 84th annual meeting & exhibition of the air & waste management association
Philip JA (1999) Reducing the emissions of dioxins from sinter plants. In: Workshop proceedings, steel research and development on environmental issues, Bilbao
Poveromo JJ (2006) Agglomeration processes-pelletizing and sintering. In: Kogel JE, Trivedi NC, Barker JM, Krukowski ST (eds) Industrial minerals & rocks: commodities, markets, and uses. Society for Mining, Metallurgy, and Exploration, Inc. (SME), Littleton
U.S. Environmental Protection Agency (1988) Air emissions species manual volume I: volatile organic compound species profiles (April)
US EPA (1994) Alternative control techniques document - NOx emissions from iron and steel mills
World Steel Association (2015) Annual crude steel production per country and region 1980–2014. http://www.worldsteel.org. Accessed 27 Nov 2015
Wu XC, Zhao LJ, Zhang YX, Zheng CH, Gao X, Cen KF (2015) Primary air pollutant emissions and future prediction of iron and steel industry in China. Aerosol Air Qual Res 15:1422–1432
Yaroshevskii S, Baoich A, Tereshchenko V, Nozdrachev V (1995) In: 3rd international conference on combustion technologies for a clean environment, 3–6 July 1995, Lisbon, vol 1, 28.11, pp 60–90
Yu YM, Zheng MH, Li XW, He XL (2012) Operating condition influences on PCDD/Fs emissions from sinter pot tests with hot flue gas recycling. J Environ Sci 24:875–881
Zahl R, Haas L, Engesser J (1995) Formation of NOX in iron oxide pelletizing. Iron Ore Cooperative Research (MnDNR), Minnesota Department of Natural Resources
Zhang WH, Wei CH, Chai XS, He JY, Cai Y, Ren M, Yan B, Peng PA, Fu JM (2012) The behaviors and fate of polycyclic aromatic hydrocarbons (PAHs) in a coking wastewater treatment plant. Chemosphere 88:174–182

Chapter 20
CO_2 Emission in China's Iron and Steel Industry

Tingyu Zhu, Wenqing Xu, and Mingpan Shao

Abstract CO emissions have become a serious problem in China because of the country's heavy reliance on fossil fuels as an energy source. The iron and steel industries, the energy consumptions of which are high compared to the rest of the world, are confronted with an increasing demand to reduce CO emissions. Data on CO emissions from iron and steel industries is a basic requirement for a certificate of CO reduction. By analyzing the production process and the influence factors of CO emissions during iron and steel production process, the scope of CO emissions were defined. Material Flow Analysis (MFA) was used to analyze carbon flow from iron and steel production process, and the CO emissions of a typical enterprise were calculated. The existing processing CO emissions reduction technologies were also analyzed, such as blast furnace top gas pressure recovery turbine (TRT), sintering waste heat power generation, converter low pressure saturated steam generation and so on. The technologies including blast furnace stock gas circulation technology, coke oven gas injection technology after reforming, carbon capture and storage technologies and so forth are considered to have a better prospect of application for CO emissions reduction.

Key words Carbon • Emission • Material Flow Analysis • Iron and steel industry • Reduction Technology

20.1 Introduction

The world is experiencing a global warming as the prominent symbol of climate change; in the last 100 years, the global average surface temperature has increased by 0.74 °C (Change 2007). Intergovernmental Panel on Climate Change (IPCC) assessment report indicated that atmospheric CO_2 concentration has been increased from 0.0280 % before the industrial revolution to 0.0379 % (Change 2007) in 2005. The issue of climate change has become the focus of the international community; greenhouse gas emissions data is the basis for the allocation of emissions reduction task. Iron and steel industry is the third largest industry CO_2 emissions source after thermal power and cement industry

T. Zhu (✉) • W. Xu • M. Shao
Institute of Process Engineering, Chinese Academy of Sciences, Beijing, China
e-mail: tyzhu@ipe.ac.cn

P. Cavaliere (ed.), *Ironmaking and Steelmaking Processes*,
DOI 10.1007/978-3-319-39529-6_20

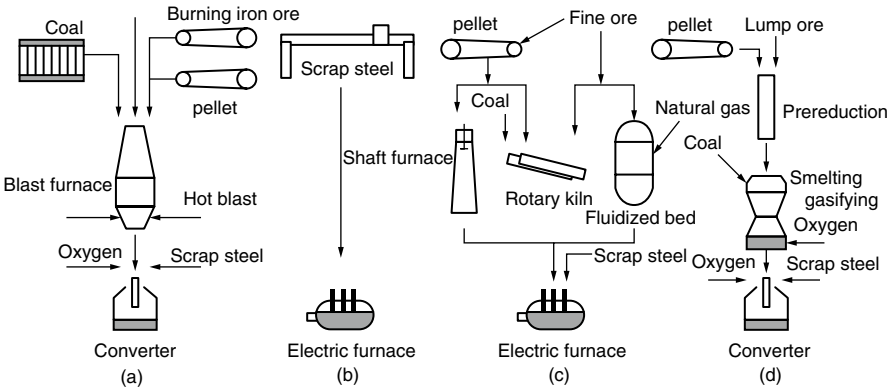

Fig. 20.1 Iron and steel production process

in China. Due to the high ratio of iron and steel, low concentration degree of iron and steel industry, the small capacity of metallurgical equipment, etc., iron and steel industry CO_2 emissions account for about 15 % of the national total emissions in China (Kim and Worrell 2002), far higher than 5–6 % of the world.

Institute of Process Engineering, Chinese Academy of Sciences was supported by the "Strategic Priority Research Program" of the Chinese Academy of Sciences, Climate Change: Carbon Budget and Relevant Issues. 190 procedures of 21 representative steel enterprises with different size, region, production process and product types were sampled and monitored. Based on the material flow analysis process and enterprise level, the carbon emissions calculation method was established, and the carbon emissions of process and enterprise level were calculated and obtained, which can provide guidance for the iron and steel emissions reduction.

20.2 Factors Affecting Carbon Emissions in Iron and Steel Industry

20.2.1 The Production Process

Typical iron and steel production process is shown in Fig. 20.1, including blast furnace-converter, scrap steel-electric furnace, direct reduction-electric furnace and smelting reduction-converter four kinds of the production process (Chu 2015).

Because of the difference in iron material, energy type, production process, equipment, crude steel production, and other aspects, the CO_2 emissions are different (Eggelston et al. 2006). The direct CO_2 emissions from blast furnace-converter technology is 1.46 t/tsteel, from scrap steel-electric furnace technology is 0.08 t/tsteel, from reduction-electric furnace technology is 0.7 t/tsteel, and from smelting reduction iron technology is 1.212 t/tsteel (Changqing et al. 2009).

20.2.2 Energy Structure

Coal is the main energy in China, accounts for about 70 % of the total energy of our country, much higher than the world's 30 % (Jiang 2008). CO_2 emissions of different kinds of energy are very wide; the coal required to obtain a unit of heat caused by CO_2 emission is higher than that of oil and natural gas by 36 and 61 % (Zhuang 2008) respectively. In addition, iron and steel production consumes a lot of power, while Chinese power generation mainly depends on coal power, accounting for 80 % of Chinese total electricity, much higher than the world's 40 % (Bureau 2010).

20.2.3 Energy Efficiency

Iron and steel production process produces much secondary energy sources, such as waste heat, residual pressure, and gas. Making full use of the secondary energy sources and improving the utilization rate of input carbon can directly or indirectly reduce the CO_2 emissions of steel production. The total amount of waste heat generated per ton steel accounted for about 37 % of the energy consumption per ton of steel; the utilization rate of waste heat resource of foreign advanced iron and steel enterprises is more than 80 %, while the utilization rate of waste heat resources of large and medium iron and steel enterprises in China is 30–50 % (Jiuju 2009).

20.2.4 Production Equipment

Large-scale equipment has an advantage of advanced technology, high output, low cost, and so on, and can reduce the energy consumption of iron and steel production and CO_2 emissions. The energy consumption of the dated production equipment is higher than that of the large-scale equipment of 10–15 %; material consumption is higher than 7–10 % (Feng et al. 2008).

20.2.5 Quality of Raw Material

Blast furnace iron-making is the largest process of CO_2 emissions in blast furnace-converter technology, accounting for about 65 % of the total emissions of ton steel. Fine material is the foundation of energy saving. In order to reduce the emission of CO_2 in blast furnace iron-making, the high quality of iron concentrate with high grade, low content of harmful impurities and high reduction of metallurgical reducing should be preferred. The iron-making theory and practice had shown that iron

ore grade on every 1 % increase, iron-making fuel ratio will decreased by 1.5 %, tons of iron slag will reduce the amount of 30 kg (Feng et al. 2008).

20.2.6 Low Carbon Production Technology

At present, the USA, the European Union, Japan, South Korea, and other developed countries and regions have begun to develop low carbon steel production technology to reduce CO_2 emissions in the production of steel (World Steel Association 2010). The low carbon technology can be divided into two categories according to the reduction media category. One is based on carbon metallurgy of low carbon technology, including blast furnace top gas recycling, carbon capture technology (CCS), etc. Of which, the blast furnace top gas recycling technology can reduce CO_2 emissions by 30 %; by CCS removal of CO_2 can reduce emissions by 20–30 %. The other is based on non-carbon metallurgy in low carbon technology, mainly including reforming coke oven gas circulation, non-carbon iron alkali liquid leaching, and thermoelectric solution.

20.3 Carbon Emissions in Iron and Steel Industry

In the national greenhouse gas inventories provided by IPCC, iron and steel production includes two parts: steel and metallurgical coke production. In this chapter, the iron and steel production includes three parts: iron-making, steelmaking, and cast rolling.

CO_2 emissions from iron and steel production include direct emissions, indirect emissions, and carbon offset; so the total amount of CO_2 emissions can be calculated by the following equation:

$$\text{Total } CO_2 \text{ emissions} = \text{direct emissions} + \text{indirect emissions} - \text{carbon offset}$$

Figure 20.2 illustrates the system boundary of CO_2 emissions in the iron and steel production process. Direct CO_2 emissions are caused by the consumption of fossil fuel and raw material in the process of conduction. Fossil fuels include coal, coke, fuel oil, coke oven gas, blast furnace gas, converter furnace gas, and so on. Raw materials include iron ore, limestone, dolomite, dust (from sintering, blast furnace iron-making, and converter furnace steelmaking), slag (from blast furnace iron making and converter furnace steelmaking), and so on. Indirect CO_2 emissions are caused by other external processes, for the use of outsourcing power and the calcination of some flux. The carbon offset come from the sales of byproducts and the self-generating electricity process.

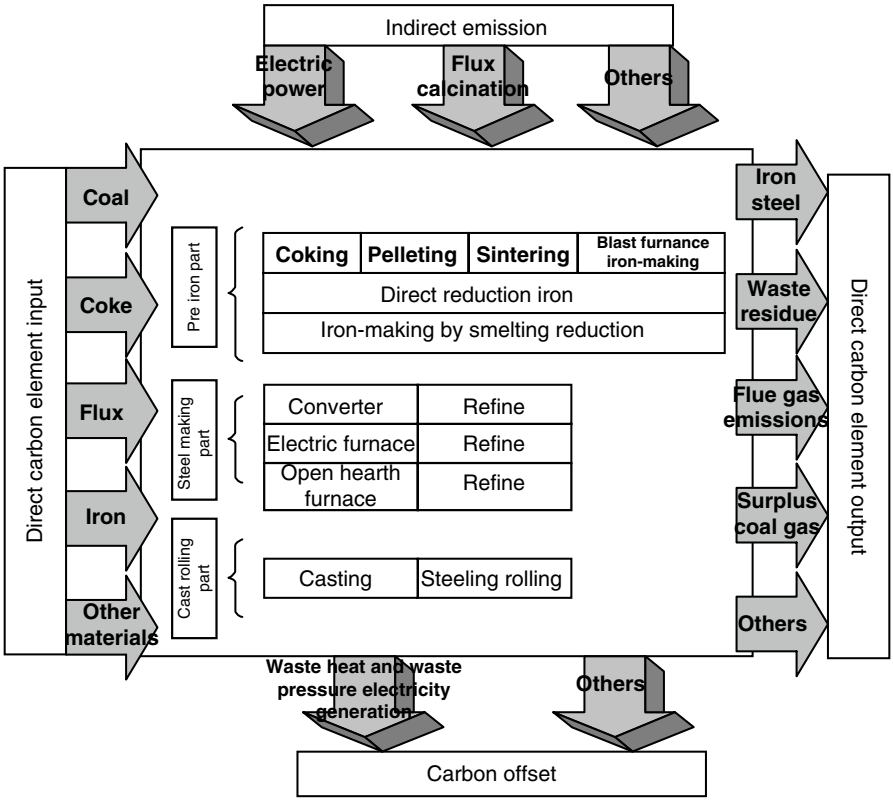

Fig. 20.2 Iron and steel production and CO_2 emission limits

20.3.1 Coke Oven Process

According to coke oven process, the carbon flow analysis is shown in Fig. 20.3.

Direct CO_2 emission from coking process was analyzed by carbon flow and obtained by carbon element conservation, that is, input amount of carbon element minus the output amount of carbon element in products form, the reduced portions of carbon element is transformed to CO_2 (the same principle as follow), that is:

$$E_{CO_2,direct} = \begin{bmatrix} CC \cdot C_{CC} - CO \cdot C_{CO} - FC \cdot C_{FC} - Bz \cdot C_{Bz} \\ -CT \cdot C_{CT} - DS \cdot C_{DS} - COG_1 \cdot C_{COG1} \\ +\left(PM_a \cdot C_a\right) \end{bmatrix} \times 44/12 \quad (20.1)$$

Where:

$E_{CO_2,direct}$ = Direct CO_2 emissions in coke production, kg (CO_2)/t (coke);
CC = Coking coal consumption in coking process, kg/t (coke);
CO = Quantity of coke in coking process, kg/t (coke);

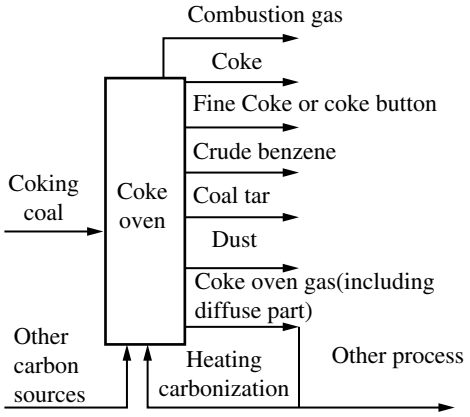

Fig. 20.3 Carbon flow analysis of coke oven process

FC = The amount of coke button or fine coke in coking process, kg/t (coke);
Bz = The number of crude benzene in coking process, kg/t (coke);
CT = The amount of coal tar in coking process, kg/t (coke);
DS = The amount of dust in coking process, kg/t (coke);
COG_1 = Coke oven gas quantity in the other process of production of coke, kg/t (coke);
PM_a = The amount of carbonization of coal and carbonaceous materials in the cove oven process, kg/t (coke);
C_x = The carbon content of x in the input or output material, kg(C)/kg (material).

The indirect CO_2 emissions are calculated by the consumption of secondary energy. In this chapter, we only consider the indirect CO_2 emissions from power consumption, see Eq. (20.2).

$$E_{CO_2,\text{indirect}} = \Sigma_i \left(M_i \cdot EF_{CO_2} \right) \tag{20.2}$$

$E_{CO_2,\text{indirect}}$ = Indirect CO_2 emissions in coke production, kg (CO_2)/t (coke);
M_i = The consumption of electricity to product 1 t coke, kW·h/t (coke);
EF_{CO_2} = CO_2 emissions in the process of 1 kW·h electric power production, =1.02 kg CO_2.

Carbon offset is calculated by the generated amount of secondary energy sources or secondary product; in this chapter, we only consider the CO_2 emissions from the power of carbon offset, as shown in Eq. (20.3).

$$E_{CO_2,\text{deduction}} = \Sigma_i \left(P_i \cdot EF_{CO_2} \right) \tag{20.3}$$

$E_{CO_2,\text{deduction}}$ = CO_2 deduction of tons coke, kg (CO_2)/t (coke);
P_i = The consumption of electricity to product 1 t coke, kW·h/t (coke);
EF_{CO_2} = CO_2 emissions in the process of 1 kW·h electric power production, =1.02 kg CO_2.

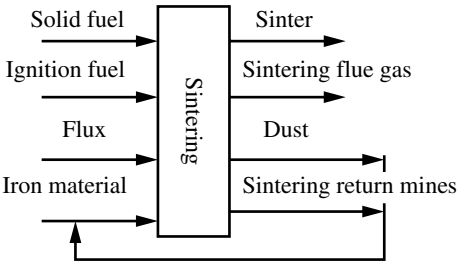

Fig. 20.4 Carbon flow analysis of the sintering process

20.3.2 Sintering Process

According to the production process of the sintering process, the carbon flow analysis of the sintering process is shown in Fig. 20.4.

Equation for calculation of direct CO_2 emission of sintering process is shown in Eq. (20.4).

$$E_{CO_2,direct} = \left[\begin{array}{l} \Sigma(SF \cdot C_{SF}) + \Sigma(IG \cdot C_{IG}) + \Sigma(FA \cdot C_{FA}) \\ + \Sigma(IM \cdot C_{IM}) + \Sigma(SF \cdot C_{SF}) + \Sigma(PM_a \cdot C_a) \\ - SN \cdot C_{SN} - FA \cdot C_{FA} \end{array} \right] \times 44/12 \quad (20.4)$$

$E_{CO_2,direct}$ = Direct CO_2 emission in sintering production, kg (CO_2)/t (sinter);
SF = The amount of consumed solid fuel, kg/t (sinter);
IG = The amount of consumed ignition fuel, kg/t (sinter);
FA = The amount of flux consumption in sintering production, kg/t (sinter);
IM = The amount of iron bearing material consumed in the sintering production, kg/t (sinter);
PM_a = The amount of other materials *a* consumed in sintering production, kg/t (sinter);
SN = Quantity of sinter from departure to steel production facilities or other facilities, kg/t (sinter);
FA = The amount of fly ash not caught in the sintering production, kg/t (sinter);
C_x = The carbon content of *x* in the input or output material, kg (C)/kg (material).

20.3.3 Pelletizing Process

According to the production process of the pelletizing process, the carbon flow analysis is shown in Fig. 20.5.

For direct CO_2 emission calculation equation of the process of pelletizing see Eq. (20.5).

$$E_{CO_2,direct} = \left[\begin{array}{l} \Sigma(FL \cdot C_{FL}) + \Sigma(AD \cdot C_{AD}) + \Sigma(IM \cdot C_{IM}) - PL \cdot C_{PL} \\ - FA \cdot C_{FA} \end{array} \right] \times 44/12 \quad (20.5)$$

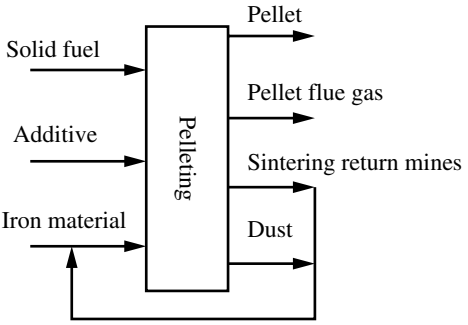

Fig. 20.5 Carbon flow analysis of pelletizing process

$E_{CO_2,direct}$ = Direct CO_2 emissions from the production of pelletizing, kg(O_2)/t (pellet);
FL = The amount of solid fuel consumed in the production of pelletizing, kg/t (pellet);
AD = The amount of additive in the production of pelletizing, kg/t (pellet);
IM = The amount of consumed iron bearing material, kg/t (pellet);
PL = The amount of pellets from the field to the steel production facilities or other facilities, kg/t (pellet);
FA = The amount of fly ash not caught in pelletizing production, kg/t (pellet);
C_x = The carbon content of x in the input or output material, kg (C)/kg (material).

20.3.4 The Blast Furnace Iron-Making Process

According to the work flow of blast furnace iron-making, the carbon flow analysis is shown in Fig. 20.6.

The computational equation for direct CO_2 emissions during blast furnace is shown in Eq. (20.6).

$$E_{CO_2,direct} = [CO \cdot C_{CO} + £\left(IM \cdot C_{IM}\right) + CI \cdot C_{CI} + PM_a \cdot C_a + PM_b \cdot C_b - MI \cdot C_{MI} - SA \cdot C_{SA} - DS \cdot C_{DS} - BFG_1 \cdot C_{BFG1}] \times 44/12 \quad (20.6)$$

$E_{CO_2,direct}$ = The direct CO_2 emissions during blast furnace process, kg (CO_2)/t (molten iron);
CO = The amount of wasting iron, kg/t (molten iron);
IM = The wasting Ferro-material during blast furnace production, contains iron ore and other material, kg/t (molten iron);
CI = The amount of coal injection in the blast furnace, kg/t (molten iron);
PM_a = The amount of other carbon-containing dust injection in the blast furnace, kg/t (molten iron);

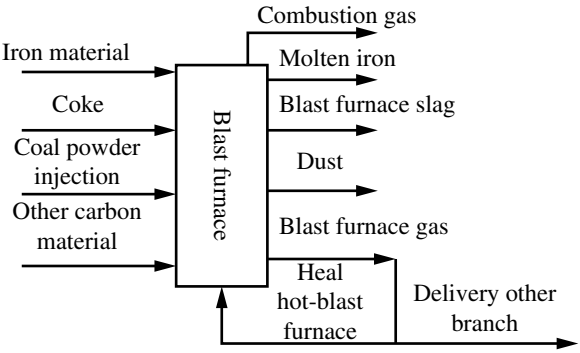

Fig. 20.6 Carbon flow analysis of blast furnace iron-making process

PM_b = The wasting material during blast furnace warming Cowper stove, kg/t (molten iron);
MI = The amount of molten iron, kg/t (molten iron);
SA = The amount of slag, kg/t (molten iron);
DS = The amount of fly ash, kg/t (molten iron);
BFG_1 = The amount of delivery of blast furnace gas, kg/t (molten iron);
C_x = The carbon content for input and put material *x*, kg/t (molten iron).

20.3.5 The Converter Steelmaking Process

According to the converter steelmaking process, the carbon flow analysis is shown in Fig. 20.7.

The computational equation of direct CO_2 emissions during the converter process is shown in Eq. (20.7).

$$E_{CO_2,direct} = \left[\begin{array}{c} \Sigma\left(IM \cdot C_{IM}\right) + \Sigma\left(FM \cdot C_{FM}\right) + CB \cdot C_{CB} + \Sigma PM_a \cdot C_a \\ -MS \cdot C_{MS} - BOS \cdot C_{BOS} - BOG_1 \cdot C_{BOG1} \end{array} \right] \times 44/12 \quad (20.7)$$

$E_{CO_2,direct}$ = The direct CO_2 emissions during converter process, kg (CO_2)/t (molten steel);
IM = The amount of wasting iron charge, kg/t (molten steel);
FM = The amount of slagging constituent, kg/t (molten steel);
CB = The amount of wasting carburant, kg/t (molten steel);
MS = The amount of molten steel, kg/t (molten steel);
BOS = The output of fly ash, kg/t (molten steel);
PM_a = The wasting amount of fuel, kg/t (molten steel);
BOG_1 = The amount of delivery converter gas, kg/t (molten steel);
C_x = The carbon content for input and put material *x*, kg/t (molten iron).

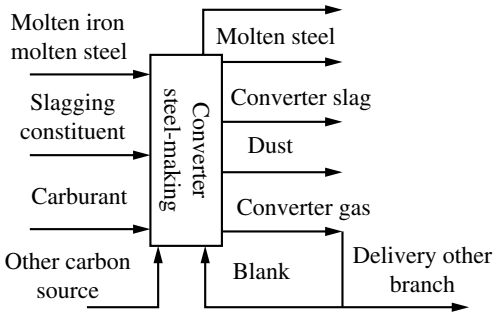

Fig. 20.7 Carbon flow analysis for converter steelmaking process

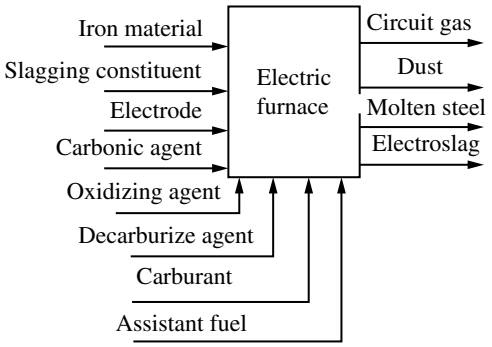

Fig. 20.8 Carbon flow analysis for electric steelmaking process

20.3.6 The Electric Steelmaking Process

According to the electric steelmaking process, the carbon flow analysis is shown in Fig. 20.8.

The calculation equation of direct CO_2 emissions for electric furnace process is shown in Eq. (20.8).

$$E_{CO_2,direct} = \left[\begin{array}{l} IS \cdot C_{IS} + FM \cdot C_{FM} + EI \cdot C_{EI} + CA \cdot C_{CA} \\ + OX \cdot Cox + DA \cdot C_{DA} + CAR \cdot C_{CAR} + AF \cdot C_{AF} \\ - S \cdot C_S - SI \cdot C_{SI} - D \cdot C_D \end{array} \right] \times 44/12 \quad (20.8)$$

$E_{CO_2,direct}$ = The direct CO_2 emissions for electric steelmaking process, kg (CO_2)/t (molten steel);

IS = The amount of wasting iron charge for steelmaking process, kg (CO_2)/t (molten steel);

FM = The amount of wasting slagging constituent, kg (CO_2)/t (molten steel);

EI = The amount of wasting electrode for steelmaking, kg (CO_2)/t (molten steel);

CA = The amount of wasting carbon-mixed for steelmaking process, kg (CO_2)/t (molten steel);

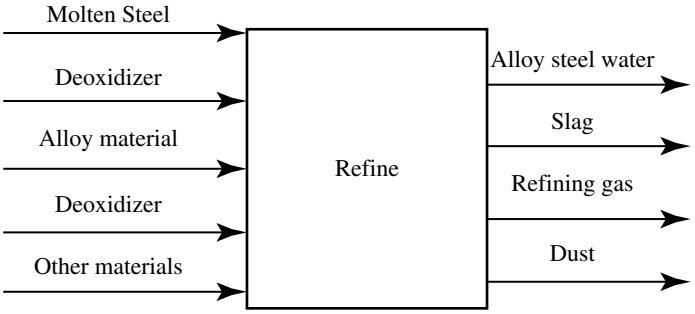

Fig. 20.9 Carbon flow analysis of refining process

OX = The amount of wasting oxidizing agent for steelmaking, kg (CO_2)/t (molten steel);
DA = The amount of wasting deoxidizing agent and alloy material for steelmaking process, kg (CO_2)/t (molten steel);
CAR = The amount of wasting carburant for steelmaking, kg/t (molten steel);
AF = The amount of wasting assistant fuel for steelmaking, kg/t (molten steel);
S = The amount of producing crude steel, kg/t (molten steel);
SI = The amount of producing slag, kg/ (molten steel);
D = The amount of producing fly ash, kg/t (molten steel);
C_x = The carbon content for input and put material x, kg (C)/kg material);

20.3.7 The Refining Process

According to the refining process, the carbon flow analysis is shown in Fig. 20.9.

The direct CO_2 emissions calculation equation of electric furnace is shown in Eq. (20.9).

$$E_{CO_2,direct} = \begin{bmatrix} MS \cdot C_{MS} + DO \cdot C_{DO} + AM \cdot C_{AM} \\ + DF \cdot C_{DF} + OC \cdot C_{OC} - AS \cdot C_A \\ - SI \cdot C_{SI} - D \cdot C_D \end{bmatrix} \times 44/12 \quad (20.9)$$

$E_{CO_2,direct}$ = The direct CO_2 emissions for electric steelmaking process, kg (CO_2)/t (molten steel);
MS = The amount of material alloy molten steel for refined process, kg/t (alloy molten steel);
DO = The amount of wasting deoxidizing agent for refined process, kg/t (alloy molten steel);

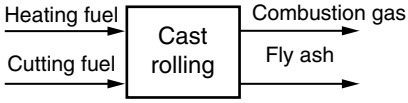

Fig. 20.10 Carbon flow analysis for casting process

AM = The amount of wasting alloy material for refined process, kg/t (alloy molten steel);
DF = The amount of wasting desulfurizer for refined process, kg/t (alloy molten steel);
OC = The amount of wasting other carbonic material for steelmaking process, kg/t (alloy molten steel);
AS = The amount of producing alloy steel, kg/t (alloy molten steel);
SI = The amount of producing slag, kg/t (alloy molten steel);
D = The amount of producing fly ash, kg/t (alloy molten steel);
C_x = The carbon content for input and output material x, kg (C)/kg material);

20.3.8 Casting and Rolling Process

The carbon flow of cast and steeling rolling process is from the fuel for heating and incising; carbon sink is the tail gas after burning the fuel (Fig. 20.10).

The direct CO_2 emissions calculation equation of cast rolling process is shown in Eq. (20.10).

$$E_{CO_2,direct} = \left[\Sigma\left(PM_a \cdot C_{PM_a}\right) + \Sigma\left(PM_b \cdot C_{PM_b}\right) - \Sigma\left(FA_i \cdot C_{FA}\right)\right] \times 44/12 \quad (20.10)$$

$E_{CO_2,direct}$ = The direct CO_2 emissions for casting and steel rolling, kg (CO_2)/t blank (molten steel);
PM_a = The amount of wasting heating fuel a of casting and steel rolling, kg (CO_2)/t blank (molten steel);
PM_b = The amount of wasting incision fuel b of casting and steel rolling, kg (CO_2)/t blank (molten steel);
FA_i = The amount without completely oxidized coke and other PM, use code as fuel for casting and steelmaking process, kg (CO_2)/t blank (molten steel);
C_x = The carbon content for input and put material x, kg (C)/kg material);

Synthesize each process carbon, get the quantitative analysis diagram of carbon for the steelmaking process for all the companies, and provide data foundation for the statistics of carbon emission and designation of carbon emission reduction measures. Take company *A* for an example; the analyze result is shown in Fig. 20.11 and Table 20.1.

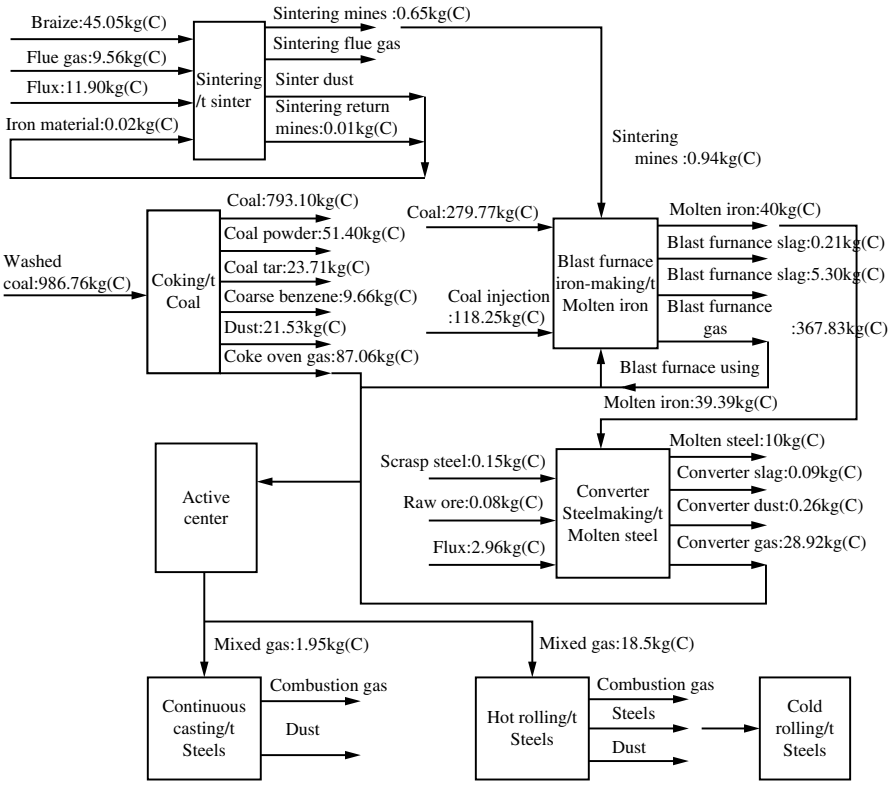

Fig. 20.11 Carbon flow analysis for iron and steelmaking process of *A* steel company

Table 20.1 Essential information for main process production equipment of *A* steel company

	Coke oven process	Sintering process	Blast furnace iron-making process	Converter steelmaking process
Specification of equipment	65 hole	210 m^2	2000 m^3	150 t
Yearly capacity (kiloton)	10	3420	1700	1500

20.4 CO_2 Emissions Reduction Technology

The existing processing equipment for CO_2 emissions reduction technology takes advantage of residual heat resources to generate electricity and to deduce the CO_2 emissions, such as blast furnace top gas pressure recovery turbine (TRT), sintering waste heat power generation, converter low-pressure saturated steam generation technology, and coke dry quenching technology. The iron and steel industry's better

CO_2 emissions reduction technology with good application prospect in the future are blast furnace stock gas circulation technology, coke oven gas injection technology after reforming, H_2/O_2 smelting reduction technology, and carbon capture and storage technologies. According to the survey of IPCC and CCS, it can reduce 20–40 % CO_2 emissions to have a positive influence on slowing down the change of climatic. The CCS technology of China is on a start step, and most of them adopt burned trapping method; the use of industry is also mainly improving petroleum recovery efficient (Tom 2009).

References

Bureau CS (2010) China statistical yearbook. Chinese Statistical Bureau, Beijing

Change IPOC (2007) Climate change 2007: the physical science basis. Agenda 6(07):333

Changqing HU, Xiaowei HAN et al (2009) Comparison of CO_2 emission between COREX and blast furnace iron-making system. J Environ Sci 21:S116–S120

Chu MS (2015) Iron and steel metallurgy fuel and auxiliary materials. Metallurgical Industry Press, Beijing

Eggelston SBL, Miwa K et al (2006) 2006 IPCC guidelines for national greenhouse gas inventories [M]. IGES

Feng JH, Wang ZG, Zhu XH (2008) The analysis of environmental pollution conditions in Chinese steel industry and the countermeasures. J Hebei Polytech Univ (Nat Sci Ed) 30(01)

Jiang ZM (2008) Reflections on energy issues in China. J Shanghai Jiaotong Univ (Sci) 13: 257–274

Jiuju CAI (2009) The energy and resources saving technologies employed in Chinese iron and steel industry and their development. World Iron Steel 4:002

Kim Y, Worrell E (2002) International comparison of CO_2 emission trends in the iron and steel industry. Energy Policy 30(10):827–838

Tom K (2009) Technology roadmap: carbon capture and storage. International Energy Agency 303–308

World Steel Association (2010) Breaking through the technology barriers. http://worldsteel.org/publications/fact-sheets.html

Zhuang G (2008) Energy saving and emission reductions: their significance to China's transition to a low-carbon economy. Adv Climate Change Res 4(05)

Chapter 21
Particulate Matter Emission in Iron and Steelmaking Plants

Wenqiang Sun, Liang Zhao, Xiaoling Li, and Yueqiang Zhao

Abstract This chapter describes the emission and control of primary particulate matter (PM) in iron and steelmaking plants. The organized and unorganized emission sources of total suspended particulates (TSP) are presented and their emission amounts are reported. Considering the increasingly strict environmental air quality requirements, the emissions of inhalable particles (PM_{10}) and fine particles ($PM_{2.5}$) during the iron and steelmaking processes are further discussed. For a sustainable and green iron and steel production, effective dust removal technologies adopted at present and should be developed and promoted in the future are also presented in this chapter.

21.1 Introduction of Steel Production Process and Particle Emission

Modern steel production process includes several steps such as smelting iron ore in a blast furnace to produce pig iron, converting the hot metal to steel, casting molten steel slab into continuously cast bloom, and producing steel materials of different use through plastic deformation processes like rolling. In modern integrated steelworks, the manufacturing process consists of sintering, coking, iron-making, steelmaking, and rolling, thus being a complex and lengthy production system.

W. Sun (✉) • L. Zhao
State Environmental Protection Key Laboratory of Eco-Industry, Northeastern University, Shenyang 110819, China
e-mail: neu20031542@163.com

X. Li
State Environmental Protection Key Laboratory of Eco-Industry, Northeastern University, Shenyang 110819, China

Faculty of Thermal Engineering, College of Petroleum Engineering, Liaoning Shihua University, Fushun 113001, China

Y. Zhao
Shandong Iron & Steel Co., Ltd., Jinan Company, Jinan 250101, Shandong, China

P. Cavaliere (ed.), *Ironmaking and Steelmaking Processes*,
DOI 10.1007/978-3-319-39529-6_21

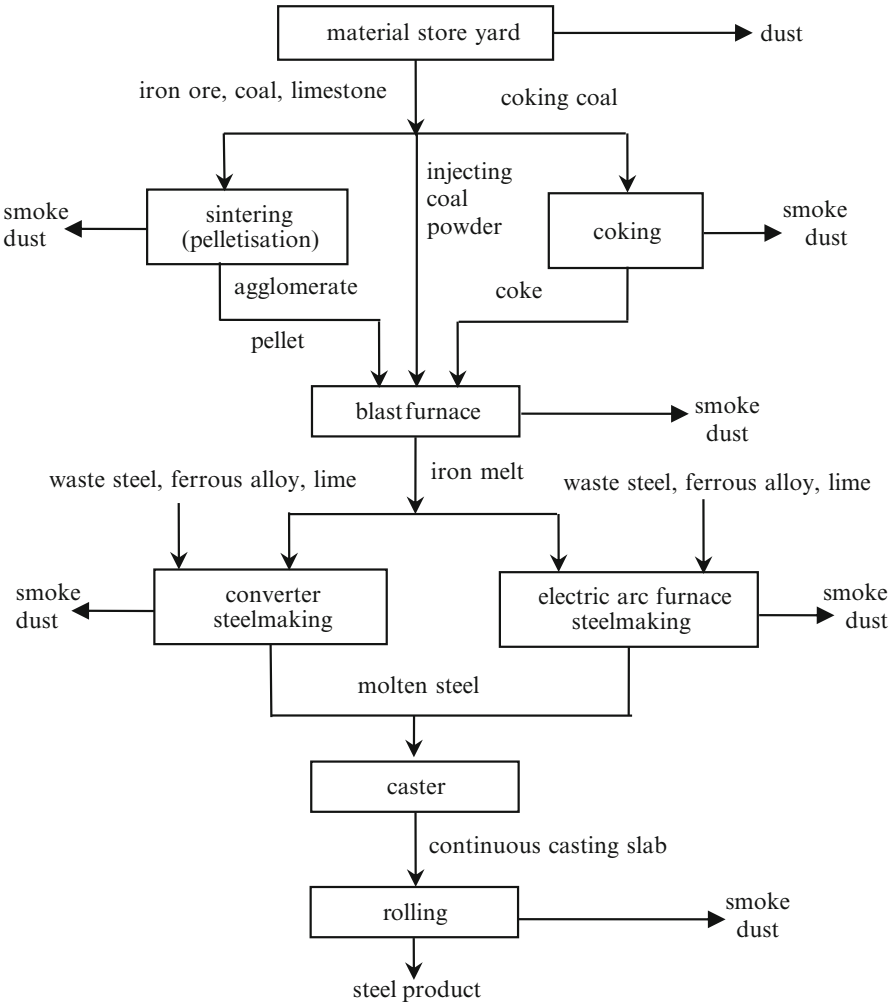

Fig. 21.1 Emission of smoke dust in the different steps of steel production

Concerning the source of dust in the steel industry, the smoke dust contained in exhaust gas expelled in chemical reactions such as sintering, coking, iron-making, steelmaking, and rolling process is regarded as the primary, followed by the exhaust gas from the combustion of fuels in the furnace. The smog particles are generally very small with particle sizes ranging from 0.01 to 1 μm, generated by condensation of gaseous substances produced by the molten material that volatilizes during the metallurgical and chemical processes. The third source is the dust distributed randomly in processes like fuel transportation, stevedoring, and machining, of which the particle size is within the range 1–200 μm. The emission of smoke dust in steel

Table 21.1 Statistics of smoke dust emission sources in steelworks

Procedure	Main contaminant	Emission source
Material store yard	Dust	Material store yard
Sintering (pelletization)	Smoke	Sintering machine nosing
	Smoke	Agglomerate cooling
	Dust	Sintering machine screening
	Smoke	Pelletization shaft furnace
Coking	Dust	Quenching device
	Smoke	Coke oven
Iron-making	Dust	Ore storage tank
	Smoke	Hot-blast stove
	Dust	Blast furnace casting house
Steelmaking	Smoke	Mixer
	Smoke, dust	Converter or electric arc furnace
	Dust	Auxiliary material crushing
Rolling	Smoke	Heating furnace

production process is illustrated in Fig. 21.1, while statistics of smoke and dust emission sources in several steelworks are shown in Table 21.1.

Thus, smoke dust is produced all along the production process in steelworks. Pollutant sources are widely distributed, characterized by the emission of high quantity of dust-containing gas, the high concentration of dust in the emitted gas and a complex composition (Wang et al. 2014). During the process of smelting and machining, huge amounts of iron ore, fuel, and auxiliary materials are consumed. About 6–7 t of raw materials are consumed to produce 1 t of steel, and about 80 % of these raw materials are converted into waste (Yu et al. 2012). For example, in an enterprise producing a million tons of crude steel annually, about 8 billion m^3 of smoke with huge amounts of CO, CO_2, and SO_2 and 100,000 t of dust are produced annually only from the sintering, iron-making, and steelmaking procedures (Wang and Zhang 2006).

21.2 Distribution of Particle Emission Sources in Steelworks

The primary sources of smoke dust in the steel production process are as follows.

21.2.1 The Sintering Procedure

The quantity of smoke dust produced during the sintering process is of around 20–40 kg/t of agglomerate while the emission quantity is about 1.02 kg/t, representing about 40 % of the total emission in steel manufacturing (Shi et al. 2006). The sources of smoke dust during the sintering procedure are:

1. *Preparation of raw materials*. Namely, the dust produced during downloading, crushing, sieving, and transportation systems.
2. *Sintering of materials*. Water rapidly evaporates when it is mixed with the mixed materials containing hot returning ore in the mixer by contact with the hot metal. This water vapor escapes with an enormous amount of dust, in the form of very humid exhaust gas with a high dust concentration.
3. *Sintering machine nosing*. When the ignition is started, the drawing fan ventilates the chamber from the lower part of materials, thus initiating the combustion of the fuel contained in the sintering materials. As a result, the smoke produced by combustion contains a huge amount of smoke dust.
4. *Sintering machine tail*. Dust is produced when the agglomerate is crushed by the single roll crusher. During this step, a huge amount of very hot dust-containing exhaust gas is produced when the agglomerate is ventilated and cooled by an annular cooler.
5. *Product size stabilization*. The stabilization system includes crushing and multistage screening, during which a huge amount of dust is produced.

21.2.2 The Coking Procedure

The quantity of smoke dust generated during the coking step is 4–13 kg/t of coke. The smoke dust emission quantity in this stage accounts for about 10 % of the total emissions in steelworks (You 2013). The smoke dust sources during the coking procedure are:

1. *Coal loading process*. Since coal occupies the space in the carbonization chamber during loading, and positive pressure is formed as a part of coal is burnt in the carbonization chamber, raw gas along with soot are pushed out from the coal-loading hole, contaminating the environment.
2. *Coking process*. During this stage, the smoke mainly comes from the leakage of furnace bodies such as the furnace door, the coal-loading hole cover, and the ascension pipe cover. Smoke produced in this step is characterized by its wide distribution, being produced continuously and having a large contaminant range.
3. *Coke pushing process*. The red hot coke shrinks and cracks when it is placed in contact with air due to its high surface area and high temperature. Thus, this oxidation and combustion process generates a strong convection movement of the surrounding air and produces a huge amount of smoke.
4. *Coke quenching process*. During wet quenching process, a huge amount of smoke dust is discharged from the quenching tower top. Similarly, a huge amount of smoke dust is discharged from the dry quenching tank top and the coke outlet during the dry quenching process.
5. *Coke sieving and transportation*. During this stage, a huge amount of dust is also produced.

21.2.3 The Iron-Making Procedure

The quantity of smoke dust produced during the iron-making procedure ranges between 9 and 12 kg/t of steel. The smoke dust emission quantity in this stage represents about 15 % of the total emission quantity in steelworks. The smoke dust sources during the iron-making procedure are:

1. *Ore tank and preparation of coal powders*. Iron-making raw material enters the blast furnace through the ore tank, conveyor belt, shale shaker, charging wagon, hoisting feeder storage, transportation, and loading system. Dust is also produced during the running of devices such as the charging machine and shale shaker. Additionally, coal is sprayed into the blast furnace after it is crushed and ground into powder, where the ball grinder and the hoists originate a huge amount of dust (Yang and Wu 2004).
2. *Blast furnace cast house*. When iron is cast out, a huge amount of high-temperature smoke containing dust is produced at the tapping hole, skimmer, trough and slag spout, as well as when the pig iron is loaded into a hot metal ladle and the tapping hole is opened.
3. *Hot-blast stove discharge*. Smoke is produced during combustion occurred in the regenerator.

21.2.4 The Steelmaking Procedure

The quantity of smoke dust produced during the manufacturing of steel procedure is of about 10–20 kg/t of steel, which correspond to about 20 % of the total emission quantity in steelworks (Jia 2012). The sources of smoke dust during the steelmaking procedure are:

1. *Pouring and pretreatment of molten iron*. When molten iron is poured from the molten iron car or torpedo car into the pretreatment tank, slag is skimmed, and sulfur is removed from the molten iron. During this step, a huge amount of dust-containing high-temperature smoke is produced.
2. *Primary smoke*. A huge amount of dust-containing smoke is produced during blowing in the converter, melting in an electric arc furnace or the oxidation stage.
3. *Secondary smoke*. A huge amount of dust-containing smoke is produced due to molten steel spraying during hot metal pouring, loading of materials, blowing, slag tapping, and steel tapping procedures.
4. *Refining*. During the refining process of molten steel, slag residue and alloy are added according to the process requirements. Thus, physical changes and chemical reactions can take place, producing a huge amount of dust-containing smoke.

21.3 Intensity of Smoke and Dust Emission in Steelworks

Thermal power generation and steel industry are great particle emission hosts. Currently, the particle size distribution before and after the dust precipitator for the boiler in a coal-fired power plant is studied by researchers all over the world, as well as the classification efficiency of dust removal (Lighty et al. 2000; Kauppinen and Kappanen 1990). As has been previously described, the production procedures in the steel industry are fairly complicated, and particles generate in each production stage, with contaminant sources distributed rather widely. Thus, a systematic and thorough study on particle emission characteristics in steelworks is very difficult. Therefore, neither studies about the particle size distribution before and after the dust precipitator in steelworks, nor the classification efficiency of dust precipitators is frequently reported.

Emission factors including TSP, PM_{10}, and $PM_{2.5}$ in steelworks from China, USA, and EU are given in Table 21.2 (Ma 2009). According to these data, it is clear that even if TSP emission during each production procedures is well characterized for steelworks in the different countries, very little is known about the differentiation of the corresponding particle emissions regarding PM_{10} and $PM_{2.5}$ fractions.

Figures 21.2, 21.3, and 21.4 show the comparison of the emission factors of TSP, PM_{10}, and $PM_{2.5}$ in steelworks from China, USA, and EU. According to the data presented in these figures, smoke dust emission factors of Chinese steelworks are higher than those of the USA and EU in all the production stages. There are several reasons that may influence the value of such emission factors, including differences in the production processes in steelworks, in the production techniques or terminal management technologies, etc.

The United States Environmental Protection Agency (EPA) has organized substantial measurements against contaminant sources and published the handbook of air contaminant emission factors (AP-42) (USEPA 1996) on this basis. AP-42 summarizes the vast majority of anthropogenic contaminant source emission factors and describes the main emission processes. Emission coefficients in AP-42 are classified into five levels like A, B, C, D, and E according to their reliability and accuracy levels. Thus, the classification standard is defined so that when the same measurement technique is employed, the emission coefficients based on measuring at least 10 contaminant sources is regarded as level A, whereas the emission coefficients based on measuring fewer contaminant sources are regarded as level B. Emission coefficients based on survey and collection or derived from emission coefficients of other processes similar to the contaminant emission processes are regarded as levels C, D, and E.

Table 21.3 lists the optimal practical smoke dust purification techniques applied by steelworks in EU and their environmental benefits.

Table 21.4 shows the production procedures, emission sources, and data corresponding to the emission factors of integrated steelworks given by “Best Available Techniques Reference Document on the Production of Iron and Steel.”

Table 21.2 Smoke dust emission factors in steelworks from China, USA, and EU

	Coking			Sintering			Iron-making			Steelmaking			Rolling		
Item	CN	USA	EU	CN	USA	EU	CN	USA	EU	CN	USA	EU	CN	USA	EU
TSP	0.24	0.19	0.016–0.30	0.15–0.21	0.085–0.8	0.071–0.85	0.16	0.15	0.0054–0.20	0.124	0.045–0.065	0.014–0.15	0.02	–	–
PM_{10}	–		–	0.13	0.05–0.104	<0.18	0.03		0.00026–0.026	0.014	0.0023	–	–	–	–
$PM_{2.5}$	–		–	0.062–0.131	0.028–0.041	–	0.03–0.085	0.10	–	0.012	0.0022	–	–	–	–

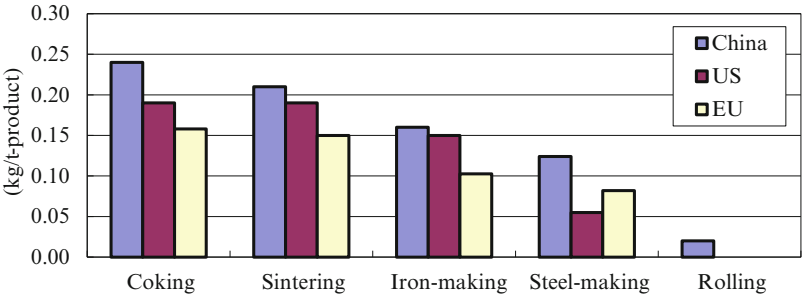

Fig. 21.2 Comparison of the TSP emission factors of steelworks from China, USA, and EU

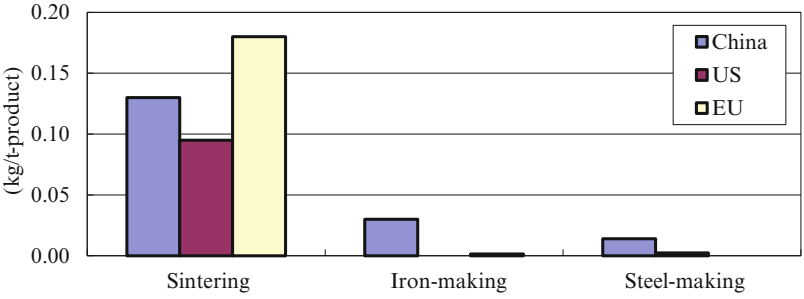

Fig. 21.3 Comparison of the PM_{10} emission factors of steelworks from China, USA, and EU

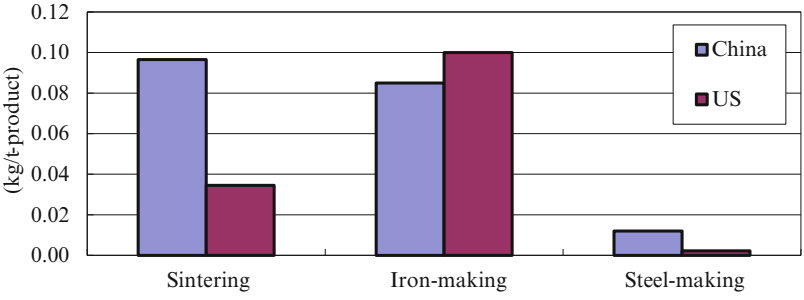

Fig. 21.4 Comparison of the $PM_{2.5}$ emission factors of steelworks from China and the USA

China's "Industrial pollution source discharge coefficient manual of the first national pollution source census" gives the most comprehensive data of the country's smoke dust emission in the steel industry. However, the data are obtained based on the emission level in 2007.

According to references from countries all over the world, few studies on PM_{10} and $PM_{2.5}$ produced during each procedure in steelworks are reported, so it is difficult to obtain detailed data and information. Therefore, field research of steelworks is necessary to gain a more comprehensive knowledge about the smoke dust emission in steelworks.

21.4 Control Measures to Reduce Particle Emission in Steelworks

Dust removal techniques have been widely applied in industries as an important measure to protect the ecological environment and recycle the resources. Thus, using a dust precipitator can significantly reduce the emission of smoke, recycle

Table 21.3 Optimal practical smoke dust purification techniques applied by steelworks in EU and the environmental benefits

Procedure	Target	Technique	Benefit	Example
Sintering		Energy pulse superposition electrostatic precipitator	43–77 mg/m^3	POSCO, Kwangyang, Rep. of Korea; Thyssenkrupp GmbH, Duisburg, Germany; Arcelor Mittal Co., Fos & Dunkirk, France; Arcelor Mittal Co., Gent, Belgium
		Moving electrode electrostatic precipitator	20–50 mg/m^3	Japan; Taranto, Italy; Arcelor Mittal Co., Eisenhüttenstadt, Germany
		Extra space electrostatic vacuum cleaner	<40 mg/m^3	Sintering factory, JFE Co., Yawata, Japan
		Bag dust collector (generally located at the downstream of electrostatic precipitator or cyclone separator)	1–10 mg/m^3	DK Recycling Co., Duisburg, Germany; Voestalpine GmbH, Donawitz, Austria; Arcelor Mittal Co., Fos, France; Inland Steelworks, East Chicago, USA, etc.
		Cyclone separator (particle size >10 μm)	300–600 mg/m^3	Corus Co., Ijmuiden, Holland; JFE Co., Japan
		High quality wet air fine	40–80 mg/m^3	Voestalpine GmbH, Linz, Austria; Corus Co., Ijmuiden, Holland
Pallet ization	Grinder (dry grinding)	Electrostatic precipitator	<20 mg/m^3	Pelletization factory, Corus Co., Ijmuiden, Holland
		Wet cleaner (drying stage) + Electrostatic precipitator (calcination stage)	<10 mg/m^3	KK3 pelletization factory, LKAB Co., Sweden; Corus Co., Ijmuiden, Holland
		Gas suspension absorber (semi drying method)	2 mg/m^3	KK3 pelletization factory, LKAB Co., S-Kiruna, Sweden

(continued)

Table 21.3 (continued)

Procedure	Target	Technique	Benefit	Example
Coking	Coke pushing and dust removing	Bag precipitator ("staples from system to system")	5–10 mg/m^3	Coking factory, US Steel Co., Clairton, USA; coking factory, Arcelor Mittal Co., Gent, Belgium; Arcelor Mittal Co., Dunkirk, France, etc.
	Coke dry quenching	Bag precipitator	<20 mg/m^3	Working quantity of dry coke quenching (up to 2008): East Asia: 104; Central Asia: 12; South America: 5; Europe: 21; Hungary: 5; Finland: 3; Poland: 4; Romania: 4; Turkey: 5
	Coke wet quenching	Shutter baffle	<25 g/t	Coking factory, Arcelor Mittal Co., Gent, Belgium; coking factory, Arcelor Mittal Atlantique, Dunkirk, France
		Coke stable quenching	6–12 g/t	Schwelgern coking factory, KBS GmbH, Duisburg, Germany
	Coke treatment, including crushing, grinding, and sieving	Bag precipitator	0.5–4.5 mg/m^3	
Iron-making	Cast house (tapping hole, trough, slag skimmer, torpedo ladle)	Moving cap to cover trough or using nitrogen to cover liquid iron + bag filter	3–10 mg/m^3	Cast house (tapping hole, trough, slag skimmer, torpedo ladle)

(continued)

useful materials in the smoke, and improve the utilization of resources. Also, the gas purified in the dust precipitator can be recycled, thus indirectly saving resources. Along with the advance of dust removal techniques, multiple removal measures occur. Meanwhile, the removal efficiency is improved obviously and reached 99 % or more for some dust precipitators.

Table 21.3 (continued)

Procedure	Target	Technique	Benefit	Example
Steel making by converter	Dust produced by blowing oxygen (primary dust removal)	Dry, wet, or electrostatic precipitator	10–50 mg/m^3	Steelworks in Germany, Austria, Belgium, Spain, Italy, etc.
	Secondary dust removal	Electrostatic or bag precipitator	6 mg/Nm^3 <2–13 mg/m^3	
	Pretreatment of molten steel (sulfur removal, separating slag from ore, converting molten steel, weighing)	Bag precipitator or electrostatic precipitator	<1–10 mg/m^3	Many plants on the world
	Ingot and continuous casting	Bag filter	0.5 mg/m^3	EAF factory, Germany; UK
Steel making by electric arc furnace	Slag treatment	Bag precipitator (crushing and sieving) + enclosing conveyor + wet treatment of temporary stack and yard	10–20 mg/m^3	Steelworks, Kehl, BSW GmbH, Germany
	Primary and secondary emissions discharged from electric arc furnace	Bag filter or electrostatic precipitator	0.35–3.4 mg/m^3 1.8 mg/m^3	Steelworks in Luxembourg, Austria, Germany, and Finland

The gas–solid or liquid–solid separation mechanisms based on two mobile phases are employed in dust removal techniques to capture solid or liquid particles in gas. In industry, there are many frequently used dust precipitators, which can be classified as the mechanical precipitator, wet precipitator, electrostatic precipitator, filtration collector, and electrostatic precipitation-bag filtration comprehensive dust collector according to the capturing mechanism.

Table 21.4 The production procedures, emission sources and emission factors of integrated steelworks

Procedure	Target	Emission factor
Coking	Loading coal	0.3–10 g/t
	Combustion chamber	–
	Coking door	0.3–6 g/t
	Coking cover	0.2–1 g/t
	Pushing coke	–
	Quenching coke	10–50 g/t
	Tamping coke	3 g/t
	Total dust	15.7–298 g/t
Sintering	Mixing raw materials	0.5–37.7 g/t (TSP) 5.6–18.9 g/t (PM_{10})
	Agglomerate	40.7–559.4 g/t (TSP) 66.3–177.1 g/t (PM_{10})
	Hot sieving	14.5–40 g/t (TSP) 7.7–25.1 g/t (PM_{10})
	Cold sieving	14–212 g/t (TSP) 1.3–42.8 g/t (PM_{10})
Iron-making	Preparing materials	2–54 g/t
	Loading materials	2.7–81.4 g/t (TSP) 0.2–11 g/t (PM_{10})
	Cast house	0.42–41.95 g/t (TSP) 0.26–25.92 g/t (PM_{10})
	Hot-blast stove	0.4–18 g/t
Steelmaking	Pretreating molten iron	1 g/t
	Loading material	2–60 g/t
	Blowing	0.3–55 g/t
	Top emission	8–120 g/t
	Secondary refining	0.1–50 g/t
	Total dust	14–143 g/t

21.4.1 Mechanical Precipitator

Mechanical precipitator separates particles from air flow and makes them precipitate by effects such as gravity, inertia, and centrifugation. It can be classified as gravity settling chamber, inertia dust precipitator and cyclone dust precipitator, etc. Mechanical precipitator, with an efficiency of generally between 40 and 90 %, is a kind of standard dust removal equipment, and is characterized by simple, less investment, convenient operation, and low power consumption. However, due to the small dust removal efficiency, they are usually applied to pretreating the dust only. The application of cyclone precipitator is the widest among them (Chen 2006).

21.4.2 Wet Dust Precipitator

Wet dust precipitator is a device in which exhaust gas containing dust touches either water or other solutions, and particles are separated from the exhaust gas by washing, adsorption, and inertial impaction effects caused by the liquid layer, liquid drop, and liquid membrane. According to the purification mechanism, wet dust precipitators can be classified into seven types: wet cyclone precipitator, wet foam precipitator, self-excited spraying wet precipitator, packed bed wet precipitator, gravity spraying wet precipitator, mechanical induced spraying wet precipitator, and Venturi wet precipitator (Yuan and Wang 2011).

Wet dust precipitators have advantages of simple structure, low cost, safe running, and high dust removal efficiency. They can not only be applied to treating dust-containing gas with high temperature, high humidity, high specific resistance, and high flammability, but also to removing hazardous materials in the exhaust gas. However, wet dust precipitators also have the following disadvantages: the power consumption is high; the waste liquid touched with exhaust gas easily leads to secondary pollution; gas containing fog drops may cause the device corrosion or scaling; lowered quality of the exhaust gas and waste of the power resource; also, when wet dust precipitators are employed in cold areas, freezing may occur.

21.4.3 Electrostatic Precipitator

An electrostatic precipitator is a dust removal device in which the electric field is formed by high voltage imposed between the discharge electrode and the dust collection plate. When the dust-containing gas comes through the electric field, the dust particles are electrified and precipitated on the dust collection plate due to the effect of the electric field force. Compared with other dust removal mechanisms, the separation force in the electric dust removal process is directly imposed on particles rather than on the whole airflow. Thus, this method has the advantages of high dust removal efficiency, low power consumption, low airflow resistance, and large smoke treatment quantity. Additionally, it can be applied to capturing particles at the sub-micro level (0.1 μm) and be controlled by a micro-computer in remote operation. This measure has been widely used in industrial departments like electricity, cement, and metallurgy (Wei 2000).

However, electrostatic precipitators have the disadvantages of requiring a high initial investment, large space occupation, and a high cost of operation and management. It is not suitable to purify gas with high dust concentration directly by electrostatic precipitator because dust-containing exhaust gas with high-temperature loads stable corona charges only at high voltage conditions. There are also some other challenges in using electrostatic precipitators, such as insulation, electrode corrosion, and sensitivity to characteristics like dust particular resistance and gas composition. Moreover, using electrostatic precipitators calls for a very high quality of manufacture and installation, in which high voltage transformer and rectifier control devices are indispensable.

21.4.4 Filtration Collector

Filtration collector is a dust removal device in which dust-containing airflow comes through the filtration material, and dust is thus separated and captured. Bag style dust collector is a typical representative of filtration collector and applied most widely. Materials like cotton, wool, or man-made fibers are handled to textile and then used as filtering media in bag style dust collector to filter dust-containing gas. The filtration bag blocks particles in the smoke when the dust-containing gas passes the pores of filtering media, whereas clean airflow comes through the filtration bag and is discharged. Dust precipitated on the filtration bag is then detached from the filtering media surface using back flushing or vibration and then falls into the ash bucket. Since the blocked particles in smoke form a pancake filtering layer at the tiny meshes on the filtration bag surface (it seems like a "bridging" phenomenon), fine particles can be filtered effectively when the exhaust gas passes the pancake filtering layer. Thus, the dust removal efficiency of bag style collector can reach higher than 99 %, making bag style collector the most widely used dust removal method at present. The advantages of bag style dust collector include stable running performance, simple operation and maintenance, and multiple functions of capturing various dry clouds of dust. However, it has disadvantages such as a narrowly applicable temperature range. Also, phenomena like bag burning and break are easy to occur when the collector is employed to filter high-temperature smoke (Zhang and Li 2005).

The steel industry is a critical particle emission host. Particle treatment in steel industry must follow the comprehensive treatment principle. Reduction of power and resource consumption is one of the fundamental means to lessen the particle emission. This process should be improved, and advanced production devices should be employed to reduce the production of particles in the manufacturing process. Efficient dust removal devices should be applied so as to improve the treatment, recycling, and reuse of particles.

Steelworks adopt the corresponding control measures against the primary contaminant sources of particles. Detailed information is given in Table 21.5.

21.5 Development Directions of Particle Emission Control in Steelworks

Currently, the study of fine particle control technique in the world can be classified in two directions. One studies on efficient dust removal technologies, including the development of efficient dust precipitators and improvement of traditional dust precipitators. The other is the study of the aggregation techniques of fine particles, including applying external effects like electric field and magnetic field and adding chemical nucleating agents to aggregate fine particles to large particles.

Table 21.5 Main contaminant sources of particles in steelworks and the control measures

Procedure	Contaminant source	Control measure
Sintering	Sintering materials	Electrostatic dust removal, bag style dust removal
	Sintering machine nosing	Electrostatic dust removal, wet dust removal
	Sintering machine tail	Electrostatic dust removal, bag style dust removal, wet dust removal
	Product size stabilization	Electrostatic dust removal, bag style dust removal, wet dust removal
Coking	Loading coal	Removing smoke and dust on furnace top, removing smoke on furnace top + wet dust removal on the ground, removing smoke on furnace top + dry dust removal on the ground, dry dust removal on the ground, etc.
	Pushing coke	Dust removal using thermal buoyancy shield, wet dust removal on the ground, dry dust removal on the ground
	Coke dry quenching	Dry dust removal on the ground
	Sieving coke and transportation	Bag style dust removal
Iron-making	Blast furnace ore tank	Dust collector hood + electrostatic dust removal, Dust collector hood + bag style dust removal
	Blast furnace cast house	Dust collector hood + electrostatic dust removal, Dust collector hood + bag style dust removal
Steelmaking	Inversing bottle and pretreatment	Dust collector hood + bag style dust removal
	Primary smoke dust	BOF: OG, LT; EAF: dust collector hood + bag style dust removal
	Secondary smoke dust	Dust collector hood + bag style dust removal
	Refining	Bag style dust removal

21.5.1 Efficient Dust Removal Techniques

1. *Electrostatic precipitation-bag style filtration comprehensive dust collector*. Electrostatic precipitation-bag style filtration integral dust collector is a new dust removal method based on two developed dust removal theories (electrostatic dust removal and bag style dust removal). Electrostatic-bag style dust collector can be classified into three types according to composition style, as for electrostatic-back bag style, electrostatically enhanced the style and electrostatic-bag integrated style. The advantages of electrostatic precipitator and bag style dust collector such as high dust removal efficiency and excellent running reliability are integrated into electrostatic-bag style dust collector. However, considering that the coordination between the electrostatic collection zone and the bag filtration zone can hardly be maintained for a long time, the application of this technique is limited. Until now, the electrostatic-back bag style has been

employed in several coal-fired power plants with removal efficiency of higher than 99.9 %. However, since basic research is not sufficient, yet many critical problems have not been solved, so the running of dust collectors is still not stable enough.

2. *Electrostatic cyclone dust collector*. In electrostatic cyclone dust collector, cyclone capturing technique and electrostatic capturing technique are integrated organically. Dust is separated in the collector due to the effect of centrifugation as well as electrostatic force. Big particle size dust is captured by the cyclone effect whereas fine dust is captured by an electrostatic force field, and fixtures on the wall are cleared by the rapid spinning airflow which causes a flushing effect on the wall and collision effect between dust particles. Due to the advantages such as simple structure, low running cost, and high dust removal efficiency, electrostatic cyclone dust collector has been studied by many researchers in previous years. However, this technique remains at the mechanism exploring and performance research stage and has not been applied to industry at present.
3. *Electrostatic particle layer dust collector*. In electrostatic particle layer dust collector, an external electric field is imposed on the space in particle layer dust collector, which charges dust particles or filtering media. Thus, the particle coagulation and the filtration effect of particle layer are promoted, improving the removal efficiency of fine dust particles. Electrostatic particle layer dust collector has the advantages such as high-temperature resistance and high dust removal efficiency while the disadvantages of the system include rather high resistance, low filtration rate, and complicated dust cleaning procedure. Limited by the above factors, this technique remains at the experimental study stage.

21.5.2 Fine Particle Coagulation Techniques

1. *Electrostatic coagulation*. In the electrostatic coagulation process, due to different moving rate and direction, the dust particles collide one with each other and then nucleation occurs under the effect of the electrostatic force. The result of electrostatic coagulation depends on dust concentration, particle size, charge distribution, and the intensity of the external electric field. Based on the electrostatic coagulation mechanism, Australia Indigo Technology Co. Ltd. has developed the Indigo coagulation collector. The Indigo coagulation collector integrates the electrostatic effect and flowing process, which makes fine particles entering the collector adhere to larger particles, improving the fine particle removal efficiency of a traditional dust collector. This device has been employed by several countries in the world and has achieved favorable results.
2. *Sound coagulation*. In sound coagulation process, a high-frequency sound wave is applied to making the relative motion of fine aerosol particles so that the collision frequency in unit time is increased and fine particles are coagulated to large particles during a very short period. The removal efficiency of fine particles by the traditional dust collector can be improved by the sound coagulation effect.

Researchers from Southeast University, China, have intensely studied the kinetic characteristics and coagulation result of combustion-produced inhalable particulate matters under external sound field and obtained some innovative results. However, the application of this technique to industry is limited because of the high power consumption the lack of sound sources suitable for long-term use in high temperature, and the dusty environment.

3. *Magnetic coagulation*. Magnetic coagulation means the magnetized particles move against each other under the effects like magnetic dipole force and magnetic field gradient force, and then they coagulate with each other so that the particle granularity increases. After that, the coagulated particles are removed by a traditional dust collector. Fine particle removal efficiency of the traditional dust collector is thus improved. Until now, few studies on magnetic coagulation of ultrafine particles are reported, indicating the initial stage of research.
4. *Chemical coagulation*. Chemical coagulation means promoting the fine particle removal by adding chemical coagulation promotion agent. The main mechanism is the combination of physical adsorption and chemical reaction. According to the difference of adding the position of chemical coagulation promotion agent, this technique can be divided into chemical coagulation during combustion and chemical coagulation after combustion. Until now, few studies on chemical coagulation are reported. The existing few studies mainly focus on fine particle coagulation by usual substances like kaolinite and bauxite. Chemical coagulation is very effective in removing fine particles, and it can eliminate multi-contaminants simultaneously.

21.6 Suggestions on Smoke Dust Pollution Control in Steelworks

Promoting the Application of Advanced Dust Removal Techniques Reformation and consummation of environmental protection devices require a substantial capital investment, environmental protection investment per ton of steel in steelworks differs obviously in different countries. Therefore, steelworks in developing countries should further increase the environmental protection investment. Additionally, they should promote the application of advanced techniques such as stock yard dust inhibition, blast furnace gas dust removal by the dry process, converter gas dust removal by dry method, and coke dry quenching, so as to reduce the emission quantity of smoke dust.

Speed Up the Elimination of Backward Capacity Eliminating the backward capacity is the most direct measure for steelworks to reduce smoke dust emission. China's "National power saving and emission reduction planning during the 12th five-year" points that the steel industry needs to eliminate 48 million tons of backward ironmaking capacity and 48 million tons of backward steelmaking capacity. Until now, several steelworks in China have not yet eliminated much backward capacity on time, so they should quicken the elimination steps.

Developing Fine Particle Control Techniques Along with the increasingly improvement of environmental protection standards in countries worldwide, seeking high total dust removal efficiency only cannot meet the requirements of environmental protection. Low-cost efficient dust removal techniques and fine particle coagulation techniques should be developed, which is an important developing direction for future steelworks to control the smoke dust pollution. This will improve the filtration accuracy and capturing efficiency of fine particles.

Acknowledgments This work is partially supported by the Scientific Research Foundation for PhD of Liaoning Province, China (201501156) and the financial support from the item sponsored by National Special Fund for Environment Protection Research in the Public Interest, China (201409023). The authors also gratefully acknowledge the support and understanding of Prof. Pasquale Cavaliere, University of Salento, Italy.

References

Chen HJ (2006) Research on mechanism and performance of cyclone separator. Dissertation, Jiangnan University

Jia XY (2012) Treatment of 120 t BOF in Jinan Iron and Steel Company. Shandong Met 34(6):52–53

Kauppinen EI, Kappanen TA (1990) Coal combustion aerosols: a field study. Environ Sci Technol 24:1811–1818

Lighty JS, Veranth JM, Sarofim AF (2000) Combustion aerosols: factors governing their size and composition and implications to human health. Air Waste Manag Assoc 50:1565–1618

Ma JH (2009) Emission characteristics of particulates from typical production process of iron and steel enterprises. Dissertation, Southwest University

Shi Y, Dang XQ, Han XM, Wang D (2006) Characteristics & applications of electrostatic precipitator for sintering dust. Heavy Machinery 3:27–34

Wang YZ, Zhang DY (2006) Development trend of dust removal technologies in modern iron and steel industry. Met Environ Prot 6:14–17

Wang XY, Yan L, Lei Y (2014) Review on emission and control of particulate matters for iron and steel industry in China. Environ Sustain Dev 39(5):21–25

Wei JX (2000) Discussion on the research development of ESP. J Guangxi Univ 22(2):193–195

Yang MC, Wu SY (2004) Technology innovation of deposit to the taphole factory of the second blast furnace of Shougang puddling refinery. China Met 6:15–17

You WR (2013) Treatment of dust and flue-dust in coke plant. Hebei Met 4:74–75

Yu FL, Wang HT, Wang G, Zhang DY (2012) Smoke and dust reduction and recycle. Chemical Industry Press, Beijing

Yuan YP, Wang HN (2011) Study on efficient wet dust separator. Mining Res Dev 31(3):52–54

Zhang HX, Li M (2005) Development and application of bay filter dust removal. Environ Prot Saf 26(2):126–128

Chapter 22
Recent Progress and Future Trends of CO_2 Breakthrough Iron and Steelmaking Technologies for CO_2 Mitigation

M. Abdul Quader, Shamsuddin Ahmed, and Raja Ariffin Raja Ghazillaa

Abstract Iron and steel manufacturing is one of the most energy-intensive and CO_2 emitting industries in the world. In order to contribute to the prevention of global warming, the reduction of CO_2 from the steel works becomes a major issue imposed on the steel industry. A number of technologies have been developed in the past decade under worldwide CO_2 breakthrough program for the reduction of carbon emissions. This chapter focuses on present needs, recent progress, and future trends of energy efficient new iron and steelmaking technologies. This study presents a comparative analysis of CO_2 breakthrough programs including the present technological development and effects of application, economic feasibility, and environmental impact assessment. In addition, a brief analysis on ULCOS innovative ironmaking technologies has been done. Finally, significant CO_2 reductions can be achieved by combining a number of the available energy efficient technologies with Bio-CCS.

22.1 Introduction

The iron and steel manufacturing is one of the most energy- and carbon-intensive industries in the world. Iron and steelmaking processes are still mostly coal-based and thus highly dependent on fossil fuels, releasing substantial amount of fossil CO_2 (Abbasi et al. 2015). According to the Intergovernmental Panel on Climate Change (IPCC), the steel industry accounts for 6 % of the total world CO_2 emission.

M.A. Quader (✉)
Energy Lab, Faculty of Engineering, University of Malaya, 50603 Kuala Lumpur, Malaysia
e-mail: maquader.me@gmail.com

S. Ahmed
Department of Mechanical and Chemical Engineering, Islamic University of Technology (IUT), Dhaka, Bangladesh

R.A.R. Ghazillaa
Department of Mechanical Engineering, Faculty of Engineering, University of Malaya, 50603 Kuala Lumpur, Malaysia

P. Cavaliere (ed.), *Ironmaking and Steelmaking Processes*,
DOI 10.1007/978-3-319-39529-6_22

International Energy Agency (IEA) reported CO_2 emissions from manufacturing industry account for approximately 40 % of the total CO_2 emissions worldwide and iron and steel manufacturing industry contributes the biggest share of around 27 % of the global manufacturing sectors (Kasahara et al. 2012).

However, steel is considered to be one of the most important and useful metals in the world, and it continues to be the dominant material in global metal production. Therefore, controlling and reducing CO_2 emissions from this industry is now a pressing issue (Lin and Wang 2015). Over the last decade, a number of researches and development initiatives around the world under the 'CO_2 breakthrough Programs' (ULCOS,[1] AISI,[2] POSCO,[3] COURSE50,[4] etc.) have been investigated for carbon-free green and sustainable iron and steel production. The target is to develop CO_2 breakthrough technologies in combination with top gas recycling for the blast furnace (TGR-BF), direct reduction (DR) with electric arc furnace (EAF), iron ore electrolysis also called electro-winning (EW), carbon capture and sequestration (CCS) by using fossil fuels, biomass, hydrogen, and electricity as innovative reducing agents for the reduction process. Among all of these research programs, the Ultra-low CO_2 Steelmaking (ULCOS) is the most extensive research program with big budget. It is a consortium of 48 European companies and organizations from 15 European countries and is supported by European Commission. ULCOS consists of all major European Union steel plants, engineering partners, research institutes, and universities. It is divided into two phases: ULCOS I in 2004 and ULCOS II in 2010. It is proactively looking for solutions to the threat of global warming. The main aim of this massive project is to reduce CO_2 emission by at least 50 %, i.e., to reduce CO_2 emission from 2 t CO_2 per ton steel to 1 t CO_2 per ton steel production (Birat 2009a, b). In addition, for large scale industrial production it will develop potential and feasible ultra-low CO_2 steel production technologies that must be sustainable, i.e. environmentally friendly, economically viable, and socially acceptable.

This chapter illustrates the current development and future prospect of worldwide CO_2 breakthrough ironmaking technologies. This chapter, hopefully, will be useful for engineers, researchers, steel companies, policy makers, investors, and other interested parties to build sustainable green iron and steel industry.

22.2 Key Challenges for CCS Implement in Iron and Steel Industry

Having known the increasing importance of the development and deployment of CCS technology into the iron and steel industry, a large number of studies have focused on various issues. For instance, a technology strategy for reducing CO_2

[1] ULCOS = Ultra-Low CO_2 Steelmaking (EU).

[2] AISI = American Iron and Steel Institute with technology roadmap programme.

[3] POSCO = CO_2 Breakthrough Framework (Korea).

[4] COURSE50 = CO_2 Ultimate Reduction in Steelmaking process by innovative technology for cool Earth 2050.

emissions, socio-technical analysis, techno-economic and scenario assessment, hydrogen-based steelmaking, using biomass, technology selection, chemical absorption process modeling, physical adsorption process modeling and simulation with environmental impact assessment have been undertaken with respect to the implementation of different emerging ironmaking technologies with CCS. From these studies, and the IEA Greenhouse Gas R&D Program (IEA Greenhouse Gas R&D Programme) and CO_2 breakthrough program (i.e. ULCOS, AISI, POSCO, COURSE50, etc.), we can summarize some of the key challenges to the development of the CO_2 capture technologies for the iron and steel industry:

- to handle impurities, other than CO_2 in the flue gas stream;
- unlike power plants, where CO_2 is emitted from a single source, an integrated steel mill has multiple sources of CO_2 emissions from several stacks and occurs from the start to the end of iron and steel production;
- cost competitive and energy efficient CO_2 capture methods and processes;
- efficient, permanent, and cost-effective storage;
- effective design and operation of CO_2 transport systems; and
- implementation of CCS in steel production that requires a worldwide solution that would offer a level playing field—which is critical to make CCS in the iron and steel industry workable.

22.3 CO_2 Emission Sources in the Iron and Steel Industry

An integrated iron and steel mill consists of a number of complex series of interconnected plants, in which emissions are produced from many sources (10 or more) (Birat and Maizière lès Metz 2010). Large amounts of CO_2 are produced by the reduction reaction in the blast furnace and the combustion reaction of carbonaceous materials (coke breeze, etc.) and carbon-containing gases, such as blast furnace gas (B gas) and coke oven gas (C gas) in the sintering machine, coke ovens, and hot stoves. Thus, iron oxides are chemically converted into molten iron (Fe), which produces massive amounts of CO_2 and carbon monoxide (CO) as a by-product gas or blast furnace gas (BFG). The basic chemistry of the ironmaking processes is listed as the following equations (Germeshuizen and Blom 2013):

$$C + \tfrac{1}{2}O_2 \rightarrow CO$$

$$C + O_2 \rightarrow CO_2$$

$$Fe_2O_3 + 3CO \rightarrow 2Fe + 3CO_2$$

$$2Fe + O_2 \rightarrow 2FeO$$

$$Si + O_2 \rightarrow SiO_2$$

$$2\mathrm{Mn} + \mathrm{O}_2 \rightarrow 2\mathrm{MnO}$$

$$2\mathrm{P} + 5\mathrm{FeO} \rightarrow \mathrm{P2O}_5 + 5\mathrm{Fe}$$

$$\mathrm{CnHm} + \left(\mathrm{n} + \mathrm{m}/4\right)\mathrm{O}_2 \rightarrow \mathrm{nCO}_2 + \left(\mathrm{m}/2\right)\mathrm{H}_2\mathrm{O}$$

There are mainly eight direct emission points of sources grouped into two sections: (1) iron production (i.e., power plant stack, COG, blast furnace stoves, sinter plant stack, and lime kiln stack) and (2) steel production (i.e., BOF stack, hot strip mill stack, plate mill stack). The composition and volume of the exhaust gases for each emission point of the sources are different (Hasanbeigi et al. 2014; Ho et al. 2013). The proportion of CO_2 in flue gases (such as CO_2, N_2, O_2, H_2O, H_2 CO, CH_4, SOx, NOx) is different, based on the applied emerging technologies in the different routes of iron and steel production. Furthermore, other impurities that affect the capture process are also different in terms of CO_2 capture performance. Therefore, during the reducing process of pig iron production CO_2 technologies have to be implemented by the properties of the flue gases (Choi 2013) shown in Fig. 22.1.

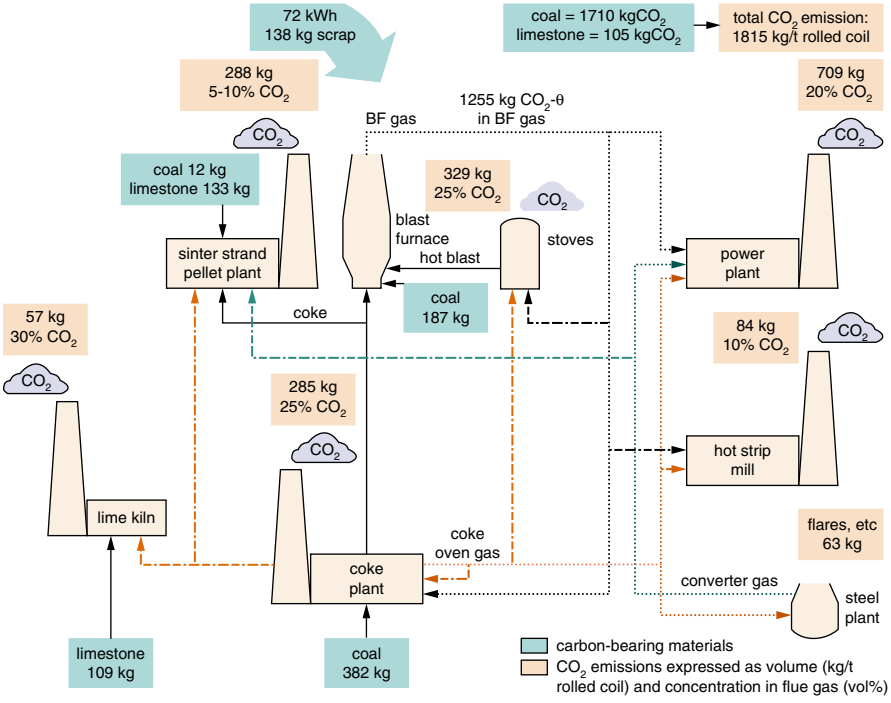

Fig. 22.1 CO_2 emissions from a typical iron and steel industry

22.4 CO_2 Breakthrough Programs

A number of programs along with ULCOS as a part of WorldSteel CO_2 breakthrough program and international Iron & Steel Association are working together to exchange knowledge and information for sustainable green iron and steel manufacturing. Extensive researches and investment are taking place in:

- The EU (ultra-low CO_2 steelmaking, or ULCOS I and ULCOS II)
- The USA (American Iron and Steel Institute)
- Canada (Canadian Steel Producers Association)
- Australia (BlueScope Steel/One Steel CSIRO coordination)
- South America (ArcelorMittal Brazil)
- Japan (Japanese Iron and Steel Federation)
- Korea (POSCO)
- China (Baosteel) and Taiwan (China Steel) and

COURSE 50 is a national CO_2 breakthrough program in Japan led by the Japan Iron and Steel Federation (JISF). It aims to decrease CO_2 emissions by around 30 % through suppression of CO_2 emissions from blast furnaces besides capture—separation and recovery of CO_2 from blast furnace gas (BFG) by launching a new amine scrubbing technology. The ready to use technology concepts would be available by 2030 and the final goal of industrializing and transferring the developed technologies by 2050. Moreover, POSCO (Pohang Iron and Steel Company) has also been developing an ammonia-based scrubbing CCS technology for the adaption to the FINEX and to the COREX processes (Birat 2010).

The USA started AISI (American Iron and Steel Institute) CO_2 breakthrough program organized by some top universities in the USA to promote carbon reduction in steel industry. It includes the use of several kinds of clean energy and development of CO_2 capture and separation technology. For example, high temperature electrolysis was examined at Massachusetts Institute of Technology (MIT), hydrogen reduction of iron ore in the laboratory, preparatory to transposing to a flash furnace reactor at Utah University, mineral sequestration at Columbia University, and CO_2 collection from EAF fumes using lime at Missouri Rolla University. According to the AISI CO_2 Breakthrough Program, two innovative technologies have been identified to cut CO_2 emissions: (1) Molten Oxide Electrolysis (MOE)—Reduction of iron ore through electrolysis. (2) Hydrogen Flash Smelting—Reduction of iron ore in a suspension, with hydrogen as a reducing agent (Table 22.1).

Table 22.1 Comparison among the projections for steel production in 2050

Source of estimates	Annual production (Mt/yr)	Comments
ULCOS-LEPII	2450/2550	POLES estimates
RITE	2200	Markal model
Tokyo University	1800	MFA model
IEA Blue Maps (low/high)	2350/2700	

However, Canadian program, run by Canadian Steel Producers Association (CSPA) and Arcelor Brazil separately has been developing biomass-based steel production. There are also ongoing programs in Australia (such as Bluescope + OneSteel consortium) and Taiwan (China Steel) which are either ambitious in terms of mitigation level or still at a conceptual level in academic work carried out in universities. Timeline of these programs is not published except ULCOS and COURSE-50. Besides, what is happening in China about CO_2 breakthrough program is not described clearly and India has decided to participate with the program, but not yet physically contributed (Chen et al. 2012).

All of these programs are similar to ULCOS program but they are less advanced in terms of developing breakthrough technologies and their progresses are not yet widely reported. A brief comparison among worldwide major CO_2 breakthrough programs is given in Table 22.2.

22.4.1 Ultra-Low Carbon Dioxide Steelmaking (ULCOS) Program

The EU CO_2 breakthrough program, ULCOS proposed a concept in terms of CO_2 breakthrough technologies as shown in Fig. 22.2. This triangle matrix explains how reducing agents and fuels can be selected from three possibilities such as carbon, hydrogen, and electrons. The mock ternary diagram represents all existing energy sources where coal is near to carbon on the carbon-hydrogen line, natural gas is near to hydrogen, and hydrogen from electrolysis of water is on the hydrogen-electricity line, etc.

The existing steel technologies are based on fossil fuels, i.e. mostly on carbon, natural gas, mix of carbon and hydrogen, and electric arc furnaces are shown in red boxes in Fig. 22.2. On the other hand, for CO_2 lean process routes, ULCOS has identified three major ways of solutions: (1) decarbonizing whereby coal would be replaced by hydrogen or electricity in hydrogen reduction or electrolysis of iron ore processes (2) CCS technology introduction, and (3) use of sustainable biomass are presented in yellow boxes in the diagram.

22.4.2 ULCOS CO_2 Breakthrough Technologies

From the beginning quite a few breakthrough technologies for the reduction of CO_2 emissions from iron and steelmaking industry have been investigated in the context of Ultra Low CO_2 Steelmaking (ULCOS) program. Finally, ULCOS has selected four process concepts that could lead to a drastic reduction of CO_2 emissions by more than 50 % compared to the present best practices. Those four cutting-edge technologies are: (1) Top Gas Recycling Blast Furnace with CO_2 Capture and

Table 22.2 A brief comparison among CO_2 breakthrough programs

Programs	Involving	Aim & target	Best result
AISI—technology roadmap programme 1 (US)	AISI and the US Department of Energy's (Doe), Office of Industrial Technology	Program designed to (1) increase energy efficiency, (2) increase competitiveness of North American steel industry, (3) improve the environment	(1) Suspension hydrogen reduction of iron oxide concentrate; (2) Molten oxide electrolysis
POSCO CO_2 breakthrough framework (Korea)	POSCO, RIST, POSLAB, POSTECH	Under framework contains six projects: (1) Pre-reduction and heat recovery of hot sinter, (2) CO_2 absorption using ammonia solution, (3) Bio-slag utilization for the restoration of marine environments, (4) Hydrogen production using COG and wastes, (5) Iron ore reduction using hydrogen-enriched syngas, and (6) Carbon-lean FINEX process	(1) CO_2 absorption using ammonia solution; (2) Carbon-lean FINEX process
COURSE50 (Japan)	Japanese iron and steel federation (JISF), Japan Ministry of economy, trade and industry	Development of innovative technologies for solving global environmental problems including R&D projects, public relations activities and promotes industry/institute cooperation.	(1) Scenario-making for global warming mitigation; (2) CO_2 separation, capture and storage; (3) CO_2 fixation by plants and its effective use
ULCOS—ultra-low carbon dioxide steelmaking-1&2 (EU)	All major EU steel companies, energy and engineering partners, research institutes and universities, European Commission	Cooperative R&D initiative to research rapid CO_2 emissions reduction from steel production including process science, engineering, economics and foresight studies in climate change	(1) Top gas recycling blast furnace with CO_2 capture and storage (CCS); (2) ISARNA with CCS; (3) Advanced direct reduction with CCS; (4) Electrolysis

Storage (CCS), (2) HIsarna with CCS, (3) ULCORED with CCS, and (4) Electrolysis. Additionally, hydrogen-based steelmaking and the use of biomass as reducing agent have been evaluated as supporting technology to decrease CO_2 emissions (Birat et al. 2010).

The ULCOS experiment and program structure has been illustrated in Fig. 22.3. The key strategies of ULCOS have been included in this program as described below.

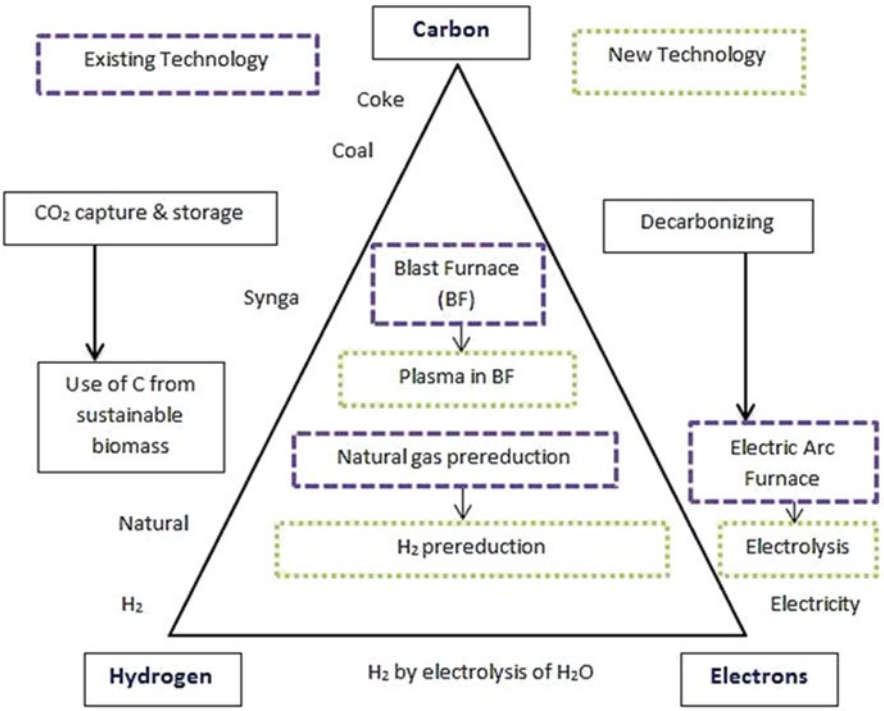

Fig. 22.2 Pathways of ULCOS breakthrough technology

22.4.2.1 ULCOS Blast Furnace Process (SP1 & SP2)

Blast Furnace (BF) is the most energy consuming process in integrated steel plants. So it is essential to reduce fossil CO_2 emissions from this process. ULCOS has invented top gas recycling blast furnace (TGR-BF) is a blast furnace gas separation technology for clean steel production. Top gas used to absorb CO_2 inside blast furnace acts as a reducing agent. It effectively reduces carbon emission around 50 %. The integrated use of TGR-BF and CO_2 capture and storage (CCS) technologies is helpful to remove nitrogen from the TGR-BF and oxygen injection into BF can also effectively recover CO_2. After extraction of CO_2 from recycled gas by using VPSA CCS technology, the cryogenic technique is applied to store. The following three different versions were tested:

- Version 4, the treated is a recycled gas in the main tuyeres and additional tuyeres located in lower stack at 12,500 and 9000 °C, respectively. The expected carbon saving is 26 %.
- Version 3, the treated gas is recycled through the main tuyeres only and expected carbon saving is 24 %.
- Version 1 has the same flow sheet like version 4 but the recycled gas is cold and expected carbon saving is 22 %.

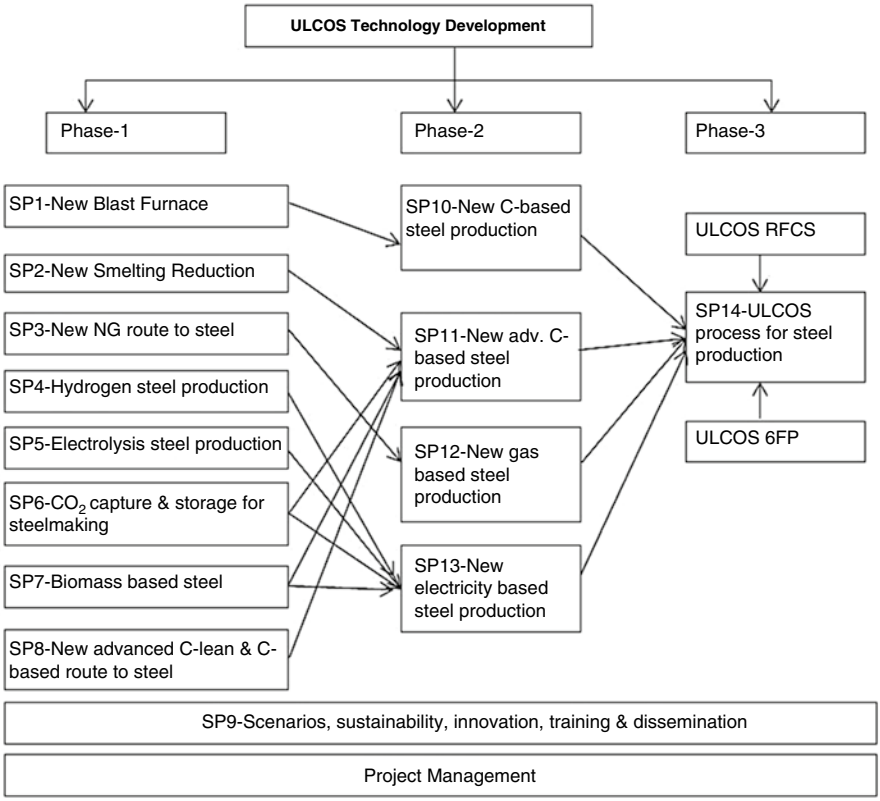

Fig. 22.3 ULCOS Program experimental setup and structure

In 2007 the first experiment was successfully done at LKAB's Experimental Blas Furnace (EBF) in Lulea, Sweden and it ran efficiently with high thermal stability, including up to 24 % CO_2 reduction. After this for the second phase ULCOS 2, EU invested hundreds of million euros for the promotion and planning of TRG-BF. It was successful, this technology will hopefully mitigate CO_2 emission of almost 1.5 Mt per year, i.e. about 1/3 for a BF (Fig. 22.4).

22.4.2.2 HIsarna Smelter

The HIsarna process is based on a modified version of the HIsmelt smelter technology. It is a concept using a combination of three new ironmaking technologies: (a) coal preheating and partial pyrolysis in a reactor, (b) melting cyclone for ore melting, and (c) melter vessel for final ore reduction and iron production.

HIsarna is a bath-smelting technology that combines coal preheating and partial pyrolysis in a reactor. It uses a smelter vessel for final ore reduction and a melting cyclone for ore smelting. By removing sintering and coking processes it reduces CO_2 emission. Moreover, by using biomass or natural gas instead of coal, process-

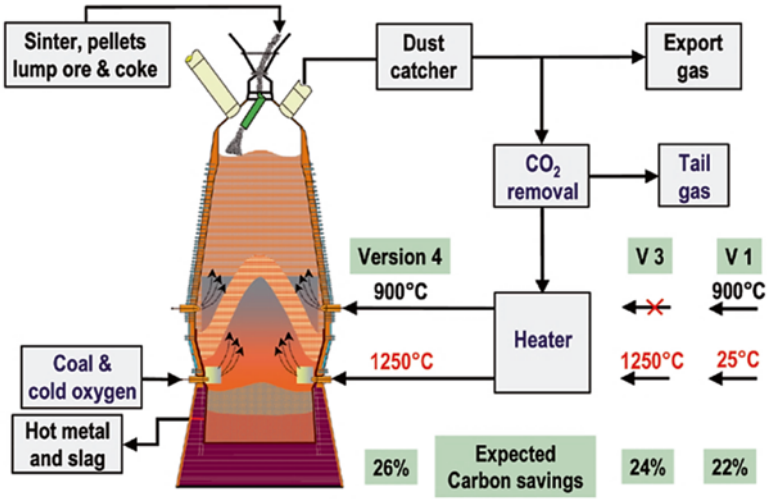

Fig. 22.4 Different types of the ULCOS Blast Furnace with process flow

ing combustion gases, storing CO_2, and recycling heat energy, HIsarna technology reduces almost 70 % CO_2 emission [45]. The benefits of the HIsarna process are

- Reduction of the CO_2 emissions per ton with 20 %
- Reduction of the CO_2 emissions per ton with 80 % if the process is combined with CCS
- Elimination of coke and sinter/pellet plant emissions
- Use of non-coking coal qualities
- Use of low cost iron ores, outside the blast furnace quality range
- Economically attractive even at small unit size (0.8–1.2 M thm/y)

A pilot plant of this technology was set up by TATA Iron and Steel Group of European Companies in Holland IJmuiden in September 2010 with 65 kt annual outputs under ULCOS II project Design output of TATA Steel HIsarna pilot plant is 8 t/h of hot metal. Ore and coal injection capacity is 8 and 15 t/h, respectively. However, if it is going to be successful, the technology will be used at a commercial level after 10–20 years (Fig. 22.5).

22.4.2.3 Direct-Reduced Iron with Natural Gas (ULCORED) (SP3)

The project ULCORED is built up for iron ore pretreatment especially for sintering and preheating. To produce direct-reduced iron (DRI) for sending to electric arc furnace (EAF) the reducing agent such as natural gas or biomass gas is used in a reactive level for the iron ore sintering process. In gas purification process traditional reducing agent is replaced by natural gas. Top gas recycling and preheating processes reduce natural gas consumption (Fig. 22.6). Using this technology, we can reduce 60 % CO_2 emission and also it is an economical and efficient process since natural gas is expensive.

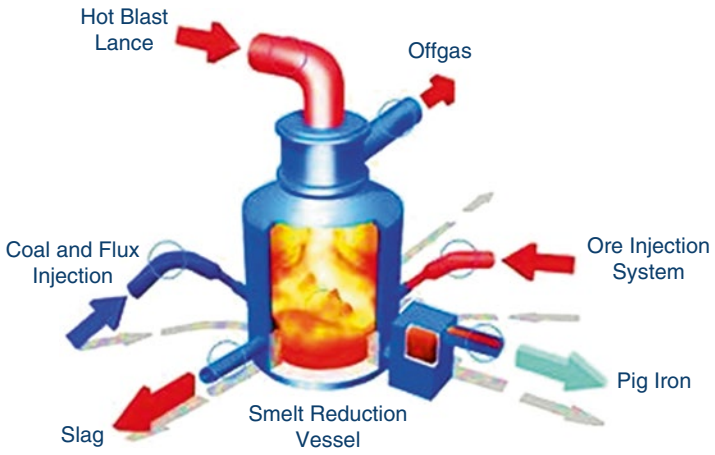

Fig. 22.5 Overview of HIsmelt smelter technology

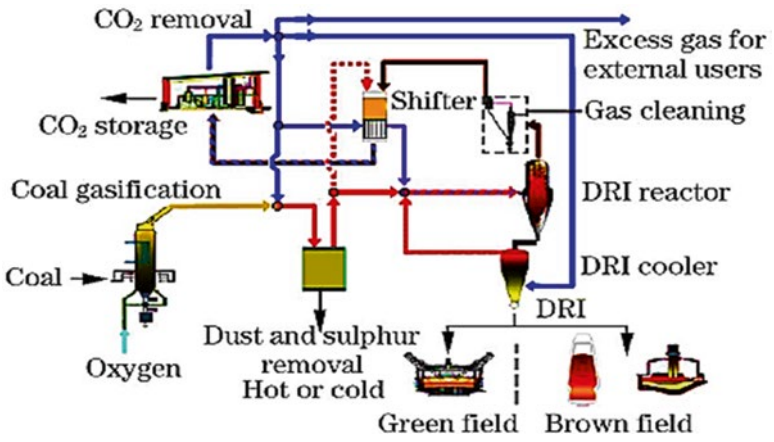

Fig. 22.6 ULCORED direct reduction process

22.4.2.4 Direct Electrolysis of Iron Ore (ULCOwin & ULCOlysis) (SP5)

The principle of the direct electrolysis of iron ore has been applied in ULCOWIN project, whose products are iron and oxygen with zero carbon emission. The ULCOWIN technology is different from other conventional smelting process which employs a new method for steel production. Its reaction temperature is around 110 °C where iron ore and iron are used as an anode and cathode precipitation, respectively. Electrolysis of iron ore does not emit CO_2 (Fig. 22.7).

Although its initial production rate is very low efficiency production efficiency, only 5 kg iron per day, but its cost is reasonable. Hence, the ULCOS team developed a process named ULCOLYSIS for melting iron ore at 16,000 °C by using electric direct reduction. This is the least developed technology in contrast with other three alternatives.

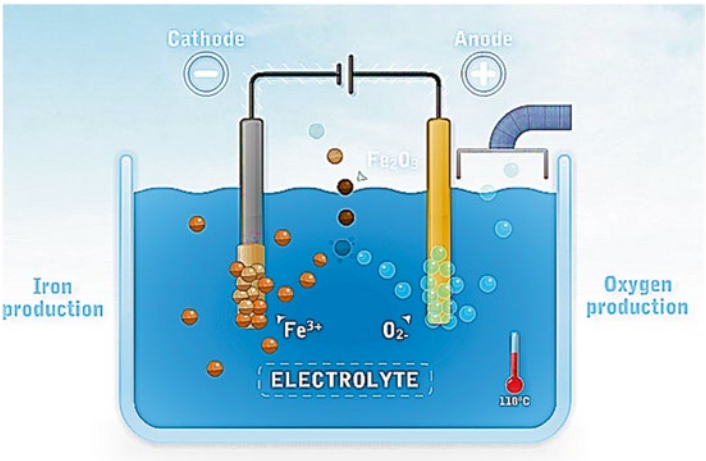

Fig. 22.7 Electrolysis of iron ore

22.4.2.5 Hydrogen-Based Steelmaking (SP4)

By hydrogen-based steelmaking route, CO_2 emissions would be reduced by more than 80 %. Hydrogen steelmaking will depend profoundly on the availability of green hydrogen. It can be generated from natural gas by steam reforming (SMR) or from water by electrolysis. Today hydrogen-based steelmaking is a potential low carbon and economically attractive route in a few countries where natural gas is cheap.

A few number of studies have been done focusing on utilization of hydrogen in industrial furnace, H_2 production from BFG (Blast Furnace Gas) and COG (Coke oven gas), nuclear hydrogen steelmaking system in different countries out of ULCOS. In 2013, Ranzani da Costa et al. proposed pure H_2 based steelmaking process by developing mathematical modeling where pure hydrogen (H_2) used as reducing agent in the direct reduction (DR) process. It might be the core process of a new and cleaner way to produce steel with lower CO_2 emissions. ULCOS studied a hydrogen-based steelmaking breakthrough route where H_2 would be generated by water electrolysis using hydraulic or nuclear electricity. In a shaft furnace, by using H_2 iron ore would be reduced to direct reduced iron (DRI) and carbon-free DRI would be processed in an electric arc furnace (EAF) to produce steel (Fig. 22.8). This route would be a promising breakthrough technology regarding CO_2 emissions up to 300 kg CO_2/ton steel, as well as the CO_2 cost of electricity, and emissions from the DR furnace almost zero. It shows an 84 % cut in CO_2 emissions compared to the current 1850 kg CO_2/ton steel of the best blast furnace route (Chen et al. 2012).

This new route would be a more sustainable way for iron and steel production. Nevertheless, its future development and deployment is largely dependent on the emergence of a so-called H_2 economy, when this gas would become available in large quantities, at competitive cost, and with low CO_2 emissions for its production.

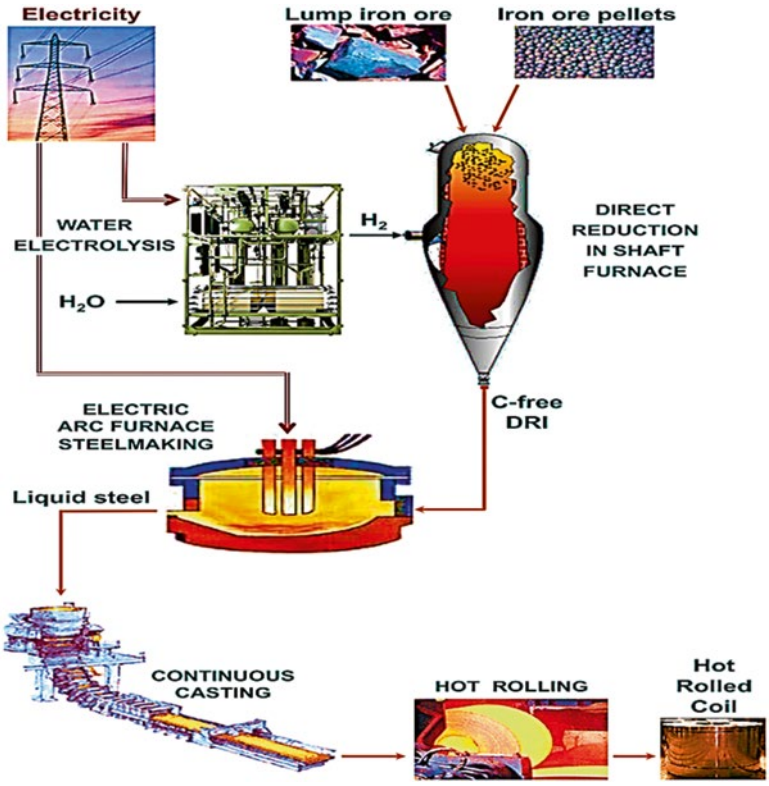

Fig. 22.8 Hydrogen-based steelmaking route

In addition, the uncertainties lay with the competition of other sectors for hydrogen consumption, for example, transportation sector would be ready to pay much higher prices for it than the steel industry.

22.4.2.6 Biomass-Based Steel Production (SP7)

Using biomass as a bioreducer in the blast furnace could be one of the processes to reduce the fossil CO_2 emissions of steelmaking. Biomass constitutes mainly carbon (C), hydrogen (H), oxygen (O), nitrogen (N), and sulfur (S) and 50 wt% (dry matter, dm) shear of carbon in the wood. The carbon content in the wood biomass is low compared to fossil fuels, for example coal, coke, or oil used in iron and steelmaking. Besides, the sulfur content is also low approximately 0.01–0.1 wt% (dm) which is advantageous for blast furnace ironmaking. The key challenges in using biomass whether it might be considered sustainable are: (1) the cultivation of biomass does not damage the environment in terms of deforestation, air and water pollution, and reduction of biodiversity (2) the use of biomass will not be occurring undesirable

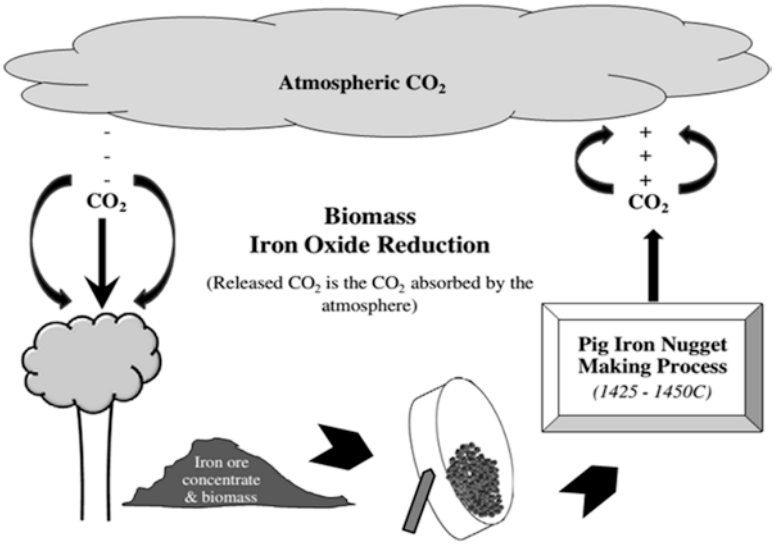

Fig. 22.9 The use of biomass as a reducing agent for ironmaking process

social and economic impact such as food price increment and removal of the original people from their land (Onarheim et al. 2015).

The most prospective solution for biomass production for the steel industry is charcoal by planting eucalyptus trees in tropical countries (e.g., Brazil or Angola). In Brazil eucalyptus plantation technology is mature and has advanced conversion process. A small size BF with 100 % charcoal is being run in Brazil (e.g., Acesita) and bringing a version of this technology to Europe is the challenge for ULCOS. However, it is difficult to sustain high hot strength of coke required in blast furnace when charcoal is added in the coal blend (Fig. 22.9).

22.4.2.7 ULCOS CCS Project (SP6)

Carbon capture and storage (CCS) presents one of the most promising options for large scale CO_2 emission reduction for the future. Iron and steel plants are suitable for CCS because emissions generated from single fixed and easily accessible points. In order to capture CO_2, it is needed to separate from flue gases from emission and then compressed and/or cooled and transported by pipelines network for underground storage.

ULCOS incorporated different CCS technologies in its ongoing experimental projects in Europe. A new CCS technology named VPSA (Vacuum Pressure Swing Adsorption) built by Air Liquide has been deployed in Lulea TGR-BF experimental project. For a larger scale experiment, a commercial blast furnace will be set up

under ULCOS II. In this plant the flue gases will be stored in deep saline aquifer where higher level of purity in CO_2 is required. By using cryogenics further purification of the steam would be done in the BF. Here, the optimized system consists of a combination of a PSA and of a cryogenics. ULCOS TGR-BF experiments show that chemisorption technologies such as amine scrubbing, physisorption, the VPSA or PSA and cryogenics have different fields of optimality. The level of CO_2 concentration of the gas stream to be treated in the TGR-BF for physisorption systems are the best in terms of technical performance and economical operation. It has also been efficient if CCS is applied in ULCORED (Siitonen et al. 2010). For HIsarna only a cryogenics unit is enough because it directly delivers a very-high concentration of CO_2. In contrast, if CCS is deployed in others stack of the steel mill, and then an amine scrubbing unit would be the best solution.

22.5 Conclusions

Although CCS is considered a promising solution for emission reduction, it contributes to reducing the overall efficiency of a steel plant due to the high energy consumption for solvent regeneration during capture processes. Therefore, combination of CO_2 capture and utilization (CCU) technologies with waste heat recovery from flue gas and molten steelmaking slag could be critical in the near-term to support longer-term objectives for deployment of CCS in steel industry from the year 2035 onwards. The utilization of CO_2 includes: CO_2 to fuels, enhanced commodity production, enhanced hydrocarbon production, CO_2 mineralization and chemicals production will produce a lot of profits, while CCS is an only waste mitigation technology. With CCU the CO_2 is converted to value added products.

However, hydrogen and biomass-based steelmaking also offer very attractive perspectives, while raising lots of major challenges. They will also require much research and development before they can be proven and implemented commercially. Finally, it is clear that CO_2 breakthrough technology has not fairly reached the level of being technology for the deployment in steel industry as it is still a concept that needs to be fleshed out and authenticated at a credible scale. Therefore, the initial gap and barrier for making this technology available, is the requirement of an enduring research and development effort through larger scale laboratory, pilot and demonstrator.

Acknowledgement The authors would like to extend their heartiest gratitude to the Ministry of Education, Malaysia for the financial support under the project of UM.C/625/1/HIR/MOHE/ENG/40- High Impact Research (HIR) Grant, Faculty of Engineering, University of Malaya, Malaysia.

References

Abbasi M, Farniaei M, Rahimpour M, Shariati A (2015) A feasibility study for synthesis gas production by considering carbon dioxide capturing in an industrial-scale methanol synthesis plant. Arab J Sci Eng 40(5):1255–1268. doi:10.1007/s13369-015-1598-9

Birat JP (2009a) Addressing the climate change challenge: ULCOS breakthrough program. Paper presented at the 157th ISIJ meeting, international organized sessions, environmental and energy technology/high temperature processes, Tokyo, Japan

Birat JP (2009b) CCS and the steel industry. Paper presented at the international conference on CCS regulation for the EU and China

Birat JP (2010) Carbon dioxide (CO_2) capture and storage technology in the iron and steel industry. Woodhead Publishing Limited. Cambridge, UK.

Birat J, Maizière lès Metz D (2010) Steel sectoral report. Contribution to the UNIDO roadmap on CCS1-fifth draft JP. Birat, Arcelor Mittal Global R and D, Maizières-lès-Metz, France

Chen WH, Lin MR, Yu A, Du SW, Leu TS (2012) Hydrogen production from steam reforming of coke oven gas and its utility for indirect reduction of iron oxides in blast furnace. Int J Hydrog Energy 37(16):11748–11758

Choi HD (2013) Hybrid life cycle assessment of steel production with carbon capture and storage. Institutt for energi- og prosessteknikk, 76

Germeshuizen LM, Blom P (2013) A techno-economic evaluation of the use of hydrogen in a steel production process, utilizing nuclear process heat. Int J Hydrog Energy 38(25):10671–10682

Hasanbeigi A, Arens M, Price L (2014) Alternative emerging ironmaking technologies for energy-efficiency and carbon dioxide emissions reduction: a technical review. Renew Sustain Energy Rev 33:645–658

Ho MT, Bustamante A, Wiley DE (2013) Comparison of CO_2 capture economics for iron and steel mills. Int J Greenhouse Gas Control 19:145–159

Kasahara S, Inagaki Y, Ogawa M (2012) Flow sheet model evaluation of nuclear hydrogen steel-making processes with VHTR-IS (very high temperature reactor and iodine-sulfur process). ISIJ Int 52(8):1409–1419

Lin B, Wang X (2015) Carbon emissions from energy intensive industry in China: evidence from the iron & steel industry. Renew Sustain Energy Rev 47:746–754

Onarheim K, Mathisen A, Arasto A (2015) Barriers and opportunities for application of CCS in Nordic industry—a sectorial approach. Int J Greenhouse Gas Control 36:93–105

Siitonen S, Tuomaala M, Ahtila P (2010) Variables affecting energy efficiency and CO_2 emissions in the steel industry. Energy Policy 38(5):2477–2485

Chapter 23
Manganese Emissions From Steelmaking

Donghui Li, Jack Young, Sina Mostaghel, and Kinnor Chattopadhyay

Abstract Manganese emission from pyrometallurgical furnaces is becoming an important issue with more and more stringent environmental restrictions on hazardous air pollutant (HAP) metals across the globe. Manganese is going to become the next pollutant in focus from 2016 onward. Mn emission from steelmaking or ferromanganese furnaces mainly depend on factors such as input load, gas flow rate, blowing practice, and finally the operating conditions of the dust capture systems which control particulate matter emissions. In the present study, several mechanisms of dust formation have been reviewed, and a manganese mass balance was performed to understand the distribution of Mn between liquid metal, slag, and dust for a few BOFs in operation. Operational parameters such as oxygen flow rate, blowing time, hot metal (HM) Mn content, scrap Mn content, end blow Mn%, and conditions of the electrostatic precipitator (ESP) were considered and correlated to plant measurements of Mn emission. Issues related to emissions from EAFs, ferromanganese furnaces, and high-Mn steels have been discussed as well.

Nomenclature

ESP	Electrostatic precipitator
HAP	Hazardous air pollutant
HM	Hot metal
LCA	Lifecycle assessment
LMF	Ladle metallurgical furnace
LRF	Ladle refining furnace
PM	Particulate matter

D. Li • K. Chattopadhyay (✉)
Department of Materials Science and Engineering, Process Metallurgy and Modeling Group (PM2G), University of Toronto, Toronto, ON, Canada, M5S3E4
e-mail: donghui.li@utoronto.ca; Kinnor.chattopadhyay@utoronto.ca

J. Young • S. Mostaghel
HATCH Ltd, 2800 Speakman Drive, Mississauga, ON, Canada, L5K2R7
e-mail: JYoung@hatch.ca; SMostaghel@hatch.ca

P. Cavaliere (ed.), *Ironmaking and Steelmaking Processes*,
DOI 10.1007/978-3-319-39529-6_23

23.1 Introduction

Manganese emission to the environment is becoming a major concern for all environmental regulatory bodies around the world, and stringent limits are being imposed. Manganese is among the trace elements least toxic to mammals; however, exposure to abnormally high concentrations, resulting from anthropogenic sources, has resulted in adverse human health effects related to neurotoxicity and may be possible reprotoxicity. Manganese poisoning is characterized by progressive deterioration of the central nervous system, sometimes accompanied by unrelated pneumonitis. The majority of cases have been associated with the breathing of manganese dust or fumes from mining and metallurgical operations. An outbreak of a form of pneumonia in inhabitants of Sauda, Norway, was attributed to manganese emissions from a ferromanganese furnace. Absorption via the gastrointestinal tract and through the skin has also been reported. An outbreak of manganese poisoning in Japan was attributed to ingestion of manganese-contaminated well water. In the early stages of poisoning, removal of the victim from the polluted environment usually clears up manganese; however, in chronic cases, the effects on the central nervous system are not completely reversible. Exposure to high concentrations of Mn may lead to Parkinson disease.

On the review of literature and environmental guidelines from different countries, it was found that the permit limits are very different in each country, and in most cases a local municipal permit limit applies which overrules the federal standards. Table 23.1 introduces some permit limits of manganese in air around the world. The USA has the strictest limit on manganese emissions in air.

The principal sources of ambient environmental pollution by manganese are emissions from metallurgical processing plants and reprocessing waste materials. Emissions to the atmosphere from industrial plants and processes will vary considerably, depending upon the process involved and the degree of control exercised. Manganese has been found in measurable amounts in practically all samples of suspended particulate matter collected by the National Air Surveillance Networks (NASN) from the air of some 300 urban areas. The highest concentrations, as expected, are found in the vicinity of ferromanganese alloy plants or related activities. The NASN urban average manganese concentration is less than 0.2 microgram per cubic meter ($\mu g/m^3$), but several cities have annual averages in the 0.5–3.3 $\mu g/m^3$ range. Occasional 24-hour concentrations as high as 14.0×10^3 $\mu g/m^3$ have been measured. Annual averages as high as 8.3 $\mu g/m^3$ have occurred in small communities located near a large point source in the highly industrialized Kanawha River Valley of West Virginia. In Norway, concentrations of over 46 $\mu g/m^3$ have been reported in the vicinity of a ferromanganese plant. Approximately 80 % of manganese in the suspended particulate matter from six large cities in the USA was associated with particles in the respirable size range—that is, 5 μm or less in diameter. The existence of manganese in the smaller particles favors a widespread distribution of this pollutant. Such distribution has been confirmed by the analysis of precipitation samples collected at many remote locations in the USA (Singh 2005; Vasu 2006).

It has been estimated that over 80 % of the total national manganese emissions in 1968 was from iron, steel, and ferroalloy production. Dust from the handling of raw materials in metallurgical processing and other production activities, such as the manufacture of chemicals, fertilizers, fungicides, and dry cell batteries, may result in local manganese pollution problems (1975). Table 23.2 shows the Mn emission factors for various ferrous and ferroalloy processes.

Table 23.1 Review of some permit limits of manganese in air around the world

Country	Regulatory body	Type	Element	Description of the limit	Value
Canada	Health Canada	Air	Manganese	Reference concentration to which the population could be exposed for a lifetime without appreciable risk of adverse health effects	0.11 μg/m^3
USA	Environmental Protection Agency (EPA)	Air	Manganese	Reference concentration	0.05 μg/m^3
Global	World Health Organization (WHO)	Air	Manganese	Recommended air quality guideline values—TWA—for individual substances based on effects other than cancer or odor/annoyance using an averaging time of 1 year (annual)	0.15 μg/m^3

Table 23.2 Mn emission factors for various ferrous and ferroalloy processes (Singh 2005)

Process	Factor	Unit
Mining	0.09	kg/ton of Mn ore mined
Mn metal	11.36	kg/ton of Mn processed
Mn blast furnace	10.86	kg/ton of FeMn produced
Si-Mn	31.55	kg/ton of SiMn produced
Ironmaking blast furnace	10.22	kg/1000 tons of hot metal produced
BOF	35.45	kg/1000 tons of steel produced
Electric furnace	35.45	kg/1000 tons of steel produced
Welding rods	7.27	kg/ton of Mn processed
Nonferrous alloys	5.45	kg/ton of Mn processed
Batteries	4.54	kg/ton of Mn processed
Chemicals	4.54	kg/ton of Mn processed
Coal	3.5	kg/ton of coal burned

Emissions from oxygen steelmaking furnaces are in the form of solid filterable particulate matter and condensable gasses. One of the largest sources of filterable particulate matter (PM) and hazardous air pollutant (HAP) metals is the BOF electrostatic precipitator (ESP) during the oxygen blowing period, and a feasible option for reducing these emissions is to upgrade the ESPs to improve emission control performance. Consequently, reducing the filterable PM emissions from these sources would result in co-control of HAP metals. Feasible controls have been demonstrated at several steel mills in North America, Europe, and Japan. These mills use hoods exhausted to bag houses to capture emissions that occur when the blast furnace is tapped and when the BOF is charged and tapped. An efficiently designed and operated fume control system can achieve a reduction of 95 % or more (from the uncontrolled case) in HAP metal emissions from these sources. Review of historical test data suggests that, if variability in operating parameters is minimized and if the ESPs perform consistently at their lowest measured emission rates, emissions could be reduced by 50 % or more from current operating levels.

Manganese has been listed as one of the top hazardous air pollutant (HAP) metals by environmental regulatory boards in Europe and North America. In a recent report by RTI international (Vasu 2006), it is seen that in the Detroit area, manganese tops the list among all HAP metals at 13 t per year with much lesser quantities of nickel, chromium, and lead. Table 23.3 shows the exact numbers. Because of the high temperatures of steelmaking operations (1600 °C), the more volatile metals are removed and concentrated in the PM. The primary metal HAP is manganese, which was reported in an EPA survey as about 1 % of the BOF dust. Other analyses of BOF dust averaged 1.1 % manganese, 0.74 % lead, 0.03 % chromium, and 0.01 % nickel. BOF slag contains about 4.3 % manganese, 0.001 % each lead and nickel, and 0.1 % chromium.

23.2 Theoretical Considerations

23.2.1 Mechanisms of Dust Formation During Steelmaking

There are several hypotheses for the mechanism of dust formation in basic oxygen furnaces (BOFs). They are direct hot metal vaporization, hot metal/slag ejection by CO bubble bursting, metal/slag ejection by mechanical action of the impinging

Table 23.3 Total HAP metals emissions from two steel works and one coke battery

HAP metal	Total emissions ton/year	HAP in $PM_{2.5}$ ton/year
Mn	13	7.2
Pb	1.9	0.7
Ni	0.04	0.01
Cr	0.2	0.1
Hg	0.4	0.4
Total	15.5	8.4

oxygen jet, and entrainment of solid particles during top charging. It is difficult to say which is the dominant mechanism, but studies indicate that the mechanism changes during the blow time. Vaporization typically occurs due to local hot spots that are generated by highly exothermic reactions during oxygen blowing in the BOF process. Various studies indicated that the local hot spot temperature could be in the range of 2100–3050 °C (Goetz 1980). When fume particles are formed entirely by the condensation of vapors, then the highly volatile elements (e.g., Mn) get enriched in the fume. In the temperature range of 1400–2100 °C, the vapor pressure of Mn is 100–1000 times higher than that of iron; hence, analyses of fumes produced solely due to vaporization show Mn/Fe ratios in the order of 30–150 times compared to the Mn/Fe ratio in the bath. The dust particles formed as a result of the vaporization mechanism can be identified by their octagonal ($FeFe_2O_4$) or rhombohedral (Fe_2O_3) shape.

The other mechanism is dust formation by hot metal/slag ejection by CO bubble bursting or mechanical action of the impinging jet. In either case, the dust particles are spherical in shape. Also, the Mn/Fe ratio in the fume is almost equal to the Mn/Fe ratio in the bath as there is no vaporization involved. In reality, BOF dust is formed by a combination of both mechanisms and that can be tracked by plotting the Mn/Fe ratio in fume to the Mn/Fe ratio in bath with blowing time. Goetz (1980) in his studies indicated that large ratios imply a mechanism of direct vaporization, whereas a low ratio indicates metal/slag ejection as the mechanism of dust formation. Figure 23.1 shows a typical Mn/Fe ratio plot with blowing time.

Evidently, metal/slag ejection by CO bubble bursting or mechanical action is the dominant mechanism of dust formation at the beginning of the blow. However, toward the end of the blow, vaporization becomes more dominant. This finding of 1980 was also reconfirmed by Tsujino et al. (1989) in 1989, Nedar (1996) in 1996, and Gritzan and Neuschutz in 2001. Nedar also concluded that 60–70 % of the dust

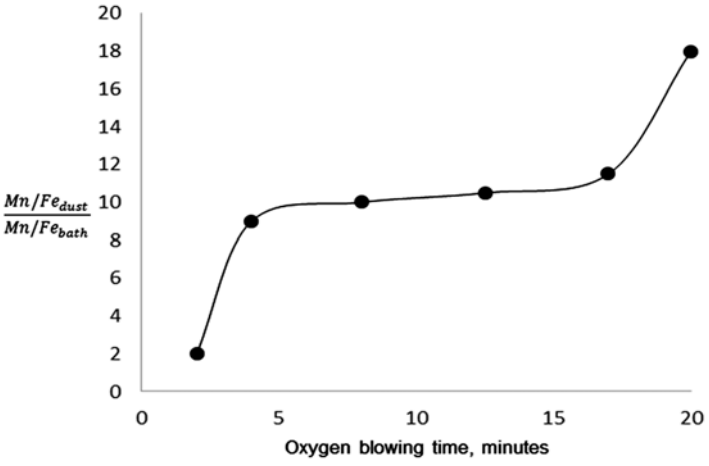

Fig. 23.1 Variation of Mn/Fe ratio of the dust over that of the bath with blowing time

is formed by metal/slag ejection (bubble bursting) mechanism, whereas other mechanisms contribute to the rest 30 %. Gritzan and Neuschutz (2001) also advocated for metal/slag ejections to be the primary mechanism for dust generation in BOF operations.

Based on Mn/Fe ratios, Goetz (1980) summarized that the amount of BOF dust generated by vaporization mechanism during the decarburization period is about 1.8 % by weight, whereas the degree of vaporization during preignition and re-blow is about 10 %. So it can be concluded that direct vaporization during the re-blow and preignition periods is about five times larger than that during decarburization period of the blow. However, the major mechanism of fume formation remains that of metal/slag ejection and bubble bursting.

Another probable cause of dust generation is top charging of lime during the blowing period. However, it is seen that top charging increases the dust generation rate only momentarily, i.e., it only affects the instantaneous dust generation rate and not on the total amount of dust generated. The possible reason for momentary increase in dust generation rate during top charging is because the slag layer collapses due to solid lumps falling upon the slag. On the other hand, the early period of lime charging takes place before the slag starts to foam, and it is during this period that the increase in dust generation is particularly strong. Also, the top charged material are usually rough surfaced solid lumps which act as nucleation sites for CO bubbles and enhances bubble bursting and dust generation momentarily. Goetz, in his thesis, also discussed the effect of bath temperature and bath carbon content on fuming rates in a BOF. For a fixed carbon content, the lower the bath temperature (lower the superheat), the greater the metal/slag ejection and hence higher the fume rate. Lower bath temperatures also result in lower slag temperature and higher slag viscosities, which impedes the formation of a stable foamy slag cover and helps in entrapping a part of the metal ejections. This also results in higher fume rates. It can also be inferred that all parameters which contribute to stable foaming in the slag can reduce the dust emission rates from the furnace. Based on the extensive research effort conducted by Fruehan and his team (1995), a higher viscosity and lower density and surface tension of the slag lead to formation of foams with more height, which are also more stable and last longer, hence reducing the emission rates from the furnace.

The dust generation rate in the BOF decreases rapidly with blowing time. Goetz showed some typical curves (Fig. 23.2) to represent dust generation rate versus blowing time in an experimental BOF.

The general trend of a decreasing dust generation rate with blow time was confirmed in all cases of normal practice, and this phenomenon has been repeatedly reported in literature (Gritzan and Neuschutz 2001) (Figs. 23.3 and 23.4).

Figure 23.5 shows the dust generation rate as a function of top-blown oxygen flow rate during the middle stages of the blowing (one fourth to three fourth blowing period) in a 250 and 300 t BOF with combined blowing practices (Tsujino et al. 1989). Higher flow rates of oxygen results in increased dust generation rate.

There is a direct relation between the dust generation rate and carbon content of the melt and this has been reported by several investigators (Knaggs and Slater

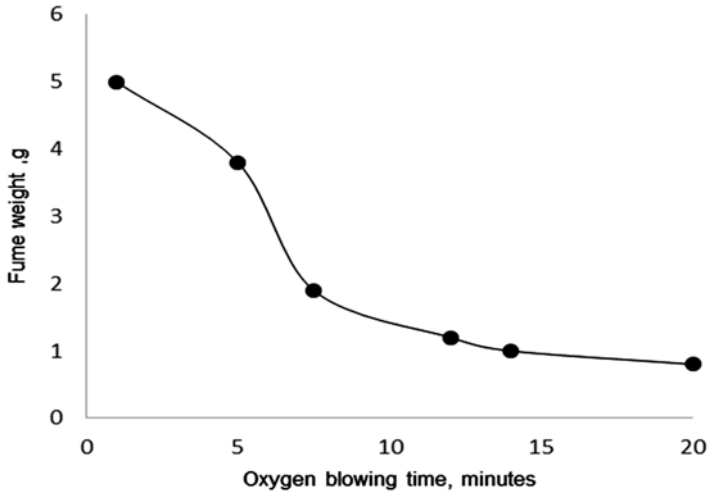

Fig. 23.2 Fume weight versus blowing time (Goetz 1980)

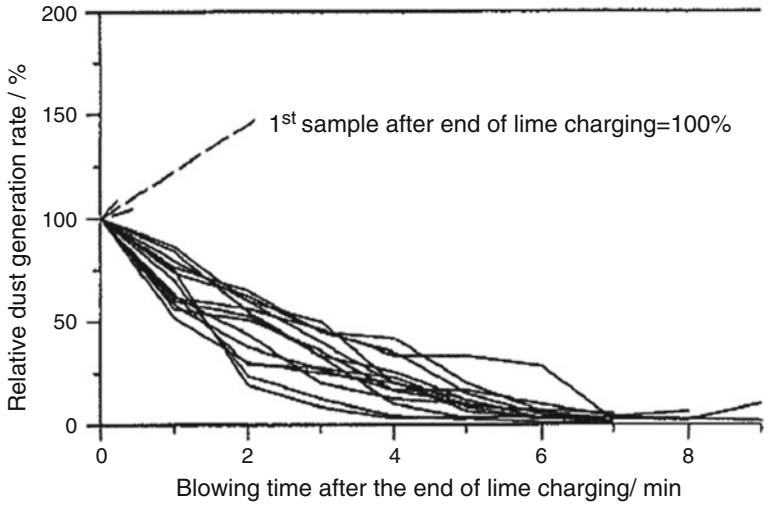

Fig. 23.3 Relative dust generation rate versus blowing time in a 200 t BOF at ThyssenKrupp Dortmund (oxygen flow rate was constant throughout the blow period)

1959; Turkdogan and Leake 1959; Ellis and Glover 1971; Ohno et al. 1986; Herwig 1995). In fact, the only variable that changes with blow time is the carbon content of the bath. Gritzan and Neuschutz (2001) based on their observations explained the steady decrease of dust generation rate with blowing time in a BOF. At the beginning of the blow, due to high momentum and velocity of the oxygen jet impinging on the melt surface, large quantity of splashes are formed and ejected into the gas atmosphere above the melt. The droplets are greater than 10 mm, i.e., much larger

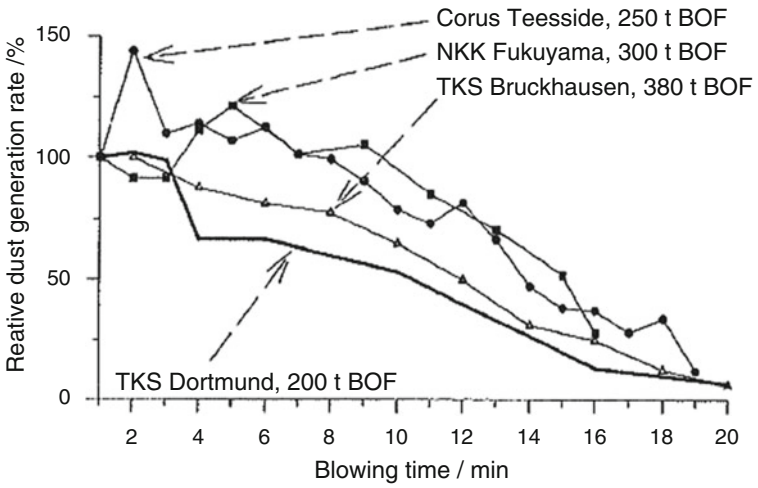

Fig. 23.4 Relative dust generation rate versus blowing time for different vessel sizes (oxygen flow rate was constant throughout the blow period)

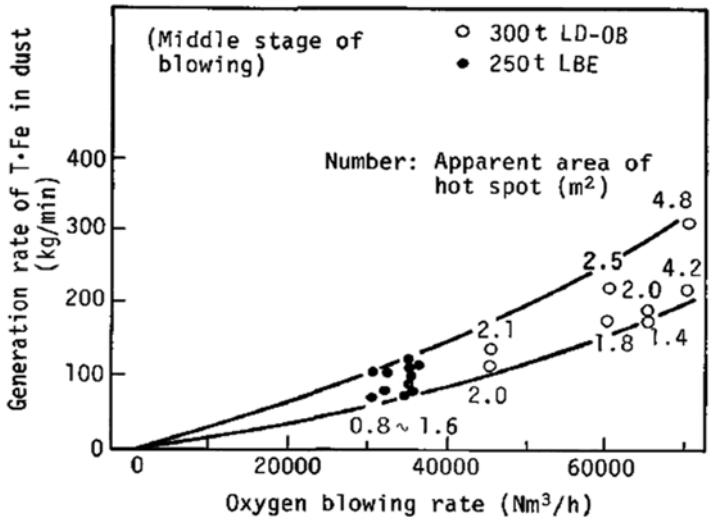

Fig. 23.5 The dust generation rate as a function of top-blown oxygen flow rate during the middle stages of the blowing (one fourth to three fourth blowing period; combined blowing was performed)

than dust particles. Most of the splashes/droplets return back to the melt after a parabolic flight. As long as they contain sufficient carbon, their liquidus temperature is relatively low, and so they remain liquid during the entire flight time. In that state, the droplets rapidly dissolve oxygen, which reacts with carbon to form CO bubbles inside the droplets/splashes. The CO bubbles rise to the splash surface, burst, and

form smaller film and jet droplets, which are immediately carried away by the off-gas. Now the liquidus/solidus temperatures of these splashes will rise steadily with blow time as the carbon content of the melt decreases. With lower carbon content the formation of a solid shell around the splash starts earlier in its flight above the bath. Then, the rapid dissolution of oxygen into the liquid splashes is restricted to a shorter period of time. This reduces the overall dust generation rate. With increasing blowing time, a stable layer of slag forms on the top surface of the melt, which also entraps most of the droplets formed by CO bubble bursting. Therefore, the overall, dust generation rate decreases with blow time.

23.2.2 Size Distribution and Chemistry

Since this chapter's focus is on manganese, the dust chemistry was reviewed in terms of Mn, MnO, and Mn/Fe ratio content in BOF dust. Some observations were also reported on dust particle size range and its relationship to dust chemistry. Goetz (1980) reported on dust chemistry from industrial BOFs. The fume particles that result from vaporization are either hexagonal or octagonal in shape and exist over a limited size range of 0.05–0.2 μm in diameter. Fumes resulting from vaporization also have a very high concentration of volatile elements like Mn (50–150 times) than the bulk bath from which it originated. On the other hand, the dust particles which are formed by the process of metal spray/ejection are spherical in shape and exist over a larger size range from 0.05 to 5 μm in diameter. In these dust/fumes, the concentration of Mn is the same as that in the bulk. Krichevtsov (1970) reported on the evolution of fume chemistry with blowing time. From Krichevtsov's calculations, the average Mn/Fe ratio in the fume is around 0.033. In a BOF, the majority of the manganese is oxidized in the first few minutes of the blow, and then the Mn level in the bath ranges between 0.15 and 0.3 depending on the initial hot metal Mn content. Assuming the Fe content of the bath greater than 95 %, the Mn/Fe ratio in the bath is 10–15 times lower than that in the fume. From Krichevtsov's results, the calculated Mn content of the fume ranges between 0.9 and 3.3 %. These calculations were used and the evolution of Mn content in the dust with blow time is plotted in Fig. 23.6. It is clearly seen that the Mn content in the dust is not constant and varies along the blow period. The major chemical components of BOF dust are (FeO_x), CaO, MgO, and MnO.

Nedar (1996) reported on dust chemistry based on his tests on a 100 t BOF operation at SSAB Tunnplat AB, in Luleå, Sweden. He showed that Mn levels vary significantly in the two stages of the blow. The first part of the blow was for 7 min, while the second part lasted for another 6–10 min.

From a previous study by Laciak (1977) based on an operation at ArcelorMittal Dofasco, the Mn% in the fume versus blow time was also plotted and is shown Fig. 23.7. Average Mn/Fe ratio in the fume is 0.46/61.7 = 0.007, whereas for the second part of the blow, it is 1.16/66.9 = 0.017 which is almost 2.5 times higher. So the dust is enriched with manganese in the second stage of the blow.

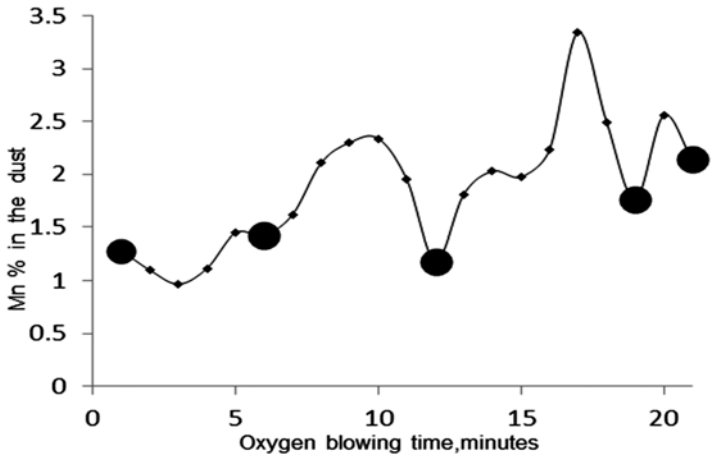

Fig. 23.6 Variation of Mn% in BOF dust with blowing time (the *black circles* are the times at which lime were added)

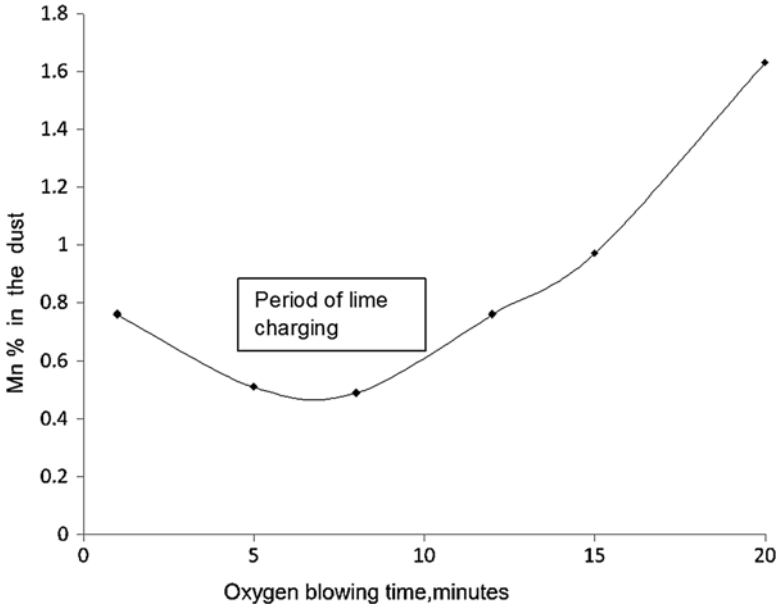

Fig. 23.7 Variation of Mn% in BOF dust with blowing time

Gritzan and Neuschutz (2001) reported on dust size and chemistry from their studies on a 200 t BOF operating at ThyssenKrupp, Dortmund. The Mn content of the dust varies between 0.077 and 0.38 wt%. A typical size distribution of the dust particles is shown in Fig. 23.8. The observed size distribution breaks down to four distinct classes with their individual maxima at 1, 12, 50, and 140 μm. The particle size distribution did not vary significantly with blowing time or with top charging.

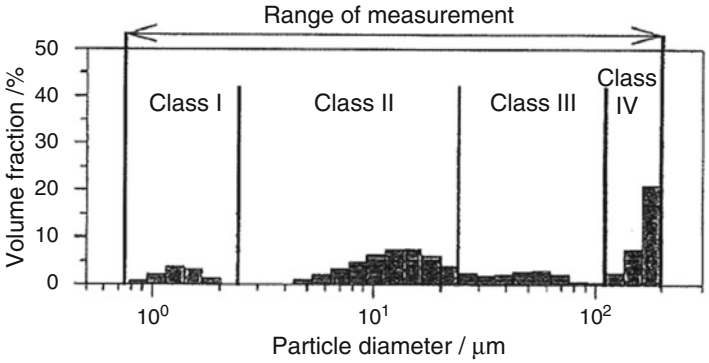

Fig. 23.8 Particle size distribution from the dust samples as reported by Gritzan and Neuschutz (2001)

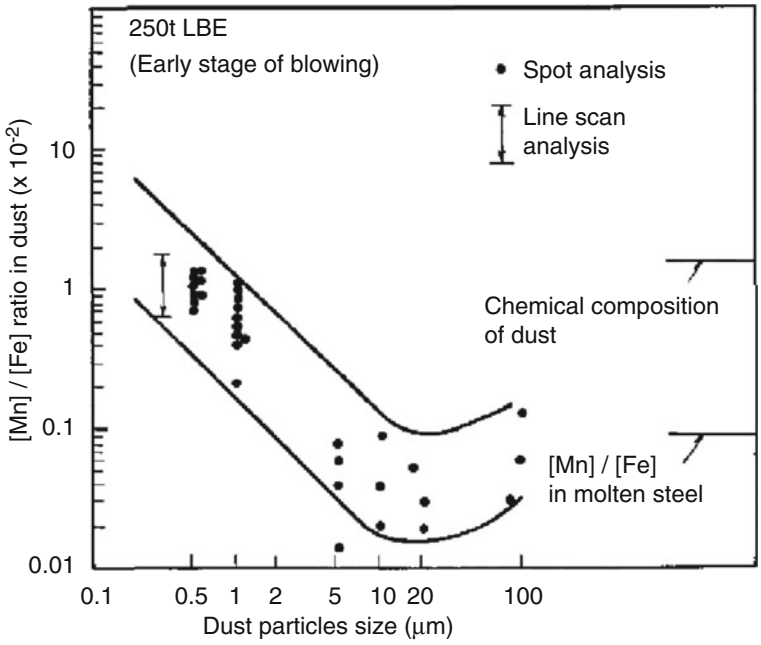

Fig. 23.9 Relation between Mn/Fe ratio in the dust and dust particle size (early stage of blowing)

Tsujino et al. (1989) reported on dust composition and size range from their studies in 175, 250, and 300 t BOFs with minimum slag practice. Figures 23.9 and 23.10 show the Mn/Fe ratio in the dust versus particle size for the early stages of blow and the end of the blow, respectively. When the dust particle size is as fine as 5 μm or less, the smaller the dust particle size, the higher is the Mn/Fe ratio. The Mn/Fe ratio in dust whose particle size is 1 μm or less is about 5–20 times as much as that in the

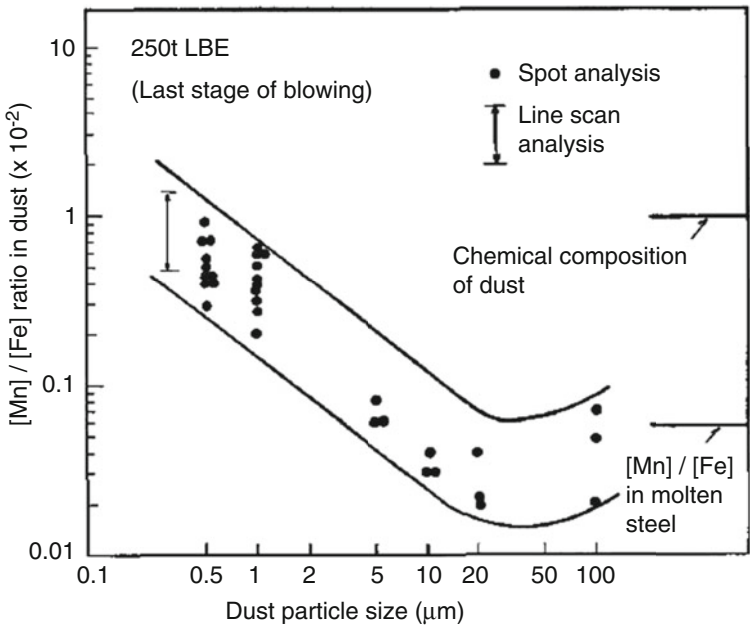

Fig. 23.10 Relation between Mn/Fe ratio in the dust and dust particle size (later stage of blowing)

melt. Also, with respect to dust having particle size of 5–10 μm, the Mn/Fe ratio in dust is lower than that in the bath, which is minimum for all particle sizes. When the particle size becomes larger, the Mn/Fe ratio in dust is approximately equal to that of the bath. At any dust generation rate, the smaller the dust particle size, the higher the concentration of Mn in the dust.

23.2.3 Factors Affecting End Blow Mn Content

The major operational parameters that influence the end blow manganese behavior in the BOF are hot metal manganese input, slag volume, oxidation level, and temperature (Dias Barao et al. 2008). Manganese oxidation in the BOF occurs by either direct oxygen or by indirect oxidation via FeO. The manganese oxidation reaction is exothermic implying lower equilibrium constant values with increasing temperatures. So from a thermodynamic point of view, higher temperatures would lead to larger amounts of Mn recovery. However, manganese recovery is also affected by dissolved oxygen content. At the end of the blow, dissolved oxygen content is higher, and this leads to manganese oxidation. Manganese oxidation is mainly dictated by lower temperatures, increasing FeO content and increasing the activity coefficients ratio of FeO and MnO. For a given slag composition and a known blow

temperature profile, the theoretical manganese partition can be calculated at every instant during the blow. Figure 23.11 shows the variation of Mn partition with blowing time. It shows a good degree of fitting starting from the second period of blowing (approximately at 40 %, when the oxygen lance height is increased, and the oxygen flow rate is reduced), meaning that from this moment on, the manganese oxidation is controlled by slag/metal reaction and FeO oxidation. Figure 23.12 shows the relationship between hot metal Mn content and end blow Mn concentration from data collected from ten steel plants in Brazil. There is definitely an increase

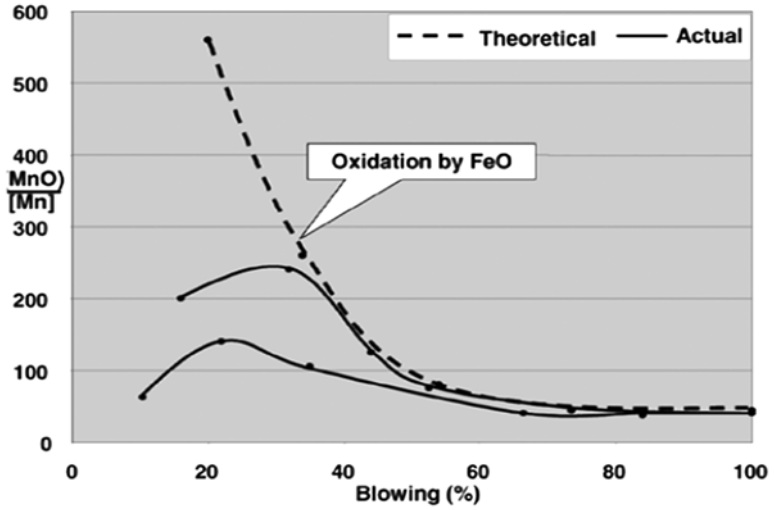

Fig. 23.11 Variation of Mn partition with blowing time (linear time dependence of temperature was assumed)

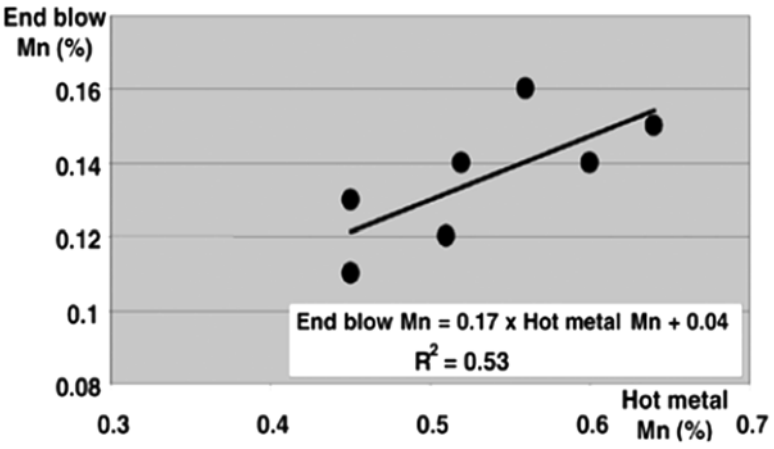

Fig. 23.12 Hot metal Mn concentration versus end blow Mn content

in end blow manganese concentration if hot metal Mn content is high. It is evident that only a small fraction (17 %) of the hot metal manganese is recovered in the steel. The influence of hot metal Mn content on end blow Mn is higher at higher carbon contents. The slag/metal manganese partition ratio decreases for increasing hot metal manganese content. The higher the temperature, the smaller the slag/metal manganese partition ratio; this effect adds up to the effect of hot metal manganese content. The effect of hot metal Si on end blow Mn is not disturbed by the oxidation level, and it is lesser than the effect of hot metal Mn content. Several factors that influence the Mn partition between slag and metal are FeO and CaF_2 contents of the slag, and temperature (Jung et al. 2002). The Mn distribution ratio increases with FeO content linearly in the FeO concentration range of (6–25 mass %). The Mn partition ratio decreases with increasing CaF_2 content in the slag. However, most plants do not use CaF_2 due to the environmental issues.

Detailed data analysis was performed at a BOF shop in North America with two BOFs in operation, and similar trends on end blow Mn were observed. The results are presented in Fig. 23.13 (Chattopadhyay et al.).

23.3 Results and Discussion

23.3.1 Mn Emissions From BOFs

One of the major reasons for increased focus on Mn is the quality of the raw materials including iron ore pellets and scrap. The BOFs are usually receiving higher Mn hot metal than before, and this is obviously related to high-Mn hot metal production

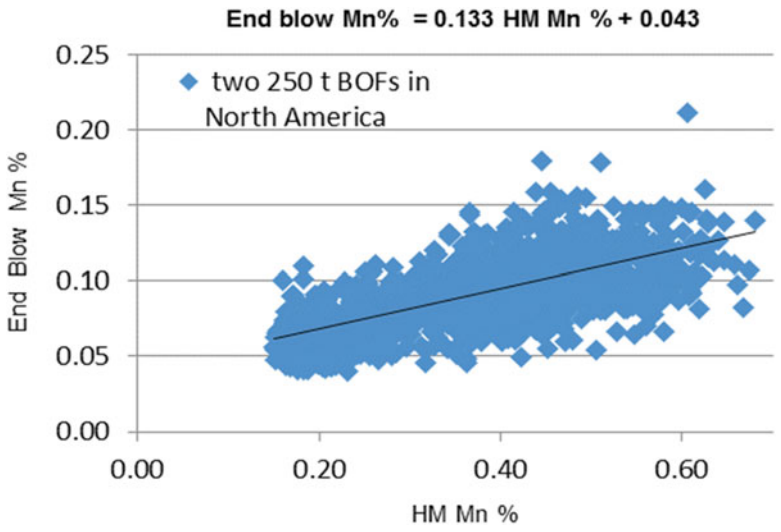

Fig. 23.13 Manganese concentration in the end blow as a function of hot metal Mn content for two North American BOFs

at the blast furnaces. As the iron ore mines are digging deeper and deeper into the earth's crust, the Mn content of the ore keeps on increasing. Figure 23.14 shows the trend for an iron ore mine in North America.

Plants operate with varying levels of hot metal Mn (AIST 2012), and this is illustrated in Fig. 23.15. HM Mn concentration can range between 0.2 and 1.0 wt% and depending on the Mn input load, the amount of Mn in the dust and fumes will be affected based on the partition ratio. Some data from steel plants were considered for the Mn mass balance analysis and the details are shown in Table 23.4. The mass balance was performed based on plant data, including steel and slag analysis and ESP dust analysis and stack test data. It is clear from Table 23.5 that for BOFs, 25–28 % of the Mn goes into the liquid steel, 69–71 % into the slag as MnO, and

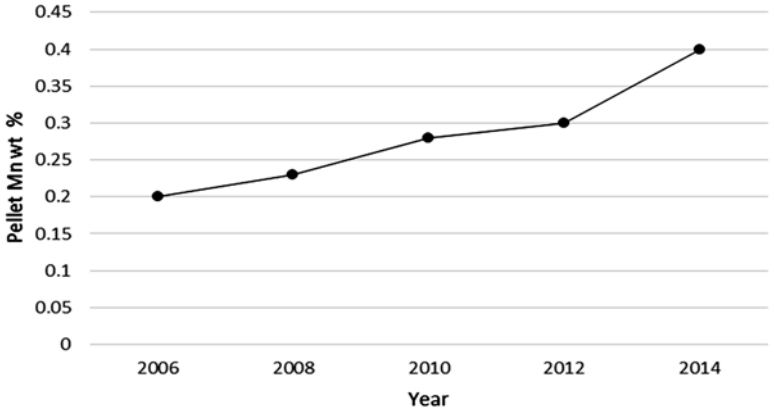

Fig. 23.14 Increase in Mn content of the pellets over the past decade

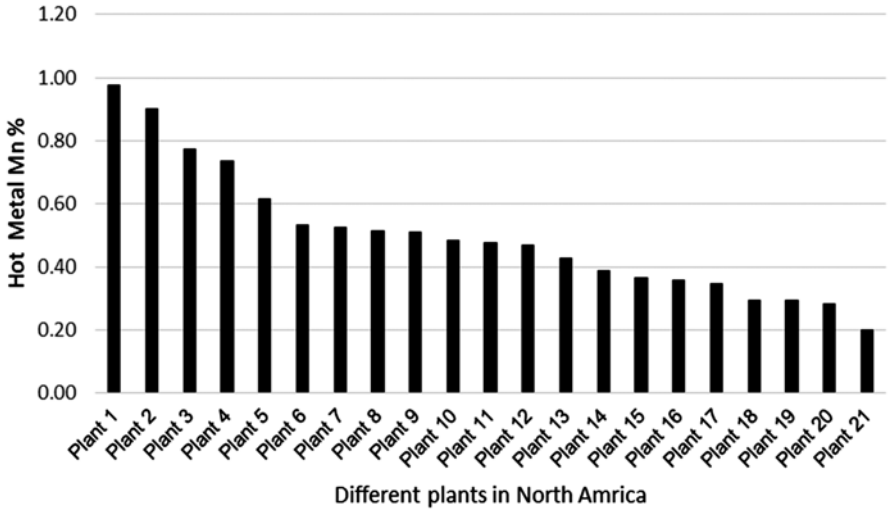

Fig. 23.15 Different levels of Mn in hot metal (AIST 2012)

Table 23.4 Manganese concentration in hot metal for plants considered

	HM Mn wt%
Range for BOFs in North America	0.2–1 %
Range for BOFs in Brazil	0.4–0.7

Table 23.5 The distribution of Mn among liquid steel, slag, and dust/fumes

	% of Mn in *outputs*		
	Liquid steel	slag	dust
Average of two BOFs in North America	28	69	3
Average of BOFs in Brazil	25	71	4

Table 23.6 PM and Mn emission rates from different ESPs

	Mn kg/h	Permit limit kg/h	PM in kg/h	PM permit limit kg/h
ESP with minimal maintenance	0.15	0.046	10	23
Upgraded ESP	0.06	0.046	6	23
Upgraded and well maintained ESP	0.04	0.046	3.5	23

Table 23.7 HM Mn % versus dust Mn %

HM Mn wt%	Dust Mn wt%	Ratio
0.28	0.45	1.61
0.44	0.68	1.55
0.45	0.83	1.84
0.49	0.86	1.76
0.52	0.90	1.73

3–4 % goes into the dust. Of course these partition ratios vary depending on the furnace operating conditions including temperature and partial pressure of oxygen. Considering the highly oxidizing nature in BOF furnaces, it is expected to have more Mn in the slag.

About 3–4 % of Mn goes into the dust for BOFs, most of the dust should be captured by the ESP system. A good ESP that is well maintained can easily prevent Mn emissions by capturing most of the solid dust particles. Data was collected from a steel plant and PM and Mn emission rates (kg/h) were correlated with ESP operating condition. A summary of which is presented in Table 23.6.

Table 23.7 shows the ratio between the Mn% in the dust to the hot metal Mn%, and the ratio is fairly constant for various hot metal Mn levels. It ranges between 1.5 and 1.9.

23.3.2 *Manganese Emission From High Mn Steels and Other Pyrometallurgical Processes*

Most steel grades contain only about 0.5–1.0 % manganese, which as discussed above by itself is a safety and environmental concern. Obviously, production of Mn-rich ferroalloys (i.e., ferromanganese or silicomanganese) or specialty high-Mn alloys (e.g., twinning induced plasticity (TWIP) or transformation induced plasticity (TRIP) steels) can emit more Mn to the atmosphere (if not controlled).

Recently, Paymandar et al. (2014) have investigated the interfacial reactions between slag and high manganese and aluminum alloy steels between 1500 and 1550 °C. They experimentally measured the manganese loss due to evaporation from four different steel compositions: V1, 17%Mn-1.5%Al; V2, 22%Mn-1.5%Al; V3, 22%Mn-3%Al; and V4, 17%Mn-3%Al. They have concluded that the total manganese loss from these steels can be between 0.59 and 1.8 % of the total manganese content (Fig. 23.16), which is significant and necessarily needs to be controlled.

Emission of Mn from high-Mn ferroalloys is also a significant concern. High-carbon ferromanganese, which is primarily produced in submerged-arc electric furnaces, contains up to 80 wt-% Mn and 7.5 % carbon. The recovery of Mn in the alloy is about 70–80 %; the remainder reports to slag as MnO or to the off-gas as Mn-containing species. The slag generated during FeMn production may contain as high as 42 wt-% Mn and is used to produce silicomanganese, containing 12.5–18.5 wt-% silicon and ~65–68 wt-% Mn, which will in turn be used for to alloy low-carbon steel.

Hatch and the International Manganese Institute (IMnI) have recently completed the first life cycle assessment (LCA) of global manganese alloy production. The study considered 17 manganese mines and smelters providing a standard measure of average environmental performance for the release of greenhouse gasses, particulate

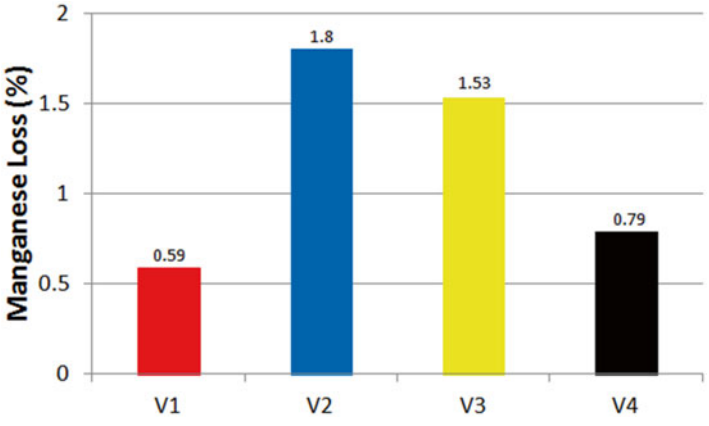

Fig. 23.16 Manganese loss by oxidation and evaporation from different steel compositions

matter (PM), NO_X and SO_X, as well as water and energy consumption and waste generation (Westfall et al. 2015). In this analysis, the LCA supply chain has been grouped into the following categories, which also represent sources of Mn emission:

1. Mineral extraction and hauling.
2. Ore processing, beneficiation, and delivery.
3. Sinter production and delivery.
4. Smelting (furnace production), in all three types of electric arc furnace, i.e., open, semi-open, and sealed. This unit process is the major source of Mn emission. To address this issue, the following controlling equipment have been used:
   - Fabric filters with particulate capturing efficiency of over 99 %
   - High-pressure-drop venturi scrubbers with particulate capturing efficiencies between 94 and 98 %
   - Wet scrubbers, including both multistage centrifugal scrubbers and venture scrubbers, with particulate removal efficiency of 99 %
5. Metal casting, crushing and screening, materials handling, and other auxiliary smelter activities.

The United States Environmental Protection Agency (EPA) (1985) has derived emission factors for ferromanganese production furnaces, assuming an average Mn ore grade of 45 % and production of 80 wt-% Mn FeMn, listed in Table 23.8.

Most of the alloying in steel is done at the LRF, and thus it is important to see the partition ratio of Mn in the LRF. Data was collected from two LRFs in operation at a steel plant in North America. These particular LRFs had a very low oxygen level as Al was added in majority of the heats. Because of low oxygen potential, very little Mn was lost in the slag as MnO. Table 23.9 shows the distribution of Mn in the LRF. It is clearly seen that 99 % of the Mn is retained in the liquid steel, 0.78 % goes into the slag and 0.001 % goes into the dust. The stirring energy and oxygen potential is very little at the LRF when compared to the BOF. As the major mechanism of Mn emissions is by CO bubble bursting and mechanical action, these results are very reasonable.

Table 23.8 Emission factors derived for ferromanganese production furnaces

Source		Mn emission factor kg/ton of ore processed/metal produced
Raw material processing	Receipt and storage of Mn ore	0.45
	Crushing and sizing	0.45
	Weighting and feeding	0.4
Smelting (uncontrolled)	Open furnace	6.6
	Semi-sealed	2.6
	Sealed	9.6

Table 23.9 Distribution of Mn in the ladle refining furnace (LRF)

	Wt (lbs)	Mn%	Wt of Mn (lbs)	% Input
Input				
Incoming steel ladle	506,017	0.21	1,062	60.22
Ferroalloys added	780	90.00	702	39.78
Total Mn input			*1,764*	
Output				
Mn in liquid steel	500,000	0.35	1,750	99.22
Dust	Based on dust generation rate and treatment time		0.02	0.001
Mn going in LRF slag	The balance		13.8	0.78
Total Mn output			*1,764*	

23.3.3 Manganese Consumption

The manganese consumption in the steel industry is not projected to increase substantially in the next 10 years, estimated consumption per ton of crude steel will remain at ~7 kg/t. Some new steel grades with higher Mn are being developed; however, it is not anticipated that these products will have a significant impact on the overall Mn consumption rate. There are some other TRIP and TWIP steel grades with Mn levels in excess of 20 % which are being developed for small niche products; however, special continuous casters are required to cast such product, and this will not have a significant impact on overall Mn consumption. Overall crude steel production is projected to increase in the next 10 years; the expected annual growth rates in steel are ~3.0 % which will ultimately translate into an overall increase in manganese consumption. To put this into perspective, the projected annual increase in crude steel production is 45 million ton per year, which will impact Mn consumption. Increased BOF steel production will increase the consumption of higher Mn-containing iron ores, which can potentially increase the Mn emission levels from the BOF if environmental systems are not maintained properly. However, the majority of the increased Mn associated with this increase in steel production will be in ferroalloys added typically when the steelmaking furnaces are tapping or subsequently at secondary ladle metallurgy facilities (ladle furnaces and vacuum degassers). Emissions associated with these manganese additions should be captured by the secondary emission systems at the steelmaking furnace or with fume capture equipment at the secondary treatment facilities.

23.4 Conclusions

Mn emission is a concern because of its detrimental effects related to neurotoxicity and perhaps reprotoxicity. The steel industry is one of the major sources of Mn emissions, and in today's scenario, the raw materials have more Mn content in them

than before. The higher Mn content in the ore is attributed to the increased amount of Mn in the earth's crust, as it is being mined deeper and deeper. The higher Mn in the ore results in higher Mn in the hot metal which in turn causes the problem of Mn emissions during basic oxygen steelmaking. The dominant mechanism of Mn emission in the BOF is by mechanical action due to the supersonic jet, as well as CO bubble bursting, due to high oxygen potential. The results show that as the hot metal Mn is increased, the Mn in the slag and dust have also increased proportionally. For a BOF, typically 25–30 % Mn is retained in the steel, and 65–70 % goes into the slag, and around 3–4 % goes into the dust. However, it is not a concern as long as the off-gas cleaning systems are well maintained. This study showed that, for an upgraded and well maintained ESP, the stringent permit limits can be achieved.

Emission of Mn from high-Mn ferroalloys is also a significant concern: High-carbon ferromanganese, which is primarily produced in submerged-arc electric furnaces, contains up to 80 wt-% Mn and 7.5 % carbon. The recovery of Mn in the alloy is about 70–80 %; the remainder reports to slag as MnO or to the off-gas as Mn-containing species.

When alloying is performed at the LRF/LMF, the conditions are significantly different. The oxygen potential and the stirring energy at the LRF/LMF are way lower than the BOF, and hence retention of Mn alloy in the steel is almost 99 %, and very little ends up in the emissions. Therefore, for the production of high-Mn steels, majority of the alloying should be performed at the LRF/LMF, resulting in little Mn dust emission.

References

AIST (2012) Internal report, Ironmaking Committee

Chattopadhyay K, Johnson D, Young J, Vieira J, Bachenheimer S, Kumar S (2014) Evaluation of air emissions in steel plants with focus on heavy metals emission. AISTech 2014, Indianapolis

Dias Barao C, da Silva CA, da Silva IA (2008) Analysis of parameters affecting end blow manganese content at oxygen steelmaking. La Reveue de Metallurgie 105:556–561

Ellis AF, Glover J (1971) Mechanism of fume formation in oxygen steelmaking. J Iron Steel Inst 209:593–599

Goetz F (1980) The mechanism of B.O.F. fume formation. Dissertation, McMaster University

Gritzan A, Neuschutz D (2001) Rates and mechanisms of dust generation in oxygen steelmaking. Steel Res 72:324–330

Jung S-M, Rhee C-H, Min D-J (2002) Thermodynamic properties of manganese oxide in BOF slags. ISIJ Int 42:63–70

Knaggs K, Slater JM (1959) Some factors affecting fume evolution in molten steel during oxygen injection. J Iron Steel Inst 193:211–216

Krichevtsov E (1970) Special operating procedures during the blowing of high-phosphorus hot metal in the ld-ac shop at the huckingen works of Mannesmann AG. Stal 2:113–118

Laciak S (1977) A study of the kinetics and mechanisms of materials ejection from a basic oxygen furnace. Dissertation, McMaster University

Nedar L (1996) Dust formation in a BOF converter. Steel Res 67:320–327

Ohno T, Ono H, Okajima M (1986) Pure steel droplet ejection. Trans ISIJ 26:B-312

Paymandar M, Schmuck S, Schweinichen P, Senk D (2014) Interfacial reactions between slag and melt in the new world of high manganese steels. EPD Congress, TMS Annual meeting

Schurmaan E, Polch A, Pfilipsen HD, Herwig U (1995) Chemical-composition, generation mechanism and formation rate of converter dust. Stahl und Eisen 115:55–61
Scientific and Technical Assessment Report on Manganese (1975) Program Element No. 1 AA001 ROAP No. 26AAA, US EPA
Singh VP (2005) Toxic metals and environmental issues. Sarup & Sons, New Delhi
Tsujino R, Hiral M, Ohno T, Ishiwata N, Inoshita T (1989) Mechanism of dust generation in a converter with minimum slag. ISIJ Int 29:291–299
Turkdogan ET, Leake LE (1959) Preliminary studies on the evolution of fumes from iron at high temperatures. J Iron Steel Inst 192:162–170
U.S. Environmental Protection Agency (1985) Locating and estimating air emissions from sources of manganese, U.S. EPA Report No. EPA-450/4-88-007h
Vasu A (2006) RTI report, U.S. Environmental Protection Agency, pp 36–50
Westfall LA, Cramer MH, Davourie J, McGough D, Ali M (2015) In: 14th International Ferroalloy Congress, INFACONXIV, Ukraine, pp 626–635
Zhang Y, Fruehan RJ (1995) Effect of the bubble size and chemical reactions on slag foaming. Metall Mater Trans B 26B:803–812

Chapter 24
Potential of Best Available and Radically New Technologies for Cutting Carbon Dioxide Emissions in Ironmaking

Volodymyr Shatokha

Abstract Transition to a low-carbon economy requires modernisation of the iron and steel industry. Improvement of energy efficiency of blast furnace ironmaking, development of new and rapid commercialisation of currently developed innovative ironmaking technologies and deployment of carbon capture and storage/utilisation technologies are required to reach sustainability targets. Four scenarios with various combinations of energy efficiency enhancement and different market penetration of breakthrough ironmaking technologies have been developed and analysed. Deployment of the best available technologies is indispensable though not sufficient for cutting CO_2 emissions to an extent required by the climate change mitigation targets established by the International Energy Agency. Increased share of secondary steel produced via EAF method using gradually decarbonised electricity also is a prerequisite for substantial cutting of CO_2 emissions. Rapid and wide commercialisation of currently developed innovative ironmaking technologies after 2020 allows for reaching emission levels consistent with the targets up to 2030–2040, depending upon the market penetration. However, in the following years even in the most radical modernisation scenario, new impulse is needed to align CO_2 emissions with sustainability targets. Hydrogen-based ironmaking, enhanced material efficiency, greater share of secondary steel production and CCS/CCU technologies can play the role of such impulse. Delayed and limited mitigation actions will result in much greater amounts of CO_2 emitted to atmosphere with unavoidable impact on climate.

V. Shatokha (✉)
National Metallurgical Academy of Ukraine, Dnipropetrovsk, Ukraine
e-mail: shatokha@metal.nmetau.edu.ua; shatokha@gmail.com

P. Cavaliere (ed.), *Ironmaking and Steelmaking Processes*,
DOI 10.1007/978-3-319-39529-6_24

24.1 Introduction

Reducing carbon dioxide emissions becomes increasingly important driver behind the technology advancement of the iron and steel industry under emerging paradigm of industrial transformation towards meeting the climate change mitigation targets (Rynikiewicz 2008).

Iron and steel industry is responsible for 6.7 % of all global anthropogenic CO_2 emissions (Worldsteel Assoc. 2015a). In the EU its share in total industrial CO_2 emissions is 21 % (Croezen and Korteland 2010). In the countries where iron and steel sector plays more dominant role in the economy, its share is more essential—e.g., 30.6 % in Ukraine (Shatokha 2015). Therefore, cutting CO_2 emissions in the iron and steel industry is indispensable for reaching the climate change mitigation targets. Ambitious 2DS[1] of the International Energy Agency (IEA 2014) envisages reduction of CO_2 emissions in the iron and steel industry (including cokemaking) by 28 % in 2050 compared to 2011 is envisaged despite an expected increase in crude steel production by 51 % within the same period. This target is difficult to reach, and the fact that the 2DS contradicts both historical and current development trends in this industry has been noted (IEA 2014).

In Fig. 24.1 the statistic data on crude steel production and total CO_2 emissions, calculated using CO_2 intensity data (Worldsteel Assoc. 2015a) for the period from 2003 (a year starting from which global data for CO_2 emissions are being collected by Worldsteel) to 2014, are shown together with the IEA model for the period of 2020–2050 based on low-demand and high-demand variants of 2DS (IEA 2014). Steel production growth decelerates in both IEA variants but—to some extent—

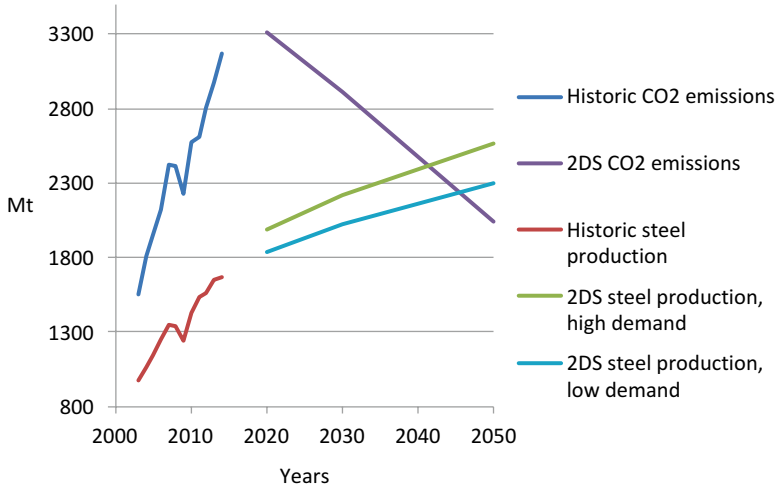

Fig. 24.1 Data on crude steel production and CO_2 emissions: historic and predicted in IEA 2DS

[1] A scenario where global warming shall be limited to 2 °C.

might be considered as a continuation of the current trend. However, the levels and the trend for predicted CO_2 emissions fully contradict historic data: unlike in any previous period, the production growth and CO_2 emissions have to be decoupled from each other. Obviously, such a transition can hardly be possible on the business as usual basis. Even implementation of the best available technologies might not be sufficient, and a disruptive innovation will be required.

The integrated steel production route where a blast furnace is used as the major technology to produce iron represents 71 % of world steel production, standing for 82 % of energy consumption and 88 % of CO_2 emissions (Laplace Conseil 2013). More specifically, the blast furnace itself consumes nearly a half of energy of the integrated steelmaking factory (Gutowski et al. 2013). Energy sources in the iron and steel industry are almost completely associated with consumption of fossil fuels; hence, substantial cutting of carbon dioxide emission requires delivery of the following targets:

- Improvement of energy efficiency of the blast furnace ironmaking
- Development of new and rapid commercialisation of currently developed radically innovative ironmaking technologies allowing to phase out an iron ore agglomeration and a cokemaking
- Implementation of carbon capture and storage/utilisation technologies

Current paper explores potential of these options and their combinations for decoupling of carbon dioxide emissions from production growth and for reaching the climate change mitigation targets.

24.2 Methodology

Steelmaking routes considered in this study, their market shares and CO_2 emission intensities are presented in Table 24.1. Data on market shares for 2013 are taken based on the Worldsteel statistics (Worldsteel Assoc. 2015c). In 2013 (final data for 2014 are unavailable at a time of this study), 1.8 t CO_2 was emitted to atmosphere per tonne of crude steel (Worldsteel Assoc. 2015b); however, emissions for specific steel production routes are not reported by Worldsteel. Literature data on CO_2 emission intensity for specific steel production routes vary in very wide range. With the production levels of blast furnace pig iron, DRI products and crude steel in 2013

Table 24.1 Market shares and CO_2 intensities for various steel production routes

	Market share		CO_2 intensity per 1 tonne of crude steel	
Route	2013	2050	2013	2050
BF-BOF/OHF	74.0	60.0	2.20	1.89
Scrap-EAF	22.2	36.9	0.70	0.35
Gas-based DRI-EAF	3.0	3.1	1.40	0.70
Coal-based DRI-EAF	0.8	0.0	3.50	2.50

(via BOF, OHF, EAF and other methods) reported by Worldsteel, we found it possible to balance CO_2 emission intensity for the steel production routes by using the figures represented in Table 24.1 in order to obtain the reported 1.8 t CO_2 per tonne of crude steel. Share of scrap in the BOF steelmaking was taken as 15 %.

Figures for 2050 are based on the assumptions on the best available technologies' deployment (discussed in Sect. 24.3.1 below).

In order to simplify the analysis, BOF and OHF are considered in a combination where the OHFs are gradually phased out being fully replaced by BOF. For the same reason, production of liquid iron in blast furnaces is combined with that in Corex apparatus. Production of all solid reduced iron products via different (current and future) routes is combined to DRI.

The figures for future CO_2 emissions per tonne of crude steel required to reach 2DS targets were taken from the paper of Krabbe et al. (2015) where corporate industrial targets are aligned with the IEA model (IEA 2014).

Penetration of the best available technologies (BAT) and the breakthrough technologies (BT) was calculated based on the S-curve model with following assumptions:

- All technologies reach saturation levels by 2050.
- The year of rapid penetration growth is taken as 2025 for the BAT and as 2030 for the BT.

24.3 Technologies and Scenarios

24.3.1 Best Available Energy-Saving Technologies

Improvement of the efficiency and reducing of the carbon footprint for existing processes through modernisation of the equipment, energy system optimisation and energy recovery based on the proven solutions require less capital investment compared to implementation of novel technologies and can be easily multiplied through the technology transfer (Lee 2013). In the IEA 2DS energy efficiency improvements play a major role, providing 42 % of the total predicted emission reduction in the iron and steel industry. Significant share of this amount is to be reached through blast furnace improvements, notably in India, China and Ukraine (IEA 2014).

Within the period from 1960 to 2014, the iron and steel industry has reduced its energy consumption per tonne of steel produced by 60 %; however, it is commonly recognised that there is little room for further improvement of energy efficiency on the basis of existing technology (Worldsteel Assoc. 2015a). From 2000 to 2011, energy intensity per one tonne of crude steel decreased by 4.6 % (from 20.7 to 21.7 GJ/t crude steel), although probably more essential improvement was offset by a decline in recycling as a share of total crude steel production from 47 % in 2000 to 29 % in 2011—mostly because China's steel industry has been developed based on less scrap-intensive BF-BOF route rather than the EAF due to insufficient scrap

availability (IEA 2014). Gutowski et al. (2013) show that energy intensity to produce pig iron through blast furnace technology already approaches thermodynamic limit; however, as it can be seen from Fig. 24.2 (data by the IEA), the potential to cut energy consumption varies from country to country in very wide range: for Japan, South Korea, Europe (OECD) and the USA, energy-saving potential is limited within 1–2 GJ per tonne of crude steel, whereas for Ukraine it exceeds 7 GJ per tonne of crude steel. This variety relates to several factors, among which the most important are structure of the industry, conditions of the equipment, BAT penetration and quality of raw materials. As it is seen from Fig. 24.2, blast furnace improvements still have to play a major role in reducing world's average energy consumption in the iron and steel industry.

The best available technologies, considered for modernisation of ironmaking in two representative studies by the US Environmental Protection Agency (EPA 2012) and a Reference Report by the Joint Research Centre (JRC) of the European Commission (Pardo et al. 2012), are summarised in Table 24.2. It should be noted that some of these technologies are truly energy saving, whereas some other represent fuel switch from more carbon-intensive coke to coal or hydrocarbons.

In this study we do not distinguish carbon dioxide emissions cutting potential for each technology but consider instead cumulative effect from the BAT deployment in all sub-sectors of the iron and steel industry including iron ore agglomeration, coke-making, iron and steel making, casting and rolling. According to the IEA modelling (IEA 2010), CO_2 emission reduction potential achieved through the BAT deployment accounts for 420 $MtCO_2$ per year, representing 19 % of CO_2 emissions in the sector in 2010. Milford et al. (2013) in their forecast use more conservative figure of 14 % based on earlier estimation (IEA 2008). In our study we modelled the effect of BAT deployment for both variants—with 14 and 19 % reduction of CO_2 emissions (Table 24.3).

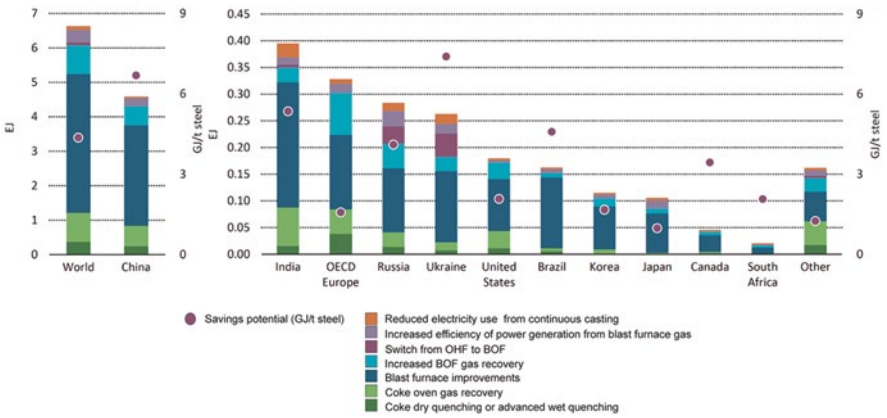

Fig. 24.2 Energy-saving potential of the best available technologies (in GJ/t of crude steel and EJ per year) for the world's major steel-producing countries (IEA 2014)

Table 24.2 The best available ironmaking technologies considered in JRC and EPA analyses

Technology	JRC	EPA
Top gas recovery turbine	+	+
Stove waste gas heat recovery	+	+
Hot blast stove automation		+
Improvement of combustion in hot stove		+
BF top charging system improvement	+	
Recovery of blast furnace gas	+	+
Optimised sinter/pellet ratio	+	
Charging carbon composite agglomerates		+
Pulverised coal injection	+	+
Natural gas injection	+	+
Injection of oil		+
Injection of COG and BOF gas		+
Improved blast furnace control		+

Table 24.3 Market shares of BT in the modelled variants

		Market share				
			2050			
Route		2014	BAT only	BAT + scrap	BAT + scrap + InnoM	BAT + scrap + InnoR
Ironmaking technologies	BF	100	99	99	65	0
	TGR BF	0	0	0	5	5
	HIsarna	0	0	0	20	85
	Finex	≈0	1	1	10	10
Share of EAF in crude steel production		25.8	25.8	40	40	40

24.3.2 The Breakthrough Technologies

The technologies under development with greater degree of radicalness are identified in our study as follows.

Top gas recycling blast furnace (TGR BF) is one of the key technologies initiated in ULCOS project of the EU. It implies an oxygen blast with the PCI injection, separation of the top gas into CO_2 and $CO + N_2$ with returning the latter after preheating either into conditional tuyeres or to the lower shaft. TGR BF might be an option for both new enterprises and for brown field modernisation. Technological aspects were worked out at the experimental LKAB blast furnace in Luleå, Sweden. With recirculation ratio of 90 %, coke consumption was down by 25 % which corresponds to cutting 24 % of CO_2 (ULCOS 2014).

Authors of comprehensive study (Croezen and Korteland 2010) state that "the TGR process does not give a net reduction in energy consumption as reduced coke consumption is balanced by an increased electric power requirement for CO_2 separation. Greenhouse gas emissions are reduced if CO_2 is sequestered". However, modelling by Jin et al. (2015) demonstrates possibility to cut energy consumption by 12.2 % and to reduce net CO_2 emissions by 35.7 %, even taking into account CO_2 emissions related to energy consumed to separate increased quantity of O_2 from the air (to produce oxygen blast) and CO_2 from the top gas. However, in cited paper all the top gas produced is either separated or burned to reheat the recycled CO, with zero amount of gas entering energy network of an enterprise, which is hardly economically feasible: at an integrated steelwork, blast furnace top gas is indispensable component of energy mix. Reduction of CO_2 emissions by 15 % per tonne of final product is considered in paper by van der Stel (2013), and this figure is taken in our analysis.

Pilot implementation of this technology was planned in 2015 at ArcelorMittal Florange (France); however, in 2013 the project has been suspended. Currently it is being continued in the frames of Low Impact Steelmaking project funded by ArcelorMittal and French government, though future timeline for its commercialisation is unclear.

HIsarna is a reduction smelting technology that combines Cyclone Converter Furnace (CCF) and Smelt Reduction Vessel (SRV). Both CCF and SRV apparatuses have a long history of development. The CCF has been developed by then Hoogovens company in the 1990s with pilot plant processing 15–20 t of iron ore per hour. Iron ore and oxygen were injected into the cyclone where the burning of gas occurs (initially an artificial gas imitating the gas produced in the SRV was used). The product—partially molten and reduced for 10–20 % ore with temperature of 1450 °C under force of gravity—flows down along the walls (in the pilot plan, it was discharged to the slag ladle).

The SRV HIsmelt (high-intensity iron smelting) dates back to oxygen bottom blowing converter KOBM (Klockner Oxygen Blown Maxhutte) modified to produce iron. First HIsmelt pilot plant with 2 t of hot metal per hour was launched in Maxhutte in the 1980s. Next pilot plant with 8 t of hot metal per hour was erected in Kwinana (Australia), and a larger plant with design capacity of 0.80 Mt of hot metal per year was launched in 2005 and operated till the end of 2008 as the result of collaboration between Rio Tinto, Nucor Corporation, Mitsubishi Corporation and Shougang Corporation (Rio Tinto 2016). Later on HIsmelt has been relocated from Australia to China. Although commissioning of first Chinese HIsmelt plant with 0.5 Mt capacity was planned yet in 2014, we found no information concerning current status of this project. Moreover, according to the IEA data (IEA 2014), 1.0–1.2 Mt HIsmelt-based steelwork was planned to be operational by 2016 in India, but no further information available for this project as well. However, obviously there exists a long-term experience in scaling up and industrial operation for HIsmelt.

In Europe HIsarna (hybrid of the CCF and HIsmelt) is being developed by Tata Steel in IJmuiden as part of the former ULCOS project in collaboration with Rio Tinto as well as with other steelmaking and engineering companies such as

ArcelorMittal, ThyssenKrupp Steel, voestalpine Stahl and Paul Wurth. A former hot metal desulphurisation plant has been revamped with erection of HIsarna pilot plant producing 8 t of pig iron per hour. During pilot campaigns in 2012–2014, a possibility of using various coal grades and an upper limit of productivity were studied. For 2015 it was planned to study peculiarities of long-term operation in order to explore possible drawbacks of design and to prepare upscaling. Reaching of 7 t of pig iron per hour benchmark has been reported constituting 88 % of initially designed productivity (Meijer et al. 2015). Demonstration is planned to finish by 2018 with further upscaling and commercialisation after 2020.

Compared to blast furnace ironmaking, the following advantages of HIsarna are noted:

– Production cost reduces owing to phasing out coking and sintering/pelletising and possibility to use lower-grade coals and other solid fuels.
– Adaptability to wide range of raw materials including phosphorous ores, titanomagnetites and quartzites.
– Low inertia and possibility to adjust operation towards availability of materials and other factors without affecting the product quality.

Another reduction smelting technology, Romelt, is under commercialisation in Myanmar by Russian supplier with production capacity of 0.2 million tonnes per year and commissioning expected in 2016 (Tyazhpromexport 2016). However, very little information about current state of Romelt (technology is being developed since the 1980s) is available; therefore, HIsarna is taken to represent the category of reduction smelting technologies in this study.

HIsarna emits more CO_2 than a blast furnace; however, thanks to phasing out cokemaking and sintering, the aggregate CO_2 emissions per tonne of crude steel are estimated to be 20 % lower compared to conventional BF-BOF route (Croezen and Korteland 2010).

Finex is the ironmaking technology developed by POSCO in collaboration with Siemens VAI. The prototype of Finex is Corex technology developed by Siemens VAI and commercialised in 1989 in SAR and later in India. Corex has two parts: a shaft furnace for iron ore prereduction and a melter gasifier. Relatively low efficiency of utilising reductive potential of the gas in Corex is followed by much higher CO content in a top gas compared to a blast furnace. Therefore, in terms of energy efficiency and CO_2 emission reduction, this technology can compete with traditional blast furnace only if (1) top gas is completely utilised for production of electricity in very efficient generators and (2) if CO_2 emission factor at power generation of the grid is above 0.9 kg CO_2/kWh (Hu et al. 2009), a case for countries where the electricity generation is mostly coal based.

In 1992 POSCO started the development of a novel Finex technology where—in lieu of a shaft furnace—a cascade of fluidised bed reactors is used to heat up and pre-reduce the ore and a briquetting machine is used to compact pre-reduced ore and coal. These novelties enabled the use of low-grade and fine raw materials. Constructed in 1996 laboratory installation with productivity of 15 t pig iron per day was upscaled in 1999 to a pilot plant with productivity of 150 t per day. In 2003

demonstration plant with Finex apparatus producing 0.6 Mt of pig iron per year has been erected, followed by launching in 2007 of the first commercial plant with production capacity of 1.5 Mt in 2007 at Pohang works. Experience attained allowed to simplify the design and to launch in January 2014 Finex plant with productivity of 2 Mt per year (Lee 2009).

The best result achieved so far is 700 kg of solid fuel per tonne of pig iron that corresponds to 97 % of average fuel consumption in blast furnace technology. With the help of better process control, it is expected to reach in the nearest future the benchmark of 680 kg per tonne with further decrease to 660 kg per tonne that will correspond to 93 and 90 % CO_2 emissions compared to blast furnace. Longer-term plans envisage application of the CCS with extraction of 0.7 т CO_2 per tonne of pig iron that will cut CO_2 emissions by 53 % compared to blast furnace. Finex is oxygen-based technology; hence, the CCS efficiency must be better than for the blast furnace top gas (Yi and Lee 2015). In our paper we consider carbon dioxide cutting potential of Finex as 10 %.

Other innovative technologies such as Ironmaking by Hydrogen Flash Smelting and Molten Oxide Electrolysis being developed under the aegis of the American Iron and Steel Institute, as well as ULCOWIN and ULCOLYSIS initiated in the EU-funded ULCOS project (Wins 2012; Sohn 2008). Hydrogen-based ironmaking is also part of the Japan's COURSE 50 project (Tonomura 2013). However, these technologies are currently still on early R&D stage with commercialisation planned beyond 2030 or even 2050. Although these technologies are not included to our model, a need to develop them is revealed in the discussion below.

24.3.3 Scenarios

In this study we explore the pathways towards reaching the sustainability targets, established by the International Energy Agency (IEA 2014).

The IEA considers two options—with low and high demand for steel. The direct CO_2 emission reduction target is the same in both options, so greater emission reductions are needed in the high-demand case. In 2 °C scenario (2DS), global population and economic growth are decoupled from energy demand. It optimistically assumes technology development, considering that low-carbon technologies will be cost-effective and that barriers associated with regulatory frameworks and social acceptance will be overcome (IEA 2014).

In the 2DS, by 2050 the largely decarbonised electricity mix depends on fossil fuels just for 20 %—down from 70 % in 2011. Based on this assumption, we consider decreasing of CO_2 emissions in the non-integrated EAF-based steelmaking route also by 50 % in 2050 (see Table 24.1). The overall share of the EAF in total crude steel production increases to 37 % by 2025 in 2DS (IEA 2014). In our model the EAF share follows the S-curve, reaching this target as envisaged by the IEA in 2025 and arriving to 40 % in 2050.

We studied four scenarios (Table 24.3) where iron and steelmaking technologies are represented as follows:

- *BAT only* scenario involves adoption of the BAT; however, it doesn't envisage deployment of any breakthrough technologies. Steel production structure doesn't change: the share of secondary steel production through the EAF method is limited at current 25.8 % level (2014). Finex attains limited commercialisation gaining 1 % of the primary iron production market.
- *BAT+scrap* scenario in addition to *BAT only* implies greater availability of scrap resulting at 40 % of steel production through EAF (36.9 % in *scrap EAF* and 3.1 % in *DRI-EAF*; see also Table 24.1) in 2050.
- *BAT+scrap+InnoM* scenario in addition to *BAT+scrap* envisages moderate level of BT deployment. In this scenario 65 % of liquid iron still produced in conventional blast furnaces, 5 % in blast furnaces modified for top gas recycling, 20 % in HIsarna and 10 % in Finex.
- *BAT+scrap+InnoR* is the most radical scenario where all remaining blast furnaces are modified to produce just 5 % of total liquid iron with top gas recycling, 85 % of liquid iron is produced in HIsarna and 10 % in Finex.

Two variants are modelled—with 14 and 19 % CO_2 cutting achieved via BAT deployment.

24.4 Results and Discussion

Results of modelling of the scenarios described above are shown in Fig. 24.3. It is obvious that the results achieved via *BAT only* scenario are very far from the IEA targets. However, increased share of steel production via the EAF (in case if electricity generation is decarbonised to a planned level) in *BAT+scrap* scenario drastically changes the situation, making CO_2 emissions very close to the IEA target in 2030–2033 even in case if BATs' carbon-cutting efficiency is to 14 %. However, further CO_2 emission reduction becomes limited arriving at 1.28 t of CO_2 per tonne of crude steel in 2050. This behaviour is connected to the features of the model: both decarbonisation of the EAF production and share of secondary steel production follow the S-curve.

Moderate deployment of breakthrough technologies in *BAT+scrap+InnoM* scenario only slightly improves the result compared to *BAT+scrap*: deviation from the IEA target is delayed for about 5 years, and the emission intensity decreases to 1.22 t of CO_2 per tonne of crude steel in 2050.

Most radical modernisation with global deployment of breakthrough technologies in *BAT+scrap+InnoR* scenario allows for reaching the results consistent with the IEA targets during 2033–2040. However, after that, owing to saturation of the market with BTs, emission intensity also deviates from the IEA target achieving the level of 1.07 t of CO_2 per tonne of crude steel in 2050.

For the case where BATs will allow cutting CO_2 emissions by 19 % (Fig. 24.3b), the results improve quantitatively both in terms of the emissions intensity achieved

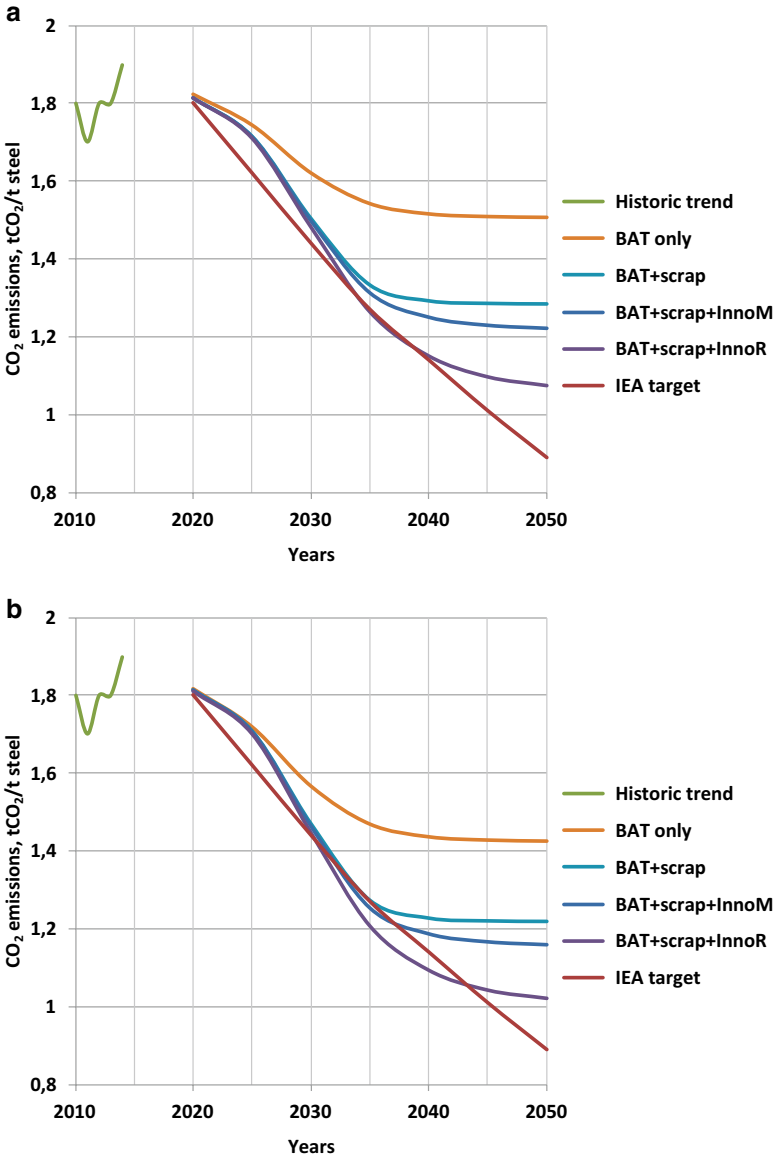

Fig. 24.3 Historic trend and modelling of CO_2 emissions for the variants with 14 % (**a**) and 19 % (**b**) of CO_2 emission reduction achieved by BAT deployment

and delayed deviation from the IEA pathway. Moreover, for the *BAT + scrap + InnoR* scenario, CO_2 emissions' cutting essentially exceeds the IEA targets within more than 10-year period. However, even for this scenario, neither BATs nor BTs can deliver result established by IEA by 2050 and beyond.

The results of modelling for all scenarios show that well before 2050 another radically new technology (in addition to those analysed in this study and with much

higher CO_2 cutting potential) shall be developed and rapidly commercialised and/or carbon capture and sequestration/utilisation (CCS/CCU) technologies shall be deployed in order to avoid further increase of greenhouse gases concentration in the atmosphere.

Several ironmaking technologies with very low- or zero-carbon intensity are being developed. In particular, in the mentioned above ULCOLYSIS and Molten Oxide Electrolysis processes, electric potential is used to separate iron and oxygen in molten electrolyte producing liquid iron and oxygen gas by the following summary reaction:

$$4Fe^{3+} + 6O^{2-} \rightarrow 4Fe + 3O_2$$

However, this technology still on its fundamental development phase needed to overcome such challenges as stability of anode material (graphite is not acceptable owing to unavoidable CO_2 emission carbon, whereas iridium, considered as most promising, is scarce and expensive) and reoxidation of reduced liquid iron. Moreover, this technology is sensible only if the electricity source is fully decarbonised (Wang et al. 2011; Kim et al. 2010).

Several hydrogen-based ironmaking technologies are under development worldwide. In particular flash ironmaking process is being developed by the University of Utah in collaboration with several industrial companies (Sohn 2008). This process is analogue to flash smelting technology, well proven in copper industry and also adapted for production of nickel and lead (Outotec 2016). It has a potential to reduce energy consumption compared to blast furnace ironmaking by 38 %. In case if hydrogen is used as reductant, CO_2 emissions will be decreased by 96 %, for natural gas this figure goes down to 61 % and for coal to 31 % (Sohn 2008; Chen et al. 2015). Currently this technology is on the phase of fundamental laboratory experiments and modelling. High cost of hydrogen is mentioned by the developers as the major barrier for commercialisation of this technology (Sohn and Choi 2009).

Generally, the use of hydrogen for metal smelting is considered by the Intergovernmental Panel for Climate Change (IPCC) as a longer-term option for mitigating the industrial CO_2 emissions, capable to enter the marketplace only beyond 2030 (IPCC 2007). Various technologies aimed to produce affordable hydrogen with zero- or very low-carbon intensity are being developed nowadays; however, other barriers such as transportation and storage of hydrogen in large quantities shall also be noted (Fekete et al. 2015; Le Duigou et al. 2013).

Other approaches for decreasing carbon footprint from steel industry can also be considered—such as substantially enhanced material efficiency (resulting in the demand for steel decreased below the IEA low-demand model) and more essential share of secondary steel production. Material efficiency scenarios and greater scrap availability scenarios are studied comprehensively in the works by Pauliuk et al. (2013) and Allwood et al. (2010, 2011). Even though both options can be considered as plausible, several challenges are noted such as insufficient quality of secondary steel and lack of control over the capacities to be built in the developing countries despite the availability of unutilised capacities in the developed world (so-called capacity follow demand scenario).

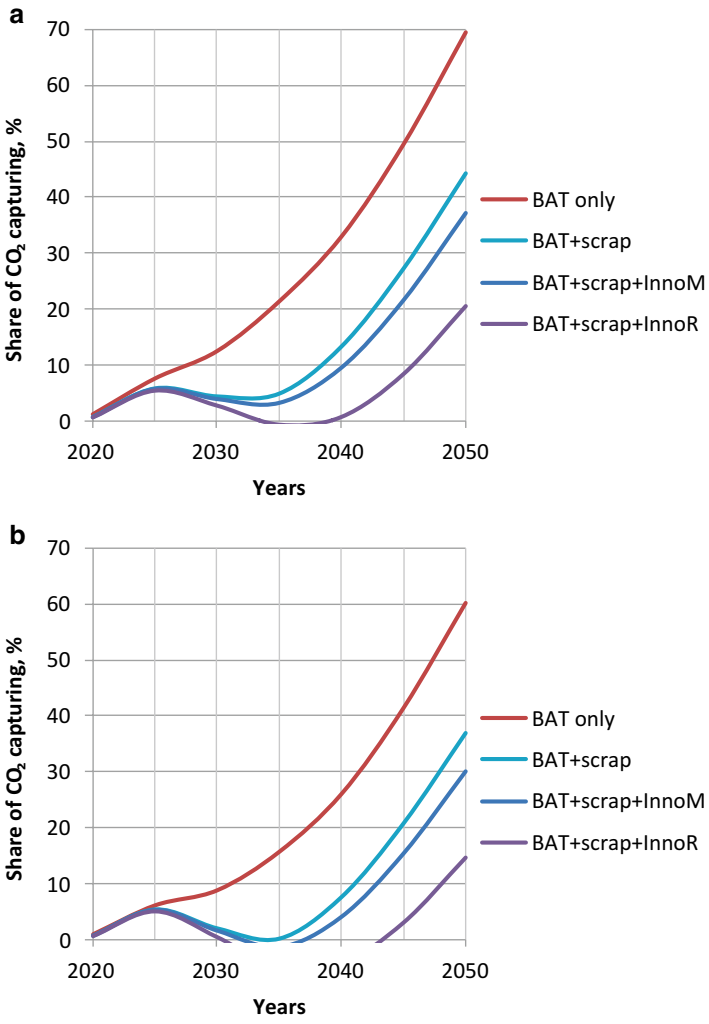

Fig. 24.4 Share of CO_2 capturing in total CO_2 emissions for the variants with 14 % (**a**) and 19 % (**b**) of CO_2 emission reduction achieved by BAT deployment

The share of CO_2 emissions to be treated through carbon cutting and sequestration or utilisation technologies is shown in Fig. 24.4. Obtained results are generally consistent with IEA scenario envisaging capturing 40 % of the sector's direct CO_2 emissions by 2050 (IEA 2014). In any scenario, to avoid excess of the emissions over IEA targets, CCS/CCU technologies shall be deployed in case if no technology with the carbon intensity lower than that of the technologies included in current analysis is developed and implemented. It should be noted that CCS/CCU technologies still are on early development phase and deployment of CCS may face also social acceptance factor owing to unpredictable effect on the environment.

24.5 Conclusions

The following conclusions are drawn from the results of this study:

1. Transition to a low-carbon economy in line with the objectives established by the IEA requires rapid and radical modernisation of iron and steel industry.
2. Deployment of the best available technologies is indispensable though not sufficient for cutting CO_2 emissions to the extent required by climate change mitigation targets.
3. Increased share of secondary steel produced via the EAF method using gradually decarbonised electricity is a prerequisite for substantial cutting the CO_2 emissions. However, problems of scrap availability and quality of secondary steel product shall be addressed.
4. Rapid and wide commercialisation of currently developed innovative technologies after 2020 allows for reaching emission level consistent with the IEA targets up to 2030–2040, depending upon market penetration. However, even in the most radical modernisation scenario, new impulse is needed to align the emissions with sustainable targets. Hydrogen-based ironmaking, enhanced material efficiency, greater share of secondary steel production and CCS/CCU technologies can play the role of such an impulse.
5. Delayed and limited mitigation actions will result in much greater amounts of CO_2 emitted to the atmosphere with unavoidable impact on climate.

Acknowledgements This work is partially supported by the European Commission through the EUClim project 564689-EPP-1-2015-1-UAEPPJMO-MODULE funded under Erasmus+Programme (Jean Monnet Modules).

References

Allwood JM, Cullen JM, Milford RL (2010) Options for achieving a 50% cut in industrial carbon emissions by 2050. Environ Sci Technol 44:1888–1894

Allwood JM, Ashby MF, Gutowski TG, Worrell E (2011) Material efficiency: a white paper. Resour Conserv Recycl 55:362–381

Chen F, Mohassab Y, Jiang T, Sohn HY (2015) Hydrogen reduction kinetics of hematite concentrate particles relevant to a novel flash ironmaking process. Metall Mater Trans B 46:1133–1145

Croezen H, Korteland M (2010) Technological developments in Europe: a long-term view of CO2 efficient manufacturing in the European region. Commissioned by Climate Action Network Europe CAN, CE Delft

EPA (2012) Available and emerging technologies for reducing greenhouse gas emissions from the iron and steel industry. US Environmental Protection Agency, North Carolina

Fekete JR, Sowards JW, Amaro RL (2015) Economic impact of applying high strength steels in hydrogen gas pipelines. Int J Hydrog Energy 40:10547–10558

Gutowski TG, Sahni S, Allwood JM, Ashby MF, Worrell E (2013) The energy required to produce materials: constraints on energy-intensity improvements, parameters of demand. Phil Trans R Soc A 371:20120003. doi:10.1098/rsta.2012.0003

Hu C, Han X, Li Z, Zhang C (2009) Comparison of CO_2 emission between COREX and blast furnace iron-making system. J Environ Sci Suppl 21:S116–S120
IEA (2008) Energy technology transitions for industry: strategies for the next industrial revolution. OECD/IEA, Paris
IEA (2010) Energy technology perspectives: scenarios & strategies to 2050. OECD/IEA, Paris
IEA (2014) Energy technology perspectives: harnessing electricity's potential. OECD/IEA, Paris
IPCC (2007) IPCC fourth assessment report: climate change 2007. 7.12.1 Longer-term mitigation options. https://www.ipcc.ch/publications_and_data/ar4/wg3/en/ch7s7-12.html. Accessed 01 Jan 2016
Jin P, Jiang Z, Bao C, Lu Y, Zhang J, Zhang X (2015) Mathematical modeling of the energy consumption and carbon emission for the oxygen blast furnace with top gas recycling. Steel Res Int 86. doi:10.1002/srin.201500054
Kim H, Paramore J, Allanore A, Sadoway DR (2010) Stability of iridium anode in molten oxide electrolysis for ironmaking: influence of slag basicity. ECS Trans 33:219–230
Krabbe O, Linthorst G, Blok K, Crijns-Graus W, van Vuuren DP, Höhne N, Faria P, Aden N, Pineda AC (2015) Aligning corporate greenhouse-gas emissions targets with climate goals. Nat Clim Chang 5:1057–1060. doi:10.1038/nclimate2770
Laplace Conseil (2013) Impacts of energy market developments on the steel industry. In: 74th session of the OECD Steel Committee, Paris
Le Duigou A, Quéméré M-M, Marion P et al (2013) Hydrogen pathways in France: results of the HyFrance3 project. Energy Policy 62:1562–1569
Lee K-H (2009) POSCO solutions towards low carbon & green growth. Australia-Korea/Korea-Australia Green Business Forum, Sydney
Lee S-Y (2013) Existing and anticipated technology strategies for reducing greenhouse gas emissions in Korea's petrochemical and steel industries. J Clean Prod 40:83–92
Meijer K, Zeilstra C, Treadgold C, van der Stel J, Peeters T, Borlée J, Skorianz M, Feilmayr C, Goedert P, Dry R (2015) The HIsarna ironmaking process. In: METEC & 2nd ESTAD, Düsseldorf
Milford RL, Pauliuk S, Allwood JM, Müller DB (2013) The Roles of Energy and Material Efficiency in Meeting Steel Industry CO_2 Targets Environ Sci Technol 47: 3455–3462
Outotec (2016) http://www.outotec.com/en/About-us/Our-technologies/Smelting/Flash-smelting-Flash-converting/. Accessed 01 Jan 2016
Pardo N, Moya JA, Vatopoulos K (2012) Prospective scenarios on energy efficiency and CO_2 emissions in the EU Iron & Steel Industry. EUR 25543 - Joint Research Centre - Institute for Energy and Transport. doi:10.2790/64264
Pauliuk S, Milford RL, Müller DB, Allwood JM (2013) The steel scrap age. Environ Sci Technol 47:3448–3454
Rio Tinto (2016). HIsmelt process. http://www.riotinto.com/ironore/hismelt-process-10659.aspx. Accessed 01 Jun 2016
Rynikiewicz C (2008) The climate change challenge and transitions for radical changes in the European steel industry. J Clean Prod 16:781–789. doi:10.1016/j.jclepro.2007.03.001
Shatokha V (2015) The sustainability of the iron and steel industries in Ukraine: challenges and opportunities. J Sustain Metall. doi:10.1007/s40831-015-0036-2
Sohn HY (2008) AISI/DOE technology roadmap program for the steel industry. TRP 9953: Suspension hydrogen reduction of iron oxide concentrate: final project report, Utah. http://www.osti.gov/scitech/servlets/purl/929441/. Accessed 01 Jan 2016
Sohn HY, Choi ME (2009) A novel green ironmaking technology with greatly reduced CO_2 emission and energy consumption. In: Gupta GS, Lollchund MR (eds) international conference on the advances in theory of ironmaking and steelmaking. Allied Publishers Pvt. Ltd, Bangalore, pp 9–27
Tonomura S (2013) Outline of course 50. Energy Procedia 37:7160–7167
Tyazhpromexport (2016) http://www.tyazh.ru/en/projects/metallurgicheskij_kompleks9/. Accessed 01 Jan 2016

ULCOS (2014) ULCOS top gas recycling blast furnace process. Final report. European Commission, EUR 26414. doi:10.2777/59481

van der Stel J (2013) Top gas recycling blast furnace developments for 'green' and sustainable ironmaking. Ironmak Steelmak 40:483–489

Wang D, Gmitter AJ, Sadoway DR (2011) Production of oxygen gas and liquid metal by electrochemical decomposition of molten iron oxide. J Electrochem Soc 158:51–54

Wins T (2012) The low carbon future of the European steel sector: presentation for the EU Parliament. http://ccap.org/resource/the-low-carbon-future-of-the-european-steel-sector/

Worldsteel Assoc. (2015a) Steel's contribution to a low carbon future and climate resilient societies. Worldsteel position paper. https://www.worldsteel.org/publications/position-papers/Steel-s-contribution-to-a-low-carbon-future.html. Accessed 01 Jan 2016

Worldsteel Assoc. (2015b) Sustainability indicators. https://www.worldsteel.org/statistics/Sustainability-indicators.html. Accessed 01 Jan 2016

Worldsteel Assoc. (2015c) Statistics archive. https://www.worldsteel.org/statistics/statistics-archive.html. Accessed 01 Jan 2016

Yi S-H, Lee H-G (2015) The recent update of innovative ironmaking process FINEX. In: 2nd international conference advances in metallurgical processes & materials, Kyiv

Chapter 25
Greenhouse Gas Emissions and Energy Consumption of Ironmaking Processes

Hong Yong Sohn and Yousef Mohassab

Abstract The emissions of greenhouse gases (GHG), mainly carbon dioxide, and energy consumption levels of a number of ironmaking processes including several new technologies that are currently under development worldwide are analyzed and compared. In terms of total emissions of greenhouse gas, energy consumption is important because the production of fuels and energy indirectly adds to the total amount of emissions. The relevant levels of emissions and energy requirements are compared with those of an average blast furnace, which is currently the dominant ironmaking process. The article will also discuss the needs for alternate ironmaking processes and present the descriptions of major alternate ironmaking processes, including important novel technologies under development. Finally, different methods for calculating process energy vs total energy requirement in ironmaking will be discussed.

25.1 Introduction

Iron is produced worldwide via blast furnace (BF), direct reduction (DR), and recently smelting reduction (SR). The BF is the dominant means for making iron, after which comes DR. Currently, smelting reduction shares a relatively small portion of global iron production; however, increasing attention is being paid to this process as a competitor to the BF process. The BF technology is well established and dominates the commercial ironmaking industry. Some DR and SR processes, however, have already been adopted in ironmaking plants. In addition to these three technologies, there are electrolysis-based technologies to produce iron, which are currently under research; we will refer to it as EI in this text. These ironmaking processes will be discussed in some details in the following sections.

H.Y. Sohn (✉) • Y. Mohassab
University of Utah, 135 S 1460 E RM 412, Salt Lake City, UT 84112, USA
e-mail: h.y.sohn@utah.edu; yousef.mohassab@gmail.com

P. Cavaliere (ed.), *Ironmaking and Steelmaking Processes*,
DOI 10.1007/978-3-319-39529-6_25

A novel process, Flash Ironmaking Technology (FIT), is under development at the University of Utah and will be discussed in some detail and compared with the current processes as well as with some of those that are under research.

25.2 Blast Furnace and Needs for Alternate Ironmaking Processes

The blast furnace process has been the major method of iron production for over 600 years (Strassburger et al. 1969), and currently produces approximately 94 % of the primary iron, also known as pig iron (WSA 2012). The smallest blast furnaces have a capacity of 0.550 Mt pig iron per year; however, the state-of-the-art ones produce 2–4 Mt pig iron per year.

The blast furnace ironmaking is a countercurrent process occurring in a shaft furnace. Iron-bearing raw materials such as sinter, pellets, or lump ore of mostly magnetite (Fe_3O_4), hematite (Fe_2O_3), and goethite ($Fe_2O_3.H_2O$) (Yellishetty et al. 2010), coke, and flux (limestone) are fed into a shaft furnace from the top, and preheated air (blast) is blown into the bottom through tuyeres to burn and provide the heat required for the smelting process. Coke is made by pyrolyzing the coal (i.e., heating in the absence of oxygen at high temperatures). In the BF, coke functions as: (1) the main chemical reductant of iron ore to iron, (2) fuel, and (3) strong and permeable support for the burden, allowing an adequate flow of gases through the furnace. Coke retains its strength at high temperatures in contrast to coal that tends to soften at elevated temperatures. Fine ores cannot be directly charged to the blast furnace; rather, they have to be sintered or pelletized. The purpose of sintering and pelletizing is to render the fine charge into strong but porous clinker and agglomerated balls (pellets) with a size of ~1.5 cm to enhance the burden permeability and facilitate the reduction (Worrell et al. 2010). Supplementary fuels, such as pulverized coal, natural gas (NG), and oil, are also injected into the furnace through the tuyeres to reduce the consumption of coke, which is expensive. The hot air reacts with coke and injected fuels, forming 2273–2773 K (2000–2500 °C) hot gas. This hot gas rises and passes through the raw materials that descend from the top. While the hot gases (mostly N_2, CO, and CO_2) ascend, their sensible heat is transferred to the descending materials and as a result the gas temperature decreases, while the descending charge is heated and experiences a series of physicochemical changes, most importantly the partial reduction of iron oxides. The final reduction to iron, the desulfurization, and silica reduction occur in the lower part of the bosh and the crucible where the temperature is high. The reduction takes place by CO and H_2 in the gas and solid carbon in coke. Liquid hot metal (pig iron) and molten slag are formed in the hearth of the furnace. The blast furnace is a chemically and thermally efficient reactor. Moreover, there have been efforts to improve the BF process in terms of increasing productivity and energy efficiency, decreasing coke consumption, developing better cokemaking processes, reducing CO_2 emissions, increasing pulverized

coal injection, and injecting natural gas and plastics. Many of these steps to improve the BF process have already been commercialized. Furthermore, R&D efforts to improve the BF process are continuing. Examples are the reformation of coke oven gas with the aid of catalysts (Course 50), top gas recycling, CO_2 capture and storage, avoiding gas flaring, and heat recovery from slag (IETD 2012a).

Despite aforementioned merits and improvements, the blast furnace process still suffers from drawbacks. As long as the blast furnace is used, the needs for sintering/pelletizing of the ore and high-grade coking coal cannot be avoided. Other materials preparation contributes significantly to the energy consumption as well as CO_2 emissions in the blast furnace process. Figure 25.1 indicates that ore and coke preparation emits ~20 % of the total CO_2 in the BF–BOF route and the BF contributes ~70 %, whereas the steelmaking step adds only ~11 % of the total emissions (Orth et al. 2007) from a typical integrated steel plant. Moreover, the BF process is energy intensive and requires a high capital cost as it entails large infrastructure. Table 25.1 compares the primary energy intensity, defined as the energy used for the production facility as well as to generate the electricity consumed at the facility, to produce a metric ton of mild steel for three steelmaking technologies (Worrell et al. 2008). It is seen that the BF consumes around 78 % of the total energy required in the BF–BOF route (Worrell et al. 2008).

Since the Kyoto protocol (38 nations agreed in 1997 to reduce greenhouse gas emissions on average by 5.2 % by 2012) was announced, greenhouse gases (GHG) emissions and the resulting climate change have continued to be a significant environmental issue for the steel industry and, in particular, the BF process, as will be discussed later.

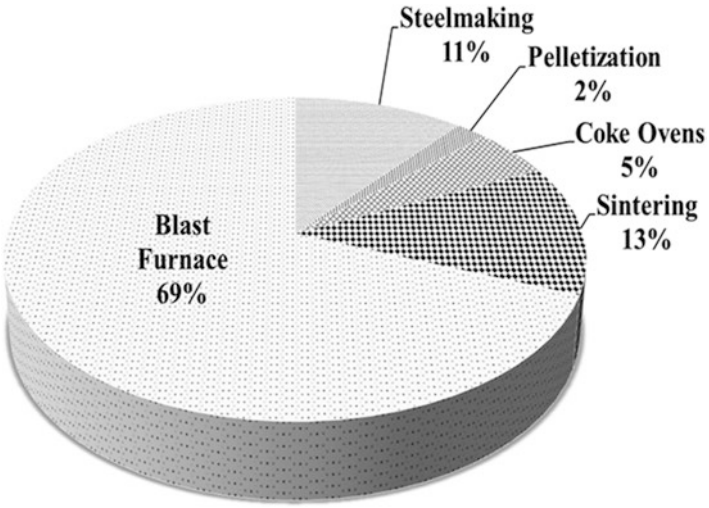

Fig. 25.1 The CO_2 emissions in primary steelmaking (BF–BOF), (total = 2227 kg CO_2/t steel) (Orth et al. 2007)

Table 25.1 World best practice primary energy intensity values for iron and steel

Production step	Process	BF–BOF	SR–BOF	DRI–EAF	Scrap–EAF
Material preparation	Sintering	2.2		2.2	
	Pelletizing		0.8	0.8	
	Coking	1.1			
Ironmaking	Blast furnace	12.4			
	Smelting reduction		17.9		
	Direct reduced iron			9.2	
Steelmaking	Basic oxygen furnace	–0.3	–0.3		
	Electric arc furnace			5.9	5.5
	Refining	0.4	0.4		
Total (GJ/metric ton steel)		15.8	18.8	18.1	5.5

Values are GJ per metric ton of steel and the primary energy includes electricity generation, transmission, and distribution losses of 67 % (adapted from Worrell et al. 2008)

25.3 Major Alternate Ironmaking Processes

25.3.1 Direct Reduction

Direct reduction processes are mostly gas-based, which are globally dominated by Midrex technology (63 % of world DR) (IPTS 2009). Ore (fines, pellets, or lumps) is reduced in solid state—unlike BF process where a liquid metal is produced. Direct reduced iron (DRI) or sponge iron offers an alternative steel production route to BF–BOF and Scrap–EAF routes. DRI production is common in the Middle East, South America, India, and Mexico. DR offers an attractive route due to its low capital investment and its suitability to local raw material situations (IETD 2012a, b). Despite the aforementioned advantages, the DR route suffers from drawbacks such as the small scale of operations, which acts as a barrier for energy efficiency investments. Also, DRI is prone to re-oxidation unless passivated or briquetted. The energy requirement of the DR–EAF route is compared with the BF–BOF route in Table 25.1, which shows that the former route requires ~2 GJ per metric ton of steel more than the latter.

The quality of DRI is highly dependent on the feed quality, unlike hot metal produced by the BF with stable and dependable quality (IPTS 2009). In DR, natural gas and coal are the two primary fuels. More than 90 % of the global DRI plants use natural gas, whereas production in India is mainly coal based.

DRI processes can be grouped according to the type of reactor used, namely (IETD 2012a, b):

- Shaft furnaces (Midrex, Energiron)
- Rotary kilns (SL/RN process)
- Rotary hearth furnaces (Fastmet/Fastmelt, and ITmk3)
- Fluidized bed reactors (Circored)

In DR, iron oxide is reduced below the melting point of iron, involving no molten slag phase. Therefore, all gangue elements of the iron ore remain in the DRI and need to be separated via the slag in the EAF. This increases the electrical energy and electrode consumption of the EAF compared to steel scrap melting (secondary steelmaking). This energy consumption can be reduced by immediate transfer of hot DRI to the EAF melt shop. By doing this, the heat from the direct reduction process lowers the cost of melting the DRI in the EAF, considerably cutting the energy costs and electrode consumption (IETD 2012b).

The most widely used technologies for DRI production are Midrex and Energiron, both using natural gas. The energy consumption in natural gas-based DRI production is well known and established to be 10–11.4 GJ/t-DRI. Natural gas-based DRI production also leads to lower CO_2 emissions, with emissions ranging from 0.77 to 0.92 t of CO_2 per ton of steel (compared with ~1.9 t of CO_2 per ton of steel for the BF–BOF route), depending on the type of electricity used (IETD 2012a, b). At present, this process is more expensive than the BF process and it also demands better quality iron ore, which increases the cost and limits its flexibility. The amount of electricity required for melting DRI in EAF also makes the process less efficient in terms of energy use (18 GJ/t of crude steel compared with 16 GJ/t in the BF–BOF route, as shown in Table 25.1). The clear potential of this proven technology, however, is the removal of the need for coke ovens and reducing CO_2 emissions.

Table 25.2 summarizes reported information on the levels of energy consumption and CO_2 emissions associated with various direct reduction technologies together with the development status.

25.3.2 Smelting Reduction

Smelting reduction (SR) processes are the latest development in pig iron production. The SR emerged during the 1990s. In SR, iron ore and coal are added directly to a metal-slag bath where the ore is reduced. The SR combines the gasification of coal with the melt reduction of iron ore. Energy consumption of smelting reduction is lower than that of blast furnace, as coking step is avoided and the need for ore preparation is reduced. Examples of this process are Finex and HIsmelt. Although SR reduces GHG emissions, the process demands higher energy for ironmaking step (18.7 GJ/t of crude steel) that exceeds the total energy required for the entire steelmaking process through the BF–BOF route (15.8 GJ/t) (Worrell et al. 2008).

In 2003, Birat et al. (2004) made a benchmarking study that was based on process calculations. This study was aimed to visualize the future scenarios of steelmaking technologies beyond Kyoto protocol. Based on their study, the results of which are presented in Fig. 25.2, the share of different ironmaking technologies which could be in place in 2050 was forecasted with a total steel make in excess of 2300 Mt (compared with 1518 Mt in 2011) (Gupta and Sahajwalla 2005; WSA 2012). The BF is expected still to be the largest process for iron production; however, it is expected to drop from 94 % in 2011 to 60 % in 2050. Based on the same

Table 25.2 Summary of common direct reduction technologies (adapted from IETD 2012)

Technology	Energy consumption	CO_2 emissions	Development status
Midrex process	Total ~10.4 GJ/t-DRI. Natural gas consumption in high-efficiency Midrex plants ~9.6 GJ/t-DRI.	Some Midrex plant/ EAF facilities emit only one-third of the CO_2 of a BF/BOF complex	Commercial
HYL III process	10.4 GJ/t-DRI.	IEA: from steelmaking with natural gas-based DRI 0.77–0.92 t-CO_2/t--steel.	Commercial
FASTMET & FASTMELT	12.3 GJ/t-HM	Reduces CO_2 emissions by 1.24 t/t-HM.	Commercial
ITmk3 process	Reduces energy consumption by 3 and 10 GJ/t-HM compared to large- and small blast furnaces. No electricity is used.	Reduction of 1 tCO_2/t-HM expected.	Commercial
SL/RN process	Decreases because no coke oven and sinter plants are required. Total electricity consumption is 1000 kWh/t liquid steel.	3.2 t/t-liquid steel.	Commercial
Finmet	Process gas usage = 12.4 GJ/t-DRI		Commercial
Iron carbide process	12.6 GJ/t-product.	Total emissions 2.17 tCO_2/t-steel.	Commercial
Circored	Gas usage 11.5 GJ/t Electricity consumption for Circored-HBI-EAF 901 kWh/t-steel.	Total (including electricity) 1.2 and 2.0 t/t-steel.	Commercial
Redsmelt	No coke oven required. Electricity consumption ~690 kWh/t-steel.	Total 1.99 tCO_2/t-steel.	Commercial
Sustainable steelmaking using biomass and waste oxides	Productivity gains (DRI production rate per unit area of hearth) as high as 50 % by replacing coal with wood charcoal.	Less than 5 % increase in total carbon consumption.	Research
ULCORED	Insufficient information	Insufficient information	Research

(continued)

Table 25.2 (continued)

Technology	Energy consumption	CO_2 emissions	Development status
Paired straight hearth furnace	With a smelter, 30 % less energy than BF/ coke oven.	Decrease by one third compared with BF.	Demonstration
Flash Ironmaking Technology (FIT)	~38 % less energy than the blast furnace or 7.4 GJ/t of hot metal.	With natural gas, reduction of 39 % compared with blast furnace	Research

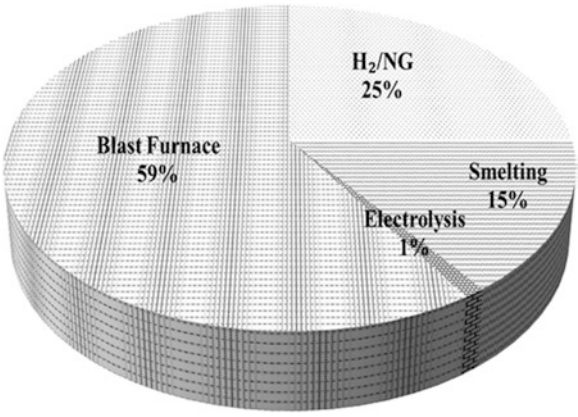

Fig. 25.2 Predicted share of ironmaking routes in 2050 (Birat et al. 2004)

study, GHG emission is expected to be 39 % less than that in 2003. Also, they presented examples of these future processes such as those based on the increased use of hydrogen for reduction, low carbon fuels such as natural gas, and smelting processes.

Table 25.3 summarizes reported information on the levels of energy consumption and CO_2 emissions associated with various smelting reduction technologies together with the development status.

25.4 Major Novel Technologies Under Development

25.4.1 Flash Ironmaking Technology

25.4.1.1 Process Description

Despite the dominance of the blast furnace ironmaking process, increasing attention is paid to the development of a new technology with lower energy consumption and CO_2 emissions. It should also require much less capital investment than the blast furnace/coke oven combination. At the University of Utah, an alternative technology to meet these demands, called the FIT, has been under development (Sohn 2007; Pinegar et al. 2011, 2012a, b; Mohassab Ahmed 2013; Chen et al. 2015a).

Table 25.3 Summary of common smelting reduction technologies (adapted from IETD 2012)

Technology	Energy consumption	CO_2 emission reduction potential	Development status
Corex process	Dry fuel consumption with and without off-gas recycling is reported to be 770 and 940 kg/t-HM.	CO_2 emissions of combined product (hot metal + DRI) ~20 % lower than blast furnace route	Commercial
	With a combined cycle power plant and off-gas recycling, net thermal and electrical energy consumption for a one million t/y capacity plant is 450 and 45 MW, respectively.	Total CO_2 emissions for steel produced with 60 % hot metal from Corex and 40 % DRI is around 3.78 t/t-steel.	
Finex process	Coal consumption of the process <700 kg/t-HM.	4 % less CO_2 than blast furnace.	Commercial
	An additional energy reduction of 1.3 GJ/t-HM by utilizing off-gases after CO_2 removal.		
HIsmelt	With no raw material processing required, the process uses less energy.	Can reduce CO_2 emissions by ~20 % compared to BF route.	Commercial
Dios process	Lower by 3–4 %. Low electrical power consumption. Coal consumption 950 kg/t-HM.	4–5 % lower.	Demonstration
Hisarna	20 % improvement.	20 % reduction of CO_2/t-hot rolled coil (HRC) without carbon capture and storage (CCS) expected. Reduction of up to 80 % possible with CCS.	Research
Romelt	Coal consumption ~900–1200 kg/ton.	With no coke oven plant, sinter or pellet plant required, emissions lower than conventional process.	Demonstration

This novel technology eliminates the highly problematic cokemaking and pelletization/sintering steps by directly utilizing iron ore concentrate, which is in abundance in the USA and elsewhere. In this article, recent advances on this work are discussed.

The FIT is an innovative process that uses iron ore concentrate directly without further treatment. The fineness of the concentrate particles allows a very rapid reaction rate, thus requiring residence times measured in seconds instead of the minutes and hours it takes to reduce pellets and even iron ore fines.

Other processes for the gaseous reduction of iron oxide can be grouped into two broad types: (1) shaft furnaces [Midrex (Cheeley 1999) and Energiron (Duarte et al. 2008)] and (2) fluidized bed reactors [FINMET and the earlier FIOR (Hassan et al. 1994), CIRCORED process (Husain et al. 1999), and SPIREX (Macauley 1997)]. Shaft furnaces require pellets or sinter, which are 10–12 mm in size and require minutes or even hours to be fully reduced. The fluid bed processes use "iron ore fines," particles in the range of +0.1 mm to −10 mm. These processes are slow because the larger pellets and particles react slowly and the process cannot be operated at high temperatures, under which they suffer the problems of sticking and fusion of particles. Processes that can replace the blast furnace must be sufficiently intensive to meet the large production rates required for economic competitiveness. The FIT reduces iron ore concentrates of <100 μm sizes, which are even smaller than fines by one or two orders of magnitude. Historically, fluidized bed processes using iron ore fines have been less than successful. Compared with concentrate particles, even ore "fines" used in a fluidized bed take much longer time to reduce than the time available in a typical flash reduction process.

The FIT removes many of the limitations associated with the other processes discussed above. Specifically, (1) it uses iron oxide concentrates directly without the need for pelletization or sintering; (2) coke ovens are not required; (3) high temperatures can be used because there will be little particle sticking or fusion problems (and thus, the process can be operated at high temperatures); (4) it is possible to produce either solid or molten iron; and (5) the raw materials can be fed continuously. The process also has the possibility of direct steelmaking in a single unit, as depicted in Fig. 25.3.

In this paper we will describe major progresses made so far on the Flash Ironmaking research, especially the kinetics of the reduction process, the chemistry of the slag, and the economic and environmental aspects of the process.

25.4.1.2 Reduction Kinetics

As an integral part of the development of this novel process, Sohn and coworkers (Chen et al. 2015a, b; Choi and Sohn 2010) have determined the kinetics of the gaseous reduction of magnetite concentrate particles aimed at generating a database to be used for the design of a flash ironmaking reactor—before their work, there had been little research reported on this subject under the conditions of the FIT. Their work included the measurement of the particle kinetics of the reduction of magnetite or hematite concentrate particles by hydrogen or carbon monoxide in the temperature range of 1423–1673 K (1150–1400 °C) (Chen et al. 2015a, b; Choi and Sohn 2010; Wang and Sohn 2013). Most importantly, they established that magnetite concentrate can be reduced to a degree higher than 90 pct within several seconds, which presents sufficiently rapid kinetics for a flash reduction process. They obtained the following rate expression for the hydrogen reduction of magnetite concentrate particle in the temperature range 1423 K (1150 °C) to 1623 K (1350 °C) which is given by

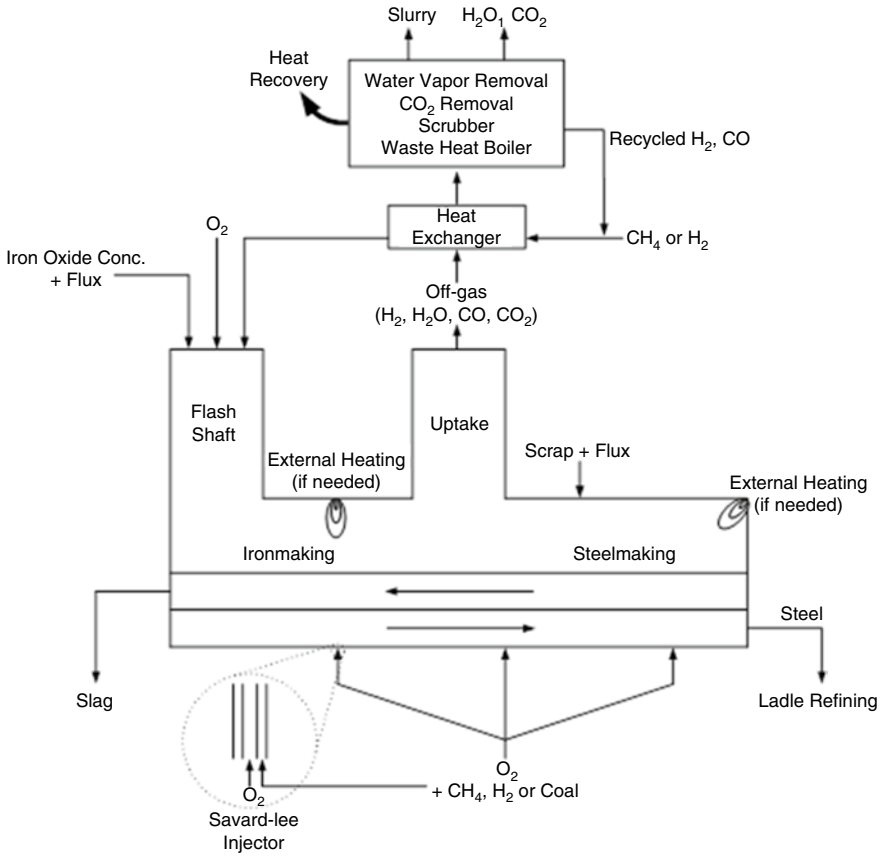

Fig. 25.3 A schematic diagram of a possible direct steelmaking process based on the Flash Ironmaking Technology (FIT) (Sohn and Choi 2012)

$$-Ln\left(1-X\right)=1.23\times10^{7}\times e^{-196000/RT}\times\left(pH_2-\frac{pH_2O}{K}\right)_{\text{lm}}\times t \qquad (25.1)$$

where, R is 8.314 J mol^{-1} K^{-1}, p is in atm, and t is in seconds.

Although the FIT is being developed for magnetite concentrate, it is expected to be equally applicable to hematite concentrate. Thus, Sohn and coworkers (Chen et al. 2015a) studied the hydrogen reduction kinetics of hematite concentrate particles of average size 21.3 μm in the temperature range 1423–1623 K (1150–1400 °C). The results clearly indicated that the hematite concentrate can also be reduced to greater than 90 pct degree by hydrogen in the several seconds of residence time typically available in a flash reactor. In their work (Chen et al. 2015a), results at various temperatures and partial pressures of hydrogen showed that the nucleation and growth rate equation with an Avrami parameter of 1 well describes the kinetics of hematite reduction. The reduction rate has a first-order dependence on the partial

pressure of hydrogen. The activation energy of hydrogen reduction of hematite concentrate is 214 kJ/mol (Chen et al. 2015a). The following rate equation was obtained, which satisfactorily represents the reduction kinetics of hematite particles:

$$-Ln(1-X) = 4.41\times 107\times e^{-214000/RT}\times\left(pH_2 - \frac{pH_2O}{K}\right)_{lm}\times t \qquad (25.2)$$

where R is 8.314 J/mol K, T is in K, p is in atm, and t is in seconds.

Compared with the activation energy of the hydrogen reduction of magnetite concentrate of 196 kJ/mol in the temperature range 1423–1673 K (1150–1400 °C), the reduction of hematite concentrate has a lower activation energy of 214 kJ/mol in the similar temperature range.

Hematite reduction kinetics by $CO+H_2$ mixtures was also investigated to represent the case of using natural gas or coal gas as the reductant/fuel in the flash ironmaking process (Mohassab et al. 2016). The kinetics in this case is complicated due to the simultaneous reduction by the two reductants. It was, however, found that within a few seconds of residence time, a reduction degree of over 90 pct was achieved using either $CO+H_2$ at temperatures above 1573 K (1300 °C), as shown in Fig. 25.4. It is also clear that adding CO to the H_2 boosts the reduction kinetics as compared with the reduction by a single gas H_2 or CO. Increasing CO partial

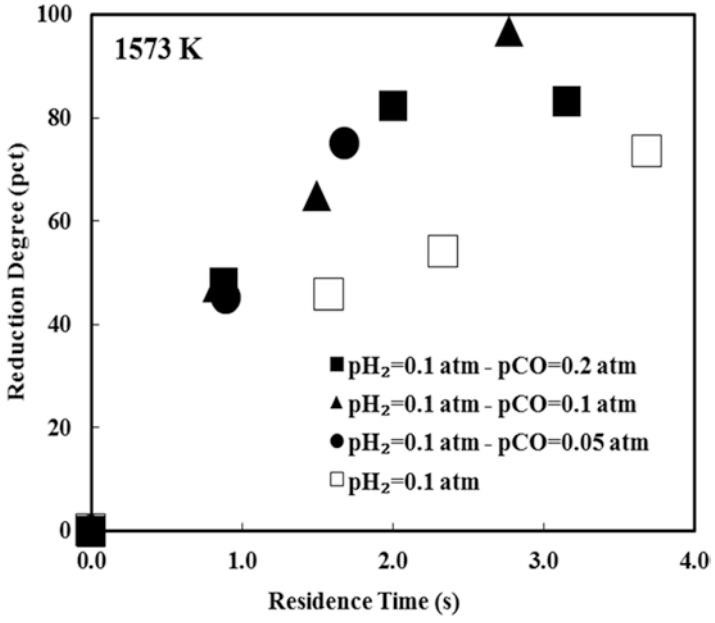

Fig. 25.4 Reduction degree comparisons between single reductant gas (H_2) and $CO+H_2$ mixtures at 1573 K (1300 °C) [adapted from (Mohassab et al. 2016)]

pressure from 0.05 to 0.2 atm while holding hydrogen partial pressure at 0.2 atm did not affect the reduction kinetics of hematite concentrate, as Fig. 25.4 shows.

The measurement of the kinetics of the flash reduction continues to determine the rate equation for the reduction of magnetite and hematite concentrate with mixtures of CO and H_2 gases to be used in designing flash reactor that will run on natural gas.

On the other hand, Sohn and coworkers (Yuan and Sohn 2014; Yuan et al. 2013) studied the kinetics of the re-oxidation of iron particles produced by the FIT in various oxidizing gas mixtures. As the gas–particle mixture cools down in the lower part of the flash reactor, the re-oxidation of iron could take place because of the decreasing equilibrium constant and the high reactivity of the freshly reduced fine iron particles. The last stage of hydrogen reduction of iron oxide, i.e., the reduction of wustite, is significantly limited by equilibrium. The effects of temperature [823–973 K (550–700 °C)] and H_2O partial pressure (40–100 pct.) on the re-oxidation rate were examined. The nucleation and growth model was shown to best describe the re-oxidation kinetics. Pressure dependence was first order with respect to water vapor, and the activation energy was 146 kJ/mol. A complete rate equation that adequately represents the experimental data was developed (Yuan et al. 2013). They also studied the oxidation in pure CO_2 gas in the temperature range of 873–1073 K (600–800 °C). Their findings indicated that within the several seconds of residence time typically available in a flash reduction process the re-oxidation degree of iron particles in water vapor should be <0.24 % in the temperature range of 823–973 K (550–700 °C) and the results implied that the oxidation will be negligible in the flash reduction process where CO_2 from partial combustion of natural gas with oxygen accounts for less than 10 % in the gas mixture. In the collector where product iron particles may be kept for up to one hour at around 673 K (400 °C), the expected re-oxidation degree would be around 0.02 % (Yuan 2013; Yuan and Sohn 2014; Yuan et al. 2013). This indicates that re-oxidation within the reactor due to the shifting of equilibrium as temperature decreases toward the bottom of the reactor is of no concern.

The pyrophoricity of DRI when it comes into contact with air is of concern during storage or transportation. Thus, oxidation of flash reduced iron in O_2–N_2 gas mixtures was investigated to determine the effects of temperature [673–873 K (400–600 °C)] and O_2 partial pressure (5–21 pct.). The rate data were analyzed based on the nucleation and growth model, which resulted a pressure dependence of first order with respect to oxygen and an activation energy of 14.4 kJ/mol (Yuan and Sohn 2014). Most importantly, it was concluded that flash reduced iron is much less vulnerable to oxidation than conventional DRI particles. This is because the flash ironmaking process uses higher reduction temperatures, leading to a lower specific surface area of the product iron. This can be clearly seen from the micrographs presented in Fig. 25.5 which shows iron oxide reduced at a lower temperature at which conventional DRI is produced (Fig. 25.5a) compared with iron produced at a flash ironmaking temperature (Fig. 25.5b). This work determined that at temperatures lower than 573 K (300 °C), the oxidation of flash reduced iron is not of great concern (Yuan and Sohn 2014).

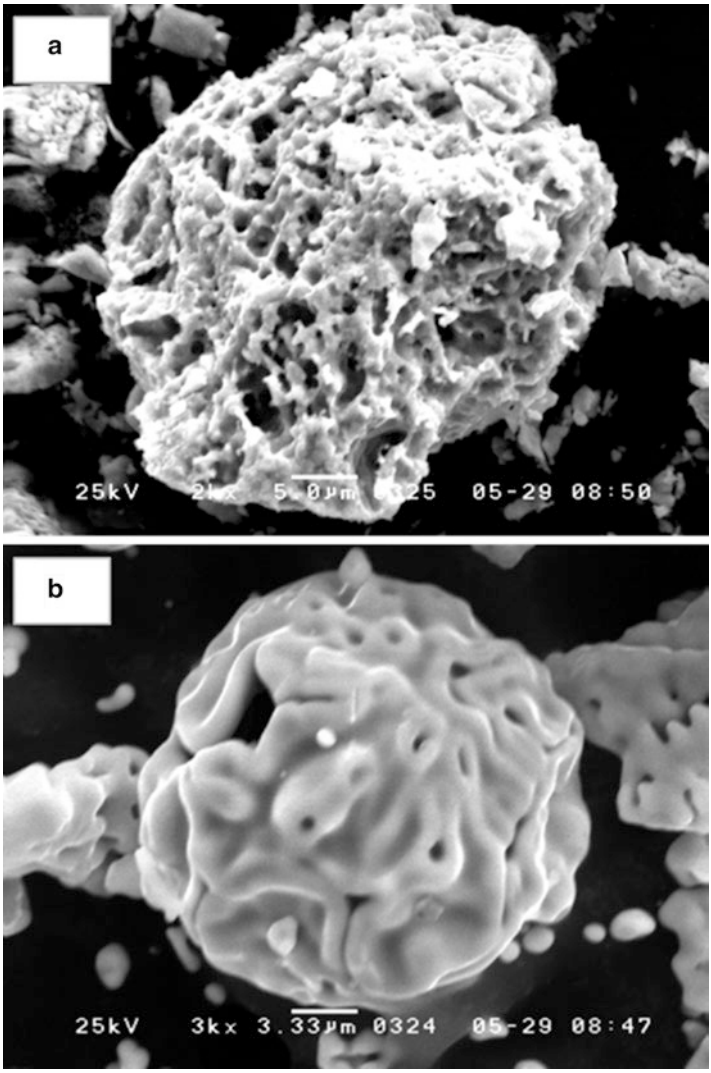

Fig. 25.5 Comparison of microstructures of different iron particles: (**a**) H_2-reduced iron at 1073 K (800 °C); (**b**) flash reduced iron produced at 1623 K (1350 °C) (Yuan and Sohn 2014)

25.4.1.3 Slag Chemistry

In addition, the slag chemistry was studied under the conditions of the FIT. Sohn and coworkers (Mohassab-Ahmed and Sohn 2014a, b; Mohassab-Ahmed et al. 2012a, b; Mohassab-Ahmed et al. 2014; Mohassab and Sohn 2014a, b, 2015) have applied a number of analytical techniques to determine the structures and properties of the slags formed under the conditions of flash ironmaking. These techniques

have been proved to be highly useful for this purpose. Several features of such instrumental analysis have direct correlations with important properties of slag such as its affinity to impurities. These techniques were applied to slags of interest for the FIT, especially in terms of the effects of water vapor expected to be present in high contents in the new process (Mohassab Ahmed 2013). Water vapor was found to be advantageous for lowering FeO in slag (Mohassab and Sohn 2014a), and manganese (Mohassab-Ahmed and Sohn 2014b). Moreover they found that water vapor in the atmosphere of the new process would keep lining wear low based on the low MgO solubility in slag under its expected operating conditions (Mohassab and Sohn 2014a). The research on slag also found that water vapor decreased sulfur (Mohassab and Sohn 2014b) and phosphorus (Mohassab and Sohn 2015) in produced molten iron.

25.4.1.4 Economic and Environmental Aspects

The economic and environmental aspects of the FIT were also studied. Process simulation for the FIT was carried out by Sohn and coworkers using the METSIM software to assess the economic feasibility for different process configurations (Pinegar et al. 2012a, b, c). Major results are summarized in Figs. 25.6 and 25.7. Figure 25.6 shows potential energy saving, lower carbon footprint, and economic feasibility (except when purchased H_2 is used) relative to the BF. However, application of a $50 per ton of CO_2 credit should make the use of hydrogen economically feasible at the 2010 price of hydrogen, as Fig. 25.6 indicates (Pinegar et al. 2012a, b, c).

In summary, this transformative technology has significant energy saving and reduced CO_2 emissions compared with the blast furnace process. It has been proved that iron particles of more than 95 % metallization can be obtained by reduction with hydrogen or a mixture of carbon monoxide and hydrogen in 2–7 s at temperatures of 1573 K (1300 °C) or above. The product of FIT, which is expected to operate at temperatures higher than 1273 K (1000 °C), is significantly less reactive towards oxygen compared with DRI produced by the current technologies. Also, the molten iron to be produced by the FIT will contain less impurities and the relevant slag would be less corrosive to furnace lining.

25.4.2 Electrolytic Ironmaking

In principle, iron oxide can be reduced by aqueous or molten electrolysis. There are two processes that are currently under research: (1) molten oxide electrolysis (MOE) and (2) aqueous electrolysis.

ULCOLYSIS (ULCOS 2012) and the Sadoway process (Kim et al. 2011) are the two molten electrolysis processes under research to reduce iron from iron oxide in a molten bath. In MOE processes, iron ore is dissolved in a molten oxide mixture at 1823–1973 K (1550–1700 °C). The anode, made of a material inert towards the

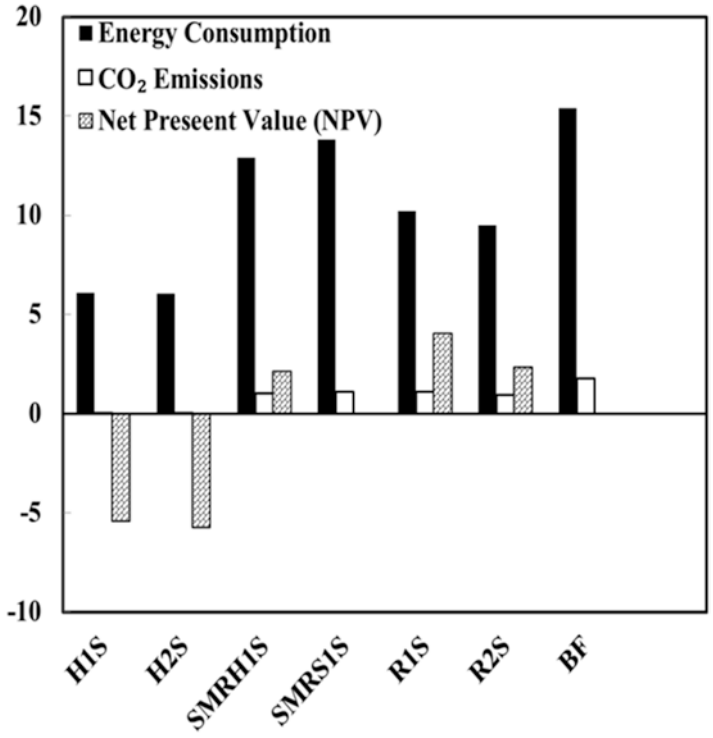

Fig. 25.6 Energy consumption (GJ/ton of iron), CO_2 emission (tons/ton of iron), and NPV (in 2010 dollars and conditions) in million dollars for a 1 Mt/year plant of the different configurations of the FIT in addition to the blast furnace applying \$0 CO_2 credit. [*H1S* H_2-based 1-step process, *H2S* H_2-based 2-step process, *SMRH1S* 1-step process with hydrogen production from SMR (Steam-Methane Reforming), *SMRS1S* 1-step process with syngas production from SMR, *R1S* Reformerless 1-step process, *R2S* Reformerless 2-step process] (Pinegar et al. 2012a, b, c)

oxide mixture, is dipped in this solution. Electrical current is passed between this anode and a liquid iron pool connected to the circuit as the cathode. Oxygen evolves as a gas at the anode and iron is produced as a liquid metal at the cathode.

ULCOWIN (ULCOS 2012) is an example of a research project to study the aqueous electrolysis, often referred to as electrowinning, as a means to produce iron on a large scale. Unlike MOE, aqueous electrolysis uses an alkaline solution (mostly aqueous NaOH) as the electrolyte. In addition, two inert electrodes are used. On the cathode, the iron cations are reduced and iron is plated.

Electrolysis still involves CO_2 generation as the process relies intensively on electrical energy which is largely produced by the consumption of carbon-based fuels. Also, there are other obstacles to be overcome in MOE, such as the high temperature required to maintain the electrolyte liquid as well as the electrode material for large scale. For aqueous electrolysis, in addition to the requirement of electrical energy, the major challenge is the large-scale solution treatment and purification as well as other problems associated with hydrometallurgical processes.

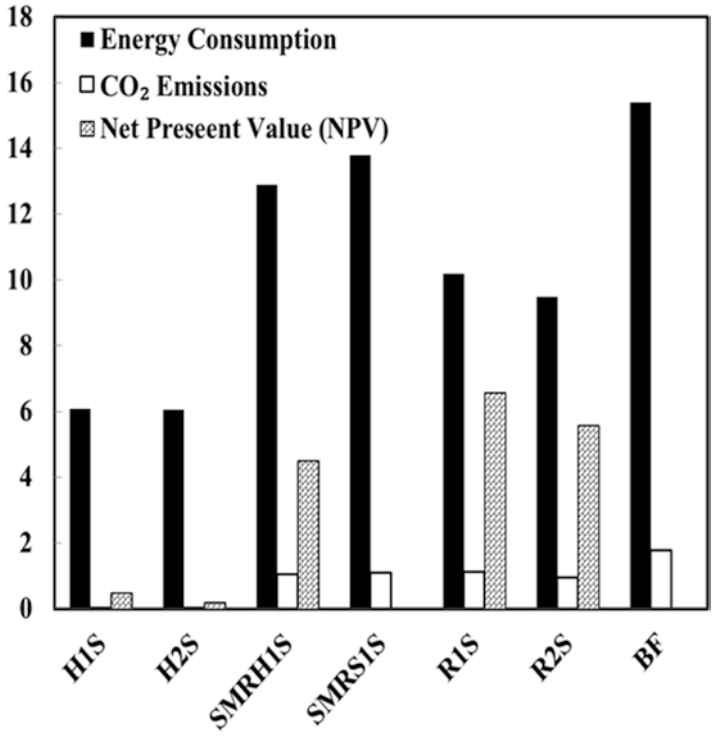

Fig. 25.7 The energy consumption (GJ/ton of iron), CO_2 emission (tons/ton of iron), and NPV of the different configurations of the FIT in addition to the BF applying \$50 CO_2 credit (Pinegar et al. 2012a, b, c)

25.5 Methods for Calculating Energy Requirements: Need for Standardization

25.5.1 Introduction

Energy consumption is inseparably coupled with CO_2 emissions under the current conditions in which most energy production relies on the combustion of fossil fuels. There are currently different ways to calculate and present energy requirements for ironmaking. Although the differences in energy requirements among different processes are largely unaffected by the methods of calculation, as will be shown subsequently, the absolute values are affected by them. Thus, it deserves considerable attention to clearly understand what these different methods involve. It is also important to distinguish different types of energy in terms of relating them to associated carbon footprint.

When a process involves both endothermic chemical reactions and heat generation from the combustion of fuels, the choice of endothermic reactions to include in computing the "energy requirement" for the overall process is rather arbitrary and can be a source of confusion. It is shown that the essential question becomes whether

the heat of combustion of a reactant, which can be used as a fuel, should be included in the energy requirement value. It is noted that the choice is a matter of convention, but it is important to clearly state what convention is followed in presenting the results of energy calculations. There is a need to select a standard approach because the presented value of "energy requirement" of a process depends on this choice (Sohn and Olivas-Martinez 2014).

Different approaches are used for performing energy balance calculations and perhaps more significantly in presenting the "energy requirement" of a process. The question becomes more involved for a process in which one or more reactants are also used to generate the process heat by combustion. Often the key issue is which heat of chemical reaction to include in computing (or presenting) the "energy requirement" of the process.

We will use the example of ironmaking processes to illustrate the problem. In these processes, as currently practiced or under development, carbon and/or hydrocarbons (including hydrogen) are used as the fuel as well as the reactant for reducing the iron oxide mineral (Sohn and Olivas-Martinez 2014). The different approaches for calculating the energy requirement in this case essentially boil down to the following question: Does one include the combustion heat of the reductant used in the reduction reaction or treat the reductant portion as just a reactant? Depending on the viewpoint, either approach can be considered acceptable. There is a need, however, to select a standard approach because the absolute value of "energy requirement" of an ironmaking process depends on such a choice. It is particularly important to clearly state the specific approach used when the energy requirement of ironmaking is compared with those of other industrial processes such as petrochemicals production.

25.5.2 Energy Requirement in Ironmaking Processes

25.5.2.1 General Energy Balance and Total Energy Requirement

To determine the energy requirement of a steady-state process, we start from the general statement of energy balance:

$$\begin{Bmatrix}\text{Energy Input}\\ \text{with Input Streams}\end{Bmatrix}-\begin{Bmatrix}\text{Energy Output}\\ \text{with Output Streams}\end{Bmatrix}+\begin{Bmatrix}\text{Energy Generation}\\ \text{within System}\end{Bmatrix}\mp\begin{Bmatrix}\text{Energy Leaving}\\ \text{or Added to System}\end{Bmatrix}=0 \tag{25.3}$$

Mathematically,

$$\left(-\Delta H_{T_r}^{'}\right)+\sum_i n_i\left(H_T-H_{T_r}\right)_i=\sum_j n_j\left(H_T-H_{T_r}\right)_j+Q_{\text{loss}}+Q_{\text{recovered}} \tag{25.4}$$

where n_i and n_j denote the amounts of the ith reactant and the jth product, respectively, and $(H_T - H_{Tr})$ is the sensible enthalpy of a given species at the system temperature (T). The first term on the left-hand side (LHS) of Eq. (25.4) represents the total enthalpy of the reactions occurring in the system at the reference temperature (T_r). When the overall chemical reaction is exothermic, this term is positive (i.e., energy input to the system). The opposite is true for overall endothermic reactions. In ironmaking process, this term is positive since energy is added to the system by the combustion of fuels.

The second term in the LHS of Eq. (25.4) is the energy *added* to the system in the form of sensible heat of the reactants [if the reactants enter the system at the reference temperature, this term is zero]. The first term on the right-hand side (RHS) represents the energy *removed* from the system in the form of sensible heat in the products. The second term on the RHS is the energy *removed* from the system in the form of heat losses to the surroundings. The last term in the RHS is the *recoverable* heat from the process (e.g., recovery of sensible heat of the off-gases). When some of the products contain a fuel value, it should be included in this term.

For a process involving chemical reactions to produce useful products and combustion of fuels to generate process heat, the total reaction enthalpy is a sum of the two general terms shown in the following equation:

$$\left(-\Delta H_{T_r}^{'}\right) = \left(-\Delta H_{T_r}^{'}\right)_{\text{reaction}} + \left(-\Delta H_{T_r}^{'}\right)_{\text{combustion}} \tag{25.5}$$

where $\left(-\Delta H_{T_r}^{'}\right)_{\text{reaction}}$ is the heat of reaction which is usually endothermic (negative term) for a process that has a "heat requirement" and $\left(-\text{"}\, H_{T_r}^{'}\right)_{\text{combustion}}$ is the combustion heat (positive term) of the fuel used to generate process heat. Substituting Eqs. (25.5) into (25.4), the energy balance becomes

$$\begin{aligned}\left(-\Delta H_{T_r}^{'}\right)_{\text{combustion}} + \sum_i n_i \left(H_T - H_{T_r}\right)_i &= \left(\Delta H_{T_r}^{'}\right)_{\text{reaction}} \\ + \sum_j n_j \left(H_T - H_{T_r}\right)_j + Q_{\text{loss}} + Q_{\text{recovered}}&\end{aligned} \tag{25.6}$$

To calculate and compare energy requirements of different processes producing the same desired product, the system boundaries for the different processes should be drawn so that all input materials enter the system at the reference temperature (i.e., 298 K). Thus, the second term on the LHS of Eq. (25.6) is zero. The "total energy requirement" is then given by the following equation, taking into consideration that $Q_{\text{recovered}}$ is credited to decrease energy requirement either by preheating some of the input stream or simply recovered as a useful energy source. The energy requirement is then given by

$$\begin{aligned}\text{Energy Requirement} = \left(-\Delta H_{T_r}^{'}\right)_{\text{combustion}} - Q_{\text{recovered}} &= \left(\Delta H_{T_r}^{'}\right)_{\text{reduction}} \\ + \sum_j n_j \left(H_T - H_{T_r}\right)_j + Q_{\text{loss}}&\end{aligned} \tag{25.7}$$

This equation assumes that the sensible heat contained in the products is unrecoverable and thus is discarded.

In ironmaking processes, the choice of endothermic reactions, i.e., $\left(-\Delta H'_{T_r}\right)_{\text{reduction}}$, to include in computing the "total energy requirement" [Eq. (25.7)] for the overall process is rather arbitrary and can be a source of confusion. In the following sections, the choice of the endothermic reactions on the resulting energy requirement is discussed and two approaches for calculating the energy requirement are described.

25.5.2.2 Definitions of Chemical Energy Terms

To reduce iron oxides to iron, the energy requirement for the reduction reaction can be defined in two ways: One is to consider the reduction as decomposing iron oxide to iron and oxygen (reverse of the energy of formation of iron oxide); the other is to consider it as a reaction of iron oxide with a reductant. [As shown below, the former is equivalent to including the heat of combustion of the fuel/reductant acting as a reductant in the total energy requirement, whereas the latter is equivalent to not including it.] The following is a simplified demonstration of these equivalences.

The demonstration is made just for the energy involved with chemical changes at a reference temperature (usually 298 K), excluding sensible heat and other energy terms [see Eq. (25.7)] which do not affect the argument discussed here.

Basis of the Simplified Demonstration

1. The solid charge is composed of pure iron oxide. No flux materials are considered.
2. Carbon is used as the fuel/reductant. However, this methodology can easily be extended to the case in which hydrogen or a hydrocarbon is used as the fuel/reductant.
3. The total carbon input is divided into two groups: fuel carbon and reductant carbon.
4. The heat balance is performed over the entire system. The process outputs are iron and the complete combustion product (CO_2) of fuel carbon plus the reduction product (CO_2), all at 298 K.

25.5.2.3 Chemical Reactions

The overall chemical reaction taking place to reduce iron oxide to iron using carbon as the fuel/reductant is

$$\left[\mathrm{Fe_3O_4} + 2\left(\mathrm{C}\right)_r\right] + \left[x\left(\mathrm{C}\right)_f + x\left(\mathrm{O_2}\right)_f\right] = 3\mathrm{Fe} + 2\left(\mathrm{CO_2}\right)_r + x\left(\mathrm{CO_2}\right)_f \qquad (25.8)$$

where $(C)_r$ is the carbon consumed by the reduction reaction, $(C)_f$ is the carbon burned to generate heat, $(O_2)_f$ is the oxygen for reaction with the fuel carbon, $(CO_2)_r$ is the carbon dioxide produced by the reduction reaction, $(CO_2)_f$ is the carbon dioxide produced by combustion of the fuel carbon, and x is the number of moles of the fuel portion of carbon required to generate the heat for the reduction process.

The enthalpy change of the overall reaction (25.8) is a combination of the energy required to reduce iron oxide and the energy produced by combustion of the fuel/reductant. As mentioned in the Introduction, different definitions of "energy requirement" are possible depending on what one considers as the reduction reaction between the following two reactions:

$$\mathrm{Fe_3O_4} = 3\mathrm{Fe} + 2\left(\mathrm{O_2}\right)_r \tag{25.9}$$

and

$$\mathrm{Fe_3O_4} + 2\left(\mathrm{C}\right)_r = 3\mathrm{Fe} + 2\left(\mathrm{CO_2}\right)_r \tag{25.10}$$

Approach 1: Energy Requirement for Reduction Reaction Based on Oxide Decomposition

When the reduction of iron oxide is considered to be the decomposition of the iron oxide [Eq. (25.9)], the energy requirement for reduction process is the difference between the heats of reactions (25.8) and (25.9), which is equivalent to the heat of the following combustion reaction:

$$\left[2\left(\mathrm{C}\right)_r + x\left(\mathrm{C}\right)_f\right] + \left[2\left(\mathrm{O_2}\right)_r + x\left(\mathrm{O_2}\right)_f\right] = \left[2\left(\mathrm{CO_2}\right)_r + x\left(\mathrm{CO_2}\right)_f\right] \tag{25.11}$$

The heat of this reaction $\left[\left(-\Delta H_{T_r}^{'}\right)_{\text{combustion}}\right]$ corresponds to the chemical heating value of the total amount of carbon supplied to the system. A number of reports (Remus et al. 2013; Fruehan et al. 2000; Stubbles 2000) on energy use in the iron-making industry follow this approach.

Approach 2: Energy Requirement Based on Oxide Reaction with Reductant

When the reduction of iron oxide is considered as the reaction of iron oxide with carbon [Eq. (25.10)], the energy requirement for reduction process is the difference between the heats of reactions (25.8) and (25.10), which is equivalent to the heat of the following combustion reaction:

$$x\left(\mathrm{C}\right)_f + x\left(\mathrm{O_2}\right)_f = x\left(\mathrm{CO_2}\right)_f \tag{25.12}$$

The heat of this combustion reaction [$\left(-\Delta H'_{T_r}\right)_{\text{combustion}}$] corresponds to the chemical heating value of just the fuel portion of carbon $(C)_f$. Some energy balance calculations (Pinegar et al. 2011, 2012a, b) have used this approach.

25.5.3 Results

The application of the above two approaches to the calculation of energy requirement is illustrated using as an example a novel flash ironmaking process under development at the University of Utah, described in Sect. 4.1, and an average blast furnace operation. For this purpose, a material and energy flow diagram prepared by Pinegar and coworkers (Pinegar et al. 2012a) for a commercial-scale reformerless flash ironmaking process producing one million tons of iron per year and operating with natural gas using the commercially available software METSIM is used.

25.5.3.1 Material and Energy Flows: System Boundary

Energy balance calculations start with material balance around a clearly defined system boundary. A system boundary can be drawn around different parts of a process, depending on the purpose of the calculation. An illustration is given in Fig. 25.8. The solid lines represent material flow with associated sensible and latent heats, and the open arrows indicate the flow of heat only. Once the boundary is defined, any open-ended streams that cross it are the input and output streams. Any streams entirely inside a boundary (e.g., the off-gas in Fig. 25.8 in the case of the outer boundary) are not included in the balance calculations around that boundary.

It is noted that the heat contents of any output streams that can be recovered for a useful purpose, such as steam, should be credited to reduce the input amount of energy or "energy requirement." This is equivalent to placing that term as a negative input item in the energy balance [Eq. (25.7)]. Heat losses and the sensible heat of an output stream that are not recovered are output items and increase the input amount and thus the "energy requirement." Further, all heats of chemical reaction (chemical heat contents), including heat of combustion, are calculated at 298 K and all sensible heat in input or output streams is calculated relative to this temperature.

25.5.3.2 Energy Balances for Ironmaking Processes

Tables 25.4 and 25.5 present energy inputs and outputs, respectively, in terms of Approaches 1 and 2 for the flash ironmaking process using natural gas or hydrogen and for the average blast furnace operation. These values were calculated around the outer boundary in Fig. 25.8, depicted by the dashed line. The annual production rates in all the cases are one million tons of iron from a single unit of the ironmaking

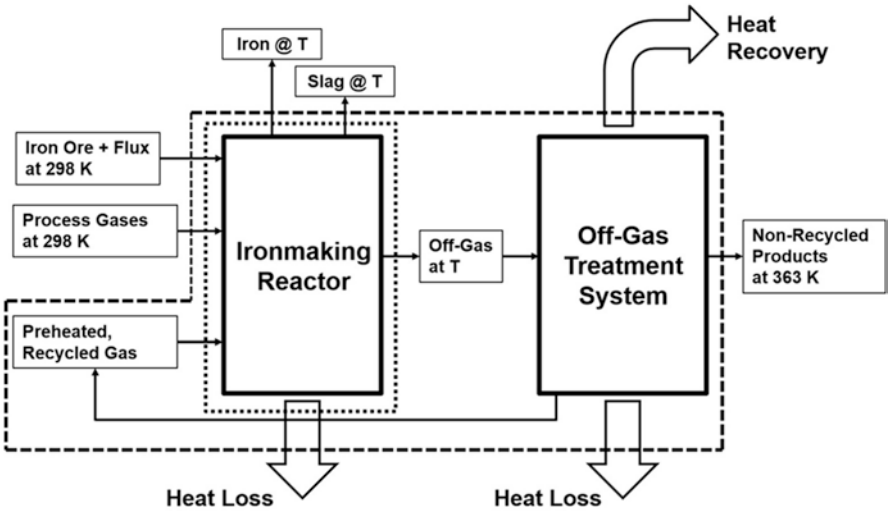

Fig. 25.8 Examples of a system boundary for material and energy balance calculations for an ironmaking process [adapted from Sohn and Olivas-Martinez (2014)]

reactor. The energy balance for the flash ironmaking process is based on the flow sheet presented by Pinegar et al. (2012a). Higher heating values (HHV) of natural gas and hydrogen were used to be conservative in calculating the energy requirements, respectively, of reformerless flash ironmaking and hydrogen-based flash ironmaking. The energy balance for an average blast furnace operation was calculated using published material balance data and applying the same method of calculating energy values as for the flash ironmaking process. Although not shown here, Sohn and Olivas-Martinez (2014) also presented the energy balances for the reformerless flash ironmaking process and for the average blast furnace as Sankey diagrams (Schlesinger 1995).

In the blast furnace process, the energy consumed by sintering, pelletizing, and cokemaking operations, which are not required in flash ironmaking, is part of the energy requirement and represents a significant portion of the overall energy requirement for the blast furnace operation. The ore/coke preparation accounts for 30 and 40 % of the total energy input (which is defined as the sum of the input streams) in terms of Approaches 1 and 2, respectively (Sohn and Olivas-Martinez 2014).

For the flash ironmaking process, the cases of using two different reductants/fuels—natural gas or hydrogen—have been analyzed. The results of applying Approach 2 were adapted from Pinegar et al. (2011, 2012a) and those of applying Approach 1 were calculated by modifying the "Fuel combustion" term in the input category and the "Reduction" term in the output category, which are the only numbers that are different between Approaches 1 and 2.

In terms of the descriptions of Approaches 1 and 2 formulated above, the "fuel combustion" energy input was calculated by adding the energy (subtracting reaction

Table 25.4 Energy input items for a commercial-scale flash ironmaking process using natural gas or hydrogen compared with those for an average blast furnace process (production rate=1 million tons of iron) [adapted from Pinegar et al. (2011, 2012a)]

Process		Reformerless natural gas		Hydrogen[d]		Blast furnace[a,e]	
Approach		1	2	1	2	1	2
ITEMIZED INPUT (GJ/t Fe)	Fuel combustion[b]	19.22	13.45	14.05	8.28	13.60	8.33
	Heat recovery (sum of next 2)	−4.77		−2.80		−1.32	
	(Waste heat boiler)	(−3.39)					
	(Steam not used)	(−1.38)					
	Sub-total	14.45	8.68	11.25	5.48	12.28	7.01
	Ore/Coke preparation[c]					5.68	
	$CaCO_3$ and $MgCO_3$ calcination (external)	0.26		0.26			
	Total	14.71	8.94	11.51	5.74	17.96	12.69

[a]Energy balance was calculated by METSIM based on the published material balance
[b]Fuel combustion energy input was calculated by adding the energy (subtracting reaction enthalpy) for iron ore reduction from the difference of heats of formation of all output components and input components [Eq. (25.8)]. This amount is equivalent to the heat of reaction (25.11) for Approach 1 and reaction (25.12) for Approach 2. Higher heating values (HHV) of the natural gas and hydrogen were used for this calculation
[c]See Sohn and Olivas-Martinez (2014) for references
[d]Energy requirement for hydrogen production was not included for this calculation. It is anticipated that the energy required for hydrogen production will strongly depend on the production process such as steam-methane reforming, coal gasification, or water splitting
[e]In fairness to excluding the energy requirement of hydrogen production in the energy balance of flash ironmaking, the energy required for producing coking coal was not included either for the blast furnace

enthalpy) for iron ore reduction from the difference of heats of formation of all output components and input components [Eq. (25.8)]. This amount is equivalent to the heat of combustion of reaction (25.11) for Approach 1 and reaction (25.12) for Approach 2.

The "reduction" energy in the output category (i.e., Table 25.5) corresponds to the decomposition of magnetite (Fe_3O_4) [reaction (25.9) (6.68 GJ/t Fe)] for Approach 1 for the flash ironmaking process. For the blast furnace, it corresponds to the heat of decomposition of hematite (Fe_2O_3) (7.37 GJ/t Fe). [Magnetite concentrate must be pelletized or sintered to be used in a blast furnace during which it is converted to hematite, generating heat. This heat generation is reflected in the energy requirement for pelletization. Thus, it is appropriate to use hematite as the feed material in blast furnace operations.] In Approach 2, the "reduction" energy corresponds to the heat of reduction reaction by hydrogen (0.91 GJ/t Fe) for flash ironmaking [even when natural gas is used, essentially all reduction is done by hydrogen produced

Table 25.5 Energy output items for a commercial-scale flash ironmaking process using natural gas or hydrogen compared with those for an average blast furnace process (production rate = 1 million tons of iron) [adapted from Pinegar et al. (2011, 2012a)]

Process		Reformerless natural gas		Hydrogen		Blast furnace[a]	
Approach		1	2	1	2	1	2
Itemized output (GJ/t Fe)	Reduction[b]	6.68	0.91	6.68	0.91	7.37	2.10
	Sensible heat of iron	1.27 (1773 K)				1.35 (1873 K)	
	Sensible heat of slag	0.24 (1773 K)				0.47 (1873 K)	
	Slurry (H_2O (l))	2.25 (323 K)		1.93			
	Hot water not used	1.57 (493 K)					
	Flue gas	0.79 (573 K)				0.26 (363 K)	
	Removed water vapor			0.01			
	$CaCO_3$ decomposition					0.33	
	Slagmaking					−0.17	
	Heat loss in the reactor	0.78		0.78		2.60	
	Heat loss in the heat exchangers (sum of next 3)	0.73		0.34		0.07	
	(Reactor feed gas heater)	(0.40)					
	(Natural gas heater)	(0.21)					
	(WGS reactor feed gas heater)	(0.12)					
	Steam not used (363 K)	0.14					
	Sub-total	14.45	8.68	11.25	5.48	12.28	7.01
	Pelletizing[c]					3.01	
	Sintering[c]					0.65	
	Cokemaking[c]					2.02	
	$CaCO_3$ and $MgCO_3$ calcination (external)	0.26		0.26			
	Total	14.71	8.94	11.51	5.74	17.96	12.69

[a]Energy balance was calculated by METSIM based on the published material balance

[b]For flash ironmaking process, the reduction energy corresponds to the decomposition of magnetite (25.10) (6.68 GJ/t Fe) for Approach 1. For the blast furnace, it corresponds to the heat of decomposition of Fe_2O_3 (7.37 GJ/t Fe). In Approach 2, reduction energy corresponds to the heat of reduction reaction (25.11) (0.91 GJ/t Fe) for flash ironmaking and the heat of the reaction $Fe_2O_3 + 3/2C = 2Fe + 3/2CO_2$ for the blast furnace [see discussion in the text for the justification of using hematite for the blast furnace]

[c]See Sohn and Olivas-Martinez (2014) for references

from partial combustion of natural gas] and it is the heat of the reaction $Fe_2O_3 + 3/2C = 2Fe + 3/2CO_2$ for the blast furnace.

The energy requirement calculated using Approach 2 is the "process energy requirement" and the difference between the total input energy by Approach 1 and the process energy requirement may be termed "reductant energy" ["feedstock energy" in petrochemicals production] (Sohn and Olivas-Martinez 2014).

25.5.4 Discussion

As can be seen in Tables 25.4 and 25.5, the difference in the energy requirements between each ironmaking process and the blast furnace remains largely the same regardless of the treatment given to the fuel used as a reductant.

The "energy requirements" of these processes can be obtained directly from the total amounts of energy inputs in Table 25.4 and outputs in Table 25.5. This is possible because in Table 25.4 the recovered heat is presented as a negative input item, as indicated by Eq. (25.7). The energy balance results can be presented with such an item listed as a positive output item in Table 25.5, in which case the "balance" is still achieved, as indicated by Eq. (25.6).

In some reports (De Beer et al. 2000; Sohn and Olivas-Martinez 2014), the energy required for decomposing iron oxide to iron and oxygen, reaction (25.9), is used as the "theoretically lowest" or "theoretical minimum" energy requirement. It is noted that this reaction, which does not actually take place under ironmaking processes, involves the largest enthalpy change (energy requirement) of any chemical reactions involved in the production of iron from iron oxide. This decomposition reaction requires more than 30 % of the energy input in both processes. The energy required for this reaction is used as an item of energy requirement in Approach 1 above. In Approach 2, the endothermic heat of the reduction reaction [e.g., reaction (25.10)] is used for calculating energy requirement. This energy represents only 7 and 15 % of the energy input when Approach 2 is used for determining the energy requirement for the flash ironmaking process and blast furnace, respectively.

A simple food-for-thought question: If we consider a process in which the reaction

$$2/3Fe_2O_3 + C = 4/3Fe + CO_2 \tag{25.13}$$

occurs at room temperature, what do we consider as the energy requirement for the process? Is it the heat of reaction (25.13), or should it include the heat of combustion of the carbon used as a reactant just because it has a heating value?

When calculating "energy requirements" and presenting the results, it is essential to clearly state the approach used. Specifically and most importantly, it should be stated whether or not the chemical heat content (the heat of combustion) of a reactant that can also be used as a fuel is included in the calculated value of energy

requirement. Even with these clarifications of approaches, it will make it much clearer to present distinct values for "process energy requirement" that includes only the heating value of the fuel and "reductant energy" ("feedstock energy" in petrochemicals production) that represents the chemical heating value of the material used as a reactant.

It is advocated using just the "process energy requirement" as the standard value of the energy requirement for a process in which a reactant is also a fuel, which is equivalent to using Approach 2.

In addition, a statement regarding whether the higher heating value (HHV; assumes liquid water in the combustion products) or the lower heating value (LHV; assumes water vapor in the combustion products at 298 K) should be included when the fuel contains hydrogen. Another item of information often neglected that must be provided is the system boundary around which the material and energy balances are performed; that is, clear definitions of input and output streams and conditions.

25.6 Conclusions

According to the International Energy Association (IEA), the iron and steel sector accounts for 6.7 % of the world CO_2 emissions. Also, the iron and steel industry is the second-largest industrial user of energy, consuming 2.58×10^7 TJ in 2007 and the largest industrial source of CO_2 emissions (30 %). On average, 1.9 t of CO_2 are emitted for every ton of steel produced coming mostly from the BF process as mentioned earlier.

Reduction in energy use and CO_2 emissions in the steel industry is rapidly reaching the limits defined by the laws of physics and chemistry. In order to make major reductions in future energy consumption and CO_2 emissions, new methods of making steel will require completely fresh and innovative thinking. Breakthrough technologies based on radically new routes will be required in order to fulfill the environmental regulations and energy consumption reduction plans.

Given the limited efficiency potential inherent in existing best technologies and based on the driving force discussed above, an FIT was conceived as a novel ironmaking process at the University of Utah. This technology is based on fine particle reduction using a reductant gas such as hydrogen, natural gas, coal gas, or a combination thereof. It is the first flash-type ironmaking process converting iron ore concentrate directly to metallic iron in-flight, which would be suitable for an industrial-scale operation. This process will produce iron without requiring pelletization or sintering and thus avoids the need for coke. In addition, this process concept allows an intensive operation, unlike other alternate ironmaking routes, taking a full advantage of the fine particle size of the concentrate with a large surface area which permits rapid reduction by a gas. Another potential benefit of this process is the possibility of steelmaking in a single continuous process. This transformative technology is expected to allow significant energy saving and reduced CO_2 emissions compared with the blast furnace process.

Finally, when calculating "energy requirements" and presenting the results, it should be stated whether or not the chemical heat content (the heat of combustion) of a reactant that can also be used as a fuel is included in the calculated value of energy requirement. It is advocated using just the "process energy requirement" as the standard value of the energy requirement for a process in which a reactant is also a fuel.

Acknowledgments The authors thank both previous and current members of the Sohn laboratory whose work was cited in this paper. The authors acknowledge the financial support from American Iron and Steel Institute (AISI) through a Research Service Agreement with the University of Utah under AISI's CO_2 Breakthrough Program. This material also contains results of work supported by the US Department of Energy under Award Number DE-EE0005751 with cost share by AISI and the University of Utah.

References

Birat J-P, Hanrot F, Danloy G (2004) CO_2 mitigation technologies in the steel industry: a benchmarking study based on process calculation. Canadian Institute of Mining, Metallurgy and Petroleum

Cheeley R (1999) Gasification and the Midrex direct reduction process. In: 1999 Gasification technologies conference, San Francisco, California

Chen F, Mohassab Y, Jiang T, Sohn HY (2015a) Hydrogen reduction kinetics of hematite concentrate particles relevant to a novel flash ironmaking process. Metall Mater Trans B 46(3): 1133–1145

Chen F, Mohassab Y, Zhang S, Sohn H (2015b) Kinetics of the reduction of hematite concentrate particles by carbon monoxide relevant to a novel flash ironmaking process. Metall Mater Trans B 46B(4):1716–1728

Choi ME, Sohn HY (2010) Development of green suspension ironmaking technology based on hydrogen reduction of iron oxide concentrate: rate measurements. Ironmaking Steelmaking 37(2):81–88

De Beer J, Worrell E, Blok K (1998) Future technologies for energy-efficient iron and steel making. Annu Rev Energy 23:123–205

Duarte PE, Becerra J, Lizcano C, Martinis A (2008) ENERGIRON direct reduction technology-economical, flexible, environmentally friendly. Acero LatinoAmericano 6:52–58

Fruehan RJ, Fortini O, Paxton HW, Brindle R (2000) Theoretical minimum energies to product steel for selected conditions. U.S. Department of Energy. http://energy.gov/sites/prod/files/2013/11/f4/theoretical_minimum_energies.pdf. Accessed 01 June 2016

Gupta S, Sahajwalla V (2005) The scope for fuel rate reduction in ironmaking. In: Burgess J (ed) Technical note 16. Cooperative Research Centre for Coal in Sustainable Development QCAT Technology Transfer Centre, Pullenvale

Hassan A, Whipp R, Millionis K, Zeller S (1994) Development of an improved fluid bed reduction process. In: Ironmaking conference proceedings. Iron and Steel Society of AIME, Warrendale, pp 481–490

Husain R, Sneyd S, Weber P (1999) Circored and Circofer - two new fine ore reduction processes. Publ. Australas. Inst. Min. Metall. 3/99 (ICARISM '99, Proceedings of the International Conference on Alternative Routes of Iron and Steelmaking), pp 123–129

Industrial Efficiency Technology Database (IETD) (2012a) Iron and steel. http://www.ietd.iipnetwork.org/content/iron-and-steel. Accessed 16 Oct 2012

Industrial Efficiency Technology Database (IETD) (2012b) Direct reduced iron. http://www.ietd.iipnetwork.org/content/direct-reduced-iron. Accessed 13 Oct 2012

Institute for Prospective Technological Studies (IPTS) (2009) Integrated pollution prevention and control: draft reference document on best available techniques for the production of iron and steel. http://old.vpvb.gov.lv/ippc/bat/bat_ES1/EdzelzsTerauds_Pr200907.pdf. Accessed 13 Oct 2012

Kim H, Paramore J, Allanore A, Sadoway DR (2011) Electrolysis of molten iron oxide with an iridium anode: the role of electrolyte basicity. J Electrochem Soc 158(10):E101–E105

Macauley D (1997) Options increase for non-BF ironmaking. Steel Times Int 21(1):20

Mohassab Ahmed MY (2013) Phase equilibria between iron and slag in $CO/CO_2/H_2/H_2O$ atmospheres relevant to a novel flash ironmaking technology. PhD Dissertation, The University of Utah

Mohassab Y, Sohn HY (2014a) Analysis of slag chemistry by FTIR-RAS and raman spectroscopy: effect of water vapor content in H_2-H_2O-CO-CO_2 mixtures relevant to a novel green ironmaking technology. Steel Res Int 86(7):740–752

Mohassab Y, Sohn HY (2014b) Effect of water vapor on sulfur distribution between liquid Fe and MgO-saturated slag relevant to a flash ironmaking technology. Steel Res Int 86(7):753–759

Mohassab Y, Sohn HY (2015) Effect of water vapour on distribution of phosphorus between liquid iron and MgO saturated slag relevant to flash ironmaking technology. Ironmaking Steelmaking 42(5):346–350

Mohassab Y, Chen F, Elzohiery M, Abelghany A, Zhang S, Sohn HY (2016) Reduction kinetics of hematite concentrate particles by CO+H mixture relevant to a novel flash ironmaking process. In: 7th international symposium on high temperature metallurgical processing, TMS 145 annual meeting & exhibition, Nashville

Mohassab-Ahmed MY, Sohn HY (2014a) Effect of water vapor content in H_2-H_2O-CO-CO_2 mixtures on the activity of iron oxide in slags relevant to a novel flash ironmaking technology. Ironmaking Steelmaking 41(9):665–675

Mohassab-Ahmed MY, Sohn HY (2014b) Effect of water vapor content in H_2–H_2O–CO–CO_2 mixtures on the equilibrium distribution of manganese between CaO–MgO_{sat}–SiO_2–Al_2O_3–FeO–P_2O_5 slag and molten iron. Steel Res Int 85(5):875–884

Mohassab-Ahmed MY, Sohn HY, Kim HG (2012a) Phosphorus distribution between liquid iron and magnesia-saturated slag in H_2/H_2O atmosphere relevant to a novel ironmaking technology. Ind Eng Chem Res 51(20):7028–7034

Mohassab-Ahmed MY, Sohn HY, Kim HG (2012b) Sulfur distribution between liquid iron and magnesia-saturated slag in H_2/H_2O atmosphere relevant to a novel green ironmaking technology. Ind Eng Chem Res 51(9):3639–3645

Mohassab-Ahmed MY, Sohn HY, Zhu L (2014) Effect of water vapour content in H_2–H_2O–CO–CO_2 mixtures on MgO solubility in slag under conditions of novel flash ironmaking technology. Ironmaking Steelmaking 41(8):575–582

Orth A, Anastasijevic N, Eichberger H (2007) Low CO_2 emission technologies for iron and steelmaking as well as Titania slag production. Miner Eng 20(9):854–861

Pinegar HK, Moats MS, Sohn HY (2011) Process simulation and economic feasibility analysis for a hydrogen-based novel suspension ironmaking technology. Steel Res Int 82(8):951–963

Pinegar H, Moats M, Sohn H (2012a) Flowsheet development, process simulation and economic feasibility analysis for novel suspension ironmaking technology based on natural gas: Part 1 –

Flowsheet and simulation for ironmaking with reformerless natural gas. Ironmaking Steelmaking 39(6):398–408
Pinegar H, Moats M, Sohn H (2012b) Flowsheet development, process simulation and economic feasibility analysis for novel suspension ironmaking technology based on natural gas: Part 2 – Flowsheet and simulation for ironmaking combined with steam methane reforming. Ironmaking Steelmaking 40:44–49
Pinegar H, Moats M, Sohn HY (2012c) Flowsheet development, process simulation and economic feasibility analysis for novel suspension ironmaking technology based on natural gas: Part 3 – economic feasibility analysis. Ironmaking Steelmaking 40:44–49
Remus R, Aguado Monsonet MA, Roudier S, Delgado Sancho L (2013) Best available techniques (BAT) reference document for iron and steel production. Industrial Emissions Directive 2010/75/EU (Integrated Pollution Prevention and Control), Joint Research Centre (JRC) of the European Union, Spain, pp 304–305
Schlesinger MA (1995) Mass and energy balances in materials engineering. Prentice Hall College Div, Saddle River
Sohn HY (2007) Suspension ironmaking technology with greatly reduced energy requirement and CO_2 emissions. Steel Times Int 31(3):68–72
Sohn HY, Choi ME (2012) Steel industry and carbon dioxide emissions - a novel ironmaking process with greatly reduced carbon footprint. In: Carpenter M, Shelton EJ (eds) Carbon dioxide emissions: new research, vol. 11788. Nova Science Publishers, Hauppauge
Sohn H, Olivas-Martinez M (2014) Methods for calculating energy requirements for processes in which a reactant is also a fuel: need for standardization. JOM 66(9):1557–1564
Strassburger JH, Brown DC, Dancy TE, Stephenson RL (1969) Blast furnace-theory and practice. Gordon and Breach Science
Stubbles J (2000) Energy use in the U.S. Steel Industry: an historical perspective and future opportunities. U.S. Department of Energy. http://energy.gov/sites/prod/files/2013/11/f4/steel_energy_use.pdf. Accessed 01 June 2016
Ultra-Low CO_2 Steelmaking (ULCOS) (2012) from http://www.ulcos.org/en/research/electrolysis.php. Accessed 17 Oct 2012
Wang H, Sohn H (2013) Hydrogen reduction kinetics of magnetite concentrate particles relevant to a novel flash ironmaking process. Metall Mater Trans B 44(1):133–145
World Steel Association (WSA) (2012) World Steel in Figures 2012. from http://www.worldsteel.org/dms/internetDocumentList/bookshop/WSIF_2012/document/World%20Steel%20in%20Figures%202012.pdf. Accessed 08 Oct 2012
Worrell E, Price L, Neelis M, Galitsky C, Nan Z (2008) World best practice energy intensity values for selected industrial sectors. Lawrence Berkeley National Laboratory. Berkeley, CA, LBNL-62806
Worrell EBP, Neelis M, Blomen E, Masanet E (2010) Energy efficiency improvement and cost saving opportunities for the U.S. iron and steel industry: an ENERGY STAR® guide for energy and plant managers. 10/08/2012, from http://ies.lbl.gov/drupal.files/ies.lbl.gov.sandbox/4779E.pdf
Yellishetty M, Ranjith PG, Tharumarajah A (2010) Iron ore and steel production trends and material flows in the world: is this really sustainable? Res Conserv Recycl 54(12):1084–1094
Yuan Z (2013) Re-oxidation kinetics of flash-reduced iron particles relevant to a novel flash ironmaking process. MS, University of Utah
Yuan Z, Sohn HY (2014) Re-oxidation kinetics of flash reduced iron particles in O –N gas mixtures relevant to a novel flash ironmaking process. ISIJ Int 54(6):1235–1243
Yuan Z, Sohn HY, Olivas-Martinez M (2013) Re-oxidation kinetics of flash-reduced iron particles in H_2-H_2O(g) atmosphere relevant to a novel flash ironmaking process. Metall Mater Trans B 44(6):1520–1530

Index

P. Cavaliere (ed.), *Ironmaking and Steelmaking Processes*,
DOI 10.1007/978-3-319-39529-6